Exhibit 1

US010775376B2

(12) **United States Patent**
Singhal et al.

(10) **Patent No.: US 10,775,376 B2**
(45) **Date of Patent: *Sep. 15, 2020**

(54) **METHODS FOR ASSAYING CELLULAR BINDING INTERACTIONS**

(71) Applicant: **The University of British Columbia**, Vancouver, BC (CA)

(72) Inventors: **Anupam Singhal**, Mississauga (CA); **Carl L. G. Hansen**, Vancouver (CA); **John W. Schrader**, Vancouver (CA); **Charles A. Haynes**, Vancouver (CA); **Daniel J. Da Costa**, Pitt Meadows (CA)

(73) Assignee: **THE UNIVERSITY OF BRITISH COLUMBIA**, Vancouver (CA)

(*) Notice: Subject to any disclaimer, the term of this patent is extended or adjusted under 35 U.S.C. 154(b) by 0 days.

This patent is subject to a terminal disclaimer.

(21) Appl. No.: **16/746,540**

(22) Filed: **Jan. 17, 2020**

(65) **Prior Publication Data**

US 2020/0150119 A1 May 14, 2020

Related U.S. Application Data

(63) Continuation of application No. 16/579,561, filed on Sep. 23, 2019, now Pat. No. 10,578,618, which is a (Continued)

(51) **Int. Cl.**
B01L 3/00 (2006.01)
G01N 33/569 (2006.01)
(Continued)

(52) **U.S. Cl.**
CPC .. ***G01N 33/56966*** (2013.01); ***B01L 3/502738*** (2013.01); ***B01L 3/502761*** (2013.01);
(Continued)

(58) **Field of Classification Search**
None
See application file for complete search history.

(56) **References Cited**

U.S. PATENT DOCUMENTS

5,874,085 A 2/1999 Mond et al.
6,007,690 A 12/1999 Nelson et al.
(Continued)

FOREIGN PATENT DOCUMENTS

WO 2003085379 A3 12/2003
WO 2005069980 A2 8/2005
(Continued)

OTHER PUBLICATIONS

Jerne (1984) "The generative grammar of the immune system" EMBO J. 4(4):847-852.
(Continued)

Primary Examiner — Rebecca M Giere
(74) *Attorney, Agent, or Firm* — Potomac Law Group, PLLC

(57) **ABSTRACT**

There are provided methods, and devices for assaying for a binding interaction between a protein, such as a monoclonal antibody, produced by a cell, and a biomolecule. The method may include retaining the cell within a chamber having an aperture; exposing the protein produced by the cell to a capture substrate, wherein the capture substrate is in fluid communication with the protein produced by the cell and wherein the capture substrate is operable to bind the protein produced by the cell; flowing a fluid volume comprising the biomolecule through the chamber via said aperture, wherein the fluid volume is in fluid communication with the capture substrate; and determining a binding interaction between the protein produced by the cell and the biomolecule.

27 Claims, 29 Drawing Sheets

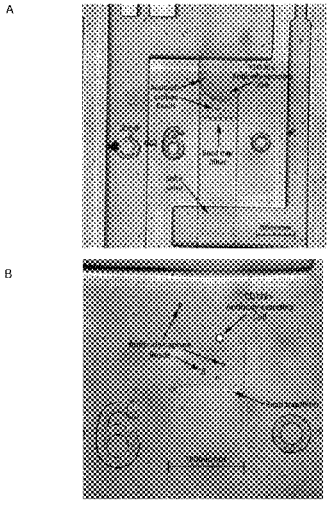

Related U.S. Application Data

continuation of application No. 16/290,751, filed on Mar. 1, 2019, now Pat. No. 10,466,241, which is a continuation of application No. 16/129,555, filed on Sep. 12, 2018, now Pat. No. 10,274,494, which is a continuation of application No. 14/879,791, filed on Oct. 9, 2015, now Pat. No. 10,107,812, which is a continuation of application No. 13/184,363, filed on Jul. 15, 2011, now Pat. No. 9,188,593.

(60) Provisional application No. 61/365,237, filed on Jul. 16, 2010.

(51) **Int. Cl.**

G01N 33/68	(2006.01)
G01N 33/577	(2006.01)
G01N 33/58	(2006.01)

(52) **U.S. Cl.**

CPC ***G01N 33/577*** (2013.01); ***G01N 33/582*** (2013.01); ***G01N 33/6854*** (2013.01); *B01L 2200/0668* (2013.01); *B01L 2300/0681* (2013.01); *B01L 2300/0861* (2013.01); *B01L 2300/0864* (2013.01); *B01L 2300/0867* (2013.01); *B01L 2400/0481* (2013.01)

(56) **References Cited**

U.S. PATENT DOCUMENTS

7,143,785	B2	12/2006	Maerkl et al.
8,124,015	B2	2/2012	Diercks et al.
9,188,593	B2	11/2015	Singhal et al.
10,107,812	B2	10/2018	Singhal et al.
10,274,494	B2	4/2019	Singhal et al.
2002/0164656	A1	11/2002	Hoeffler et al.
2009/0068170	A1	3/2009	Weitz et al.
2010/0086919	A1	4/2010	McKeon
2011/0262906	A1	10/2011	Dimov et al.
2011/0294678	A1	12/2011	Jin et al.
2013/0130301	A1	5/2013	Yoon et al.

FOREIGN PATENT DOCUMENTS

WO	2009012340	A2	1/2009
WO	2010046775	A2	4/2010
WO	2012162779	A1	12/2012

OTHER PUBLICATIONS

Abdiche et al. (2008) "Determining kinetics and affinities of protein interactions using a parallel real-time label-free biosensor, the Octet" Analytical Biochemistry 377(2):209-217.

Babcook et al. (1996) "A novel strategy for generating monoclonal antibodies from single, isolated lymphocytes producing antibodies of defined specificities" Proc. Natl. Acad. Sci. USA 93(15):7843-7848.

Bates & Quake (2009) "Highly parallel measurements of interaction kinetic constants with a microfabricated optomechanical device" Appl. Phys. Lett. 95(7):73705.

Batista & Neuberger (1998) "Affinity dependence of the B cell response to antigen: a threshold, a ceiling, and the importance of off-rate" Immunity 8(6):751-759.

Biacore Life Sciences—Biacore 3000 System Information. (2012). Website: http://www,biacore.com/lifesciences/products/svstems_overview/3000/svstem_information/index.html.

Biacore Life Sciences—Single-Cycle Kinetics. (2012). Website: https://www.biacore.com/lifesciences/technology/introduction/data_interaction/SCK/index.html.

Bornhop et al. (2007) "Free-solution, label-free molecular interactions studied by back-scattering interferometry" Science 317(5845):1732-1736.

Cai et al. (2006) "Stochastic protein expression in individual cells at the single molecule leve" Nature 440(7082):358-362.

Dlugosz et al. (2009) "pH-dependent association of proteins. The test case of monoclonal antibody HyHEL-5 and its antigen hen egg white lysozyme" The Journal of Physical Chemistry 113(47):15662-15669.

England et al. (1999) "Functional characterization of the somatic hypermutation process leading to antibody D1.3, a high affinity antibody directed against lysozyme" J. Immunol. 162(4):2129-2136.

Hansen et al. (2002) "A robust and scalable microfluidic metering method that allows protein crystal growth by free interface diffusion" Proc. Natl. Acad. Sci. USA 99(26):16531-16536.

Hansen et al. (2004) "Systematic investigation of protein phase behavior with a microfluidic formulator" Proc. Natl. Acad. Sci. USA 101(40):14431-14436.

He & Niemeyer (2003) "A novel correlation for protein diffusion coefficients based on molecular weight and radius of gyration" Biotechnol. Prog. 19(2):544-548.

Homola et al. (1999) "Surface plasmon resonance sensors: review" Sensors and Actuators B: Chemical 54:3-15.

Huang et al. (2007) "Counting low-copy number proteins in a single cell" Science 315(5808):81-84.

Ito et al. (1995) "Mutations in the complementarity-determining regions do not cause differences in free energy during the process of formation of the activated complex between an antibody and the corresponding protein antigen" J. Mol. Biol. 248(4):729-732.

Jin et al. (2009) "A rapid and efficient single-cell manipulation method for screening antigen-specific antibody-secreting cells from human peripheral blood" Nat. Med.15(9):1088-1092.

Karpas et al. (2001) "A human myeloma cell line suitable for the generation of human monoclonal antibodies" Proc. Natl. Acad. Sci. USA 98(4):1799-1804.

Kohler & Milstein (1975) "Continuous cultures of fused cells secreting antibody of predefined specificity" Nature 256(5517):495-497.

Lanzavecchia et al. (2007) "Human monoclonal antibodies by immortalization of memory B cells" Current Opinion in Biotechnology 18(6):523-528.

Lecault et al. (2011) "High-Throughput Analysis of Single Hematopoietic Stem Cell Proliferation in Microfluidic Cell Culture Arrays" Nat Methods 8(7):581-586.

Lee et al. (2009) "High-sensitivity microfluidic calorimeters for biological and chemical applications" Proc. Natl. Acad. Sci. USA 106(36):15225-15230.

Maerkl & Quake (2007) "A systems approach to measuring the binding energy landscapes of transcription factors" Science 315(5809):233-237.

Marcus et al. (2006) "Microfluidic single-cell mRNA isolation and analysis" Anal. Chem. 78(9):3084-3089.

McDonald et al. (2000) "Fabrication of microfluidic systems in poly(dimethylsiloxane)" Electrophoresis 21: 27-40.

McKinney et al. (1995) "Optimizing antibody production in batch hybridoma cell culture" J.Biotechnol. 40(1):31-48.

Pasqualini & Arap (2004) "Hybridoma-free generation of monoclonal antibodies" Proc. Natl. Acad. Sci. USA 101(1):257-259.

Poulson et al. (2007) "Kinetic, affinity, and diversity limits of human polyclonal antibody responses against tetanus toxoid" J. Immunol. 179(6):3841-3850.

Raschke et al. (2003) "Biomolecular Recognition Based on Single Gold Nanoparticle Light Scattering" Nano Letters 3(7):935-938.

Sonnichsen et al. (2000) "Spectroscopy of single metallic nanoparticles using total internal reflection microscopy" App. Phys. Letters 77(19): 2949-2951.

Spieker-Polet et al. (1995) "Rabbit monoclonal antibodies: generating a fusion partner to produce rabbit-rabbit hybridomas" Proc. Natl. Acad. Sci. USA 92(20):9348-9352.

Squires & Quake (2005) "Microfluidics: Fluid physics at the nanoliter scale" Reviews of Modern Physics 77(3):977-1026.

Story et al. (2008) "Profiling antibody responses by multiparametric analysis of primary B cells" Proc. Natl. Acad. Sci. U.S.A. 105(46):17902-17907.

(56) **References Cited**

OTHER PUBLICATIONS

Thorsen et al. (2002) "Microfluidic large-scale integration" Science 298(5593):580-584.
Tiller et al. (2009) "Cloning and expression of murine Ig genes from single B cells" J. Immunol. Methods 350(1-2):183-193.
Traggiai et al. (2004) "An efficient method to make human monoclonal antibodies from memory B cells: potent neutralization of SARS coronavirus" Nat Med 10(8):871-875.
Tyn & Gusek (1990) "Prediction of diffusion coefficients of proteins" Biotechnol. Bioeng. 35(4):327-338.
Ueno et al. (2010) "Simple dark-field microscopy with nanometer spatial precision and microsecond temporal resolution" Biophysical J. 98(9):2014-2023.
Unger et al. (2000) "Monolithic microfabricated valves and pumps by multilayer soft lithography" Science 288 (5463)113-116.
Wang et al. (2005) "Label-free detection of small-molecule-protein interactions by using nanowire nanosensors" Proc. Natl. Acad. Sci. USA 102(9):3208-3212.
Xavier & Willson (1998) "Association and dissociation kinetics of anti-hen egg lysozyme monoclonal antibodies HyHEL-5 and HyHEL-10" Biophys. J. 74(4):2036-2045.

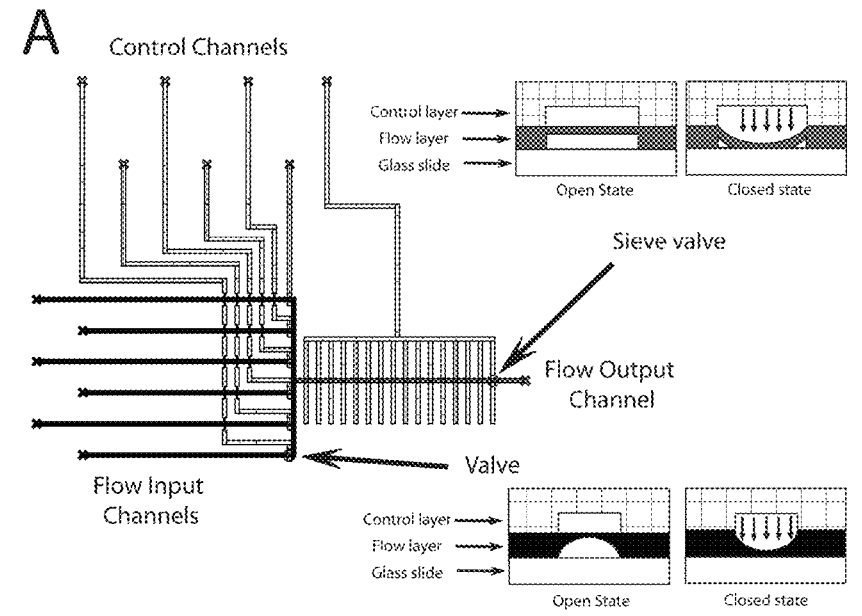
A
Control Channels
Control layer
Flow layer
Glass slide
Open State
Closed state
Sieve valve
Flow Output Channel
Valve
Flow Input Channels
Control layer
Flow layer
Glass slide
Open State
Closed state

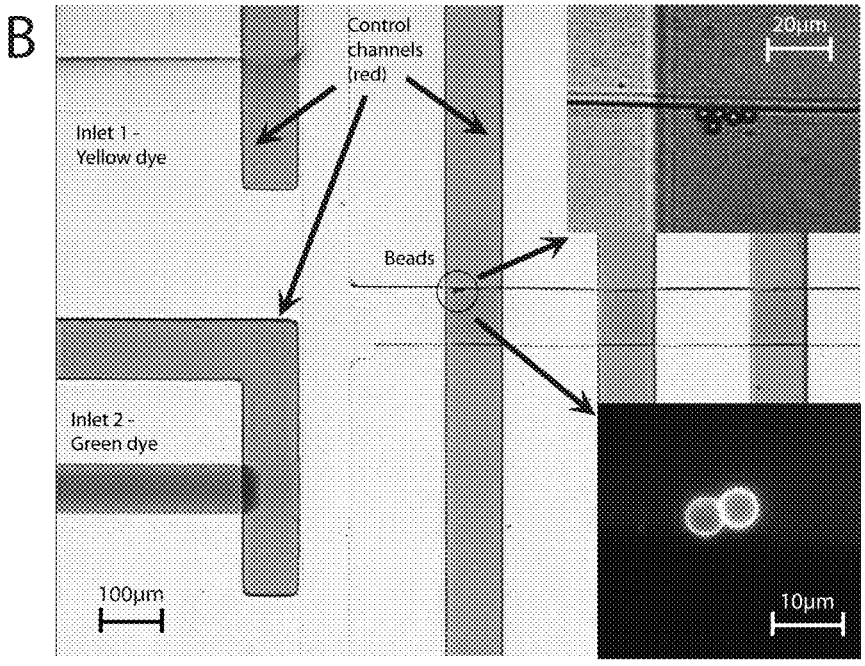
B
Control channels (red)
20µm
Inlet 1 - Yellow dye
Beads
Inlet 2 - Green dye
100µm
10µm

Figure 1

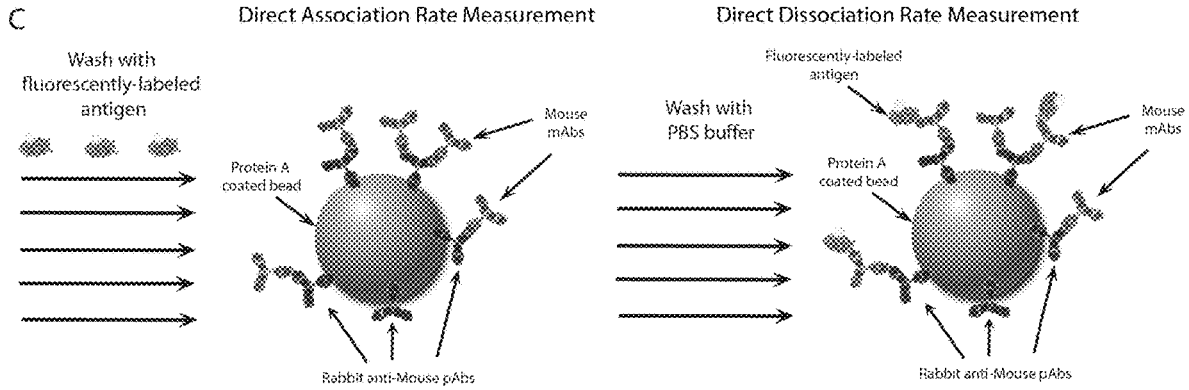

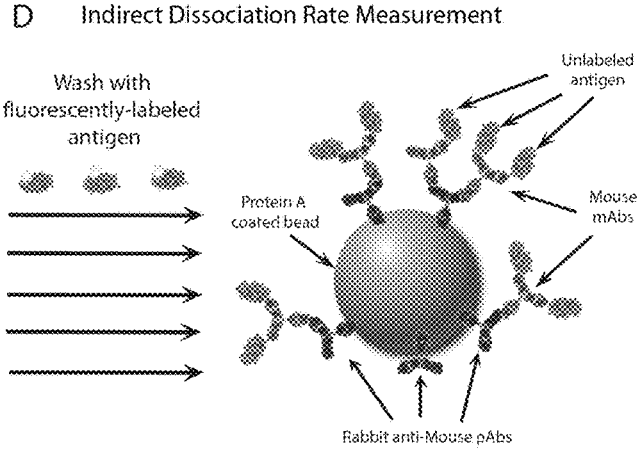

Figure 1 cont'd

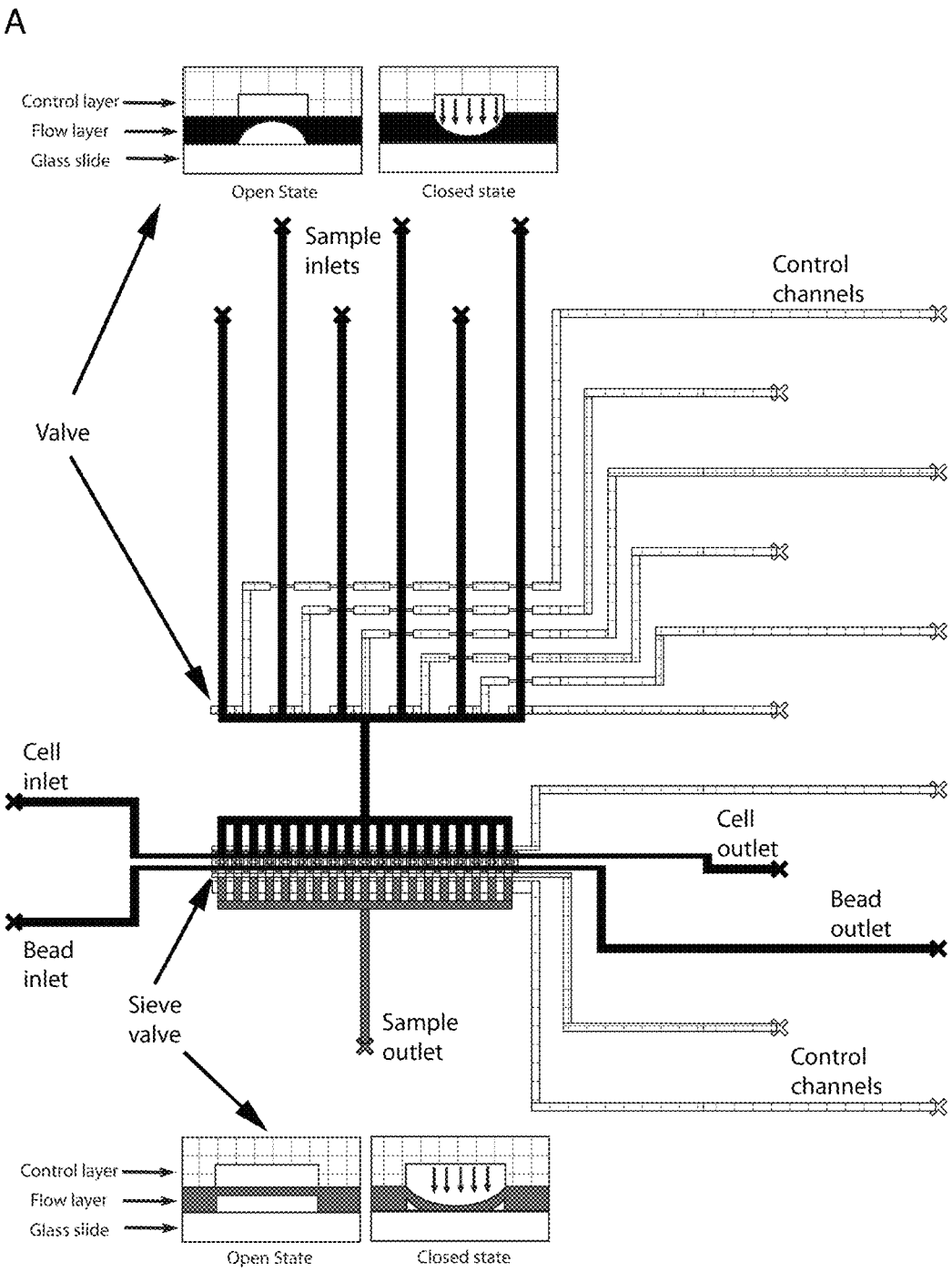
A
Control layer
Flow layer
Glass slide
Open State
Closed state
Sample inlets
Control channels
Valve
Cell inlet
Cell outlet
Bead outlet
Bead inlet
Sieve valve
Sample outlet
Control channels
Control layer
Flow layer
Glass slide
Open State
Closed state

Figure 2

B

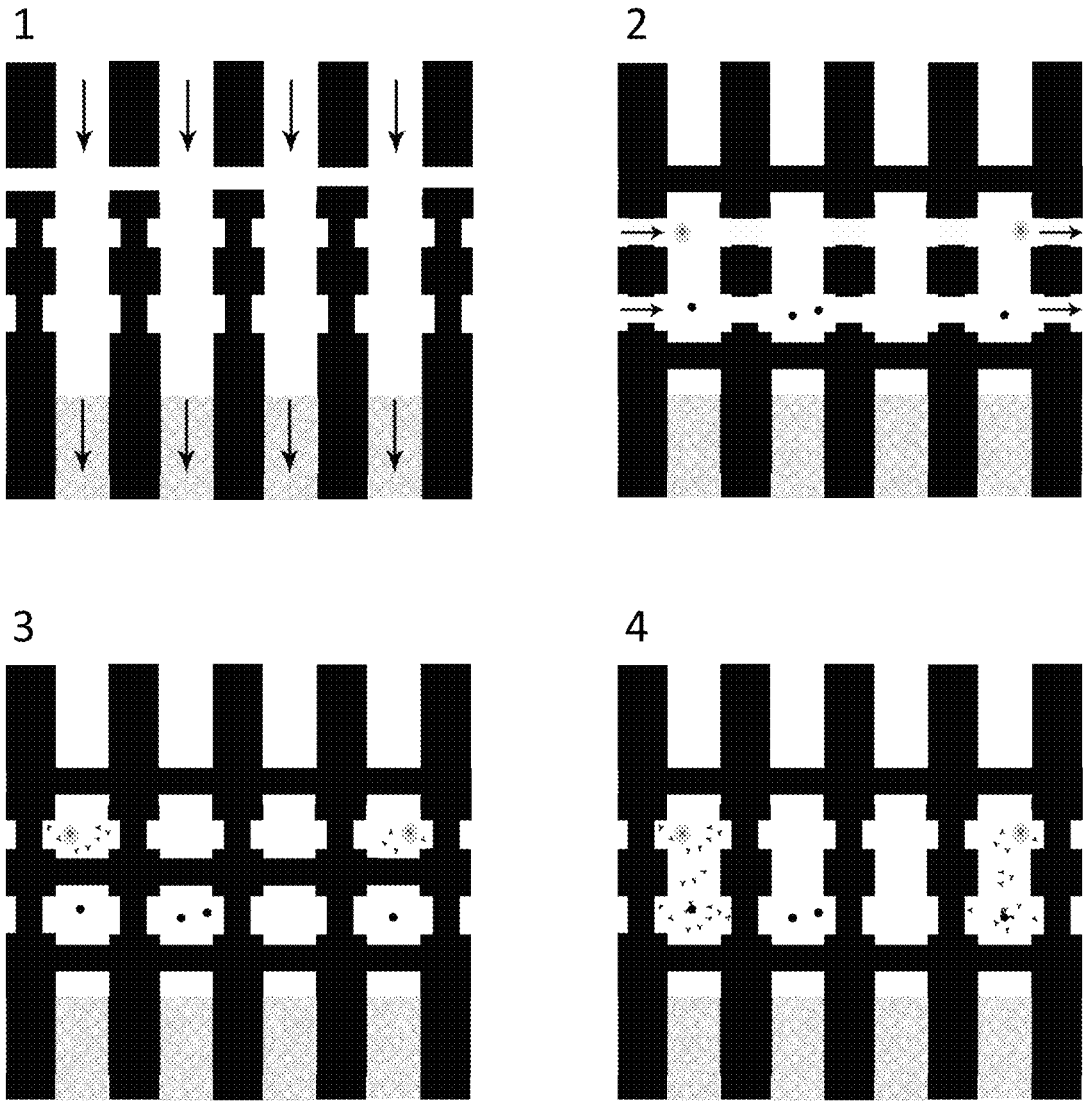

Figure 2 cont'd

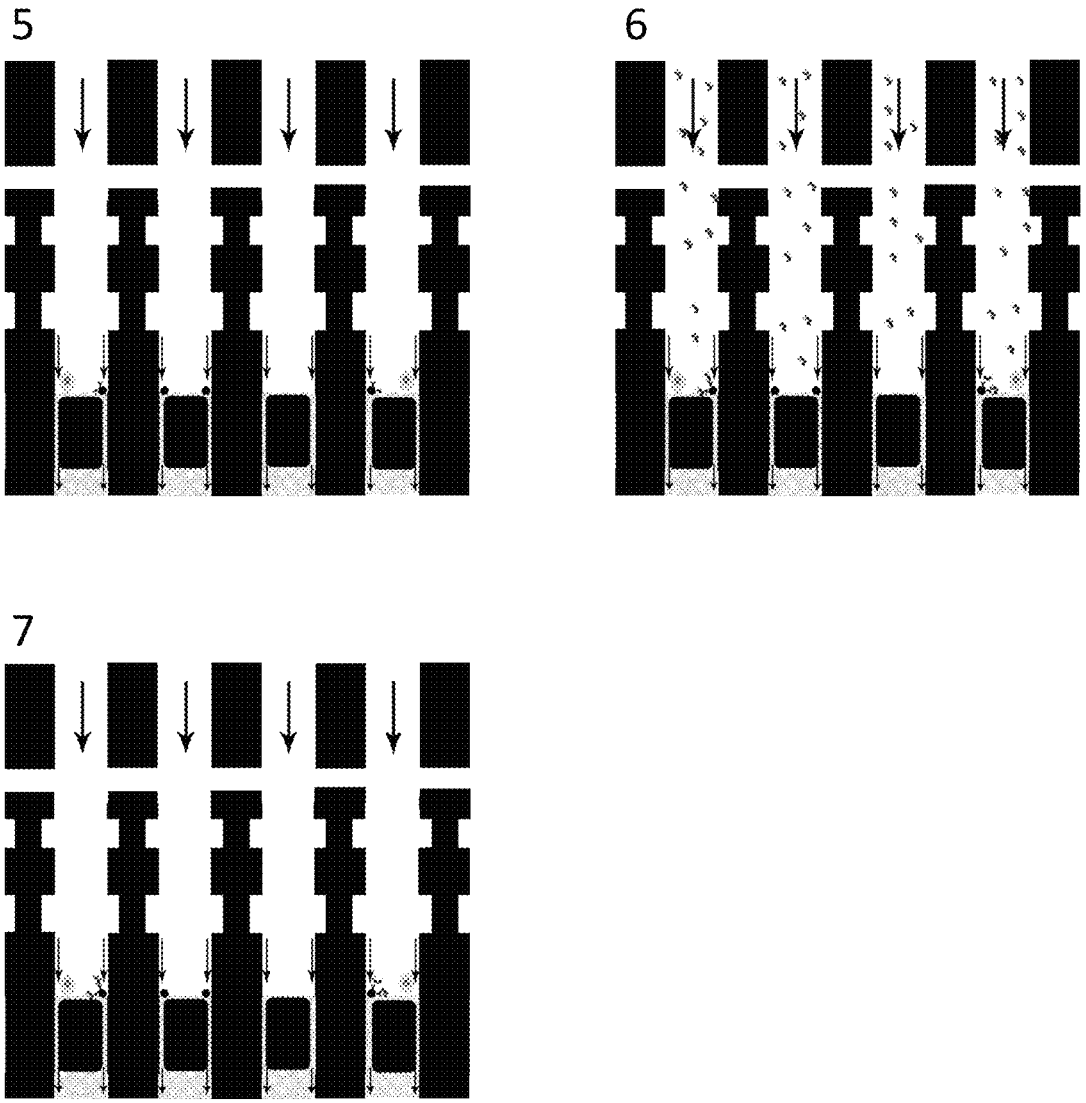

Figure 2 cont'd

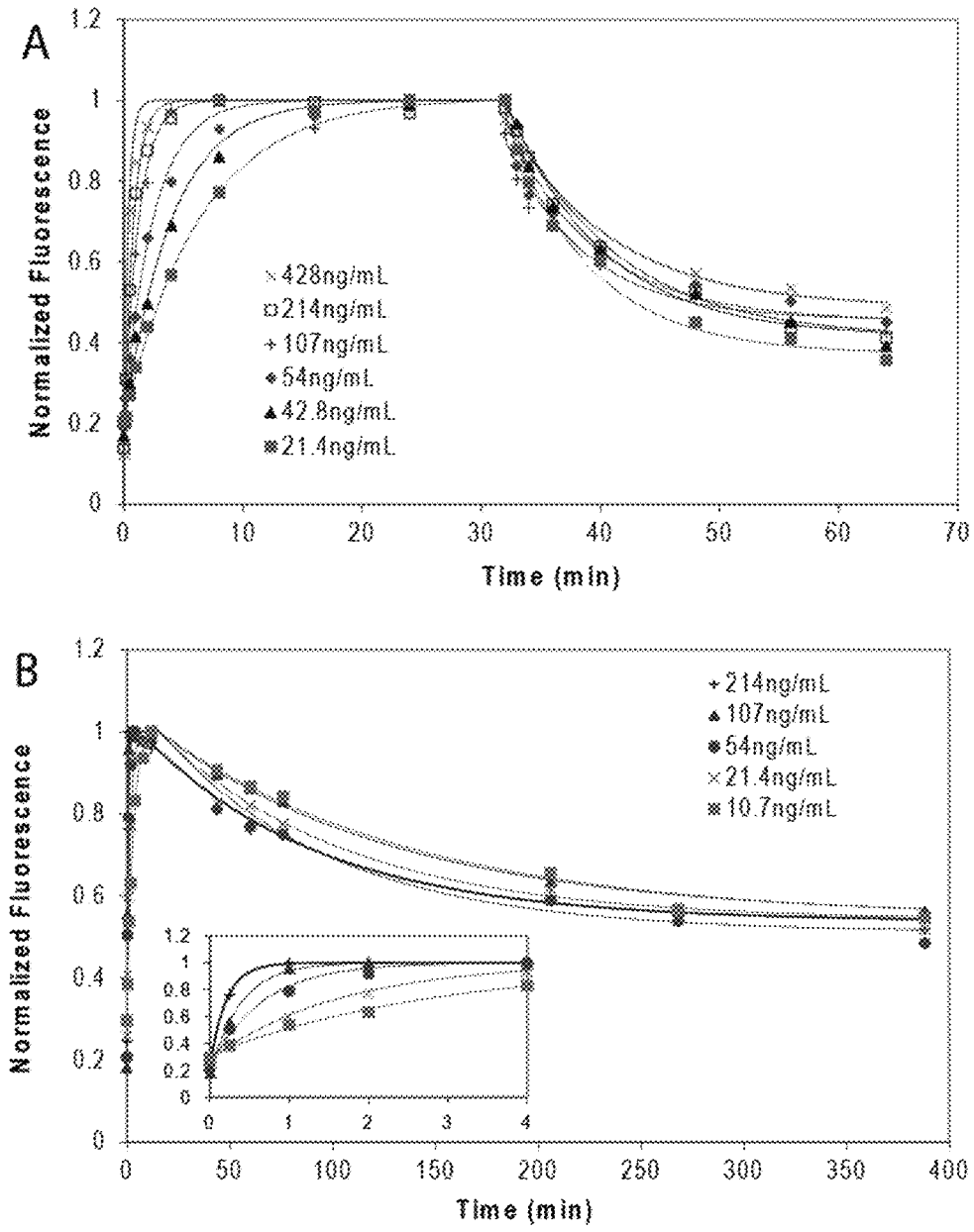
A
Normalized Fluorescence
Time (min)
428ng/mL
214ng/mL
107ng/mL
54ng/mL
42.8ng/mL
21.4ng/mL
B
Normalized Fluorescence
Time (min)
214ng/mL
107ng/mL
54ng/mL
21.4ng/mL
10.7ng/mL

Figure 3

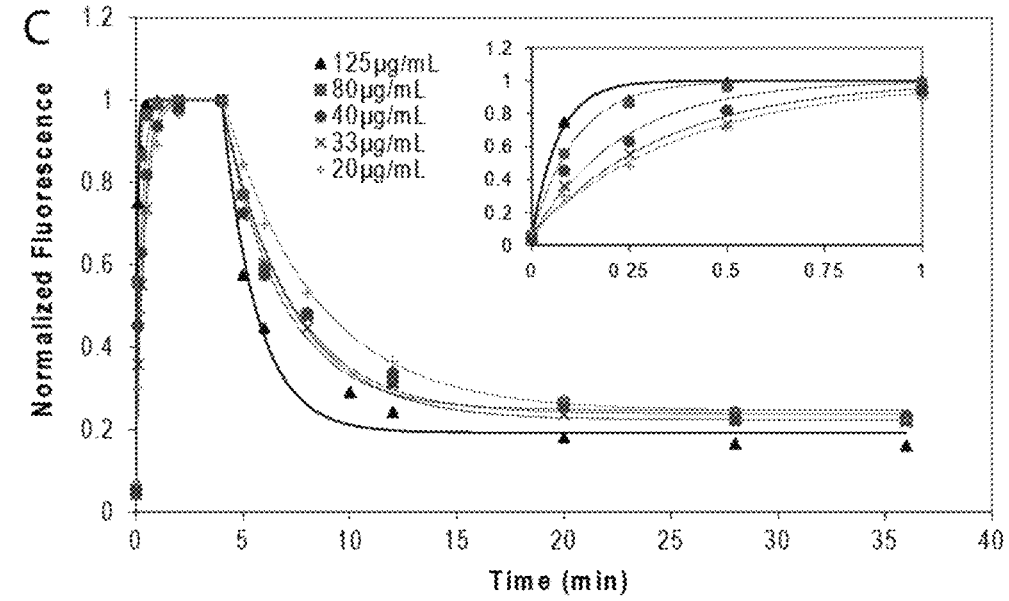

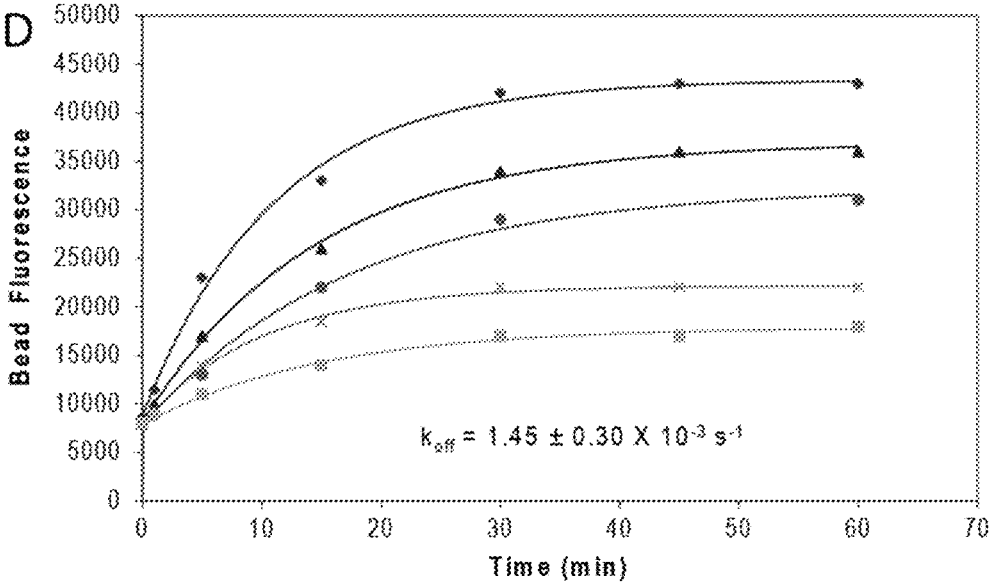

Figure 3 cont'd

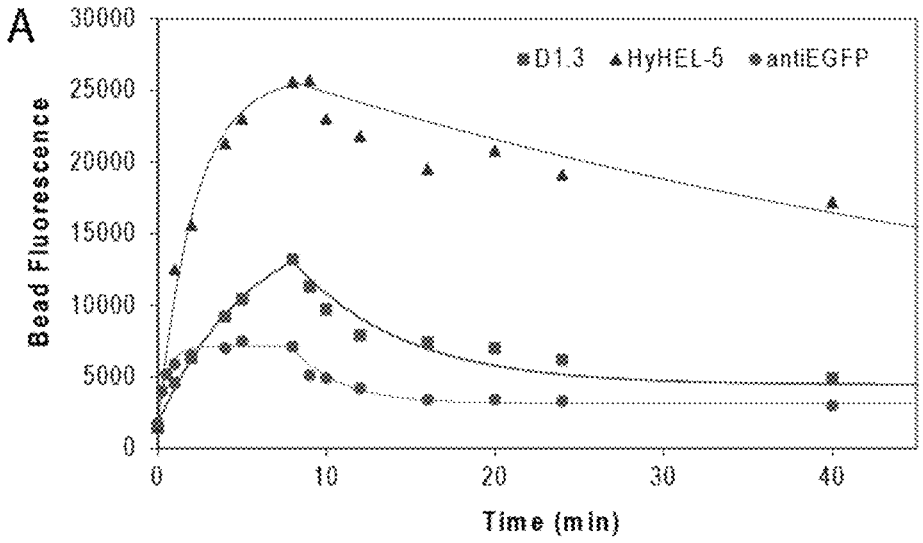
A
30000
25000
20000
15000
10000
5000
0
Bead Fluorescence
D1.3
HyHEL-5
antiEGFP
0
10
20
30
40
Time (min)

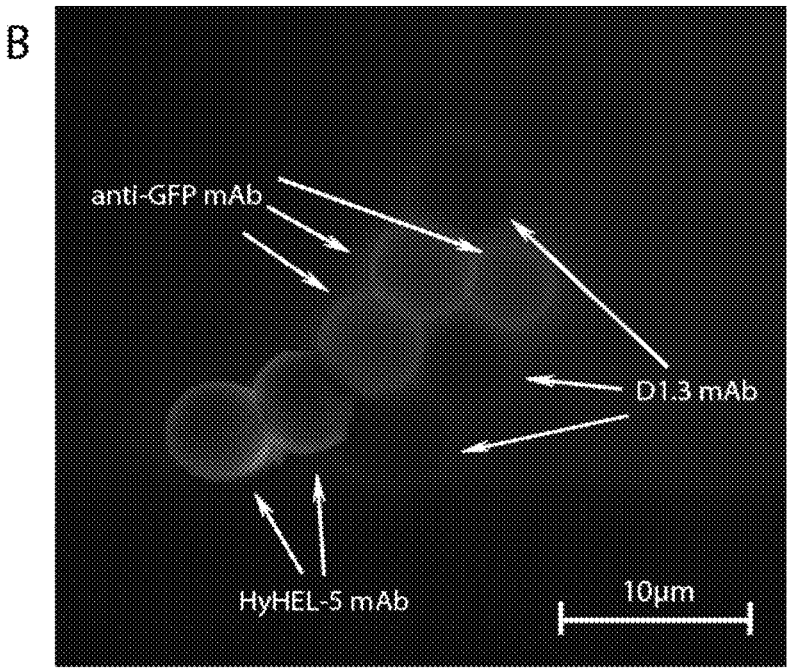
B
anti-GFP mAb
D1.3 mAb
HyHEL-5 mAb
10μm

Figure 4

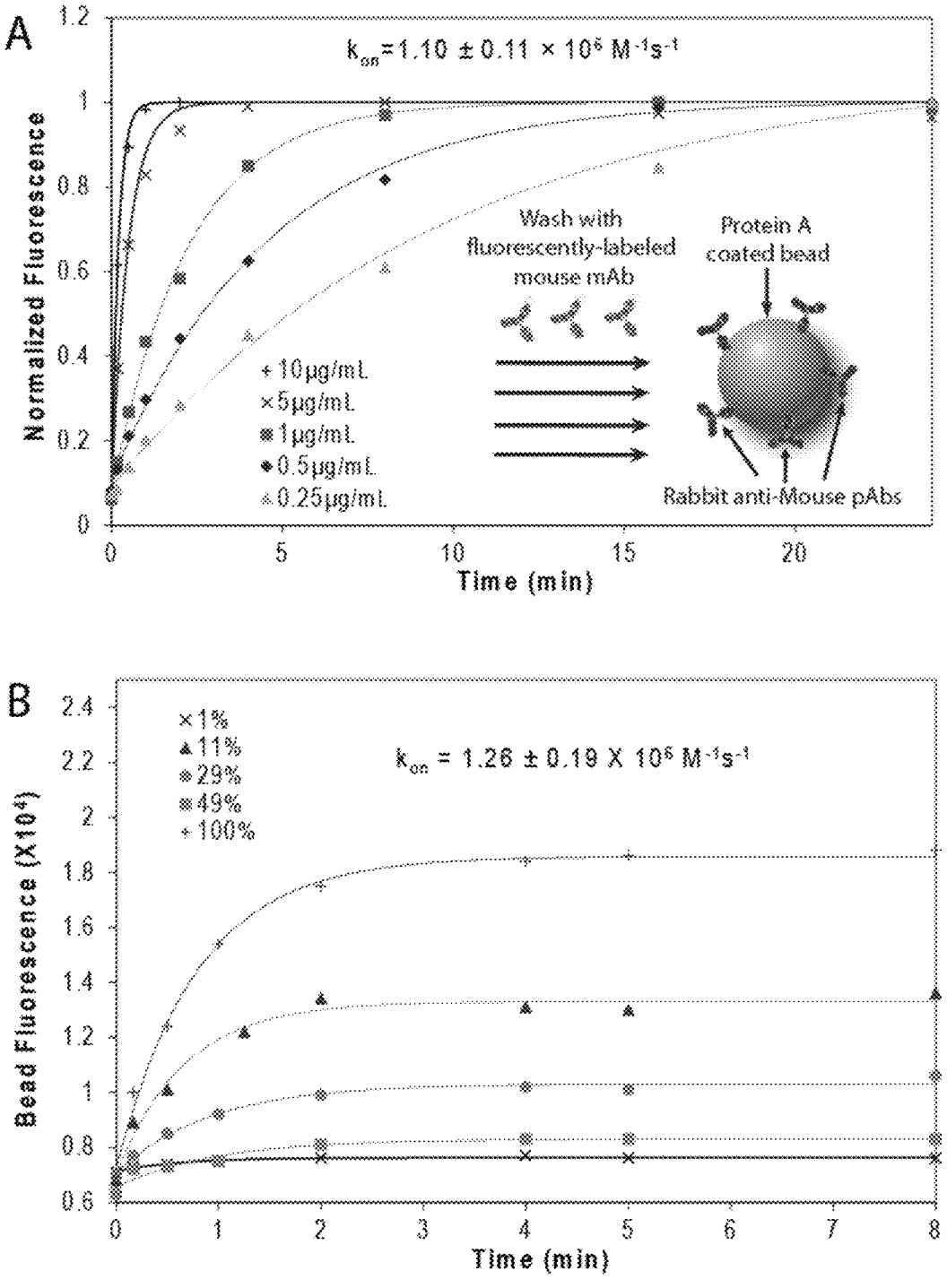
A
k_{on}=1.10 ± 0.11 × 10^5 $M^{-1}s^{-1}$
Normalized Fluorescence
Time (min)
+10μg/mL
×5μg/mL
✱1μg/mL
◆0.5μg/mL
△0.25μg/mL
Wash with fluorescently-labeled mouse mAb
Protein A coated bead
Rabbit anti-Mouse pAbs
B
×1%
▲11%
✱29%
✱49%
+100%
k_{on} = 1.26 ± 0.19 X 10^5 $M^{-1}s^{-1}$
Bead Fluorescence (X10^4)
Time (min)

Figure 5

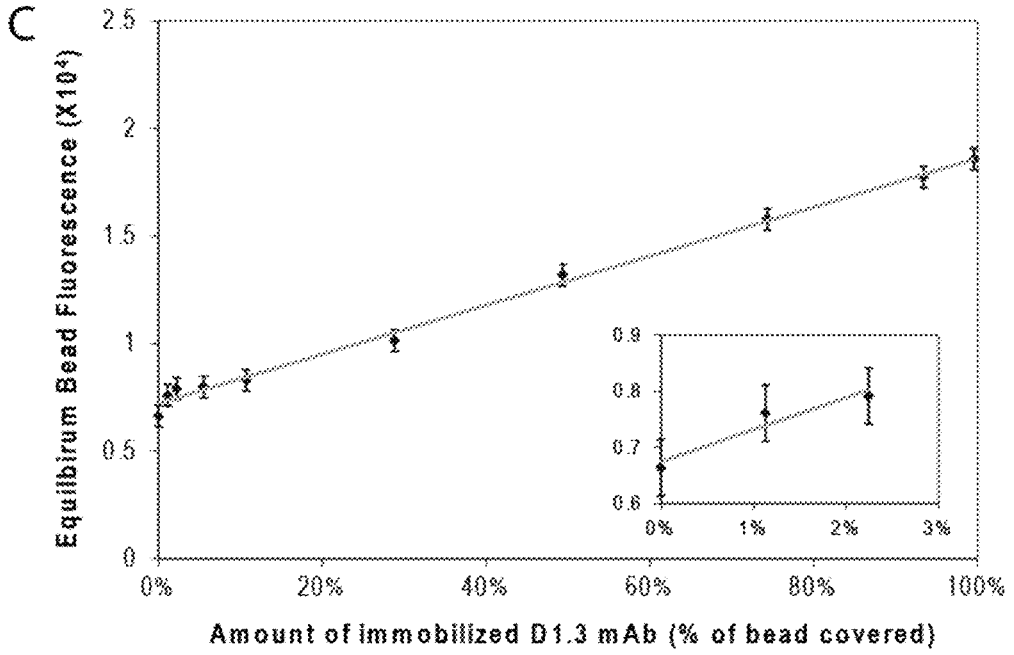

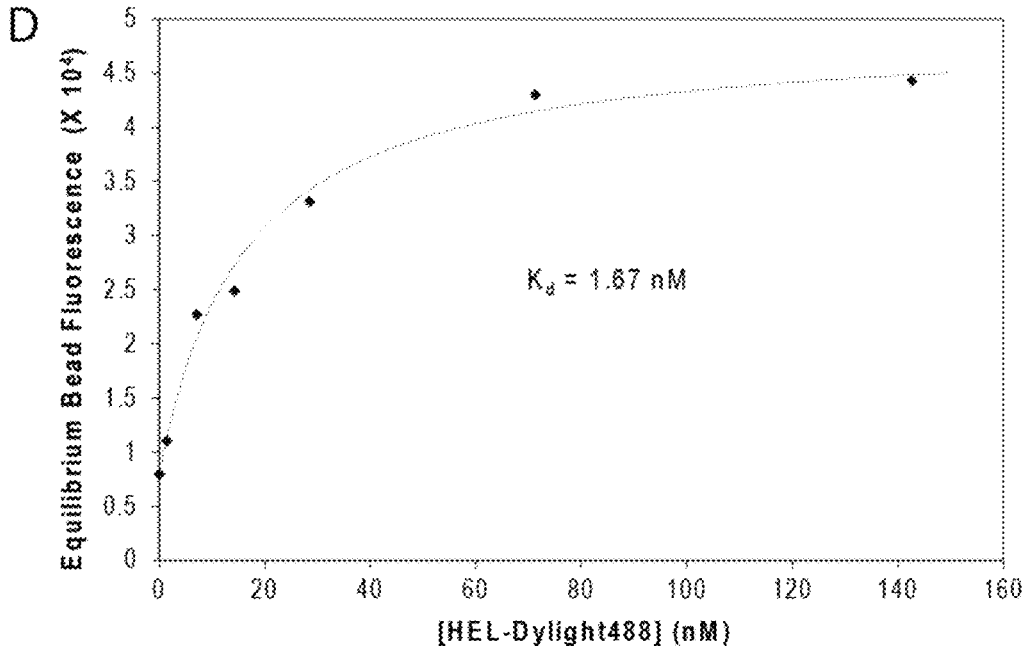

Figure 5 cont'd

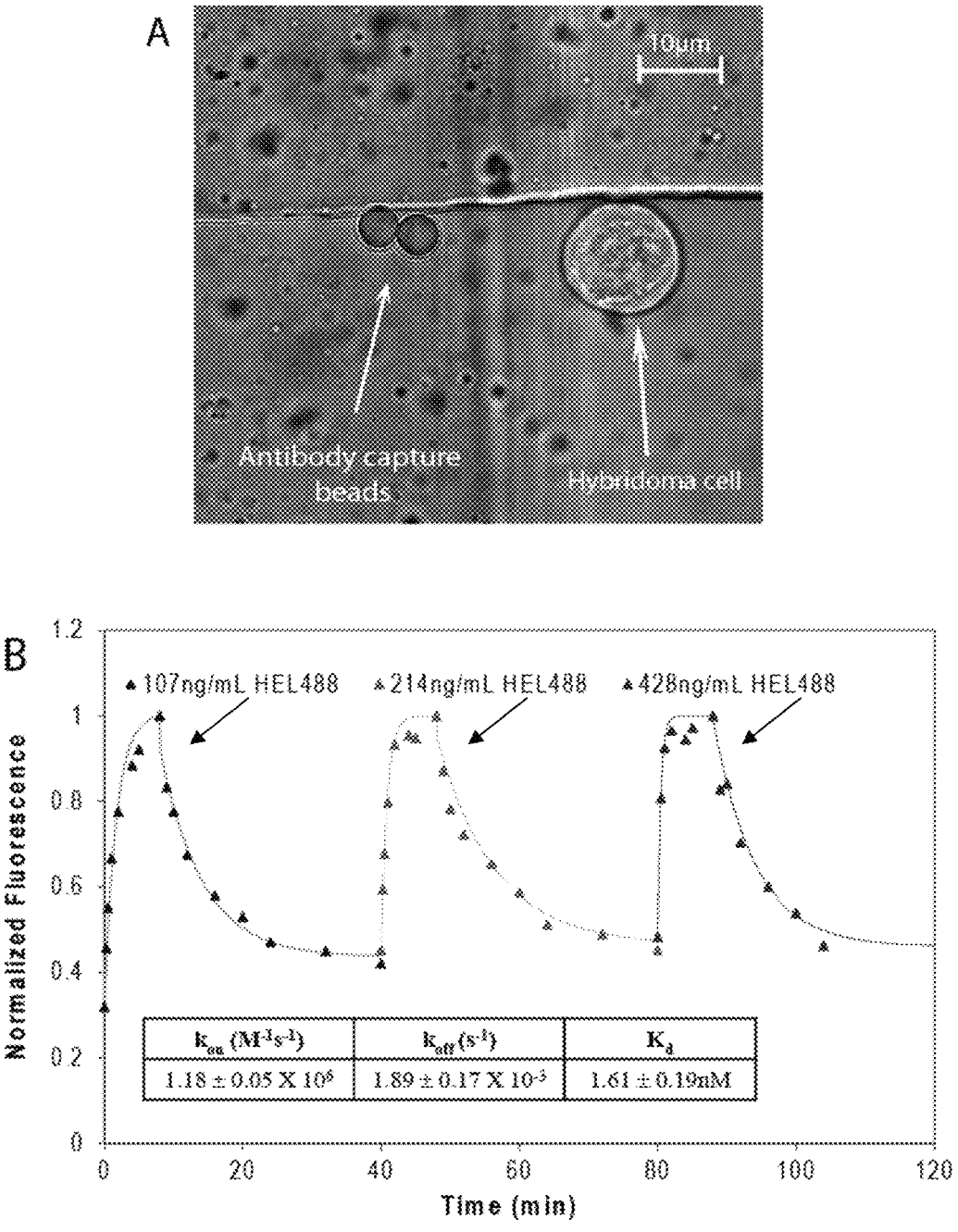
A
10μm
Antibody capture beads
Hybridoma cell
B
107ng/mL HEL488
214ng/mL HEL488
428ng/mL HEL488
Normalized Fluorescence
Time (min)
0
0.2
0.4
0.6
0.8
1
1.2
0
20
40
60
80
100
120
k_{on} ($M^{-1}s^{-1}$)
k_{off} (s^{-1})
K_d
1.18 ± 0.05 X 10^6
1.89 ± 0.17 X 10^{-5}
1.61 ± 0.19nM

Figure 6

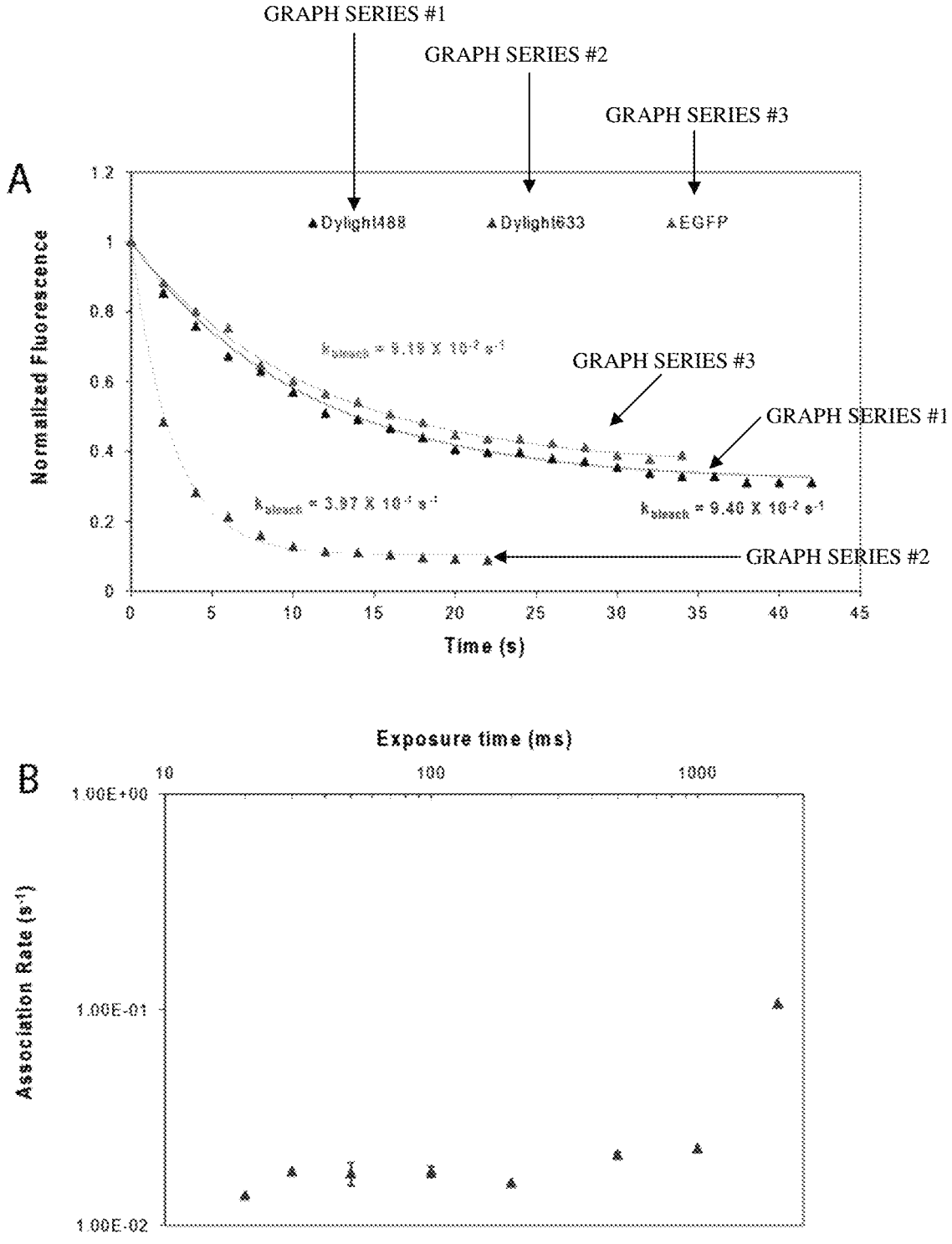
A
GRAPH SERIES #1
GRAPH SERIES #2
GRAPH SERIES #3
Dylight488
Dylight633
EGFP
Normalized Fluorescence
Time (s)
GRAPH SERIES #3
GRAPH SERIES #1
GRAPH SERIES #2
B
Exposure time (ms)
Association Rate (s-1)
1.00E+00
1.00E-01
1.00E-02

Figure 7

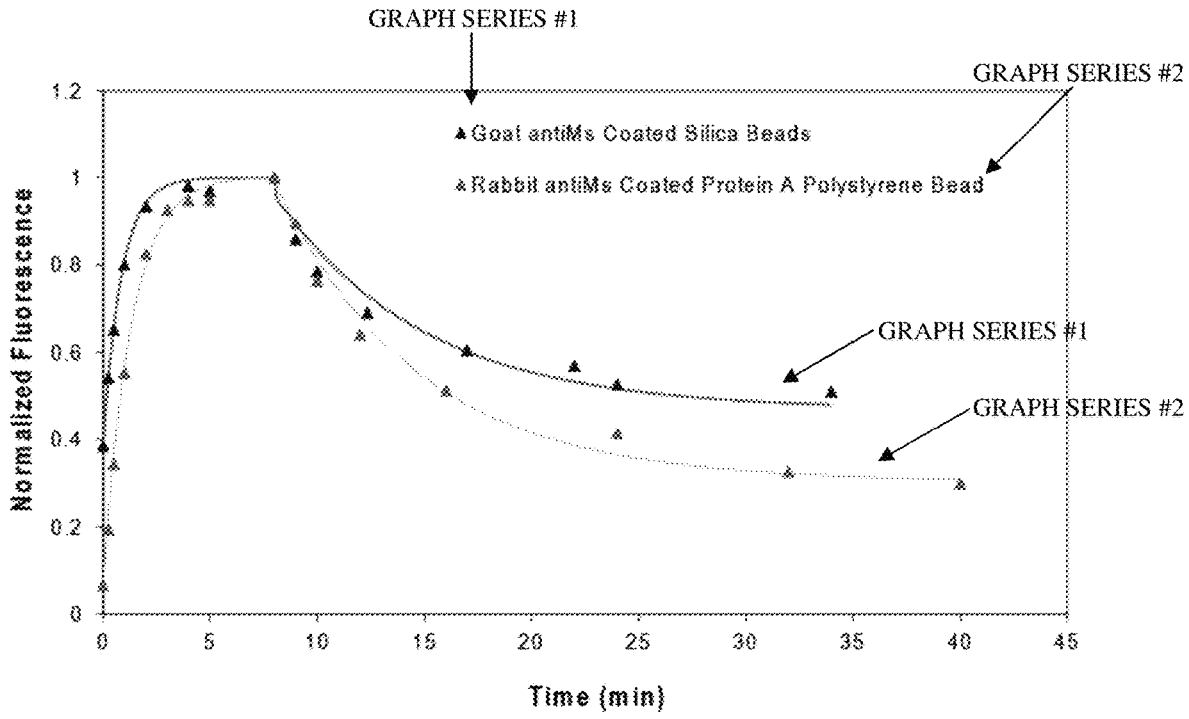
GRAPH SERIES #1
GRAPH SERIES #2
Goat antiMs Coated Silica Beads
Rabbit antiMs Coated Protein A Polystyrene Bead
GRAPH SERIES #1
GRAPH SERIES #2
Normalized Fluorescence
Time (min)
0
0.2
0.4
0.6
0.8
1
1.2
0
5
10
15
20
25
30
35
40
45

Figure 8

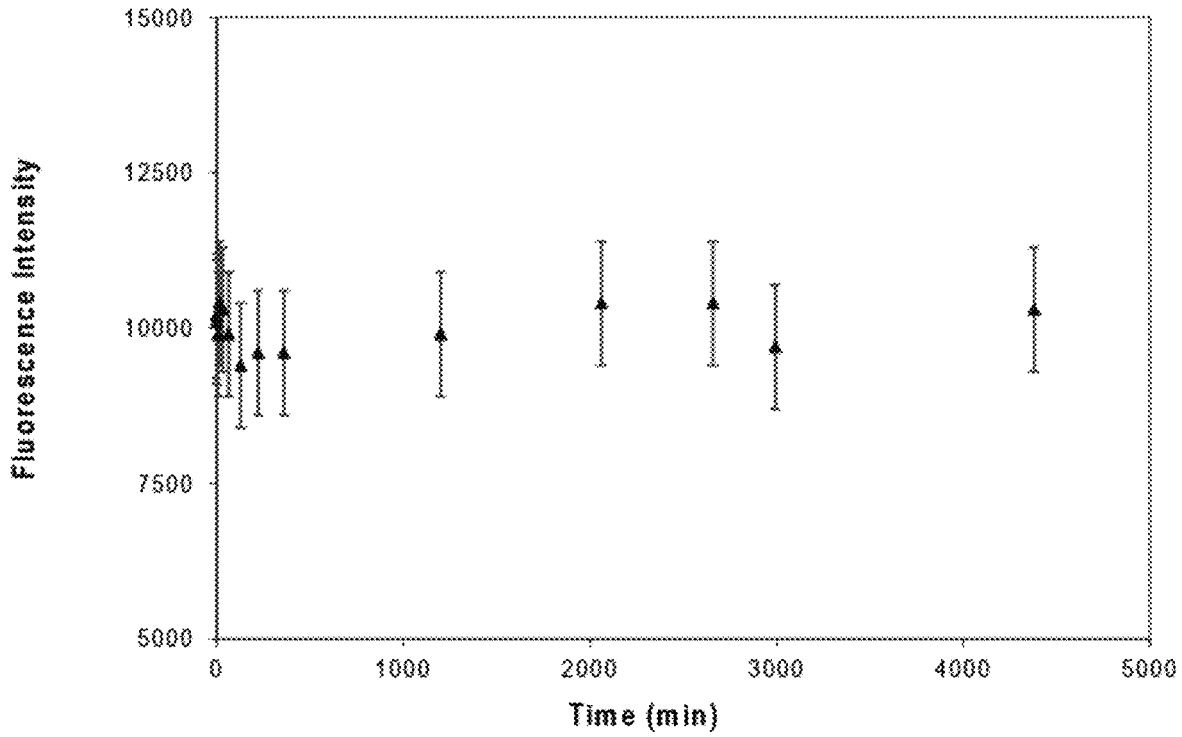
15000
12500
10000
7500
5000
Fluorescence Intensity
0
1000
2000
3000
4000
5000
Time (min)

Figure 9

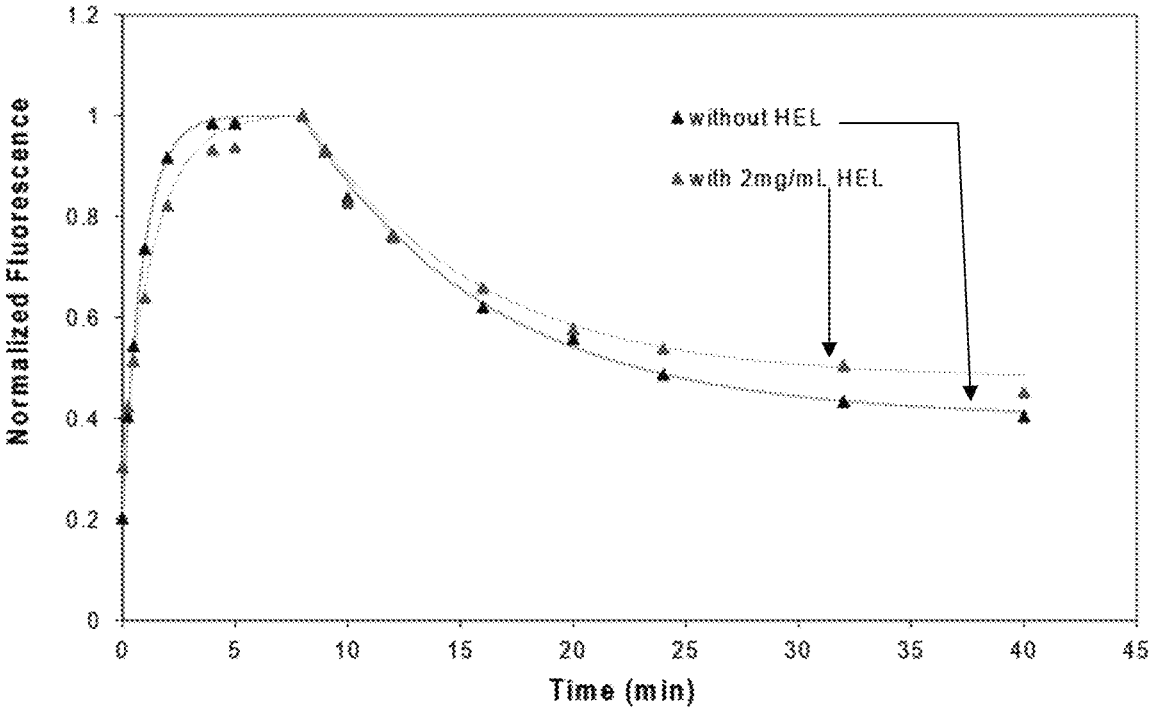
Normalized Fluorescence
1.2
1
0.8
0.6
0.4
0.2
0
0
5
10
15
20
25
30
35
40
45
Time (min)
without HEL
with 2mg/mL HEL

Figure 10

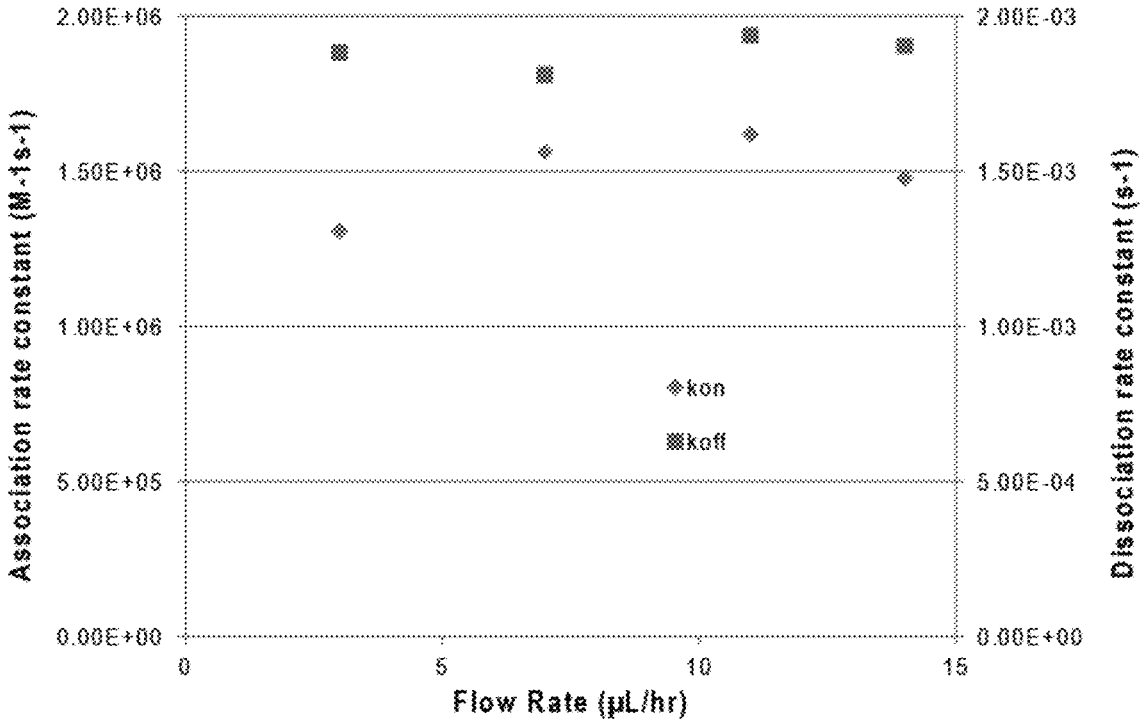
2.00E+06
1.50E+06
1.00E+06
5.00E+05
0.00E+00
Association rate constant (M-1s-1)
2.00E-03
1.50E-03
1.00E-03
5.00E-04
0.00E+00
Dissociation rate constant (s-1)
kon
koff
0
5
10
15
Flow Rate (µL/hr)

Figure 11

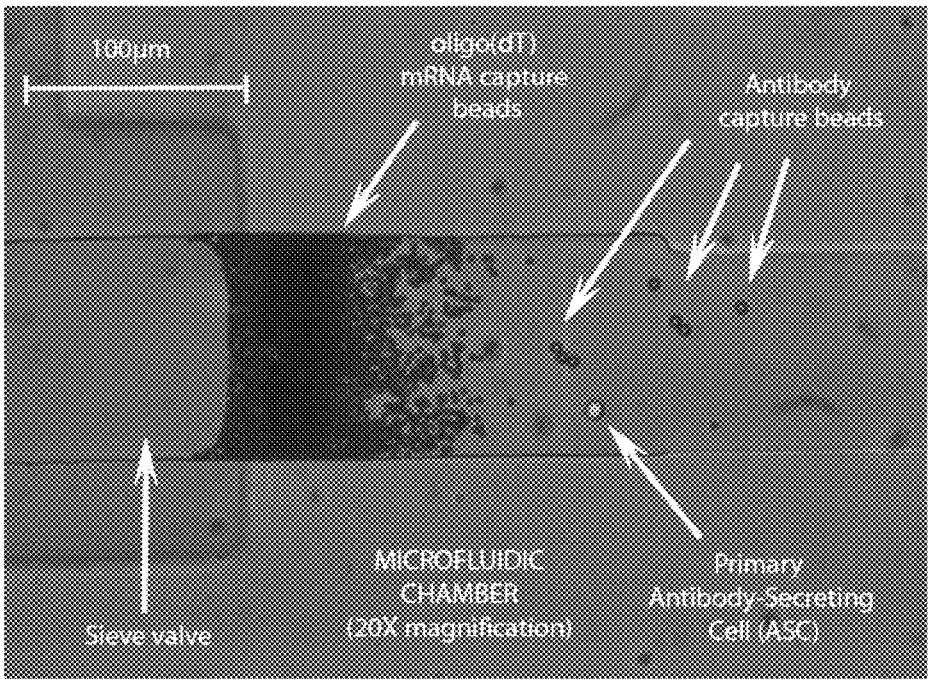
100μm
oligo(dT) mRNA capture beads
Antibody capture beads
Sieve valve
MICROFLUIDIC CHAMBER (20X magnification)
Primary Antibody-Secreting Cell (ASC)

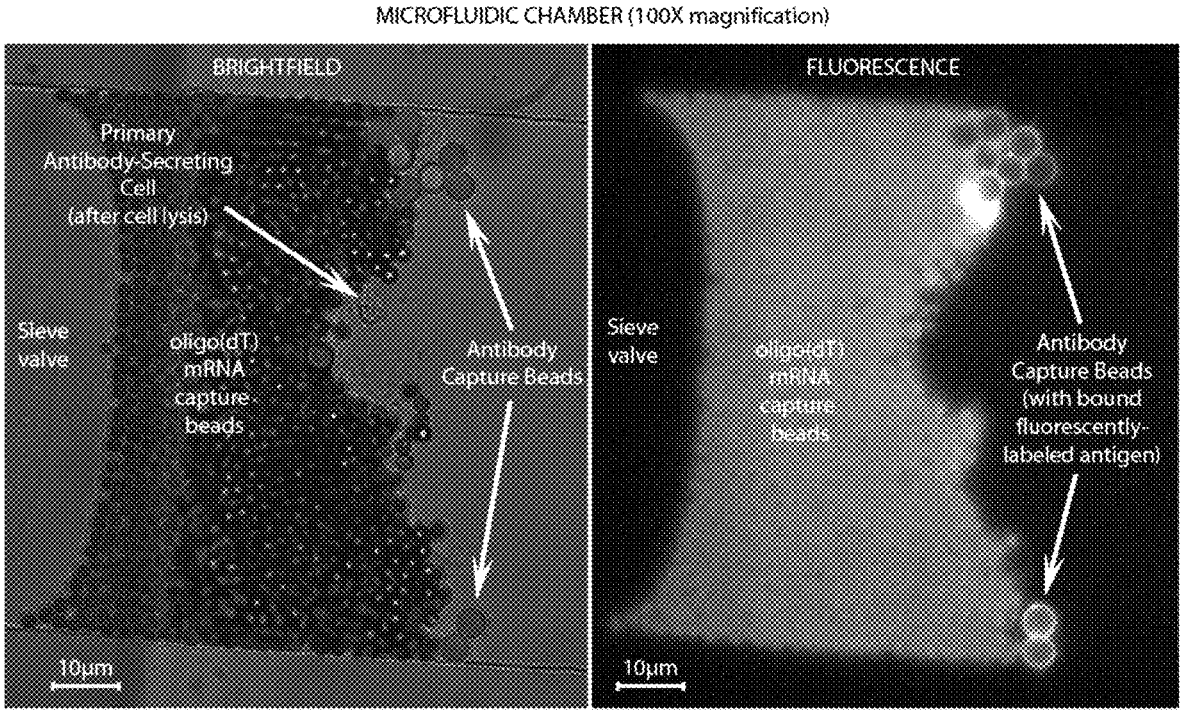
MICROFLUIDIC CHAMBER (100X magnification)
BRIGHTFIELD
FLUORESCENCE
Primary Antibody-Secreting Cell (after cell lysis)
Sieve valve
oligo(dT) mRNA capture beads
Antibody Capture Beads
Antibody Capture Beads (with bound fluorescently-labeled antigen)
10μm
10μm

Figure 12

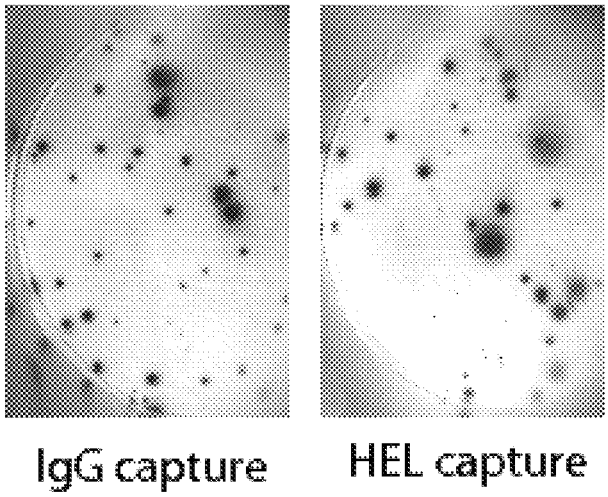

Figure 13

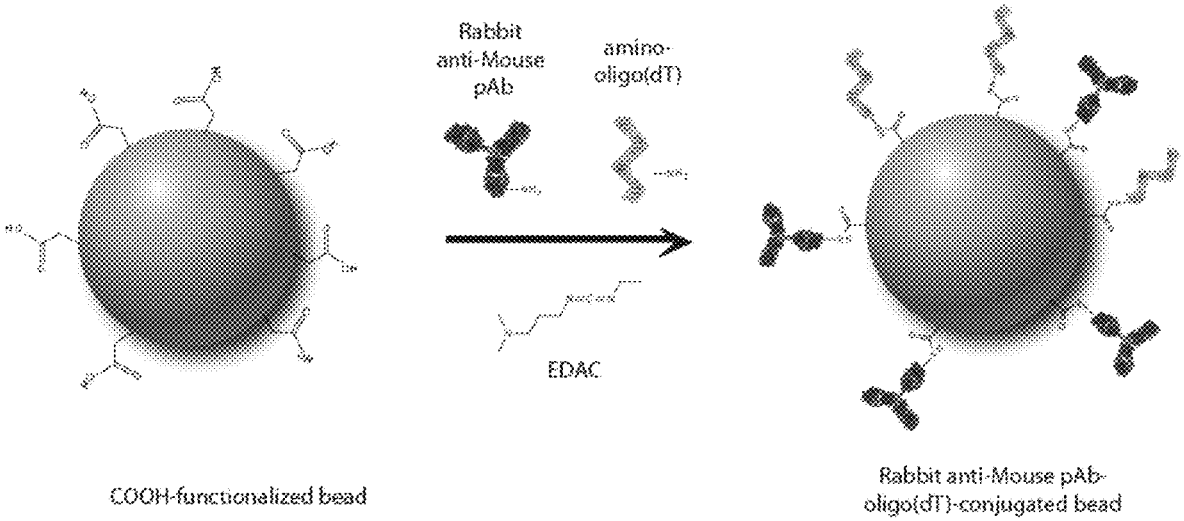
Rabbit anti-Mouse pAb
amino-oligo(dT)
EDAC
COOH-functionalized bead
Rabbit anti-Mouse pAb-oligo(dT)-conjugated bead

Figure 14

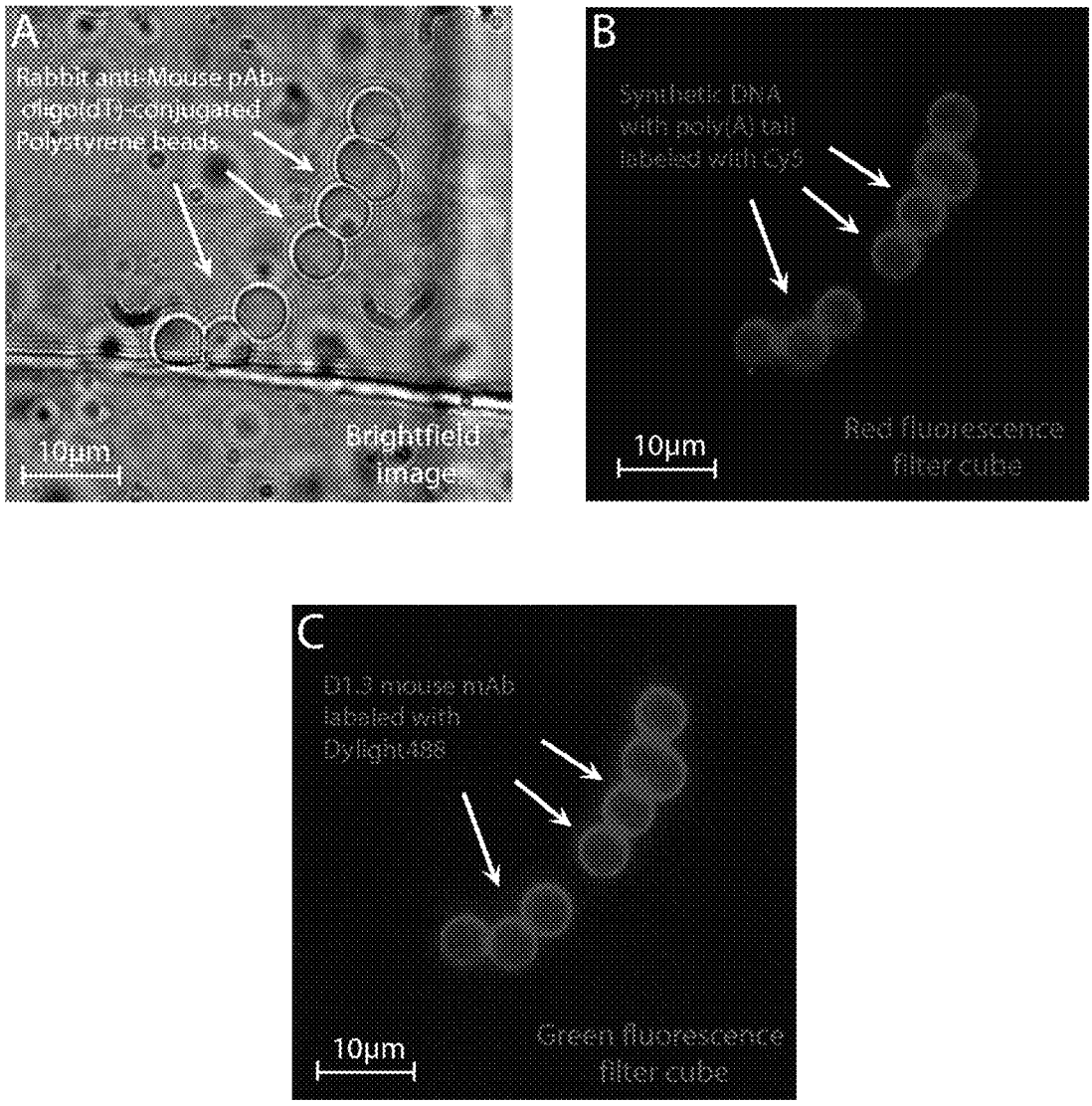
A
Rabbit anti-Mouse pAb-
oligo(dT)-conjugated
Polystyrene beads
10μm
Brightfield
image
B
Synthetic DNA
with poly(A) tail
labeled with Cy5
10μm
Red fluorescence
filter cube
C
D1.3 mouse mAb
labeled with
Dylight 488
10μm
Green fluorescence
filter cube

Figure 15

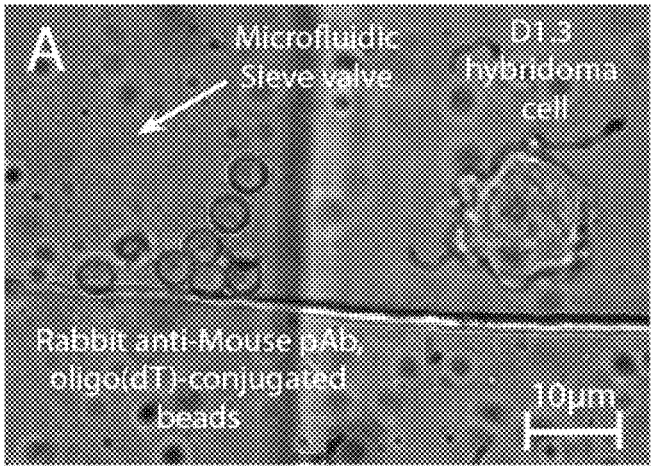
A
Microfluidic
Sieve valve
D1.3
hybridoma
cell
Rabbit anti-Mouse pAb,
oligo(dT)-conjugated
beads
10μm

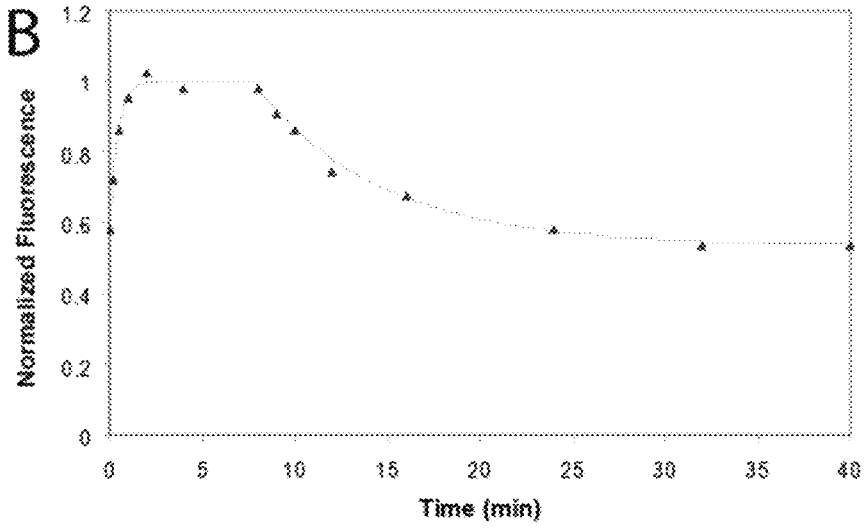
B
Normalized Fluorescence
1.2
1
0.8
0.6
0.4
0.2
0
0
5
10
15
20
25
30
35
40
Time (min)

Figure 16

A

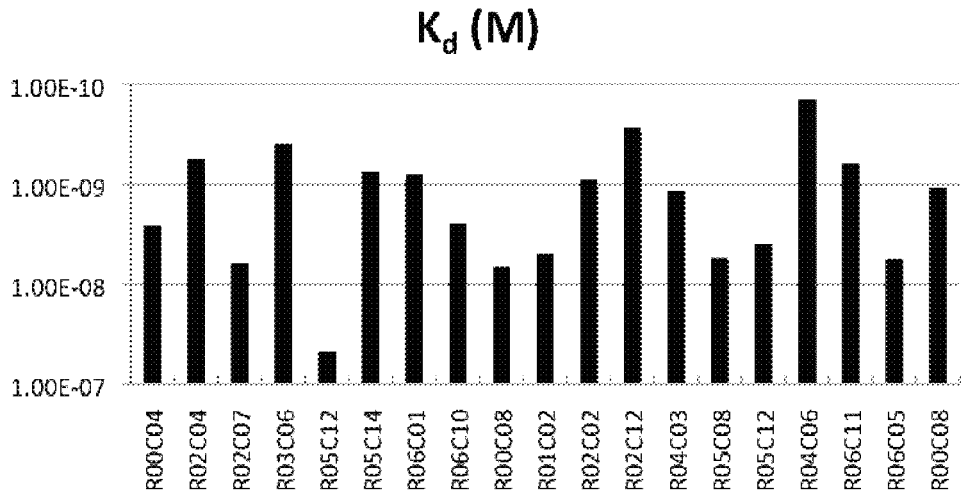

B

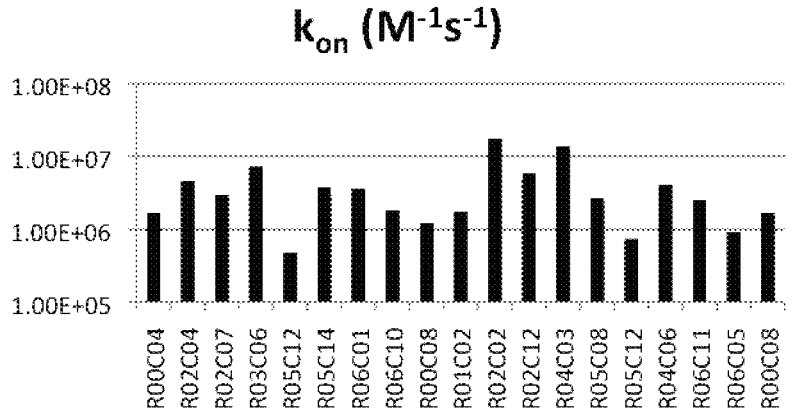

C

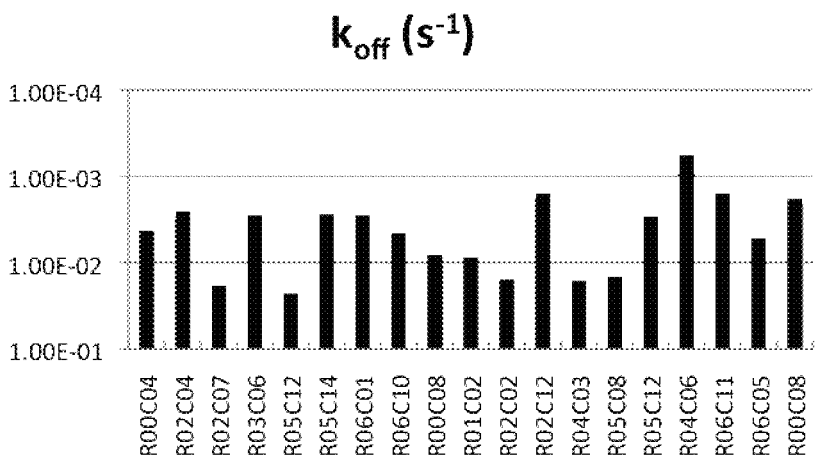

Figure 17

A

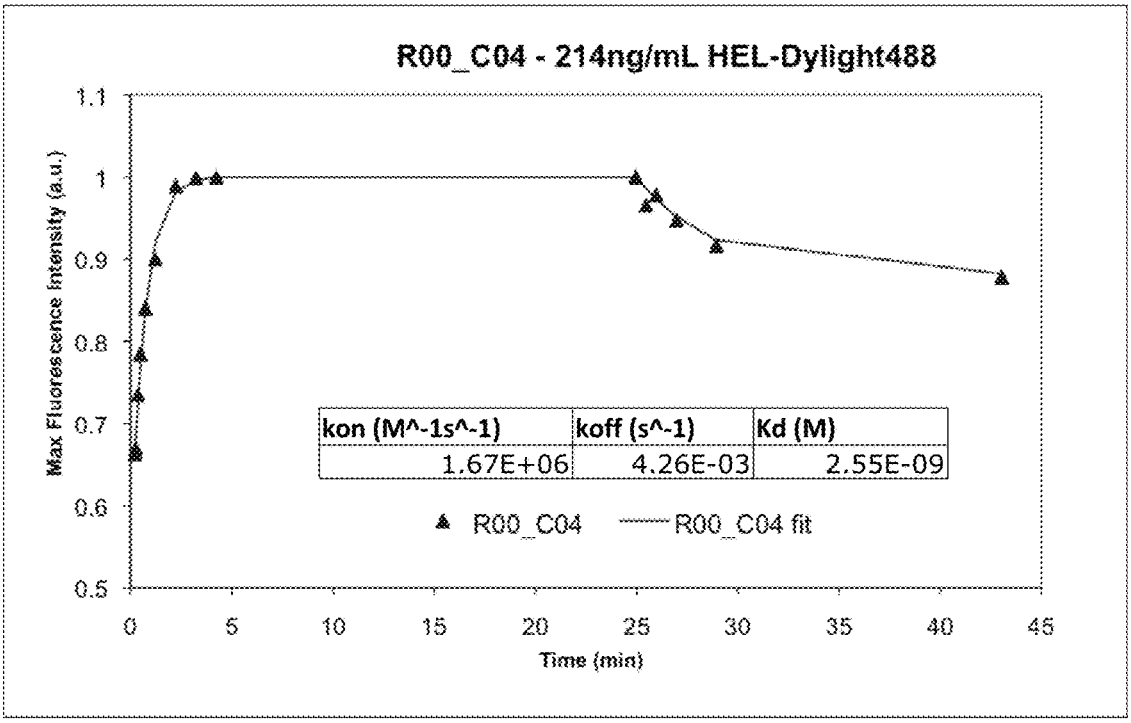
R00_C04 - 214ng/mL HEL-Dylight488
Max Fluorescence Intensity (a.u.)
Time (min)
kon (M^-1s^-1) koff (s^-1) Kd (M)
1.67E+06 4.26E-03 2.55E-09
R00_C04
R00_C04 fit

B

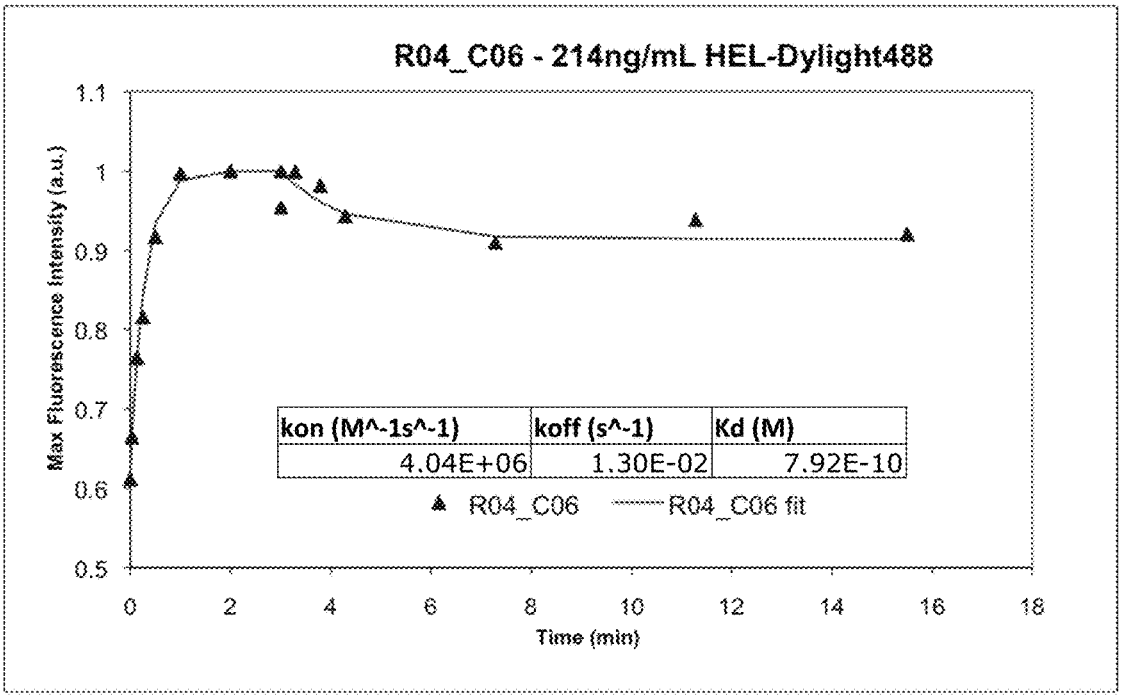
R04_C06 - 214ng/mL HEL-Dylight488
Max Fluorescence Intensity (a.u.)
Time (min)
kon (M^-1s^-1) koff (s^-1) Kd (M)
4.04E+06 1.30E-02 7.92E-10
R04_C06
R04_C06 fit

Figure 18

A

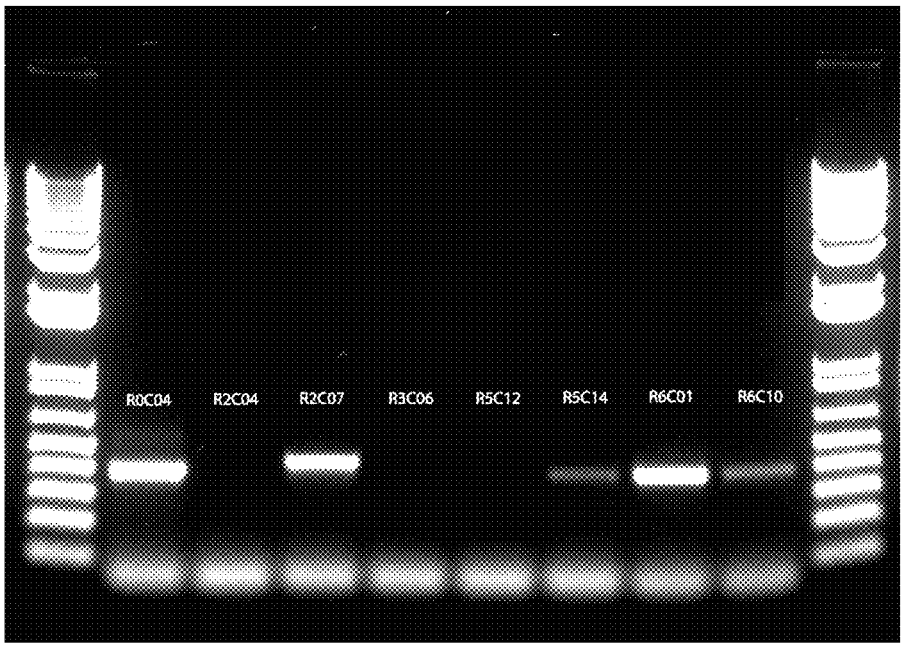
R0C04
R2C04
R2C07
R3C06
R5C12
R5C14
R6C01
R6C10

B

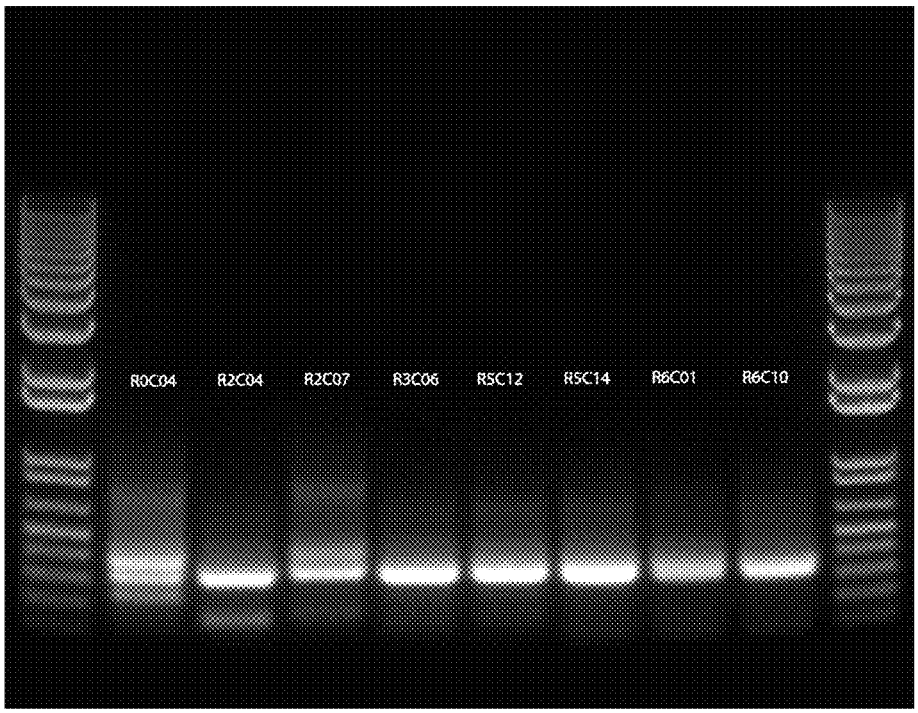
R0C04
R2C04
R2C07
R3C06
R5C12
R5C14
R6C01
R6C10

Figure 19

C

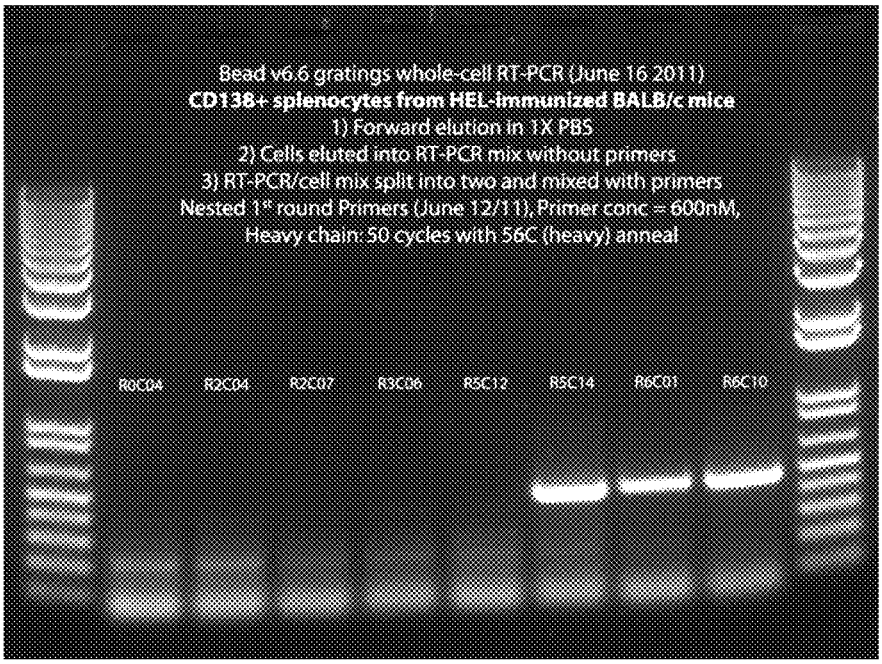

D

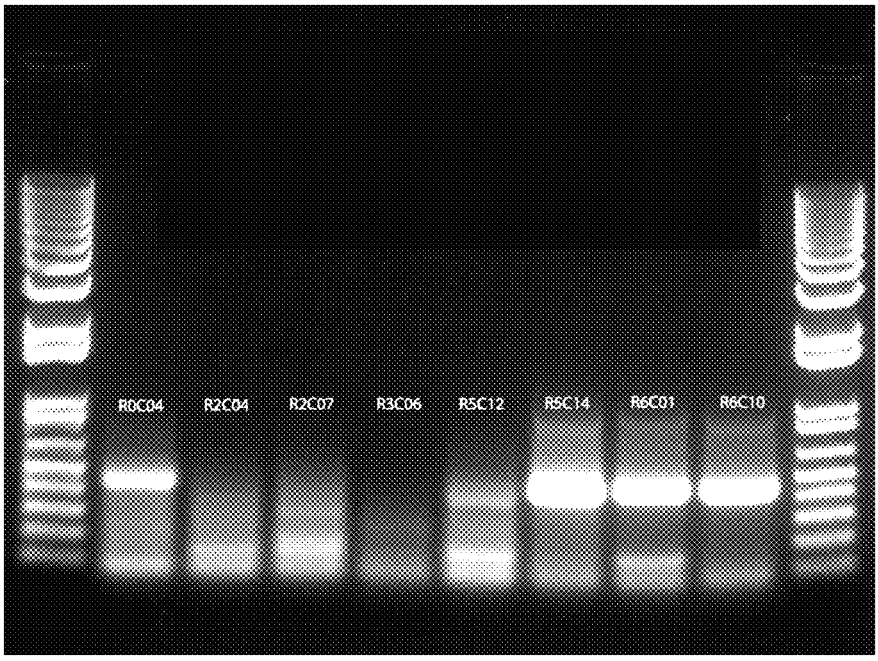

Figure 19 cont'd

A

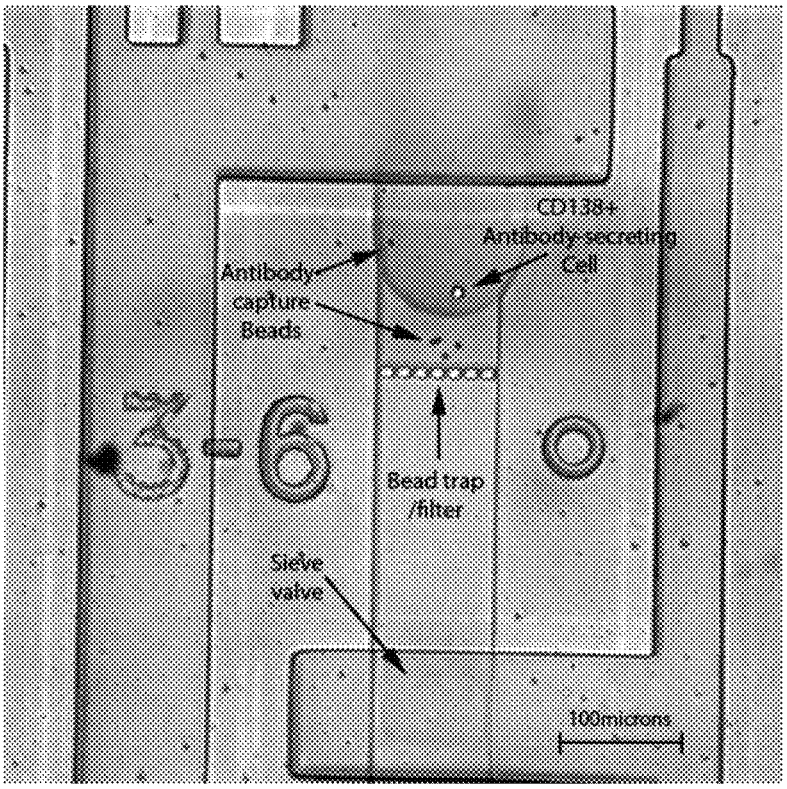
CD138+
Antibody-secreting
Cell
Antibody-
capture
Beads
Bead trap
/filter
Sieve
valve
100microns

B

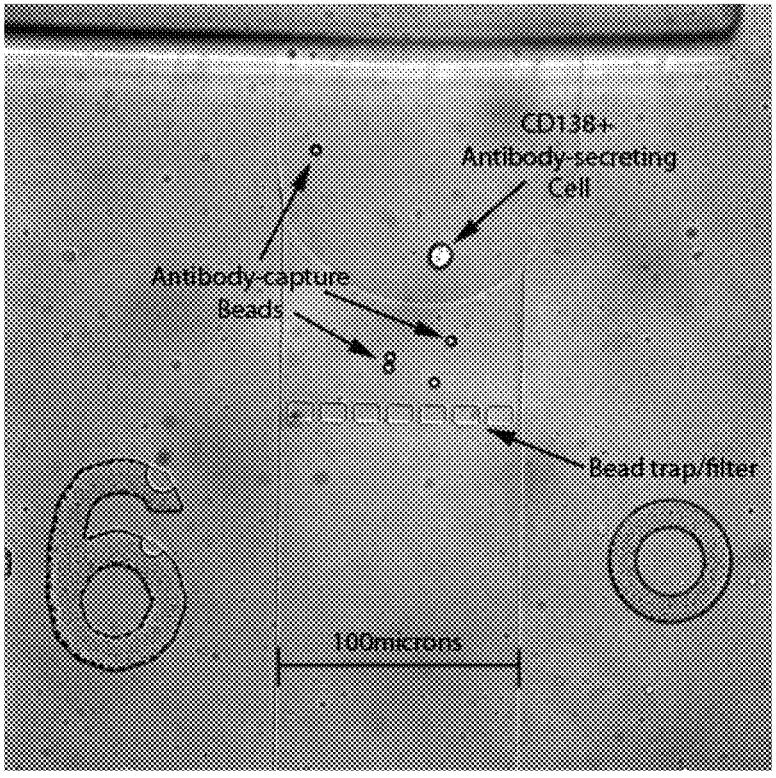
CD138+
Antibody-secreting
Cell
Antibody-capture
Beads
Bead trap/filter
100microns

Figure 20

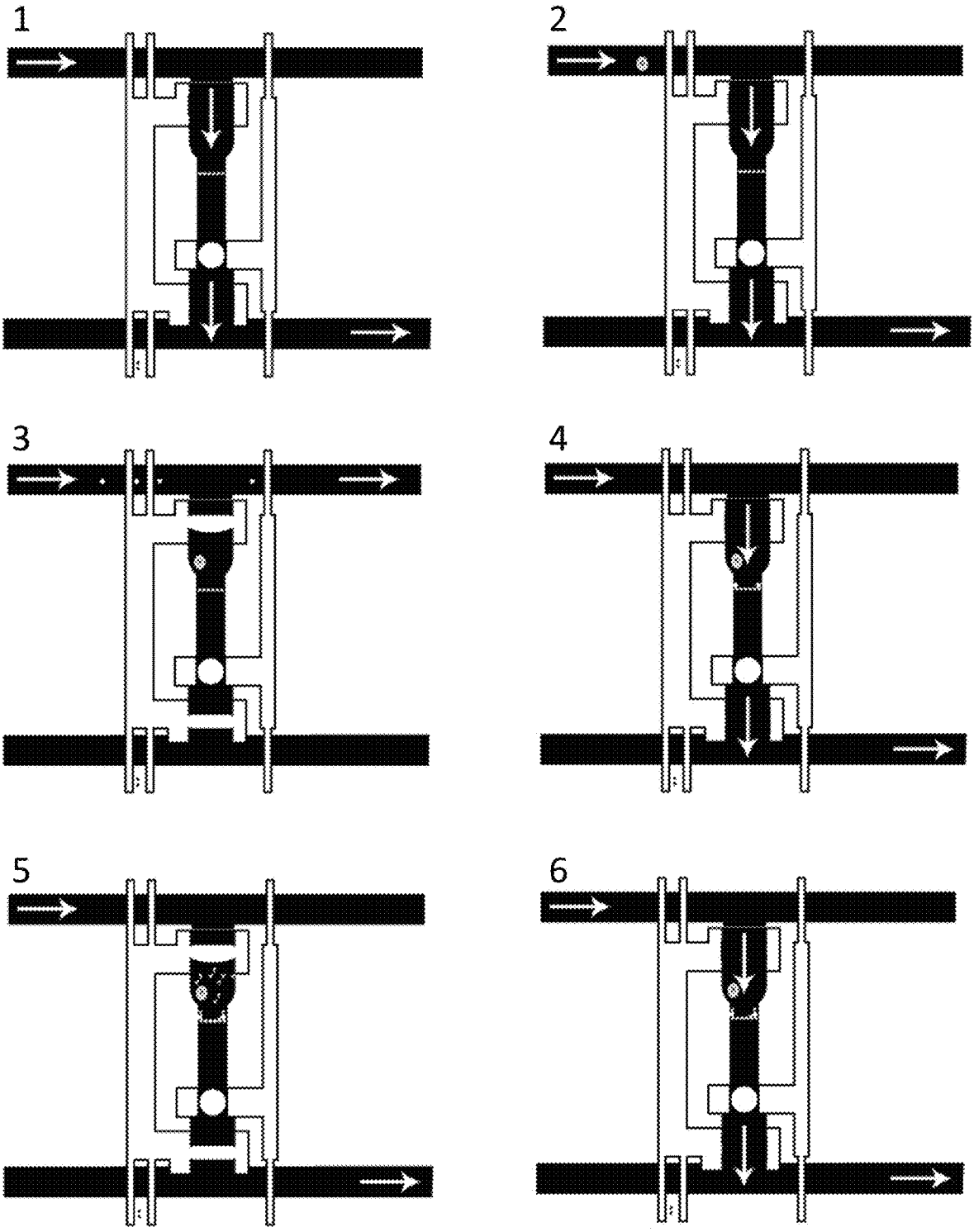

Figure 21

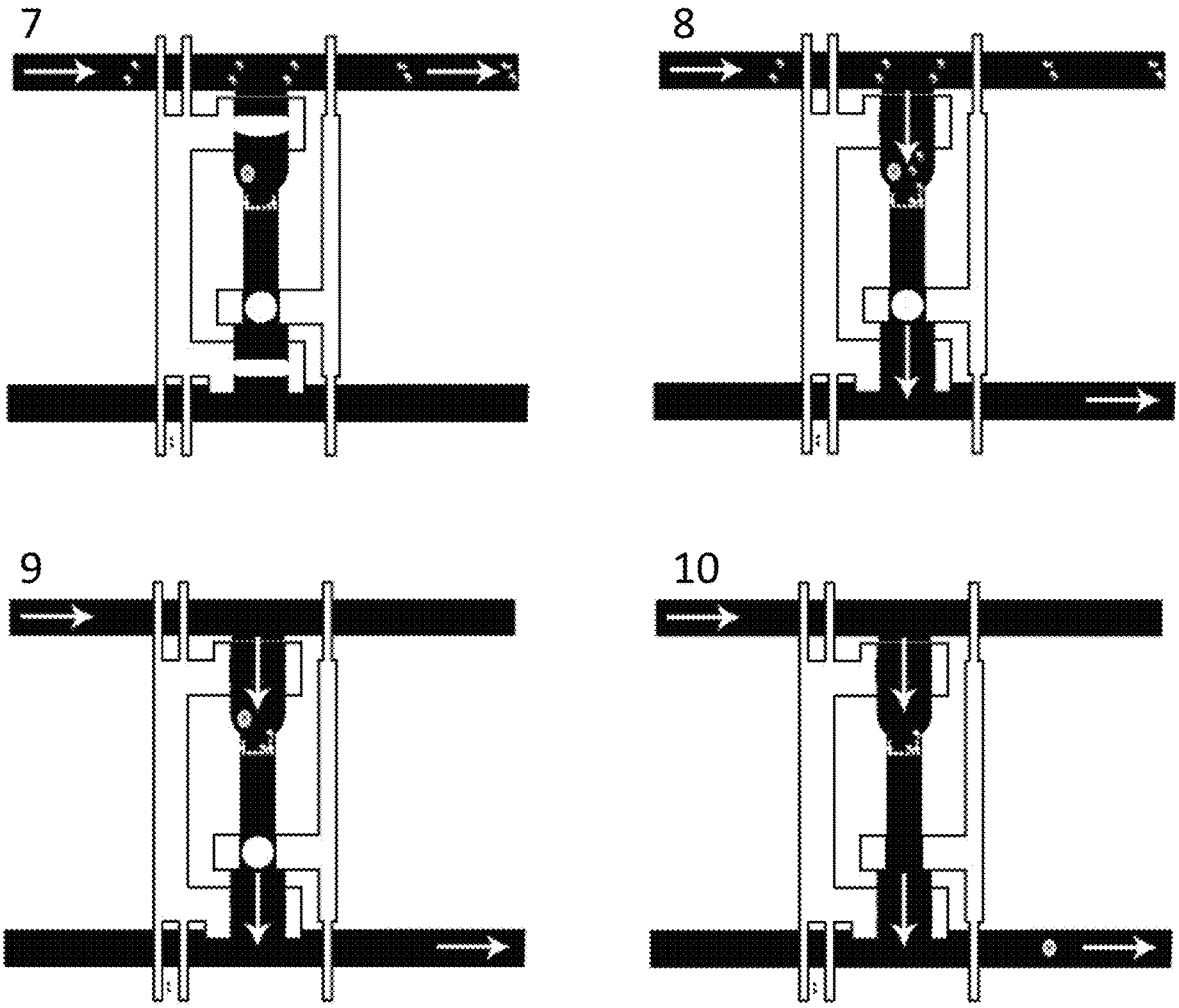

Figure 21 cont'd

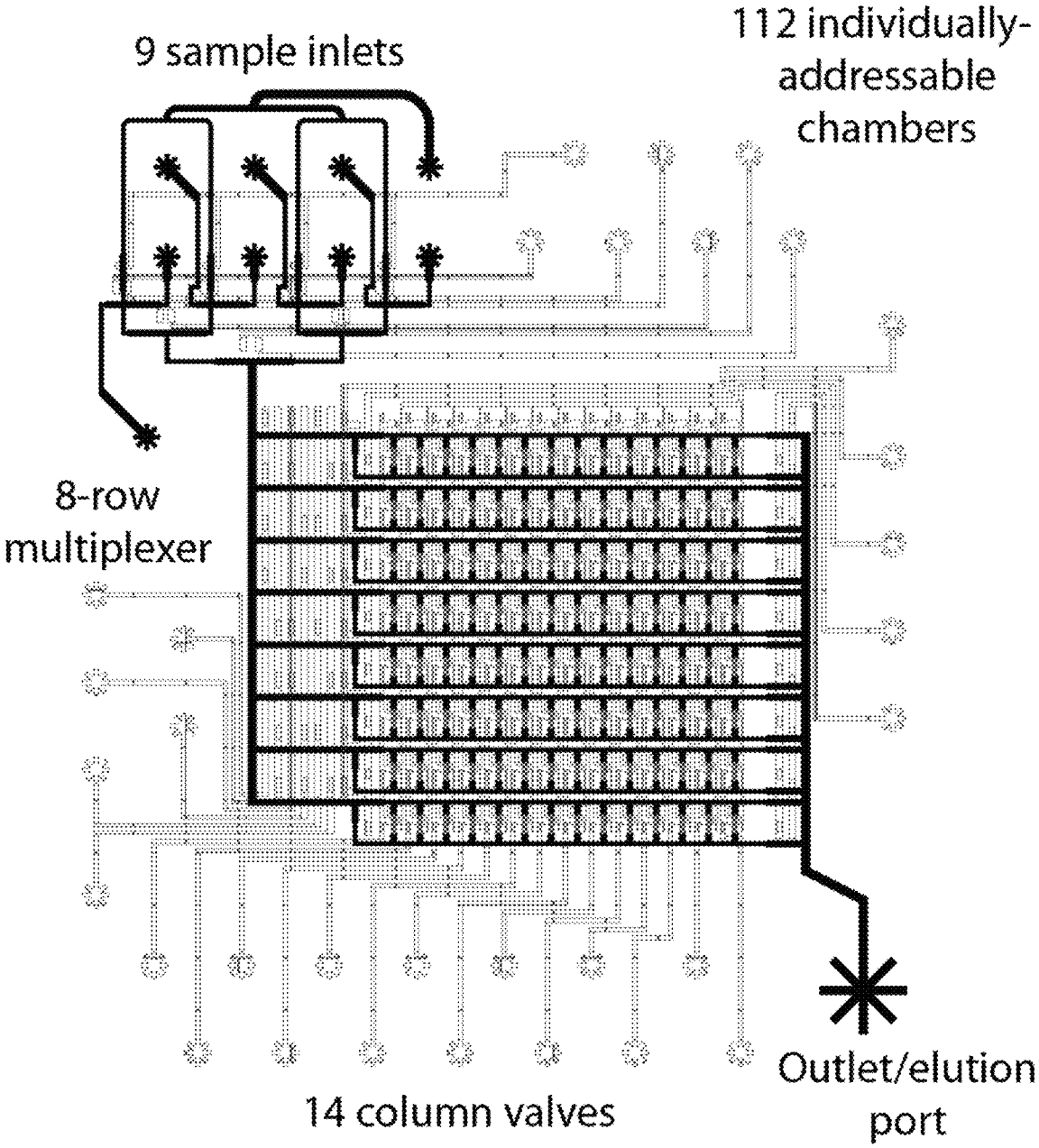
9 sample inlets
112 individually-addressable chambers
8-row multiplexer
14 column valves
Outlet/elution port

Figure 22

METHODS FOR ASSAYING CELLULAR BINDING INTERACTIONS

CROSS REFERENCE TO RELATED APPLICATIONS

This application is a continuation of U.S. patent application Ser. No. 16/579,561, filed Sep. 23, 2019, which application is a continuation of U.S. patent application Ser. No. 16/290,751, filed Mar. 1, 2019, now U.S. Pat. No. 10,466,241 issued Nov. 5, 2019, which application is a continuation of U.S. patent application Ser. No. 16/129,555, filed Sep. 12, 2018, now U.S. Pat. No. 10,274,494 issued Apr. 30, 2019, which application is a continuation of U.S. patent application Ser. No. 14/879,791, filed Oct. 9, 2015, now U.S. Pat. No. 10,107,812 issued Oct. 23, 2018, which application is a continuation of U.S. patent application Ser. No. 13/184,363, filed Jul. 15, 2011, now U.S. Pat. No. 9,188,593 issued Nov. 17, 2015, which application claims the benefit of U.S. Provisional Patent Application Ser. No. 61/365,237 entitled "METHODS FOR ASSAYING CELLULAR BINDING INTERACTIONS" filed Jul. 16, 2010, the disclosure of each of which is incorporated herein by reference in its entirety.

FIELD OF INVENTION

This invention relates to the field of microfluidics and protein binding, more specifically, binding interaction between biomolecules.

BACKGROUND

Antibodies are defense proteins produced by the vertebrate adaptive immune system for the purposes of binding and targeting for clearance of a diverse range of bacteria, viruses, and other foreign molecules (collectively referred to as antigens) (see, for e.g., Abbas et al. (1997), *Cellular and Molecular Immunology*, 3rd Ed., Chapter 3, pp. 37-65). As a result of their ability to bind target antigens selectively and with high affinity, antibodies are useful tools for protein purification, cell sorting, diagnostics, and therapeutics.

Conventional antibody production has involved the immunization of animals (i.e., mice) with a target antigen, such as a virus, bacteria, foreign protein, or other molecule. The immunized mice produce on the order of 10^4-10^5 antibody secreting cells (ASCs), each with the capacity to produce a unique (monoclonal) antibody specific to the target antigen (see, for e.g., Poulson et al. (1997), *J. Immunol.* 179: 3841-3850; and Babcock et al. (1996), *Proc. Natl. Acad. Sci. USA* 93: 7843-7848).

The ASCs are then harvested from the immunized animals and screened in order to select which cells are producing antibodies of desired affinity and selectivity to the target antigen. Since single ASCs do not produce antibodies in sufficiently large quantities for binding affinity measurements, each ASC is clonally expanded. Primary ASCs do not grow efficiently in laboratory tissue cultures; thus, clonal expansion may be achieved by fusing ASCs to murine myeloma (cancer) cells to produce immortalized, antibody-secreting (hybridoma) cells (see, for e.g., Kohler, G. and Milstein, C. (1975), *Nature* 256: 495-497). Using this method, expansion of each successfully created hybridoma then produces a monoclonal antibody in sufficiently high concentrations to measure its affinity and selectivity to a target antigen.

It has been recognized that a limitation of hybridoma technology is the low efficiency of the fusion process. For example, whereas an immune response may produce on the order of 10^4-10^5 antibody secreting cells, a typical fusion will yield less than 100 viable hybridomas. (see, for e.g., Kohler, G. and Milstein, C. (1975), *Nature* 256: 495-497; Karpas et al. (2001), *Proc. Natl. Acad. Sci. USA* 98: 1799-1804; and Spieker-Polet et al. (1995), *Proc. Natl. Acad. Sci. USA* 92: 9348-9352). Therefore, fusions from hundreds to thousands of animals are required to fully sample the diversity of antibodies produced in an immune response, making the hybridoma approach both time-consuming and expensive. Attempts to circumvent hybridoma generation by immortalizing antibody-producing cells using viral transformations have resulted in modest gains in the efficiency of ASC immortalization. However, these approaches still require costly and time-consuming clonal expansion in order to produce sufficient quantities of monoclonal antibodies to screen for affinity and selectivity to target antigens (see for e.g., Pasqualini, R. and Arap, W. (2004), *Proc. Natl. Acad. Sci. USA* 101: 257-259; Lanzavecchia et al. (2007), *Current Opinion in Biotechnology* 18: 523-528; and Traggiai et al. (2004), *Nat Med* 10: 871-875).

Devices have been developed to estimate the equilibrium dissociation constants of antibodies secreted from single antibody-secreting cells (Story, C. M. et al. *Proc. Natl. Acad. Sci. U.S.A.* (2008) 105(46):17902-17907; and Jin, A. et al. *Nat. Med.* (2009) 15(9):1088-1092), but do not measure antibody-antigen binding kinetics using antibodies secreted from single cells.

SUMMARY

In a first embodiment, there is provided a method of assaying for a binding interaction between a protein produced by a cell and a biomolecule: (a) retaining the cell within a chamber having an inlet and an outlet; (b) exposing the protein produced by the cell to a capture substrate, wherein the capture substrate is in fluid communication with the protein produced by the cell and wherein the capture substrate is operable to bind the protein produced by the cell; (c) flowing a first fluid volume comprising the biomolecule through the inlet into the chamber and out the outlet, wherein the first fluid volume is in fluid communication with the capture substrate; and (d) determining binding interactions between the protein produced by a cell and the biomolecule.

The cell may be an antibody producing cell (APC), the protein produced by the cell is an antibody and the biomolecule is an antigen. The cell may be a single cell. The biomolecule may be a fluorescently labeled antigen. The determining binding interactions may be a measure of antigen-antibody binding kinetics. The determining the antigen-antibody binding kinetics may include fluorescence imaging of antigen-antibody binding. The determining the binding interactions may be by one or more of the following techniques: surface plasmon resonance (SPR) spectroscopy, fluorescence anisotropy, interferometry, or fluorescence resonance energy transfer (FRET). The determining of the binding interaction may be by a nanocalorimeter or a nanowire nanosensor. The measure of antigen-antibody binding kinetics may be the K_{on} rate. The measure of antigen-antibody binding kinetics may be the K_{off} rate. The measure of antigen-antibody binding kinetics may be the both the K_{on} rate and the K_{off} rate. The protein produced by the cell may be an antibody. The antibody may be a monoclonal antibody. The protein produced by the cell may be an antigen. The biomolecule may be an antigen. The biomolecule may be selected from one of the following: an

antibody, a whole cell, a cell fragment, a bacterium, a virus, a viral fragment, and a protein. The protein produced by the cell may not be secreted by the cell, and the method may further include a step of cell lysis prior to exposing the protein produced by the cell to the capture substrate. The protein produced by the cell may not be secreted by the cell, and the method may further include a step of cell lysis after exposing the protein produced by the cell to the capture substrate. The capture substrate may be a removable capture substrate. The removable capture substrate may be an anti-Ig bead. The removable capture substrate may be an anti-Ig bead and/or oligo (dT) bead. The removable capture substrate may include a capture substrate capable of capturing both nucleic acids and antibodies. The removable capture substrate may include a capture substrate capable of capturing nucleic acids and a capture substrate capable of capturing antibodies. The removable capture substrate may include a capture substrate capable of capturing nucleic acids. The binding of the antibodies may be further tested by viral inactivation. The binding of the antibodies may be further tested by bacterial inactivation. The binding of the antibodies may be further tested by cell inactivation. The method may further include adding the cell to a reverse transcription polymerase chain reaction (RT-PCR) reaction to amplify the heavy and light chain genes. The amplification may be performed in a number of ways. For example, 1) the cells may be eluted into RT-PCR mix containing primers for both heavy and light chain genes for multiplex amplification of both genes in a single reaction. Alternatively, the cells may be eluted into RT-PCR mix without primers, the mix may then be split into two equal volume aliquots and the respective heavy and light chain primers may be added to the two aliquots for single-plex amplification. Both methods have been shown to work to amplify the heavy and light chains from a single cell. The exposing the protein produced by the cell to the capture substrate may include flowing a removable capture substrate into the chamber. The method may further include washing the cell prior to flowing a removable capture substrate into the chamber. The protein produced by the cell may be an antigen and the biomolecule may be an antibody. The antibody may be a monoclonal antibody. The biomolecule may be a fluorescently labeled antibody. The fluorescently labeled antibody may be a monoclonal antibody. The determining binding interactions may be a measure of antigen-antibody binding kinetics. The measure of antigen-antibody binding kinetics may be any one or both of: a K_{on} rate; and a K_{off} rate. The APC may be from one of the following: a human, a rabbit, a rat, a mouse, a sheep, an ape, a monkey, a goat; a dog, a cat, a camel, or a pig. The removable capture substrate may be a carboxylic acid (COOH) functionalized bead. The removable capture substrate may be capable of binding the protein produced by the cell and the nucleic acids encoding the protein produced by the cell. The method may further include washing the cell prior to exposing the protein produced by the cell to a capture substrate. The APC may be selected from one of the following: a primary B cell and a memory B cell.

In a further embodiment, there is provided a cell assay method, the method including: distributing an antibody producing cell (APC) to a chamber, wherein the APC is in a first fluid; replacing the first fluid with a second fluid while maintaining the APC in the chamber; placing the antibodies produced by the APC in fluid communication with an antigen; and determining the antigen-antibody binding kinetics of the antibodies produced by the APC with the antigen.

In a further embodiment, there is provided a method of assaying for a binding interaction between a protein produced by a cell and a biomolecule, the method including: (a) retaining the cell within a chamber having an aperture; (b) exposing the protein produced by the cell to a capture substrate, wherein the capture substrate is in fluid communication with the protein produced by the cell and wherein the capture substrate is operable to bind the protein produced by the cell; (c) flowing a fluid volume comprising the biomolecule through the chamber via said aperture, wherein the fluid volume is in fluid communication with the capture substrate; and (d) determining a binding interaction between the protein produced by the cell and the biomolecule.

The measure of antigen-antibody binding kinetics may be the K_{on} rate. The measure of antigen-antibody binding kinetics may be the K_{off} rate. The measure of antigen-antibody binding kinetics may be the both the K_{on} rate and the K_{off} rate. The binding of the antibodies may be further tested by viral inactivation. The binding of the antibodies may be further tested by bacterial inactivation. The binding of the antibodies may be further tested by cell inactivation. The determining of antigen-antibody binding kinetics may be by one or more of the following techniques: surface plasmon resonance (SPR) spectroscopy, fluorescence anisotropy, interferometry, or fluorescence resonance energy transfer (FRET). The determining of antigen-antibody binding kinetics may be by a nanocalorimeter or a nanowire nanosensor. The method may further include adding the cell to a reverse transcription polymerase chain reaction (RT-PCR) reaction to amplify the heavy and light chain genes. The placing the antibodies produced by the APC in fluid communication with an antigen may include flowing a removable capture substrate into the chamber. The method may further include washing the cell prior to flowing a removable capture substrate into the chamber. The APC may be from one of the following: a human, a rabbit, a rat, a mouse, a sheep, an ape, a monkey, a goat; a dog, a cat, a camel, or a pig. The removable capture substrate may be a carboxylic acid (COOH) functionalized bead. The removable capture substrate may be capable of binding the protein produced by the cell and the nucleic acids encoding the protein produced by the cell. The method may further include washing the cell prior to exposing the protein produced by the cell to a capture substrate. The APC may be selected from one of the following: a primary B cell and a memory B cell. The method may further include adding a removable capture substrate to the chamber to capture the antibodies produced by the APC prior to placing the antibodies produced by the APC in fluid communication with an antigen. The placing of the antibodies produced by the APC in fluid communication with an antigen may include flowing a fluorescently labeled antigen through the chamber. The method may further include collecting the mRNA from the cell for a reverse transcription polymerase chain reaction (RT-PCR) reaction to amplify the heavy and light chain genes. The determining the antigen-antibody binding kinetics may include fluorescence imaging of antigen-antibody binding.

In a further embodiment, there is provided a microfluidic device for assaying for a binding interaction between a protein produced by a cell and a biomolecule, the device comprising: a chamber, having: (i) at least one inlet; (ii) at least one outlet; and (iii) a reversible trap having spaced apart structural members extending across the chamber to separate the at least one inlet and at least one outlet wherein the spaced apart structural members are operable to allow

fluid flow through the chamber from the inlet to the outlet while providing size selection for a particle within the fluid flow.

In a further embodiment, there is provided a microfluidic device for assaying for a binding interaction between a protein produced by a cell and a biomolecule, the device comprising: a chamber, having: (i) at least one inlet; (ii) at least one outlet; and (iii) a reversible trap, wherein the reversible trap is a narrowing of the chamber from to allow fluid flow through the chamber from the inlet to the outlet while providing size selection for a particle within the fluid flow.

In a further embodiment, there is provided a microfluidic device for assaying a binding interaction between a protein produced by a cell and a biomolecule, the device including: a chamber having an aperture and a channel for receiving a flowed fluid volume through the chamber via said aperture, the channel providing size selection for a particle within said fluid volume.

In a further embodiment, there is provided a microfluidic device for assaying a binding interaction between a protein produced by a cell and a biomolecule, the device including: a chamber having an aperture; a reversible trap having spaced apart structural members extending across the chamber, the structural members being operable to allow a fluid volume to flow through the chamber while providing size selection for a particle within said fluid volume.

The distance between the spaced apart structural members may be less than or equal to about 4.6 microns. The distance between the spaced apart structural members may be less than or equal to about 4.5 microns. The distance between the spaced apart structural members may be less than or equal to about 4.4 microns. The distance between the spaced apart structural members may be less than or equal to about 4.3 microns. The distance between the spaced apart structural members may be less than or equal to about 4.2 microns. The distance between the spaced apart structural members may be less than or equal to about 4.1 microns. The distance between the spaced apart structural members may be less than or equal to about 4.0 microns. The distance between the spaced apart structural members may be less than or equal to about 3.9 microns. The distance between the spaced apart structural members may be less than or equal to about 3.8 microns. The distance between the spaced apart structural members may be less than or equal to about 3.7 microns. The distance between the spaced apart structural members may be less than or equal to about 3.6 microns. The distance between the spaced apart structural members may be less than or equal to about 3.5 microns. The distance between the spaced apart structural members may be less than or equal to about 3.4 microns. The distance between the spaced apart structural members may be less than or equal to about 3.3 microns. The distance between the spaced apart structural members may be less than or equal to about 3.2 microns. The distance between the spaced apart structural members may be less than or equal to about 3.1 microns. The distance between the spaced apart structural members may be less than or equal to about 3.0 microns. The distance between the spaced apart structural members may be less than or equal to about 2.9 microns. The distance between the spaced apart structural members may be less than or equal to about 2.8 microns. The distance between the spaced apart structural members may be less than or equal to about 2.7 microns. The distance between the spaced apart structural members may be less than or equal to about 2.6 microns. The distance between the spaced apart structural members may be less than or equal to about 2.5 microns. The distance between the spaced apart structural members may be less than or equal to about 2.4 microns. The distance between the spaced apart structural members may be less than or equal to about 2.3 microns. The distance between the spaced apart structural members may be less than or equal to about 2.2 microns. The distance between the spaced apart structural members may be less than or equal to about 2.1 microns. The distance between the spaced apart structural members may be less than or equal to about 2.0 microns. The distance between the spaced apart structural members may be less than or equal to about 1.9 microns. The distance between the spaced apart structural members may be less than or equal to about 1.8 microns. The distance between the spaced apart structural members may be less than or equal to about 1.7 microns. The distance between the spaced apart structural members may be less than or equal to about 1.6 microns. The distance between the spaced apart structural members may be less than or equal to about 1.5 microns. The distance between the spaced apart structural members may be less than or equal to about 1.4 microns. The distance between the spaced apart structural members may be less than or equal to about 1.3 microns. The distance between the spaced apart structural members may be less than or equal to about 1.2 microns. The distance between the spaced apart structural members may be less than or equal to about 1.1 microns. The distance between the spaced apart structural members may be less than or equal to about 1.0 microns. The distance between the spaced apart structural members may be less than or equal to about 0.9 microns. The distance between the spaced apart structural members may be less than or equal to about 0.8 microns. The distance between the spaced apart structural members may be less than or equal to about 0.7 microns. The distance between the spaced apart structural members may be less than or equal to about 0.6 microns. The distance between the spaced apart structural members may be less than or equal to about 0.5 microns. The spaced apart structural members may be posts. The spaced apart structural members may be between 5 to 30 microns in width. The spaced apart structural members may be between 10 to 20 microns in width. The spaced apart structural members may be between 5 to 30 microns in width. The spaced apart structural members may be between 5 to 20 microns in width. The spaced apart structural members may be between 5 to 10 microns in width.

The narrowing of the chamber may be from greater than about 10 microns to less than about 5.0 microns. The narrowing of the chamber may be from greater than about 10 microns to less than about 4.9 microns. The narrowing of the chamber may be from greater than about 10 microns to less than about 4.8 microns. The narrowing of the chamber may be from greater than about 10 microns to less than about 4.7 microns. The narrowing of the chamber may be from greater than about 10 microns to less than about 4.6 microns. The narrowing of the chamber may be from greater than about 10 microns to less than about 4.5 microns. The narrowing of the chamber may be from greater than about 10 microns to less than about 4.4 microns. The narrowing of the chamber may be from greater than about 10 microns to less than about 4.3 microns. The narrowing of the chamber may be from greater than about 10 microns to less than about 4.2 microns. The narrowing of the chamber may be from greater than about 10 microns to less than about 4.1 microns. The narrowing of the chamber may be from greater than about 10 microns to less than about 4.0 microns.

It will be appreciated by a person of skill in the art that the distance between the spaced apart structural members and the narrowing of the chamber to produce the reversible trap,

will depend on the size of the cells being assayed and the size of the removable capture substrate, and the flow velocity through the chamber, whereby the cell and the removable capture substrate are retained in the chamber at a first flow velocity and whereby the removable capture substrate is retained in the chamber and the cell is able to deform and fit through the reversible trap at a second flow velocity. Alternatively, there may be different sized removable capture substrates and some may be permitted to pass through the reversible trap, while other may be retained. Furthermore, there may be further flow velocities possible with a given device, whereby the reversible trap may deform to allow the removable capture substrates to pass through the chamber. Alternatively, the chamber may be pierced to remove the removable substrate and/or cells. The narrowing of the chamber may correspond to the channel size selection.

The particle may be selected from one or more of the cell, the biomolecule, the protein, the protein bound to a removeable capture substrate, and the removeable capture substrate. The size selection of the reversible trap may prevent the cell and the removeable capture substrate from passing through the reversible trap, and may allow the biomolecule and the protein to pass through the reversible trap at a first flow velocity, and the size selection of the reversible trap may prevent the removeable capture substrate from passing through the reversible trap, while allowing the cell, the biomolecule and the protein to pass through the reversible trap at a second flow velocity. The outlet may be a sieve valve and the flow velocity through the chamber when the valve is in an open position may be sufficient to allow the cell to deform and pass through the reversible trap. The device may be operable to provide two or more flow velocities through the chamber. The device may be operable to provide two flow velocities through the chamber. The device may be operable to provide three flow velocities through the chamber. The device may be operable to provide four flow velocities through the chamber. The microfluidic device may be operable to allow for removal of the removeable capture substrate. The microfluidic device may be operable to allow for removal of the cell.

The cells get trapped in the chambers when the sieve valves are closed. However, as with the posts, the cells deform when the sieve valve is opened and there is increased flow through the chambers. Both implementations of the reversible trap have worked, but the bead post design is slightly more robust at retaining the beads. The cells being used in the present experiments are about 10 microns in diameter, the beads are 5 microns in diameter, and the space between the posts is less than 3 microns.

A chamber may be in fluid communication with a first auxiliary chamber, wherein there is may be a valve between the chamber and the first auxiliary chamber. The first auxiliary chamber may be in fluid communication with a second auxiliary chamber, wherein there is a valve between the first and second auxiliary chambers, wherein the valve has an open position to allow fluid flow from the first auxiliary chamber to the second auxiliary chamber and a closed position to prevent fluid flow from the first auxiliary chamber to the second auxiliary chamber. The first auxiliary chamber may be in fluid communication with a second auxiliary chamber and the second auxiliary chamber is in fluid communication with a third auxiliary chamber, wherein there is a valve between the first and second auxiliary chambers, wherein the valve has an open position to allow fluid flow from the first auxiliary chamber to the second auxiliary chamber and a closed position to prevent fluid flow from the first auxiliary chamber to the second auxiliary chamber, wherein there is a valve between the second and third auxiliary chambers, wherein the valve has an open position to allow fluid flow from the second auxiliary chamber to the third auxiliary chamber and a closed position to prevent fluid flow from the second auxiliary chamber to the third auxiliary chamber. The volumes of the first second and third auxiliary chambers relative to the chamber may be such that fluid may be flowed into these chambers such that subsequent RT and PCR or other reactions may be carried out without exchanging the fluid (for example, where a first outlet is in a closed position).

The volume of the auxiliary chambers may be expandable. The volume of the chamber may be between 0.1 nL to 100.0 nL. The unexpanded volume of the expandable the chamber may be between 0.1 nL to 100.0 nL. The volume of the chamber may be 0.6 nL. The unexpanded chamber may be 0.6 nL. The effective volume of a given chamber may be increased by expanding the initial chamber or by opening a valve to provide fluid flow into one or more auxiliary chambers. The ratio between the second auxiliary chamber and the first auxiliary chamber may be 5:1. The ratio between the second auxiliary chamber and the first auxiliary chamber may be at least 5:1. The ratio between the expanded chamber and the unexpanded chamber may be 5:1 or the ratio between the expanded first auxiliary chamber unexpanded first auxiliary chamber may be 5:1. The ratio between the expanded chamber and the unexpanded chamber may be at least 5:1 or the ratio between the expanded first auxiliary chamber unexpanded first auxiliary chamber may be at least 5:1. The ratio between the second auxiliary chamber and the first auxiliary chamber, or between the expanded chamber and the unexpanded chamber, or between the expanded first auxiliary chamber unexpanded first auxiliary chamber may vary depending on the reaction mixtures chosen, the concentrations of the components of the mixture and the concentration of the material being assayed. Alternatively, the chamber may be between 0.05 nL and 100.0 nL. Alternatively, the chamber may be between 0.05 nL and 90.0 nL. Alternatively, the chamber may be between 0.1 nL and 95.0 nL. Alternatively, the chamber may be between 0.1 nL and 90.0 nL. Alternatively, the chamber may be between 0.1 nL and 85.0 nL. Alternatively, the chamber may be between 0.1 nL and 80.0 nL. Alternatively, the chamber may be between 0.1 nL and 75.0 nL. Alternatively, the chamber may be between 0.1 nL and 70.0 nL. Alternatively, the chamber may be between 0.1 nL and 65.0 nL. Alternatively, the chamber may be between 0.1 nL and 60.0 nL. Alternatively, the chamber may be between 0.1 nL and 55.0 nL. Alternatively, the chamber may be between 0.1 nL and 50.0 nL. Alternatively, the chamber may be between 0.1 nL and 45.0 nL. Alternatively, the chamber may be between 0.1 nL and 40.0 nL. Alternatively, the chamber may be between 0.1 nL and 35.0 nL. Alternatively, the chamber may be between 0.1 nL and 30.0 nL. Alternatively, the chamber may be between 0.1 nL and 25.0 nL. Alternatively, the chamber may be between 0.1 nL and 20.0 nL. Alternatively, the chamber may be between 0.1 nL and 15.0 nL. Alternatively, the chamber may be between 0.1 nL and 10.0 nL. Alternatively, the chamber may be between 0.1 nL and 9.0 nL. Alternatively, the chamber may be between 0.1 nL and 8.0 nL. Alternatively, the chamber may be between 0.1 nL and 7.0 nL. Alternatively, the chamber may be between 0.1 nL and 6.0 nL. Alternatively, the chamber may be between 0.1 nL and 5.0 nL. Alternatively, the chamber may be between 0.1 nL and 4.0 nL. Alternatively, the chamber may be between 0.1

nL and 3.0 nL. Alternatively, the chamber may be between 0.1 nL and 2.0 nL. Alternatively, the chamber may be between 0.1 nL and 1.0 nL.

In a further embodiment, there is provided a method of assaying for a protein of interest produced by a cell, the method comprising: incubating the cell with a removable capture substrate in a buffer, wherein the removable capture substrate is capable of binding the protein of interest and nucleic acids encoding the protein of interest; and screening the bound removable capture substrate to determine whether the cell produces the protein of interest.

In a further embodiment, there is provided a method of assaying for a protein of interest produced by a cell, the method comprising: incubating the cell with a removable capture substrate in a buffer, wherein the removable capture substrate is capable of binding the protein of interest; and screening the bound removable capture substrate to determine whether the cell produces the protein of interest.

In a further embodiment, there is provided a method of identifying a monoclonal antibody of interest, the method comprising: incubating an APC with a removable capture substrate in a suitable buffer, wherein the removable capture substrate is capable of binding the monoclonal antibody produced by the APC and nucleic acids encoding the variable regions of the monoclonal antibody; and screening the bound removable capture substrate to determine whether the APC produces the monoclonal antibody of interest.

In a further embodiment, there is provided a cell assay method, the method comprising: distributing an APC to a chamber, wherein there is on average one APC in the chamber, wherein the APC is incubated with a removable capture substrate in a first solution, and wherein the removable capture substrate is capable of binding an antibody of interest produced by the APC and nucleic acids encoding the variable regions of the antibody of interest; replacing the first solution with a second solution while maintaining the APC in the chamber; placing the antibody of interest produced by the APC in fluid communication with an antigen; and screening the bound removable capture substrate to determine whether the APC produces the antibody of interest.

In a further embodiment, there is provided a method of assaying for a chemical interaction between a protein produced by a cell and a biomolecule, the method comprising: distributing the cell to a chamber, wherein the cell is in a first solution; replacing the first solution with a second solution while maintaining the cell in the chamber; placing the protein in fluid communication with the biomolecule; and testing the chemical interaction of the protein produced by the cell with the biomolecule.

In a further embodiment, there is provided a method of identifying a monoclonal antibody of interest, the method comprising: incubating an antibody producing cell (APC) with a removable capture substrate in a suitable buffer, wherein the removable capture substrate is capable of binding the monoclonal antibody produced by the APC and nucleic acids encoding the variable regions of the monoclonal antibody; and screening the bound removable capture substrate to determine whether the APC produces the monoclonal antibody of interest.

In a further embodiment, there is provided a cell assay method, the method comprising: distributing an antibody producing cell (APC) to a chamber, wherein there is on average one APC in the chamber, wherein the APC is incubated with a removable capture substrate in a first solution, and wherein the removable capture substrate is capable of binding an antibody of interest produced by the APC and nucleic acids encoding the variable regions of the antibody of interest; replacing the first solution with a second solution while maintaining the APC in the chamber; placing the antibody of interest produced by the APC in fluid communication with an antigen; and screening the bound removable capture substrate to determine whether the APC produces the antibody of interest.

In a further embodiment, there is provided a method of assaying for a protein of interest produced by a cell. The method involves incubating the cell with a removable capture substrate in a suitable buffer, wherein the removable capture substrate is capable of binding the protein of interest; and screening the bound removable capture substrate to determine whether the cell produces the protein of interest.

The method may involve determining the binding affinity of the protein of interest. The method may involve determining a dissociation rate; and association rate and dissociation rate. The method may involve lysing the cell prior to incubation with the removable capture substrate, wherein the protein of interest is not secreted by the cell.

In a further embodiment, there is provided an device for selecting a cell that produces a protein having a binding affinity for a biomolecule. The device may include a microfluidic device as described herein operably configured to hold an aliquot, wherein the aliquot on average contains one cell, and wherein the protein produced by the cell is in fluid communication with the biomolecule; and a detector for detecting the binding affinity of the protein produced by the cell.

The device may include a detector that is a fluorescence imager for detecting the binding affinity. The device may include a detector that is a surface plasmon resonance (SPR) spectroscopy apparatus, or a fluorescence anisotropy apparatus, or an interferometry apparatus, or a FRET apparatus. Further, the device may include a detector that is a nanocalorimeter or a nanowire nanosensor.

In a further embodiment, there is provided a kit for identifying a cell that produces antibodies having a binding affinity for an antigen. The kit includes a microfluidic device as contemplated herein; and a removable capture substrate. The kit may include the removable capture substrate being capable of binding proteins, or nucleic acids, or proteins and nucleic acids. The kit may include the removable capture substrate being a microsphere. Further, the kit may include the microsphere being a polystyrene bead or a silica bead. Further, the kit may include the microsphere being a carboxylic acid (COOH) functionalized bead.

The kit may include an antigen label. The kit may include an antigen label that is a fluorescent label. Further, the kit may include instructions for the use of the device contemplated herein to identify a cell that produces proteins having a desired binding affinity. Further, the kit may include instructions for immunizing an animal and collecting APCs. Further, the kit may include an antigen.

BRIEF DESCRIPTION OF THE DRAWINGS

FIG. **1** shows a microfluidic device and schematics for bead-based measurements of antibody-antigen binding kinetics. Panel (A) is an illustration of a microfluidic device containing control channels for individually selecting six reagent inlets and actuating sieve valves on the reagent outlet channel. Panel (B) shows a microscopic image of the device with food coloring to visualize distinct reagent inlets (as shown) and control channels (as shown) (5× magnification); Top inset depicts a close-up of beads trapped using sieve valves (20× magnification; Bottom inset depicts fluo-

rescence image of beads during binding kinetic measurements (100× magnification). Panel (C) shows a schematic of a bead assay for direct measurement of association and dissociation kinetics of immobilized mAbs and fluorescently-labeled antigen. Panel (D) shows a variation of a bead assay for indirect measurement of dissociation kinetics of immobilized mAbs and unlabeled antigen molecules.

FIG. **2** shows a schematic diagram of an embodiment of a microfluidic device for the detection of antibody secreted from single cells. (A) Hydraulic pressure is applied to valves (fully-closing) and sieve valves (partially-closing) formed by the intersection of actuation control channels with rounded- or square-profile flow channels, respectively. (B) An expanded view of an embodiment of a microfluidic device for the detection of antibody secreted from single cells. (1) chip is flushed with 1× PBS; (2) antibody-secreting cells and antibody-capture beads are loaded into chambers; (3) cells are incubated for one hour to allow for antibody secretion; (4): mix valve is opened to allow for secreted antibody to bind to beads; (5) beads and cells are captured against sieve valve and unbound antibody is washed out; (6) chambers flushed with fluorescently-labeled antigen; image and measure antibody-antigen association kinetics; and (7) flushed out unbound antigen with 1× PBS; image and measure antibody-antigen dissociation kinetics.

FIG. **3** shows plots of microfluidic bead-based measurements of antibody-antigen binding kinetics. Direct fluorescent measurements of association and dissociation kinetics of (A) D1.3 mAb and HEL-Dylight488 conjugate, (B) HyHEL-5 mAb and HEL-Dylight488 conjugate, (C) LGB-1 mAb and enhanced green fluorescent protein (EGFP) are demonstrated. (D) Indirect measurement of dissociation kinetics of D1.3 mAb and HEL using HEL-Dylight488 conjugate is demonstrated.

FIG. **4** shows simultaneous measurement of multiple antibody-antigen binding kinetics using optical and spatial multiplexing. (A) Plots measured association and dissociation kinetics of 3 distinct mAbs (HyHEL-5, D1.3, and LGB-1 mAb) interacting with 2 different antigens (HEL-Dylight633 conjugate and EGFP) is demonstrated. (B) A micrograph showing false-coloured, overlay of images taken with distinct fluorescence filter cubes to identify anti-lysozyme mAbs and anti-EGFP mAbs is demonstrated.

FIG. **5** shows plots of sensitivity and detection limit of antibody-antigen binding kinetics measurements. (A) Measured association kinetics of D1.3 mAb-Dylight488 conjugate on rabbit anti-mouse pAb coated beads is demonstrated. Inset demonstrates a schematic of bead assay for measuring binding kinetics of fluorescently-labeled mouse mAb and rabbit anti-mouse pAb coated beads. (B) Association kinetics of HEL-Dylight488 conjugate on beads with varying amounts of immobilized D1.3 mAb is demonstrated. (C) Equilibrium bead fluorescence varies linearly with the amount of immobilized D1.3 mAb. Inset shows a close-up of the graph to highlight detection limit of 1% bead coverage. (D) Direct measurement of equilibrium dissociation constants by measuring equilibrium bead fluorescence using immobilized D1.3 mAb and varying concentrations of HEL-Dylight488.

FIG. **6** shows antibody-antigen binding kinetics measured using antibodies secreted from a single cell. (A) Microscope image of D1.3 hybridoma cell loaded into a microfluidic device adjacent to rabbit anti-mouse pAb coated beads trapped using a sieve valve is shown. (B) "Single-cycle" binding kinetics from a single bead containing D1.3 mAbs secreted from a single cell and subject to increasing concentrations of HEL-Dylight488 conjugate is demonstrated.

FIG. **7** shows the effect of fluorophore stability on measured antibody-antigen binding kinetics. (A) Photobleaching rates of fluorescent dye molecules under 100 W Hg lamp illumination using 100× oil-immersion objective (NA 1.30) are plotted. (B) Effect of fluorescent exposure times on measured association kinetics of D1.3 mAb and HEL-Dylight488 are plotted.

FIG. **8** shows the effect of different bead immobilization chemistries on measured antibody-antigen binding kinetics. Measured kinetics are unaffected by bead composition (silica or polystyrene) or by different polyclonal capture antibodies (rabbit or goat pAbs).

FIG. **9** shows a plot of measured dissociation kinetics of mouse mAb from antibody capture beads. No dissociation of D1.3 mAb-Dylight488 conjugate from Rabbit anti-Ms pAb coated beads was observed over 3 days.

FIG. **10** shows a plot of the effect of antigen re-binding on measured antibody-antigen dissociation kinetics. Dissociation kinetics of D1.3 mAb and HEL-Dylight488 conjugate were unaffected by the presence of a large concentration of competitive antigen (2 mg/mL HEL).

FIG. **11** shows a plot of the effect of mass transport on measured antibody-antigen binding kinetics. Association and dissociation kinetics of D1.3 mAb and HEL-Dylight488 conjugate were unaffected by varying flow rates over a range of ~3-15 μL/hr.

FIG. **12** shows representative microscopic images of primary ASCs in a microfluidic chamber in fluid communication with antibody capture beads and oligo(dT) beads.

FIG. **13** shows an image of an ELISPOT control assay confirming that the cells depicted in FIG. **12** are ASCs. The left image represents cells that secreted any antibody; the right image represents only those cells that secreted HEL-specific antibodies.

FIG. **14** shows a scheme for preparing dual-capture (i.e., dual-function) beads using carbodiimide chemistry.

FIG. **15** shows images of dual-function beads. Polystyrene COOH beads were conjugated with rabbit anti-mouse pAb and amine functionalized oligo$(dT)_{25}$ using carbodiimide chemistry. (A) Brightfield image of dual-function beads trapped using microfluidic sieve valve. (B) Fluorescence image of synthetic single-stranded DNA molecules captured on dual-function beads. Synthetic DNA molecules are labeled with Cy5 fluorophore for visualization and also contain a poly(A) tail that binds to the oligo(dT) on the bead surface. (C) Fluorescence image of mouse D1.3 monoclonal antibody (mAb) captured on dual-function beads. D1.3 mAbs are labeled with Dylight488 fluorophore for visualization and bind to the Rabbit anti-Mouse pAb on the bead surface.

FIG. **16** shows a microscopic image (A) and antibody-antigen binding kinetics (B) as determined from a microfluidic device for dual purpose beads.

FIG. **17** depicts (A) K_d, (B) K_{on}, and (C) K_{off} rates determined from specific eluted chambers according to Example 9 herein.

FIG. **18** shows representative fluorescence intensity data over time for specific eluted chambers according to Example 9 herein. (A) depicts data for R00C04; (B) depicts data for R04C06.

FIG. **19** shows Kappa chain results from the first round of RT-PCR are shown in FIG. **19**, Panel A. Kappa chain results from the second round of RT-PCR are shown in FIG. **19**, Panel B. Heavy chain results from the first round of RT-PCR are shown in FIG. **19**, Panel C. Heavy chain results from the second round of RT-PCR are shown in FIG. **19**, Panel D.

FIG. **20** shows a microfluidic device according to an embodiment of the invention described herein, showing a reversible trap. (A) brightfield image at 20× magnification; (B) brightfield image at 40× magnification.

FIG. **21** shows a schematic whereby a microfluidic device according to an embodiment of the invention described herein is used as described herein. (1) Flush chip with 1× PBS; (2) Load antibody-secreting cells into chambers; (3) Load antibody-capture beads into inlet channel; (4) Load antibody-capture beads into chamber against bead filter; (5) Incubate cells for 1 hour to allow antibody secretion and capture on beads; (6) Wash out unbound antibody; (7) Load fluorescently-labeled antigen into inlet channel; (8) Flush chambers with fluorescently-labeled antigen; image and measure antibody-antigen association kinetics; (9) Flush our unbound antigen with 1× PBS; image and measure antibody-antigen dissociation kinetics; and (10) Open sieve valve and flush cell out of the chamber to the elution port for recovery from device.

FIG. **22** shows a schematic diagram of an alternative embodiment of the microfluidic device for assaying binding interactions.

DETAILED DESCRIPTION

A binding interaction, as referred to herein, includes a molecular interaction. A molecular interaction is commonly understood as referring to a situation when two or more molecules are attracted to one another by a force, where the force could be for example, electrostatic, dipole-dipole, hydrogen bonding, covalent, or hydrophobic in nature. A binding affinity is commonly understood as referring to an average strength of a molecular interaction. Similarly, "avidity" is used to describe the combined strength of multiple interactions. When used in the present application, "affinity" is meant to encompass one or more interactions, including avidity. The methods described herein may involve determining the binding affinity of the protein of interest. The methods described herein may also involve determining a dissociation rate; and association rate and dissociation rate. Alternatively, the methods described herein may include determining binding kinetics.

The method may involve testing the antigen binding affinity by fluorescence imaging. The method may involve testing the antigen binding affinity using any of the following techniques plasmon resonance (SPR) spectroscopy, fluorescence anisotropy, or interferometry. These techniques are understood to measure antibody-antigen binding kinetics, including, but not limited to surface plasmon resonance (SPR) spectroscopy, fluorescence anisotropy, interferometry, or fluorescence resonance energy transfer (FRET). See, for e.g., Bornhop et al. (2007), *Science* 317: 1732-1736; Homola et al. (1999) *Sensors and Actuators B: Chemical* 54: 3-15; and Xavier, K. A. and Willson, R. C. (1998), *Biophys. J.* 74: 2036-2045. Further, the method may involve testing the antigen binding affinity by a nanocalorimeter or a nanowire nanosensor. See, for e.g., Wang et al. (2005), *Proc. Natl. Acad. Sci. USA* 102: 3208-3212 and Lee et al. (2009) *Proc. Natl. Acad. Sci. USA* 106: 15225-15230. Another method that could be employed would be to use a technique such as dark-field microscopy and use antigens or antibodies labeled with gold nanoparticles. This could be used to detect single molecules and generate on/off rates by counting the molecules. See, for e.g., Ueno et al. (2010) *Biophysical J.* 98: 2014-2023; Raschke et al. (2003) *Nano Letters* 3: 935-938; and Sönnischen et al. (2000) *App. Phys. Letters* 77: 2949-2951. Further methods for labeling and detecting binding events and/or binding kinetics would be known to a person of skill in the art. For example, binding assays may include determining the number of binding events.

A protein, as referred to herein, refers to organic compounds made of amino acids, including both standard and non-standard amino acids. Standard amino acids include the following: alanine, cysteine, aspartic acid, glutamic acid, phenylalanine, glycine, histidine, isoleucine, lysine, leucine, methionine, asparagine, proline, glutamine, arginine, serine, threonine, valine, tryptophan, and tyrosine. An example of a protein is an antibody.

A biomolecule, as referred to herein, may include, but is not limited to, an antibody, or an antibody fragment, or a whole cell, or a cell fragment, or a bacterium, or a virus, or a viral fragment, a nucleic acid or a protein.

A "chamber", as used herein, refers to an enclosed space within a microfluidic device in which a cells may be retained. Each chamber may have at least one inlet for permitting fluid, including fluid containing a cell, to enter the chamber, and at least one outlet to permit fluid and/or the cell to exit the chamber (depending on the design of the chamber and/or the flow through the chamber). Persons skilled in the art will understand that an inlet or an outlet can vary considerably in terms of structure and dimension, and may be characterized in a most general sense as an aperture that can be reversibly switched between an open position, to permit fluid to flow into or out of the chamber, and a closed position to seal the chamber and thereby isolate and retain its contents. Alternatively, the aperture may also be intermediate between the open and closed positions to allow some fluid flow or may be a sieve valve that allows for fluid flow out of the cell, but not other particles (for example, the cell, the beads etc.). A chamber, as referred to herein, refers to a portion of a microfluidic device which is designed to hold, for example, a cell. As used herein, the chamber is of an exceptionally small and discrete sizing. Typical volumes are in the range of ~100 pl to ~100 nl. For example, a chamber can be designed with a volume of approximately 500 pL (less than 1 nL), with dimensions of approximately 100 microns (width), 500 microns (length), and 10 microns (height).

The direction of fluid flow through the chamber dictates an "upstream" and a "downstream" orientation of the chamber. Accordingly, an inlet will be located at an upstream position of the chamber, and an outlet will be generally located at a downstream position of the chamber. A person skilled in the art will understand, however, that a single aperture could function as both an inlet and an outlet.

An "inlet" or an "outlet", as used herein, may include any aperture whereby fluid flow is restricted through the inlet or outlet. There may be a valve to control flow, or flow may be controlled by separating the channels with a layer which prevents flow (for example, oil). Alternatively, an aperture may serve as both an inlet and outlet. Furthermore, an aperture (i.e. inlet or outlet) as used herein is meant to exclude the surface opening of a microwell.

A "microfluidic device", as used herein, refers to any device that allows for the precise control and manipulation of fluids in a geometrically constrained structure. For example, where at least one dimension of the structure (width, length, height) is less than 1 mm.

A solution, as referred to herein, may include, but is not limited to, a solution that can maintain the viability of a cell. Further, the solution may include a suitable buffer that can both retain the viability of a cell such that binding interactions can be obtained or allow for an effective lysis of the cell to obtain nucleic acids from the cell and/or antibodies or

other proteins depending on the application. Alternatively, the solution may be suitable for performing an assay.

A capture substrate, as referred to herein, is meant to encompass a wide range of substrates capable of capturing a protein or biomolecule of interest. These substrates may be modified to alter their surface (internal and external) properties depending on the desired use. For example, a substrate may be bound to antibodies or antigens to capture an antibody of interest. A capture substrate may be, for example, a microsphere or a nanosphere or other microparticles including, but not limited to a polystyrene bead or a silica bead (for example, antibody capture beads and oligo (dT) mRNA capture beads). In an alternate arrangement, instead of modifying the beads with oligo(dT), specific primers could be utilized instead. Optionally, the microsphere may be a carboxylic acid (COOH) functionalized bead. Beads which make use of alternate chemical interactions can fall within this definition. See: for e.g., G. T. Hermanson (2008), *Bioconjugate Techniques, 2nd Edition*, Published by Academic Press, Inc. For example, an alternate scheme for preparing these beads would be to use streptavidin coated beads and to mix these beads with biotinylized rabbit anti-mouse pAbs and biotinylated oligo(dT). A capture substrate can also be an anti-Ig bead which binds an antibody to the capture substrate. A capture substrate can be modified such that it binds multiple biomolecules of interest, for example both mRNA and protein. Alternately, each capture substrate could be limited to a particular biomolecule, for example, one capture substrate being limited to binding mRNA and a second capture substrate being limited to binding a protein. Capture substrates are commercially available or may be made de novo and/or modified as needed for the particular application. Capture substrates may be removable, as in the case of beads. However, capture substrates may also be fixed (and thus, non-removable).

Nucleic acids, as referred to herein, include macromolecules composed of chains of monomeric nucleotides. Common examples of nucleic acids include deoxyribonucleic acid (DNA) and ribonucleic acid (RNA).

In a further embodiment, a cell assay method is provided. The method involves distributing an antibody producing cell (APC) to a chamber, wherein the APC is in a first solution, and wherein there is on average one APC in the chamber; replacing the first solution with a second solution while maintaining the APC in the chamber; placing the antibodies produced by the APC in fluid communication with an antigen; and testing the binding of the antibodies produced by the APC with the antigen. Optionally, the method may involve adding anti-Ig beads to the chamber to capture the antibodies produced by the APC. Optionally, the method may involve lysing the APC to capture antibodies produced by the APC wherein the antibodies are not secreted by the APC.

A cell as referred to herein includes an antibody producing cell (also referred to herein as an "APC"). An APC refers to a cell that can produce an antibody. An antibody producing cell is not limited to cells that secrete antibodies, which are also referred to herein as antibody secreting cells (also referred to herein as an "ASC"). For example, it will be understood from the relevant art that memory B cells, without stimulation, do not normally secrete antibodies. See, for e.g., Abbas et al. (1997), *Cellular and Molecular Immunology,* 3rd Ed., pp. 22-23). Examples of antibody producing cells (APCs) include B cells, memory B cells, primary B cells (which are also known in the art as naïve B cells), and B cell hybridomas. A primary B cell can be harvested from the spleen, blood, or bone marrow of an animal, for example from a mouse, by FACS sorting for a cell surface marker, for example, the CD138+ marker (See: for e.g., Smith et al. (1996) *Eur. J. Immunol.* 26: 444-448).

Antibodies are defense proteins produced by the vertebrate adaptive immune system for the purposes of binding and targeting for clearance a diverse range of bacteria, viruses, and other foreign molecules (antigens). As a result of their ability to bind target antigens selectively and with high affinity, antibodies are invaluable tools for protein purification, cell sorting, and diagnostics. Antibodies are produced by B cells and are secreted by activated B cells. (See generally, for e.g., Abbas et al. (1997), *Cellular and Molecular Immunology,* 3rd Ed., Chapter 3, pp. 37-65). Antibodies are also referred to herein as immunoglobulin (also referred to herein as Ig). An antibody, as referred to herein, can include, but is not limited to polyclonal antibodies and monoclonal antibodies. Unlike polyclonal antibodies, monoclonal antibodies are monospecific antibodies that are the same because they are made by one type of immune cell that are all clones of a unique parent cell. A single APC or ASC can serve as the source of a monoclonal antibody. Antibodies are not limited to a specific isotype and can include, but are not limited to the following isotypes: IgM, IgG, IgD, IgE, and IgA. Typically, it is understood that antibodies are comprised of light and heavy chains that have variable and constant regions therein (see generally, for e.g., Abbas et al. (1997), *Cellular and Molecular Immunology,* 3rd Ed., Chapter 3, pp. 37-65).

In a further embodiment, a method of identifying a monoclonal antibody of interest is provided. The method involves incubating an APC with a removable capture substrate (RCS) in a suitable buffer, wherein the removable capture substrate is capable of binding the monoclonal antibody produced by the APC and nucleic acids encoding the variable regions of the monoclonal antibody; and screening the bound removable capture substrate to determine whether the APC produces the monoclonal antibody of interest.

In a further embodiment, a cell assay method is provided. The method involves distributing an APC to a chamber, wherein there is on average one APC in the chamber, wherein the APC is incubated with a removable capture substrate in a first solution, and wherein the removable capture substrate is capable of binding an antibody of interest produced by the APC and nucleic acids encoding the variable regions of the antibody of interest; replacing the first solution with a second solution while maintaining the APC in the chamber; placing the antibody of interest produced by the APC in fluid communication with an antigen; and screening the bound removable capture substrate to determine whether the APC produces the antibody of interest.

In a further embodiment an apparatus for selecting a cell that produces a protein having a binding affinity for a biomolecule is provided. The apparatus includes a microfluidic device operably configured to hold an aliquot, wherein the aliquot on average contains one cell, and wherein the protein produced by the cell is in fluid communication with the biomolecule; and a detector for detecting the binding affinity of the protein produced by the cell. However, the microfluidic device may also hold more than one cell, particular in an assay where the antigen or biomolecule of interest is a cell, or a cell fragment. Similarly, the antigen may be a virus or a bacterial cell.

In a further embodiment, a kit for identifying a cell that produces antibodies having a binding affinity for an antigen is provided. The kit includes a microfluidic device and a removable capture substrate.

An antigen, as referred to herein, refers to a molecule recognized by the immune system. As such, an antigen can include a molecule that can elicit an immune response in an organism, including in an animal. Examples of antigens include, but are not limited to bacterial antigens and viral antigens.

A method is provided for identifying antibody secreting cells (ASCs) that produce antibodies having a particular binding affinity for an antigen or functional attributes. The method involves distributing an ASC within a discrete aliquot wherein there is on average one ASC in the aliquot, placing the antibodies in fluid communication with the antigen; and testing the antigen binding affinity of the antibodies produced by the ASC. The method is based in part on the discovery that a single ASC, without clonal expansion, is capable of producing enough antibodies to test binding affinity for an antigen or to test other functional attributes. Furthermore, the method is also based, in part, on the discovery that clonal expansion via the production of hybridomas is not required for larger scale production of monoclonal antibodies, whereby the variable regions for the antibodies of interest may be sequenced from an ASC of interest or collected with antibodies.

By way of example, a sensitive, low-cost microfluidic bead-based fluorescence assay is described herein for measuring antibody-antigen binding kinetics within low abundance samples. Direct measurements of antibody-antigen binding kinetics may be made by time-course fluorescence microscopy of antibody-conjugated beads retained in microfluidic chambers and subject to a series of wash cycles with fluorescently-labeled antigen and buffer. A variation of the bead-based assay may include measuring the dissociation kinetics of unlabeled antibody and antigen molecules. As disclosed herein, multiple antibody-antigen interactions were measured spanning nearly four orders of magnitude in equilibrium binding affinity. The rate constants measured by way of the assay disclosed herein were validated with previously published values using SPR spectroscopy.

The methods provided herein are also contemplated for being used to screen mutagenic B cell lines. Further, the methods provided herein are contemplated for being used to screen the selectivity and specificity of antibodies to multiple different antigens.

Antibody Binding Kinetics

The affinity or binding strength of an antibody for its target antigen is an important parameter when selecting an antibody for a given application. Although the affinity of an antibody-antigen interaction is typically quantified by an equilibrium binding constant (K_d), which describes the dynamic equilibrium between binding and unbinding events, the kinetic rate constants (k_{on} and k_{off}) provide a more complete characterization of an antibody-antigen interaction. Two antibodies with identical K_d values may exhibit dramatically different binding kinetics which, in turn, will determine their respective suitability for a given application. For instance, antibodies with rapid association and dissociation kinetics may be desirable for sensing applications, whereas antibody-antigen interactions with very long half-lives may be critical for histological staining, enzyme-linked immunosorbent assays (ELISA), and Western blotting. Similarly, therapeutic antibodies that bind their target antigens with long half-lives could, in principle, be administered in lower dosages, reducing the cost and side-effects of these therapies. Direct measurement of binding kinetic constants can be a critical factor for selecting antibodies for both clinical and research applications. Examples of kinetic assays include, but are not limited to viral and other pathogenic neutralization, cell signaling and growth inhibition, modulation of enzymatic activity (inhibit or enhance).

Microfluidics

Microfluidics refers to a multidisciplinary field dedicated to the design of systems in which small volumes of fluids will be used for a variety of purposes, including lab-on-a-chip technology. See: for e.g., Squires and Quake (2005), *Reviews of Modern Physics* 77: 977-1026. Microfluidic technologies enable small-scale (picoliter to nanoliter) fluid handling operations for high-throughput biochemical analyses with low reagent costs and rapid analysis times. In particular, microfluidic devices fabricated from a silicone rubber, polydimethylsiloxane (PDMS), can be designed and fabricated in 24-48 hours, enabling rapid prototyping of devices. See: for e.g., McDonald, J. C. et al. (2000), *Electrophoresis* 21: 27-40. Microfluidic devices that integrate valves into pumps, mixers, fluidic multiplexers (MUXes), and other fluid-handling components have been successfully applied for protein crystallization, chemical synthesis, protein and DNA detection and single cell analysis. See, for e.g., Thorsen et al. (2002), *Science* 298: 580-584; Hansen, et al. (2002), *Proc. Natl. Acad. Sci. USA* 99: 16531-16536; Maerkl, S. J. & Quake, S. R. (2007) *Science* 315: 233-237; Hansen et al. (2004), *Proc. Natl. Acad. Sci. USA* 101, 14431-14436; Huang, B. et al. (2007) *Science* 315, 81-84; and Cai et al. (2006) *Nature* 440: 358-362. Microfluidic devices, as described herein, can include chambers of varying sizes. For example, chambers can be designed with a volume of approximately 500 pL (less than 1 nL), with dimensions of approximately 100 microns (width), 500 microns (length), and 10 microns (height).

As disclosed herein, antibody-antigen binding kinetics were measured with approximately 4×10^4 antibody molecules (~66 zeptomoles) immobilized on a single bead and less than 2×10^6 antibodies (~3 attomoles) loaded into the microfluidic device. This represents a reduction of greater than four orders of magnitude in both detection limit and sample consumption compared to SPR spectroscopy and a recently reported microfluidic fluorescence assay for measuring protein-protein binding kinetics. See, for e.g., Bates, S. R.; Quake, S. R. (2009), *Appl. Phys. Lett.* 95, 073705. Since each antibody-antigen interaction can be characterized on a single bead, millions of distinct antibody-antigen interactions can be characterized with a single lot of commercially available beads (i.e., 1 mL at 10^7-10^8 beads/mL). By using the bead surface rather than the chip surface as the sensor, a single microfluidic device may be re-used indefinitely and may be imaged using a standard inverted fluorescence microscope. However, a person of skill in the art could also apply the basic methods described herein to a microfluidic system having antigen and/or antibodies bound to the surface of a chip. It is further shown herein that an assay applying a method described herein may be used to perform simultaneous kinetic measurements of multiple antibody-antigen interactions using spatial and optical multiplexing. By comparison, characterization of each antibody-antigen interaction using SPR spectroscopy requires specialized instrumentation and a unique flow cell on comparatively expensive sensor chips. The low detection limit of the microfluidic bead assay coupled with small volume compartmentalization was exploited in order to measure the antigen binding kinetics of antibodies secreted by a single ASC. It is contemplated that the microfluidic

bead assay described herein could be used for measuring antibody-antigen binding kinetics from rare blood samples, for screening scarce antibodies produced by primary plasma cells from immunized animals, as well as for selecting clones for recombinant protein production. Additionally, it is contemplated that in addition to its utility for measuring antibody-antigen binding kinetics, the microfluidic bead-based assay described herein can be used for measuring other protein-protein and biomolecular interactions with a wide range of binding affinities, such as protein-carbohydrate binding, protein-DNA (i.e., transcription factor binding) and protein-RNA interactions. It is also contemplated that upon identifying an ASC that secretes antibodies which are optimal for a particular purpose, the ASC in question can be cloned by reverse-transcriptase PCR and standardized cloning techniques.

Experimental Methods

Microfluidic Device Fabrication and Control

All microfluidic devices were fabricated using multilayer soft lithography (see, for e.g., Unger, M. A. et al. (2000), *Science,* 288: 113-116 and Thorsen, T. et al. (2002), *Science* 298: 580-584. Devices were composed of two layers of poly(dimethylsiloxane) (PDMS) elastomer (GE RTV 615) bonded to No 1.5 glass coverslips (Ted Pella, Inc.). The devices were designed in AutoCAD software (Autodesk) and printed on high resolution (20,000 dpi) transparency masks (CAD/Art Services). Master molds were fabricated in photoresist on silicon wafers (Silicon Quest) by standard optical lithography. The control master molds were fabricated out of 20-25 μm high SU-8 2025 photoresist (Microchem). The flow master molds were fabricated with 12 μm rounded SPR220-7.0 photoresist channels (Rohm and Haas) and 6 μm SU-8 5 photoresist (Microchem) channels with rectangular cross-section. Microfluidic valves were actuated at 30 psi pressure which was controlled using off-chip solenoid valves (Fluidigm Corp) controlled using LabView 7.1 software and a NI-6533 DAQ card (National Instruments). Compressed air (3-4 psi) was used to push reagent solutions into the device.

Reagent Preparation

Protein A-coated 5.5 μm diameter polystyrene beads (Bangs Labs) were incubated with 1 mg/mL solutions of Rabbit anti-mouse polyclonal antibodies (pAbs) (Jackson Immunoresearch). All antibody and antigen solutions were prepared in PBS/BSA/Tween solution consisting of 1× PBS, pH 7.4 (Gibco) with 10 mg/mL BSA (Sigma) and 0.5% Polyoxyethylene (20) sorbitan monolaurate (similar to Tween-20, EMD Biosciences). Lysozyme from chicken egg white (HEL) was purchased from Sigma, and the D1.3 and HyHEL-5 mouse monoclonal antibodies to lysozyme were generously provided by Dr. Richard Willson (University of Houston). The anti-GFP mouse monoclonal antibody (LGB-1) was purchased from Abcam. Fluorescent protein conjugates were prepared using Dylight488 and Dylight633 NHS esters (Pierce) and were purified using Slide-A-Lyzer dialysis cassettes (Pierce). The concentration of fluorescent conjugates was measured by spectrophotometry (Nanodrop). In order to minimize protein denaturation, fluorescent HEL conjugates were labeled at dye-to-protein (D/P) ratios of less than 1, whereas the D1.3-Dylight488 conjugate was prepared at a D/P ratio of ~5.

Microscopy

The microfluidic devices were imaged on a Nikon TE200 Eclipse inverted epifluorescence microscope equipped with green (470/40 nm excitation, 535/30 nm emission) and red (600/60 nm excitation, 655 nm long-pass emission) fluorescence filter cubes (Chroma Technology). Fluorescence images were taken using a 16-bit, cooled CCD camera (Apogee Alta U2000) and a 100× oil immersion objective (N.A. 1.30, Nikon Plan Fluor). The sensitivity of the fluorescence measurements was tuned by binning pixels on the CCD detection camera and modulating the fluorescence exposure times (20 ms-1 s) with a computer-controlled mechanical shutter (Ludl).

Cell Culture

Mouse D1.3 hybridoma cells were cultured in RPMI 1640 media (Gibco) with 10% FCS. Prior to loading into microfluidic devices, cells were washed by centrifugation at 1500 rpm and re-suspended in fresh media in order to remove antibodies secreted in the cell media.

Microfluidic Bead-Based Fluorescence Assay

A microfluidic device was designed and fabricated to perform bead-based fluorescence measurements of antigen-antibody binding kinetics (see FIGS. **1**A and B herein). The device consists of six fluidic inlets, each used for loading a distinct reagent and controlled with an independent control valve, which join into a common fluidic outlet. The fluidic outlet can be partitioned into discrete ~200 pL chambers by actuating a set of microfluidic "sieve" valves which, when actuated, act as filters to immobilize large particles (>1 micron) while still allowing fluid exchange. See, for e.g., Marcus, J. S. et al. (2006) *Analytical Chemistry* 78: 3084-3089.

At the start of the experiment, the fluidic outlet was flushed with a PBS/BSA/Tween solution from the top and bottom fluidic inlets in order to pre-coat channel walls and reduce nonspecific binding. Next, 5.5 μm diameter Protein A beads coated with Rabbit anti-mouse pAb were loaded through the device to the fluidic outlet. The microfluidic sieve valves were then actuated and the fluidic outlet was again washed with PBS/BSA/Tween solution to immobilize the beads against the traps and wash out any free rabbit pAb in solution. The beads were then washed with the mouse antibody selected for kinetic characterization. Again, free mouse antibody was washed out of the fluidic outlet using PBS/BSA/Tween. Finally, the beads were washed with fluorescently-labeled antigen and fluorescently imaged at defined time intervals to measure the rate of antibody-antigen association (see FIG. **1**C herein). When chemical equilibrium between the antibody and antigen was reached, as detected by a plateau in bead fluorescence, the beads were flushed with PBS buffer and imaged to measure the rate of antibody-antigen dissociation. The process was repeated with varying concentrations of fluorescently-labeled antigen, each loaded onto the microfluidic device from a separate fluidic inlet.

A second version of the microfluidic bead assay was implemented to indirectly measure dissociation kinetics between antibodies and unlabeled antigen molecules by displacement with fluorescently labeled antigen (see FIG. **1**D herein). In this assay, after the antibody of interest was captured on Rabbit anti-mouse pAb-coated Protein A beads, beads were washed with unlabeled antigen at high concentration (>1 μM) to saturate all antibody binding sites. Beads were then washed with fluorescently labeled antigen while imaging at defined time intervals. Dissociation of the unlabeled antigen was then inferred by accumulated fluorescence on the beads.

In order to measure the antigen binding kinetics from antibodies secreted from single cells, Protein A beads coated with Rabbit anti-mouse pAb were first immobilized in the fluidic outlet channel using the microfluidic sieve valves. A solution of RPMI-1640 media containing 10^5 hybridoma cells/mL was then loaded into the device from a separate

fluidic inlet and the control valve was momentarily opened to allow for a single hybridoma cell to be brought in close proximity with beads immobilized in the first sieve trap in the fluidic outlet channel. The hybridoma cell was then allowed to incubate next to the beads for 1 hour, and subsequently washed with PBS/BSA/Tween buffer to wash out any free antibody in solution and halt antibody secretion from the cell. Kinetic measurements of antigen binding were then performed in the same manner as with purified antibodies.

FIG. **2** shows a schematic diagram of a microfluidic device operable for detecting antibody secreted from antibody secreting cells. The steps utilized are, for example, as follows: (1) flush microfluidic channels with cell culture media; (2) load channels with antibody secreting cells (top) and capture beads (bottom); (3) incubate cells with beads to capture secreted antibody; (4) trap cells and beads with sieve valves and flush out unbound antibody by blowing buffer over cell-bead mixture; (5) flow fluorescently-labeled antigen over trapped cells and beads; and (6) flush out unbound antigen by blowing buffer over trapped cells and beads and image fluorescent beads.

Data Analysis.

Fluorescent images were analyzed using MaximDL 4 imaging software. Fluorescent intensities were measured by selecting line profiles through the beads and recording the maximum intensity at the bead surface. During protein binding experiments, line profiles were constructed through the same beads at each measurement time point in order to avoid any systemic variations caused by differences in bead-to-bead binding capacity, variation in position in the flow channel and non-uniform illumination over the field of view. The measured fluorescence bead intensities were assumed to be proportional to the concentration of antibody-antigen complex ([AbAg]) and were fit to the following first-order, mass action and Langmuir isotherm equations using nonlinear least squares minimization:

$$F(t) = (F_{max} - F_0)\frac{[Ag]_0}{[Ag]_0 + K_d}\left(1 - e^{-(k_{on}[Ag]_0 + k_{off})t}\right) + F_0 \quad \text{(equation 1)}$$

$$F(t) = (F_{max} - F_0)\frac{[Ag]_0}{[Ag]_0 + K_d}e^{-k_{off}t} + F_0 \quad \text{(equation 2)}$$

$$F(t) = (F_{max} - F_0)\frac{[Ag]_0}{[Ag]_0 + K_d} + F_0 \quad \text{(equation 3)}$$

where F(t) represents the measured bead fluorescence at time t, F_0 and F_{max} represent the background and maximum bead fluorescence, respectively, $[Ag]_0$ represents the solution concentration of antigen (in M), and, k_f and k_r represent the intrinsic association and dissociation rate constants, in units of $M^{-1}s^{-1}$ and s^{-1}, respectively.

EXAMPLES

The following examples describe embodiments of the invention detailed herein.

Example 1. Measurement of Antibody-Antigen Binding Kinetics on Beads

The binding kinetics of the D1.3 mouse monoclonal antibody (mAb) to fluorescently-labeled hen egg lysozyme (HEL) was measured using the methodologies and techniques described herein. See: FIG. **3**A and Table 1 herein.

TABLE 1

Antibody-antigen binding kinetics measured using the microfluidic fluorescence bead assay.

Antibody/Antigen interaction	k_{on} ($M^{-1}s^{-1}$)	k_{off} (s^{-1})	K_d
D1.3 mAb/HEL-Dylight488	$1.87 \pm 0.48 \times 10^6$	$2.10 \pm 0.25 \times 10^{-3}$	1.20 ± 0.42 nM
D1.3 mAb/HEL-Dylight633	$1.27 \pm 0.22 \times 10^6$	$2.15 \pm 0.23 \times 10^{-3}$	1.75 ± 0.46 nM
HyHEL-5 mAb/HEL-Dylight633	$5.75 \pm 0.71 \times 10^6$	$1.69 \pm 0.30 \times 10^{-4}$	30.0 ± 7.4 pM
LGB-1 mAb/EGFP	$5.00 \pm 0.72 \times 10^4$	$5.15 \pm 0.89 \times 10^{-3}$	106 ± 28 nM

The measured association and dissociation rate constants for the D1.3/HEL interaction were $1.87\pm0.48\times10^6$ $M^{-1}s^{-1}$ and $2.10\pm0.25\times10^{-3}$ s^{-1}, respectively, and were consistent with values of $1.0\text{-}2.0\times10^6$ $M^{-1}s^{-1}$ and $1.15\text{-}3.04\times10^{-3}s^{-1}$ previously measured using surface plasmon resonance (SPR) spectroscopy, stopped-flow fluorescence quenching, and competitive ELISA. See, for e.g., Batista, F. D. and Neuberger, M. S. (1998), *Immunity* 8: 751-759 and Ito, W. et al. (1995), *Journal of Molecular Biology* 248: 729-732. A ten-fold smaller association rate constant previously reported for the D1.3/HEL interaction (1.67×10^5 $M^{-1}s^{-1}$) can likely be attributed to differences between the full D1.3 mAb used in our microfluidic bead-based measurements and the recombinant single-chain antibody fragment used by Bedouelle and coworkers (England et al. (1999) *J. Immunol.* 162: 2129-2136).

Additionally, indirect, label-free measurements of the D1.3 mAb/HEL dissociation rate constant using a variation of our microfluidic bead assay were performed using the methodologies and techniques described herein. See: FIGS. **1**D and **3**D herein. In this assay, D1.3 mAbs immobilized on beads were first saturated with unlabeled HEL and subsequently washed with fluorescently-labeled HEL. Measurements of the accumulated bead fluorescence faithfully reflected the D1.3/HEL dissociation kinetics provided the labeled HEL was at a sufficiently high concentration to ensure that dissociation was rate-limiting (i.e. $k_{on}[Ag]>k_{off}$, or, equivalently, $[Ag]>K_d$). Using this method, the dissociation rate constant of D1.3 and unlabeled HEL was measured to be $1.45\pm0.30\times10^{-3}$ s^{-1}, in close agreement with direct dissociation measurements between D1.3 and fluorescently-labeled HEL. See Table 1 herein.

The microfluidic bead assay was used to measure the binding kinetics of HEL and HyHEL-5, a distinct mouse mAb with significantly stronger binding affinity to HEL than D1.3. In comparison to the D1.3 mAb, HyHEL-5 bound HEL with a nearly four-fold larger association rate constant ($5.75\pm0.71\times10^6$ $M^{-1}s^{-1}$) and ten-fold smaller dissociation rate constant ($1.69\pm0.30\times10^{-4}$ s^{-1}). See: FIG. **3**B herein. Thus, HyHEL-5 bound HEL with a ~40-fold smaller equilibrium dissociation constant than D1.3 (30 pM vs. 1.2 nM). See: Table 1 herein. Compared with the microfluidic bead assay, previous measurements of the HyHEL-5/HEL inter-

action using solution-phase fluorescence anisotropy resulted in a similar dissociation rate constant (2.2×10^{-4} s^{-1}), but a three- to five-fold larger association rate constant ($1.5\text{-}3.3\times10^{7}$ $M^{-1}s^{-1}$). See, for e.g., Xavier, K. A. and Willson, R. C. (1998) *Biophys. J.* 74: 2036-2045. Since HyHEL-5 mAb binds HEL with near diffusion-limited association kinetics, immobilization of the mAb in the microfluidic bead assay could potentially result in slower association kinetics when compared with solution-phase fluorescence anisotropy measurements. However, since the diffusion constant of HEL is approximately three times larger than that of the mAb, immobilization of the HyHEL-5 mAb would reduce the effective diffusion coefficient ($D\cong D_{mAb}+D_{HEL}$) and, hence, the apparent association rate constant by at most 25%. See, for e.g., Tyn, M. T. and Gusek, T. W. (1990), *Biotechnology and Bioengineering* 35: 327-338 and He, L. and Niemeyer, B. (2003), *Biotechnol. Prog.* 2003, 19: 544-548. Therefore, the difference in measured and reported association rate constants is likely a result of different buffer solutions, as the HyHEL-5 and HEL binding interaction is known to be very sensitive to solution pH and buffer salt concentration. See, for e.g., Xavier, K. A. and Willson, R. C. (1998) *Biophys. J.* 74: 2036-2045 and Długosz et al. (2009), *The Journal of Physical Chemistry* 113: 15662-15669.

The binding kinetics of a commercially available mouse monoclonal antibody (LGB-1, Abcam) to enhanced green fluorescent protein (eGFP) were also measured using the methodologies and techniques described herein. See: FIG. **3** herein. This binding interaction was chosen to demonstrate that the bead-based assay can be used to measure binding kinetics of a previously uncharacterized antibody without optimizing the bead immobilization chemistry. In this instance, native eGFP fluorescence was measured without an exogenous fluorescent label. The measured association and dissociation rate constants for the LGB-1/eGFP interaction were $5.00\pm0.72\times10^{4}$ $M^{-1}s^{-1}$ and $5.15\pm0.89\times10^{-3}$ s^{-1}, respectively. See: Table 1 herein.

Collectively, the measured binding kinetics of the anti-lysozyme and anti-eGFP mAbs span nearly four orders of magnitude in equilibrium dissociation constants (30 pM-100 nM), with association rate constants varying from 5×10^{4}-10^{6} $M^{-1}s^{-1}$ and dissociation rate constants ranging from 10^{-3}-10^{-4} s^{-1}. See: Table 1 herein. In principle, the microfluidic bead-based assay can be used to characterize stronger antibody-antigen interactions than the HyHEL-5/HEL interaction; however, binding interactions with dissociation rate constants lower than $10^{-4}s^{-1}$ require measurements to be taken over several days or weeks. On the other hand, the bead-based assay can be readily used to measure binding interactions weaker than the LGB-1/eGFP interaction. Using this assay, the practical upper limit in measurable dissociation rate constants is approximately 10^{-1} s^{-1}, as a result of the time required to exchange solutions in the microfluidic device. Thus, the microfluidic bead-based assay should enable characterization of antibody-antigen interactions that span greater than six orders of magnitude in equilibrium binding affinity.

Example 2. Simultaneous Measurement of Multiple Antibody-Antigen Binding Kinetics Using Optical and Spatial Multiplexing

The binding kinetics of multiple antibody-antigen interactions were measured simultaneously using both optical and spatial multiplexing of the bead-based assay using the methodologies and techniques described herein. Each antibody was immobilized on a distinct population of beads and, subsequently, beads from each population were sequentially trapped using sieve valves on the microfluidic device. Since beads trapped by the sieve valves remain immobilized throughout the duration of each experiment, the spatial address of beads was tracked in order to identify each antibody. Subsequently, the trapped beads were washed with a mixture of antigens, each labeled with a spectrally distinct fluorophore. The beads were then imaged with different fluorescence filter sets designed to coincide with each fluorescent antigen. In this manner, the binding kinetics of 3 different monoclonal antibodies (D1.3, HyHEL-5 and LGB-1) to two different fluorescent antigens (HEL-Dylight488 and eGFP) were simultaneously measured. See: FIG. **4** herein. By employing this strategy, it was possible to spectrally distinguish which beads were coated with anti-lysozyme mAbs or anti-eGFP mAbs, whereas the two anti-lysozyme mAbs (D1.3 and HyHEL-5) were discriminated based on their unique binding kinetics for HEL. In addition, the fluorescence intensities of HyHEL-5 coated beads were significantly higher than the D1.3 coated beads, consistent with the fact that HyHEL-5 binds HEL with a significantly lower equilibrium dissociation constant than D1.3. See: FIG. **4** herein. This technique can be extended to measure any combination of m×n antibody-antigen interactions in which m antibodies are immobilized on different beads and exposed to a solution of n antigens, each with a spectrally-resolvable fluorescent label. In practice, several hundred antibody-antigen interactions could be measured simultaneously by imaging up to 100 beads in a single field of view with five to six spectrally distinct fluorophores. Multiplexed bead measurements could be used for simultaneously analyzing the binding kinetics and binding specificities of a panel of mAbs to multiple different antigens in serum and other complex mixtures.

Example 3. Microfluidic Bead-Based Fluorescence Measurements Reflect Intrinsic Antibody-Antigen Binding Kinetics

A series of experiments were performed using the methodologies and techniques described herein to verify that bead-based fluorescence measurements reflected intrinsic antibody-antigen binding kinetics, and were unaffected by artifacts arising from fluorescent labeling of the antigen, antibody immobilization, diffusion limitation or mass transport effects. Fluorescent labeling of HEL did not alter the intrinsic D1.3/HEL binding kinetics, as indicated by the agreement between microfluidic bead-based measurements using fluorescently labeled HEL and previously reported measurements using SPR spectroscopy with unlabeled HEL. See, for e.g., Batista, F. D. and Neuberger, M. S. (1998), *Immunity* 8: 751-759 and Ito, W. et al. (1995), *Journal of Molecular Biology* 248: 729-732. Moreover, no differences were observed in bead-based kinetic measurements of the D1.3 mAb binding to HEL labeled with two different fluorophores, Dylight488 and Dylight633 (Pierce). See: Table 1 herein. It was ensured that photobleaching of fluorophores did not affect the measured binding kinetics by measuring the photobleaching rates of the of the fluorescent dyes used in this study (Dylight488, Dylight633, and eGFP) and selecting fluorescence exposure times of less than 100 ms, such that each measurement resulted in less than 5% reduction in bead fluorescence. See: FIG. **7**A herein. Indeed, measured binding kinetics were consistent over a large range of fluorescence exposure times (ms), whereas exposure times of greater than 1 s resulted in substantial photobleach-

ing and an artificial increase in measured association and dissociation binding kinetics when compared to intrinsic kinetics. See FIG. **7**B herein.

To examine the effect of different antibody bead immobilization chemistries, we verified that measured association and dissociation rate constants for the D1.3/HEL interaction were the same when captured on silica or polystyrene beads coated with either rabbit or goat anti-mouse polyclonal antibody. See: FIG. **8** herein. It was further verified that multivalent binding between the rabbit anti-mouse pAbs and fluorescently-labeled D1.3 mAb resulted in no detectable dissociation over the course of 3 days, which would otherwise artificially accelerate the measured antibody-antigen binding kinetics. See: FIG. **9** herein. The nearly irreversible bond between rabbit pAb and the mouse mAbs was critical to successful antibody-antigen binding kinetic measurements as attempts to measure D1.3/HEL binding kinetics using Protein A beads without Rabbit anti-mouse pAbs were unsuccessful due to rapid dissociation (and low affinity) of protein A/mouse mAb complexes.

Several experiments were also conducted to verify that diffusion limitation and mass transport did not affect bead-based measurements of antibody-antigen binding kinetics. In the diffusion-limited regime, antibodies adjacent on the bead surface would compete for fluorescent antigen, thus reducing the apparent association rate constant. Similarly, the apparent rate of antibody-antigen dissociation would be reduced due to antigen rebinding to adjacent antibodies. See, for e.g., Berg, H. C. and Purcell, E. M. (1977), *Biophys. J.* 20: 193-219 and Lauffenburger, D. A. and Linderman, J. (1965) *Receptors: Models for Binding, Trafficking, and Signaling*; Oxford University Press. Nearly identical association and dissociation kinetics for the D1.3-HEL interaction was measured by varying the amount of bead-immobilized D1.3 mAb over two orders of magnitude. See FIG. **10**B herein. Dissociation kinetics of the D1.3 antibody and fluorescently labeled HEL were also similar both in the presence and absence of a high concentration (~2 mg/mL) of competitive unlabeled HEL antigen. See: FIG. **10** herein. Thus, there was no observable competition between antibodies adjacent to one another on the beads and, hence, no diffusion limitation. It was also confirmed that the association and dissociation rate constants of the D1.3-HEL interaction remained constant over a range of flow rates from 3-15 μL/hr, suggesting no effect of mass transport on the measured kinetics. See: FIG. **11** herein.

Example 4. Bead-Based Kinetic Measurements Exhibit Low Detection Limits and Minimal Sample Consumption

To quantify the detection limit and minimal sample consumption required for microfluidic bead-based measurements of antibody-antigen binding kinetics, antibody-antigen binding kinetics were measured using varying amounts of bead-immobilized mAb along with the methodologies and techniques described herein. The association rate constant of fluorescently-labeled D1.3 mAb binding to Rabbit anti-mouse pAb coated Protein A beads was measured. See: FIG. **5**A herein. Using the measured kinetic on-rate constant for this interaction (k_{on}=1.10±0.11×10^6 M^{-1}s^{-1}) and modulating the loading time of D1.3 mAb, the amount of bead-immobilized D1.3 mAb was varied over two orders of magnitude. Then, the antibody-antigen binding kinetics with as little as 1% of the bead surface covered with D1.3 mAb was successfully measured. See: FIG. **5**B herein. Using the manufacturer's specifications as well as steric considerations, a single 5.5 micron bead can bind 4×10^6 antibody molecules (~6.6 amol); therefore, it was estimated that the detection limit of our microfluidic fluorescence bead assay is to be ~4×10^4 antibodies or ~66 zeptomoles. See: FIG. **5**C herein. In contrast, SPR spectroscopy requires at least 200 pg (~10^9 molecules) of immobilized antibody in order to generate a detectable refractive index change. See, for e.g., Biacore Life Sciences—Biacore 3000 System Information. Website: http://www.biacore.com/lifesciences/products/systems_overview/3000/system_information/index.html. Additionally, D1.3/HEL binding kinetics were successfully measured by loading less than 2 million D1.3 mAb molecules (~3 attomoles) into the microfluidic device. In theory, the minimum sample consumption of the microfluidic bead assay could be reduced even further by reducing losses associated with channel dead volumes and optimizing the capture efficiency of antibodies on beads, as well as using microfluidic pumps to achieve flow rates less than 1 μL/hr. Thus, when compared with alternative techniques and SPR spectroscopy, our microfluidic bead-based assay can measure antigen-antibody binding kinetics with a reduction in both detection limit and sample consumption by four orders of magnitude.

Example 5. Measurement of Binding Kinetics of Antigen and Antibody Secreted from Single Cells

Based on the low detection limit of the bead-based assay and in an effort to measure the antigen binding kinetics of antibodies secreted from single antibody secreting cells, single D1.3 hybridoma cells were loaded adjacent to Rabbit anti-Mouse pAb coated Protein A beads captured in the microfluidic device, and then co-incubated the cells and beads for 1 hour at room temperature. See: FIG. **6** herein. Subsequently, antibody-antigen binding kinetics were measured by recording the fluorescence of a single bead washed with buffer and successively higher concentrations of fluorescent antigen, in a manner analogous to the single-cycle kinetics technique used with SPR spectroscopy. See, for e.g., Biacore Life Sciences—Single-Cycle Kinetics. Website: http://www.biacore.com/lifesciences/technology/introduction/data_interaction/SCK/index.html and Abdiche et al. (2008) *Analytical Biochemistry* 377: 209-217. Using the methodologies and experimental techniques described herein, the association and dissociation rate constants for the D1.3/HEL interaction were successfully measured using antibodies secreted by a single D1.3 hybridoma cell, which were consistent with measurements on purified antibodies. See: FIG. **6** and Table 1 herein.

Antibody-secreting cells are known to secrete thousands of antibodies per second at 37° C., and would, therefore, secrete enough antibodies in approximately one hour to saturate the surface of a single 5.5 μm bead with maximum binding capacity of ~4×10^6 antibody molecules. See, for e.g., Niels Jerne (1984) The Generative Grammar of the Immune System and McKinney et al. (1995) *Journal of Biotechnology* 40: 31-48. While it is reasonable to suspect that the hybridoma cells secrete antibodies at a reduced rate when incubated at room temperature; nonetheless, single D1.3 hybridoma cells secreted sufficient antibody within 1 hour at room temperature for complete kinetic characterization. However, based on the incubation time and detection limit of the assay (~4×10^4 antibodies), it can be inferred that single hybridoma cells secreted greater than 10 antibodies/second when incubated at room temperature in the microfluidic device.

Examples 1-5 show that the methods described herein are suitable for measuring antibody-antigen kinetics in a microfluidic environment from a single cell.

Example 6. Dual Function Beads

An overview of a scheme for preparing dual-capture (i.e., dual function) beads using carbodiimide chemistry is shown in FIG. **14**. A representative experiment utilizing dual function beads is shown in FIG. **15**. Briefly, polystyrene COOH beads (Bangs Labs) were conjugated with Rabbit anti-mouse pAb (Jackson ImmunoResearch) and amine-functionalized oligo(dT)$_{25}$ (Genelink) using carbodiimide chemistry. In FIG. **14**(A), a brightfield image of dual-function beads trapped using a microfluidic sieve valve is shown. In FIG. **14**(B), a fluorescence image of synthetic single-stranded DNA molecules captured on dual-function beads is shown. Synthetic DNA molecules are labeled with Cy5 fluorophore for visualization and also contain a poly(A) tail that binds to the oligo(dT) on the bead surface. In FIG. **14**(C), a fluorescence image of mouse D1.3 monoclonal antibody (mAb) captured on dual-function beads. D1.3 mAbs are labeled with Dylight488 fluorophore for visualization and bind to the Rabbit anti-Mouse pAb on the bead surface.

It will be understood that while carboxylic acid (COOH) beads are disclosed herein, other beads, which make use of alternate chemical interactions, could also be used, See: for e.g., G. T. Hermanson (2008), *Bioconjugate Techniques, 2nd Edition*, Published by Academic Press, Inc. For example, an alternate scheme for preparing thee beads would be to use streptavidin coated beads and to mix these beads with biotinylized rabbit anti-mouse pAbs and biotinylated oligo (dT).

Example 7. Multiplex RT-PCR of the Antibody Heavy and Light Chain Genes

Results from a multiplex RT-PCR of the antibody heavy and light chain genes indicated that a gene product coinciding with the proper molecular size was obtained. Briefly, D1.3 hybridoma cells were lysed using a nonionic detergent (1% NP-40 in 1× PBS) and the lysate was then mixed with rabbit anti-mouse pAb, oligo(dT)-conjugated dual-capture beads for mRNA capture. Generally, a gentle lysis buffer is preferred for cell lysis and can include, in addition to the foregoing: 0.5% NP-40 in 1× PBS or DI water or 0.5% Tween-20 in 1× PBS or DI water. Generally, it is preferable and within the knowledge of those persons skilled in the art to use lysis buffers that can sufficiently lyse the outer membrane of the cell in question, while keeping the nucleus intact. RT-PCR was performed using degenerate primers for both heavy and light chain genes and resulted in bands of the expected size for antibody heaby and light chains (date not shown). The results suggest that dual purpose RNA and antibody beads are capable of capturing RNA suitable for amplification. For comparison, RT-PCR of antibody genes was performed using commercially available oligo(dT) beads and dual-capture beads. The methodology utilized herein is generally as follows:

1) Capture oligo(dT) beads in microfluidic chambers using sieve valves.
2) Load cells in microfluidic chambers.
3) Load antibody-capture beads in chambers.
4) Incubate cells and beads.
5) Measure antibody-antigen binding kinetics.
6) Lyse cells using either a) 1% NP-40 in 1× PBS, or b) alkaline lysis solution (100 mM Tris-HCl, pH 7.5, 500 mM LiCl, 10 mM EDTA, pH 8.0 1% LiDS, 5 mM dithiothreitol (DTT)). During lysis, the cell lysate is flushed over the stack of trapped oligo(dT) beads. The oligo(dT) beads and alkaline lysis solution are from the Dynabead mRNA direct kit developed by Invitrogen, but alternatives to these reagents exist.
7) Wash beads with 1× PBS to remove lysis solution.
8) Open sieve valves.
9) Open microfluidic chamber valves and send beads to an output port (one chamber at a time).
10) Recover beads from output port using a pipette.
11) Pipette beads into 50 microL of one-step RT-PCR mix.
    i) dNTPs;
    ii) mixture of RT and DNA polymerase enzymes;
    iii) degenerate primers for both heavy and light chain genes (PCR reagents from a One-Step RT-PCR kit developed by Qiagen, but could also be prepared ourselves);
12) Perform RT and Touchdown PCR using the following protocol:
    i) RT at 50° C. for 30 min;
    ii) 95° C. for 15 min to inactivate RT enzyme and activate DNA polymerase
    iii) First ten cycles of Touchdown PCR:
    a) 94° C. for 30 s;
    b) 55° C. for 1 min (decrease by 1 C each cycle, until 45 C);
    c) 72° C. for 1 min.
    iv) 30 cycles of PCR
    a) 94° C. for 30 s;
    b) 45° C. for 1 min;
    c) 72° C. for 1 min.
13) Visualize RT-PCR amplicons on 0.5% DNA agarose gel using SYBRsafe fluorescent dye.
14) Extract amplicons from gel and purify using standard gel extraction kit (Qiagen).
15) Sequence samples.

Example 8. Microfluidic Antibody-Antigen Binding Kinetics Measured Using Dual Function Beads and Antibodies Secreted by Single Hybridoma Cells

Microscope image of D1.3 hybridoma cell adjacent to Rabbit anti-Mouse pAb, oligo(dT)-conjugated polystyrene beads trapped by a microfluidic sieve valve. After a 2 hour incubation the beads with the D1.3 cell, antibody-antigen binding kinetics were measured using fluorescently labeled HEL-Dylight488 conjugate. These results are highlighted in FIG. **16** and show that dual purpose beads are suitable for testing antibody-antigen binding kinetics.

Example 9. Mouse Experiment: Antibody Binding Kinetics and Whole-Cell Heavy Chain RT-PCR with Beads

These experiments were designed to detect antibodies from primary splenocytes harvested from BALB/c immunized mice. The cells were eluted and whole-cell single-plex RT-PCR was performed of heavy and light chain antibody genes. Thereafter, binding kinetics of the antibodies were measured.

Chip. Bead v6.6 chip with ~3 micron high sieve channels, 2 micron gratings (fabricated: May 29, 2011 with RTV615).

Reagents. The following reagents were used herein: 1× PBS for reagent flush; FACS-sorted CD138+ primary splenocytes in RPMI-10-2-ME media; 4.9 micron Rabbit anti-

Mouse Protein A beads; 5 microL of stock bead solution resuspended in 100 μL of RPMI-10-2-ME media; and 214 ng/mL HEL488 in 1× PBS.

Experimental Protocol. The following experimental protocol was followed: washed chip with 1× PBS; closed sieve valves; spun down primary cells and decanted ~400 of 500 μL of media; and re-suspended cells in remaining media.

Thereafter, the cells were loaded in all chambers sequentially with deliberate negative controls included (e.g., R1C14 and R0C02); load 4.9 micron Rabbit anti-Mouse Protein A beads in all chambers sequentially; incubate cells and beads for 1 h 20 min; and wash all chambers with 214 ng/mL HEL488 for 5 min. Thereafter, chamber intensities were analyzed using Image Analysis. Positive chambers were determined as follows: R0C04, R0C08, R2C02, R2C04, R2C07, R2C12, R2C13, R3C06, R4C01, R4C03, R4C05, R5C08, R5C09, R5C12, R5C14, R6C01, R6C02, R6C09, R6C10, R6C11, and R7C05.

RT-PCR mix without primers was prepared from a One-Step RT-PCR kit (Qiagen). The mix comprised: 10 μL 5× RT-PCR buffer×16=160 μL; 21 μL RNase-free water×16=336 μL; 2 μL dNTPs×16=32 μL; 2 μL Enzyme mix×16=32 μL. The RT-PCR mix without primers was aliquoted into 8 tubes of 70 μL each (2 reaction volumes, not including primer volume).

Prepared primer solutions to be mixed with RT-PCR after cell elution were as follows: Heavy chain—7.5 μL 8 μM 3' IgH first primer×8=60 μL; and 7.5 μL 8 μM 5' IgH first primer×8=60 μL. Kappa chain—7.5 μL 8 μM 3' IgK first primer×8=60 μL; and 7.5 μL 8 μM 5' IgK first primer×8=60 μL. 15 μL of primer mixes were aliquoted into each of 8 tubes. The primers used herein were selected based on what is taught in Table II of Tiller et al. (2009) *J. Immunol. Methods* 350: 183-193, which is incorporated herein by reference. Those persons skilled in the art that variants to the primers defined in Table II could be used under certain circumstances including, for example, the primers in Table III in Tiller et al. (2009).

Eight (8) of the brightest chambers [R0C04, R2C04, R2C07, R3C06, R5C12, R5C14, R6C01, R6C10] were eluted. The eluted cell samples were pipetted directly into 70 μL RT-PCR mix without primers. The RT-PCR/cell mix was split into two (2) equal parts of 35 μL and mixed with kappa and heavy chain primers, respectively. RT-PCR was performed using a thermal cycler. Briefly, the "NEST1ST5" protocol was used for the kappa chain reactions, comprising: RT step: 50° C. for 30 min; Hotstart/RT inactivation: 95° C. for 15 min; and 50 Cycles (denaturation: 94° C. for 30 s; anneal: 50° C. for 30 s; and extension: 72° C. for 55 s). Then, there was a final extension: 72° C. for 10 min. Heavy chain reactions performed using the "NEST1H" protocol, comprising: RT step: 50° C. for 30 min; Hotstart/RT inactivation: 95° C. for 15 min; and 50 Cycles (denaturation: 94° C. for 30 s; anneal: 56° C. for 30 s; extension: 72° C. for 55 s). Then, there was a final extension: 72° C. for 10 min.

Thereafter, kinetics were measured on each of the eluted chambers. A summary of the kinetics data is shown in FIG. **17**. Representative kinetics sample data is shown in each of FIGS. **18**A-E herein. Dissociation kinetics were measured and then association kinetics were measured using freshly loaded HEL488. Thereafter, a second round of single-plex RT-PCR was performed using nested second round primers. The heavy chain mix comprised of: 10 μL 5× RT-PCR buffer×8=80 μL; 21 μL RNase-free water×8=168 μL; 2 μL dNTPs×8=16 μL; 2 μL Enzyme mix×8=16 μL; 7.5 μL 8 μM 3' IgH second primer×8=45 μL; and 7.5 μL 8 μM 5' IgH second primer×8=45 μL. The kappa chain mix comprised of: 10 μL 5× RT-PCR buffer×8=80 μL; 21 μL RNase-free water×8=168 μL; 2 μL dNTPs×8=16 μL; 2 μL Enzyme mix×8=16 μL; 7.5 μL 8 μM 3' IgK second primer×8=45 μL; and 7.5 μL 8 μM 5' IgK second primer×8=45 μL. Thereafter, 3.5 μL of template from each of the first round reactions was added and RT-PCR was performed on a thermal cycler. Kappa chain reactions were performed using the "NEST2K" protocol. Briefly, there was no RT step; hotstart/RT inactivation was at 95° C. for 15 min followed by 50 cycles (denaturation: 94° C. for 30 s; anneal: 45° C. for 30 s; and extension: 72° C. for 55 s). Then, there was a final extension: 72° C. for 10 min.

Heavy chain reactions performed using the "NEST2H" protocol. Briefly, there was no RT step; hotstart/RT inactivation: 95° C. for 15 min, followed by 50 cycles (denaturation: 94° C. for 30 s; anneal: 60° C. for 30 s; and extension: 72° C. for 55 s). Then, there was a final extension: 72° C. for 10 min. The RT-PCR products for both first and second round reactions were run on a gel. Kappa chain results from the first round are shown in FIG. **19**A. Kappa chain results from the second round are shown in FIG. **19**B. Heavy chain results from the first round are shown in FIG. **19**C. Heavy chain results from the second round are shown in FIG. **19**D. The gel products were sequenced by standard procedures known to those skilled in the art. Based on the sequence data generated, variants in antibody sequences were detectable. As a representative example, mutations in the R00C04 sample are shown in Table 2 herein.

TABLE 2

R00C04 (9 non-synonymous mutations)

Position (from IMGT)	Situation (from IMGT)	Germline Ab residue	R00C04 Ab residue
L-36	CDR1-L	S	N
L-92	FR3-L	S	T
H-17	FR1-H	A	D
H-36	CDR1-H	S	R
H-40	FR2-H	H	L
H-64	CDR2-H	N	K
H-65	CDR2-H	T	S
H-83	FR3-H	S	I
H-94	FR3-H	P	L

Example 10. Microfluidic device A microfluidic device has been developed for assaying a binding interaction between a protein produced by a cell and a biomolecule. The device has a chamber having an aperture and a channel for receiving a flowed fluid volume through the chamber via said aperture. The channel provides for size selection for a particle within the fluid volume. Alternately, another embodiment of the microfluidic device has a chamber having an aperture and a reversible trap. The reversible trap has spaced apart structural members extending across the chamber. The structural members are operable to allow a fluid volume to flow through the chamber while providing size selection for a particle within the fluid volume. See, for example: FIG. **20** herein.

Although various embodiments of the invention are disclosed herein, many adaptations and modifications may be made within the scope of the invention in accordance with the common general knowledge of those skilled in this art. Such modifications include the substitution of known equivalents for any aspect of the invention in order to achieve the same result in substantially the same way. Numeric ranges are inclusive of the numbers defining the

range. The word "comprising" is used herein as an open-ended term, substantially equivalent to the phrase "including, but not limited to", and the word "comprises" has a corresponding meaning. As used herein, the singular forms "a", "an" and "the" include plural referents unless the context clearly dictates otherwise. Thus, for example, reference to "a thing" includes more than one such thing. Citation of references herein is not an admission that such references are prior art to the present invention. The invention includes all embodiments and variations substantially as hereinbefore described and with reference to the examples and drawings. Further, citation of references herein is not an admission that such references are prior art to the present invention nor does it constitute any admission as to the contents or date of these documents.

What is claimed is:

1. A method of assaying for a binding interaction between an antibody secreted by a single antibody secreting cell (ASC) and an antigen, the method comprising:

retaining the single ASC within a chamber having a volume of less than 500 pL, a solid wall, and an aperture that defines an opening of the chamber;

incubating the single ASC within the chamber to produce a secreted antibody;

bringing a first fluid volume comprising the antigen in fluid communication with the secreted antibody;

exposing the secreted antibody to a removeable capture substrate, wherein the removeable capture substrate is in fluid communication with the secreted antibody and wherein the removeable capture substrate is operable to bind the secreted antibody;

incubating the secreted antibody with the removeable capture substrate to produce a bound antibody; and

measuring a binding interaction between the secreted antibody and the antigen.

2. The method of claim **1**, wherein the single ASC is a single primary plasma cell.

3. The method of claim **1**, wherein the single ASC is an activated B cell.

4. The method of claim **1**, wherein the antigen is a cell or a cell fragment.

5. The method of claim **1**, wherein the antigen is a virus or a bacterial cell.

6. The method of claim **1**, wherein the antigen is a bacterial antigen or a viral antigen.

7. The method of claim **1**, wherein the antigen is fluorescently labeled.

8. The method of claim **1**, wherein measuring the binding interaction comprises measuring a binding kinetic property between the secreted antibody and the antigen.

9. The method of claim **8**, wherein the binding kinetic property is a K_{on} rate; a K_{off} rate, a dissociation constant, or a combination thereof.

10. The method of claim **1**, wherein measuring the binding interaction comprises measuring the affinity of the secreted antibody and the antigen.

11. The method of claim **1**, wherein measuring the binding interaction comprises measuring the avidity of the secreted antibody and the antigen.

12. The method of claim **1**, wherein the single ASC is maintained in the chamber with the removeable capture substrate.

13. The method of claim **1**, wherein the removeable capture substrate is a microsphere.

14. The method of claim **1**, wherein the removeable capture substrate is a nanosphere.

15. The method of claim **1**, wherein the removeable capture substrate is a polystyrene bead or a silica bead.

16. The method of claim **1**, wherein the removeable capture substrate is a carboxylic acid (COOH) functionalized bead.

17. The method of claim **1**, wherein the removeable capture substrate is an anti-Ig bead.

18. The method of claim **1**, wherein the removeable capture substrate is a Protein A coated bead.

19. The method of claim **1**, wherein the removeable capture substrate is capable of binding the secreted antibody and nucleic acids encoding the secreted antibody.

20. The method of claim **1**, wherein measuring the binding interaction comprises fluorescence imaging of the secreted antibody binding to the antigen.

21. The method of claim **1**, wherein measuring the binding interaction comprises surface plasmon resonance (SPR) spectroscopy, fluorescence anisotropy, interferometry or fluorescence resonance energy transfer (FRET).

22. The method of claim **1**, further comprising performing a reverse transcription polymerase chain reaction (RT-PCR) on nucleic acid encoding the secreted antibody to amplify the heavy and light chain genes of the antibody.

23. The method of claim **1**, wherein the single ASC is obtained from an immunized animal.

24. The method of claim **1**, wherein the chamber is fabricated out of polydimethylsiloxane (PDMS).

25. The method of claim **22**, further comprising sequencing the amplified heavy and light chain genes of the antibody.

26. The method of claim **1**, wherein the aperture serves as the inlet and the outlet of the chamber.

27. The method of claim **7**, wherein the aperture serves as the inlet and the outlet of the chamber.

* * * * *

Exhibit 2

US010775377B1

(12) **United States Patent**
Singhal et al.

(10) **Patent No.: US 10,775,377 B1**
(45) **Date of Patent: *Sep. 15, 2020**

(54) **METHODS FOR ASSAYING CELLULAR BINDING INTERACTIONS**

(71) Applicant: **The University of British Columbia**, Vancouver (CA)

(72) Inventors: **Anupam Singhal**, Mississauga (CA); **Carl L. G. Hansen**, Vancouver (CA); **John W. Schrader**, Vancouver (CA); **Charles A. Haynes**, Vancouver (CA); **Daniel J. Da Costa**, Pitt Meadows (CA)

(73) Assignee: **The University of British Columbia**, Vancouver (CA)

(*) Notice: Subject to any disclaimer, the term of this patent is extended or adjusted under 35 U.S.C. 154(b) by 0 days.

This patent is subject to a terminal disclaimer.

(21) Appl. No.: **16/912,288**

(22) Filed: **Jun. 25, 2020**

Related U.S. Application Data

(63) Continuation of application No. 16/746,540, filed on Jan. 17, 2020, which is a continuation of application
(Continued)

(51) **Int. Cl.**
B01L 3/00 (2006.01)
G01N 33/569 (2006.01)
(Continued)

(52) **U.S. Cl.**
CPC .. ***G01N 33/56966*** (2013.01); ***B01L 3/502738*** (2013.01); ***B01L 3/502761*** (2013.01);
(Continued)

(58) **Field of Classification Search**
None
See application file for complete search history.

(56) **References Cited**

U.S. PATENT DOCUMENTS

5,874,085 A 2/1999 Mond et al.
6,007,690 A 12/1999 Nelson et al.
(Continued)

FOREIGN PATENT DOCUMENTS

WO 2003085379 A3 12/2003
WO 2005069980 A2 8/2005
(Continued)

OTHER PUBLICATIONS

Abdiche et al. (2008) "Determining kinetics and affinities of protein interactions using a parallel real-time label-free biosensor, the Octet" Analytical Biochemistry 377(2):209-217.
(Continued)

Primary Examiner — Rebecca M Giere
(74) *Attorney, Agent, or Firm* — Potomac Law Group, PLLC

(57) **ABSTRACT**

There are provided methods, and devices for assaying for a binding interaction between a protein, such as a monoclonal antibody, produced by a cell, and a biomolecule. The method may include retaining the cell within a chamber having an aperture; exposing the protein produced by the cell to a capture substrate, wherein the capture substrate is in fluid communication with the protein produced by the cell and wherein the capture substrate is operable to bind the protein produced by the cell; flowing a fluid volume comprising the biomolecule through the chamber via said aperture, wherein the fluid volume is in fluid communication with the capture substrate; and determining a binding interaction between the protein produced by the cell and the biomolecule.

30 Claims, 29 Drawing Sheets

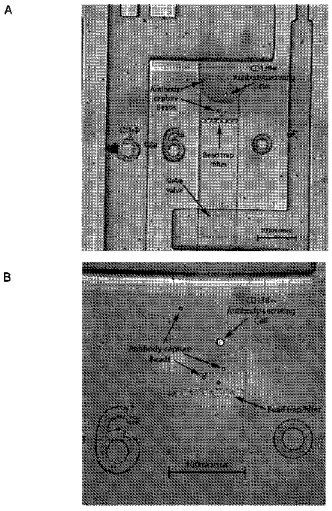

Related U.S. Application Data

No. 16/579,561, filed on Sep. 23, 2019, now Pat. No. 10,578,618, which is a continuation of application No. 16/290,751, filed on Mar. 1, 2019, now Pat. No. 10,466,241, which is a continuation of application No. 16/129,555, filed on Sep. 12, 2018, now Pat. No. 10,274,494, which is a continuation of application No. 14/879,791, filed on Oct. 9, 2015, now Pat. No. 10,107,812, which is a continuation of application No. 13/184,363, filed on Jul. 15, 2011, now Pat. No. 9,188,593.

(60) Provisional application No. 61/365,237, filed on Jul. 16, 2010.

(51) **Int. Cl.**

G01N 33/68	(2006.01)
G01N 33/577	(2006.01)
G01N 33/58	(2006.01)

(52) **U.S. Cl.**

CPC ***G01N 33/577*** (2013.01); ***G01N 33/582*** (2013.01); ***G01N 33/6854*** (2013.01); *B01L 2200/0668* (2013.01); *B01L 2300/0681* (2013.01); *B01L 2300/0861* (2013.01); *B01L 2300/0864* (2013.01); *B01L 2300/0867* (2013.01); *B01L 2400/0481* (2013.01)

(56) **References Cited**

U.S. PATENT DOCUMENTS

7,143,785	B2	12/2006	Maerkl et al.
8,124,015	B2	2/2012	Diercks et al.
9,188,593	B2	11/2015	Singhal et al.
10,107,812	B2	10/2018	Singhal et al.
10,274,494	B2	4/2019	Singhal et al.
10,466,241	B2	11/2019	Singhal et al.
10,578,618	B2	3/2020	Singhal et al.
2002/0164656	A1	11/2002	Hoeffler et al.
2009/0068170	A1	3/2009	Weitz et al.
2010/0086919	A1	4/2010	McKeon
2011/0262906	A1	10/2011	Dimov et al.
2011/0294678	A1	12/2011	Jin et al.
2013/0130301	A1	5/2013	Yoon et al.

FOREIGN PATENT DOCUMENTS

WO	2009012340 A2	1/2009
WO	2010046775 A2	4/2010
WO	2012162779 A1	12/2012

OTHER PUBLICATIONS

Babcook et al. (1996) "A novel strategy for generating monoclonal antibodies from single, isolated lymphocytes producing antibodies of defined specificities" Proc. Natl. Acad. Sci. USA 93(15):7843-7848.

Bates & Quake (2009) "Highly parallel measurements of interaction kinetic constants with a microfabricated optomechanical device" Appl. Phys. Lett. 95(7):73705.

Batista & Neuberger (1998) "Affinity dependence of the B cell response to antigen: a threshold, a ceiling, and the importance of off-rate" Immunity 8(6):751-759.

Biacore Life Sciences—Biacore 3000 System Information. (2012). Website: http://www,biacore.com/lifesciences/products/systems_overview/3000/system_information/index.html.

Biacore Life Sciences—Single-Cycle Kinetics. (2012). Website: https://www.biacore.com/lifesciences/technology/introduction/data_interaction/SCK/index.html.

Bornhop et al. (2007) "Free-solution, label-free molecular interactions studied by back- scattering interferometry" Science 317(5845):1732-1736.

Cai et al. (2006) "Stochastic protein expression in individual cells at the single molecule leve" Nature 440(7082):358-362.

Dlugosz et al. (2009) "pH-dependent association of proteins. The test case of monoclonal antibody HyHEL-5 and its antigen hen egg white lysozyme" The Journal of Physical Chemistry 113(47):15662-15669.

England et al. (1999) "Functional characterization of the somatic hypermutation process leading to antibody D1.3, a high affinity antibody directed against lysozyme" J. Immunol. 162(4):2129-2136.

Hansen et al. (2002) "A robust and scalable microfluidic metering method that allows protein crystal growth by free interface diffusion" Proc. Natl. Acad. Sci. USA 99(26):16531-16536.

Hansen et al. (2004) "Systematic investigation of protein phase behavior with a microfluidic formulator" Proc. Natl. Acad. Sci. USA 101(40):14431-14436.

He & Niemeyer (2003) "A novel correlation for protein diffusion coefficients based on molecular weight and radius of gyration" Biotechnol. Prog. 19(2):544-548.

Homola et al. (1999) "Surface plasmon resonance sensors: review" Sensors and Actuators B: Chemical 54:3-15.

Huang et al. (2007) "Counting low-copy number proteins in a single cell" Science 315(5808):81-84.

Ito et al. (1995) "Mutations in the complementarity-determining regions do not cause differences in free energy during the process of formation of the activated complex between an antibody and the corresponding protein antigen" J. Mol. Biol. 248(4):729-732.

Jerne (1984) "The generative grammar of the immune system" EMBO J. 4(4):847-852.

Jin et al. (2009) "A rapid and efficient single-cell manipulation method for screening antigen- specific antibody-secreting cells from human peripheral blood" Nat. Med.15(9):1088-1092.

Karpas et al. (2001) "A human myeloma cell line suitable for the generation of human monoclonal antibodies" Proc. Natl. Acad. Sci. USA 98(4):1799-1804.

Kohler & Milstein (1975) "Continuous cultures of fused cells secreting antibody of predefined specificity" Nature 256(5517):495-497.

Lanzavecchia et al. (2007) "Human monoclonal antibodies by immortalization of memory B cells" Current Opinion in Biotechnology 18(6):523-528.

Lecault et al. (2011) "High-Throughput Analysis of Single Hematopoietic Stem Cell Proliferation in Microfluidic Cell Culture Arrays" Nat Methods 8(7):581-586.

Lee et al. (2009) "High-sensitivity microfluidic calorimeters for biological and chemical applications" Proc. Natl. Acad. Sci. USA 106(36):15225-15230.

Maerkl & Quake (2007) "A systems approach to measuring the binding energy landscapes of transcription factors" Science 315(5809):233-237.

Marcus et al. (2006) "Microfluidic single-cell mRNA isolation and analysis" Anal. Chem. 78(9):3084-3089.

McDonald et al. (2000) "Fabrication of microfluidic systems in poly(dimethylsiloxane)" Electrophoresis 21: 27-40.

McKinney et al. (1995) "Optimizing antibody production in batch hybridoma cell culture" J.Biotechnol. 40(1):31-48.

Pasqualini & Arap (2004) "Hybridoma-free generation of monoclonal antibodies" Proc. Natl. Acad. Sci. USA 101(1):257-259.

Poulson et al. (2007) "Kinetic, affinity, and diversity limits of human polyclonal antibody responses against tetanus toxoid" J. Immunol. 179(6):3841-3850.

Raschke et al. (2003) "Biomolecular Recognition Based on Single Gold Nanoparticle Light Scattering" Nano Letters 3(7):935-938.

Sonnichsen et al. (2000) "Spectroscopy of single metallic nanoparticles using total internal reflection microscopy" App. Phys. Letters 77(19): 2949-2951.

Spieker-Polet et al. (1995) "Rabbit monoclonal antibodies: generating a fusion partner to produce rabbit-rabbit hybridomas" Proc. Natl. Acad. Sci. USA 92(20):9348-9352.

Squires & Quake (2005) "Microfluidics: Fluid physics at the nanoliter scale" Reviews of Modern Physics 77(3):977-1026.

(56) **References Cited**

OTHER PUBLICATIONS

Story et al. (2008) "Profiling antibody responses by multiparametric analysis of primary B cells" Proc. Natl. Acad. Sci. U.S.A. 105(46):17902-17907.
Thorsen et al. (2002) "Microfluidic large-scale integration" Science 298(5593):580-584.
Tiller et al. (2009) "Cloning and expression of murine Ig genes from single B cells" J. Immunol. Methods 350(1-2):183-193.
Traggiai et al. (2004) "An efficient method to make human monoclonal antibodies from memory B cells: potent neutralization of SARS coronavirus" Nat Med 10(8):871-875.
Tyn & Gusek (1990) "Prediction of diffusion coefficients of proteins" Biotechnol. Bioeng. 35(4):327-338.
Ueno et al. (2010) "Simple dark-field microscopy with nanometer spatial precision and microsecond temporal resolution" Biophysical J. 98(9):2014-2023.
Unger et al. (2000) "Monolithic microfabricated valves and pumps by multilayer soft lithography" Science 288(5463):113-116.
Wang et al. (2005) "Label-free detection of small-molecule-protein interactions by using nanowire nanosensors" Proc. Natl. Acad. Sci. USA 102(9):3208-3212.
Xavier & Willson (1998) "Association and dissociation kinetics of anti-hen egg lysozyme monoclonal antibodies HyHEL-5 and HyHEL-10" Biophys. J. 74(4):2036-2045.

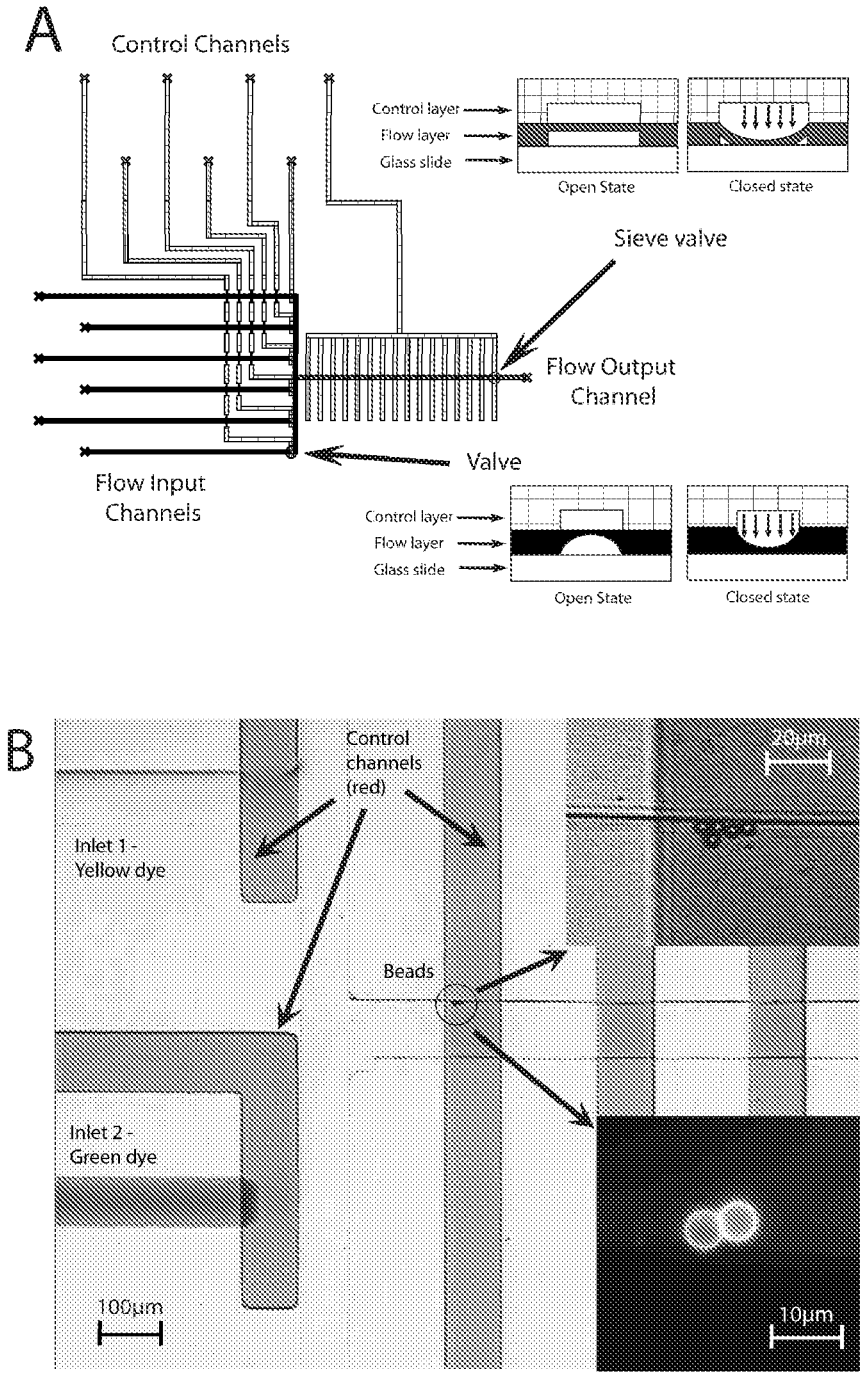
A
Control Channels
Control layer
Flow layer
Glass slide
Open State
Closed state
Sieve valve
Flow Output Channel
Valve
Flow Input Channels
Control layer
Flow layer
Glass slide
Open State
Closed state
B
Control channels (red)
20μm
Inlet 1 - Yellow dye
Beads
Inlet 2 - Green dye
100μm
10μm

Figure 1

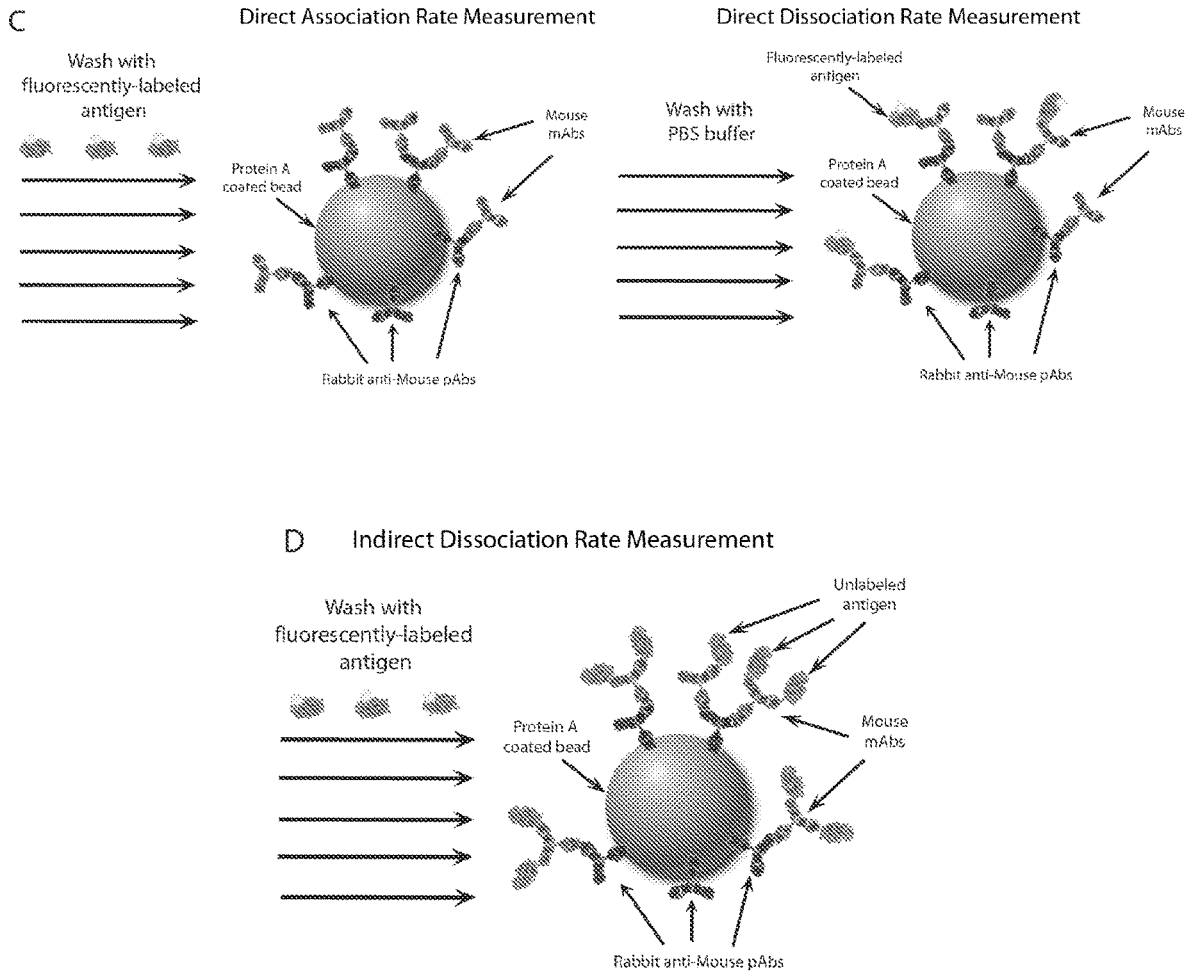

Figure 1 cont'd

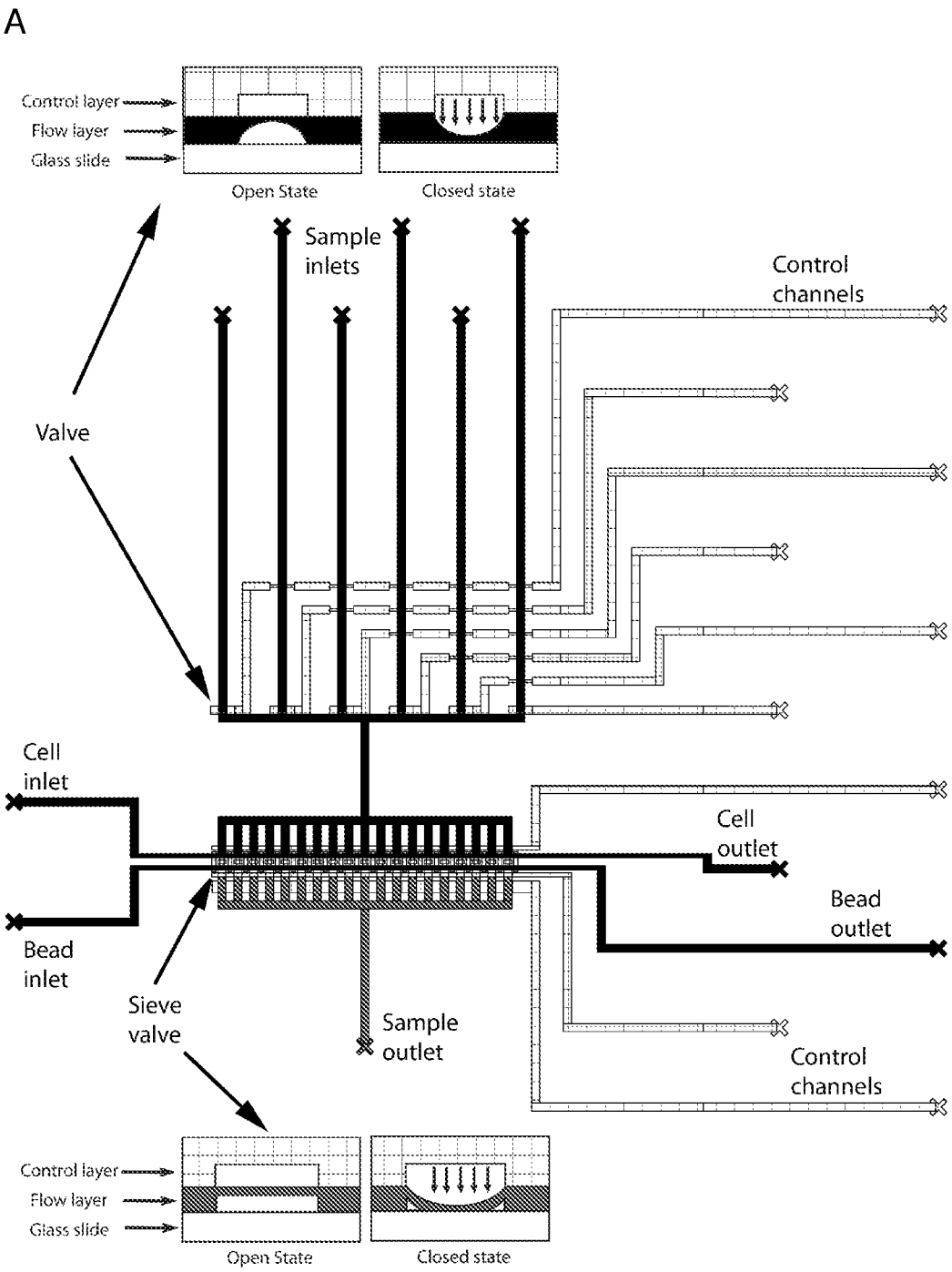
A
Control layer
Flow layer
Glass slide
Open State
Closed state
Sample inlets
Control channels
Valve
Cell inlet
Cell outlet
Bead outlet
Bead inlet
Sieve valve
Sample outlet
Control channels
Control layer
Flow layer
Glass slide
Open State
Closed state

Figure 2

B

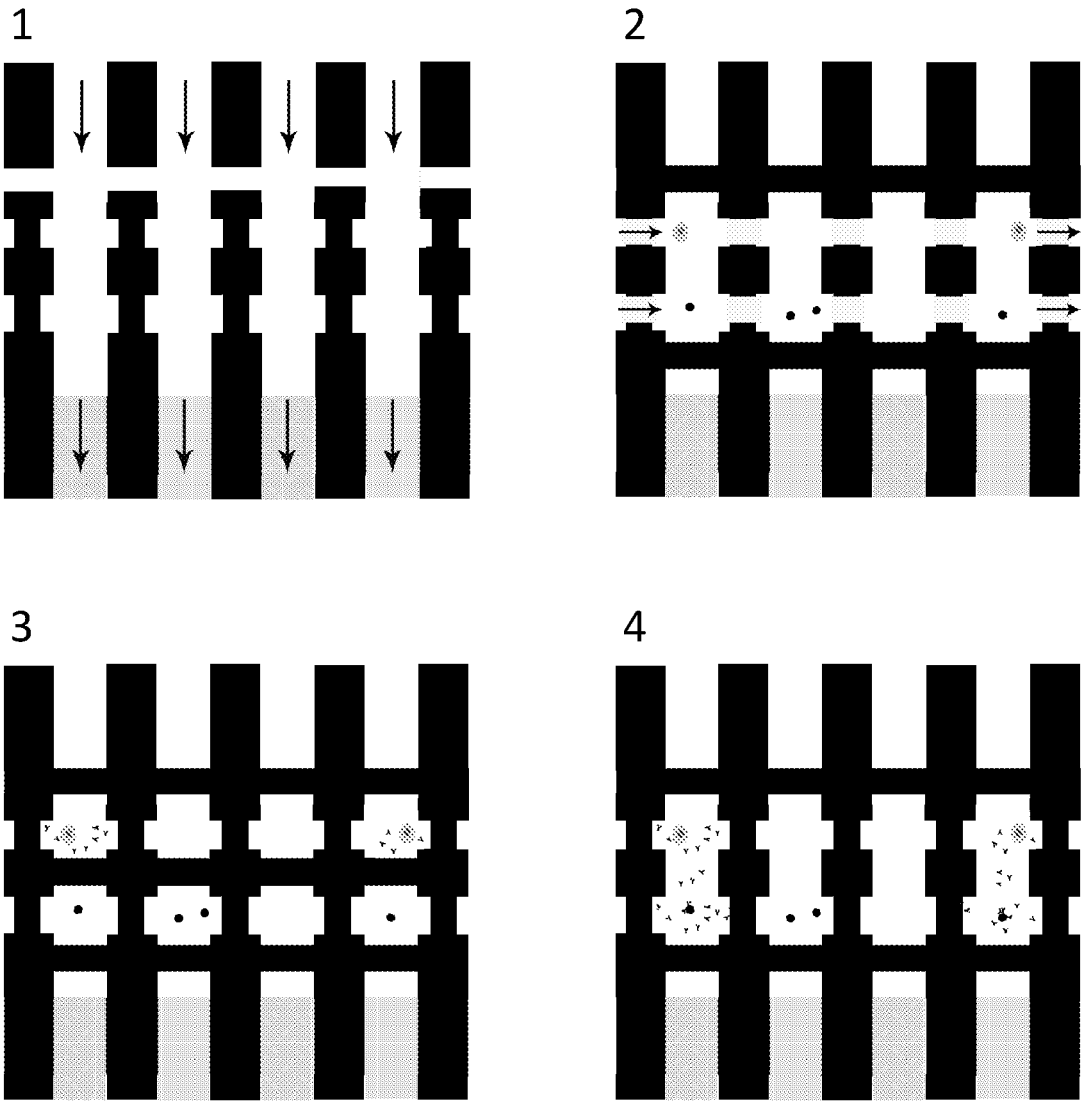

Figure 2 cont'd

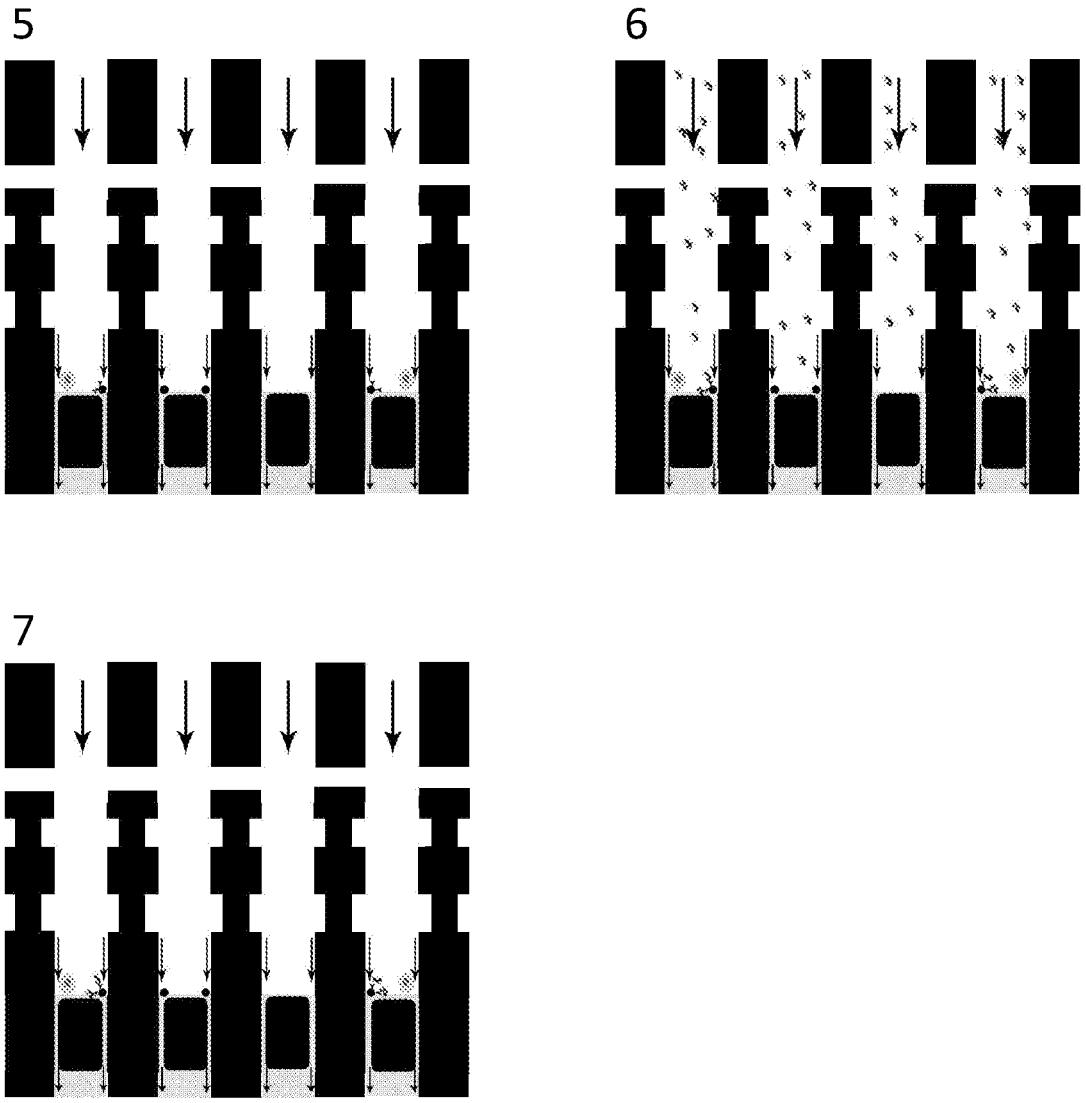

Figure 2 cont'd

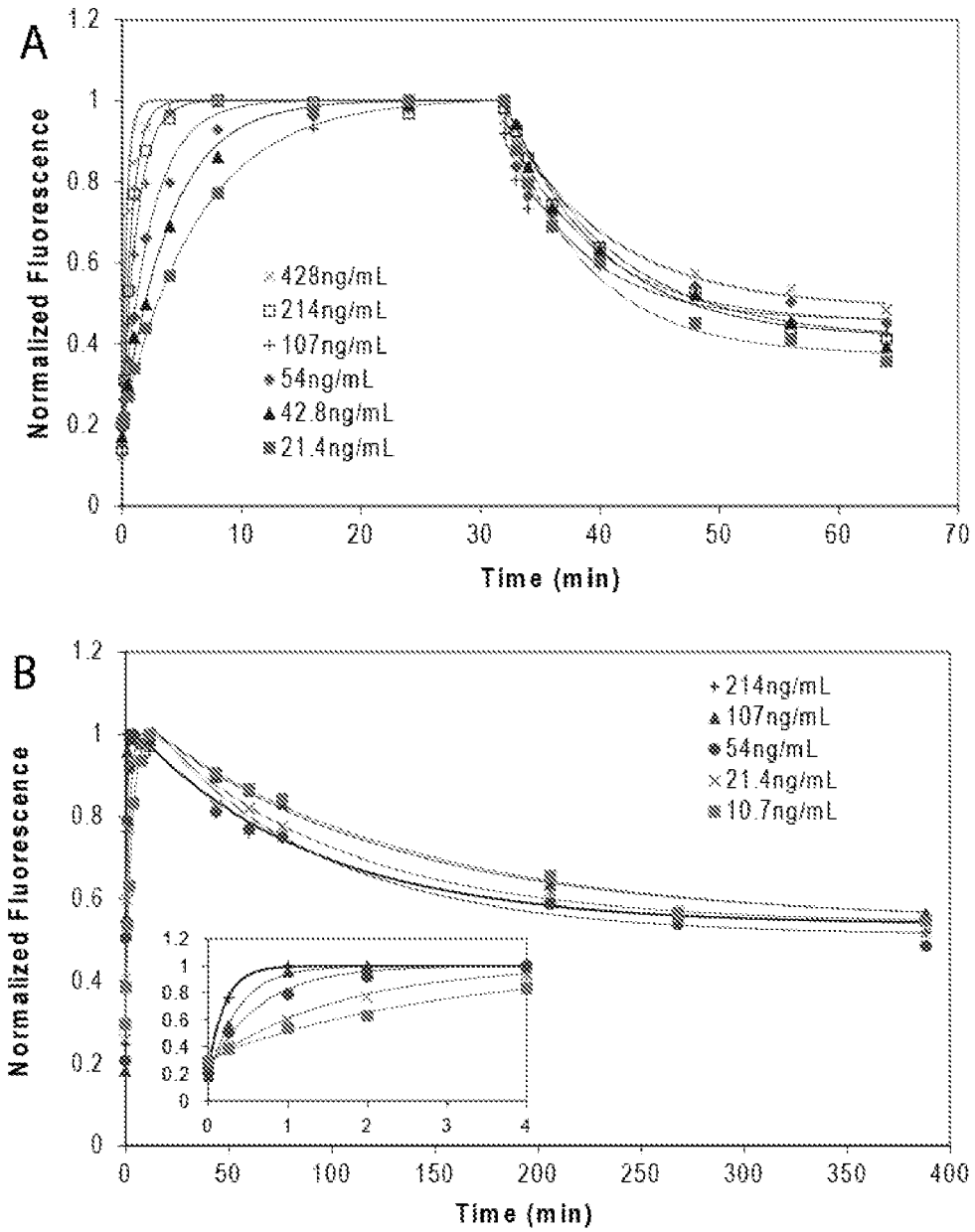
A
Normalized Fluorescence
Time (min)
428ng/mL
214ng/mL
107ng/mL
54ng/mL
42.8ng/mL
21.4ng/mL
B
Normalized Fluorescence
Time (min)
214ng/mL
107ng/mL
54ng/mL
21.4ng/mL
10.7ng/mL

Figure 3

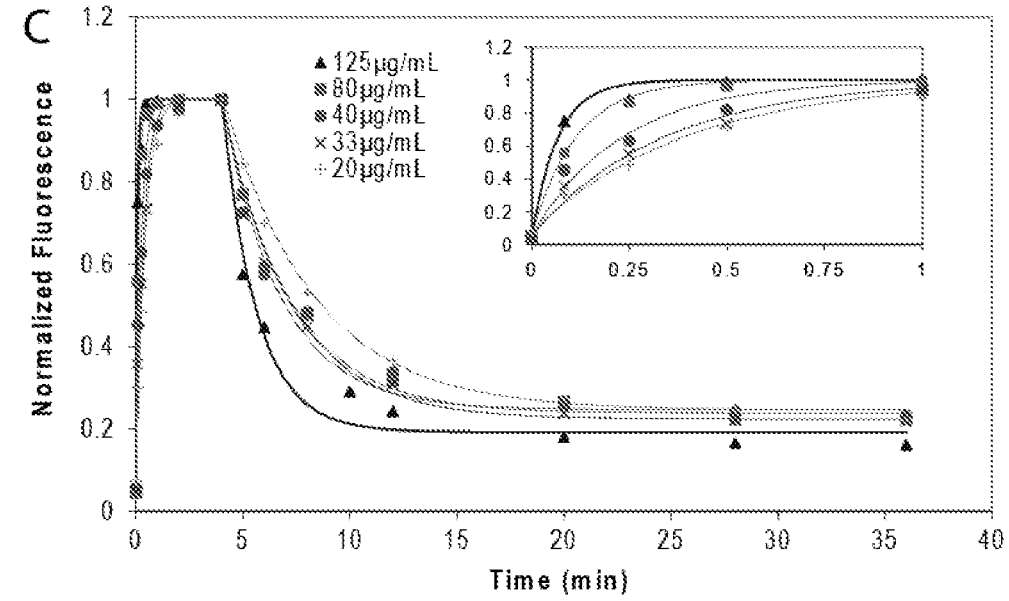

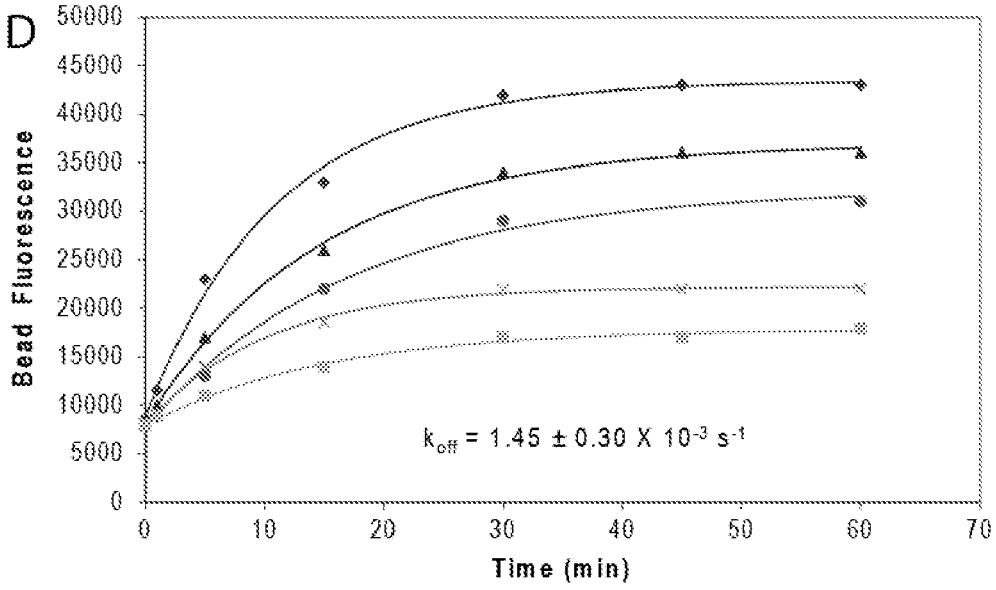

Figure 3 cont'd

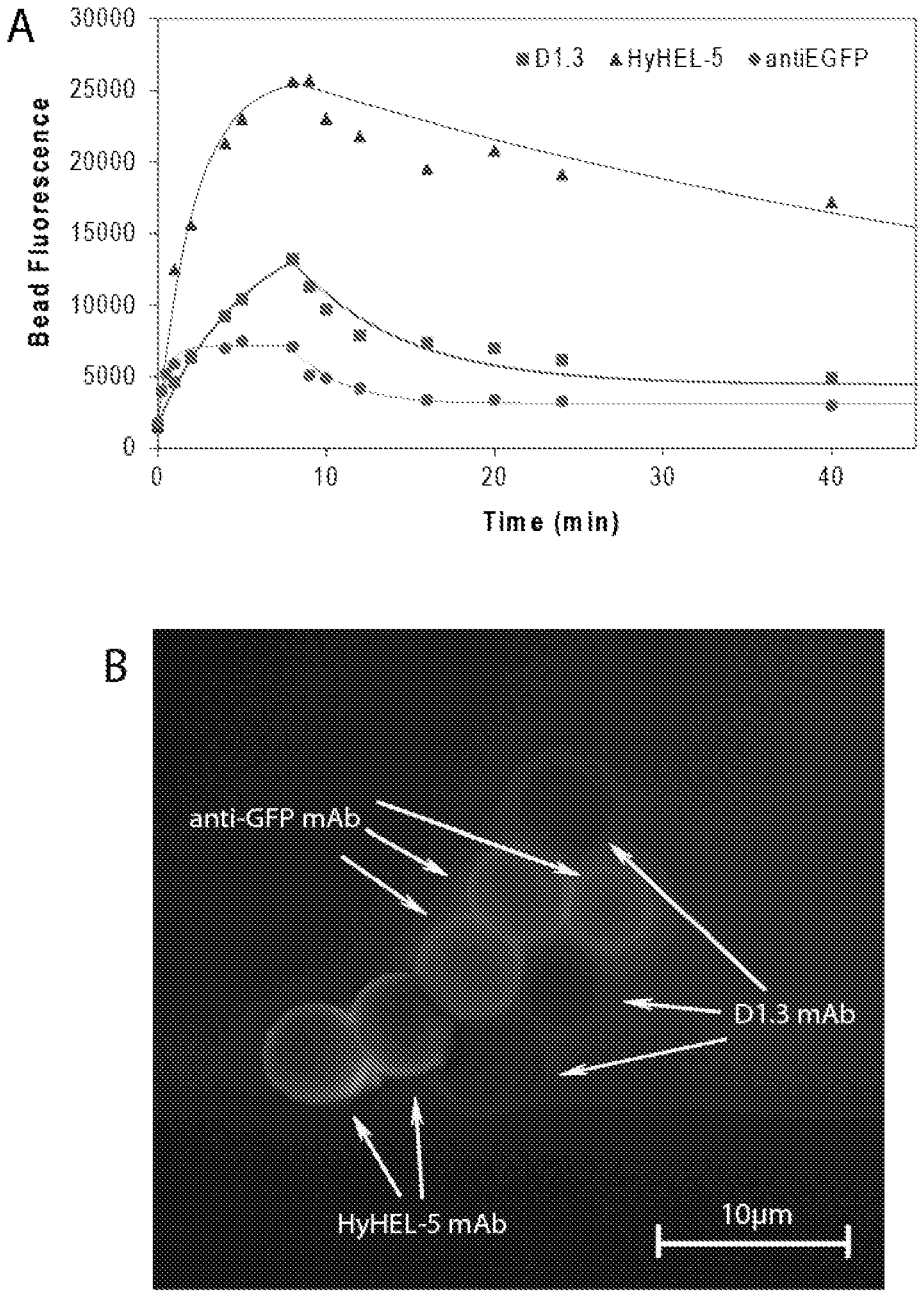
A
30000
25000
20000
15000
10000
5000
0
Bead Fluorescence
D1.3
HyHEL-5
antiEGFP
0
10
20
30
40
Time (min)
B
anti-GFP mAb
D1.3 mAb
HyHEL-5 mAb
10μm

Figure 4

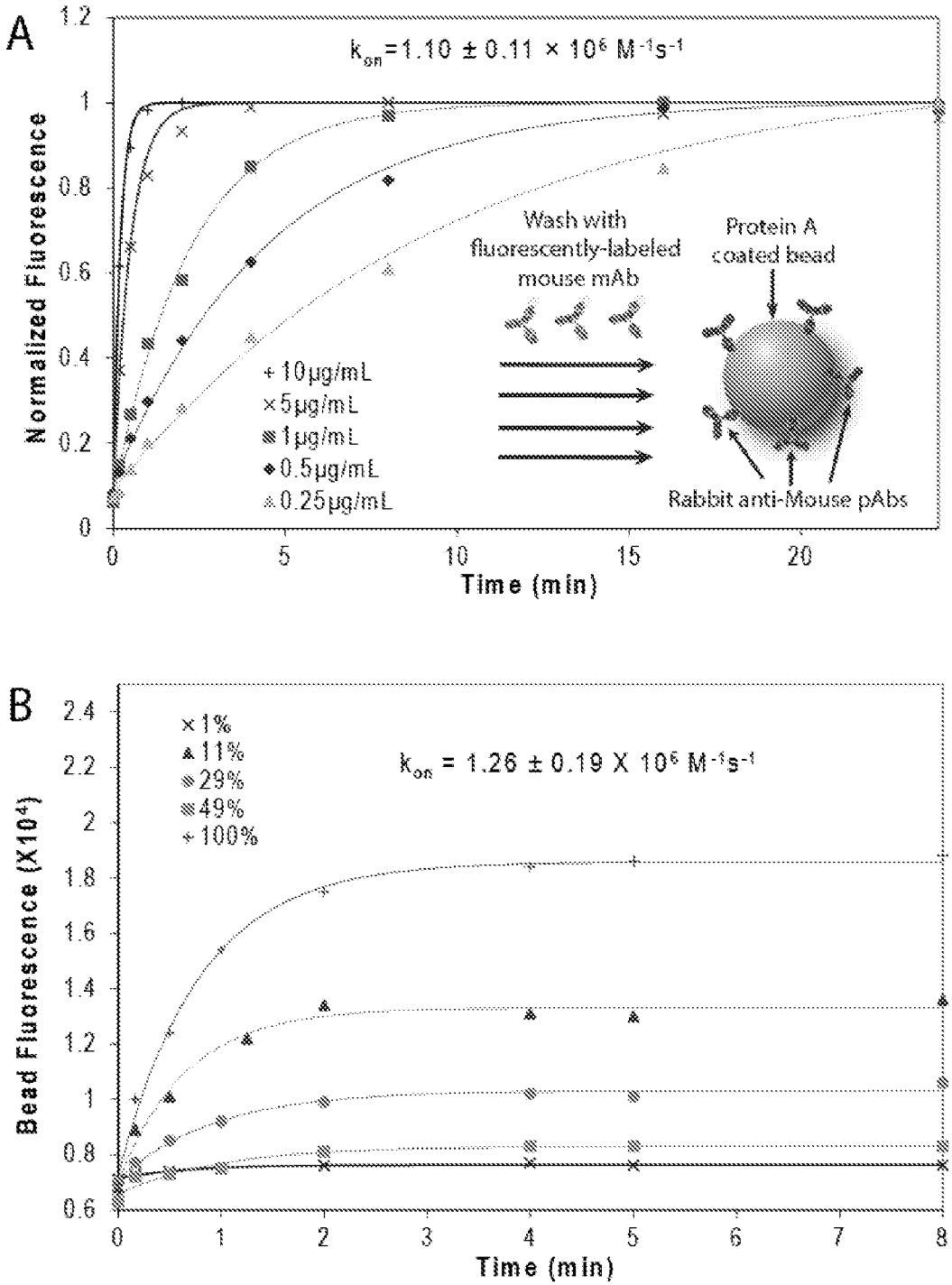
A
k_{on}=1.10 ± 0.11 × 10^6 $M^{-1}s^{-1}$
Normalized Fluorescence
Time (min)
+10μg/mL
×5μg/mL
1μg/mL
0.5μg/mL
0.25μg/mL
Wash with fluorescently-labeled mouse mAb
Protein A coated bead
Rabbit anti-Mouse pAbs
B
×1%
11%
29%
49%
+100%
k_{on} = 1.26 ± 0.19 X 10^6 $M^{-1}s^{-1}$
Bead Fluorescence (X10^4)
Time (min)

Figure 5

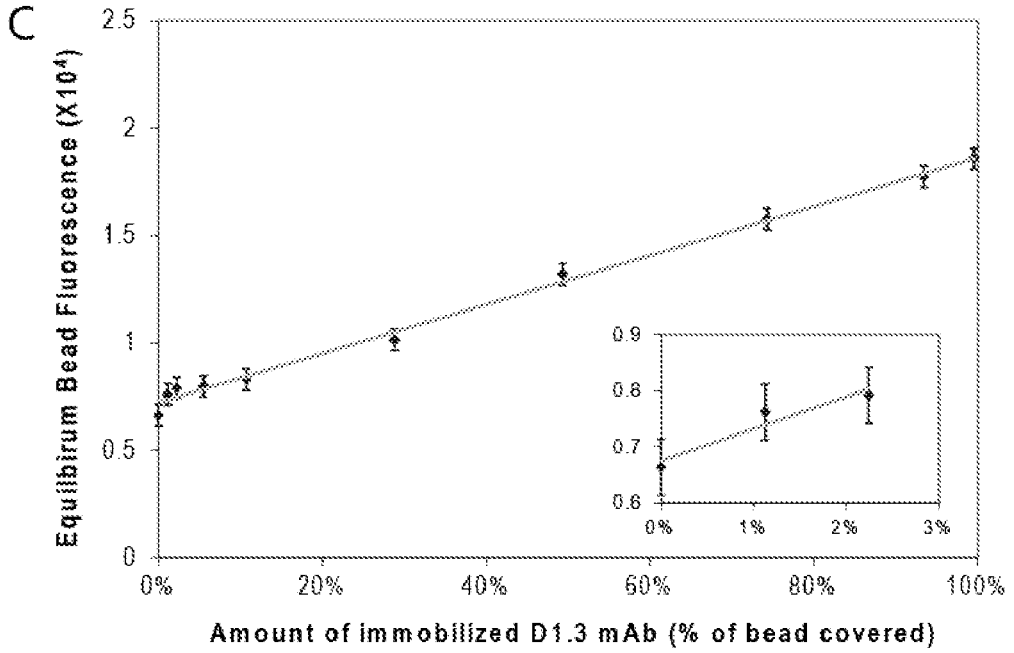

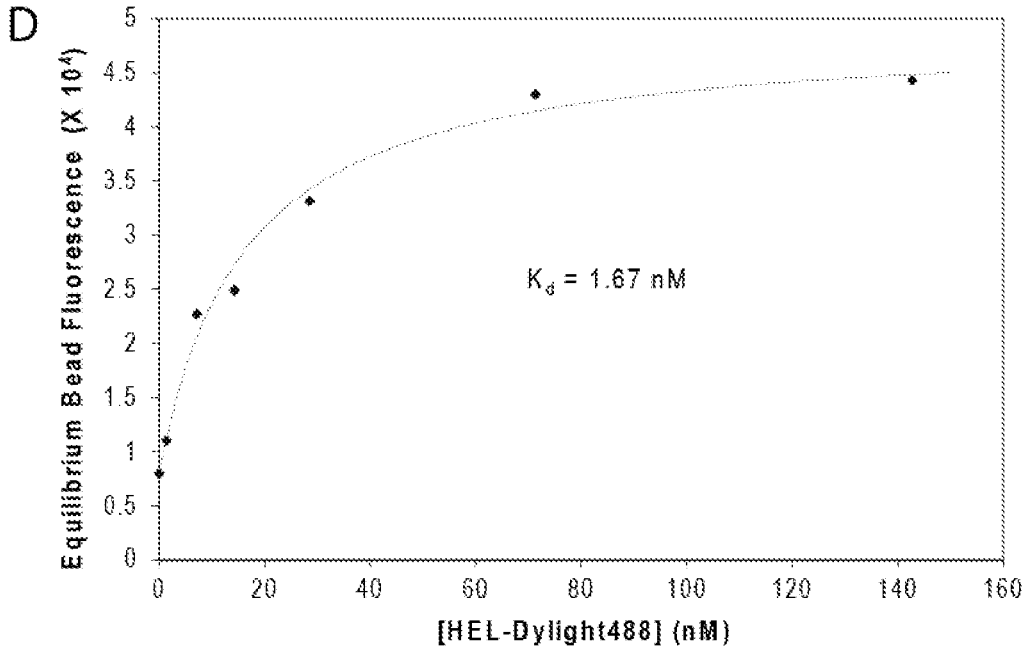

Figure 5 cont'd

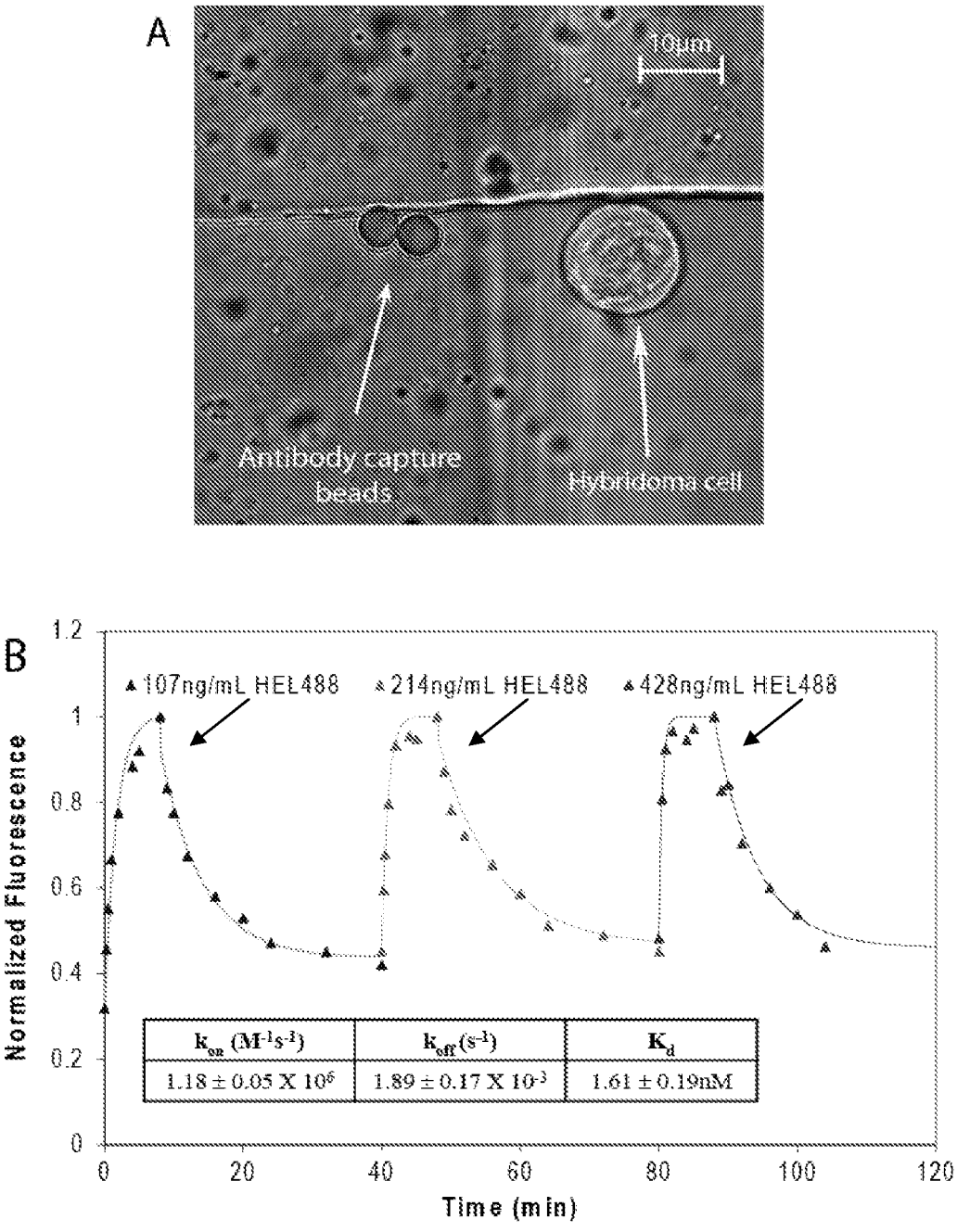
A
10μm
Antibody capture beads
Hybridoma cell
B
107ng/mL HEL488
214ng/mL HEL488
428ng/mL HEL488
Normalized Fluorescence
Time (min)
0
0.2
0.4
0.6
0.8
1
1.2
0
20
40
60
80
100
120
k_{on} ($M^{-1}s^{-1}$)
k_{off} (s^{-1})
K_d
1.18 ± 0.05 X 10^6
1.89 ± 0.17 X 10^{-3}
1.61 ± 0.19nM

Figure 6

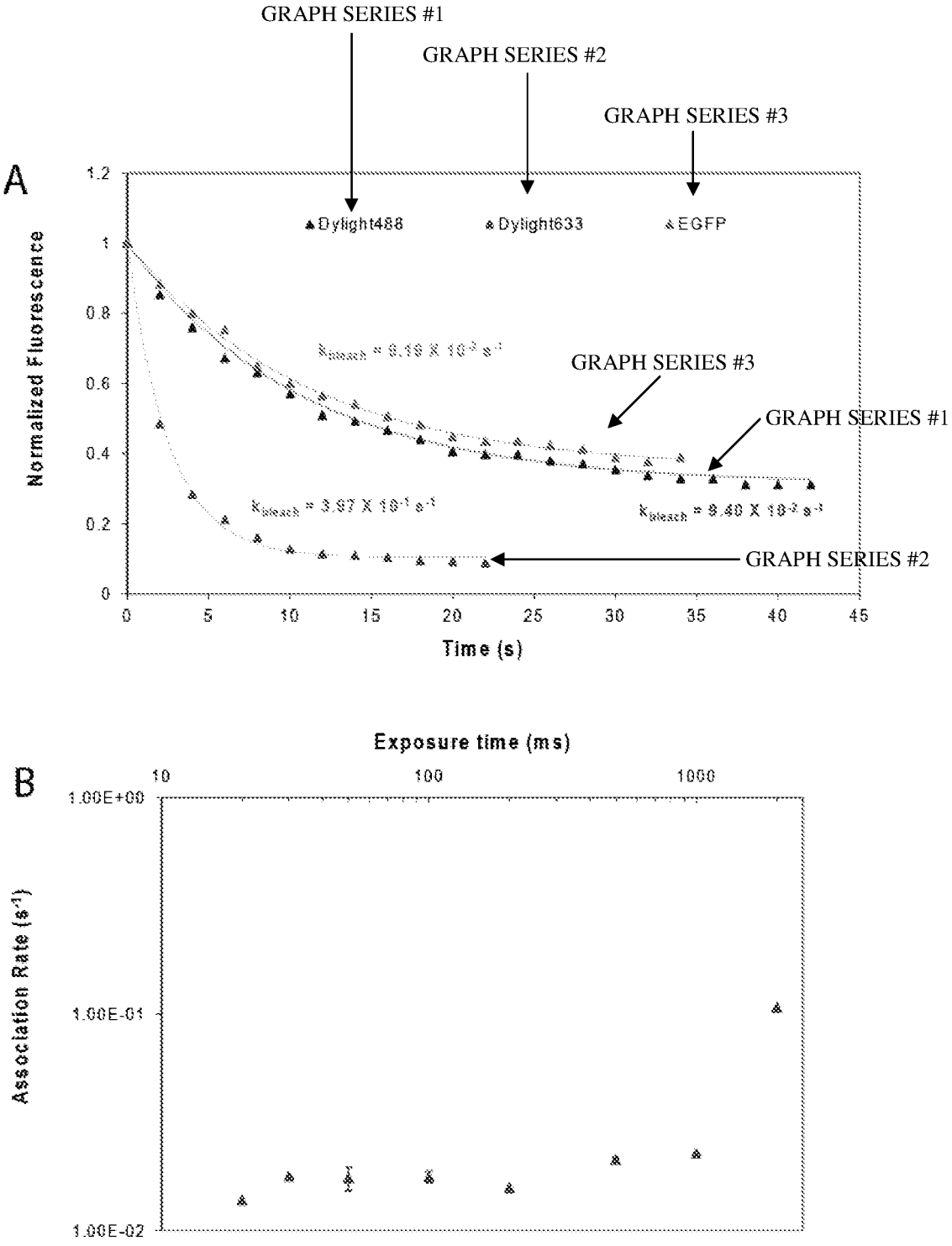
A
GRAPH SERIES #1
GRAPH SERIES #2
GRAPH SERIES #3
Dylight488
Dylight633
EGFP
Normalized Fluorescence
Time (s)
GRAPH SERIES #3
GRAPH SERIES #1
GRAPH SERIES #2
B
Exposure time (ms)
Association Rate (s-1)

Figure 7

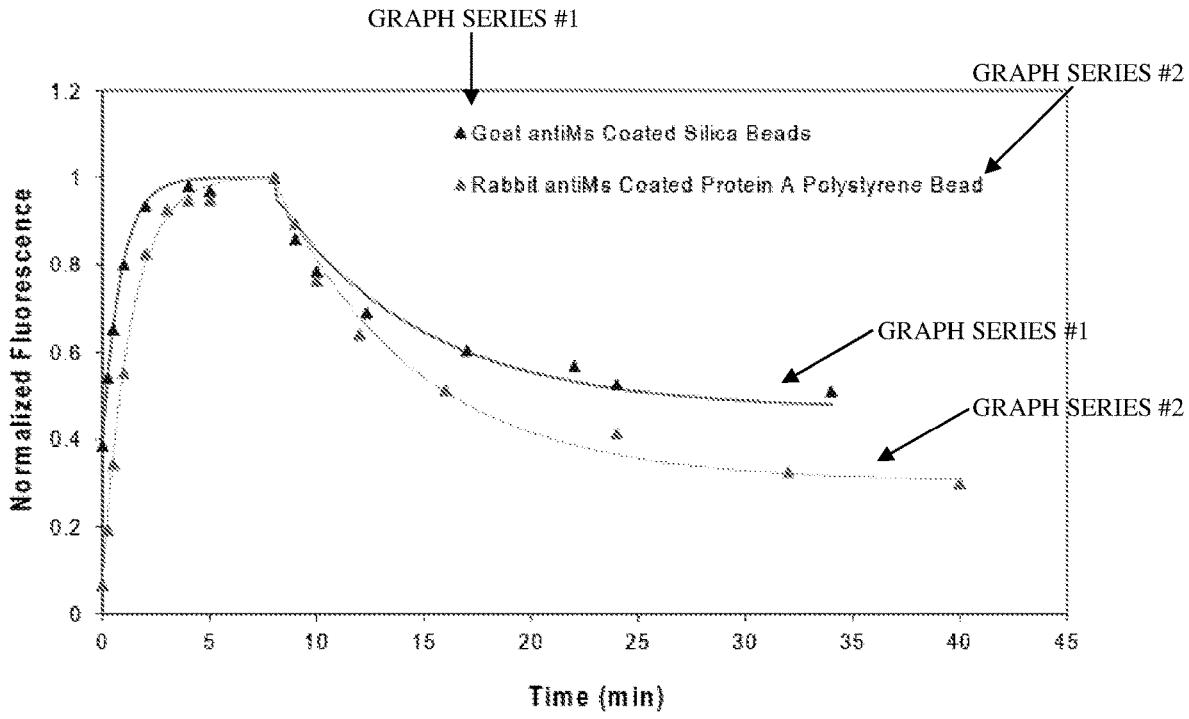
GRAPH SERIES #1
GRAPH SERIES #2
Goat antiMs Coated Silica Beads
Rabbit antiMs Coated Protein A Polystyrene Bead
GRAPH SERIES #1
GRAPH SERIES #2
Normalized Fluorescence
Time (min)
0
0.2
0.4
0.6
0.8
1
1.2
0
5
10
15
20
25
30
35
40
45

Figure 8

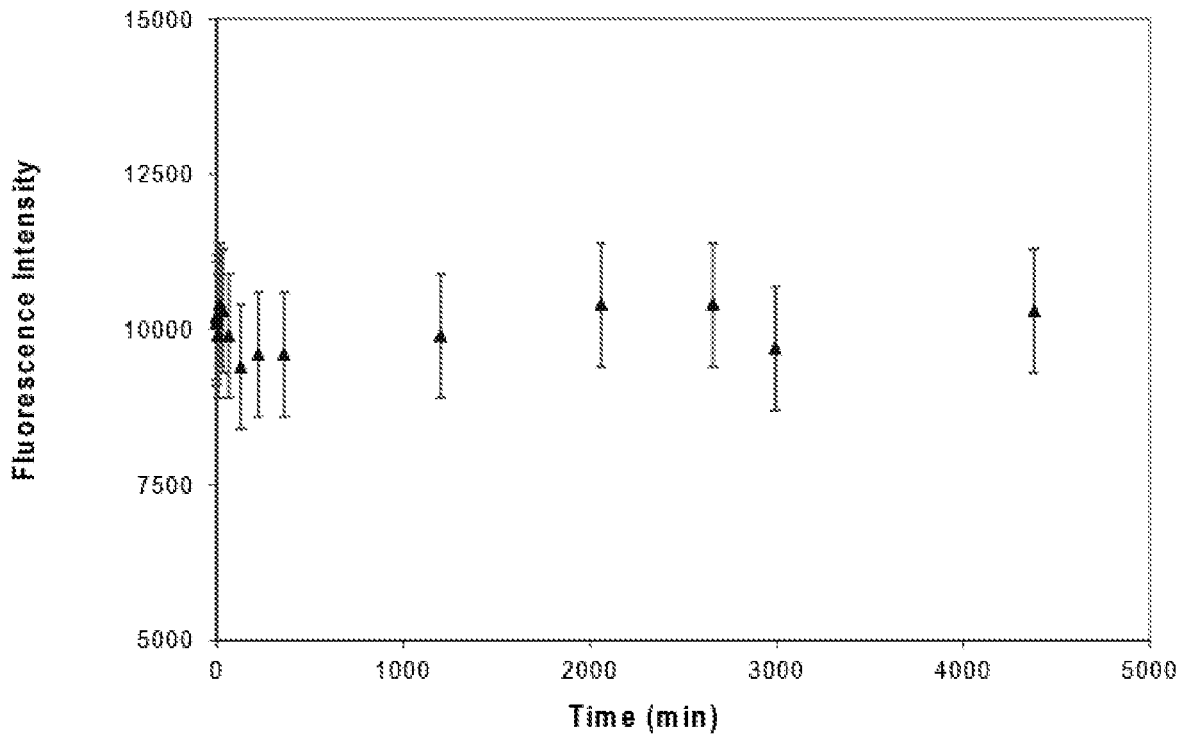
15000
12500
10000
7500
5000
Fluorescence Intensity
0
1000
2000
3000
4000
5000
Time (min)

Figure 9

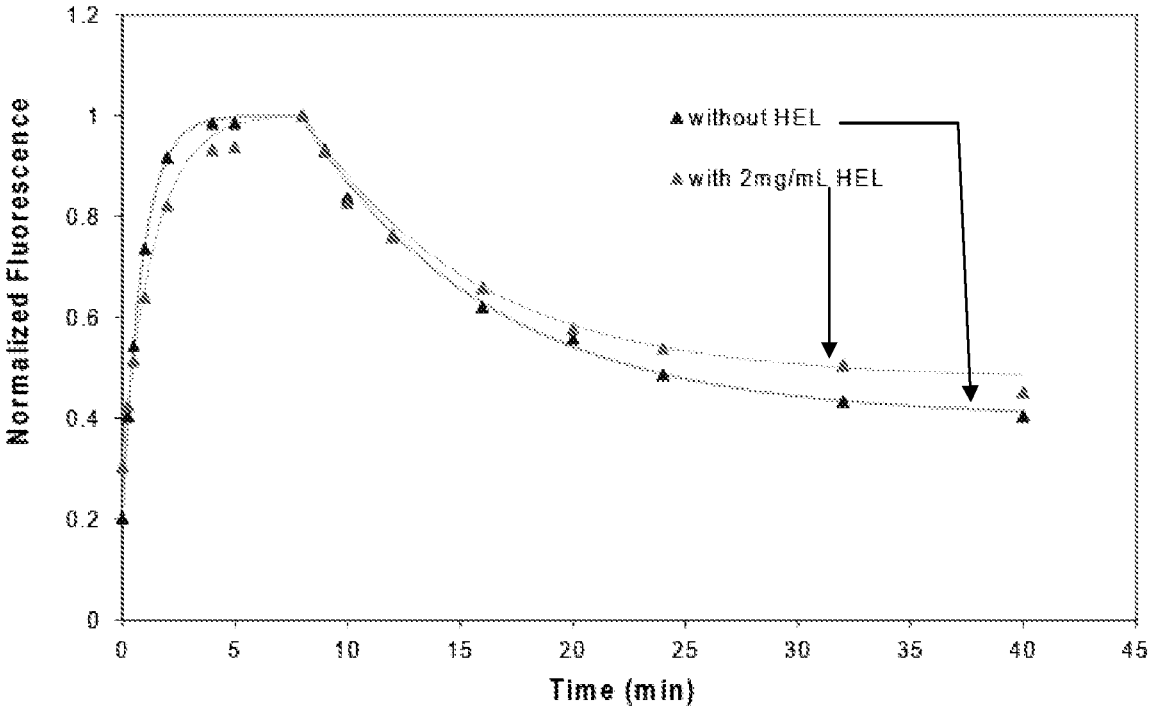
Normalized Fluorescence
Time (min)
without HEL
with 2mg/mL HEL
0
0.2
0.4
0.6
0.8
1
1.2
0
5
10
15
20
25
30
35
40
45

Figure 10

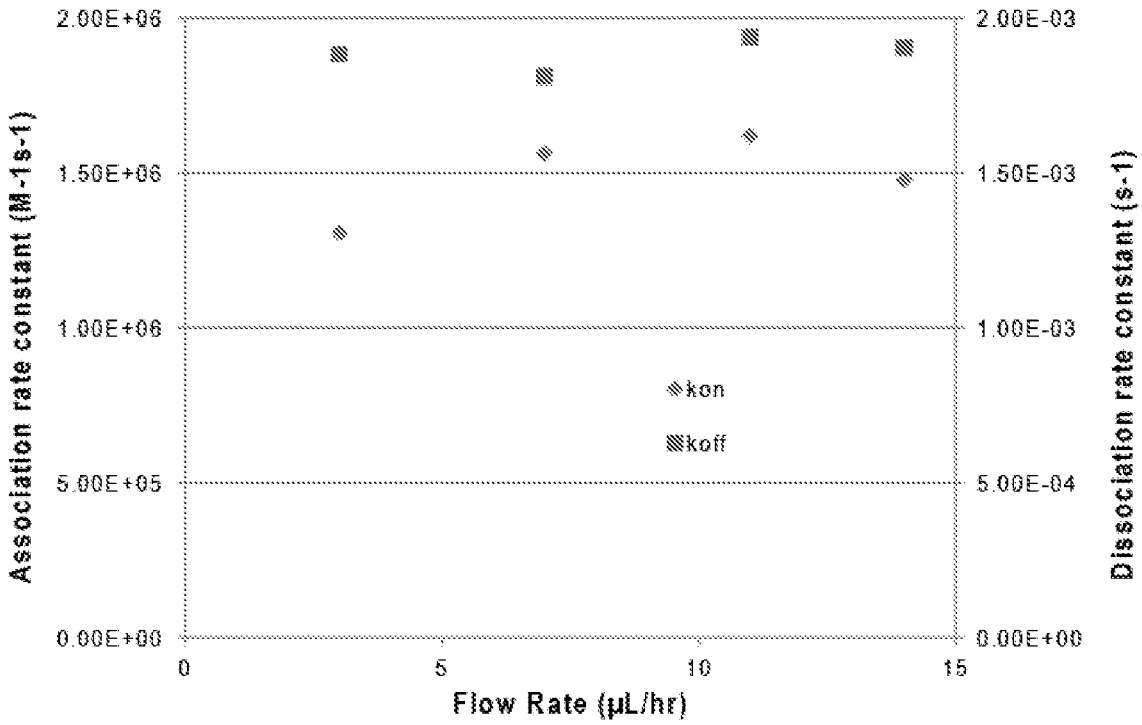
2.00E+06
1.50E+06
1.00E+06
5.00E+05
0.00E+00
Association rate constant (M-1s-1)
2.00E-03
1.50E-03
1.00E-03
5.00E-04
0.00E+00
Dissociation rate constant (s-1)
kon
koff
0
5
10
15
Flow Rate (µL/hr)

Figure 11

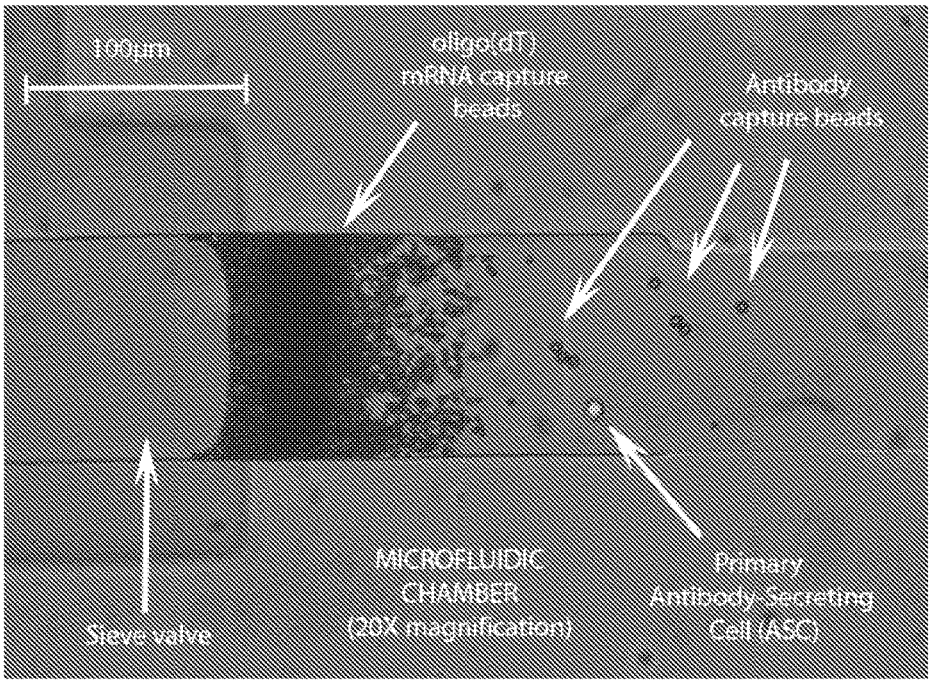
100µm
oligo(dT) mRNA capture beads
Antibody capture beads
MICROFLUIDIC CHAMBER (20X magnification)
Sieve valve
Primary Antibody-Secreting Cell (ASC)

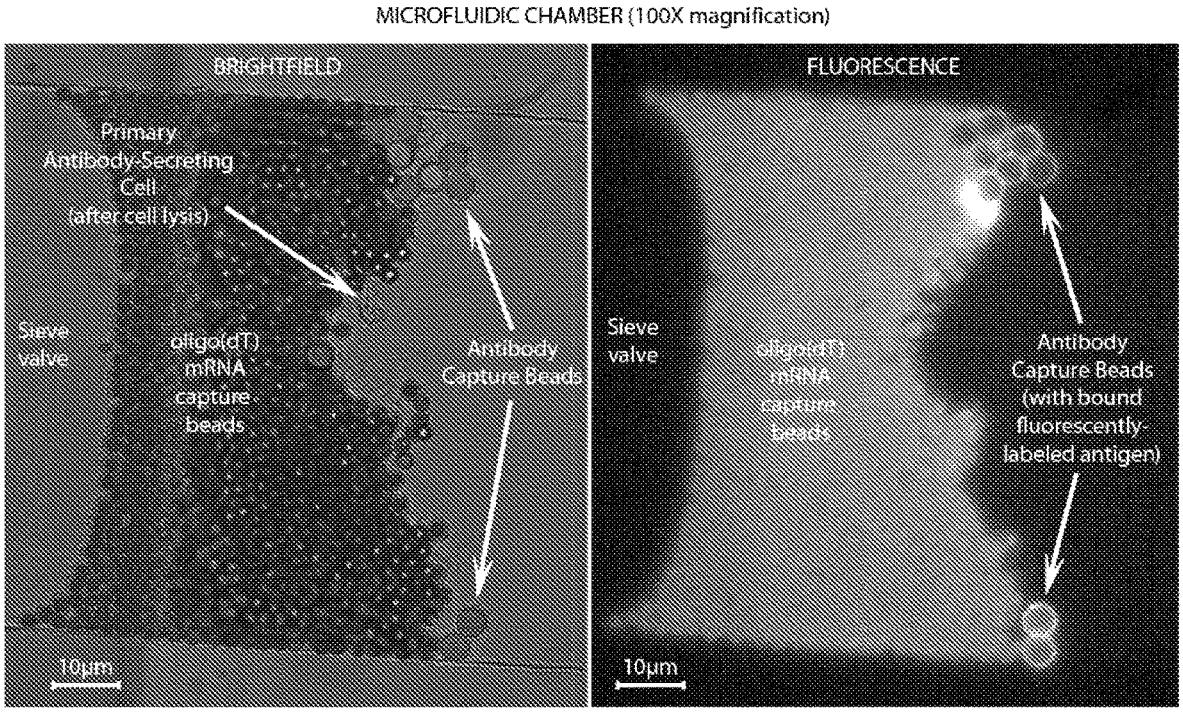
MICROFLUIDIC CHAMBER (100X magnification)
BRIGHTFIELD
Primary Antibody-Secreting Cell (after cell lysis)
Sieve valve
oligo(dT) mRNA capture beads
Antibody Capture Beads
10µm
FLUORESCENCE
Sieve valve
oligo(dT) mRNA capture beads
Antibody Capture Beads (with bound fluorescently-labeled antigen)
10µm

Figure 12

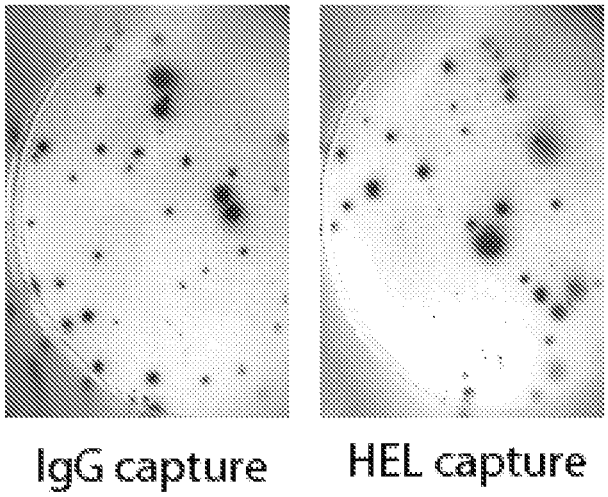

Figure 13

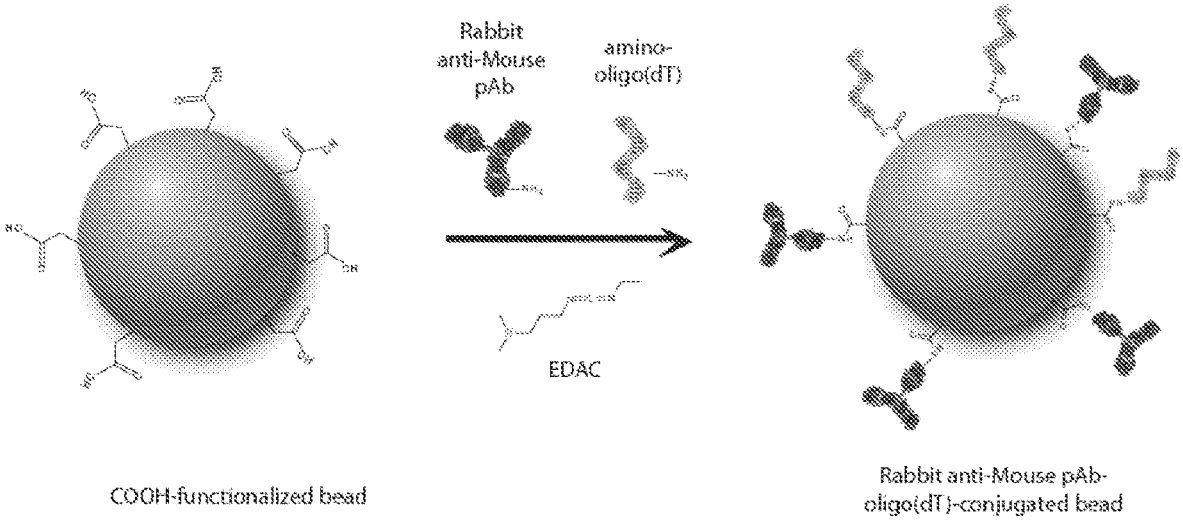
Rabbit anti-Mouse pAb
amino-oligo(dT)
EDAC
COOH-functionalized bead
Rabbit anti-Mouse pAb-oligo(dT)-conjugated bead

Figure 14

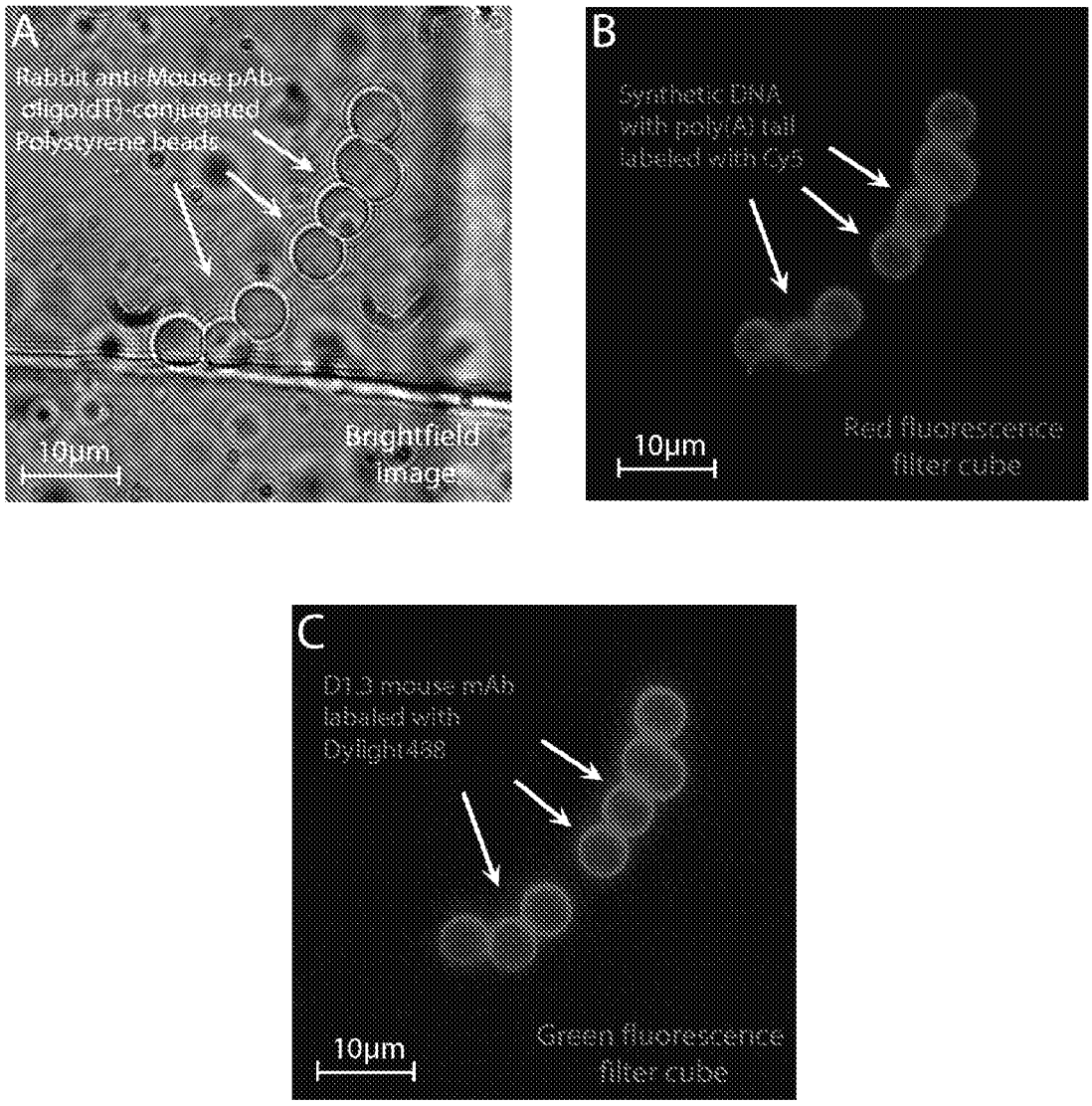
A
Rabbit anti-Mouse pAb
oligo(dT)-conjugated
Polystyrene beads
10μm
Brightfield
images
B
Synthetic DNA
with poly(A) tail
labeled with Cy5
10μm
Red fluorescence
filter cube
C
D1.3 mouse mAb
labeled with
Dylight 488
10μm
Green fluorescence
filter cube

Figure 15

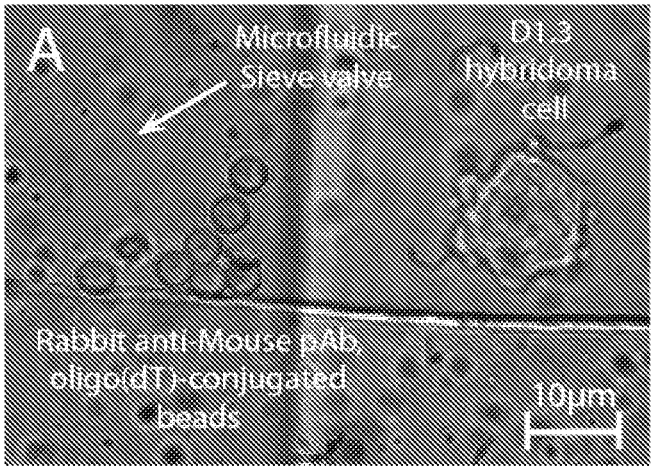
A
Microfluidic Sieve valve
D1.3 hybridoma cell
Rabbit anti-Mouse pAb oligo(dT)-conjugated beads
10μm

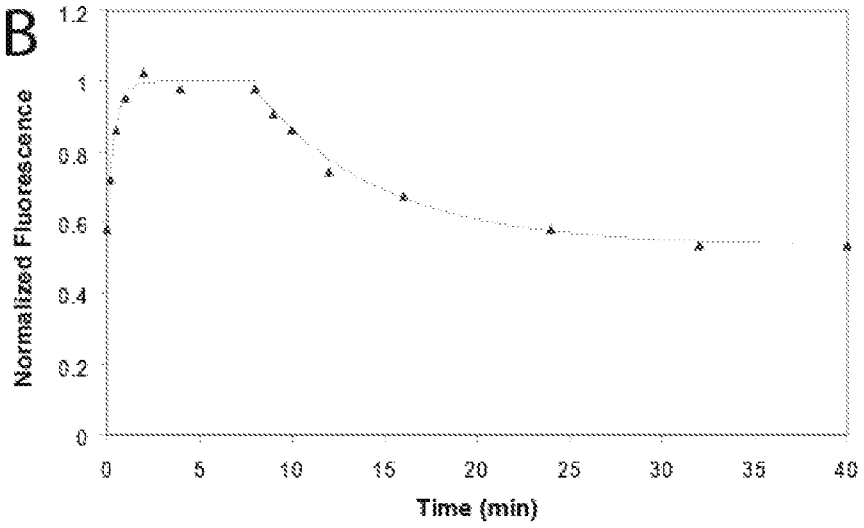
B
Normalized Fluorescence
1.2
1
0.8
0.6
0.4
0.2
0
0
5
10
15
20
25
30
35
40
Time (min)

Figure 16

A

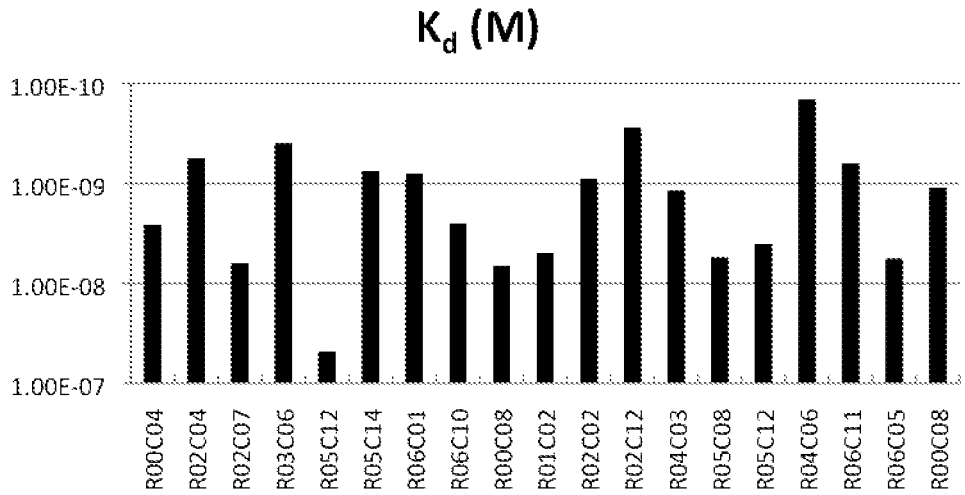

B

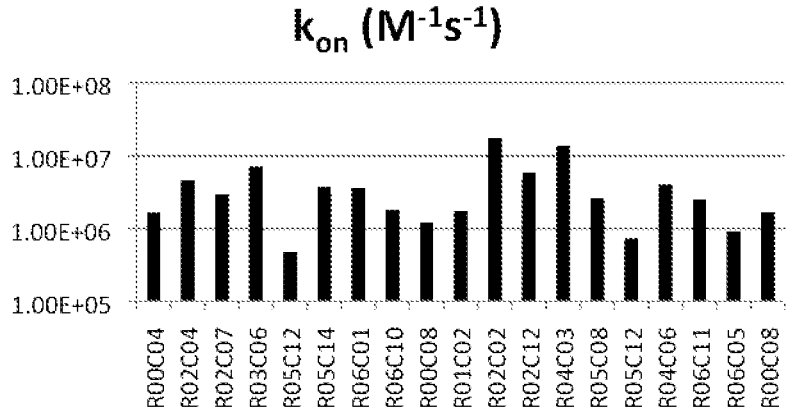

C

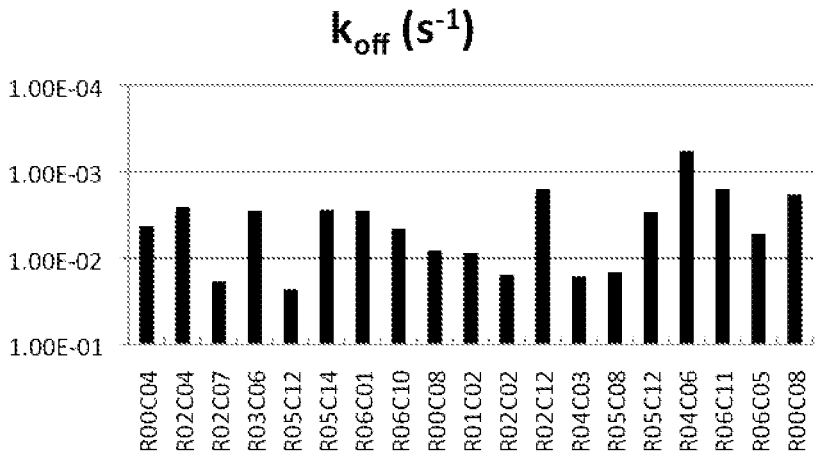

Figure 17

A

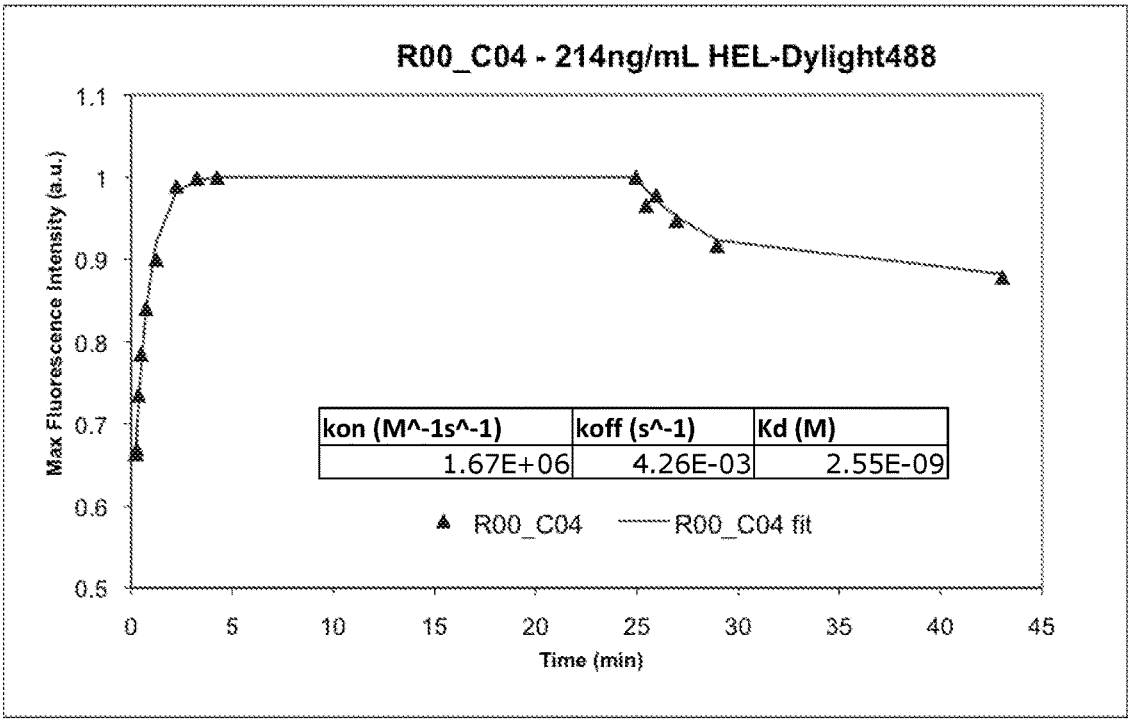
R00_C04 - 214ng/mL HEL-Dylight488
Max Fluorescence Intensity (a.u.)
Time (min)
kon (M^-1s^-1) | koff (s^-1) | Kd (M)
1.67E+06 | 4.26E-03 | 2.55E-09
R00_C04
R00_C04 fit

B

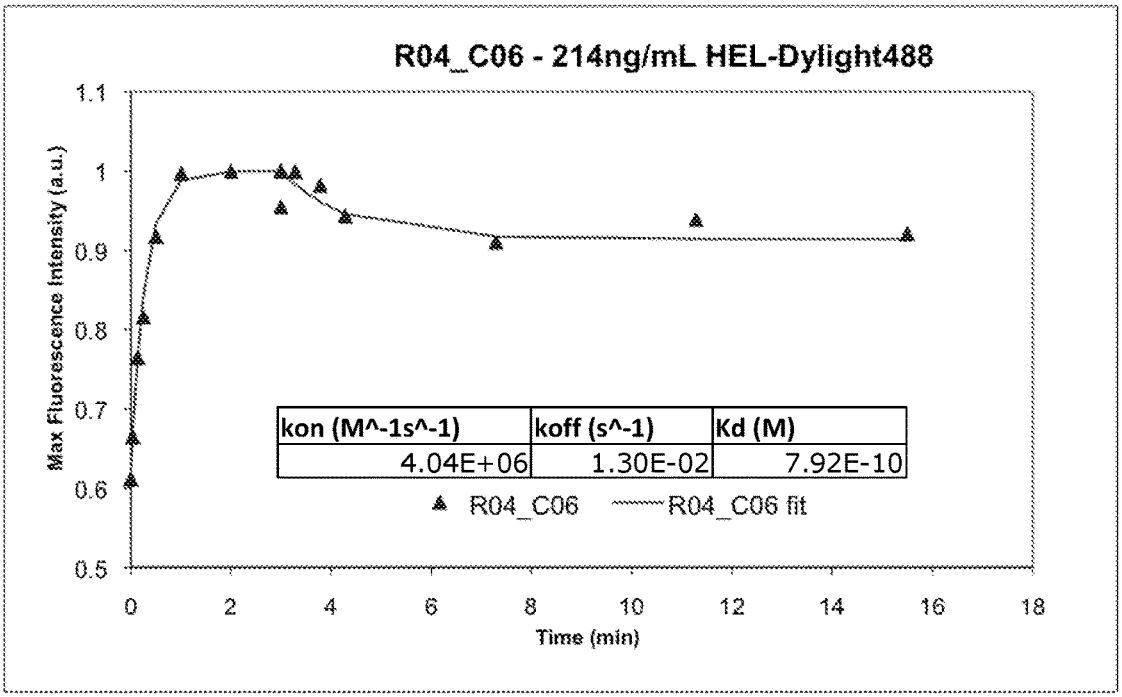
R04_C06 - 214ng/mL HEL-Dylight488
Max Fluorescence Intensity (a.u.)
Time (min)
kon (M^-1s^-1) | koff (s^-1) | Kd (M)
4.04E+06 | 1.30E-02 | 7.92E-10
R04_C06
R04_C06 fit

Figure 18

A

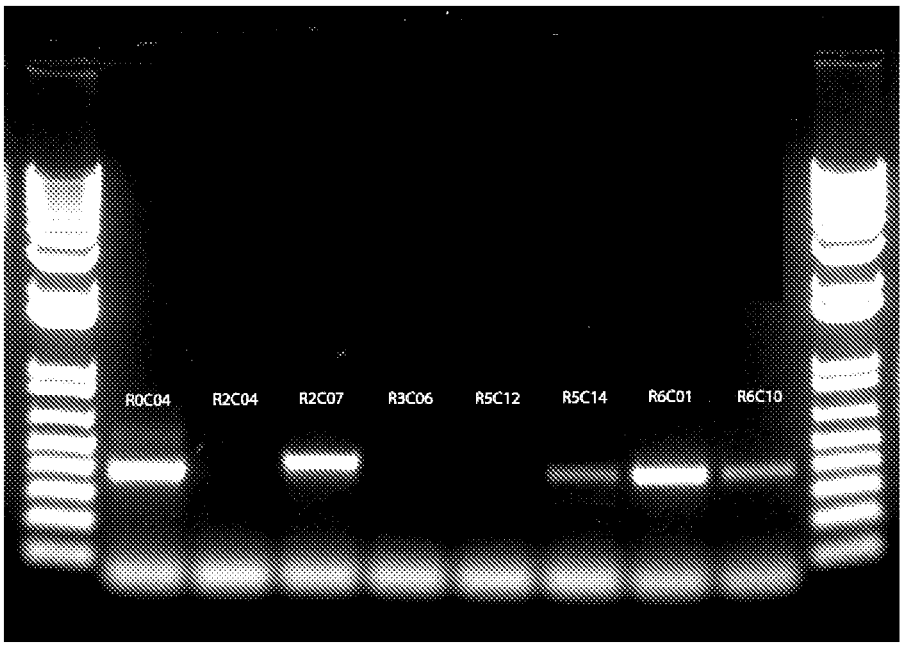
R0C04
R2C04
R2C07
R3C06
R5C12
R5C14
R6C01
R6C10

B

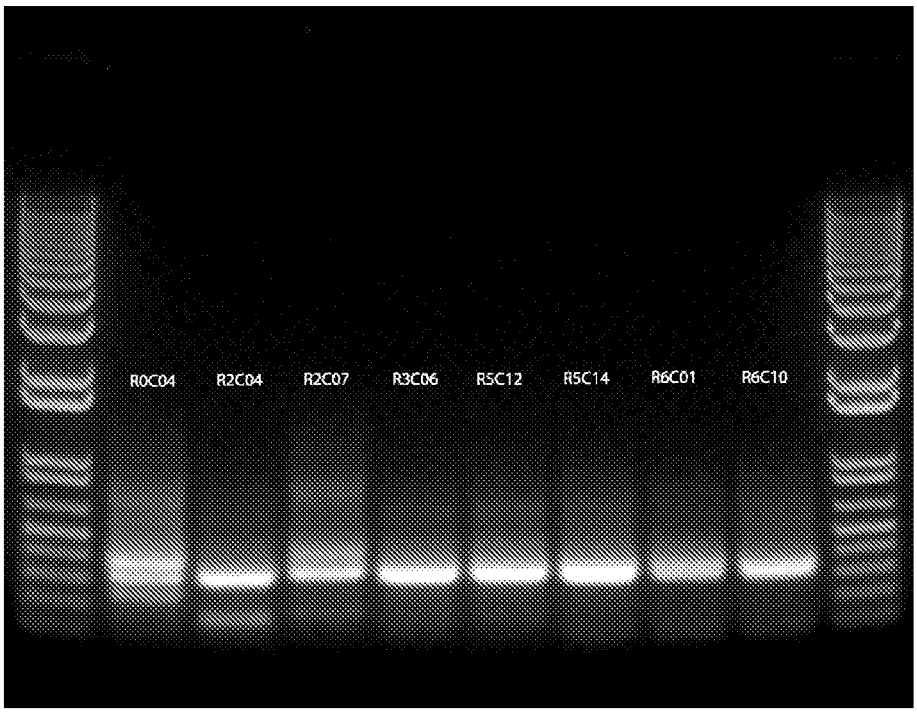
R0C04
R2C04
R2C07
R3C06
R5C12
R5C14
R6C01
R6C10

Figure 19

C

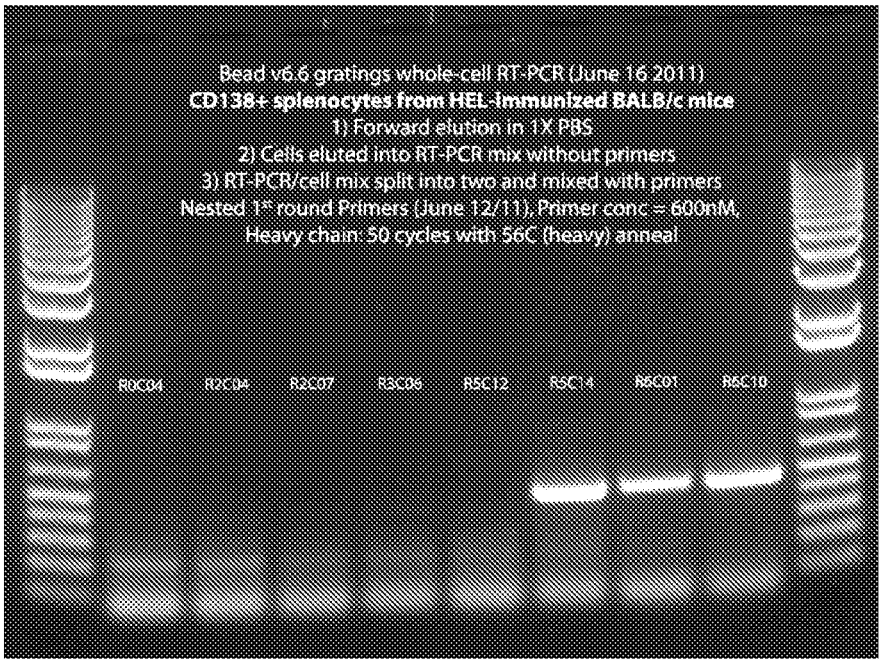

D

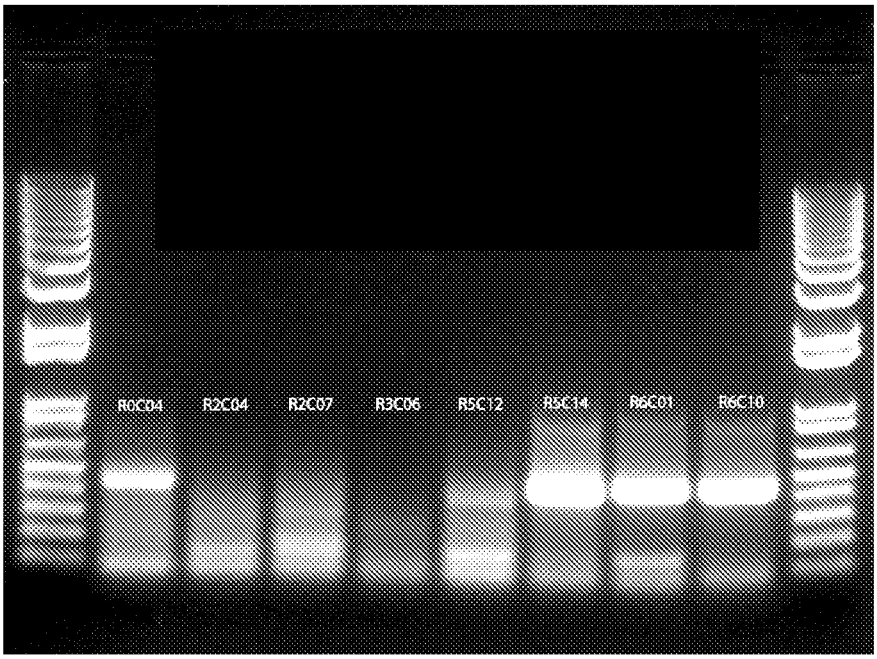

Figure 19 cont'd

A

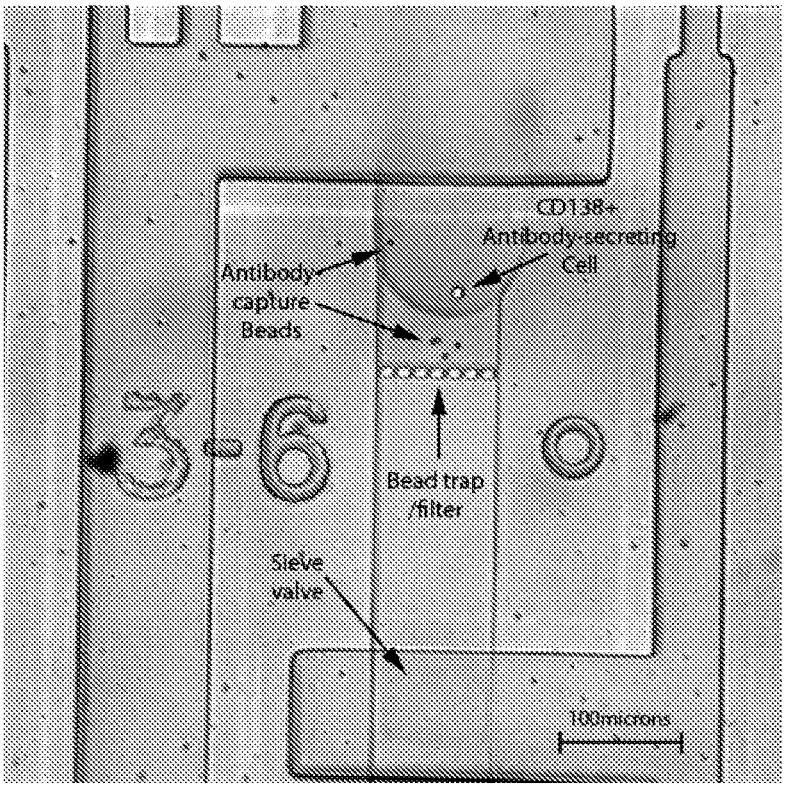
CD138+
Antibody-secreting
Cell
Antibody
capture
Beads
Bead trap
/filter
Sieve
valve
100microns

B

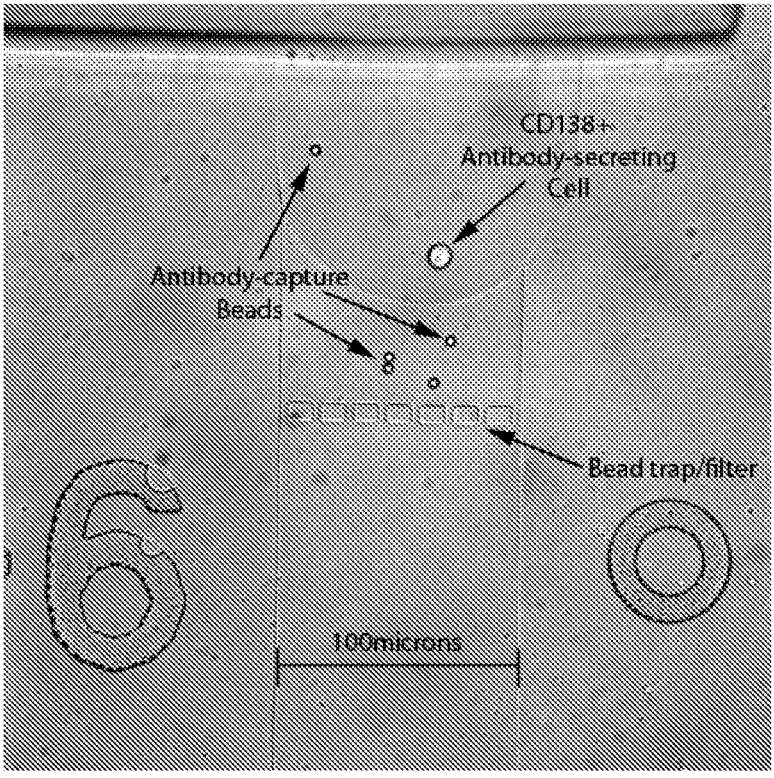
CD138+
Antibody-secreting
Cell
Antibody-capture
Beads
Bead trap/filter
100microns

Figure 20

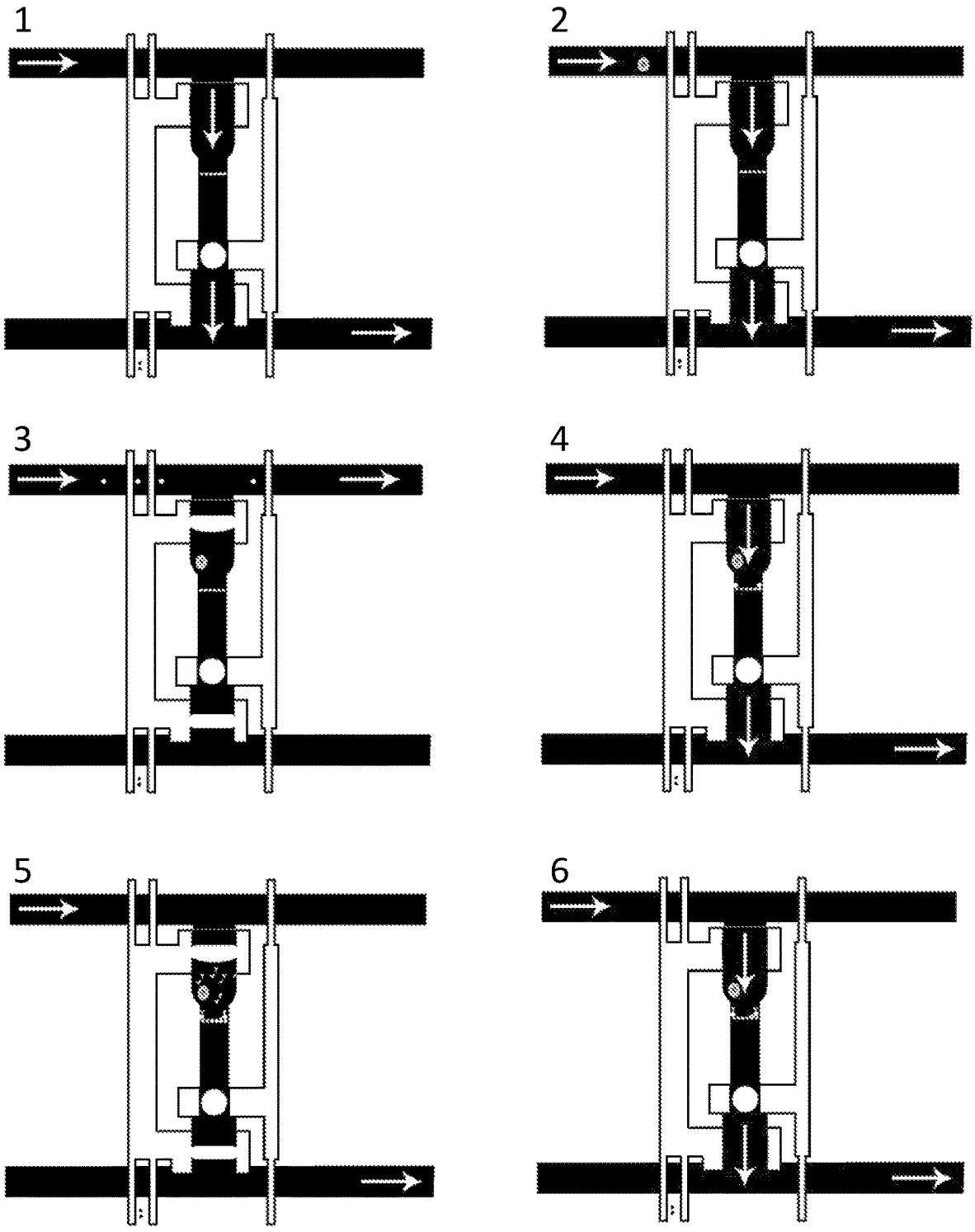

Figure 21

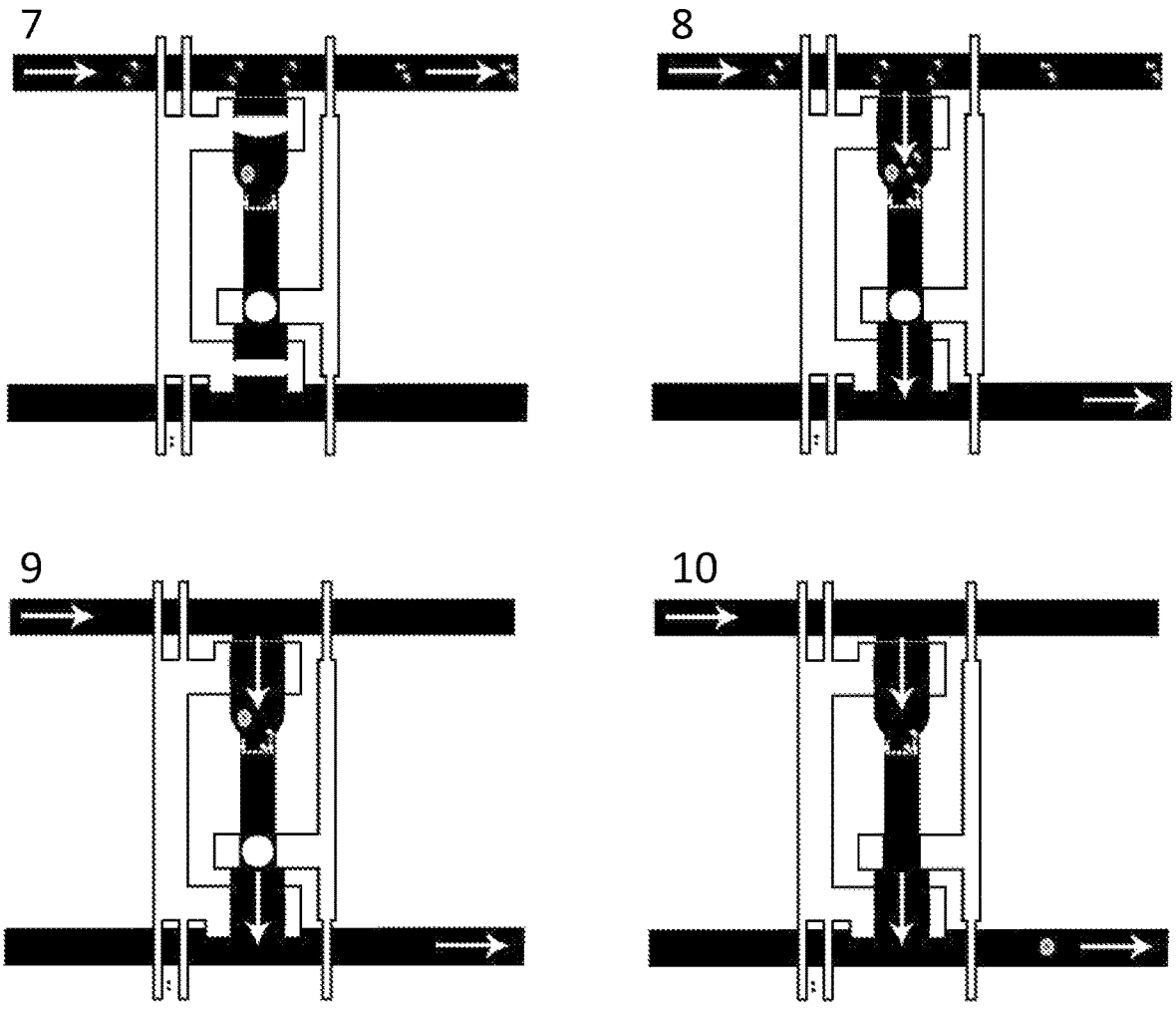

Figure 21 cont'd

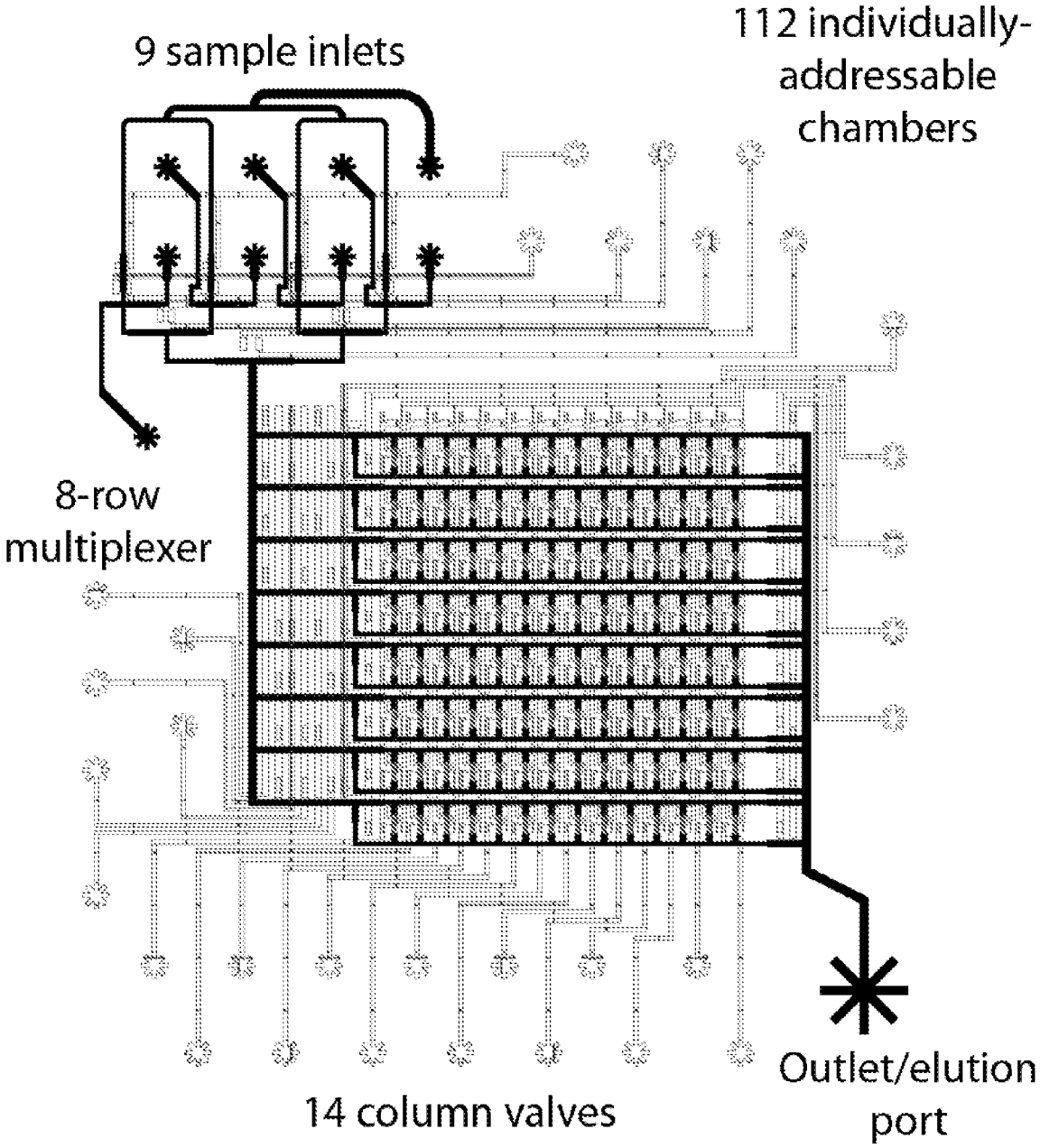
9 sample inlets
112 individually-addressable chambers
8-row multiplexer
14 column valves
Outlet/elution port

Figure 22

METHODS FOR ASSAYING CELLULAR BINDING INTERACTIONS

CROSS REFERENCE TO RELATED APPLICATIONS

This application is a continuation of U.S. patent application Ser. No. 16/746,540, filed Jan. 17, 2020, which is a continuation of U.S. patent application Ser. No. 16/579,561, filed Sep. 23, 2019, now U.S. Pat. No. 10,578,618, which is a continuation of U.S. patent application Ser. No. 16/290,751, filed Mar. 1, 2019, now U.S. Pat. No. 10,466,241, which is a continuation of U.S. patent application Ser. No. 16/129,555, filed Sep. 12, 2018, now U.S. Pat. No. 10,274,494, which is a continuation of U.S. patent application Ser. No. 14/879,791, filed Oct. 9, 2015, now U.S. Pat. No. 10,107,812, which is a continuation of U.S. patent application Ser. No. 13/184,363, filed Jul. 15, 2011, now U.S. Pat. No. 9,188,593, which claims the benefit of U.S. Provisional Patent Application Ser. No. 61/365,237 entitled "METHODS FOR ASSAYING CELLULAR BINDING INTERACTIONS" filed on Jul. 16, 2010, the disclosure of each of which is incorporated herein by reference in its entirety.

FIELD OF INVENTION

This invention relates to the field of microfluidics and protein binding, more specifically, binding interaction between biomolecules.

BACKGROUND

Antibodies are defense proteins produced by the vertebrate adaptive immune system for the purposes of binding and targeting for clearance of a diverse range of bacteria, viruses, and other foreign molecules (collectively referred to as antigens) (see, for e.g., Abbas et al. (1997), *Cellular and Molecular Immunology*, 3rd Ed., Chapter 3, pp. 37-65). As a result of their ability to bind target antigens selectively and with high affinity, antibodies are useful tools for protein purification, cell sorting, diagnostics, and therapeutics.

Conventional antibody production has involved the immunization of animals (i.e., mice) with a target antigen, such as a virus, bacteria, foreign protein, or other molecule. The immunized mice produce on the order of 10^4-10^5 antibody secreting cells (ASCs), each with the capacity to produce a unique (monoclonal) antibody specific to the target antigen (see, for e.g., Poulson et al. (1997), *J. Immunol.* 179: 3841-3850; and Babcock et al. (1996), *Proc. Natl. Acad. Sci. USA* 93: 7843-7848).

The ASCs are then harvested from the immunized animals and screened in order to select which cells are producing antibodies of desired affinity and selectivity to the target antigen. Since single ASCs do not produce antibodies in sufficiently large quantities for binding affinity measurements, each ASC is clonally expanded. Primary ASCs do not grow efficiently in laboratory tissue cultures; thus, clonal expansion may be achieved by fusing ASCs to murine myeloma (cancer) cells to produce immortalized, antibody-secreting (hybridoma) cells (see, for e.g., Kohler, G. and Milstein, C. (1975), *Nature* 256: 495-497). Using this method, expansion of each successfully created hybridoma then produces a monoclonal antibody in sufficiently high concentrations to measure its affinity and selectivity to a target antigen.

It has been recognized that a limitation of hybridoma technology is the low efficiency of the fusion process. For example, whereas an immune response may produce on the order of 10^4-10^5 antibody secreting cells, a typical fusion will yield less than 100 viable hybridomas. (see, for e.g., Kohler, G. and Milstein, C. (1975), *Nature* 256: 495-497; Karpas et al. (2001), *Proc. Natl. Acad. Sci. USA* 98: 1799-1804; and Spieker-Polet et al. (1995), *Proc. Natl. Acad. Sci. USA* 92: 9348-9352). Therefore, fusions from hundreds to thousands of animals are required to fully sample the diversity of antibodies produced in an immune response, making the hybridoma approach both time-consuming and expensive. Attempts to circumvent hybridoma generation by immortalizing antibody-producing cells using viral transformations have resulted in modest gains in the efficiency of ASC immortalization. However, these approaches still require costly and time-consuming clonal expansion in order to produce sufficient quantities of monoclonal antibodies to screen for affinity and selectivity to target antigens (see for e.g., Pasqualini, R. and Arap, W. (2004), *Proc. Natl. Acad. Sci. USA* 101: 257-259; Lanzavecchia et al. (2007), *Current Opinion in Biotechnology* 18: 523-528; and Traggiai et al. (2004), *Nat Med* 10: 871-875).

Devices have been developed to estimate the equilibrium dissociation constants of antibodies secreted from single antibody-secreting cells (Story, C. M. et al. *Proc. Natl. Acad. Sci. U.S.A.* (2008) 105(46):17902-17907; and Jin, A. et al. *Nat. Med.* (2009) 15(9):1088-1092), but do not measure antibody-antigen binding kinetics using antibodies secreted from single cells.

SUMMARY

In a first embodiment, there is provided a method of assaying for a binding interaction between a protein produced by a cell and a biomolecule: (a) retaining the cell within a chamber having an inlet and an outlet; (b) exposing the protein produced by the cell to a capture substrate, wherein the capture substrate is in fluid communication with the protein produced by the cell and wherein the capture substrate is operable to bind the protein produced by the cell; (c) flowing a first fluid volume comprising the biomolecule through the inlet into the chamber and out the outlet, wherein the first fluid volume is in fluid communication with the capture substrate; and (d) determining binding interactions between the protein produced by a cell and the biomolecule.

The cell may be an antibody producing cell (APC), the protein produced by the cell is an antibody and the biomolecule is an antigen. The cell may be a single cell. The biomolecule may be a fluorescently labeled antigen. The determining binding interactions may be a measure of antigen-antibody binding kinetics. The determining the antigen-antibody binding kinetics may include fluorescence imaging of antigen-antibody binding. The determining the binding interactions may be by one or more of the following techniques: surface plasmon resonance (SPR) spectroscopy, fluorescence anisotropy, interferometry, or fluorescence resonance energy transfer (FRET). The determining of the binding interaction may be by a nanocalorimeter or a nanowire nanosensor. The measure of antigen-antibody binding kinetics may be the K_{on} rate. The measure of antigen-antibody binding kinetics may be the K_{off} rate. The measure of antigen-antibody binding kinetics may be the both the K_{on} rate and the K_{off} rate. The protein produced by the cell may be an antibody. The antibody may be a monoclonal antibody. The protein produced by the cell may be an antigen. The biomolecule may be an antigen. The biomolecule may be selected from one of the following: an

antibody, a whole cell, a cell fragment, a bacterium, a virus, a viral fragment, and a protein. The protein produced by the cell may not be secreted by the cell, and the method may further include a step of cell lysis prior to exposing the protein produced by the cell to the capture substrate. The protein produced by the cell may not be secreted by the cell, and the method may further include a step of cell lysis after exposing the protein produced by the cell to the capture substrate. The capture substrate may be a removable capture substrate. The removable capture substrate may be an anti-Ig bead. The removable capture substrate may be an anti-Ig bead and/or oligo (dT) bead. The removable capture substrate may include a capture substrate capable of capturing both nucleic acids and antibodies. The removable capture substrate may include a capture substrate capable of capturing nucleic acids and a capture substrate capable of capturing antibodies. The removable capture substrate may include a capture substrate capable of capturing nucleic acids. The binding of the antibodies may be further tested by viral inactivation. The binding of the antibodies may be further tested by bacterial inactivation. The binding of the antibodies may be further tested by cell inactivation. The method may further include adding the cell to a reverse transcription polymerase chain reaction (RT-PCR) reaction to amplify the heavy and light chain genes. The amplification may be performed in a number of ways. For example, 1) the cells may be eluted into RT-PCR mix containing primers for both heavy and light chain genes for multiplex amplification of both genes in a single reaction. Alternatively, the cells may be eluted into RT-PCR mix without primers, the mix may then be split into two equal volume aliquots and the respective heavy and light chain primers may be added to the two aliquots for single-plex amplification. Both methods have been shown to work to amplify the heavy and light chains from a single cell. The exposing the protein produced by the cell to the capture substrate may include flowing a removable capture substrate into the chamber. The method may further include washing the cell prior to flowing a removable capture substrate into the chamber. The protein produced by the cell may be an antigen and the biomolecule may be an antibody. The antibody may be a monoclonal antibody. The biomolecule may be a fluorescently labeled antibody. The fluorescently labeled antibody may be a monoclonal antibody. The determining binding interactions may be a measure of antigen-antibody binding kinetics. The measure of antigen-antibody binding kinetics may be any one or both of: a K_{on} rate; and a K_{off} rate. The APC may be from one of the following: a human, a rabbit, a rat, a mouse, a sheep, an ape, a monkey, a goat; a dog, a cat, a camel, or a pig. The removable capture substrate may be a carboxylic acid (COOH) functionalized bead. The removable capture substrate may be capable of binding the protein produced by the cell and the nucleic acids encoding the protein produced by the cell. The method may further include washing the cell prior to exposing the protein produced by the cell to a capture substrate. The APC may be selected from one of the following: a primary B cell and a memory B cell.

In a further embodiment, there is provided a cell assay method, the method including: distributing an antibody producing cell (APC) to a chamber, wherein the APC is in a first fluid; replacing the first fluid with a second fluid while maintaining the APC in the chamber; placing the antibodies produced by the APC in fluid communication with an antigen; and determining the antigen-antibody binding kinetics of the antibodies produced by the APC with the antigen.

In a further embodiment, there is provided a method of assaying for a binding interaction between a protein produced by a cell and a biomolecule, the method including: (a) retaining the cell within a chamber having an aperture; (b) exposing the protein produced by the cell to a capture substrate, wherein the capture substrate is in fluid communication with the protein produced by the cell and wherein the capture substrate is operable to bind the protein produced by the cell; (c) flowing a fluid volume comprising the biomolecule through the chamber via said aperture, wherein the fluid volume is in fluid communication with the capture substrate; and (d) determining a binding interaction between the protein produced by the cell and the biomolecule.

The measure of antigen-antibody binding kinetics may be the K_{on} rate. The measure of antigen-antibody binding kinetics may be the K_{off} rate. The measure of antigen-antibody binding kinetics may be the both the K_{on} rate and the K_{off} rate. The binding of the antibodies may be further tested by viral inactivation. The binding of the antibodies may be further tested by bacterial inactivation. The binding of the antibodies may be further tested by cell inactivation. The determining of antigen-antibody binding kinetics may be by one or more of the following techniques: surface plasmon resonance (SPR) spectroscopy, fluorescence anisotropy, interferometry, or fluorescence resonance energy transfer (FRET). The determining of antigen-antibody binding kinetics may be by a nanocalorimeter or a nanowire nanosensor. The method may further include adding the cell to a reverse transcription polymerase chain reaction (RT-PCR) reaction to amplify the heavy and light chain genes. The placing the antibodies produced by the APC in fluid communication with an antigen may include flowing a removable capture substrate into the chamber. The method may further include washing the cell prior to flowing a removable capture substrate into the chamber. The APC may be from one of the following: a human, a rabbit, a rat, a mouse, a sheep, an ape, a monkey, a goat; a dog, a cat, a camel, or a pig. The removable capture substrate may be a carboxylic acid (COOH) functionalized bead. The removable capture substrate may be capable of binding the protein produced by the cell and the nucleic acids encoding the protein produced by the cell. The method may further include washing the cell prior to exposing the protein produced by the cell to a capture substrate. The APC may be selected from one of the following: a primary B cell and a memory B cell. The method may further include adding a removable capture substrate to the chamber to capture the antibodies produced by the APC prior to placing the antibodies produced by the APC in fluid communication with an antigen. The placing of the antibodies produced by the APC in fluid communication with an antigen may include flowing a fluorescently labeled antigen through the chamber. The method may further include collecting the mRNA from the cell for a reverse transcription polymerase chain reaction (RT-PCR) reaction to amplify the heavy and light chain genes. The determining the antigen-antibody binding kinetics may include fluorescence imaging of antigen-antibody binding.

In a further embodiment, there is provided a microfluidic device for assaying for a binding interaction between a protein produced by a cell and a biomolecule, the device comprising: a chamber, having: (i) at least one inlet; (ii) at least one outlet; and (iii) a reversible trap having spaced apart structural members extending across the chamber to separate the at least one inlet and at least one outlet wherein the spaced apart structural members are operable to allow

fluid flow through the chamber from the inlet to the outlet while providing size selection for a particle within the fluid flow.

In a further embodiment, there is provided a microfluidic device for assaying for a binding interaction between a protein produced by a cell and a biomolecule, the device comprising: a chamber, having: (i) at least one inlet; (ii) at least one outlet; and (iii) a reversible trap, wherein the reversible trap is a narrowing of the chamber from to allow fluid flow through the chamber from the inlet to the outlet while providing size selection for a particle within the fluid flow.

In a further embodiment, there is provided a microfluidic device for assaying a binding interaction between a protein produced by a cell and a biomolecule, the device including: a chamber having an aperture and a channel for receiving a flowed fluid volume through the chamber via said aperture, the channel providing size selection for a particle within said fluid volume.

In a further embodiment, there is provided a microfluidic device for assaying a binding interaction between a protein produced by a cell and a biomolecule, the device including: a chamber having an aperture; a reversible trap having spaced apart structural members extending across the chamber, the structural members being operable to allow a fluid volume to flow through the chamber while providing size selection for a particle within said fluid volume.

The distance between the spaced apart structural members may be less than or equal to about 4.6 microns. The distance between the spaced apart structural members may be less than or equal to about 4.5 microns. The distance between the spaced apart structural members may be less than or equal to about 4.4 microns. The distance between the spaced apart structural members may be less than or equal to about 4.3 microns. The distance between the spaced apart structural members may be less than or equal to about 4.2 microns. The distance between the spaced apart structural members may be less than or equal to about 4.1 microns. The distance between the spaced apart structural members may be less than or equal to about 4.0 microns. The distance between the spaced apart structural members may be less than or equal to about 3.9 microns. The distance between the spaced apart structural members may be less than or equal to about 3.8 microns. The distance between the spaced apart structural members may be less than or equal to about 3.7 microns. The distance between the spaced apart structural members may be less than or equal to about 3.6 microns. The distance between the spaced apart structural members may be less than or equal to about 3.5 microns. The distance between the spaced apart structural members may be less than or equal to about 3.4 microns. The distance between the spaced apart structural members may be less than or equal to about 3.3 microns. The distance between the spaced apart structural members may be less than or equal to about 3.2 microns. The distance between the spaced apart structural members may be less than or equal to about 3.1 microns. The distance between the spaced apart structural members may be less than or equal to about 3.0 microns. The distance between the spaced apart structural members may be less than or equal to about 2.9 microns. The distance between the spaced apart structural members may be less than or equal to about 2.8 microns. The distance between the spaced apart structural members may be less than or equal to about 2.7 microns. The distance between the spaced apart structural members may be less than or equal to about 2.6 microns. The distance between the spaced apart structural members may be less than or equal to about 2.5 microns. The distance between the spaced apart structural members may be less than or equal to about 2.4 microns. The distance between the spaced apart structural members may be less than or equal to about 2.3 microns. The distance between the spaced apart structural members may be less than or equal to about 2.2 microns. The distance between the spaced apart structural members may be less than or equal to about 2.1 microns. The distance between the spaced apart structural members may be less than or equal to about 2.0 microns. The distance between the spaced apart structural members may be less than or equal to about 1.9 microns. The distance between the spaced apart structural members may be less than or equal to about 1.8 microns. The distance between the spaced apart structural members may be less than or equal to about 1.7 microns. The distance between the spaced apart structural members may be less than or equal to about 1.6 microns. The distance between the spaced apart structural members may be less than or equal to about 1.5 microns. The distance between the spaced apart structural members may be less than or equal to about 1.4 microns. The distance between the spaced apart structural members may be less than or equal to about 1.3 microns. The distance between the spaced apart structural members may be less than or equal to about 1.2 microns. The distance between the spaced apart structural members may be less than or equal to about 1.1 microns. The distance between the spaced apart structural members may be less than or equal to about 1.0 microns. The distance between the spaced apart structural members may be less than or equal to about 0.9 microns. The distance between the spaced apart structural members may be less than or equal to about 0.8 microns. The distance between the spaced apart structural members may be less than or equal to about 0.7 microns. The distance between the spaced apart structural members may be less than or equal to about 0.6 microns. The distance between the spaced apart structural members may be less than or equal to about 0.5 microns. The spaced apart structural members may be posts. The spaced apart structural members may be between 5 to 30 microns in width. The spaced apart structural members may be between 10 to 20 microns in width. The spaced apart structural members may be between 5 to 30 microns in width. The spaced apart structural members may be between 5 to 20 microns in width. The spaced apart structural members may be between 5 to 10 microns in width.

The narrowing of the chamber may be from greater than about 10 microns to less than about 5.0 microns. The narrowing of the chamber may be from greater than about 10 microns to less than about 4.9 microns. The narrowing of the chamber may be from greater than about 10 microns to less than about 4.8 microns. The narrowing of the chamber may be from greater than about 10 microns to less than about 4.7 microns. The narrowing of the chamber may be from greater than about 10 microns to less than about 4.6 microns. The narrowing of the chamber may be from greater than about 10 microns to less than about 4.5 microns. The narrowing of the chamber may be from greater than about 10 microns to less than about 4.4 microns. The narrowing of the chamber may be from greater than about 10 microns to less than about 4.3 microns. The narrowing of the chamber may be from greater than about 10 microns to less than about 4.2 microns. The narrowing of the chamber may be from greater than about 10 microns to less than about 4.1 microns. The narrowing of the chamber may be from greater than about 10 microns to less than about 4.0 microns.

It will be appreciated by a person of skill in the art that the distance between the spaced apart structural members and the narrowing of the chamber to produce the reversible trap,

will depend on the size of the cells being assayed and the size of the removable capture substrate, and the flow velocity through the chamber, whereby the cell and the removable capture substrate are retained in the chamber at a first flow velocity and whereby the removable capture substrate is retained in the chamber and the cell is able to deform and fit through the reversible trap at a second flow velocity. Alternatively, there may be different sized removable capture substrates and some may be permitted to pass through the reversible trap, while other may be retained. Furthermore, there may be further flow velocities possible with a given device, whereby the reversible trap may deform to allow the removable capture substrates to pass through the chamber. Alternatively, the chamber may be pierced to remove the removable substrate and/or cells. The narrowing of the chamber may correspond to the channel size selection.

The particle may be selected from one or more of the cell, the biomolecule, the protein, the protein bound to a removeable capture substrate, and the removeable capture substrate. The size selection of the reversible trap may prevent the cell and the removeable capture substrate from passing through the reversible trap, and may allow the biomolecule and the protein to pass through the reversible trap at a first flow velocity, and the size selection of the reversible trap may prevent the removeable capture substrate from passing through the reversible trap, while allowing the cell, the biomolecule and the protein to pass through the reversible trap at a second flow velocity. The outlet may be a sieve valve and the flow velocity through the chamber when the valve is in an open position may be sufficient to allow the cell to deform and pass through the reversible trap. The device may be operable to provide two or more flow velocities through the chamber. The device may be operable to provide two flow velocities through the chamber. The device may be operable to provide three flow velocities through the chamber. The device may be operable to provide four flow velocities through the chamber. The microfluidic device may be operable to allow for removal of the removeable capture substrate. The microfluidic device may be operable to allow for removal of the cell.

The cells get trapped in the chambers when the sieve valves are closed. However, as with the posts, the cells deform when the sieve valve is opened and there is increased flow through the chambers. Both implementations of the reversible trap have worked, but the bead post design is slightly more robust at retaining the beads. The cells being used in the present experiments are about 10 microns in diameter, the beads are 5 microns in diameter, and the space between the posts is less than 3 microns.

A chamber may be in fluid communication with a first auxiliary chamber, wherein there is may be a valve between the chamber and the first auxiliary chamber. The first auxiliary chamber may be in fluid communication with a second auxiliary chamber, wherein there is a valve between the first and second auxiliary chambers, wherein the valve has an open position to allow fluid flow from the first auxiliary chamber to the second auxiliary chamber and a closed position to prevent fluid flow from the first auxiliary chamber to the second auxiliary chamber. The first auxiliary chamber may be in fluid communication with a second auxiliary chamber and the second auxiliary chamber is in fluid communication with a third auxiliary chamber, wherein there is a valve between the first and second auxiliary chambers, wherein the valve has an open position to allow fluid flow from the first auxiliary chamber to the second auxiliary chamber and a closed position to prevent fluid flow from the first auxiliary chamber to the second auxiliary chamber, wherein there is a valve between the second and third auxiliary chambers, wherein the valve has an open position to allow fluid flow from the second auxiliary chamber to the third auxiliary chamber and a closed position to prevent fluid flow from the second auxiliary chamber to the third auxiliary chamber. The volumes of the first second and third auxiliary chambers relative to the chamber may be such that fluid may be flowed into these chambers such that subsequent RT and PCR or other reactions may be carried out without exchanging the fluid (for example, where a first outlet is in a closed position).

The volume of the auxiliary chambers may be expandable. The volume of the chamber may be between 0.1 nL to 100.0 nL. The unexpanded volume of the expandable the chamber may be between 0.1 nL to 100.0 nL. The volume of the chamber may be 0.6 nL. The unexpanded chamber may be 0.6 nL. The effective volume of a given chamber may be increased by expanding the initial chamber or by opening a valve to provide fluid flow into one or more auxiliary chambers. The ratio between the second auxiliary chamber and the first auxiliary chamber may be 5:1. The ratio between the second auxiliary chamber and the first auxiliary chamber may be at least 5:1. The ratio between the expanded chamber and the unexpanded chamber may be 5:1 or the ratio between the expanded first auxiliary chamber unexpanded first auxiliary chamber may be 5:1. The ratio between the expanded chamber and the unexpanded chamber may be at least 5:1 or the ratio between the expanded first auxiliary chamber unexpanded first auxiliary chamber may be at least 5:1. The ratio between the second auxiliary chamber and the first auxiliary chamber, or between the expanded chamber and the unexpanded chamber, or between the expanded first auxiliary chamber unexpanded first auxiliary chamber may vary depending on the reaction mixtures chosen, the concentrations of the components of the mixture and the concentration of the material being assayed. Alternatively, the chamber may be between 0.05 nL and 100.0 nL. Alternatively, the chamber may be between 0.05 nL and 90.0 nL. Alternatively, the chamber may be between 0.1 nL and 95.0 nL. Alternatively, the chamber may be between 0.1 nL and 90.0 nL. Alternatively, the chamber may be between 0.1 nL and 85.0 nL. Alternatively, the chamber may be between 0.1 nL and 80.0 nL. Alternatively, the chamber may be between 0.1 nL and 75.0 nL. Alternatively, the chamber may be between 0.1 nL and 70.0 nL. Alternatively, the chamber may be between 0.1 nL and 65.0 nL. Alternatively, the chamber may be between 0.1 nL and 60.0 nL. Alternatively, the chamber may be between 0.1 nL and 55.0 nL. Alternatively, the chamber may be between 0.1 nL and 50.0 nL. Alternatively, the chamber may be between 0.1 nL and 45.0 nL. Alternatively, the chamber may be between 0.1 nL and 40.0 nL. Alternatively, the chamber may be between 0.1 nL and 35.0 nL. Alternatively, the chamber may be between 0.1 nL and 30.0 nL. Alternatively, the chamber may be between 0.1 nL and 25.0 nL. Alternatively, the chamber may be between 0.1 nL and 20.0 nL. Alternatively, the chamber may be between 0.1 nL and 15.0 nL. Alternatively, the chamber may be between 0.1 nL and 10.0 nL. Alternatively, the chamber may be between 0.1 nL and 9.0 nL. Alternatively, the chamber may be between 0.1 nL and 8.0 nL. Alternatively, the chamber may be between 0.1 nL and 7.0 nL. Alternatively, the chamber may be between 0.1 nL and 6.0 nL. Alternatively, the chamber may be between 0.1 nL and 5.0 nL. Alternatively, the chamber may be between 0.1 nL and 4.0 nL. Alternatively, the chamber may be between 0.1

nL and 3.0 nL. Alternatively, the chamber may be between 0.1 nL and 2.0 nL. Alternatively, the chamber may be between 0.1 nL and 1.0 nL.

In a further embodiment, there is provided a method of assaying for a protein of interest produced by a cell, the method comprising: incubating the cell with a removable capture substrate in a buffer, wherein the removable capture substrate is capable of binding the protein of interest and nucleic acids encoding the protein of interest; and screening the bound removable capture substrate to determine whether the cell produces the protein of interest.

In a further embodiment, there is provided a method of assaying for a protein of interest produced by a cell, the method comprising: incubating the cell with a removable capture substrate in a buffer, wherein the removable capture substrate is capable of binding the protein of interest; and screening the bound removable capture substrate to determine whether the cell produces the protein of interest.

In a further embodiment, there is provided a method of identifying a monoclonal antibody of interest, the method comprising: incubating an APC with a removable capture substrate in a suitable buffer, wherein the removable capture substrate is capable of binding the monoclonal antibody produced by the APC and nucleic acids encoding the variable regions of the monoclonal antibody; and screening the bound removable capture substrate to determine whether the APC produces the monoclonal antibody of interest.

In a further embodiment, there is provided a cell assay method, the method comprising: distributing an APC to a chamber, wherein there is on average one APC in the chamber, wherein the APC is incubated with a removable capture substrate in a first solution, and wherein the removable capture substrate is capable of binding an antibody of interest produced by the APC and nucleic acids encoding the variable regions of the antibody of interest; replacing the first solution with a second solution while maintaining the APC in the chamber; placing the antibody of interest produced by the APC in fluid communication with an antigen; and screening the bound removable capture substrate to determine whether the APC produces the antibody of interest.

In a further embodiment, there is provided a method of assaying for a chemical interaction between a protein produced by a cell and a biomolecule, the method comprising: distributing the cell to a chamber, wherein the cell is in a first solution; replacing the first solution with a second solution while maintaining the cell in the chamber; placing the protein in fluid communication with the biomolecule; and testing the chemical interaction of the protein produced by the cell with the biomolecule.

In a further embodiment, there is provided a method of identifying a monoclonal antibody of interest, the method comprising: incubating an antibody producing cell (APC) with a removable capture substrate in a suitable buffer, wherein the removable capture substrate is capable of binding the monoclonal antibody produced by the APC and nucleic acids encoding the variable regions of the monoclonal antibody; and screening the bound removable capture substrate to determine whether the APC produces the monoclonal antibody of interest.

In a further embodiment, there is provided a cell assay method, the method comprising: distributing an antibody producing cell (APC) to a chamber, wherein there is on average one APC in the chamber, wherein the APC is incubated with a removable capture substrate in a first solution, and wherein the removable capture substrate is capable of binding an antibody of interest produced by the APC and nucleic acids encoding the variable regions of the antibody of interest; replacing the first solution with a second solution while maintaining the APC in the chamber; placing the antibody of interest produced by the APC in fluid communication with an antigen; and screening the bound removable capture substrate to determine whether the APC produces the antibody of interest.

In a further embodiment, there is provided a method of assaying for a protein of interest produced by a cell. The method involves incubating the cell with a removable capture substrate in a suitable buffer, wherein the removable capture substrate is capable of binding the protein of interest; and screening the bound removable capture substrate to determine whether the cell produces the protein of interest.

The method may involve determining the binding affinity of the protein of interest. The method may involve determining a dissociation rate; and association rate and dissociation rate. The method may involve lysing the cell prior to incubation with the removable capture substrate, wherein the protein of interest is not secreted by the cell.

In a further embodiment, there is provided an device for selecting a cell that produces a protein having a binding affinity for a biomolecule. The device may include a microfluidic device as described herein operably configured to hold an aliquot, wherein the aliquot on average contains one cell, and wherein the protein produced by the cell is in fluid communication with the biomolecule; and a detector for detecting the binding affinity of the protein produced by the cell.

The device may include a detector that is a fluorescence imager for detecting the binding affinity. The device may include a detector that is a surface plasmon resonance (SPR) spectroscopy apparatus, or a fluorescence anisotropy apparatus, or an interferometry apparatus, or a FRET apparatus. Further, the device may include a detector that is a nanocalorimeter or a nanowire nanosensor.

In a further embodiment, there is provided a kit for identifying a cell that produces antibodies having a binding affinity for an antigen. The kit includes a microfluidic device as contemplated herein; and a removable capture substrate. The kit may include the removable capture substrate being capable of binding proteins, or nucleic acids, or proteins and nucleic acids. The kit may include the removable capture substrate being a microsphere. Further, the kit may include the microsphere being a polystyrene bead or a silica bead. Further, the kit may include the microsphere being a carboxylic acid (COOH) functionalized bead.

The kit may include an antigen label. The kit may include an antigen label that is a fluorescent label. Further, the kit may include instructions for the use of the device contemplated herein to identify a cell that produces proteins having a desired binding affinity. Further, the kit may include instructions for immunizing an animal and collecting APCs. Further, the kit may include an antigen.

BRIEF DESCRIPTION OF THE DRAWINGS

FIG. **1** shows a microfluidic device and schematics for bead-based measurements of antibody-antigen binding kinetics. Panel (A) is an illustration of a microfluidic device containing control channels for individually selecting six reagent inlets and actuating sieve valves on the reagent outlet channel. Panel (B) shows a microscopic image of the device with food coloring to visualize distinct reagent inlets (as shown) and control channels (as shown) (5× magnification); Top inset depicts a close-up of beads trapped using sieve valves (20× magnification; Bottom inset depicts fluo-

rescence image of beads during binding kinetic measurements (100× magnification). Panel (C) shows a schematic of a bead assay for direct measurement of association and dissociation kinetics of immobilized mAbs and fluorescently-labeled antigen. Panel (D) shows a variation of a bead assay for indirect measurement of dissociation kinetics of immobilized mAbs and unlabeled antigen molecules.

FIG. **2** shows a schematic diagram of an embodiment of a microfluidic device for the detection of antibody secreted from single cells. (A) Hydraulic pressure is applied to valves (fully-closing) and sieve valves (partially-closing) formed by the intersection of actuation control channels with rounded- or square-profile flow channels, respectively. (B) An expanded view of an embodiment of a microfluidic device for the detection of antibody secreted from single cells. (1) chip is flushed with 1×PBS; (2) antibody-secreting cells and antibody-capture beads are loaded into chambers; (3) cells are incubated for one hour to allow for antibody secretion; (4): mix valve is opened to allow for secreted antibody to bind to beads; (5) beads and cells are captured against sieve valve and unbound antibody is washed out; (6) chambers flushed with fluorescently-labeled antigen; image and measure antibody-antigen association kinetics; and (7) flushed out unbound antigen with 1×PBS; image and measure antibody-antigen dissociation kinetics.

FIG. **3** shows plots of microfluidic bead-based measurements of antibody-antigen binding kinetics. Direct fluorescent measurements of association and dissociation kinetics of (A) D1.3 mAb and HEL-Dylight488 conjugate, (B) HyHEL-5 mAb and HEL-Dylight488 conjugate, (C) LGB-1 mAb and enhanced green fluorescent protein (EGFP) are demonstrated. (D) Indirect measurement of dissociation kinetics of D1.3 mAb and HEL using HEL-Dylight488 conjugate is demonstrated.

FIG. **4** shows simultaneous measurement of multiple antibody-antigen binding kinetics using optical and spatial multiplexing. (A) Plots measured association and dissociation kinetics of 3 distinct mAbs (HyHEL-5, D1.3, and LGB-1 mAb) interacting with 2 different antigens (HEL-Dylight633 conjugate and EGFP) is demonstrated. (B) A micrograph showing false-coloured, overlay of images taken with distinct fluorescence filter cubes to identify anti-lysozyme mAbs and anti-EGFP mAbs is demonstrated.

FIG. **5** shows plots of sensitivity and detection limit of antibody-antigen binding kinetics measurements. (A) Measured association kinetics of D1.3 mAb-Dylight488 conjugate on rabbit anti-mouse pAb coated beads is demonstrated. Inset demonstrates a schematic of bead assay for measuring binding kinetics of fluorescently-labeled mouse mAb and rabbit anti-mouse pAb coated beads. (B) Association kinetics of HEL-Dylight488 conjugate on beads with varying amounts of immobilized D1.3 mAb is demonstrated. (C) Equilibrium bead fluorescence varies linearly with the amount of immobilized D1.3 mAb. Inset shows a close-up of the graph to highlight detection limit of 1% bead coverage. (D) Direct measurement of equilibrium dissociation constants by measuring equilibrium bead fluorescence using immobilized D1.3 mAb and varying concentrations of HEL-Dylight488.

FIG. **6** shows antibody-antigen binding kinetics measured using antibodies secreted from a single cell. (A) Microscope image of D1.3 hybridoma cell loaded into a microfluidic device adjacent to rabbit anti-mouse pAb coated beads trapped using a sieve valve is shown. (B) "Single-cycle" binding kinetics from a single bead containing D1.3 mAbs secreted from a single cell and subject to increasing concentrations of HEL-Dylight488 conjugate is demonstrated.

FIG. **7** shows the effect of fluorophore stability on measured antibody-antigen binding kinetics. (A) Photobleaching rates of fluorescent dye molecules under 100 W Hg lamp illumination using 100× oil-immersion objective (NA 1.30) are plotted. (B) Effect of fluorescent exposure times on measured association kinetics of D1.3 mAb and HEL-Dylight488 are plotted.

FIG. **8** shows the effect of different bead immobilization chemistries on measured antibody-antigen binding kinetics. Measured kinetics are unaffected by bead composition (silica or polystyrene) or by different polyclonal capture antibodies (rabbit or goat pAbs).

FIG. **9** shows a plot of measured dissociation kinetics of mouse mAb from antibody capture beads. No dissociation of D1.3 mAb-Dylight488 conjugate from Rabbit anti-Ms pAb coated beads was observed over 3 days.

FIG. **10** shows a plot of the effect of antigen re-binding on measured antibody-antigen dissociation kinetics. Dissociation kinetics of D1.3 mAb and HEL-Dylight488 conjugate were unaffected by the presence of a large concentration of competitive antigen (2 mg/mL HEL).

FIG. **11** shows a plot of the effect of mass transport on measured antibody-antigen binding kinetics. Association and dissociation kinetics of D1.3 mAb and HEL-Dylight488 conjugate were unaffected by varying flow rates over a range of ~3-15 μL/hr.

FIG. **12** shows representative microscopic images of primary ASCs in a microfluidic chamber in fluid communication with antibody capture beads and oligo(dT) beads.

FIG. **13** shows an image of an ELISPOT control assay confirming that the cells depicted in FIG. **12** are ASCs. The left image represents cells that secreted any antibody; the right image represents only those cells that secreted HEL-specific antibodies.

FIG. **14** shows a scheme for preparing dual-capture (i.e., dual-function) beads using carbodiimide chemistry.

FIG. **15** shows images of dual-function beads. Polystyrene COOH beads were conjugated with rabbit anti-mouse pAb and amine functionalized oligo$(dT)_{25}$ using carbodiimide chemistry. (A) Brightfield image of dual-function beads trapped using microfluidic sieve valve. (B) Fluorescence image of synthetic single-stranded DNA molecules captured on dual-function beads. Synthetic DNA molecules are labeled with Cy5 fluorophore for visualization and also contain a poly(A) tail that binds to the oligo(dT) on the bead surface. (C) Fluorescence image of mouse D1.3 monoclonal antibody (mAb) captured on dual-function beads. D1.3 mAbs are labeled with Dylight488 fluorophore for visualization and bind to the Rabbit anti-Mouse pAb on the bead surface.

FIG. **16** shows a microscopic image (A) and antibody-antigen binding kinetics (B) as determined from a microfluidic device for dual purpose beads.

FIG. **17** depicts (A) K_d, (B) K_a, and (C) K_{off} rates determined from specific eluted chambers according to Example 9 herein.

FIG. **18** shows representative fluorescence intensity data over time for specific eluted chambers according to Example 9 herein. (A) depicts data for R00C4; (B) depicts data for R04C06.

FIG. **19** shows Kappa chain results from the first round of RT-PCR are shown in FIG. **19**, Panel A. Kappa chain results from the second round of RT-PCR are shown in FIG. **19**, Panel B. Heavy chain results from the first round of RT-PCR are shown in FIG. **19**, Panel C. Heavy chain results from the second round of RT-PCR are shown in FIG. **19**, Panel D.

FIG. **20** shows a microfluidic device according to an embodiment of the invention described herein, showing a reversible trap. (A) brightfield image at 20× magnification; (B) brightfield image at 40× magnification.

FIG. **21** shows a schematic whereby a microfluidic device according to an embodiment of the invention described herein is used as described herein. (1) Flush chip with 1×PBS; (2) Load antibody-secreting cells into chambers; (3) Load antibody-capture beads into inlet channel; (4) Load antibody-capture beads into chamber against bead filter; (5) Incubate cells for 1 hour to allow antibody secretion and capture on beads; (6) Wash out unbound antibody; (7) Load fluorescently-labeled antigen into inlet channel; (8) Flush chambers with fluorescently-labeled antigen; image and measure antibody-antigen association kinetics; (9) Flush our unbound antigen with 1×PBS; image and measure antibody-antigen dissociation kinetics; and (10) Open sieve valve and flush cell out of the chamber to the elution port for recovery from device.

FIG. **22** shows a schematic diagram of an alternative embodiment of the microfluidic device for assaying binding interactions.

DETAILED DESCRIPTION

A binding interaction, as referred to herein, includes a molecular interaction. A molecular interaction is commonly understood as referring to a situation when two or more molecules are attracted to one another by a force, where the force could be for example, electrostatic, dipole-dipole, hydrogen bonding, covalent, or hydrophobic in nature. A binding affinity is commonly understood as referring to an average strength of a molecular interaction. Similarly, "avidity" is used to describe the combined strength of multiple interactions. When used in the present application, "affinity" is meant to encompass one or more interactions, including avidity. The methods described herein may involve determining the binding affinity of the protein of interest. The methods described herein may also involve determining a dissociation rate; and association rate and dissociation rate. Alternatively, the methods described herein may include determining binding kinetics.

The method may involve testing the antigen binding affinity by fluorescence imaging. The method may involve testing the antigen binding affinity using any of the following techniques plasmon resonance (SPR) spectroscopy, fluorescence anisotropy, or interferometry. These techniques are understood to measure antibody-antigen binding kinetics, including, but not limited to surface plasmon resonance (SPR) spectroscopy, fluorescence anisotropy, interferometry, or fluorescence resonance energy transfer (FRET). See, for e.g., Bornhop et al. (2007), *Science* 317: 1732-1736; Homola et al. (1999) *Sensors and Actuators B: Chemical* 54: 3-15; and Xavier, K. A. and Willson, R. C. (1998), *Biophys. J.* 74: 2036-2045. Further, the method may involve testing the antigen binding affinity by a nanocalorimeter or a nanowire nanosensor. See, for e.g., Wang et al. (2005), *Proc. Natl. Acad. Sci. USA* 102: 3208-3212 and Lee et al. (2009) *Proc. Natl. Acad. Sci. USA* 106: 15225-15230. Another method that could be employed would be to use a technique such as dark-field microscopy and use antigens or antibodies labeled with gold nanoparticles. This could be used to detect single molecules and generate on/off rates by counting the molecules. See, for e.g., Ueno et al. (2010) *Biophysical J.* 98: 2014-2023; Raschke et al. (2003) *Nano Letters* 3: 935-938; and Sönnischen et al. (2000) *App. Phys. Letters* 77: 2949-2951. Further methods for labeling and detecting binding events and/or binding kinetics would be known to a person of skill in the art. For example, binding assays may include determining the number of binding events.

A protein, as referred to herein, refers to organic compounds made of amino acids, including both standard and non-standard amino acids. Standard amino acids include the following: alanine, cysteine, aspartic acid, glutamic acid, phenylalanine, glycine, histidine, isoleucine, lysine, leucine, methionine, asparagine, proline, glutamine, arginine, serine, threonine, valine, tryptophan, and tyrosine. An example of a protein is an antibody.

A biomolecule, as referred to herein, may include, but is not limited to, an antibody, or an antibody fragment, or a whole cell, or a cell fragment, or a bacterium, or a virus, or a viral fragment, a nucleic acid or a protein.

A "chamber", as used herein, refers to an enclosed space within a microfluidic device in which a cells may be retained. Each chamber may have at least one inlet for permitting fluid, including fluid containing a cell, to enter the chamber, and at least one outlet to permit fluid and/or the cell to exit the chamber (depending on the design of the chamber and/or the flow through the chamber). Persons skilled in the art will understand that an inlet or an outlet can vary considerably in terms of structure and dimension, and may be characterized in a most general sense as an aperture that can be reversibly switched between an open position, to permit fluid to flow into or out of the chamber, and a closed position to seal the chamber and thereby isolate and retain its contents. Alternatively, the aperture may also be intermediate between the open and closed positions to allow some fluid flow or may be a sieve valve that allows for fluid flow out of the cell, but not other particles (for example, the cell, the beads etc.). A chamber, as referred to herein, refers to a portion of a microfluidic device which is designed to hold, for example, a cell. As used herein, the chamber is of an exceptionally small and discrete sizing. Typical volumes are in the range of ~100 pl to ~100 nl. For example, a chamber can be designed with a volume of approximately 500 pL (less than 1 nL), with dimensions of approximately 100 microns (width), 500 microns (length), and 10 microns (height).

The direction of fluid flow through the chamber dictates an "upstream" and a "downstream" orientation of the chamber. Accordingly, an inlet will be located at an upstream position of the chamber, and an outlet will be generally located at a downstream position of the chamber. A person skilled in the art will understand, however, that a single aperture could function as both an inlet and an outlet.

An "inlet" or an "outlet", as used herein, may include any aperture whereby fluid flow is restricted through the inlet or outlet. There may be a valve to control flow, or flow may be controlled by separating the channels with a layer which prevents flow (for example, oil). Alternatively, an aperture may serve as both an inlet and outlet. Furthermore, an aperture (i.e. inlet or outlet) as used herein is meant to exclude the surface opening of a microwell.

A "microfluidic device", as used herein, refers to any device that allows for the precise control and manipulation of fluids in a geometrically constrained structure. For example, where at least one dimension of the structure (width, length, height) is less than 1 mm.

A solution, as referred to herein, may include, but is not limited to, a solution that can maintain the viability of a cell. Further, the solution may include a suitable buffer that can both retain the viability of a cell such that binding interactions can be obtained or allow for an effective lysis of the cell to obtain nucleic acids from the cell and/or antibodies or

other proteins depending on the application. Alternatively, the solution may be suitable for performing an assay.

A capture substrate, as referred to herein, is meant to encompass a wide range of substrates capable of capturing a protein or biomolecule of interest. These substrates may be modified to alter their surface (internal and external) properties depending on the desired use. For example, a substrate may be bound to antibodies or antigens to capture an antibody of interest. A capture substrate may be, for example, a microsphere or a nanosphere or other microparticles including, but not limited to a polystyrene bead or a silica bead (for example, antibody capture beads and oligo (dT) mRNA capture beads). In an alternate arrangement, instead of modifying the beads with oligo(dT), specific primers could be utilized instead. Optionally, the microsphere may be a carboxylic acid (COOH) functionalized bead. Beads which make use of alternate chemical interactions can fall within this definition. See: for e.g., G. T. Hermanson (2008), *Bioconjugate Techniques,* 2nd Edition, Published by Academic Press, Inc. For example, an alternate scheme for preparing these beads would be to use streptavidin coated beads and to mix these beads with biotinylized rabbit anti-mouse pAbs and biotinylated oligo(dT). A capture substrate can also be an anti-Ig bead which binds an antibody to the capture substrate. A capture substrate can be modified such that it binds multiple biomolecules of interest, for example both mRNA and protein. Alternately, each capture substrate could be limited to a particular biomolecule, for example, one capture substrate being limited to binding mRNA and a second capture substrate being limited to binding a protein. Capture substrates are commercially available or may be made de novo and/or modified as needed for the particular application. Capture substrates may be removable, as in the case of beads. However, capture substrates may also be fixed (and thus, non-removable).

Nucleic acids, as referred to herein, include macromolecules composed of chains of monomeric nucleotides. Common examples of nucleic acids include deoxyribonucleic acid (DNA) and ribonucleic acid (RNA).

In a further embodiment, a cell assay method is provided. The method involves distributing an antibody producing cell (APC) to a chamber, wherein the APC is in a first solution, and wherein there is on average one APC in the chamber; replacing the first solution with a second solution while maintaining the APC in the chamber; placing the antibodies produced by the APC in fluid communication with an antigen; and testing the binding of the antibodies produced by the APC with the antigen. Optionally, the method may involve adding anti-Ig beads to the chamber to capture the antibodies produced by the APC. Optionally, the method may involve lysing the APC to capture antibodies produced by the APC wherein the antibodies are not secreted by the APC.

A cell as referred to herein includes an antibody producing cell (also referred to herein as an "APC"). An APC refers to a cell that can produce an antibody. An antibody producing cell is not limited to cells that secrete antibodies, which are also referred to herein as antibody secreting cells (also referred to herein as an "ASC"). For example, it will be understood from the relevant art that memory B cells, without stimulation, do not normally secrete antibodies. See, for e.g., Abbas et al. (1997), *Cellular and Molecular Immunology,* 3rd Ed., pp. 22-23). Examples of antibody producing cells (APCs) include B cells, memory B cells, primary B cells (which are also known in the art as naïve B cells), and B cell hybridomas. A primary B cell can be harvested from the spleen, blood, or bone marrow of an animal, for example from a mouse, by FACS sorting for a cell surface marker, for example, the CD138+ marker (See: for e.g., Smith et al. (1996) *Eur. J. Immunol.* 26: 444-448).

Antibodies are defense proteins produced by the vertebrate adaptive immune system for the purposes of binding and targeting for clearance a diverse range of bacteria, viruses, and other foreign molecules (antigens). As a result of their ability to bind target antigens selectively and with high affinity, antibodies are invaluable tools for protein purification, cell sorting, and diagnostics. Antibodies are produced by B cells and are secreted by activated B cells. (See generally, for e.g., Abbas et al. (1997), *Cellular and Molecular Immunology,* 3rd Ed., Chapter 3, pp. 37-65). Antibodies are also referred to herein as immunoglobulin (also referred to herein as Ig). An antibody, as referred to herein, can include, but is not limited to polyclonal antibodies and monoclonal antibodies. Unlike polyclonal antibodies, monoclonal antibodies are monospecific antibodies that are the same because they are made by one type of immune cell that are all clones of a unique parent cell. A single APC or ASC can serve as the source of a monoclonal antibody. Antibodies are not limited to a specific isotype and can include, but are not limited to the following isotypes: IgM, IgG, IgD, IgE, and IgA. Typically, it is understood that antibodies are comprised of light and heavy chains that have variable and constant regions therein (see generally, for e.g., Abbas et al. (1997), *Cellular and Molecular Immunology,* 3rd Ed., Chapter 3, pp. 37-65).

In a further embodiment, a method of identifying a monoclonal antibody of interest is provided. The method involves incubating an APC with a removable capture substrate (RCS) in a suitable buffer, wherein the removable capture substrate is capable of binding the monoclonal antibody produced by the APC and nucleic acids encoding the variable regions of the monoclonal antibody; and screening the bound removable capture substrate to determine whether the APC produces the monoclonal antibody of interest.

In a further embodiment, a cell assay method is provided. The method involves distributing an APC to a chamber, wherein there is on average one APC in the chamber, wherein the APC is incubated with a removable capture substrate in a first solution, and wherein the removable capture substrate is capable of binding an antibody of interest produced by the APC and nucleic acids encoding the variable regions of the antibody of interest; replacing the first solution with a second solution while maintaining the APC in the chamber; placing the antibody of interest produced by the APC in fluid communication with an antigen; and screening the bound removable capture substrate to determine whether the APC produces the antibody of interest.

In a further embodiment an apparatus for selecting a cell that produces a protein having a binding affinity for a biomolecule is provided. The apparatus includes a microfluidic device operably configured to hold an aliquot, wherein the aliquot on average contains one cell, and wherein the protein produced by the cell is in fluid communication with the biomolecule; and a detector for detecting the binding affinity of the protein produced by the cell. However, the microfluidic device may also hold more than one cell, particular in an assay where the antigen or biomolecule of interest is a cell, or a cell fragment. Similarly, the antigen may be a virus or a bacterial cell.

In a further embodiment, a kit for identifying a cell that produces antibodies having a binding affinity for an antigen is provided. The kit includes a microfluidic device and a removable capture substrate.

An antigen, as referred to herein, refers to a molecule recognized by the immune system. As such, an antigen can include a molecule that can elicit an immune response in an organism, including in an animal. Examples of antigens include, but are not limited to bacterial antigens and viral antigens.

A method is provided for identifying antibody secreting cells (ASCs) that produce antibodies having a particular binding affinity for an antigen or functional attributes. The method involves distributing an ASC within a discrete aliquot wherein there is on average one ASC in the aliquot, placing the antibodies in fluid communication with the antigen; and testing the antigen binding affinity of the antibodies produced by the ASC. The method is based in part on the discovery that a single ASC, without clonal expansion, is capable of producing enough antibodies to test binding affinity for an antigen or to test other functional attributes. Furthermore, the method is also based, in part, on the discovery that clonal expansion via the production of hybridomas is not required for larger scale production of monoclonal antibodies, whereby the variable regions for the antibodies of interest may be sequenced from an ASC of interest or collected with antibodies.

By way of example, a sensitive, low-cost microfluidic bead-based fluorescence assay is described herein for measuring antibody-antigen binding kinetics within low abundance samples. Direct measurements of antibody-antigen binding kinetics may be made by time-course fluorescence microscopy of antibody-conjugated beads retained in microfluidic chambers and subject to a series of wash cycles with fluorescently-labeled antigen and buffer. A variation of the bead-based assay may include measuring the dissociation kinetics of unlabeled antibody and antigen molecules. As disclosed herein, multiple antibody-antigen interactions were measured spanning nearly four orders of magnitude in equilibrium binding affinity. The rate constants measured by way of the assay disclosed herein were validated with previously published values using SPR spectroscopy.

The methods provided herein are also contemplated for being used to screen mutagenic B cell lines. Further, the methods provided herein are contemplated for being used to screen the selectivity and specificity of antibodies to multiple different antigens.

Antibody Binding Kinetics

The affinity or binding strength of an antibody for its target antigen is an important parameter when selecting an antibody for a given application. Although the affinity of an antibody-antigen interaction is typically quantified by an equilibrium binding constant (K_d), which describes the dynamic equilibrium between binding and unbinding events, the kinetic rate constants (k_{on} and k_{off}) provide a more complete characterization of an antibody-antigen interaction. Two antibodies with identical K_d values may exhibit dramatically different binding kinetics which, in turn, will determine their respective suitability for a given application. For instance, antibodies with rapid association and dissociation kinetics may be desirable for sensing applications, whereas antibody-antigen interactions with very long half-lives may be critical for histological staining, enzyme-linked immunosorbent assays (ELISA), and Western blotting. Similarly, therapeutic antibodies that bind their target antigens with long half-lives could, in principle, be administered in lower dosages, reducing the cost and side-effects of these therapies. Direct measurement of binding kinetic constants can be a critical factor for selecting antibodies for both clinical and research applications. Examples of kinetic assays include, but are not limited to viral and other pathogenic neutralization, cell signaling and growth inhibition, modulation of enzymatic activity (inhibit or enhance).

Microfluidics

Microfluidics refers to a multidisciplinary field dedicated to the design of systems in which small volumes of fluids will be used for a variety of purposes, including lab-on-a-chip technology. See: for e.g., Squires and Quake (2005), *Reviews of Modern Physics* 77: 977-1026. Microfluidic technologies enable small-scale (picoliter to nanoliter) fluid handling operations for high-throughput biochemical analyses with low reagent costs and rapid analysis times. In particular, microfluidic devices fabricated from a silicone rubber, polydimethylsiloxane (PDMS), can be designed and fabricated in 24-48 hours, enabling rapid prototyping of devices. See: for e.g., McDonald, J. C. et al. (2000), *Electrophoresis* 21: 27-40. Microfluidic devices that integrate valves into pumps, mixers, fluidic multiplexers (MUXes), and other fluid-handling components have been successfully applied for protein crystallization, chemical synthesis, protein and DNA detection and single cell analysis. See, for e.g., Thorsen et al. (2002), *Science* 298: 580-584; Hansen, et al. (2002), *Proc. Natl. Acad. Sci. USA* 99: 16531-16536; Maerkl, S. J. & Quake, S. R. (2007) *Science* 315: 233-237; Hansen et al. (2004), *Proc. Natl. Acad. Sci. USA* 101, 14431-14436; Huang, B. et al. (2007) *Science* 315, 81-84; and Cal et al. (2006) *Nature* 440: 358-362. Microfluidic devices, as described herein, can include chambers of varying sizes. For example, chambers can be designed with a volume of approximately 500 pL (less than 1 nL), with dimensions of approximately 100 microns (width), 500 microns (length), and 10 microns (height).

As disclosed herein, antibody-antigen binding kinetics were measured with approximately 4×10^4 antibody molecules (~66 zeptomoles) immobilized on a single bead and less than 2×10^6 antibodies (~3 attomoles) loaded into the microfluidic device. This represents a reduction of greater than four orders of magnitude in both detection limit and sample consumption compared to SPR spectroscopy and a recently reported microfluidic fluorescence assay for measuring protein-protein binding kinetics. See, for e.g., Bates, S. R.; Quake, S. R. (2009), *Appl. Phys. Lett.* 95, 073705. Since each antibody-antigen interaction can be characterized on a single bead, millions of distinct antibody-antigen interactions can be characterized with a single lot of commercially available beads (i.e., 1 mL at 10^7-10^8 beads/mL). By using the bead surface rather than the chip surface as the sensor, a single microfluidic device may be re-used indefinitely and may be imaged using a standard inverted fluorescence microscope. However, a person of skill in the art could also apply the basic methods described herein to a microfluidic system having antigen and/or antibodies bound to the surface of a chip. It is further shown herein that an assay applying a method described herein may be used to perform simultaneous kinetic measurements of multiple antibody-antigen interactions using spatial and optical multiplexing. By comparison, characterization of each antibody-antigen interaction using SPR spectroscopy requires specialized instrumentation and a unique flow cell on comparatively expensive sensor chips. The low detection limit of the microfluidic bead assay coupled with small volume compartmentalization was exploited in order to measure the antigen binding kinetics of antibodies secreted by a single ASC. It is contemplated that the microfluidic

bead assay described herein could be used for measuring antibody-antigen binding kinetics from rare blood samples, for screening scarce antibodies produced by primary plasma cells from immunized animals, as well as for selecting clones for recombinant protein production. Additionally, it is contemplated that in addition to its utility for measuring antibody-antigen binding kinetics, the microfluidic bead-based assay described herein can be used for measuring other protein-protein and biomolecular interactions with a wide range of binding affinities, such as protein-carbohydrate binding, protein-DNA (i.e., transcription factor binding) and protein-RNA interactions. It is also contemplated that upon identifying an ASC that secretes antibodies which are optimal for a particular purpose, the ASC in question can be cloned by reverse-transcriptase PCR and standardized cloning techniques.

EXPERIMENTAL METHODS

Microfluidic Device Fabrication and Control

All microfluidic devices were fabricated using multilayer soft lithography (see, for e.g., Unger, M. A. et al. (2000), *Science*, 288: 113-116 and Thorsen, T. et al. (2002), *Science* 298: 580-584. Devices were composed of two layers of poly(dimethylsiloxane) (PDMS) elastomer (GE RTV 615) bonded to No 1.5 glass coverslips (Ted Pella, Inc.). The devices were designed in AutoCAD software (Autodesk) and printed on high resolution (20,000 dpi) transparency masks (CAD/Art Services). Master molds were fabricated in photoresist on silicon wafers (Silicon Quest) by standard optical lithography. The control master molds were fabricated out of 20-25 μm high SU-8 2025 photoresist (Microchem). The flow master molds were fabricated with 12 μm rounded SPR220-7.0 photoresist channels (Rohm and Haas) and 6 μm SU-8 5 photoresist (Microchem) channels with rectangular cross-section. Microfluidic valves were actuated at 30 psi pressure which was controlled using off-chip solenoid valves (Fluidigm Corp) controlled using LabView 7.1 software and a NI-6533 DAQ card (National Instruments). Compressed air (3-4 psi) was used to push reagent solutions into the device.

Reagent Preparation

Protein A-coated 5.4 μm diameter polystyrene beads (Bangs Labs) were incubated with lmg/mL solutions of Rabbit anti-mouse polyclonal antibodies (pAbs) (Jackson Immunoresearch). All antibody and antigen solutions were prepared in PBS/BSA/Tween solution consisting of 1×PBS, pH 7.4 (Gibco) with 10 mg/mL BSA (Sigma) and 0.5% Polyoxyethylene (20) sorbitan monolaurate (similar to Tween-20, EMD Biosciences). Lysozyme from chicken egg white (HEL) was purchased from Sigma, and the D1.3 and HyHEL-5 mouse monoclonal antibodies to lysozyme were generously provided by Dr. Richard Willson (University of Houston). The anti-GFP mouse monoclonal antibody (LGB-1) was purchased from Abcam. Fluorescent protein conjugates were prepared using Dylight488 and Dylight633 NHS esters (Pierce) and were purified using Slide-A-Lyzer dialysis cassettes (Pierce). The concentration of fluorescent conjugates was measured by spectrophotometry (Nanodrop). In order to minimize protein denaturation, fluorescent HEL conjugates were labeled at dye-to-protein (D/P) ratios of less than 1, whereas the D1.3-Dylight488 conjugate was prepared at a D/P ratio of ~5.

Microscopy

The microfluidic devices were imaged on a Nikon TE200 Eclipse inverted epifluorescence microscope equipped with green (470/40 nm excitation, 535/30 nm emission) and red (600/60 nm excitation, 655 nm long-pass emission) fluorescence filter cubes (Chroma Technology). Fluorescence images were taken using a 16-bit, cooled CCD camera (Apogee Alta U2000) and a 100× oil immersion objective (N.A. 1.30, Nikon Plan Fluor). The sensitivity of the fluorescence measurements was tuned by binning pixels on the CCD detection camera and modulating the fluorescence exposure times (20 ms-1 s) with a computer-controlled mechanical shutter (Ludl).

Cell Culture

Mouse D1.3 hybridoma cells were cultured in RPMI 1640 media (Gibco) with 10% FCS. Prior to loading into microfluidic devices, cells were washed by centrifugation at 1500 rpm and re-suspended in fresh media in order to remove antibodies secreted in the cell media.

Microfluidic Bead-Based Fluorescence Assay

A microfluidic device was designed and fabricated to perform bead-based fluorescence measurements of antigen-antibody binding kinetics (see FIGS. **1**A and B herein). The device consists of six fluidic inlets, each used for loading a distinct reagent and controlled with an independent control valve, which join into a common fluidic outlet. The fluidic outlet can be partitioned into discrete ~200 pL chambers by actuating a set of microfluidic "sieve" valves which, when actuated, act as filters to immobilize large particles (>1 micron) while still allowing fluid exchange. See, for e.g., Marcus, J. S. et al. (2006) *Analytical Chemistry* 78: 3084-3089.

At the start of the experiment, the fluidic outlet was flushed with a PBS/BSA/Tween solution from the top and bottom fluidic inlets in order to pre-coat channel walls and reduce nonspecific binding. Next, 5.4 μm diameter Protein A beads coated with Rabbit anti-mouse pAb were loaded through the device to the fluidic outlet. The microfluidic sieve valves were then actuated and the fluidic outlet was again washed with PBS/BSA/Tween solution to immobilize the beads against the traps and wash out any free rabbit pAb in solution. The beads were then washed with the mouse antibody selected for kinetic characterization. Again, free mouse antibody was washed out of the fluidic outlet using PBS/BSA/Tween. Finally, the beads were washed with fluorescently-labeled antigen and fluorescently imaged at defined time intervals to measure the rate of antibody-antigen association (see FIG. **1**C herein). When chemical equilibrium between the antibody and antigen was reached, as detected by a plateau in bead fluorescence, the beads were flushed with PBS buffer and imaged to measure the rate of antibody-antigen dissociation. The process was repeated with varying concentrations of fluorescently-labeled antigen, each loaded onto the microfluidic device from a separate fluidic inlet.

A second version of the microfluidic bead assay was implemented to indirectly measure dissociation kinetics between antibodies and unlabeled antigen molecules by displacement with fluorescently labeled antigen (see FIG. **1**D herein). In this assay, after the antibody of interest was captured on Rabbit anti-mouse pAb-coated Protein A beads, beads were washed with unlabeled antigen at high concentration (>1 μM) to saturate all antibody binding sites. Beads were then washed with fluorescently labeled antigen while imaging at defined time intervals. Dissociation of the unlabeled antigen was then inferred by accumulated fluorescence on the beads.

In order to measure the antigen binding kinetics from antibodies secreted from single cells, Protein A beads coated with Rabbit anti-mouse pAb were first immobilized in the fluidic outlet channel using the microfluidic sieve valves. A

solution of RPMI-1640 media containing 10^5 hybridoma cells/mL was then loaded into the device from a separate fluidic inlet and the control valve was momentarily opened to allow for a single hybridoma cell to be brought in close proximity with beads immobilized in the first sieve trap in the fluidic outlet channel. The hybridoma cell was then allowed to incubate next to the beads for 1 hour, and subsequently washed with PBS/BSA/Tween buffer to wash out any free antibody in solution and halt antibody secretion from the cell. Kinetic measurements of antigen binding were then performed in the same manner as with purified antibodies.

FIG. **2** shows a schematic diagram of a microfluidic device operable for detecting antibody secreted from antibody secreting cells. The steps utilized are, for example, as follows: (1) flush microfluidic channels with cell culture media; (2) load channels with antibody secreting cells (top) and capture beads (bottom); (3) incubate cells with beads to capture secreted antibody; (4) trap cells and beads with sieve valves and flush out unbound antibody by blowing buffer over cell-bead mixture; (5) flow fluorescently-labeled antigen over trapped cells and beads; and (6) flush out unbound antigen by blowing buffer over trapped cells and beads and image fluorescent beads.

Data Analysis.

Fluorescent images were analyzed using MaximDL 4 imaging software. Fluorescent intensities were measured by selecting line profiles through the beads and recording the maximum intensity at the bead surface. During protein binding experiments, line profiles were constructed through the same beads at each measurement time point in order to avoid any systemic variations caused by differences in bead-to-bead binding capacity, variation in position in the flow channel and non-uniform illumination over the field of view. The measured fluorescence bead intensities were assumed to be proportional to the concentration of antibody-antigen complex ([AbAg]) and were fit to the following first-order, mass action and Langmuir isotherm equations using nonlinear least squares minimization:

$$F(t) = (F_{max} - F_0)\frac{[Ag]_0}{[Ag]_0 + K_d}\left(1 - e^{-(k_{on}[Ag]_0 + k_{off})t}\right) + F_0 \quad \text{(equation 1)}$$

$$F(t) = (F_{max} - F_0)\frac{[Ag]_0}{[Ag]_0 + K_d}e^{-k_{off}t} + F_0 \quad \text{(equation 2)}$$

$$F(t) = (F_{max} - F_0)\frac{[Ag]_0}{[Ag]_0 + K_d} + F_0 \quad \text{(equation 3)}$$

where F(t) represents the measured bead fluorescence at time t, F_0 and F_{max} represent the background and maximum bead fluorescence, respectively, $[Ag]_0$ represents the solution concentration of antigen (in M), and, k_f and k_r represent the intrinsic association and dissociation rate constants, in units of M^{-1} s^{-1} and s^{-1}, respectively.

EXAMPLES

The following examples describe embodiments of the invention detailed herein.

Example 1. Measurement of Antibody-Antigen Binding Kinetics on Beads

The binding kinetics of the D1.3 mouse monoclonal antibody (mAb) to fluorescently-labeled hen egg lysozyme (HEL) was measured using the methodologies and techniques described herein. See: FIG. **3**A and Table 1 herein.

TABLE 1

Antibody-antigen binding kinetics measured using the microfluidic fluorescence bead assay.

Antibody/ Antigen interaction	k_{on} ($M^{-1}s^{-1}$)	k_{off}(s^{-1})	K_d
D1.3 mAb/ HEL-Dylight488	$1.87 \pm 0.48 \times 10^6$	$2.10 \pm 0.25 \times 10^{-3}$	1.20 ± 0.42 nM
D1.3 mAb/ HEL-Dylight633	$1.27 \pm 0.22 \times 10^6$	$2.15 \pm 0.23 \times 10^{-3}$	1.75 ± 0.46 nM
HyHEL-5 mAb/ HEL-Dylight633	$5.75 \pm 0.71 \times 10^6$	$1.69 \pm 0.30 \times 10^{-4}$	30.0 ± 7.4 pM
LGB-1 mAb/ EGFP	$5.00 \pm 0.72 \times 10^4$	$5.15 \pm 0.89 \times 10^{-3}$	106 ± 28 nM

The measured association and dissociation rate constants for the D1.3/HEL interaction were $1.87\pm0.48\times10^6$ M^{-1} s^{-1} and $2.10\pm0.25\times10^{-3}$ s^{-1}, respectively, and were consistent with values of $1.0\text{-}2.0\times10^6$ M^{-1} s^{-1} and $1.15\text{-}3.04\times10^{-3}$ s^{-1} previously measured using surface plasmon resonance (SPR) spectroscopy, stopped-flow fluorescence quenching, and competitive ELISA. See, for e.g., Batista, F. D. and Neuberger, M. S. (1998), *Immunity* 8: 751-759 and Ito, W. et al. (1995), *Journal of Molecular Biology* 248: 729-732. A ten-fold smaller association rate constant previously reported for the D1.3/HEL interaction (1.67×10^5 M^{-1} s^{-1}) can likely be attributed to differences between the full D1.3 mAb used in our microfluidic bead-based measurements and the recombinant single-chain antibody fragment used by Bedouelle and coworkers (England et al. (1999) J. Immunol. 162: 2129-2136).

Additionally, indirect, label-free measurements of the D1.3 mAb/HEL dissociation rate constant using a variation of our microfluidic bead assay were performed using the methodologies and techniques described herein. See: FIGS. **1**D and **3**D herein. In this assay, D1.3 mAbs immobilized on beads were first saturated with unlabeled HEL and subsequently washed with fluorescently-labeled HEL. Measurements of the accumulated bead fluorescence faithfully reflected the D1.3/HEL dissociation kinetics provided the labeled HEL was at a sufficiently high concentration to ensure that dissociation was rate-limiting (i.e. $k_{on}[Ag]>k_{off}$, or, equivalently, $[Ag]>K_d$). Using this method, the dissociation rate constant of D1.3 and unlabeled HEL was measured to be $1.45\pm0.30\times10^{-3}$ s^{-1}, in close agreement with direct dissociation measurements between D1.3 and fluorescently-labeled HEL. See Table 1 herein.

The microfluidic bead assay was used to measure the binding kinetics of HEL and HyHEL-5, a distinct mouse mAb with significantly stronger binding affinity to HEL than D1.3. In comparison to the D1.3 mAb, HyHEL-5 bound HEL with a nearly four-fold larger association rate constant ($5.75\pm0.71\times10^6$ M^{-1} s^{-1}) and ten-fold smaller dissociation rate constant ($1.69\pm0.30\times10^{-4}$ s^{-1}). See: FIG. **3**B herein. Thus, HyHEL-5 bound HEL with a ~40-fold smaller equilibrium dissociation constant than D1.3 (30 pM vs. 1.2 nM). See: Table 1 herein. Compared with the microfluidic bead assay, previous measurements of the HyHEL-5/HEL interaction using solution-phase fluorescence anisotropy resulted in a similar dissociation rate constant (2.2×10^{-4} s^{-1}), but a three- to five-fold larger association rate constant ($1.5\text{-}3.3\times10^7$ M^{-1} s^{-1}). See, for e.g., Xavier, K. A. and Willson, R. C. (1998) *Biophys. J.* 74: 2036-2045. Since HyHEL-5 mAb

binds HEL with near diffusion-limited association kinetics, immobilization of the mAb in the microfluidic bead assay could potentially result in slower association kinetics when compared with solution-phase fluorescence anisotropy measurements. However, since the diffusion constant of HEL is approximately three times larger than that of the mAb, immobilization of the HyHEL-5 mAb would reduce the effective diffusion coefficient ($D \cong D_{mAb}+D_{HEL}$) and, hence, the apparent association rate constant by at most 25%. See, for e.g., Tyn, M. T. and Gusek, T. W. (1990), *Biotechnology and Bioengineering* 35: 327-338 and He, L. and Niemeyer, B. (2003), *Biotechnol. Prog.* 2003, 19: 544-548. Therefore, the difference in measured and reported association rate constants is likely a result of different buffer solutions, as the HyHEL-5 and HEL binding interaction is known to be very sensitive to solution pH and buffer salt concentration. See, for e.g., Xavier, K. A. and Willson, R. C. (1998) *Biophys. J.* 74: 2036-2045 and Dlugosz et al. (2009), *The Journal of Physical Chemistry* 113: 15662-15669.

The binding kinetics of a commercially available mouse monoclonal antibody (LGB-1, Abcam) to enhanced green fluorescent protein (eGFP) were also measured using the methodologies and techniques described herein. See: FIG. **3** herein. This binding interaction was chosen to demonstrate that the bead-based assay can be used to measure binding kinetics of a previously uncharacterized antibody without optimizing the bead immobilization chemistry. In this instance, native eGFP fluorescence was measured without an exogenous fluorescent label. The measured association and dissociation rate constants for the LGB-1/eGFP interaction were $5.00\pm0.72\times10^{4}$ M^{-1} s^{-1} and $5.15\pm0.89\times10^{-3}$ s^{-1}, respectively. See: Table 1 herein.

Collectively, the measured binding kinetics of the anti-lysozyme and anti-eGFP mAbs span nearly four orders of magnitude in equilibrium dissociation constants (30 pM-100 nM), with association rate constants varying from 5×10^{4}-10^{6} M^{-1} s^{-1} and dissociation rate constants ranging from 10^{-3}-10^{-4} s^{-1}. See: Table 1 herein. In principle, the microfluidic bead-based assay can be used to characterize stronger antibody-antigen interactions than the HyHEL-5/HEL interaction; however, binding interactions with dissociation rate constants lower than 10^{-4} s^{-1} require measurements to be taken over several days or weeks. On the other hand, the bead-based assay can be readily used to measure binding interactions weaker than the LGB-1/eGFP interaction. Using this assay, the practical upper limit in measurable dissociation rate constants is approximately 10^{-1} s^{-1}, as a result of the time required to exchange solutions in the microfluidic device. Thus, the microfluidic bead-based assay should enable characterization of antibody-antigen interactions that span greater than six orders of magnitude in equilibrium binding affinity.

Example 2. Simultaneous Measurement of Multiple Antibody-Antigen Binding Kinetics Using Optical and Spatial Multiplexing

The binding kinetics of multiple antibody-antigen interactions were measured simultaneously using both optical and spatial multiplexing of the bead-based assay using the methodologies and techniques described herein. Each antibody was immobilized on a distinct population of beads and, subsequently, beads from each population were sequentially trapped using sieve valves on the microfluidic device. Since beads trapped by the sieve valves remain immobilized throughout the duration of each experiment, the spatial address of beads was tracked in order to identify each antibody. Subsequently, the trapped beads were washed with a mixture of antigens, each labeled with a spectrally distinct fluorophore. The beads were then imaged with different fluorescence filter sets designed to coincide with each fluorescent antigen. In this manner, the binding kinetics of 3 different monoclonal antibodies (D1.3, HyHEL-5 and LGB-1) to two different fluorescent antigens (HEL-Dylight488 and eGFP) were simultaneously measured. See: FIG. **4** herein. By employing this strategy, it was possible to spectrally distinguish which beads were coated with anti-lysozyme mAbs or anti-eGFP mAbs, whereas the two anti-lysozyme mAbs (D1.3 and HyHEL-5) were discriminated based on their unique binding kinetics for HEL. In addition, the fluorescence intensities of HyHEL-5 coated beads were significantly higher than the D1.3 coated beads, consistent with the fact that HyHEL-5 binds HEL with a significantly lower equilibrium dissociation constant than D1.3. See: FIG. **4** herein. This technique can be extended to measure any combination of m×n antibody-antigen interactions in which m antibodies are immobilized on different beads and exposed to a solution of n antigens, each with a spectrally-resolvable fluorescent label. In practice, several hundred antibody-antigen interactions could be measured simultaneously by imaging up to 100 beads in a single field of view with five to six spectrally distinct fluorophores. Multiplexed bead measurements could be used for simultaneously analyzing the binding kinetics and binding specificities of a panel of mAbs to multiple different antigens in serum and other complex mixtures.

Example 3. Microfluidic Bead-Based Fluorescence Measurements Reflect Intrinsic Antibody-Antigen Binding Kinetics

A series of experiments were performed using the methodologies and techniques described herein to verify that bead-based fluorescence measurements reflected intrinsic antibody-antigen binding kinetics, and were unaffected by artifacts arising from fluorescent labeling of the antigen, antibody immobilization, diffusion limitation or mass transport effects. Fluorescent labeling of HEL did not alter the intrinsic D1.3/HEL binding kinetics, as indicated by the agreement between microfluidic bead-based measurements using fluorescently labeled HEL and previously reported measurements using SPR spectroscopy with unlabeled HEL. See, for e.g., Batista, F. D. and Neuberger, M. S. (1998), *Immunity* 8: 751-759 and Ito, W. et al. (1995), *Journal of Molecular Biology* 248: 729-732. Moreover, no differences were observed in bead-based kinetic measurements of the D1.3 mAb binding to HEL labeled with two different fluorophores, Dylight488 and Dylight633 (Pierce). See: Table 1 herein. It was ensured that photobleaching of fluorophores did not affect the measured binding kinetics by measuring the photobleaching rates of the of the fluorescent dyes used in this study (Dylight488, Dylight633, and eGFP) and selecting fluorescence exposure times of less than 100 ms, such that each measurement resulted in less than 5% reduction in bead fluorescence. See: FIG. **7**A herein. Indeed, measured binding kinetics were consistent over a large range of fluorescence exposure times (ms), whereas exposure times of greater than 1 s resulted in substantial photobleaching and an artificial increase in measured association and dissociation binding kinetics when compared to intrinsic kinetics. See FIG. **7**B herein.

To examine the effect of different antibody bead immobilization chemistries, we verified that measured association and dissociation rate constants for the D1.3/HEL interaction

were the same when captured on silica or polystyrene beads coated with either rabbit or goat anti-mouse polyclonal antibody. See: FIG. **8** herein. It was further verified that multivalent binding between the rabbit anti-mouse pAbs and fluorescently-labeled D1.3 mAb resulted in no detectable dissociation over the course of 3 days, which would otherwise artificially accelerate the measured antibody-antigen binding kinetics. See: FIG. **9** herein. The nearly irreversible bond between rabbit pAb and the mouse mAbs was critical to successful antibody-antigen binding kinetic measurements as attempts to measure D1.3/HEL binding kinetics using Protein A beads without Rabbit anti-mouse pAbs were unsuccessful due to rapid dissociation (and low affinity) of protein A/mouse mAb complexes.

Several experiments were also conducted to verify that diffusion limitation and mass transport did not affect bead-based measurements of antibody-antigen binding kinetics. In the diffusion-limited regime, antibodies adjacent on the bead surface would compete for fluorescent antigen, thus reducing the apparent association rate constant. Similarly, the apparent rate of antibody-antigen dissociation would be reduced due to antigen rebinding to adjacent antibodies. See, for e.g., Berg, H. C. and Purcell, E. M. (1977), *Biophys. J.* 20: 193-219 and Lauffenburger, D. A. and Linderman, J. (1965) *Receptors: Models for Binding, Trafficking, and Signaling*; Oxford University Press. Nearly identical association and dissociation kinetics for the D1.3-HEL interaction was measured by varying the amount of bead-immobilized D1.3 mAb over two orders of magnitude. See FIG. **10**B herein. Dissociation kinetics of the D1.3 antibody and fluorescently labeled HEL were also similar both in the presence and absence of a high concentration (~2 mg/mL) of competitive unlabeled HEL antigen. See: FIG. **10** herein. Thus, there was no observable competition between antibodies adjacent to one another on the beads and, hence, no diffusion limitation. It was also confirmed that the association and dissociation rate constants of the D1.3-HEL interaction remained constant over a range of flow rates from 3-15 μL/hr, suggesting no effect of mass transport on the measured kinetics. See: FIG. **11** herein.

Example 4. Bead-Based Kinetic Measurements Exhibit Low Detection Limits and Minimal Sample Consumption

To quantify the detection limit and minimal sample consumption required for microfluidic bead-based measurements of antibody-antigen binding kinetics, antibody-antigen binding kinetics were measured using varying amounts of bead-immobilized mAb along with the methodologies and techniques described herein. The association rate constant of fluorescently-labeled D1.3 mAb binding to Rabbit anti-mouse pAb coated Protein A beads was measured. See: FIG. **5**A herein. Using the measured kinetic on-rate constant for this interaction (k_{on}=1.10±0.11×10^6 M^{-1} s^{-1}) and modulating the loading time of D1.3 mAb, the amount of bead-immobilized D1.3 mAb was varied over two orders of magnitude. Then, the antibody-antigen binding kinetics with as little as 1% of the bead surface covered with D1.3 mAb was successfully measured. See: FIG. **5**B herein. Using the manufacturer's specifications as well as steric considerations, a single 5.5 micron bead can bind 4×10^6 antibody molecules (~6.6 amol); therefore, it was estimated that the detection limit of our microfluidic fluorescence bead assay is to be ~4×10^4 antibodies or ~66 zeptomoles. See: FIG. **5**C herein. In contrast, SPR spectroscopy requires at least 200 pg (~10^9 molecules) of immobilized antibody in order to generate a detectable refractive index change. See, for e.g., Biacore Life Sciences—Biacore 3000 System Information. Website: http://www.biacore.com/lifesciences/products/systems_overview/3000/system_information/index.html. Additionally, D1.3/HEL binding kinetics were successfully measured by loading less than 2 million D1.3 mAb molecules (~3 attomoles) into the microfluidic device. In theory, the minimum sample consumption of the microfluidic bead assay could be reduced even further by reducing losses associated with channel dead volumes and optimizing the capture efficiency of antibodies on beads, as well as using microfluidic pumps to achieve flow rates less than 1 μL/hr. Thus, when compared with alternative techniques and SPR spectroscopy, our microfluidic bead-based assay can measure antigen-antibody binding kinetics with a reduction in both detection limit and sample consumption by four orders of magnitude.

Example 5. Measurement of Binding Kinetics of Antigen and Antibody Secreted from Single Cells

Based on the low detection limit of the bead-based assay and in an effort to measure the antigen binding kinetics of antibodies secreted from single antibody secreting cells, single D1.3 hybridoma cells were loaded adjacent to Rabbit anti-Mouse pAb coated Protein A beads captured in the microfluidic device, and then co-incubated the cells and beads for 1 hour at room temperature. See: FIG. **6** herein. Subsequently, antibody-antigen binding kinetics were measured by recording the fluorescence of a single bead washed with buffer and successively higher concentrations of fluorescent antigen, in a manner analogous to the single-cycle kinetics technique used with SPR spectroscopy. See, for e.g., Biacore Life Sciences—Single-Cycle Kinetics. Website: http://www.biacore.com/lifesciences/technology/introduction/data_interaction/SCK/index.htm 1 and Abdiche et al. (2008) *Analytical Biochemistry* 377: 209-217. Using the methodologies and experimental techniques described herein, the association and dissociation rate constants for the D1.3/HEL interaction were successfully measured using antibodies secreted by a single D1.3 hybridoma cell, which were consistent with measurements on purified antibodies. See: FIG. **6** and Table 1 herein.

Antibody-secreting cells are known to secrete thousands of antibodies per second at 37° C., and would, therefore, secrete enough antibodies in approximately one hour to saturate the surface of a single 5.5 μm bead with maximum binding capacity of ~4×10^6 antibody molecules. See, for e.g., Niels Jerne (1984) The Generative Grammar of the Immune System and McKinney et al. (1995) *Journal of Biotechnology* 40: 31-48. While it is reasonable to suspect that the hybridoma cells secrete antibodies at a reduced rate when incubated at room temperature; nonetheless, single D1.3 hybridoma cells secreted sufficient antibody within 1 hour at room temperature for complete kinetic characterization. However, based on the incubation time and detection limit of the assay (~4×10^4 antibodies), it can be inferred that single hybridoma cells secreted greater than 10 antibodies/second when incubated at room temperature in the microfluidic device.

Examples 1-5 show that the methods described herein are suitable for measuring antibody-antigen kinetics in a microfluidic environment from a single cell.

Example 6. Dual Function Beads

An overview of a scheme for preparing dual-capture (i.e., dual function) beads using carbodiimide chemistry is shown

in FIG. **14**. A representative experiment utilizing dual function beads is shown in FIG. **15**. Briefly, polystyrene COOH beads (Bangs Labs) were conjugated with Rabbit anti-mouse pAb (Jackson ImmunoResearch) and amine-functionalized oligo(dT)$_{25}$ (Genelink) using carbodiimide chemistry. In FIG. **14**(A), a brightfield image of dual-function beads trapped using a microfluidic sieve valve is shown. In FIG. **14**(B), a fluorescence image of synthetic single-stranded DNA molecules captured on dual-function beads is shown. Synthetic DNA molecules are labeled with Cy5 fluorophore for visualization and also contain a poly(A) tail that binds to the oligo(dT) on the bead surface. In FIG. **14**(C), a fluorescence image of mouse D1.3 monoclonal antibody (mAb) captured on dual-function beads. D1.3 mAbs are labeled with Dylight488 fluorophore for visualization and bind to the Rabbit anti-Mouse pAb on the bead surface.

It will be understood that while carboxylic acid (COOH) beads are disclosed herein, other beads, which make use of alternate chemical interactions, could also be used, See: for e.g., G. T. Hermanson (2008), *Bioconjugate Techniques,* 2nd Edition, Published by Academic Press, Inc. For example, an alternate scheme for preparing thee beads would be to use streptavidin coated beads and to mix these beads with biotinylized rabbit anti-mouse pAbs and biotinylated oligo (dT).

Example 7. Multiplex RT-PCR of the Antibody Heavy and Light Chain Genes

Results from a multiplex RT-PCR of the antibody heavy and light chain genes indicated that a gene product coinciding with the proper molecular size was obtained. Briefly, D1.3 hybridoma cells were lysed using a nonionic detergent (1% NP-40 in 1×PBS) and the lysate was then mixed with rabbit anti-mouse pAb, oligo(dT)-conjugated dual-capture beads for mRNA capture. Generally, a gentle lysis buffer is preferred for cell lysis and can include, in addition to the foregoing: 0.5% NP-40 in 1×PBS or DI water or 0.5% Tween-20 in 1×PBS or DI water. Generally, it is preferable and within the knowledge of those persons skilled in the art to use lysis buffers that can sufficiently lyse the outer membrane of the cell in question, while keeping the nucleus intact. RT-PCR was performed using degenerate primers for both heavy and light chain genes and resulted in bands of the expected size for antibody heaby and light chains (date not shown). The results suggest that dual purpose RNA and antibody beads are capable of capturing RNA suitable for amplification. For comparison, RT-PCR of antibody genes was performed using commercially available oligo(dT) beads and dual-capture beads. The methodology utilized herein is generally as follows:

1) Capture oligo(dT) beads in microfluidic chambers using sieve valves.
2) Load cells in microfluidic chambers.
3) Load antibody-capture beads in chambers.
4) Incubate cells and beads.
5) Measure antibody-antigen binding kinetics.
6) Lyse cells using either a) 1% NP-40 in 1×PBS, or b) alkaline lysis solution (100 mM Tris-HCl, pH 7.5, 500 mM LiCl, 10 mM EDTA, pH 8.0 1% LiDS, 5 mM dithiothreitol (DTT)). During lysis, the cell lysate is flushed over the stack of trapped oligo(dT) beads. The oligo(dT) beads and alkaline lysis solution are from the Dynabead mRNA direct kit developed by Invitrogen, but alternatives to these reagents exist.
7) Wash beads with 1×PBS to remove lysis solution.
8) Open sieve valves.
9) Open microfluidic chamber valves and send beads to an output port (one chamber at a time).
10) Recover beads from output port using a pipette.
11) Pipette beads into 50 microL of one-step RT-PCR mix.
    i) dNTPs;
    ii) mixture of RT and DNA polymerase enzymes;
    iii) degenerate primers for both heavy and light chain genes (PCR reagents from a One-Step RT-PCR kit developed by Qiagen, but could also be prepared ourselves);
12) Perform RT and Touchdown PCR using the following protocol:
    i) RT at 50° C. for 30 min;
    ii) 95° C. for 15 min to inactivate RT enzyme and activate DNA polymerase
    iii) First ten cycles of Touchdown PCR:
    a) 94° C. for 30 s;
    b) 55° C. for 1 min (decrease by 1C each cycle, until 45C);
    c) 72° C. for 1 min.
    iv) 30 cycles of PCR
    a) 94° C. for 30 s;
    b) 45° C. for 1 min;
    c) 72° C. for 1 min.
13) Visualize RT-PCR amplicons on 0.5% DNA agarose gel using SYBRsafe fluorescent dye.
14) Extract amplicons from gel and purify using standard gel extraction kit (Qiagen).
15) Sequence samples.

Example 8. Microfluidic Antibody-Antigen Binding Kinetics Measured Using Dual Function Beads and Antibodies Secreted by Single Hybridoma Cells

Microscope image of D1.3 hybridoma cell adjacent to Rabbit anti-Mouse pAb, oligo(dT)-conjugated polystyrene beads trapped by a microfluidic sieve valve. After a 2 hour incubation the beads with the D1.3 cell, antibody-antigen binding kinetics were measured using fluorescently labeled HEL-Dylight488 conjugate. These results are highlighted in FIG. **16** and show that dual purpose beads are suitable for testing antibody-antigen binding kinetics.

Example 9. Mouse Experiment: Antibody Binding Kinetics and Whole-Cell Heavy Chain RT-PCR with Beads

These experiments were designed to detect antibodies from primary splenocytes harvested from BALB/c immunized mice. The cells were eluted and whole-cell single-plex RT-PCR was performed of heavy and light chain antibody genes. Thereafter, binding kinetics of the antibodies were measured.

Chip.

Bead v6.6 chip with ~3 micron high sieve channels, 2 micron gratings (fabricated: May 29, 2011 with RTV615).

Reagents.

The following reagents were used herein: 1×PBS for reagent flush; FACS-sorted CD138+ primary splenocytes in RPMI-10-2-ME media; 4.9 micron Rabbit anti-Mouse Protein A beads; 5 microL of stock bead solution resuspended in 100 μL of RPMI-10-2-ME media; and 214 ng/mL HEL488 in 1×PBS.

Experimental Protocol.

The following experimental protocol was followed: washed chip with 1×PBS; closed sieve valves; spun down

primary cells and decanted ~400 of 500 pt of media; and re-suspended cells in remaining media.

Thereafter, the cells were loaded in all chambers sequentially with deliberate negative controls included (e.g., R1C14 and R0C02); load 4.9 micron Rabbit anti-Mouse Protein A beads in all chambers sequentially; incubate cells and beads for 1 h 20 min; and wash all chambers with 214 ng/mL HEL488 for 5 min. Thereafter, chamber intensities were analyzed using Image Analysis. Positive chambers were determined as follows: R0004, R0008, R2C02, R2C04, R2C07, R2C12, R2C13, R3C06, R4C01, R4C03, R4C05, R5C08, R5C09, R5C12, R5C14, R6C01, R6C02, R6C09, R6C10, R6C11, and R7C05.

RT-PCR mix without primers was prepared from a One-Step RT-PCR kit (Qiagen). The mix comprised: 10 μL 5×RT-PCR buffer×16=160 μL; 21 μL RNase-free water×16=336 μL; 2 μL dNTPs×16=32 μL; 2 μL Enzyme mix×16=32 pL. The RT-PCR mix without primers was aliquoted into 8 tubes of 70 μL each (2 reaction volumes, not including primer volume).

Prepared primer solutions to be mixed with RT-PCR after cell elution were as follows: Heavy chain-7.5 μL 8 μM 3' IgH first primer×8=60 μL; and 7.5 μL 8 μM 5' IgH first primer×8=60 pt. Kappa chain-7.5 μL 8 μM 3' IgK first primer×8=60 μL; and 7.5 μL 8 μM 5' IgK first primer×8=60 μL. 15 μL of primer mixes were aliquoted into each of 8 tubes. The primers used herein were selected based on what is taught in Table II of Tiller et al. (2009) *J. Immunol. Methods* 350: 183-193, which is incorporated herein by reference. Those persons skilled in the art that variants to the primers defined in Table II could be used under certain circumstances including, for example, the primers in Table III in Tiller et al. (2009).

Eight (8) of the brightest chambers [R0004, R2C04, R2C07, R3C06, R5C12, R5C14, R6C01, R6C10] were eluted. The eluted cell samples were pipetted directly into 70 μL RT-PCR mix without primers. The RT-PCR/cell mix was split into two (2) equal parts of 35 μL and mixed with kappa and heavy chain primers, respectively. RT-PCR was performed using a thermal cycler. Briefly, the "NEST1ST5" protocol was used for the kappa chain reactions, comprising: RT step: 50° C. for 30 min; Hotstart/RT inactivation: 95° C. for 15 min; and 50 Cycles (denaturation: 94° C. for 30 s; anneal: 50° C. for 30 s; and extension: 72° C. for 55 s). Then, there was a final extension: 72° C. for 10 min. Heavy chain reactions performed using the "NEST1H" protocol, comprising: RT step: 50° C. for 30 min; Hotstart/RT inactivation: 95° C. for 15 min; and 50 Cycles (denaturation: 94° C. for 30 s; anneal: 56° C. for 30 s; extension: 72° C. for 55 s). Then, there was a final extension: 72° C. for 10 min.

Thereafter, kinetics were measured on each of the eluted chambers. A summary of the kinetics data is shown in FIG. **17**. Representative kinetics sample data is shown in each of FIGS. **18**A-E herein. Dissociation kinetics were measured and then association kinetics were measured using freshly loaded HEL488. Thereafter, a second round of single-plex RT-PCR was performed using nested second round primers. The heavy chain mix comprised of: 10 μL 5×RT-PCR buffer×8=80 μL; 21 μL RNase-free water×8=168 μL; 2 μL dNTPs×8=16 μL; 2 μL Enzyme mix×8=16 μL; 7.5 μL 8 μM 3' IgH second primer×8=45 μL; and 7.5 μL 8 μM 5' IgH second primer×8=45 μL. The kappa chain mix comprised of: 10 μL 5×RT-PCR buffer×8=80 μL; 21 μL RNase-free water×8=168 μL; 2 μL dNTPs×8=16 μL; 2 μL Enzyme mix×8=16 μL; 7.5 μL 8 μM 3' IgK second primer×8=45 μL; and 7.5 μL 8 μM 5' IgK second primer×8=45 μL. Thereafter, 3.5 μL of template from each of the first round reactions was added and RT-PCR was performed on a thermal cycler. Kappa chain reactions were performed using the "NEST2K" protocol. Briefly, there was no RT step; hotstart/RT inactivation was at 95° C. for 15 min followed by 50 cycles (denaturation: 94° C. for 30 s; anneal: 45° C. for 30 s; and extension: 72° C. for 55 s). Then, there was a final extension: 72° C. for 10 min. Heavy chain reactions performed using the "NEST2H" protocol. Briefly, there was no RT step; hotstart/RT inactivation: 95° C. for 15 min, followed by 50 cycles (denaturation: 94° C. for 30 s; anneal: 60° C. for 30 s; and extension: 72° C. for 55 s). Then, there was a final extension: 72° C. for 10 min. The RT-PCR products for both first and second round reactions were run on a gel. Kappa chain results from the first round are shown in FIG. **19**A. Kappa chain results from the second round are shown in FIG. **19**B. Heavy chain results from the first round are shown in FIG. **19**C. Heavy chain results from the second round are shown in FIG. **19**D. The gel products were sequenced by standard procedures known to those skilled in the art. Based on the sequence data generated, variants in antibody sequences were detectable. As a representative example, mutations in the R00C04 sample are shown in Table 2 herein.

TABLE 2

R00C04 (9 non-synonymous mutations)

Position (from IMGT)	Situation (from IMGT)	Germline Ab residue	R00C04 Ab residue
L-36	CDR1-L	S	N
L-92	FR3-L	S	T
H-17	FR1-H	A	D
H-36	CDR1-H	S	R
H-40	FR2-H	H	L
H-64	CDR2-H	N	K
H-65	CDR2-H	T	S
H-83	FR3-H	S	I
H-94	FR3-H	P	L

Example 10. Microfluidic Device

A microfluidic device has been developed for assaying a binding interaction between a protein produced by a cell and a biomolecule. The device has a chamber having an aperture and a channel for receiving a flowed fluid volume through the chamber via said aperture. The channel provides for size selection for a particle within the fluid volume. Alternately, another embodiment of the microfluidic device has a chamber having an aperture and a reversible trap. The reversible trap has spaced apart structural members extending across the chamber. The structural members are operable to allow a fluid volume to flow through the chamber while providing size selection for a particle within the fluid volume. See, for example: FIG. **20** herein.

Although various embodiments of the invention are disclosed herein, many adaptations and modifications may be made within the scope of the invention in accordance with the common general knowledge of those skilled in this art. Such modifications include the substitution of known equivalents for any aspect of the invention in order to achieve the same result in substantially the same way. Numeric ranges are inclusive of the numbers defining the range. The word "comprising" is used herein as an open-ended term, substantially equivalent to the phrase "including, but not limited to", and the word "comprises" has a corresponding meaning. As used herein, the singular forms "a", "an" and "the" include plural referents unless the

context clearly dictates otherwise. Thus, for example, reference to "a thing" includes more than one such thing. Citation of references herein is not an admission that such references are prior art to the present invention. The invention includes all embodiments and variations substantially as hereinbefore described and with reference to the examples and drawings. Further, citation of references herein is not an admission that such references are prior art to the present invention nor does it constitute any admission as to the contents or date of these documents.

What is claimed is:

1. A method of assaying a secreted monoclonal antibody produced by a single antibody producing cell (APC) and an antigen, the method comprising:

retaining the single APC within a chamber having a volume of from 100 pL to 100 nL, a solid wall, and an aperture that defines an opening of the chamber;

incubating the single APC within the chamber to produce a secreted monoclonal antibody;

exposing the secreted monoclonal antibody to a first removeable capture substrate bound to an antigen;

determining whether the secreted monoclonal antibody binds the antigen;

lysing the single APC and capturing the nucleic acids of the single APC on a second removeable capture substrate.

2. The method of claim **1**, wherein the single APC is a primary B cell or a memory B cell.

3. The method of claim **1**, wherein the single APC is a primary plasma cell.

4. The method of claim **1**, wherein the single APC is from a human, a rabbit, a rat, a mouse, a sheep, an ape, a monkey, a goat, a dog, a cat, a camel, or a pig.

5. The method of claim **1**, wherein the antigen is fluorescently labeled.

6. The method of claim **1**, wherein the second removeable capture substrate comprises an oligo(dT) mRNA capture bead capable of binding mRNA from the single APC.

7. The method of claim **5**, wherein the second removeable capture substrate comprises an oligo(dT) mRNA capture bead capable of binding mRNA from the single APC.

8. The method of claim **1**, wherein the second removeable capture substrate is capable of binding nucleic acids encoding the variable regions of the secreted monoclonal antibody and capturing the nucleic acids comprises capturing nucleic acids encoding the variable regions of the secreted monoclonal antibody.

9. The method of claim **5**, wherein the second removeable capture substrate is capable of binding nucleic acids encoding the variable regions of the secreted monoclonal antibody and capturing the nucleic acids comprises capturing nucleic acids encoding the variable regions of the secreted monoclonal antibody.

10. The method of claim **1**, further comprising washing the second removeable capture substrate after lysing.

11. The method of claim **5**, further comprising washing the second removeable capture substrate after lysing.

12. The method of claim **6**, further comprising washing the second removeable capture substrate after lysing.

13. The method of claim **7**, further comprising washing the second removeable capture substrate after lysing.

14. The method of claim **8**, further comprising washing the second removeable capture substrate after lysing.

15. The method of claim **1**, further comprising recovering the first removeable capture substrate and the second removeable capture substrate.

16. The method of claim **1**, further comprising recovering the second removeable capture substrate.

17. The method of claim **5**, further comprising recovering the second removeable capture substrate.

18. The method of claim **6**, further comprising recovering the second removeable capture substrate.

19. The method of claim **8**, further comprising recovering the second removable capture substrate.

20. The method of claim **19**, further comprising sequencing the nucleic acids encoding the variable regions of the secreted monoclonal antibody.

21. The method of claim **1**, wherein determining whether the secreted monoclonal antibody binds the antigen comprises measuring an antigen-antibody binding kinetic property between the antigen and secreted monoclonal antibody.

22. The method of claim **21**, wherein the antigen-antibody binding kinetic property is a K_{on} rate; a K_{off} rate, a dissociation constant, or a combination thereof.

23. The method of claim **1**, wherein determining whether the secreted monoclonal antibody binds the antigen comprises measuring the affinity of the secreted monoclonal antibody and the antigen.

24. The method of claim **1**, wherein determining whether the secreted monoclonal antibody binds the antigen comprises measuring the avidity of the secreted monoclonal antibody and the antigen.

25. The method of claim **1**, wherein the antigen is a cell fragment, a bacterium, a virus, a viral fragment, or a protein.

26. The method of claim **1**, wherein the aperture serves as the inlet and the outlet of the chamber.

27. The method of claim **1**, wherein determining whether the secreted monoclonal antibody binds the antigen comprises fluorescence imaging of the chamber.

28. The method of claim **1**, wherein determining whether the secreted monoclonal antibody binds the antigen comprises a surface plasmon resonance (SPR) spectroscopy, fluorescence anisotropy, interferometry or fluorescence resonance energy transfer (FRET) measurement.

29. The method of claim **1**, further comprising performing a reverse transcription polymerase chain reaction (RT-PCR) on the nucleic acids of the single APC to amplify the heavy and light chain genes of the secreted monoclonal antibody.

30. The method of claim **5**, further comprising performing a reverse transcription polymerase chain reaction (RT-PCR) on the nucleic acids of the APC to amplify the heavy and light chain genes of the secreted monoclonal antibody.

* * * * *

Exhibit 3

US010775378B1

(12) **United States Patent**
Singhal et al.

(10) **Patent No.: US 10,775,378 B1**
(45) **Date of Patent: *Sep. 15, 2020**

(54) **METHODS FOR ASSAYING CELLULAR BINDING INTERACTIONS**

(71) Applicant: **The University of British Columbia**, Vancouver (CA)

(72) Inventors: **Anupam Singhal**, Mississauga (CA); **Carl L. G. Hansen**, Vancouver (CA); **John W. Schrader**, Vancouver (CA); **Charles A. Haynes**, Vancouver (CA); **Daniel J. Da Costa**, Pitt Meadows (CA)

(73) Assignee: **The University of British Columbia**, Vancouver (CA)

(*) Notice: Subject to any disclaimer, the term of this patent is extended or adjusted under 35 U.S.C. 154(b) by 0 days.

This patent is subject to a terminal disclaimer.

(21) Appl. No.: **16/912,488**

(22) Filed: **Jun. 25, 2020**

Related U.S. Application Data

(63) Continuation of application No. 16/746,540, filed on Jan. 17, 2020, which is a continuation of application
(Continued)

(51) **Int. Cl.**
B01L 3/00 (2006.01)
G01N 33/569 (2006.01)
(Continued)

(52) **U.S. Cl.**
CPC .. ***G01N 33/56966*** (2013.01); ***B01L 3/502738*** (2013.01); ***B01L 3/502761*** (2013.01);
(Continued)

(58) **Field of Classification Search**
None
See application file for complete search history.

(56) **References Cited**

U.S. PATENT DOCUMENTS

5,874,085 A 2/1999 Mond et al.
6,007,690 A 12/1999 Nelson et al.
(Continued)

FOREIGN PATENT DOCUMENTS

WO 2003085379 A3 12/2003
WO 2005069980 A2 8/2005
(Continued)

OTHER PUBLICATIONS

Abdiche et al. (2008) "Determining kinetics and affinities of protein interactions using a parallel real-time label-free biosensor, the Octet" Analytical Biochemistry 377(2):209-217.
(Continued)

Primary Examiner — Rebecca M Giere
(74) *Attorney, Agent, or Firm* — Potomac Law Group, PLLC

(57) **ABSTRACT**

There are provided methods, and devices for assaying for a binding interaction between a protein, such as a monoclonal antibody, produced by a cell, and a biomolecule. The method may include retaining the cell within a chamber having an aperture; exposing the protein produced by the cell to a capture substrate, wherein the capture substrate is in fluid communication with the protein produced by the cell and wherein the capture substrate is operable to bind the protein produced by the cell; flowing a fluid volume comprising the biomolecule through the chamber via said aperture, wherein the fluid volume is in fluid communication with the capture substrate; and determining a binding interaction between the protein produced by the cell and the biomolecule.

30 Claims, 29 Drawing Sheets

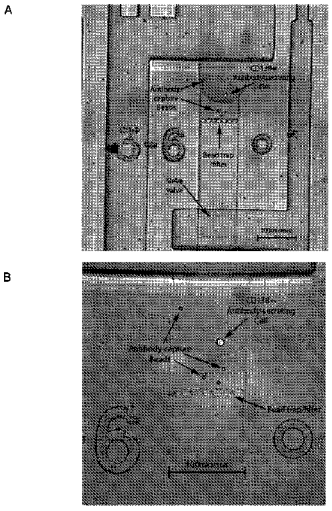

Related U.S. Application Data

No. 16/579,561, filed on Sep. 23, 2019, now Pat. No. 10,578,618, which is a continuation of application No. 16/290,751, filed on Mar. 1, 2019, now Pat. No. 10,466,241, which is a continuation of application No. 16/129,555, filed on Sep. 12, 2018, now Pat. No. 10,274,494, which is a continuation of application No. 14/879,791, filed on Oct. 9, 2015, now Pat. No. 10,107,812, which is a continuation of application No. 13/184,363, filed on Jul. 15, 2011, now Pat. No. 9,188,593.

(60) Provisional application No. 61/365,237, filed on Jul. 16, 2010.

(51) **Int. Cl.**

G01N 33/68	(2006.01)
G01N 33/577	(2006.01)
G01N 33/58	(2006.01)

(52) **U.S. Cl.**

CPC ***G01N 33/577*** (2013.01); ***G01N 33/582*** (2013.01); ***G01N 33/6854*** (2013.01); *B01L 2200/0668* (2013.01); *B01L 2300/0681* (2013.01); *B01L 2300/0861* (2013.01); *B01L 2300/0864* (2013.01); *B01L 2300/0867* (2013.01); *B01L 2400/0481* (2013.01)

(56) **References Cited**

U.S. PATENT DOCUMENTS

7,143,785	B2	12/2006	Maerkl et al.
8,124,015	B2	2/2012	Diercks et al.
9,188,593	B2	11/2015	Singhal et al.
10,107,812	B2	10/2018	Singhal et al.
10,274,494	B2	4/2019	Singhal et al.
10,466,241	B2	11/2019	Singhal et al.
10,578,618	B2	3/2020	Singhal et al.
2002/0164656	A1	11/2002	Hoeffler et al.
2009/0068170	A1	3/2009	Weitz et al.
2010/0086919	A1	4/2010	McKeon
2011/0262906	A1	10/2011	Dimov et al.
2011/0294678	A1	12/2011	Jin et al.
2013/0130301	A1	5/2013	Yoon et al.

FOREIGN PATENT DOCUMENTS

WO	2009012340	A2	1/2009
WO	2010046775	A2	4/2010
WO	2012162779	A1	12/2012

OTHER PUBLICATIONS

Babcook et al. (1996) "A novel strategy for generating monoclonal antibodies from single, isolated lymphocytes producing antibodies of defined specificities" Proc. Natl. Acad. Sci. USA 93(15):7843-7848.

Bates & Quake (2009) "Highly parallel measurements of interaction kinetic constants with a microfabricated optomechanical device" Appl. Phys. Lett. 95(7):73705.

Batista & Neuberger (1998) "Affinity dependence of the B cell response to antigen: a threshold, a ceiling, and the importance of off-rate" Immunity 8(6):751-759.

Biacore Life Sciences—Biacore 3000 System Information. (2012). Website: http://www,biacore.com/lifesciences/products/svstems_overview/3000/system_information/index.html.

Biacore Life Sciences—Single-Cycle Kinetics. (2012). Website: https://www.biacore.com/lifesciences/technology/introduction/data_interaction/SCK/index.html.

Bornhop et al. (2007) "Free-solution, label-free molecular interactions studied by back-scattering interferometry" Science 317(5845):1732-1736.

Cai et al. (2006) "Stochastic protein expression in individual cells at the single molecule leve" Nature 440 (7082):358-362.

Dlugosz et al. (2009) "pH-dependent association of proteins. The test case of monoclonal antibody HyHEL-5 and its antigen hen egg white lysozyme" The Journal of Physical Chemistry 113(47):15662-15669.

England et al. (1999) "Functional characterization of the somatic hypermutation process leading to antibody D1.3, a high affinity antibody directed against lysozyme" J. Immunol. 162(4):2129-2136.

Hansen et al. (2002) "A robust and scalable microfluidic metering method that allows protein crystal growth by free interface diffusion" Proc. Natl. Acad. Sci. USA 99(26):16531-16536.

Hansen et al. (2004) "Systematic investigation of protein phase behavior with a microfluidic formulator" Proc. Natl. Acad. Sci. USA 101(40):14431-14436.

He & Niemeyer (2003) "A novel correlation for protein diffusion coefficients based on molecular weight and radius of gyration" Biotechnol. Prog. 19(2):544-548.

Homola et al. (1999) "Surface plasmon resonance sensors: review" Sensors and Actuators B: Chemical 54:3-15.

Huang et al. (2007) "Counting low-copy number proteins in a single cell" Science 315(5808):81-84.

Ito et al. (1995) "Mutations in the complementarity-determining regions do not cause differences in free energy during the process of formation of the activated complex between an antibody and the corresponding protein antigen" J. Mol. Biol. 248(4):729-732.

Jerne (1984) "The generative grammar of the immune system" EMBO J. 4(4):847-852.

Jin et al. (2009) "A rapid and efficient single-cell manipulation method for screening antigen-specific antibody-secreting cells from human peripheral blood" Nat. Med.15(9):1088-1092.

Karpas et al. (2001) "A human myeloma cell line suitable for the generation of human monoclonal antibodies" Proc. Natl. Acad. Sci. USA 98(4):1799-1804.

Kohler & Milstein (1975) "Continuous cultures of fused cells secreting antibody of predefined specificity" Nature 256(5517):495-497.

Lanzavecchia et al. (2007) "Human monoclonal antibodies by immortalization of memory B cells" Current Opinion in Biotechnology 18(6):523-528.

Lecault et al. (2011) "High-Throughput Analysis of Single Hematopoietic Stem Cell Proliferation in Microfluidic Cell Culture Arrays" Nat Methods 8(7):581-586.

Lee et al. (2009) "High-sensitivity microfluidic calorimeters for biological and chemical applications" Proc. Natl. Acad. Sci. USA 106(36):15225-15230.

Maerkl & Quake (2007) "A systems approach to measuring the binding energy landscapes of transcription factors" Science 315(5809):233-237.

Marcus et al. (2006) "Microfluidic single-cell mRNA isolation and analysis" Anal. Chem. 78(9):3084-3089.

Mcdonald et al. (2000) "Fabrication of microfluidic systems in poly(dimethylsiloxane)" Electrophoresis 21: 27-40.

Mckinney et al. (1995) "Optimizing antibody production in batch hybridoma cell culture" J.Biotechnol. 40(1):31-48.

Pasqualini & Arap (2004) "Hybridoma-free generation of monoclonal antibodies" Proc. Natl. Acad. Sci. USA 101 (1):257-259.

Poulson et al. (2007) "Kinetic, affinity, and diversity limits of human polyclonal antibody responses against tetanus toxoid" J. Immunol. 179(6):3841-3850.

Raschke et al. (2003) "Biomolecular Recognition Based on Single Gold Nanoparticle Light Scattering" Nano Letters 3(7):935-938.

Sonnichsen et al. (2000) "Spectroscopy of single metallic nanoparticles using total internal reflection microscopy" App. Phys. Letters 77(19): 2949-2951.

Spieker-Polet et al. (1995) "Rabbit monoclonal antibodies: generating a fusion partner to produce rabbit-rabbit hybridomas" Proc. Natl. Acad. Sci. USA 92(20):9348-9352.

Squires & Quake (2005) "Microfluidics: Fluid physics at the nanoliter scale" Reviews of Modern Physics 77 (3):977-1026.

(56) **References Cited**

OTHER PUBLICATIONS

Story et al. (2008) "Profiling antibody responses by multiparametric analysis of primary B cells" Proc. Natl. Acad. Sci. U.S.A. 105(46):17902-17907.

Thorsen et al. (2002) "Microfluidic large-scale integration" Science 298(5593):580-584.

Tiller et al. (2009) "Cloning and expression of murine Ig genes from single B cells" J. Immunol. Methods 350 (1-2):183-193.

Traggiai et al. (2004) "An efficient method to make human monoclonal antibodies from memory B cells: potent neutralization of SARS coronavirus" Nat Med 10(8):871-875.

Tyn & Gusek (1990) "Prediction of diffusion coefficients of proteins" Biotechnol. Bioeng. 35(4):327-338.

Ueno et al. (2010) "Simple dark-field microscopy with nanometer spatial precision and microsecond temporal resolution" Biophysical J. 98(9):2014-2023.

Unger et al. (2000) "Monolithic microfabricated valves and pumps by multilayer soft lithography" Science 288 (5463):113-116.

Wang et al. (2005) "Label-free detection of small-molecule-protein interactions by using nanowire nanosensors" Proc. Natl. Acad. Sci. USA 102(9):3208-3212.

Xavier & Willson (1998) "Association and dissociation kinetics of anti-hen egg lysozyme monoclonal antibodies HyHEL-5 and HyHEL-10" Biophys. J. 74(4):2036-2045.

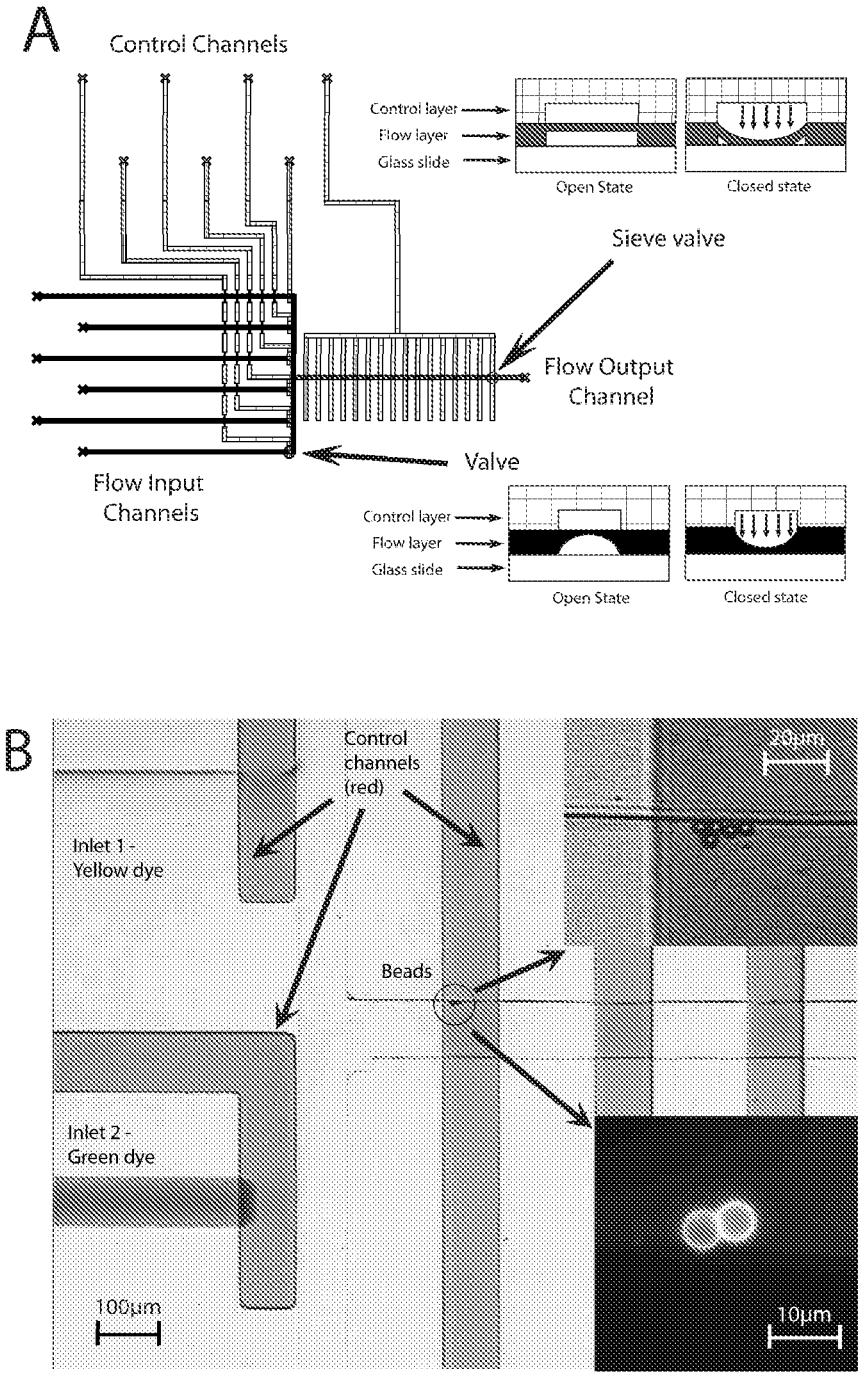
A
Control Channels
Control layer
Flow layer
Glass slide
Open State
Closed state
Sieve valve
Flow Output Channel
Valve
Flow Input Channels
Control layer
Flow layer
Glass slide
Open State
Closed state
B
Control channels (red)
20μm
Inlet 1 - Yellow dye
Beads
Inlet 2 - Green dye
100μm
10μm

Figure 1

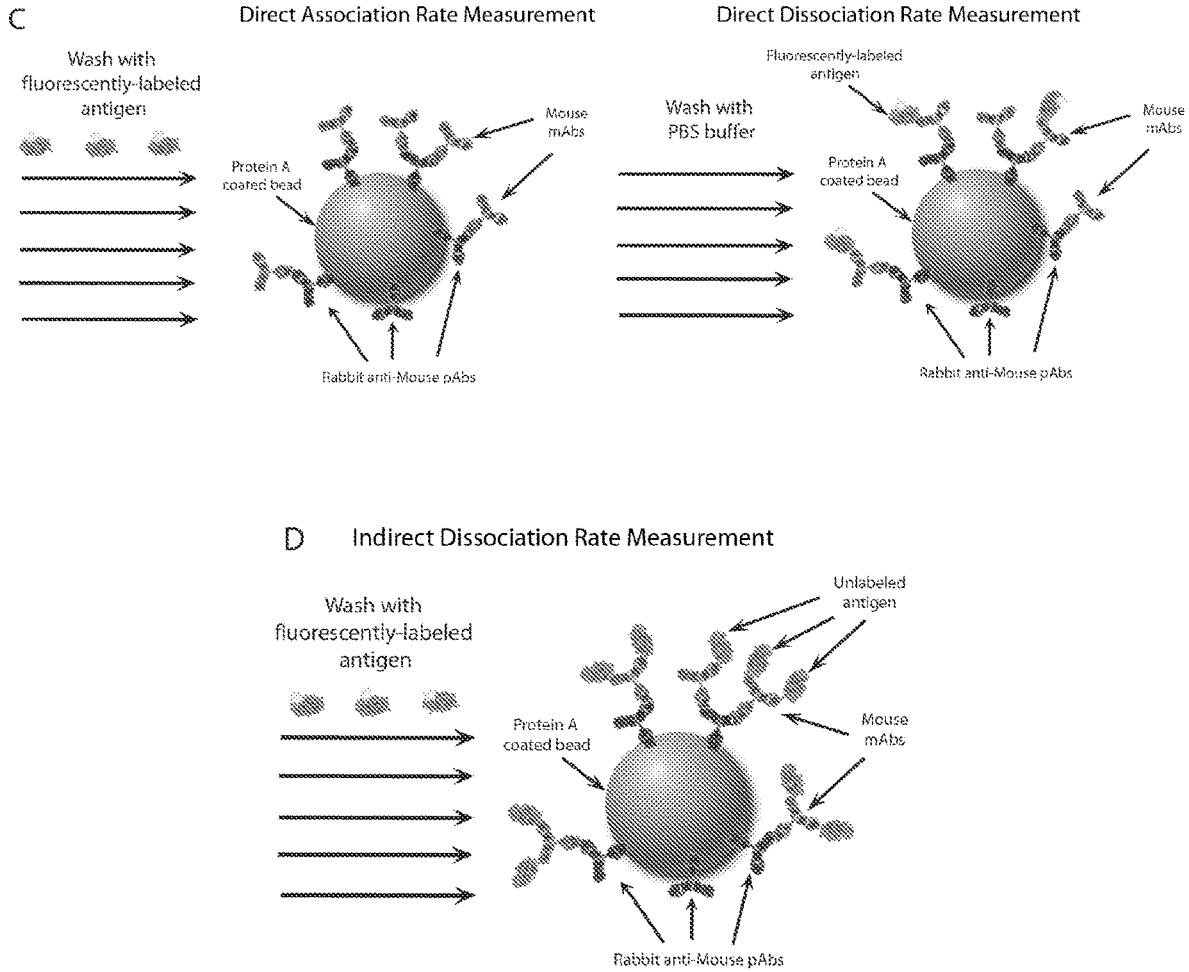

Figure 1 cont'd

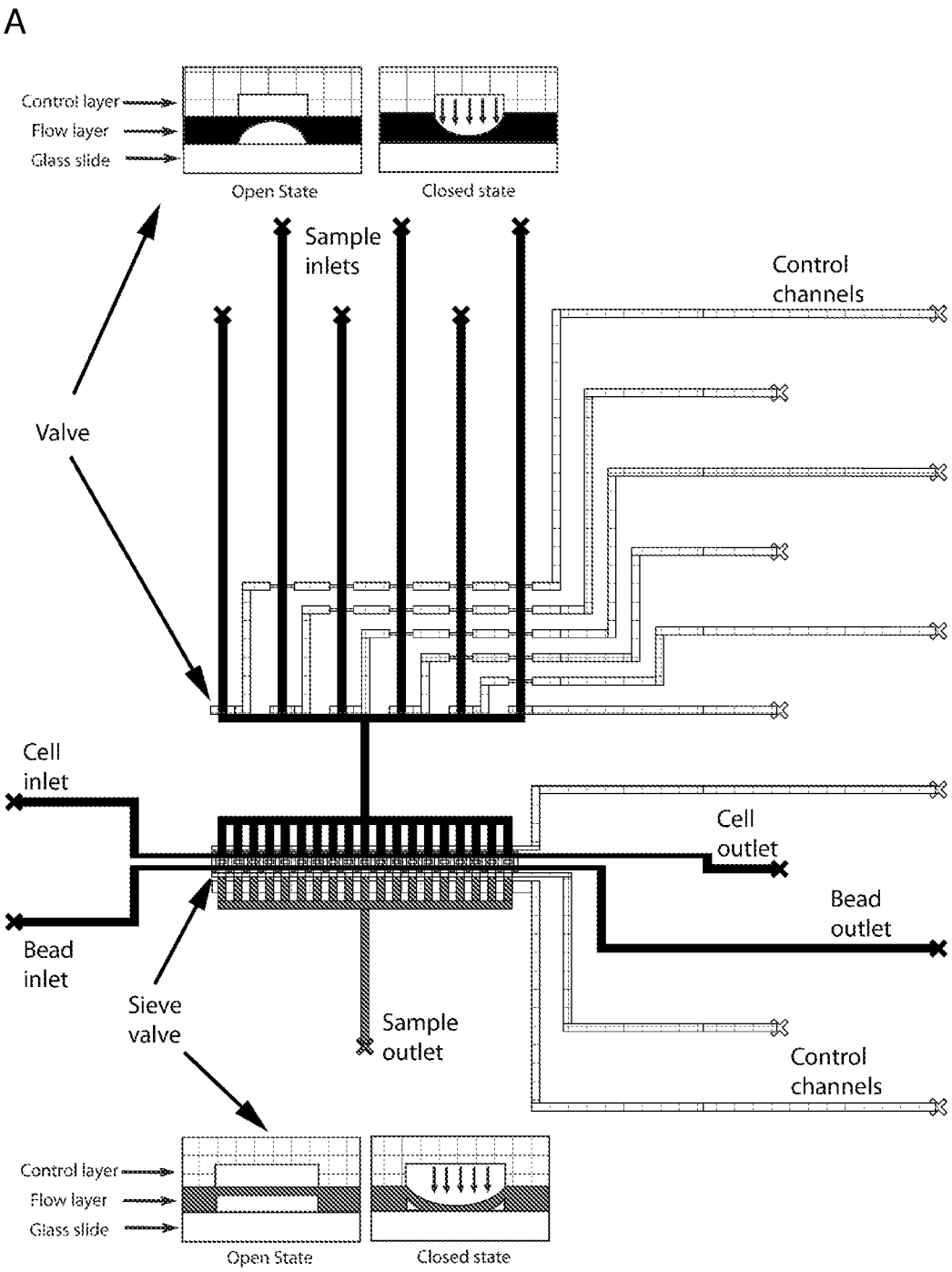
A
Control layer
Flow layer
Glass slide
Open State
Closed state
Sample inlets
Control channels
Valve
Cell inlet
Cell outlet
Bead outlet
Bead inlet
Sieve valve
Sample outlet
Control channels
Control layer
Flow layer
Glass slide
Open State
Closed state

Figure 2

B

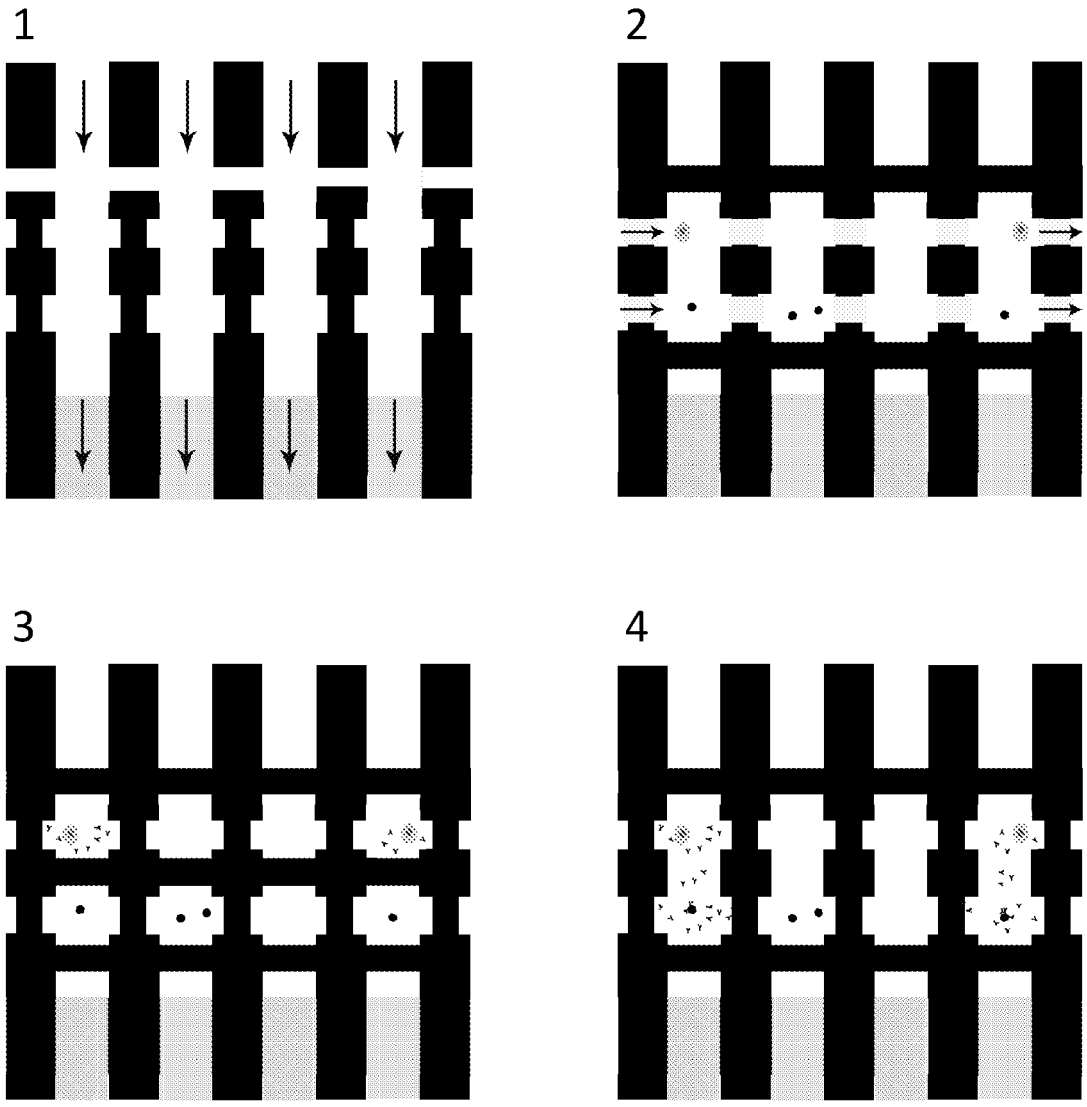

Figure 2 cont'd

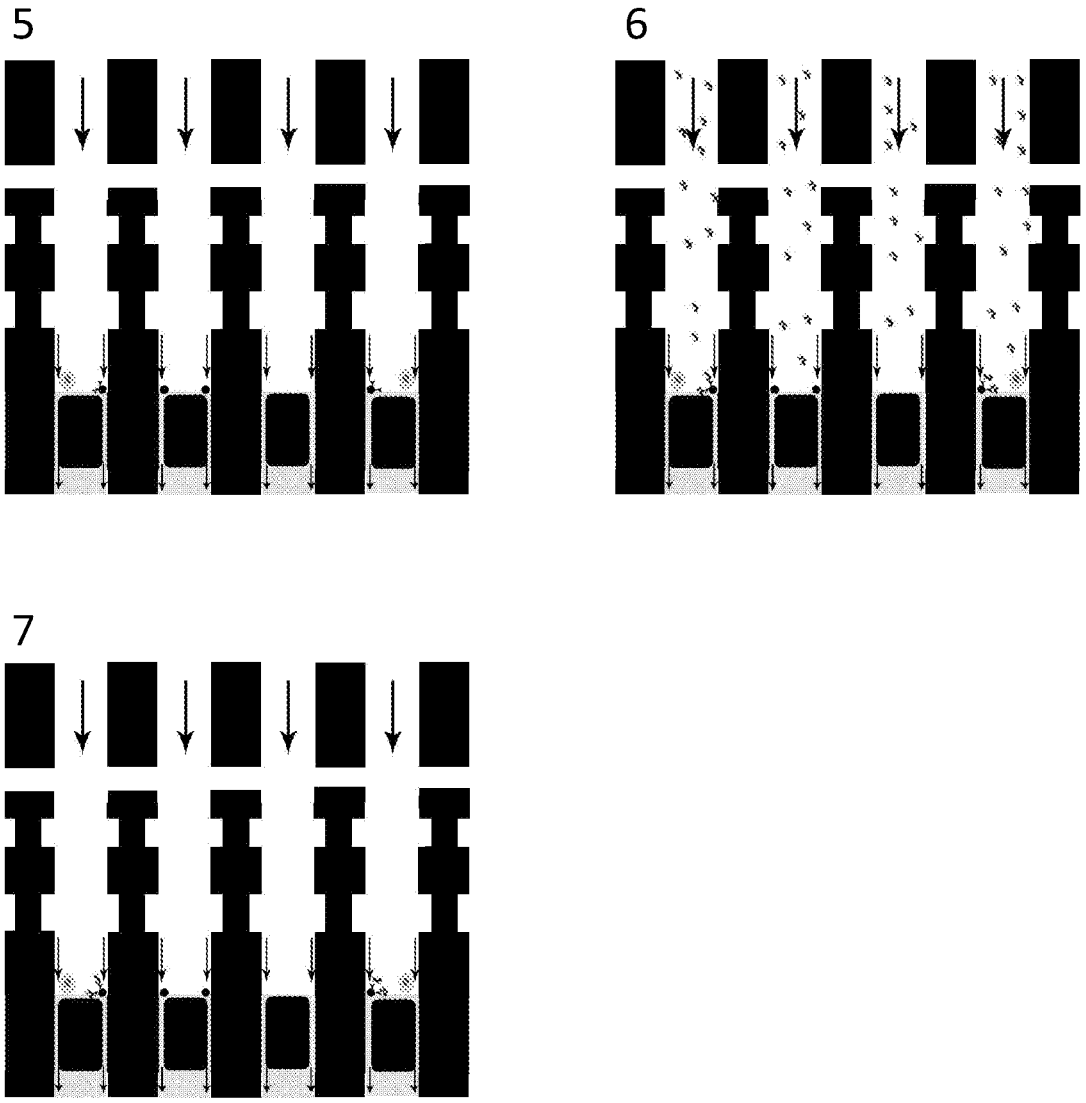

Figure 2 cont'd

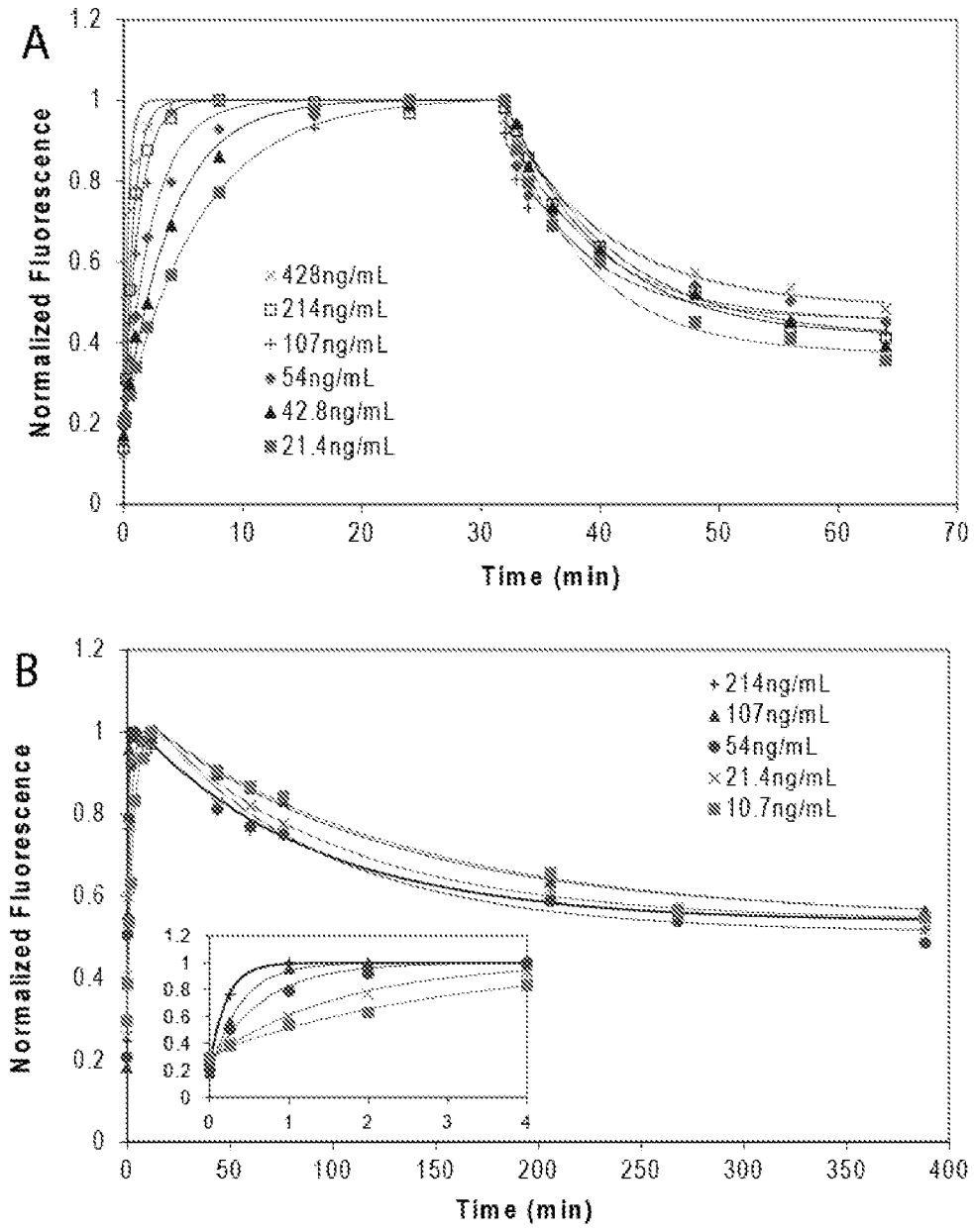
A
Normalized Fluorescence
Time (min)
428ng/mL
214ng/mL
107ng/mL
54ng/mL
42.8ng/mL
21.4ng/mL
B
Normalized Fluorescence
Time (min)
214ng/mL
107ng/mL
54ng/mL
21.4ng/mL
10.7ng/mL

Figure 3

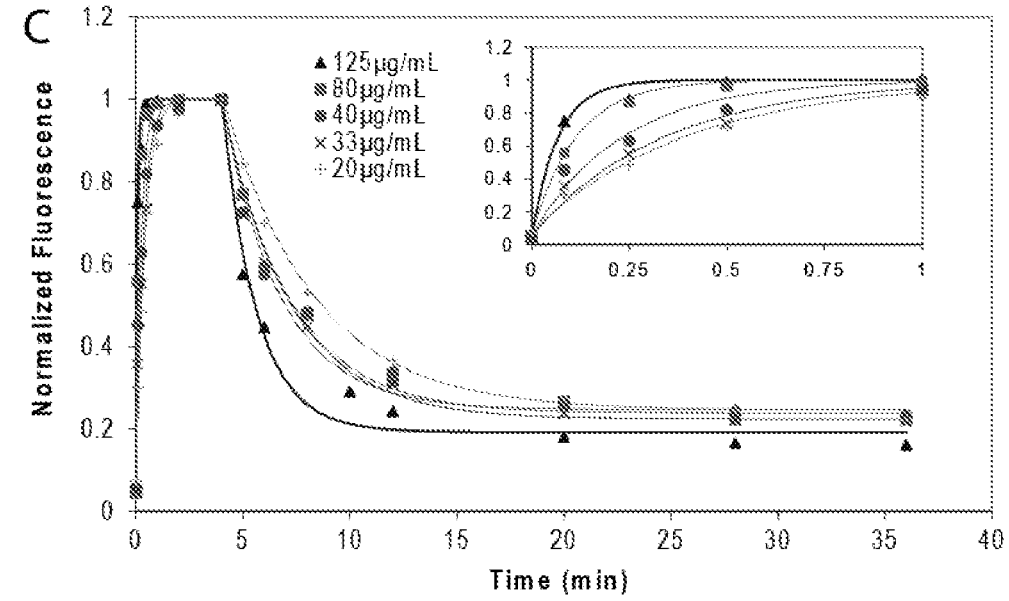

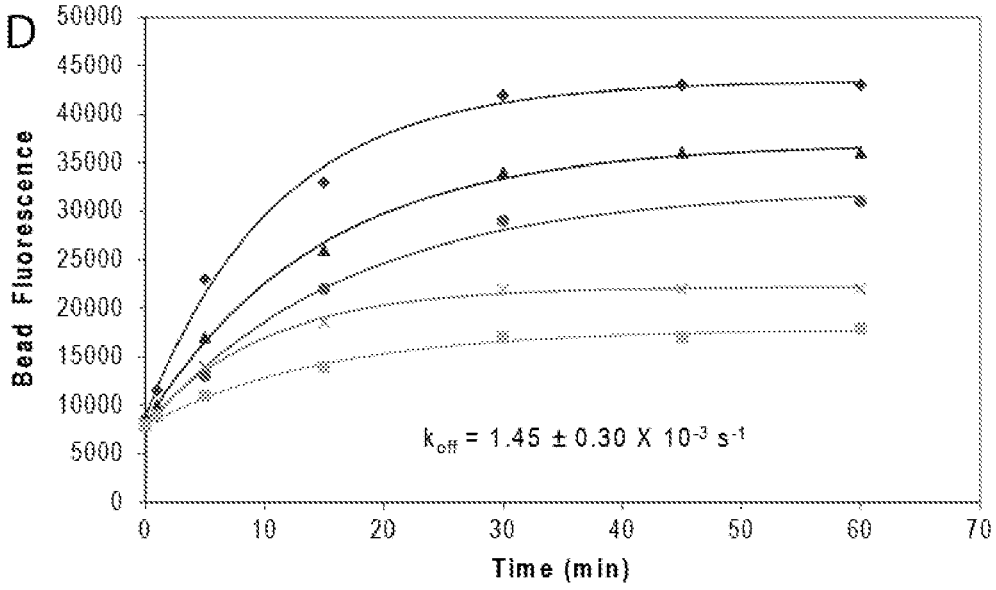

Figure 3 cont'd

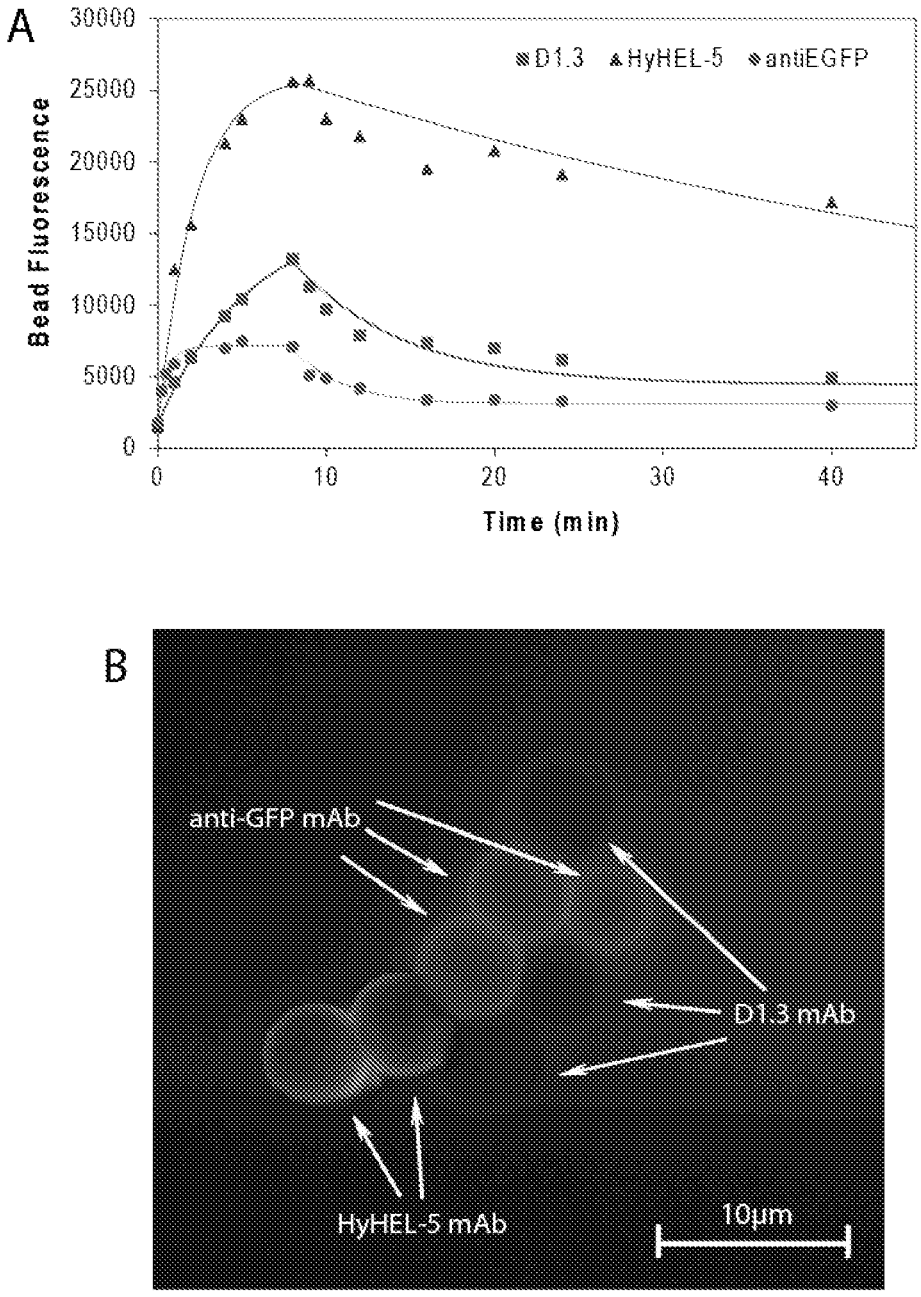
A
30000
25000
20000
15000
10000
5000
0
Bead Fluorescence
D1.3
HyHEL-5
antiEGFP
0
10
20
30
40
Time (min)
B
anti-GFP mAb
D1.3 mAb
HyHEL-5 mAb
10µm

Figure 4

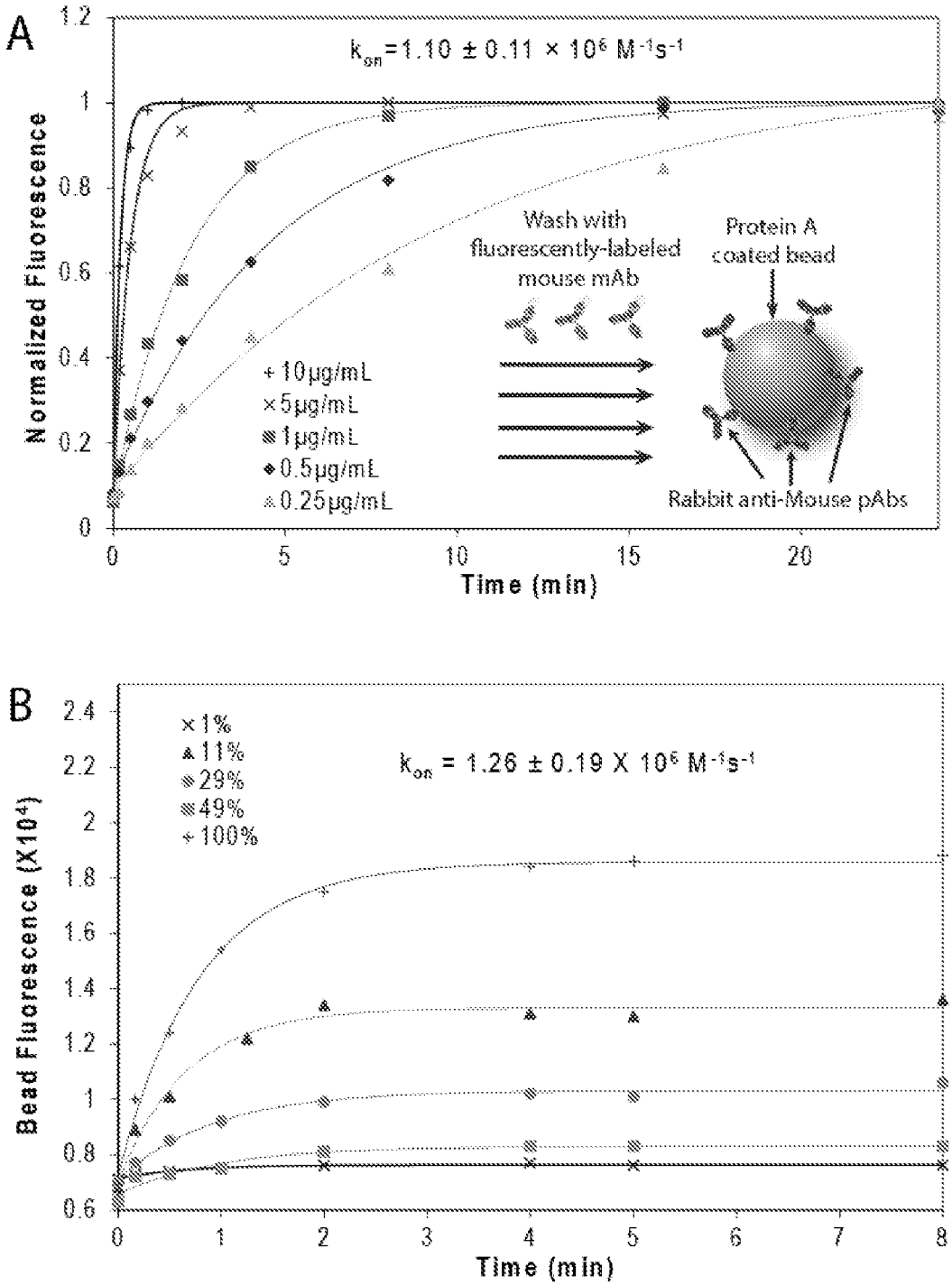
A
k_{on}=1.10 ± 0.11 × 10⁶ M⁻¹s⁻¹
Normalized Fluorescence
Time (min)
10µg/mL
5µg/mL
1µg/mL
0.5µg/mL
0.25µg/mL
Wash with fluorescently-labeled mouse mAb
Protein A coated bead
Rabbit anti-Mouse pAbs
B
1%
11%
29%
49%
100%
k_{on} = 1.26 ± 0.19 X 10⁶ M⁻¹s⁻¹
Bead Fluorescence (X10⁴)
Time (min)

Figure 5

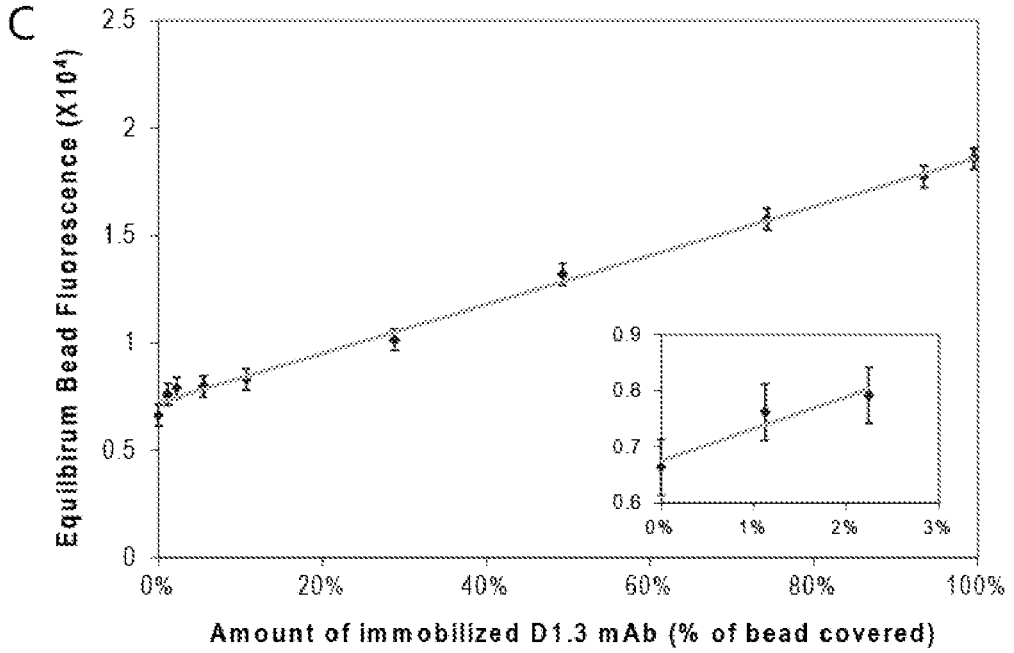

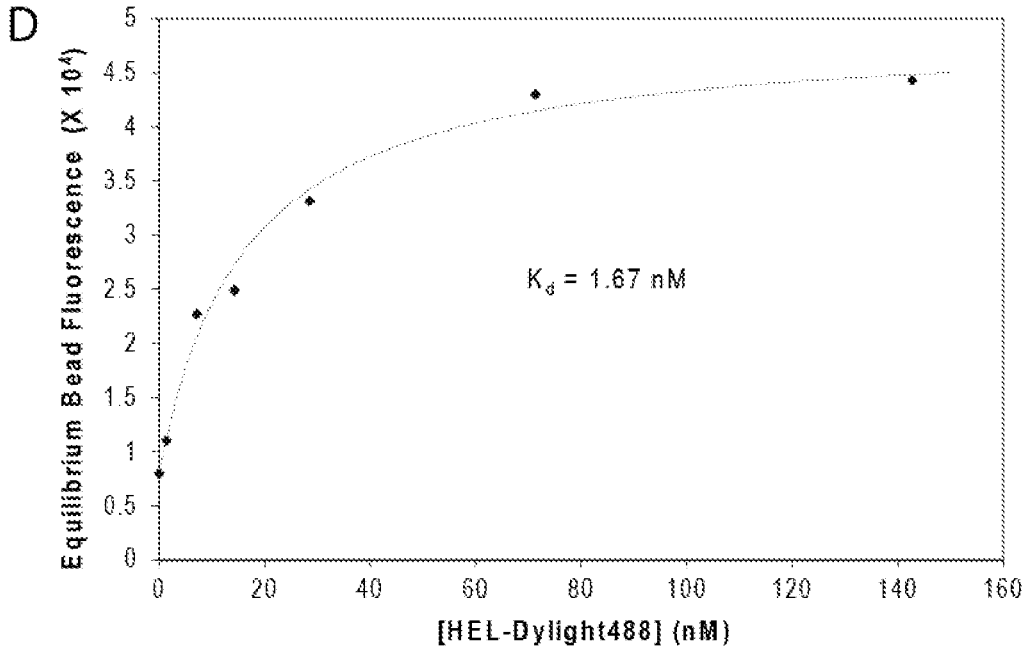

Figure 5 cont'd

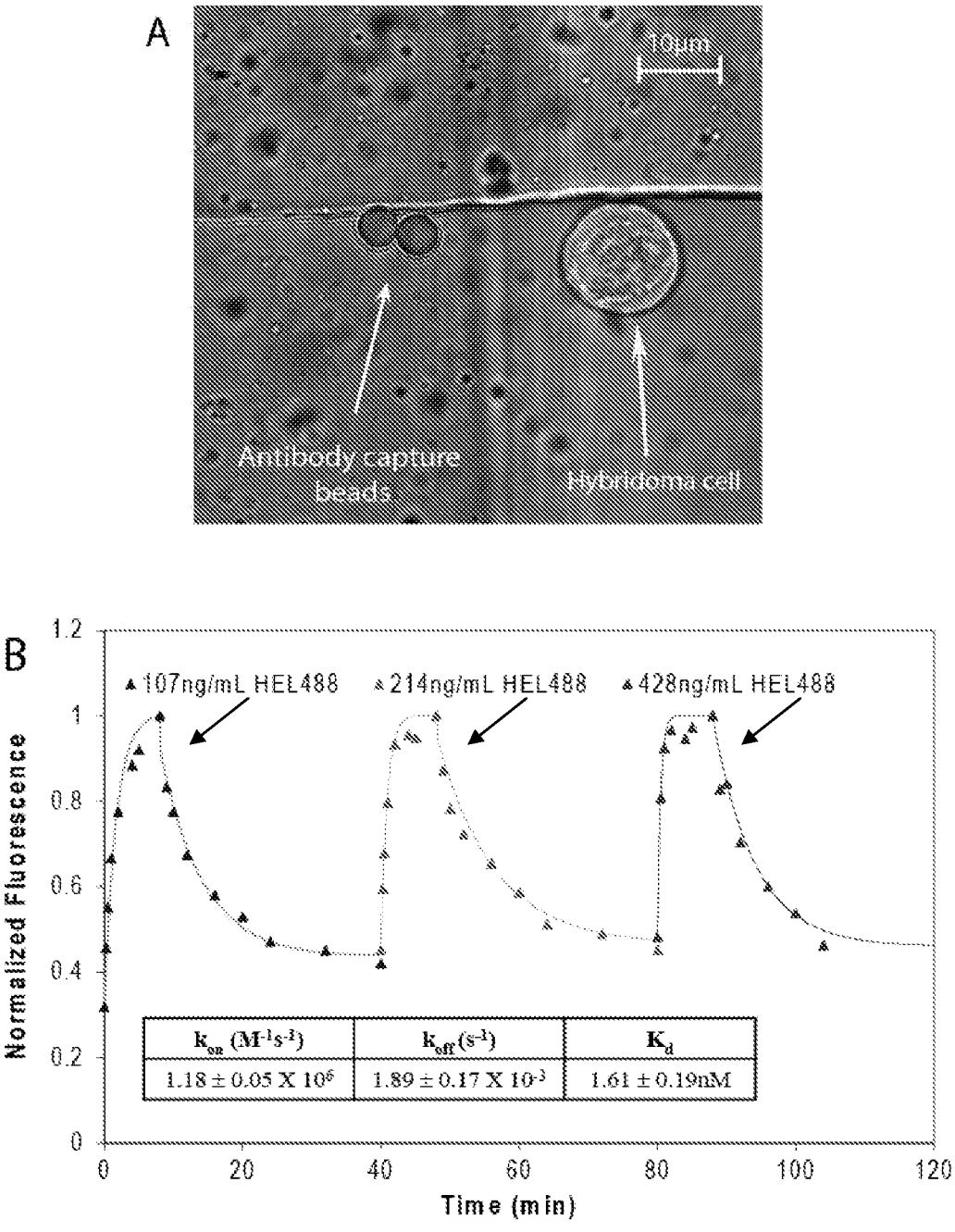
A
10μm
Antibody capture beads
Hybridoma cell
B
107ng/mL HEL488
214ng/mL HEL488
428ng/mL HEL488
Normalized Fluorescence
Time (min)
0
0.2
0.4
0.6
0.8
1
1.2
0
20
40
60
80
100
120
k_{on} ($M^{-1}s^{-1}$)
k_{off} (s^{-1})
K_d
1.18 ± 0.05 X 10^6
1.89 ± 0.17 X 10^{-3}
1.61 ± 0.19nM

Figure 6

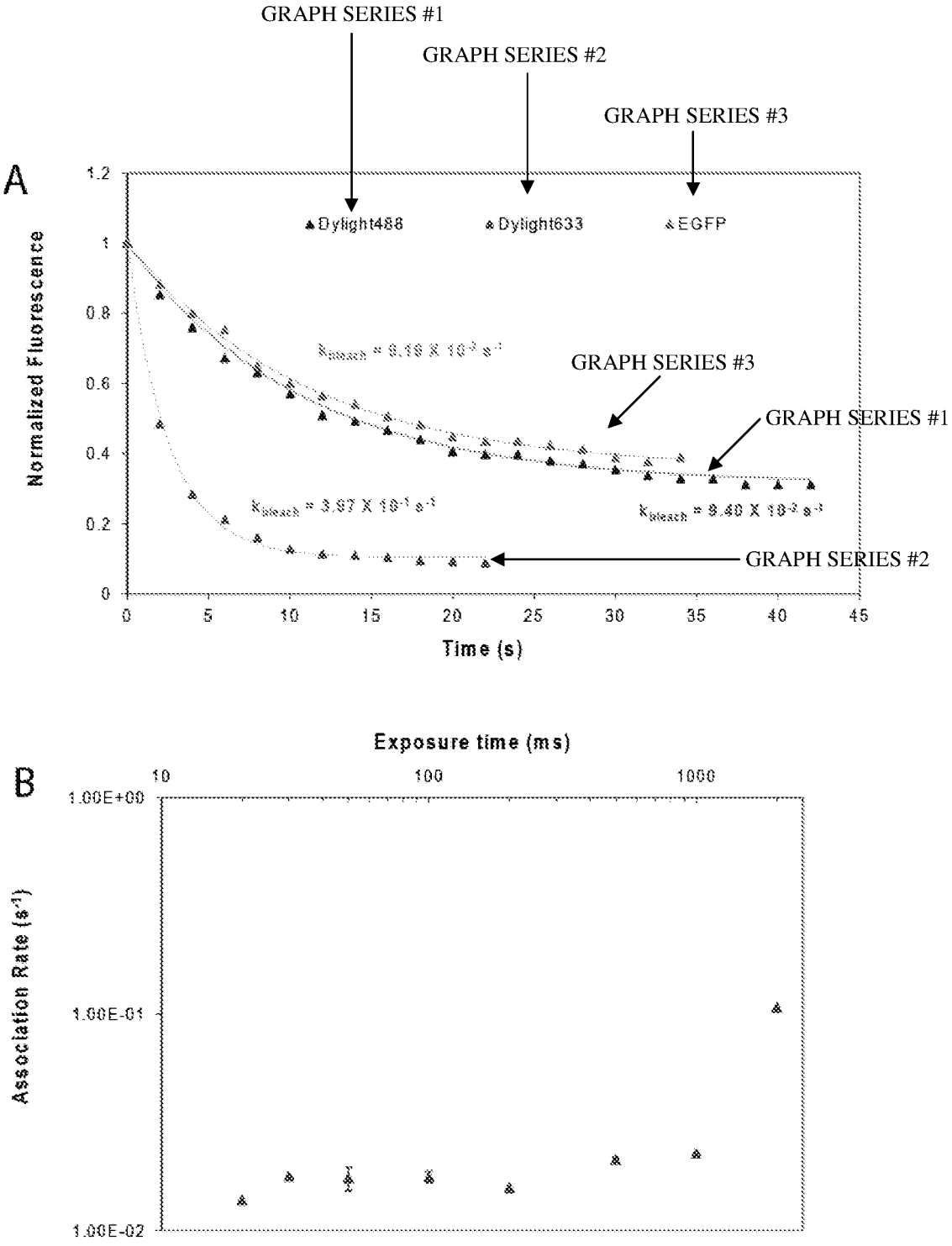
A
GRAPH SERIES #1
GRAPH SERIES #2
GRAPH SERIES #3
Dylight488
Dylight633
EGFP
Normalized Fluorescence
Time (s)
GRAPH SERIES #3
GRAPH SERIES #1
GRAPH SERIES #2
B
Exposure time (ms)
Association Rate (s-1)

Figure 7

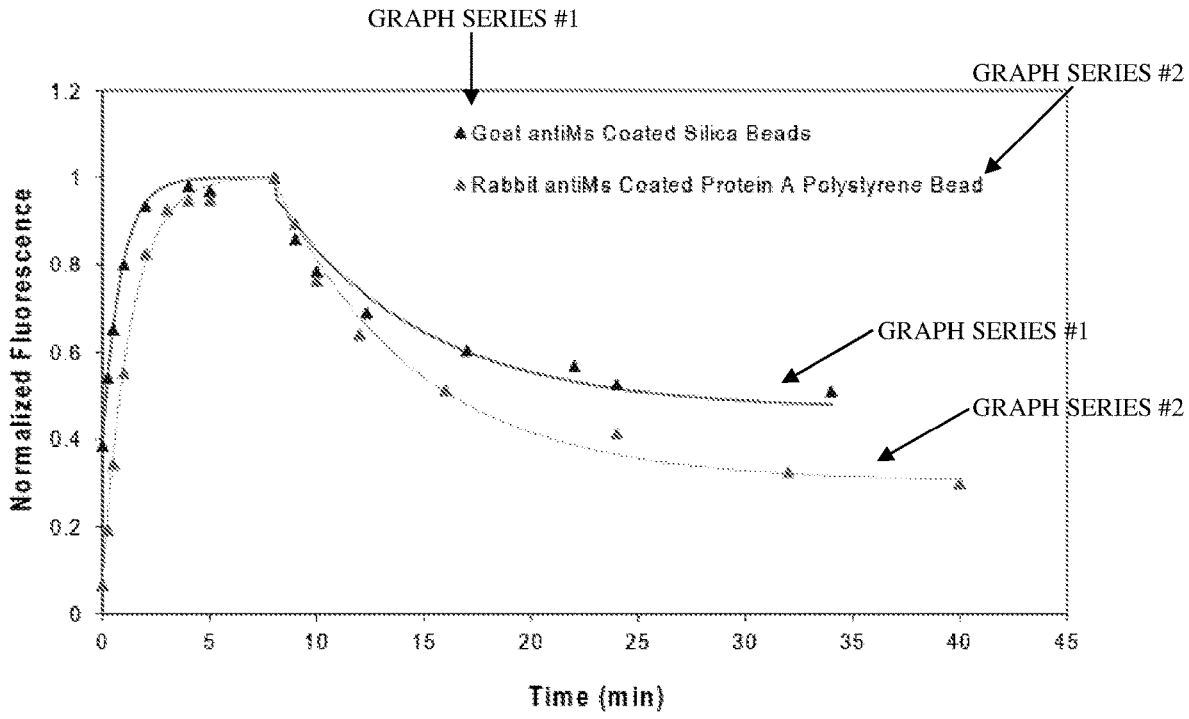
GRAPH SERIES #1
GRAPH SERIES #2
Goat antiMs Coated Silica Beads
Rabbit antiMs Coated Protein A Polystyrene Bead
GRAPH SERIES #1
GRAPH SERIES #2
Normalized Fluorescence
Time (min)
0
0.2
0.4
0.6
0.8
1
1.2
0
5
10
15
20
25
30
35
40
45

Figure 8

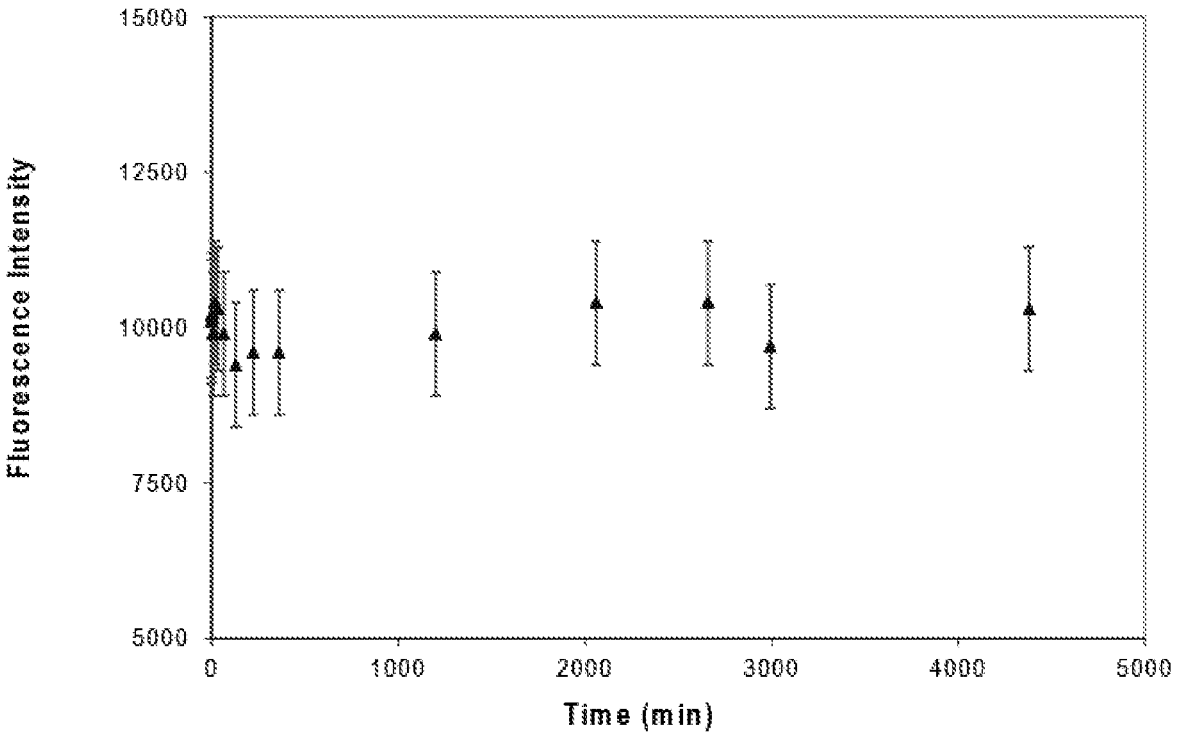
15000
12500
10000
7500
5000
Fluorescence Intensity
0
1000
2000
3000
4000
5000
Time (min)

Figure 9

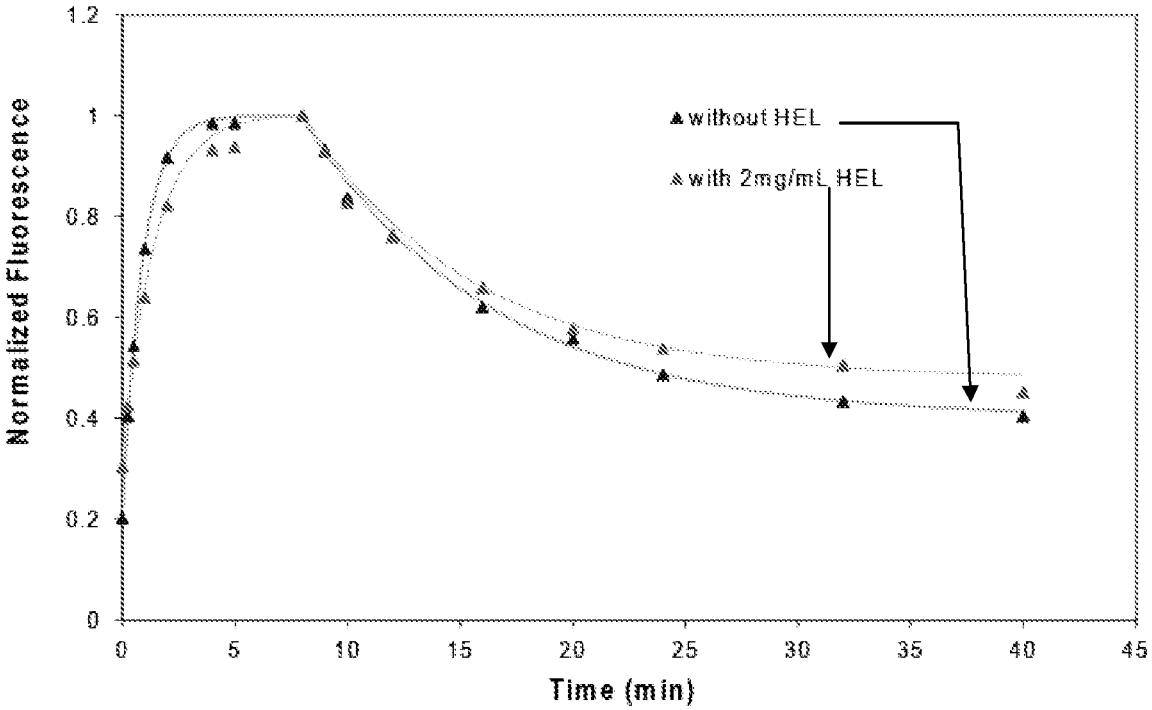
Normalized Fluorescence
1.2
1
0.8
0.6
0.4
0.2
0
0
5
10
15
20
25
30
35
40
45
Time (min)
without HEL
with 2mg/mL HEL

Figure 10

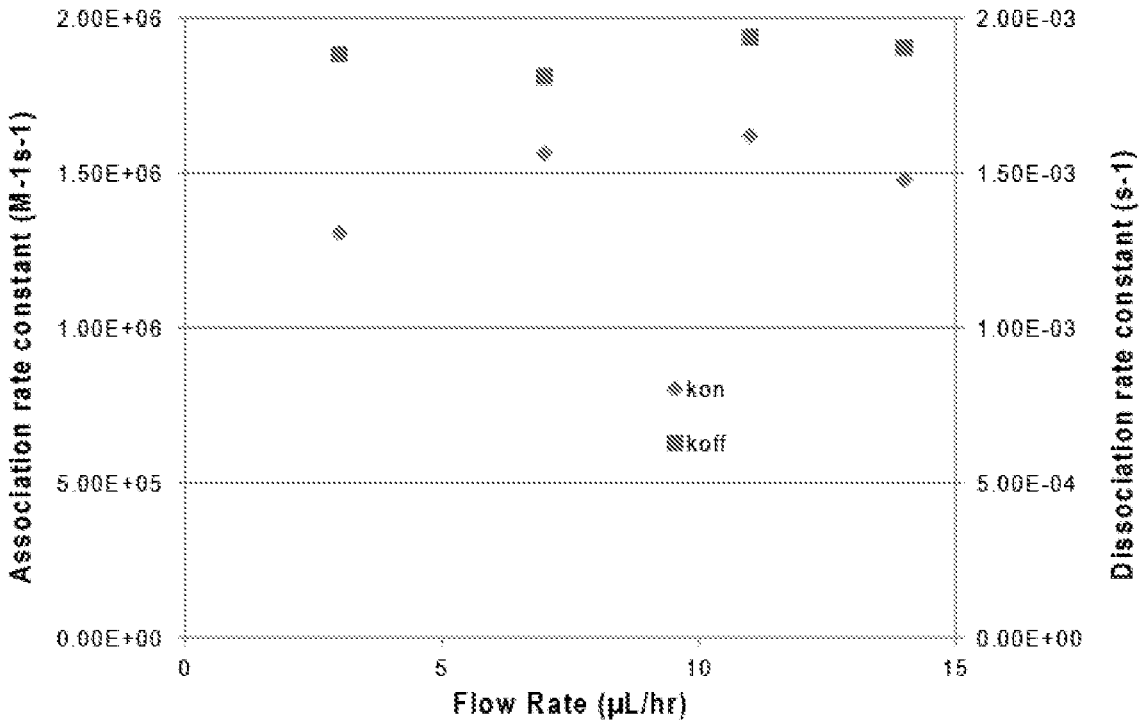
2.00E+06
1.50E+06
1.00E+06
5.00E+05
0.00E+00
Association rate constant (M-1s-1)
2.00E-03
1.50E-03
1.00E-03
5.00E-04
0.00E+00
Dissociation rate constant (s-1)
kon
koff
0
5
10
15
Flow Rate (µL/hr)

Figure 11

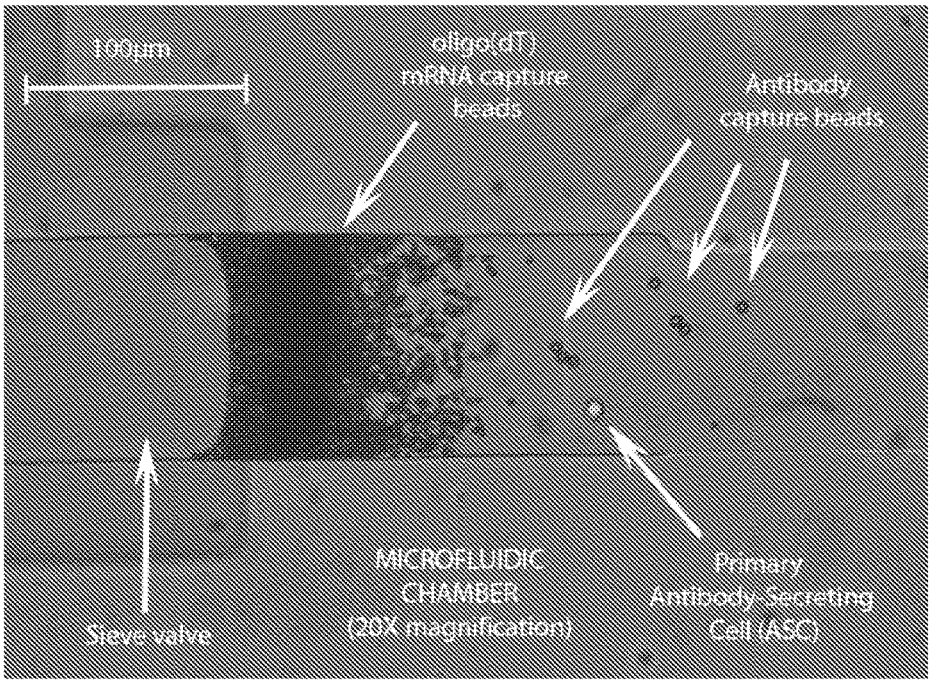
100µm
oligo(dT) mRNA capture beads
Antibody capture beads
MICROFLUIDIC CHAMBER (20X magnification)
Sieve valve
Primary Antibody-Secreting Cell (ASC)

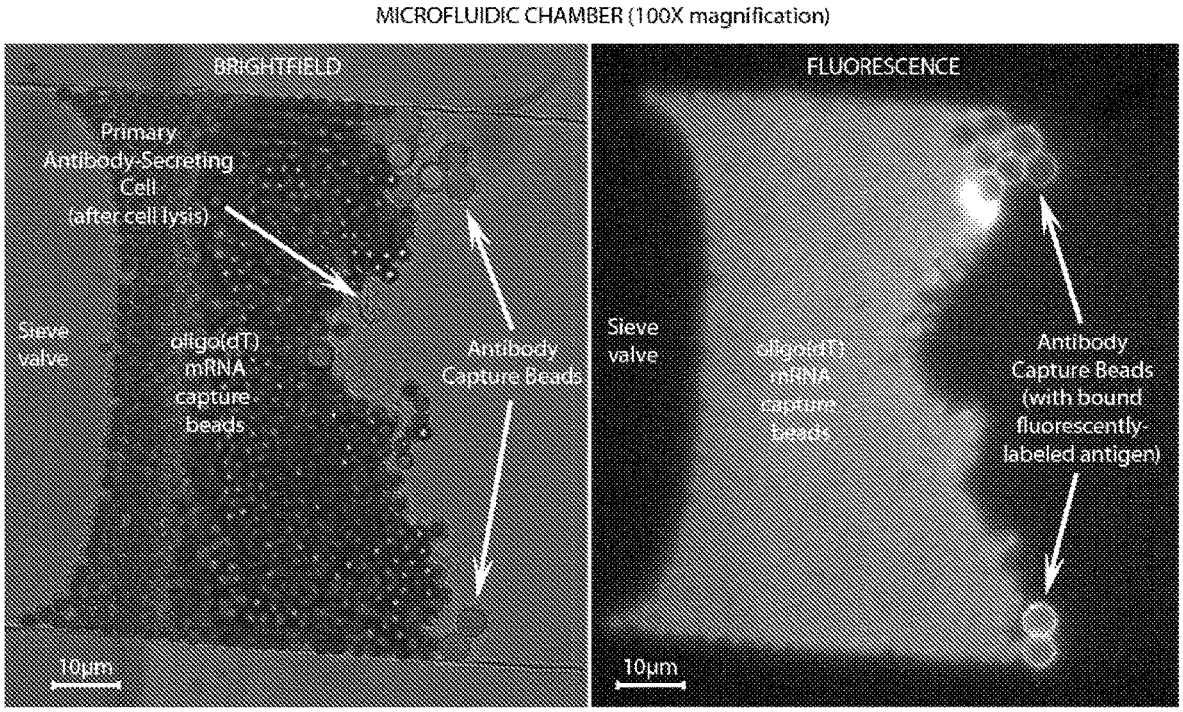
MICROFLUIDIC CHAMBER (100X magnification)
BRIGHTFIELD
Primary Antibody-Secreting Cell (after cell lysis)
Sieve valve
oligo(dT) mRNA capture beads
Antibody Capture Beads
10µm
FLUORESCENCE
Sieve valve
oligo(dT) mRNA capture beads
Antibody Capture Beads (with bound fluorescently-labeled antigen)
10µm

Figure 12

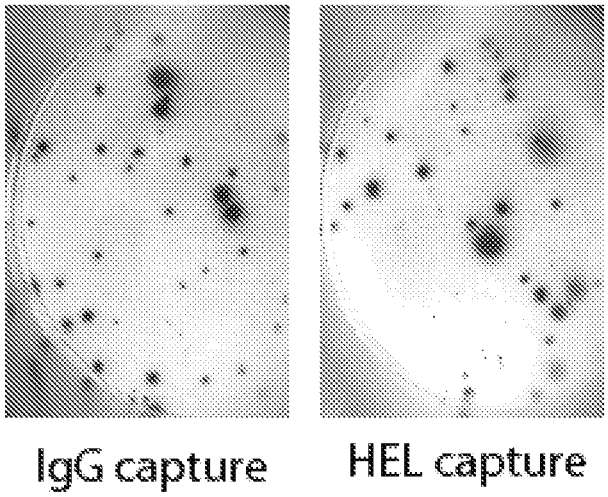

Figure 13

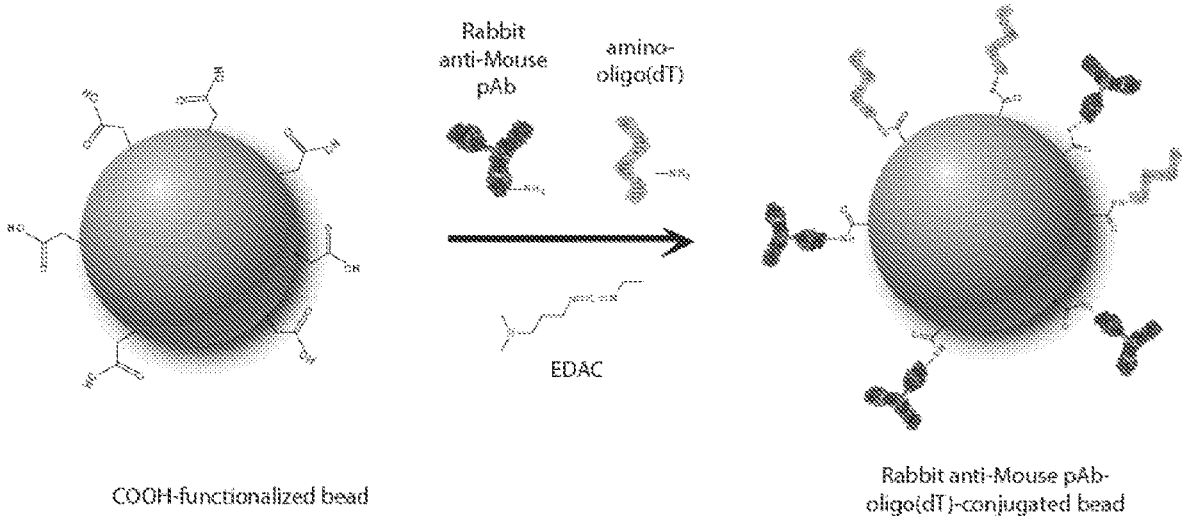
Rabbit anti-Mouse pAb
amino-oligo(dT)
EDAC
COOH-functionalized bead
Rabbit anti-Mouse pAb-oligo(dT)-conjugated bead

Figure 14

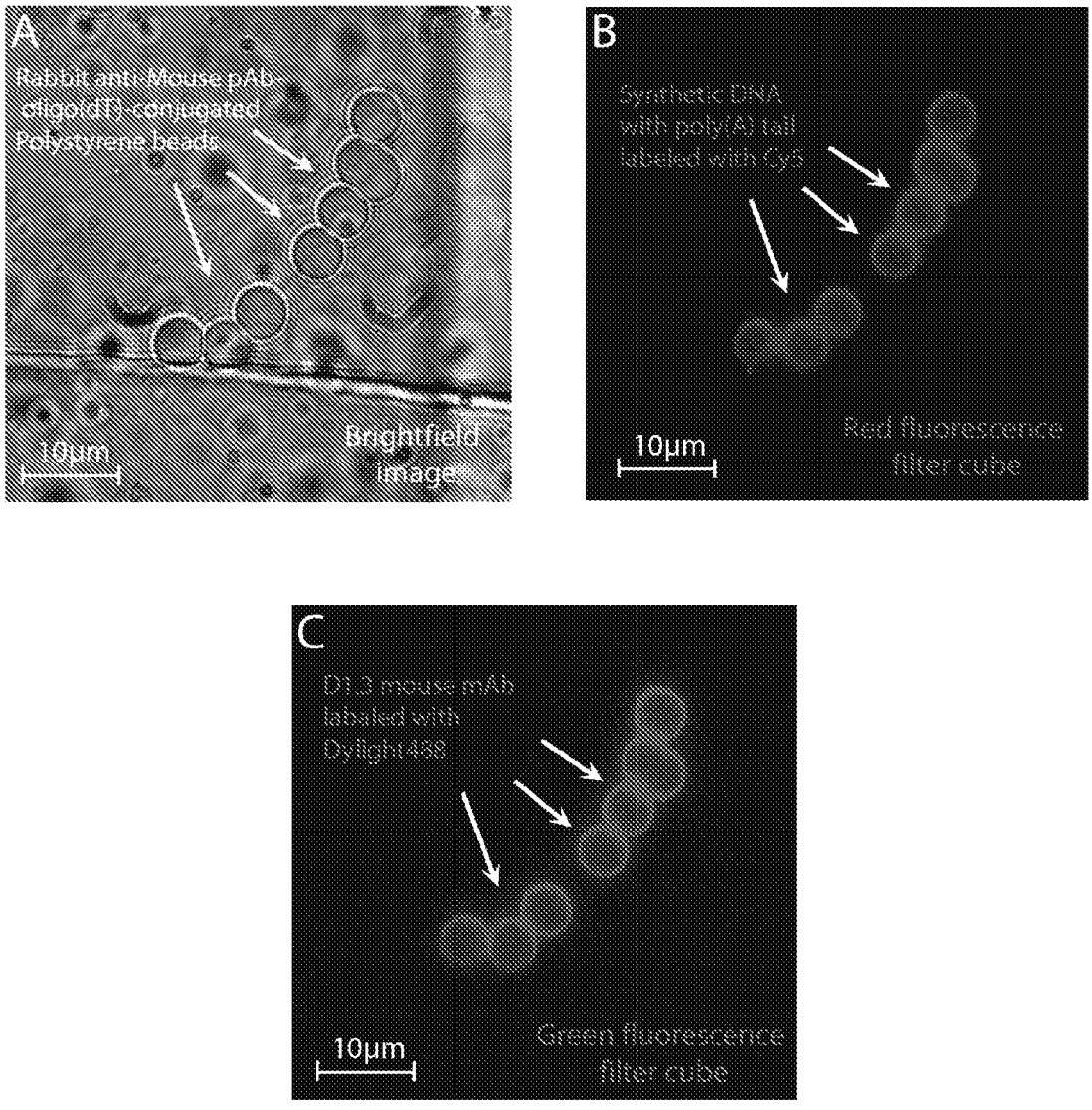
A
Rabbit anti-Mouse pAb
oligo(dT)-conjugated
Polystyrene beads
10μm
Brightfield
images
B
Synthetic DNA
with poly(A) tail
labeled with Cy5
10μm
Red fluorescence
filter cube
C
D1.3 mouse mAb
labeled with
Dylight 488
10μm
Green fluorescence
filter cube

Figure 15

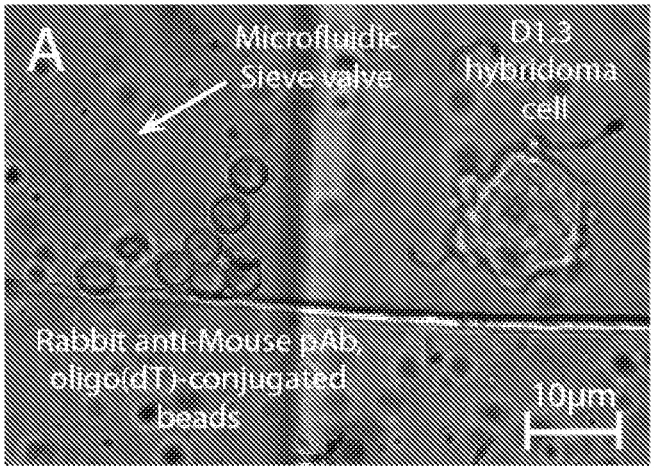
A
Microfluidic Sieve valve
D1.3 hybridoma cell
Rabbit anti-Mouse pAb oligo(dT)-conjugated beads
10μm

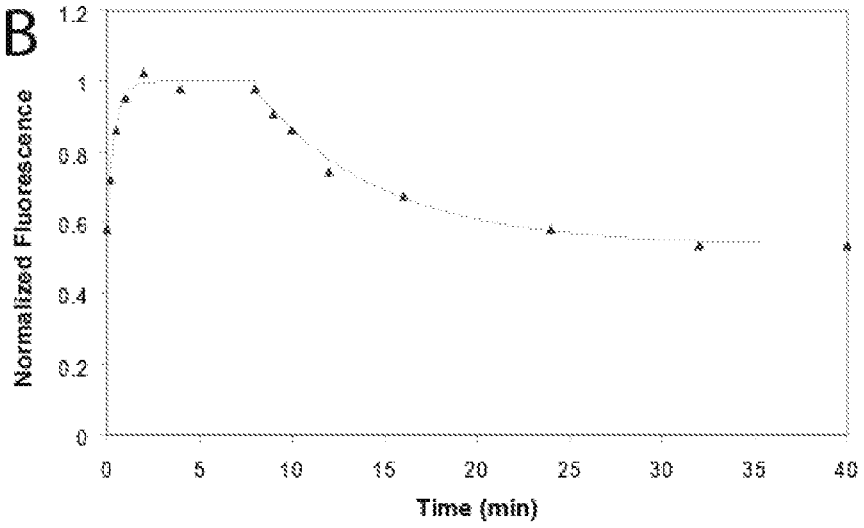
B
Normalized Fluorescence
1.2
1
0.8
0.6
0.4
0.2
0
0
5
10
15
20
25
30
35
40
Time (min)

Figure 16

A

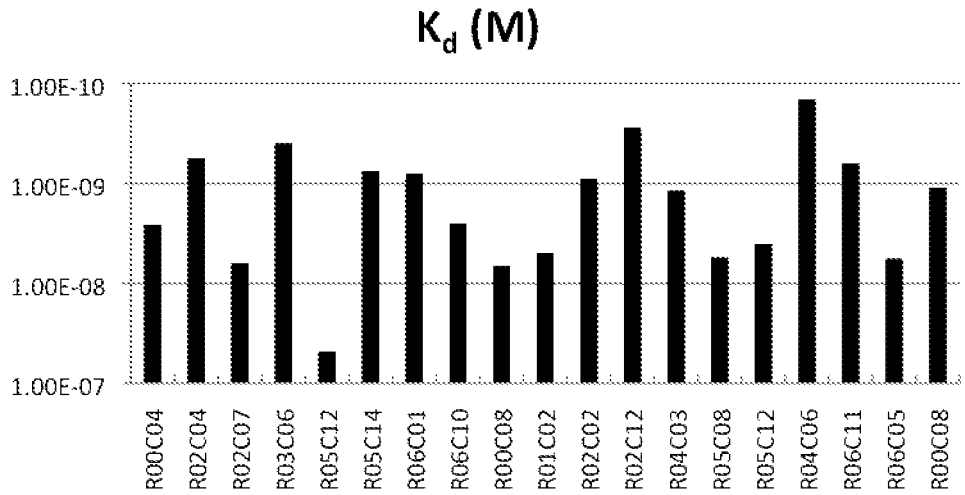

B

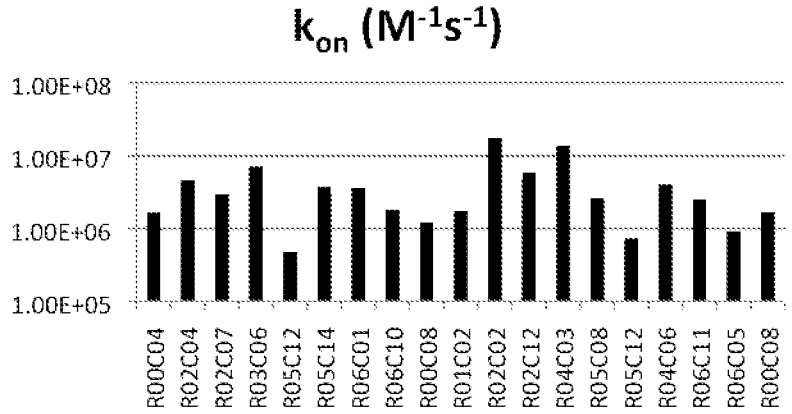

C

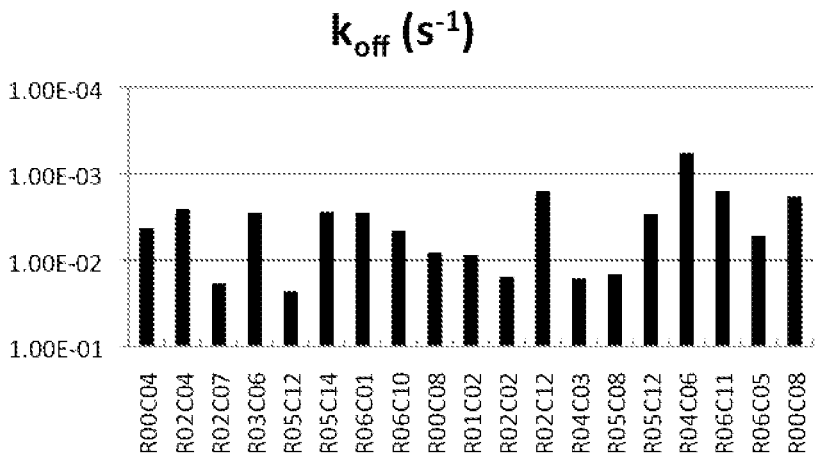

Figure 17

A

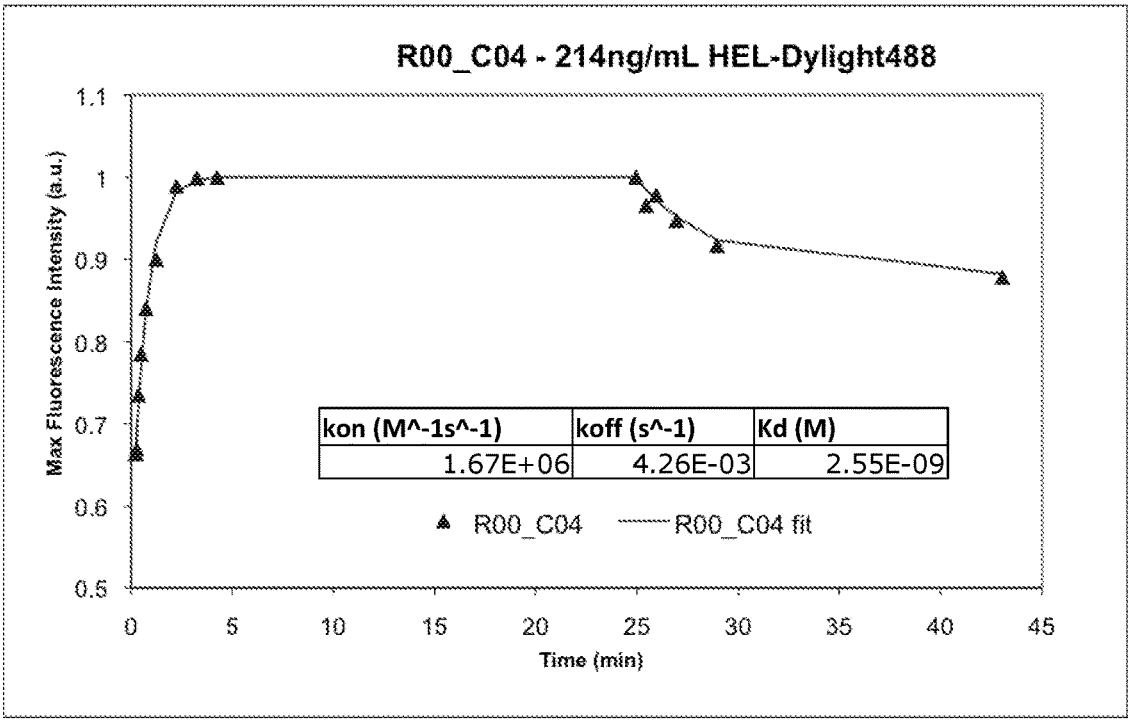
R00_C04 - 214ng/mL HEL-Dylight488
Max Fluorescence Intensity (a.u.)
Time (min)
kon (M^-1s^-1) | koff (s^-1) | Kd (M)
1.67E+06 | 4.26E-03 | 2.55E-09
R00_C04
R00_C04 fit

B

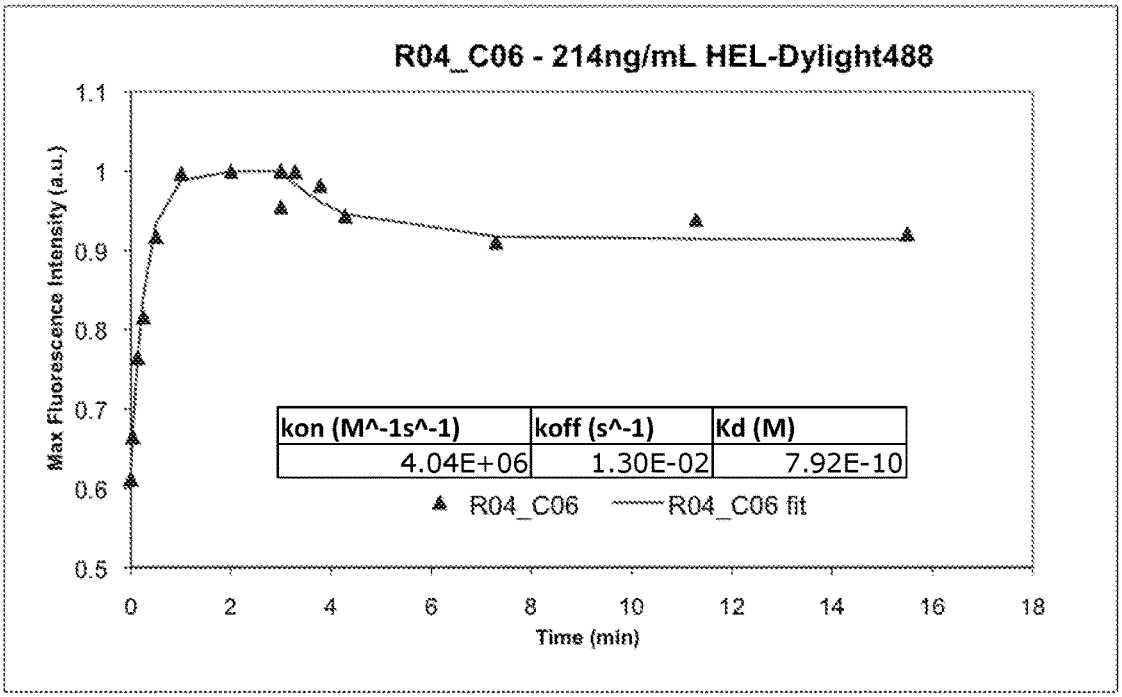
R04_C06 - 214ng/mL HEL-Dylight488
Max Fluorescence Intensity (a.u.)
Time (min)
kon (M^-1s^-1) | koff (s^-1) | Kd (M)
4.04E+06 | 1.30E-02 | 7.92E-10
R04_C06
R04_C06 fit

Figure 18

A

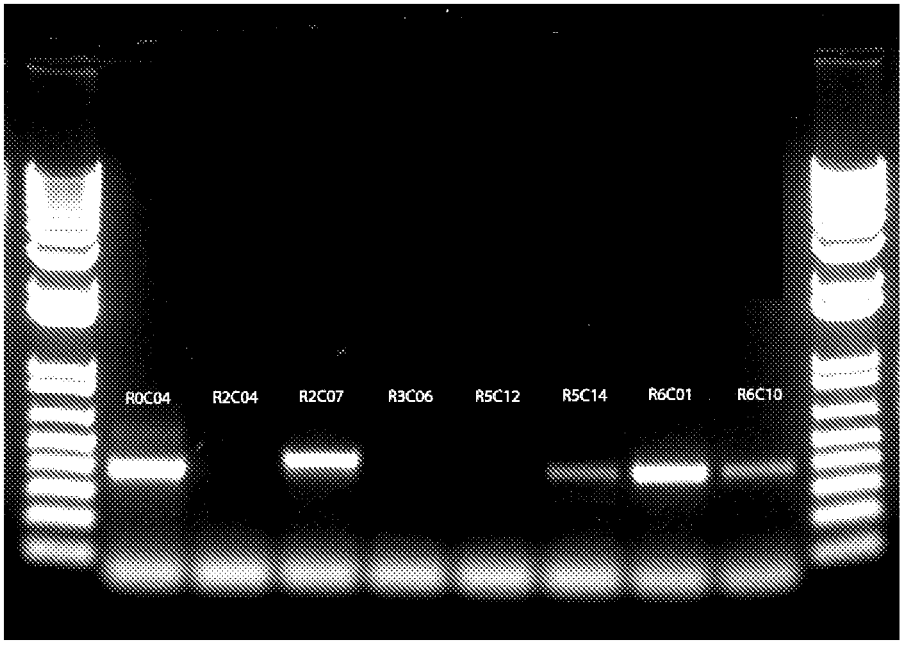
R0C04
R2C04
R2C07
R3C06
R5C12
R5C14
R6C01
R6C10

B

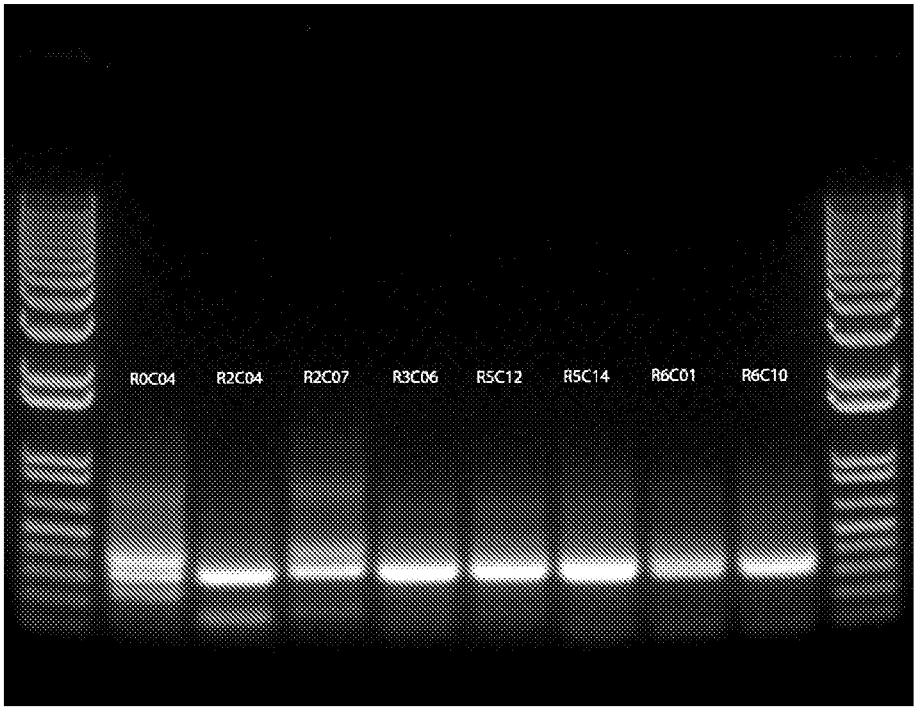
R0C04
R2C04
R2C07
R3C06
R5C12
R5C14
R6C01
R6C10

Figure 19

C

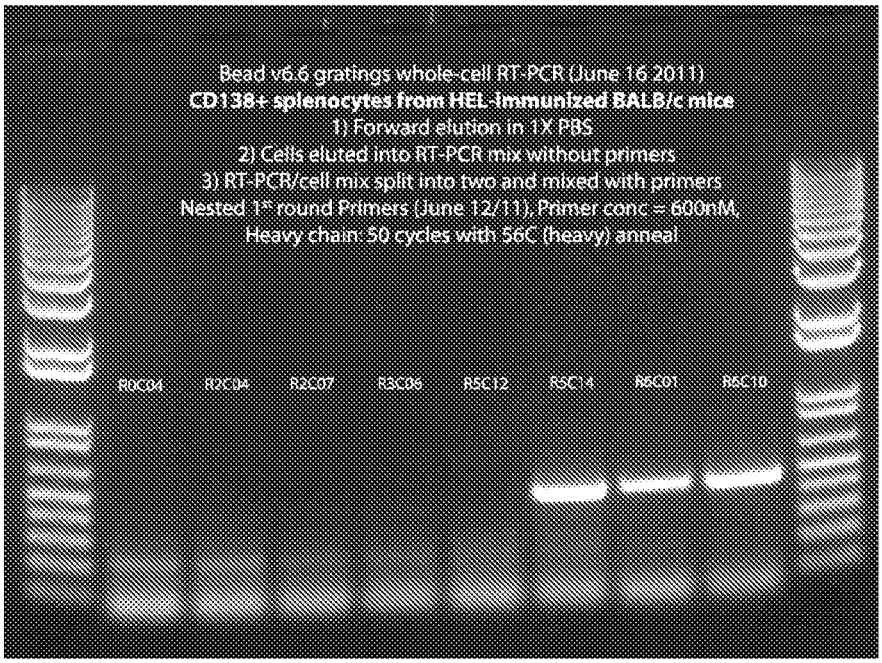

D

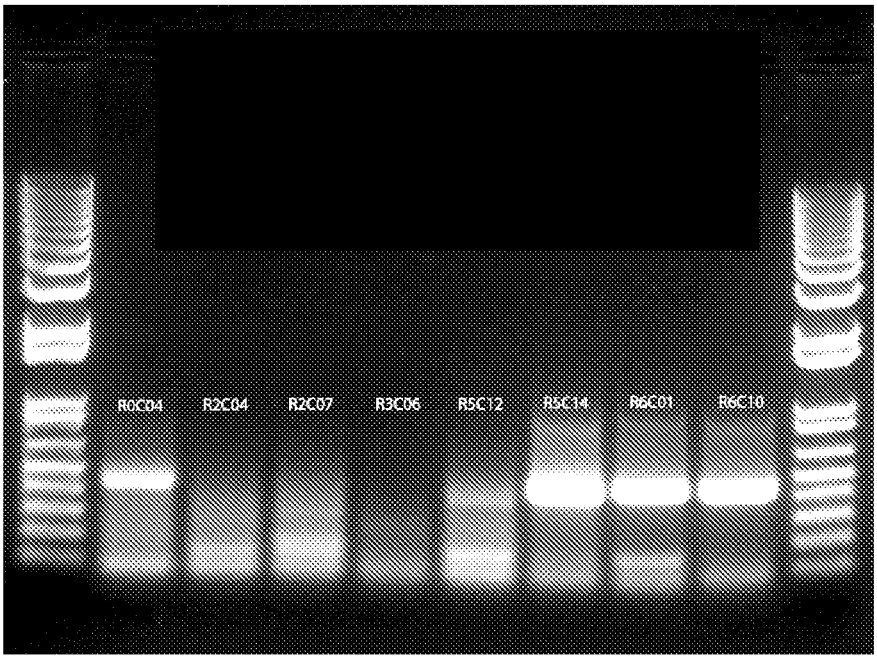

Figure 19 cont'd

A

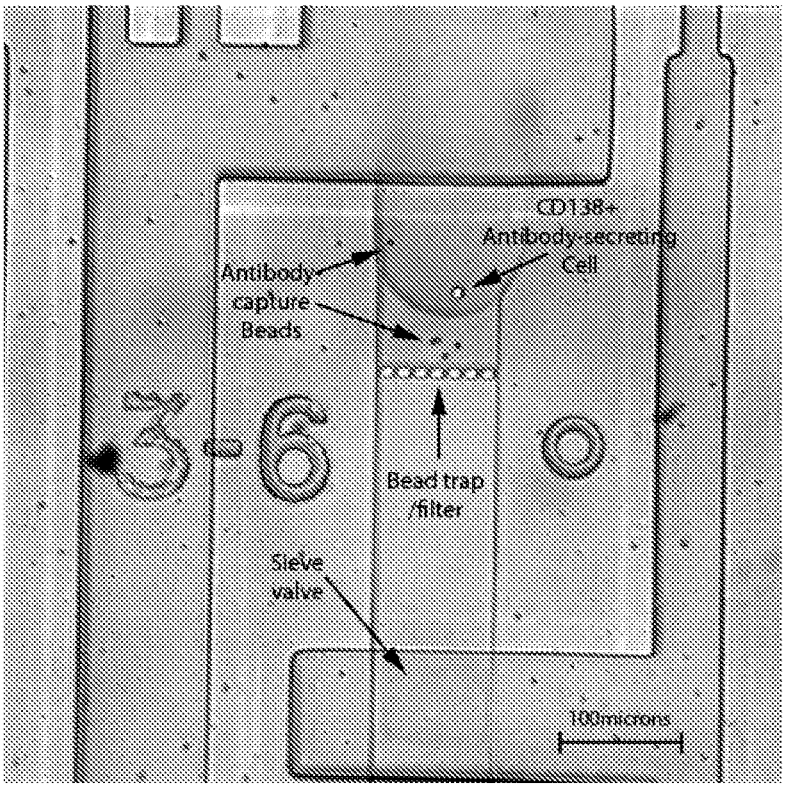
CD138+
Antibody-secreting
Cell
Antibody
capture
Beads
Bead trap
/filter
Sieve
valve
100microns

B

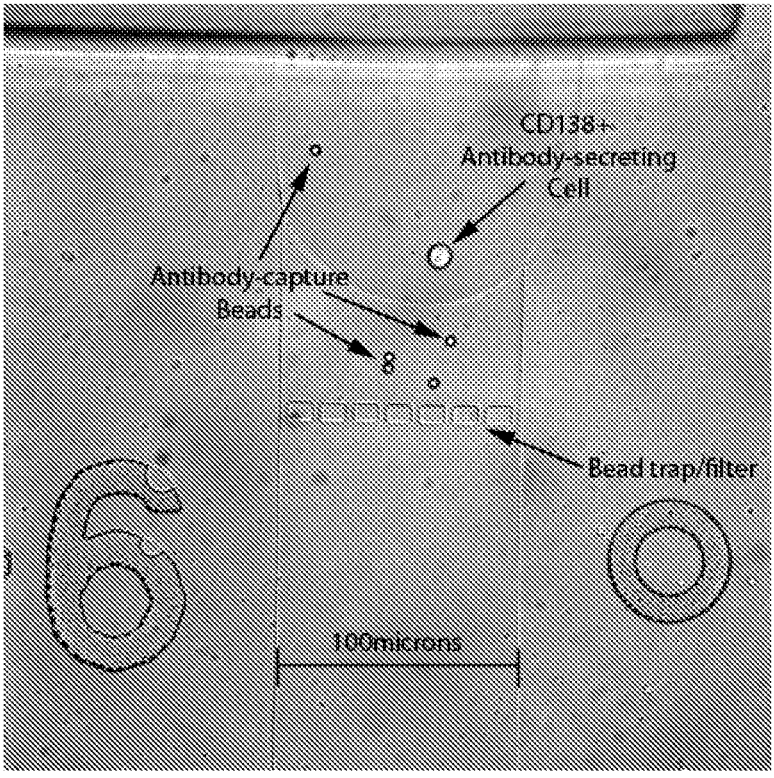
CD138+
Antibody-secreting
Cell
Antibody-capture
Beads
Bead trap/filter
100microns

Figure 20

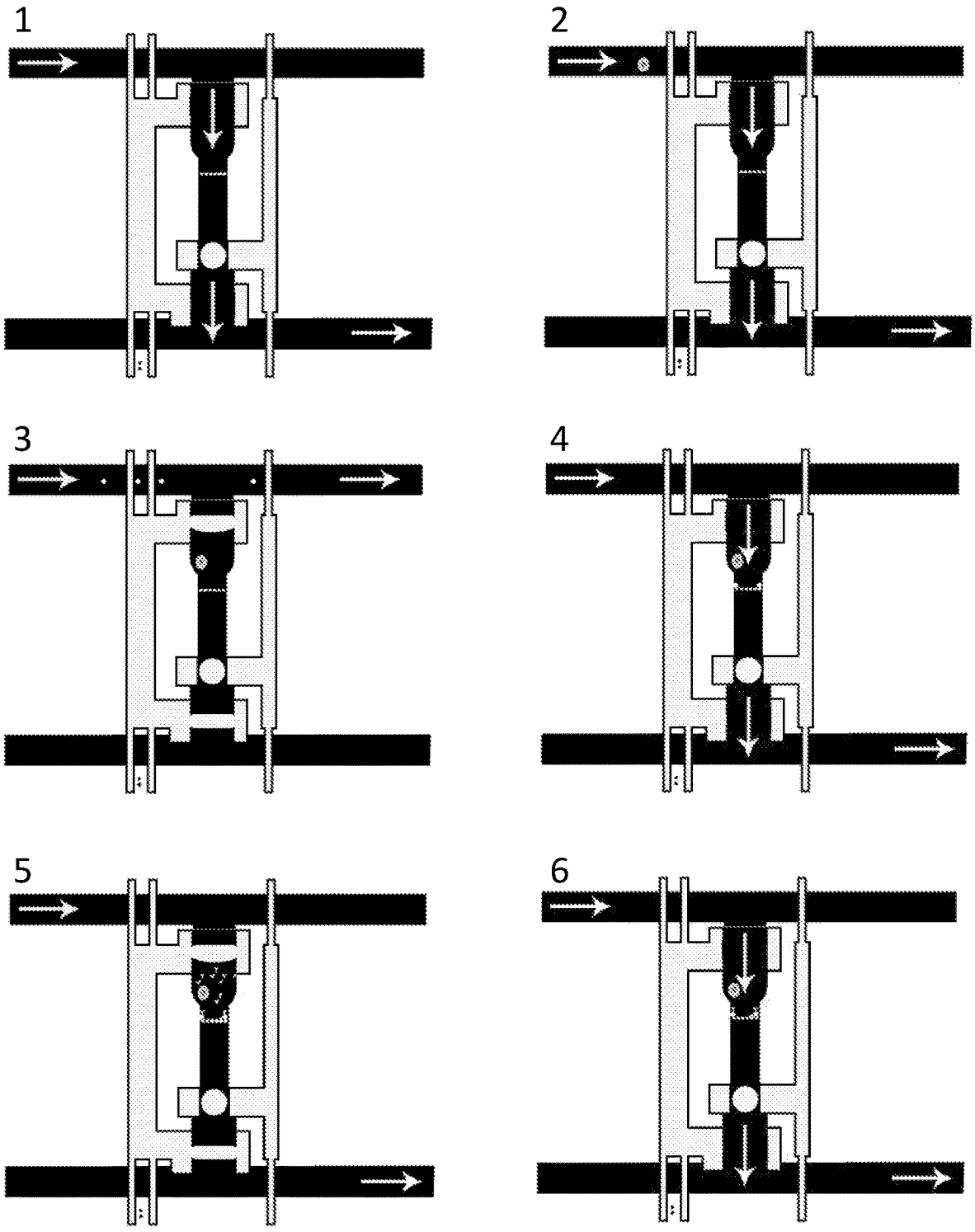

Figure 21

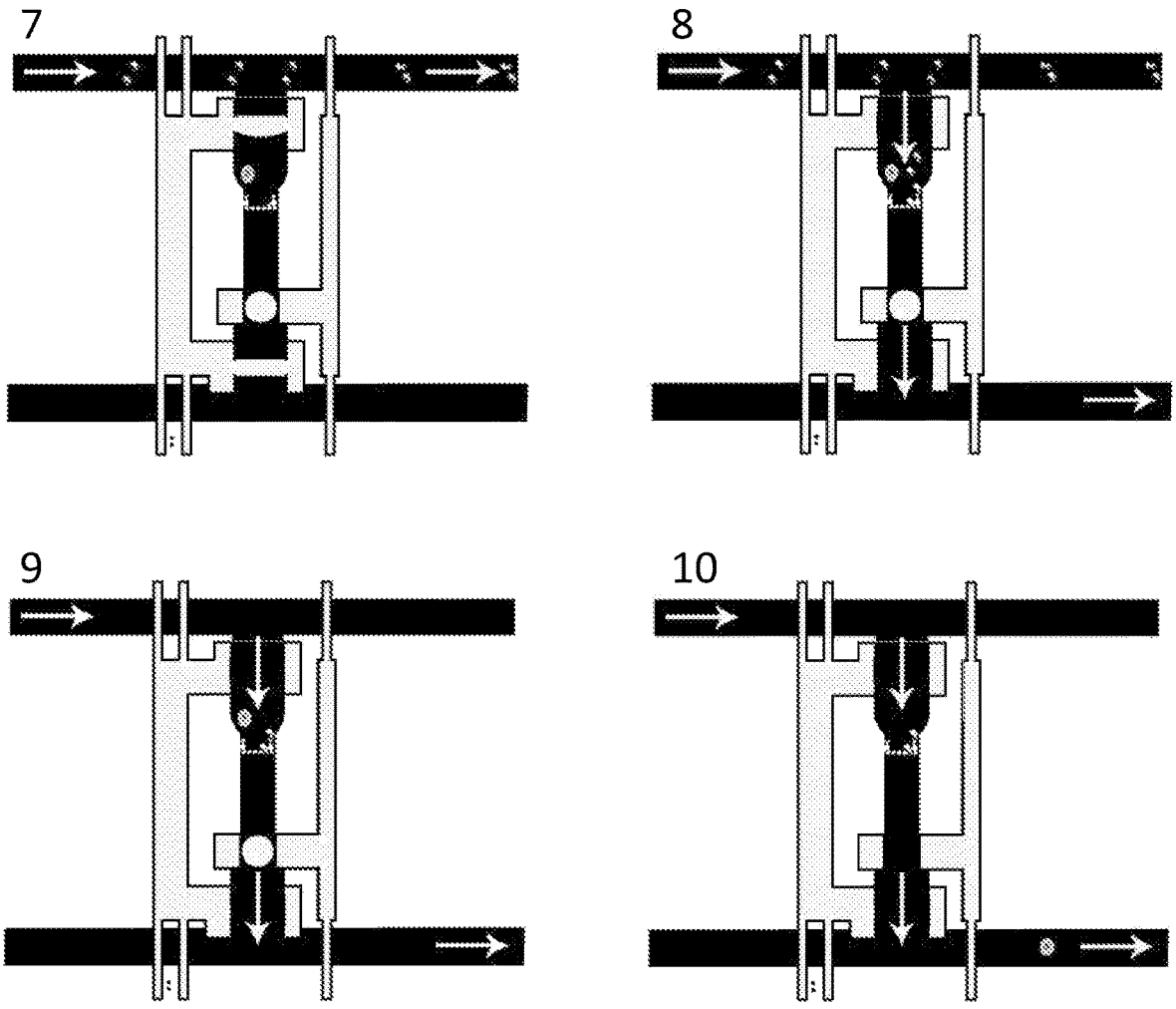

Figure 21 cont'd

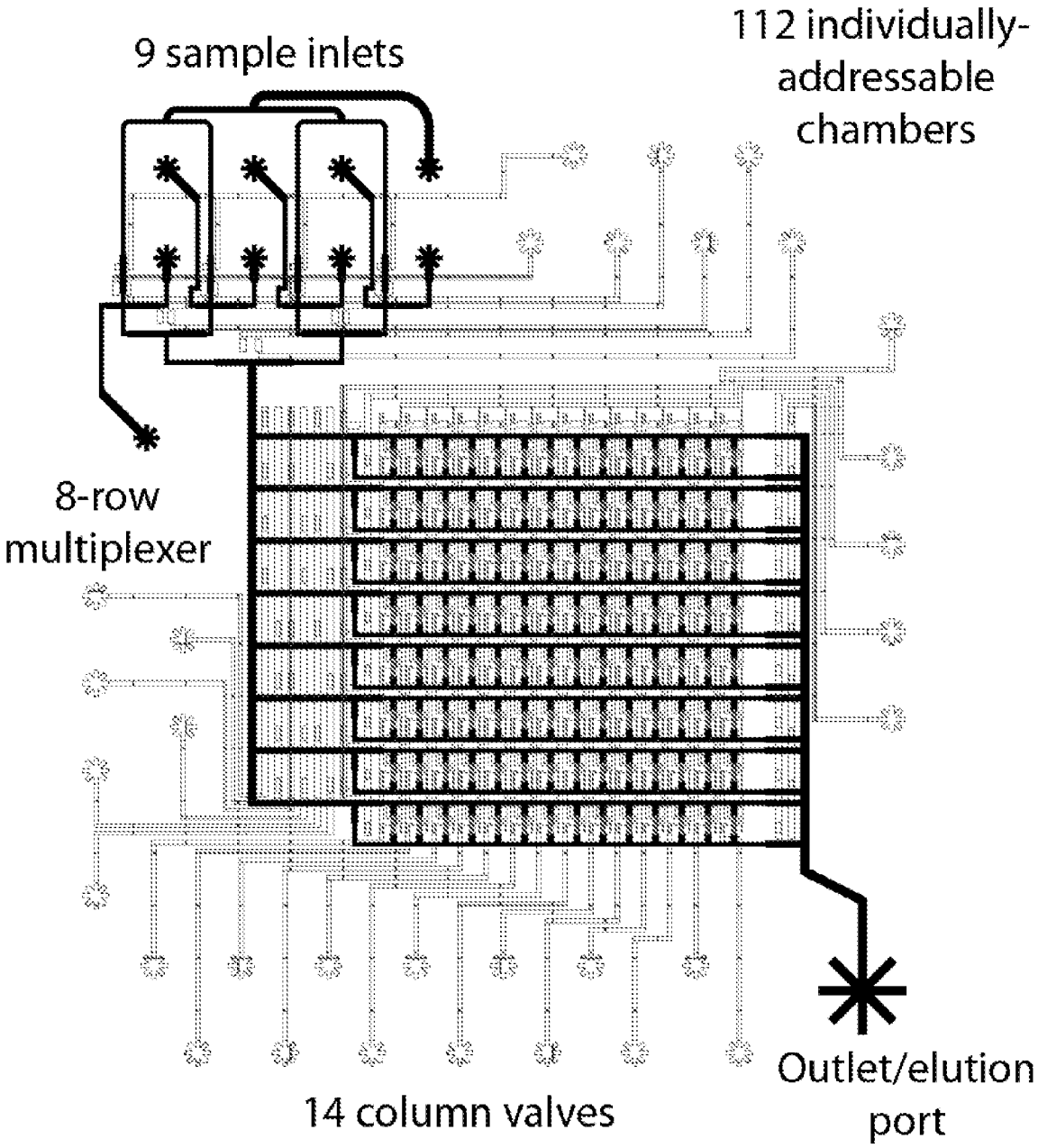
9 sample inlets
112 individually-addressable chambers
8-row multiplexer
14 column valves
Outlet/elution port

Figure 22

METHODS FOR ASSAYING CELLULAR BINDING INTERACTIONS

CROSS REFERENCE TO RELATED APPLICATIONS

This application is a continuation of U.S. patent application Ser. No. 16/746,540, filed Jan. 17, 2020, which is a continuation of U.S. patent application Ser. No. 16/579,561, filed Sep. 23, 2019, now U.S. Pat. No. 10,578,618, which is a continuation of U.S. patent application Ser. No. 16/290,751, filed Mar. 1, 2019, now U.S. Pat. No. 10,466,241, which is a continuation of U.S. patent application Ser. No. 16/129,555, filed Sep. 12, 2018, now U.S. Pat. No. 10,274,494, which is a continuation of U.S. patent application Ser. No. 14/879,791, filed Oct. 9, 2015, now U.S. Pat. No. 10,107,812, which is a continuation of U.S. patent application Ser. No. 13/184,363, filed Jul. 15, 2011, now U.S. Pat. No. 9,188,593, which claims the benefit of U.S. Provisional Patent Application Ser. No. 61/365,237 entitled "METHODS FOR ASSAYING CELLULAR BINDING INTERACTIONS" filed Jul. 16, 2010, the disclosure of each of which is incorporated herein by reference in its entirety.

FIELD OF INVENTION

This invention relates to the field of microfluidics and protein binding, more specifically, binding interaction between biomolecules.

BACKGROUND

Antibodies are defense proteins produced by the vertebrate adaptive immune system for the purposes of binding and targeting for clearance of a diverse range of bacteria, viruses, and other foreign molecules (collectively referred to as antigens) (see, for e.g., Abbas et al. (1997), *Cellular and Molecular Immunology*, 3rd Ed., Chapter 3, pp. 37-65). As a result of their ability to bind target antigens selectively and with high affinity, antibodies are useful tools for protein purification, cell sorting, diagnostics, and therapeutics.

Conventional antibody production has involved the immunization of animals (i.e., mice) with a target antigen, such as a virus, bacteria, foreign protein, or other molecule. The immunized mice produce on the order of 10^4-10^5 antibody secreting cells (ASCs), each with the capacity to produce a unique (monoclonal) antibody specific to the target antigen (see, for e.g., Poulson et al. (1997), *J. Immunol.* 179: 3841-3850; and Babcock et al. (1996), *Proc. Natl. Acad. Sci. USA* 93: 7843-7848).

The ASCs are then harvested from the immunized animals and screened in order to select which cells are producing antibodies of desired affinity and selectivity to the target antigen. Since single ASCs do not produce antibodies in sufficiently large quantities for binding affinity measurements, each ASC is clonally expanded. Primary ASCs do not grow efficiently in laboratory tissue cultures; thus, clonal expansion may be achieved by fusing ASCs to murine myeloma (cancer) cells to produce immortalized, antibody-secreting (hybridoma) cells (see, for e.g., Kohler, G. and Milstein, C. (1975), *Nature* 256: 495-497). Using this method, expansion of each successfully created hybridoma then produces a monoclonal antibody in sufficiently high concentrations to measure its affinity and selectivity to a target antigen.

It has been recognized that a limitation of hybridoma technology is the low efficiency of the fusion process. For example, whereas an immune response may produce on the order of 10^4-10^5 antibody secreting cells, a typical fusion will yield less than 100 viable hybridomas. (see, for e.g., Kohler, G. and Milstein, C. (1975), *Nature* 256: 495-497; Karpas et al. (2001), *Proc. Natl. Acad. Sci. USA* 98: 1799-1804; and Spieker-Polet et al. (1995), *Proc. Natl. Acad. Sci. USA* 92: 9348-9352). Therefore, fusions from hundreds to thousands of animals are required to fully sample the diversity of antibodies produced in an immune response, making the hybridoma approach both time-consuming and expensive. Attempts to circumvent hybridoma generation by immortalizing antibody-producing cells using viral transformations have resulted in modest gains in the efficiency of ASC immortalization. However, these approaches still require costly and time-consuming clonal expansion in order to produce sufficient quantities of monoclonal antibodies to screen for affinity and selectivity to target antigens (see for e.g., Pasqualini, R. and Arap, W. (2004), *Proc. Natl. Acad. Sci. USA* 101: 257-259; Lanzavecchia et al. (2007), *Current Opinion in Biotechnology* 18: 523-528; and Traggiai et al. (2004), *Nat Med* 10: 871-875).

Devices have been developed to estimate the equilibrium dissociation constants of antibodies secreted from single antibody-secreting cells (Story, C. M. et al. *Proc. Natl. Acad. Sci. U.S.A.* (2008) 105(46):17902-17907; and Jin, A. et al. *Nat. Med.* (2009) 15(9):1088-1092), but do not measure antibody-antigen binding kinetics using antibodies secreted from single cells.

SUMMARY

In a first embodiment, there is provided a method of assaying for a binding interaction between a protein produced by a cell and a biomolecule: (a) retaining the cell within a chamber having an inlet and an outlet; (b) exposing the protein produced by the cell to a capture substrate, wherein the capture substrate is in fluid communication with the protein produced by the cell and wherein the capture substrate is operable to bind the protein produced by the cell; (c) flowing a first fluid volume comprising the biomolecule through the inlet into the chamber and out the outlet, wherein the first fluid volume is in fluid communication with the capture substrate; and (d) determining binding interactions between the protein produced by a cell and the biomolecule.

The cell may be an antibody producing cell (APC), the protein produced by the cell is an antibody and the biomolecule is an antigen. The cell may be a single cell. The biomolecule may be a fluorescently labeled antigen. The determining binding interactions may be a measure of antigen-antibody binding kinetics. The determining the antigen-antibody binding kinetics may include fluorescence imaging of antigen-antibody binding. The determining the binding interactions may be by one or more of the following techniques: surface plasmon resonance (SPR) spectroscopy, fluorescence anisotropy, interferometry, or fluorescence resonance energy transfer (FRET). The determining of the binding interaction may be by a nanocalorimeter or a nanowire nanosensor. The measure of antigen-antibody binding kinetics may be the K_{on} rate. The measure of antigen-antibody binding kinetics may be the K_{off} rate. The measure of antigen-antibody binding kinetics may be the both the K_{on} rate and the K_{off} rate. The protein produced by the cell may be an antibody. The antibody may be a monoclonal antibody. The protein produced by the cell may be an antigen. The biomolecule may be an antigen. The biomolecule may be selected from one of the following: an

antibody, a whole cell, a cell fragment, a bacterium, a virus, a viral fragment, and a protein. The protein produced by the cell may not be secreted by the cell, and the method may further include a step of cell lysis prior to exposing the protein produced by the cell to the capture substrate. The protein produced by the cell may not be secreted by the cell, and the method may further include a step of cell lysis after exposing the protein produced by the cell to the capture substrate. The capture substrate may be a removable capture substrate. The removable capture substrate may be an anti-Ig bead. The removable capture substrate may be an anti-Ig bead and/or oligo (dT) bead. The removable capture substrate may include a capture substrate capable of capturing both nucleic acids and antibodies. The removable capture substrate may include a capture substrate capable of capturing nucleic acids and a capture substrate capable of capturing antibodies. The removable capture substrate may include a capture substrate capable of capturing nucleic acids. The binding of the antibodies may be further tested by viral inactivation. The binding of the antibodies may be further tested by bacterial inactivation. The binding of the antibodies may be further tested by cell inactivation. The method may further include adding the cell to a reverse transcription polymerase chain reaction (RT-PCR) reaction to amplify the heavy and light chain genes. The amplification may be performed in a number of ways. For example, 1) the cells may be eluted into RT-PCR mix containing primers for both heavy and light chain genes for multiplex amplification of both genes in a single reaction. Alternatively, the cells may be eluted into RT-PCR mix without primers, the mix may then be split into two equal volume aliquots and the respective heavy and light chain primers may be added to the two aliquots for single-plex amplification. Both methods have been shown to work to amplify the heavy and light chains from a single cell. The exposing the protein produced by the cell to the capture substrate may include flowing a removable capture substrate into the chamber. The method may further include washing the cell prior to flowing a removable capture substrate into the chamber. The protein produced by the cell may be an antigen and the biomolecule may be an antibody. The antibody may be a monoclonal antibody. The biomolecule may be a fluorescently labeled antibody. The fluorescently labeled antibody may be a monoclonal antibody. The determining binding interactions may be a measure of antigen-antibody binding kinetics. The measure of antigen-antibody binding kinetics may be any one or both of: a K_{on} rate; and a K_{off} rate. The APC may be from one of the following: a human, a rabbit, a rat, a mouse, a sheep, an ape, a monkey, a goat; a dog, a cat, a camel, or a pig. The removable capture substrate may be a carboxylic acid (COOH) functionalized bead. The removable capture substrate may be capable of binding the protein produced by the cell and the nucleic acids encoding the protein produced by the cell. The method may further include washing the cell prior to exposing the protein produced by the cell to a capture substrate. The APC may be selected from one of the following: a primary B cell and a memory B cell.

In a further embodiment, there is provided a cell assay method, the method including: distributing an antibody producing cell (APC) to a chamber, wherein the APC is in a first fluid; replacing the first fluid with a second fluid while maintaining the APC in the chamber; placing the antibodies produced by the APC in fluid communication with an antigen; and determining the antigen-antibody binding kinetics of the antibodies produced by the APC with the antigen.

In a further embodiment, there is provided a method of assaying for a binding interaction between a protein produced by a cell and a biomolecule, the method including: (a) retaining the cell within a chamber having an aperture; (b) exposing the protein produced by the cell to a capture substrate, wherein the capture substrate is in fluid communication with the protein produced by the cell and wherein the capture substrate is operable to bind the protein produced by the cell; (c) flowing a fluid volume comprising the biomolecule through the chamber via said aperture, wherein the fluid volume is in fluid communication with the capture substrate; and (d) determining a binding interaction between the protein produced by the cell and the biomolecule.

The measure of antigen-antibody binding kinetics may be the K_{on} rate. The measure of antigen-antibody binding kinetics may be the K_{off} rate. The measure of antigen-antibody binding kinetics may be the both the K_{on} rate and the K_{off} rate. The binding of the antibodies may be further tested by viral inactivation. The binding of the antibodies may be further tested by bacterial inactivation. The binding of the antibodies may be further tested by cell inactivation. The determining of antigen-antibody binding kinetics may be by one or more of the following techniques: surface plasmon resonance (SPR) spectroscopy, fluorescence anisotropy, interferometry, or fluorescence resonance energy transfer (FRET). The determining of antigen-antibody binding kinetics may be by a nanocalorimeter or a nanowire nanosensor. The method may further include adding the cell to a reverse transcription polymerase chain reaction (RT-PCR) reaction to amplify the heavy and light chain genes. The placing the antibodies produced by the APC in fluid communication with an antigen may include flowing a removable capture substrate into the chamber. The method may further include washing the cell prior to flowing a removable capture substrate into the chamber. The APC may be from one of the following: a human, a rabbit, a rat, a mouse, a sheep, an ape, a monkey, a goat; a dog, a cat, a camel, or a pig. The removable capture substrate may be a carboxylic acid (COOH) functionalized bead. The removable capture substrate may be capable of binding the protein produced by the cell and the nucleic acids encoding the protein produced by the cell. The method may further include washing the cell prior to exposing the protein produced by the cell to a capture substrate. The APC may be selected from one of the following: a primary B cell and a memory B cell. The method may further include adding a removable capture substrate to the chamber to capture the antibodies produced by the APC prior to placing the antibodies produced by the APC in fluid communication with an antigen. The placing of the antibodies produced by the APC in fluid communication with an antigen may include flowing a fluorescently labeled antigen through the chamber. The method may further include collecting the mRNA from the cell for a reverse transcription polymerase chain reaction (RT-PCR) reaction to amplify the heavy and light chain genes. The determining the antigen-antibody binding kinetics may include fluorescence imaging of antigen-antibody binding.

In a further embodiment, there is provided a microfluidic device for assaying for a binding interaction between a protein produced by a cell and a biomolecule, the device comprising: a chamber, having: (i) at least one inlet; (ii) at least one outlet; and (iii) a reversible trap having spaced apart structural members extending across the chamber to separate the at least one inlet and at least one outlet wherein the spaced apart structural members are operable to allow

fluid flow through the chamber from the inlet to the outlet while providing size selection for a particle within the fluid flow.

In a further embodiment, there is provided a microfluidic device for assaying for a binding interaction between a protein produced by a cell and a biomolecule, the device comprising: a chamber, having: (i) at least one inlet; (ii) at least one outlet; and (iii) a reversible trap, wherein the reversible trap is a narrowing of the chamber from to allow fluid flow through the chamber from the inlet to the outlet while providing size selection for a particle within the fluid flow.

In a further embodiment, there is provided a microfluidic device for assaying a binding interaction between a protein produced by a cell and a biomolecule, the device including: a chamber having an aperture and a channel for receiving a flowed fluid volume through the chamber via said aperture, the channel providing size selection for a particle within said fluid volume.

In a further embodiment, there is provided a microfluidic device for assaying a binding interaction between a protein produced by a cell and a biomolecule, the device including: a chamber having an aperture; a reversible trap having spaced apart structural members extending across the chamber, the structural members being operable to allow a fluid volume to flow through the chamber while providing size selection for a particle within said fluid volume.

The distance between the spaced apart structural members may be less than or equal to about 4.6 microns. The distance between the spaced apart structural members may be less than or equal to about 4.5 microns. The distance between the spaced apart structural members may be less than or equal to about 4.4 microns. The distance between the spaced apart structural members may be less than or equal to about 4.3 microns. The distance between the spaced apart structural members may be less than or equal to about 4.2 microns. The distance between the spaced apart structural members may be less than or equal to about 4.1 microns. The distance between the spaced apart structural members may be less than or equal to about 4.0 microns. The distance between the spaced apart structural members may be less than or equal to about 3.9 microns. The distance between the spaced apart structural members may be less than or equal to about 3.8 microns. The distance between the spaced apart structural members may be less than or equal to about 3.7 microns. The distance between the spaced apart structural members may be less than or equal to about 3.6 microns. The distance between the spaced apart structural members may be less than or equal to about 3.5 microns. The distance between the spaced apart structural members may be less than or equal to about 3.4 microns. The distance between the spaced apart structural members may be less than or equal to about 3.3 microns. The distance between the spaced apart structural members may be less than or equal to about 3.2 microns. The distance between the spaced apart structural members may be less than or equal to about 3.1 microns. The distance between the spaced apart structural members may be less than or equal to about 3.0 microns. The distance between the spaced apart structural members may be less than or equal to about 2.9 microns. The distance between the spaced apart structural members may be less than or equal to about 2.8 microns. The distance between the spaced apart structural members may be less than or equal to about 2.7 microns. The distance between the spaced apart structural members may be less than or equal to about 2.6 microns. The distance between the spaced apart structural members may be less than or equal to about 2.5 microns. The distance between the spaced apart structural members may be less than or equal to about 2.4 microns. The distance between the spaced apart structural members may be less than or equal to about 2.3 microns. The distance between the spaced apart structural members may be less than or equal to about 2.2 microns. The distance between the spaced apart structural members may be less than or equal to about 2.1 microns. The distance between the spaced apart structural members may be less than or equal to about 2.0 microns. The distance between the spaced apart structural members may be less than or equal to about 1.9 microns. The distance between the spaced apart structural members may be less than or equal to about 1.8 microns. The distance between the spaced apart structural members may be less than or equal to about 1.7 microns. The distance between the spaced apart structural members may be less than or equal to about 1.6 microns. The distance between the spaced apart structural members may be less than or equal to about 1.5 microns. The distance between the spaced apart structural members may be less than or equal to about 1.4 microns. The distance between the spaced apart structural members may be less than or equal to about 1.3 microns. The distance between the spaced apart structural members may be less than or equal to about 1.2 microns. The distance between the spaced apart structural members may be less than or equal to about 1.1 microns. The distance between the spaced apart structural members may be less than or equal to about 1.0 microns. The distance between the spaced apart structural members may be less than or equal to about 0.9 microns. The distance between the spaced apart structural members may be less than or equal to about 0.8 microns. The distance between the spaced apart structural members may be less than or equal to about 0.7 microns. The distance between the spaced apart structural members may be less than or equal to about 0.6 microns. The distance between the spaced apart structural members may be less than or equal to about 0.5 microns. The spaced apart structural members may be posts. The spaced apart structural members may be between 5 to 30 microns in width. The spaced apart structural members may be between 10 to 20 microns in width. The spaced apart structural members may be between 5 to 30 microns in width. The spaced apart structural members may be between 5 to 20 microns in width. The spaced apart structural members may be between 5 to 10 microns in width.

The narrowing of the chamber may be from greater than about 10 microns to less than about 5.0 microns. The narrowing of the chamber may be from greater than about 10 microns to less than about 4.9 microns. The narrowing of the chamber may be from greater than about 10 microns to less than about 4.8 microns. The narrowing of the chamber may be from greater than about 10 microns to less than about 4.7 microns. The narrowing of the chamber may be from greater than about 10 microns to less than about 4.6 microns. The narrowing of the chamber may be from greater than about 10 microns to less than about 4.5 microns. The narrowing of the chamber may be from greater than about 10 microns to less than about 4.4 microns. The narrowing of the chamber may be from greater than about 10 microns to less than about 4.3 microns. The narrowing of the chamber may be from greater than about 10 microns to less than about 4.2 microns. The narrowing of the chamber may be from greater than about 10 microns to less than about 4.1 microns. The narrowing of the chamber may be from greater than about 10 microns to less than about 4.0 microns.

It will be appreciated by a person of skill in the art that the distance between the spaced apart structural members and the narrowing of the chamber to produce the reversible trap,

will depend on the size of the cells being assayed and the size of the removable capture substrate, and the flow velocity through the chamber, whereby the cell and the removable capture substrate are retained in the chamber at a first flow velocity and whereby the removable capture substrate is retained in the chamber and the cell is able to deform and fit through the reversible trap at a second flow velocity. Alternatively, there may be different sized removable capture substrates and some may be permitted to pass through the reversible trap, while other may be retained. Furthermore, there may be further flow velocities possible with a given device, whereby the reversible trap may deform to allow the removable capture substrates to pass through the chamber. Alternatively, the chamber may be pierced to remove the removable substrate and/or cells. The narrowing of the chamber may correspond to the channel size selection.

The particle may be selected from one or more of the cell, the biomolecule, the protein, the protein bound to a removeable capture substrate, and the removeable capture substrate. The size selection of the reversible trap may prevent the cell and the removeable capture substrate from passing through the reversible trap, and may allow the biomolecule and the protein to pass through the reversible trap at a first flow velocity, and the size selection of the reversible trap may prevent the removeable capture substrate from passing through the reversible trap, while allowing the cell, the biomolecule and the protein to pass through the reversible trap at a second flow velocity. The outlet may be a sieve valve and the flow velocity through the chamber when the valve is in an open position may be sufficient to allow the cell to deform and pass through the reversible trap. The device may be operable to provide two or more flow velocities through the chamber. The device may be operable to provide two flow velocities through the chamber. The device may be operable to provide three flow velocities through the chamber. The device may be operable to provide four flow velocities through the chamber. The microfluidic device may be operable to allow for removal of the removeable capture substrate. The microfluidic device may be operable to allow for removal of the cell.

The cells get trapped in the chambers when the sieve valves are closed. However, as with the posts, the cells deform when the sieve valve is opened and there is increased flow through the chambers. Both implementations of the reversible trap have worked, but the bead post design is slightly more robust at retaining the beads. The cells being used in the present experiments are about 10 microns in diameter, the beads are 5 microns in diameter, and the space between the posts is less than 3 microns.

A chamber may be in fluid communication with a first auxiliary chamber, wherein there is may be a valve between the chamber and the first auxiliary chamber. The first auxiliary chamber may be in fluid communication with a second auxiliary chamber, wherein there is a valve between the first and second auxiliary chambers, wherein the valve has an open position to allow fluid flow from the first auxiliary chamber to the second auxiliary chamber and a closed position to prevent fluid flow from the first auxiliary chamber to the second auxiliary chamber. The first auxiliary chamber may be in fluid communication with a second auxiliary chamber and the second auxiliary chamber is in fluid communication with a third auxiliary chamber, wherein there is a valve between the first and second auxiliary chambers, wherein the valve has an open position to allow fluid flow from the first auxiliary chamber to the second auxiliary chamber and a closed position to prevent fluid flow from the first auxiliary chamber to the second auxiliary chamber, wherein there is a valve between the second and third auxiliary chambers, wherein the valve has an open position to allow fluid flow from the second auxiliary chamber to the third auxiliary chamber and a closed position to prevent fluid flow from the second auxiliary chamber to the third auxiliary chamber. The volumes of the first second and third auxiliary chambers relative to the chamber may be such that fluid may be flowed into these chambers such that subsequent RT and PCR or other reactions may be carried out without exchanging the fluid (for example, where a first outlet is in a closed position).

The volume of the auxiliary chambers may be expandable. The volume of the chamber may be between 0.1 nL to 100.0 nL. The unexpanded volume of the expandable the chamber may be between 0.1 nL to 100.0 nL. The volume of the chamber may be 0.6 nL. The unexpanded chamber may be 0.6 nL. The effective volume of a given chamber may be increased by expanding the initial chamber or by opening a valve to provide fluid flow into one or more auxiliary chambers. The ratio between the second auxiliary chamber and the first auxiliary chamber may be 5:1. The ratio between the second auxiliary chamber and the first auxiliary chamber may be at least 5:1. The ratio between the expanded chamber and the unexpanded chamber may be 5:1 or the ratio between the expanded first auxiliary chamber unexpanded first auxiliary chamber may be 5:1. The ratio between the expanded chamber and the unexpanded chamber may be at least 5:1 or the ratio between the expanded first auxiliary chamber unexpanded first auxiliary chamber may be at least 5:1. The ratio between the second auxiliary chamber and the first auxiliary chamber, or between the expanded chamber and the unexpanded chamber, or between the expanded first auxiliary chamber unexpanded first auxiliary chamber may vary depending on the reaction mixtures chosen, the concentrations of the components of the mixture and the concentration of the material being assayed. Alternatively, the chamber may be between 0.05 nL and 100.0 nL. Alternatively, the chamber may be between 0.05 nL and 90.0 nL. Alternatively, the chamber may be between 0.1 nL and 95.0 nL. Alternatively, the chamber may be between 0.1 nL and 90.0 nL. Alternatively, the chamber may be between 0.1 nL and 85.0 nL. Alternatively, the chamber may be between 0.1 nL and 80.0 nL. Alternatively, the chamber may be between 0.1 nL and 75.0 nL. Alternatively, the chamber may be between 0.1 nL and 70.0 nL. Alternatively, the chamber may be between 0.1 nL and 65.0 nL. Alternatively, the chamber may be between 0.1 nL and 60.0 nL. Alternatively, the chamber may be between 0.1 nL and 55.0 nL. Alternatively, the chamber may be between 0.1 nL and 50.0 nL. Alternatively, the chamber may be between 0.1 nL and 45.0 nL. Alternatively, the chamber may be between 0.1 nL and 40.0 nL. Alternatively, the chamber may be between 0.1 nL and 35.0 nL. Alternatively, the chamber may be between 0.1 nL and 30.0 nL. Alternatively, the chamber may be between 0.1 nL and 25.0 nL. Alternatively, the chamber may be between 0.1 nL and 20.0 nL. Alternatively, the chamber may be between 0.1 nL and 15.0 nL. Alternatively, the chamber may be between 0.1 nL and 10.0 nL. Alternatively, the chamber may be between 0.1 nL and 9.0 nL. Alternatively, the chamber may be between 0.1 nL and 8.0 nL. Alternatively, the chamber may be between 0.1 nL and 7.0 nL. Alternatively, the chamber may be between 0.1 nL and 6.0 nL. Alternatively, the chamber may be between 0.1 nL and 5.0 nL. Alternatively, the chamber may be between 0.1 nL and 4.0 nL. Alternatively, the chamber may be between 0.1

nL and 3.0 nL. Alternatively, the chamber may be between 0.1 nL and 2.0 nL. Alternatively, the chamber may be between 0.1 nL and 1.0 nL.

In a further embodiment, there is provided a method of assaying for a protein of interest produced by a cell, the method comprising: incubating the cell with a removable capture substrate in a buffer, wherein the removable capture substrate is capable of binding the protein of interest and nucleic acids encoding the protein of interest; and screening the bound removable capture substrate to determine whether the cell produces the protein of interest.

In a further embodiment, there is provided a method of assaying for a protein of interest produced by a cell, the method comprising: incubating the cell with a removable capture substrate in a buffer, wherein the removable capture substrate is capable of binding the protein of interest; and screening the bound removable capture substrate to determine whether the cell produces the protein of interest.

In a further embodiment, there is provided a method of identifying a monoclonal antibody of interest, the method comprising: incubating an APC with a removable capture substrate in a suitable buffer, wherein the removable capture substrate is capable of binding the monoclonal antibody produced by the APC and nucleic acids encoding the variable regions of the monoclonal antibody; and screening the bound removable capture substrate to determine whether the APC produces the monoclonal antibody of interest.

In a further embodiment, there is provided a cell assay method, the method comprising: distributing an APC to a chamber, wherein there is on average one APC in the chamber, wherein the APC is incubated with a removable capture substrate in a first solution, and wherein the removable capture substrate is capable of binding an antibody of interest produced by the APC and nucleic acids encoding the variable regions of the antibody of interest; replacing the first solution with a second solution while maintaining the APC in the chamber; placing the antibody of interest produced by the APC in fluid communication with an antigen; and screening the bound removable capture substrate to determine whether the APC produces the antibody of interest.

In a further embodiment, there is provided a method of assaying for a chemical interaction between a protein produced by a cell and a biomolecule, the method comprising: distributing the cell to a chamber, wherein the cell is in a first solution; replacing the first solution with a second solution while maintaining the cell in the chamber; placing the protein in fluid communication with the biomolecule; and testing the chemical interaction of the protein produced by the cell with the biomolecule.

In a further embodiment, there is provided a method of identifying a monoclonal antibody of interest, the method comprising: incubating an antibody producing cell (APC) with a removable capture substrate in a suitable buffer, wherein the removable capture substrate is capable of binding the monoclonal antibody produced by the APC and nucleic acids encoding the variable regions of the monoclonal antibody; and screening the bound removable capture substrate to determine whether the APC produces the monoclonal antibody of interest.

In a further embodiment, there is provided a cell assay method, the method comprising: distributing an antibody producing cell (APC) to a chamber, wherein there is on average one APC in the chamber, wherein the APC is incubated with a removable capture substrate in a first solution, and wherein the removable capture substrate is capable of binding an antibody of interest produced by the APC and nucleic acids encoding the variable regions of the antibody of interest; replacing the first solution with a second solution while maintaining the APC in the chamber; placing the antibody of interest produced by the APC in fluid communication with an antigen; and screening the bound removable capture substrate to determine whether the APC produces the antibody of interest.

In a further embodiment, there is provided a method of assaying for a protein of interest produced by a cell. The method involves incubating the cell with a removable capture substrate in a suitable buffer, wherein the removable capture substrate is capable of binding the protein of interest; and screening the bound removable capture substrate to determine whether the cell produces the protein of interest.

The method may involve determining the binding affinity of the protein of interest. The method may involve determining a dissociation rate; and association rate and dissociation rate. The method may involve lysing the cell prior to incubation with the removable capture substrate, wherein the protein of interest is not secreted by the cell.

In a further embodiment, there is provided an device for selecting a cell that produces a protein having a binding affinity for a biomolecule. The device may include a microfluidic device as described herein operably configured to hold an aliquot, wherein the aliquot on average contains one cell, and wherein the protein produced by the cell is in fluid communication with the biomolecule; and a detector for detecting the binding affinity of the protein produced by the cell.

The device may include a detector that is a fluorescence imager for detecting the binding affinity. The device may include a detector that is a surface plasmon resonance (SPR) spectroscopy apparatus, or a fluorescence anisotropy apparatus, or an interferometry apparatus, or a FRET apparatus. Further, the device may include a detector that is a nanocalorimeter or a nanowire nanosensor.

In a further embodiment, there is provided a kit for identifying a cell that produces antibodies having a binding affinity for an antigen. The kit includes a microfluidic device as contemplated herein; and a removable capture substrate. The kit may include the removable capture substrate being capable of binding proteins, or nucleic acids, or proteins and nucleic acids. The kit may include the removable capture substrate being a microsphere. Further, the kit may include the microsphere being a polystyrene bead or a silica bead. Further, the kit may include the microsphere being a carboxylic acid (COOH) functionalized bead.

The kit may include an antigen label. The kit may include an antigen label that is a fluorescent label. Further, the kit may include instructions for the use of the device contemplated herein to identify a cell that produces proteins having a desired binding affinity. Further, the kit may include instructions for immunizing an animal and collecting APCs. Further, the kit may include an antigen.

BRIEF DESCRIPTION OF THE DRAWINGS

FIG. **1** shows a microfluidic device and schematics for bead-based measurements of antibody-antigen binding kinetics. Panel (A) is an illustration of a microfluidic device containing control channels for individually selecting six reagent inlets and actuating sieve valves on the reagent outlet channel. Panel (B) shows a microscopic image of the device with food coloring to visualize distinct reagent inlets (as shown) and control channels (as shown) (5× magnification); Top inset depicts a close-up of beads trapped using sieve valves (20× magnification; Bottom inset depicts fluo-

rescence image of beads during binding kinetic measurements (100× magnification). Panel (C) shows a schematic of a bead assay for direct measurement of association and dissociation kinetics of immobilized mAbs and fluorescently-labeled antigen. Panel (D) shows a variation of a bead assay for indirect measurement of dissociation kinetics of immobilized mAbs and unlabeled antigen molecules.

FIG. **2** shows a schematic diagram of an embodiment of a microfluidic device for the detection of antibody secreted from single cells. (A) Hydraulic pressure is applied to valves (fully-closing) and sieve valves (partially-closing) formed by the intersection of actuation control channels with rounded- or square-profile flow channels, respectively. (B) An expanded view of an embodiment of a microfluidic device for the detection of antibody secreted from single cells. (1) chip is flushed with 1×PBS; (2) antibody-secreting cells and antibody-capture beads are loaded into chambers; (3) cells are incubated for one hour to allow for antibody secretion; (4): mix valve is opened to allow for secreted antibody to bind to beads; (5) beads and cells are captured against sieve valve and unbound antibody is washed out; (6) chambers flushed with fluorescently-labeled antigen; image and measure antibody-antigen association kinetics; and (7) flushed out unbound antigen with 1×PBS; image and measure antibody-antigen dissociation kinetics.

FIG. **3** shows plots of microfluidic bead-based measurements of antibody-antigen binding kinetics. Direct fluorescent measurements of association and dissociation kinetics of (A) D1.3 mAb and HEL-Dylight488 conjugate, (B) HyHEL-5 mAb and HEL-Dylight488 conjugate, (C) LGB-1 mAb and enhanced green fluorescent protein (EGFP) are demonstrated. (D) Indirect measurement of dissociation kinetics of D1.3 mAb and HEL using HEL-Dylight488 conjugate is demonstrated.

FIG. **4** shows simultaneous measurement of multiple antibody-antigen binding kinetics using optical and spatial multiplexing. (A) Plots measured association and dissociation kinetics of 3 distinct mAbs (HyHEL-5, D1.3, and LGB-1 mAb) interacting with 2 different antigens (HEL-Dylight633 conjugate and EGFP) is demonstrated. (B) A micrograph showing false-coloured, overlay of images taken with distinct fluorescence filter cubes to identify anti-lysozyme mAbs and anti-EGFP mAbs is demonstrated.

FIG. **5** shows plots of sensitivity and detection limit of antibody-antigen binding kinetics measurements. (A) Measured association kinetics of D1.3 mAb-Dylight488 conjugate on rabbit anti-mouse pAb coated beads is demonstrated. Inset demonstrates a schematic of bead assay for measuring binding kinetics of fluorescently-labeled mouse mAb and rabbit anti-mouse pAb coated beads. (B) Association kinetics of HEL-Dylight488 conjugate on beads with varying amounts of immobilized D1.3 mAb is demonstrated. (C) Equilibrium bead fluorescence varies linearly with the amount of immobilized D1.3 mAb. Inset shows a close-up of the graph to highlight detection limit of 1% bead coverage. (D) Direct measurement of equilibrium dissociation constants by measuring equilibrium bead fluorescence using immobilized D1.3 mAb and varying concentrations of HEL-Dylight488.

FIG. **6** shows antibody-antigen binding kinetics measured using antibodies secreted from a single cell. (A) Microscope image of D1.3 hybridoma cell loaded into a microfluidic device adjacent to rabbit anti-mouse pAb coated beads trapped using a sieve valve is shown. (B) "Single-cycle" binding kinetics from a single bead containing D1.3 mAbs secreted from a single cell and subject to increasing concentrations of HEL-Dylight488 conjugate is demonstrated.

FIG. **7** shows the effect of fluorophore stability on measured antibody-antigen binding kinetics. (A) Photobleaching rates of fluorescent dye molecules under 100 W Hg lamp illumination using 100× oil-immersion objective (NA 1.30) are plotted. (B) Effect of fluorescent exposure times on measured association kinetics of D1.3 mAb and HEL-Dylight488 are plotted.

FIG. **8** shows the effect of different bead immobilization chemistries on measured antibody-antigen binding kinetics. Measured kinetics are unaffected by bead composition (silica or polystyrene) or by different polyclonal capture antibodies (rabbit or goat pAbs).

FIG. **9** shows a plot of measured dissociation kinetics of mouse mAb from antibody capture beads. No dissociation of D1.3 mAb-Dylight488 conjugate from Rabbit anti-Ms pAb coated beads was observed over 3 days.

FIG. **10** shows a plot of the effect of antigen re-binding on measured antibody-antigen dissociation kinetics. Dissociation kinetics of D1.3 mAb and HEL-Dylight488 conjugate were unaffected by the presence of a large concentration of competitive antigen (2 mg/mL HEL).

FIG. **11** shows a plot of the effect of mass transport on measured antibody-antigen binding kinetics. Association and dissociation kinetics of D1.3 mAb and HEL-Dylight488 conjugate were unaffected by varying flow rates over a range of ~3-15 μL/hr.

FIG. **12** shows representative microscopic images of primary ASCs in a microfluidic chamber in fluid communication with antibody capture beads and oligo(dT) beads.

FIG. **13** shows an image of an ELISPOT control assay confirming that the cells depicted in FIG. **12** are ASCs. The left image represents cells that secreted any antibody; the right image represents only those cells that secreted HEL-specific antibodies.

FIG. **14** shows a scheme for preparing dual-capture (i.e., dual-function) beads using carbodiimide chemistry.

FIG. **15** shows images of dual-function beads. Polystyrene COOH beads were conjugated with rabbit anti-mouse pAb and amine functionalized oligo$(dT)_{25}$ using carbodiimide chemistry. (A) Brightfield image of dual-function beads trapped using microfluidic sieve valve. (B) Fluorescence image of synthetic single-stranded DNA molecules captured on dual-function beads. Synthetic DNA molecules are labeled with Cy5 fluorophore for visualization and also contain a poly(A) tail that binds to the oligo(dT) on the bead surface. (C) Fluorescence image of mouse D1.3 monoclonal antibody (mAb) captured on dual-function beads. D1.3 mAbs are labeled with Dylight488 fluorophore for visualization and bind to the Rabbit anti-Mouse pAb on the bead surface.

FIG. **16** shows a microscopic image (A) and antibody-antigen binding kinetics (B) as determined from a microfluidic device for dual purpose beads.

FIG. **17** depicts (A) K_d, (B) K_{on}, and (C) K_{off} rates determined from specific eluted chambers according to Example 9 herein.

FIG. **18** shows representative fluorescence intensity data over time for specific eluted chambers according to Example 9 herein. (A) depicts data for R00C04; (B) depicts data for R04C06.

FIG. **19** shows Kappa chain results from the first round of RT-PCR are shown in FIG. **19**, Panel A. Kappa chain results from the second round of RT-PCR are shown in FIG. **19**, Panel B. Heavy chain results from the first round of RT-PCR are shown in FIG. **19**, Panel C. Heavy chain results from the second round of RT-PCR are shown in FIG. **19**, Panel D.

FIG. **20** shows a microfluidic device according to an embodiment of the invention described herein, showing a reversible trap. (A) brightfield image at 20× magnification; (B) brightfield image at 40× magnification.

FIG. **21** shows a schematic whereby a microfluidic device according to an embodiment of the invention described herein is used as described herein. (1) Flush chip with 1×PBS; (2) Load antibody-secreting cells into chambers; (3) Load antibody-capture beads into inlet channel; (4) Load antibody-capture beads into chamber against bead filter; (5) Incubate cells for 1 hour to allow antibody secretion and capture on beads; (6) Wash out unbound antibody; (7) Load fluorescently-labeled antigen into inlet channel; (8) Flush chambers with fluorescently-labeled antigen; image and measure antibody-antigen association kinetics; (9) Flush our unbound antigen with 1×PBS; image and measure antibody-antigen dissociation kinetics; and (10) Open sieve valve and flush cell out of the chamber to the elution port for recovery from device.

FIG. **22** shows a schematic diagram of an alternative embodiment of the microfluidic device for assaying binding interactions.

DETAILED DESCRIPTION

A binding interaction, as referred to herein, includes a molecular interaction. A molecular interaction is commonly understood as referring to a situation when two or more molecules are attracted to one another by a force, where the force could be for example, electrostatic, dipole-dipole, hydrogen bonding, covalent, or hydrophobic in nature. A binding affinity is commonly understood as referring to an average strength of a molecular interaction. Similarly, "avidity" is used to describe the combined strength of multiple interactions. When used in the present application, "affinity" is meant to encompass one or more interactions, including avidity. The methods described herein may involve determining the binding affinity of the protein of interest. The methods described herein may also involve determining a dissociation rate; and association rate and dissociation rate. Alternatively, the methods described herein may include determining binding kinetics.

The method may involve testing the antigen binding affinity by fluorescence imaging. The method may involve testing the antigen binding affinity using any of the following techniques plasmon resonance (SPR) spectroscopy, fluorescence anisotropy, or interferometry. These techniques are understood to measure antibody-antigen binding kinetics, including, but not limited to surface plasmon resonance (SPR) spectroscopy, fluorescence anisotropy, interferometry, or fluorescence resonance energy transfer (FRET). See, for e.g., Bornhop et al. (2007), *Science* 317: 1732-1736; Homola et al. (1999) *Sensors and Actuators B: Chemical* 54: 3-15; and Xavier, K. A. and Willson, R. C. (1998), *Biophys. J.* 74: 2036-2045. Further, the method may involve testing the antigen binding affinity by a nanocalorimeter or a nanowire nanosensor. See, for e.g., Wang et al. (2005), *Proc. Natl. Acad. Sci. USA* 102: 3208-3212 and Lee et al. (2009) *Proc. Natl. Acad. Sci. USA* 106: 15225-15230. Another method that could be employed would be to use a technique such as dark-field microscopy and use antigens or antibodies labeled with gold nanoparticles. This could be used to detect single molecules and generate on/off rates by counting the molecules. See, for e.g., Ueno et al. (2010) *Biophysical J.* 98: 2014-2023; Raschke et al. (2003) *Nano Letters* 3: 935-938; and Sönnischen et al. (2000) *App. Phys. Letters* 77: 2949-2951. Further methods for labeling and detecting binding events and/or binding kinetics would be known to a person of skill in the art. For example, binding assays may include determining the number of binding events.

A protein, as referred to herein, refers to organic compounds made of amino acids, including both standard and non-standard amino acids. Standard amino acids include the following: alanine, cysteine, aspartic acid, glutamic acid, phenylalanine, glycine, histidine, isoleucine, lysine, leucine, methionine, asparagine, proline, glutamine, arginine, serine, threonine, valine, tryptophan, and tyrosine. An example of a protein is an antibody.

A biomolecule, as referred to herein, may include, but is not limited to, an antibody, or an antibody fragment, or a whole cell, or a cell fragment, or a bacterium, or a virus, or a viral fragment, a nucleic acid or a protein.

A "chamber", as used herein, refers to an enclosed space within a microfluidic device in which a cells may be retained. Each chamber may have at least one inlet for permitting fluid, including fluid containing a cell, to enter the chamber, and at least one outlet to permit fluid and/or the cell to exit the chamber (depending on the design of the chamber and/or the flow through the chamber). Persons skilled in the art will understand that an inlet or an outlet can vary considerably in terms of structure and dimension, and may be characterized in a most general sense as an aperture that can be reversibly switched between an open position, to permit fluid to flow into or out of the chamber, and a closed position to seal the chamber and thereby isolate and retain its contents. Alternatively, the aperture may also be intermediate between the open and closed positions to allow some fluid flow or may be a sieve valve that allows for fluid flow out of the cell, but not other particles (for example, the cell, the beads etc.). A chamber, as referred to herein, refers to a portion of a microfluidic device which is designed to hold, for example, a cell. As used herein, the chamber is of an exceptionally small and discrete sizing. Typical volumes are in the range of ~100 μl to ~100 nl. For example, a chamber can be designed with a volume of approximately 500 pL (less than 1 nL), with dimensions of approximately 100 microns (width), 500 microns (length), and 10 microns (height).

The direction of fluid flow through the chamber dictates an "upstream" and a "downstream" orientation of the chamber. Accordingly, an inlet will be located at an upstream position of the chamber, and an outlet will be generally located at a downstream position of the chamber. A person skilled in the art will understand, however, that a single aperture could function as both an inlet and an outlet.

An "inlet" or an "outlet", as used herein, may include any aperture whereby fluid flow is restricted through the inlet or outlet. There may be a valve to control flow, or flow may be controlled by separating the channels with a layer which prevents flow (for example, oil). Alternatively, an aperture may serve as both an inlet and outlet. Furthermore, an aperture (i.e. inlet or outlet) as used herein is meant to exclude the surface opening of a microwell.

A "microfluidic device", as used herein, refers to any device that allows for the precise control and manipulation of fluids in a geometrically constrained structure. For example, where at least one dimension of the structure (width, length, height) is less than 1 mm.

A solution, as referred to herein, may include, but is not limited to, a solution that can maintain the viability of a cell. Further, the solution may include a suitable buffer that can both retain the viability of a cell such that binding interactions can be obtained or allow for an effective lysis of the cell to obtain nucleic acids from the cell and/or antibodies or

other proteins depending on the application. Alternatively, the solution may be suitable for performing an assay.

A capture substrate, as referred to herein, is meant to encompass a wide range of substrates capable of capturing a protein or biomolecule of interest. These substrates may be modified to alter their surface (internal and external) properties depending on the desired use. For example, a substrate may be bound to antibodies or antigens to capture an antibody of interest. A capture substrate may be, for example, a microsphere or a nanosphere or other microparticles including, but not limited to a polystyrene bead or a silica bead (for example, antibody capture beads and oligo (dT) mRNA capture beads). In an alternate arrangement, instead of modifying the beads with oligo(dT), specific primers could be utilized instead. Optionally, the microsphere may be a carboxylic acid (COOH) functionalized bead. Beads which make use of alternate chemical interactions can fall within this definition. See: for e.g., G. T. Hermanson (2008), *Bioconjugate Techniques,* 2nd Edition, Published by Academic Press, Inc. For example, an alternate scheme for preparing these beads would be to use streptavidin coated beads and to mix these beads with biotinylized rabbit anti-mouse pAbs and biotinylated oligo(dT). A capture substrate can also be an anti-Ig bead which binds an antibody to the capture substrate. A capture substrate can be modified such that it binds multiple biomolecules of interest, for example both mRNA and protein. Alternately, each capture substrate could be limited to a particular biomolecule, for example, one capture substrate being limited to binding mRNA and a second capture substrate being limited to binding a protein. Capture substrates are commercially available or may be made de novo and/or modified as needed for the particular application. Capture substrates may be removable, as in the case of beads. However, capture substrates may also be fixed (and thus, non-removable).

Nucleic acids, as referred to herein, include macromolecules composed of chains of monomeric nucleotides. Common examples of nucleic acids include deoxyribonucleic acid (DNA) and ribonucleic acid (RNA).

In a further embodiment, a cell assay method is provided. The method involves distributing an antibody producing cell (APC) to a chamber, wherein the APC is in a first solution, and wherein there is on average one APC in the chamber; replacing the first solution with a second solution while maintaining the APC in the chamber; placing the antibodies produced by the APC in fluid communication with an antigen; and testing the binding of the antibodies produced by the APC with the antigen. Optionally, the method may involve adding anti-Ig beads to the chamber to capture the antibodies produced by the APC. Optionally, the method may involve lysing the APC to capture antibodies produced by the APC wherein the antibodies are not secreted by the APC.

A cell as referred to herein includes an antibody producing cell (also referred to herein as an "APC"). An APC refers to a cell that can produce an antibody. An antibody producing cell is not limited to cells that secrete antibodies, which are also referred to herein as antibody secreting cells (also referred to herein as an "ASC"). For example, it will be understood from the relevant art that memory B cells, without stimulation, do not normally secrete antibodies. See, for e.g., Abbas et al. (1997), *Cellular and Molecular Immunology,* 3rd Ed., pp. 22-23). Examples of antibody producing cells (APCs) include B cells, memory B cells, primary B cells (which are also known in the art as naïve B cells), and B cell hybridomas. A primary B cell can be harvested from the spleen, blood, or bone marrow of an animal, for example from a mouse, by FACS sorting for a cell surface marker, for example, the CD138+ marker (See: for e.g., Smith et al. (1996) *Eur. J. Immunol.* 26: 444-448).

Antibodies are defense proteins produced by the vertebrate adaptive immune system for the purposes of binding and targeting for clearance a diverse range of bacteria, viruses, and other foreign molecules (antigens). As a result of their ability to bind target antigens selectively and with high affinity, antibodies are invaluable tools for protein purification, cell sorting, and diagnostics. Antibodies are produced by B cells and are secreted by activated B cells. (See generally, for e.g., Abbas et al. (1997), *Cellular and Molecular Immunology,* 3rd Ed., Chapter 3, pp. 37-65). Antibodies are also referred to herein as immunoglobulin (also referred to herein as Ig). An antibody, as referred to herein, can include, but is not limited to polyclonal antibodies and monoclonal antibodies. Unlike polyclonal antibodies, monoclonal antibodies are monospecific antibodies that are the same because they are made by one type of immune cell that are all clones of a unique parent cell. A single APC or ASC can serve as the source of a monoclonal antibody. Antibodies are not limited to a specific isotype and can include, but are not limited to the following isotypes: IgM, IgG, IgD, IgE, and IgA. Typically, it is understood that antibodies are comprised of light and heavy chains that have variable and constant regions therein (see generally, for e.g., Abbas et al. (1997), *Cellular and Molecular Immunology,* 3rd Ed., Chapter 3, pp. 37-65).

In a further embodiment, a method of identifying a monoclonal antibody of interest is provided. The method involves incubating an APC with a removable capture substrate (RCS) in a suitable buffer, wherein the removable capture substrate is capable of binding the monoclonal antibody produced by the APC and nucleic acids encoding the variable regions of the monoclonal antibody; and screening the bound removable capture substrate to determine whether the APC produces the monoclonal antibody of interest.

In a further embodiment, a cell assay method is provided. The method involves distributing an APC to a chamber, wherein there is on average one APC in the chamber, wherein the APC is incubated with a removable capture substrate in a first solution, and wherein the removable capture substrate is capable of binding an antibody of interest produced by the APC and nucleic acids encoding the variable regions of the antibody of interest; replacing the first solution with a second solution while maintaining the APC in the chamber; placing the antibody of interest produced by the APC in fluid communication with an antigen; and screening the bound removable capture substrate to determine whether the APC produces the antibody of interest.

In a further embodiment an apparatus for selecting a cell that produces a protein having a binding affinity for a biomolecule is provided. The apparatus includes a microfluidic device operably configured to hold an aliquot, wherein the aliquot on average contains one cell, and wherein the protein produced by the cell is in fluid communication with the biomolecule; and a detector for detecting the binding affinity of the protein produced by the cell. However, the microfluidic device may also hold more than one cell, particular in an assay where the antigen or biomolecule of interest is a cell, or a cell fragment. Similarly, the antigen may be a virus or a bacterial cell.

In a further embodiment, a kit for identifying a cell that produces antibodies having a binding affinity for an antigen is provided. The kit includes a microfluidic device and a removable capture substrate.

An antigen, as referred to herein, refers to a molecule recognized by the immune system. As such, an antigen can include a molecule that can elicit an immune response in an organism, including in an animal. Examples of antigens include, but are not limited to bacterial antigens and viral antigens.

A method is provided for identifying antibody secreting cells (ASCs) that produce antibodies having a particular binding affinity for an antigen or functional attributes. The method involves distributing an ASC within a discrete aliquot wherein there is on average one ASC in the aliquot, placing the antibodies in fluid communication with the antigen; and testing the antigen binding affinity of the antibodies produced by the ASC. The method is based in part on the discovery that a single ASC, without clonal expansion, is capable of producing enough antibodies to test binding affinity for an antigen or to test other functional attributes. Furthermore, the method is also based, in part, on the discovery that clonal expansion via the production of hybridomas is not required for larger scale production of monoclonal antibodies, whereby the variable regions for the antibodies of interest may be sequenced from an ASC of interest or collected with antibodies.

By way of example, a sensitive, low-cost microfluidic bead-based fluorescence assay is described herein for measuring antibody-antigen binding kinetics within low abundance samples. Direct measurements of antibody-antigen binding kinetics may be made by time-course fluorescence microscopy of antibody-conjugated beads retained in microfluidic chambers and subject to a series of wash cycles with fluorescently-labeled antigen and buffer. A variation of the bead-based assay may include measuring the dissociation kinetics of unlabeled antibody and antigen molecules. As disclosed herein, multiple antibody-antigen interactions were measured spanning nearly four orders of magnitude in equilibrium binding affinity. The rate constants measured by way of the assay disclosed herein were validated with previously published values using SPR spectroscopy.

The methods provided herein are also contemplated for being used to screen mutagenic B cell lines. Further, the methods provided herein are contemplated for being used to screen the selectivity and specificity of antibodies to multiple different antigens.

Antibody Binding Kinetics

The affinity or binding strength of an antibody for its target antigen is an important parameter when selecting an antibody for a given application. Although the affinity of an antibody-antigen interaction is typically quantified by an equilibrium binding constant (K_d), which describes the dynamic equilibrium between binding and unbinding events, the kinetic rate constants (k_{on} and k_{off}) provide a more complete characterization of an antibody-antigen interaction. Two antibodies with identical K_d values may exhibit dramatically different binding kinetics which, in turn, will determine their respective suitability for a given application. For instance, antibodies with rapid association and dissociation kinetics may be desirable for sensing applications, whereas antibody-antigen interactions with very long half-lives may be critical for histological staining, enzyme-linked immunosorbent assays (ELISA), and Western blotting. Similarly, therapeutic antibodies that bind their target antigens with long half-lives could, in principle, be administered in lower dosages, reducing the cost and side-effects of these therapies. Direct measurement of binding kinetic constants can be a critical factor for selecting antibodies for both clinical and research applications. Examples of kinetic assays include, but are not limited to viral and other pathogenic neutralization, cell signaling and growth inhibition, modulation of enzymatic activity (inhibit or enhance).

Microfluidics

Microfluidics refers to a multidisciplinary field dedicated to the design of systems in which small volumes of fluids will be used for a variety of purposes, including lab-on-a-chip technology. See: for e.g., Squires and Quake (2005), *Reviews of Modern Physics* 77: 977-1026. Microfluidic technologies enable small-scale (picoliter to nanoliter) fluid handling operations for high-throughput biochemical analyses with low reagent costs and rapid analysis times. In particular, microfluidic devices fabricated from a silicone rubber, polydimethylsiloxane (PDMS), can be designed and fabricated in 24-48 hours, enabling rapid prototyping of devices. See: for e.g., McDonald, J. C. et al. (2000), *Electrophoresis* 21: 27-40. Microfluidic devices that integrate valves into pumps, mixers, fluidic multiplexers (MUXes), and other fluid-handling components have been successfully applied for protein crystallization, chemical synthesis, protein and DNA detection and single cell analysis. See, for e.g., Thorsen et al. (2002), *Science* 298: 580-584; Hansen, et al. (2002), *Proc. Natl. Acad. Sci. USA* 99: 16531-16536; Maerkl, S. J. & Quake, S. R. (2007) *Science* 315: 233-237; Hansen et al. (2004), *Proc. Natl. Acad. Sci. USA* 101, 14431-14436; Huang, B. et al. (2007) *Science* 315, 81-84; and Cai et al. (2006) *Nature* 440: 358-362. Microfluidic devices, as described herein, can include chambers of varying sizes. For example, chambers can be designed with a volume of approximately 500 pL (less than 1 nL), with dimensions of approximately 100 microns (width), 500 microns (length), and 10 microns (height).

As disclosed herein, antibody-antigen binding kinetics were measured with approximately 4×10^4 antibody molecules (~66 zeptomoles) immobilized on a single bead and less than 2×10^6 antibodies (~3 attomoles) loaded into the microfluidic device. This represents a reduction of greater than four orders of magnitude in both detection limit and sample consumption compared to SPR spectroscopy and a recently reported microfluidic fluorescence assay for measuring protein-protein binding kinetics. See, for e.g., Bates, S. R.; Quake, S. R. (2009), *Appl. Phys. Lett.* 95, 073705. Since each antibody-antigen interaction can be characterized on a single bead, millions of distinct antibody-antigen interactions can be characterized with a single lot of commercially available beads (i.e., 1 mL at 10^7-10^8 beads/mL). By using the bead surface rather than the chip surface as the sensor, a single microfluidic device may be re-used indefinitely and may be imaged using a standard inverted fluorescence microscope. However, a person of skill in the art could also apply the basic methods described herein to a microfluidic system having antigen and/or antibodies bound to the surface of a chip. It is further shown herein that an assay applying a method described herein may be used to perform simultaneous kinetic measurements of multiple antibody-antigen interactions using spatial and optical multiplexing. By comparison, characterization of each antibody-antigen interaction using SPR spectroscopy requires specialized instrumentation and a unique flow cell on comparatively expensive sensor chips. The low detection limit of the microfluidic bead assay coupled with small volume compartmentalization was exploited in order to measure the antigen binding kinetics of antibodies secreted by a single ASC. It is contemplated that the microfluidic

bead assay described herein could be used for measuring antibody-antigen binding kinetics from rare blood samples, for screening scarce antibodies produced by primary plasma cells from immunized animals, as well as for selecting clones for recombinant protein production. Additionally, it is contemplated that in addition to its utility for measuring antibody-antigen binding kinetics, the microfluidic bead-based assay described herein can be used for measuring other protein-protein and biomolecular interactions with a wide range of binding affinities, such as protein-carbohydrate binding, protein-DNA (i.e., transcription factor binding) and protein-RNA interactions. It is also contemplated that upon identifying an ASC that secretes antibodies which are optimal for a particular purpose, the ASC in question can be cloned by reverse-transcriptase PCR and standardized cloning techniques.

Experimental Methods

Microfluidic Device Fabrication and Control

All microfluidic devices were fabricated using multilayer soft lithography (see, for e.g., Unger, M. A. et al. (2000), *Science,* 288: 113-116 and Thorsen, T. et al. (2002), *Science* 298: 580-584. Devices were composed of two layers of poly(dimethylsiloxane) (PDMS) elastomer (GE RTV 615) bonded to No 1.5 glass coverslips (Ted Pella, Inc.). The devices were designed in AutoCAD software (Autodesk) and printed on high resolution (20,000 dpi) transparency masks (CAD/Art Services). Master molds were fabricated in photoresist on silicon wafers (Silicon Quest) by standard optical lithography. The control master molds were fabricated out of 20-25 μm high SU-8 2025 photoresist (Microchem). The flow master molds were fabricated with 12 μm rounded SPR220-7.0 photoresist channels (Rohm and Haas) and 6 μm SU-8 5 photoresist (Microchem) channels with rectangular cross-section. Microfluidic valves were actuated at 30 psi pressure which was controlled using off-chip solenoid valves (Fluidigm Corp) controlled using LabView 7.1 software and a NI-6533 DAQ card (National Instruments). Compressed air (3-4 psi) was used to push reagent solutions into the device.

Reagent Preparation

Protein A-coated 5.4 μm diameter polystyrene beads (Bangs Labs) were incubated with 1 mg/mL solutions of Rabbit anti-mouse polyclonal antibodies (pAbs) (Jackson Immunoresearch). All antibody and antigen solutions were prepared in PBS/BSA/Tween solution consisting of 1×PBS, pH 7.4 (Gibco) with 10 mg/mL BSA (Sigma) and 0.5% Polyoxyethylene (20) sorbitan monolaurate (similar to Tween-20, EMD Biosciences). Lysozyme from chicken egg white (HEL) was purchased from Sigma, and the D1.3 and HyHEL-5 mouse monoclonal antibodies to lysozyme were generously provided by Dr. Richard Willson (University of Houston). The anti-GFP mouse monoclonal antibody (LGB-1) was purchased from Abcam. Fluorescent protein conjugates were prepared using Dylight488 and Dylight633 NHS esters (Pierce) and were purified using Slide-A-Lyzer dialysis cassettes (Pierce). The concentration of fluorescent conjugates was measured by spectrophotometry (Nanodrop). In order to minimize protein denaturation, fluorescent HEL conjugates were labeled at dye-to-protein (D/P) ratios of less than 1, whereas the D1.3-Dylight488 conjugate was prepared at a D/P ratio of ~5.

Microscopy

The microfluidic devices were imaged on a Nikon TE200 Eclipse inverted epifluorescence microscope equipped with green (470/40 nm excitation, 535/30 nm emission) and red (600/60 nm excitation, 655 nm long-pass emission) fluorescence filter cubes (Chroma Technology). Fluorescence images were taken using a 16-bit, cooled CCD camera (Apogee Alta U2000) and a 100× oil immersion objective (N.A. 1.30, Nikon Plan Fluor). The sensitivity of the fluorescence measurements was tuned by binning pixels on the CCD detection camera and modulating the fluorescence exposure times (20 ms-1 s) with a computer-controlled mechanical shutter (Ludl).

Cell Culture

Mouse D1.3 hybridoma cells were cultured in RPMI 1640 media (Gibco) with 10% FCS. Prior to loading into microfluidic devices, cells were washed by centrifugation at 1500 rpm and re-suspended in fresh media in order to remove antibodies secreted in the cell media.

Microfluidic Bead-Based Fluorescence Assay

A microfluidic device was designed and fabricated to perform bead-based fluorescence measurements of antigen-antibody binding kinetics (see FIGS. **1**A and B herein). The device consists of six fluidic inlets, each used for loading a distinct reagent and controlled with an independent control valve, which join into a common fluidic outlet. The fluidic outlet can be partitioned into discrete ~200 pL chambers by actuating a set of microfluidic "sieve" valves which, when actuated, act as filters to immobilize large particles (>1 micron) while still allowing fluid exchange. See, for e.g., Marcus, J. S. et al. (2006) *Analytical Chemistry* 78: 3084-3089.

At the start of the experiment, the fluidic outlet was flushed with a PBS/BSA/Tween solution from the top and bottom fluidic inlets in order to pre-coat channel walls and reduce nonspecific binding. Next, 5.4 μm diameter Protein A beads coated with Rabbit anti-mouse pAb were loaded through the device to the fluidic outlet. The microfluidic sieve valves were then actuated and the fluidic outlet was again washed with PBS/BSA/Tween solution to immobilize the beads against the traps and wash out any free rabbit pAb in solution. The beads were then washed with the mouse antibody selected for kinetic characterization. Again, free mouse antibody was washed out of the fluidic outlet using PBS/BSA/Tween. Finally, the beads were washed with fluorescently-labeled antigen and fluorescently imaged at defined time intervals to measure the rate of antibody-antigen association (see FIG. **1**C herein). When chemical equilibrium between the antibody and antigen was reached, as detected by a plateau in bead fluorescence, the beads were flushed with PBS buffer and imaged to measure the rate of antibody-antigen dissociation. The process was repeated with varying concentrations of fluorescently-labeled antigen, each loaded onto the microfluidic device from a separate fluidic inlet.

A second version of the microfluidic bead assay was implemented to indirectly measure dissociation kinetics between antibodies and unlabeled antigen molecules by displacement with fluorescently labeled antigen (see FIG. **1**D herein). In this assay, after the antibody of interest was captured on Rabbit anti-mouse pAb-coated Protein A beads, beads were washed with unlabeled antigen at high concentration (>1 μM) to saturate all antibody binding sites. Beads were then washed with fluorescently labeled antigen while imaging at defined time intervals. Dissociation of the unlabeled antigen was then inferred by accumulated fluorescence on the beads.

In order to measure the antigen binding kinetics from antibodies secreted from single cells, Protein A beads coated with Rabbit anti-mouse pAb were first immobilized in the fluidic outlet channel using the microfluidic sieve valves. A solution of RPMI-1640 media containing 10^5 hybridoma cells/mL was then loaded into the device from a separate

fluidic inlet and the control valve was momentarily opened to allow for a single hybridoma cell to be brought in close proximity with beads immobilized in the first sieve trap in the fluidic outlet channel. The hybridoma cell was then allowed to incubate next to the beads for 1 hour, and subsequently washed with PBS/BSA/Tween buffer to wash out any free antibody in solution and halt antibody secretion from the cell. Kinetic measurements of antigen binding were then performed in the same manner as with purified antibodies.

FIG. **2** shows a schematic diagram of a microfluidic device operable for detecting antibody secreted from antibody secreting cells. The steps utilized are, for example, as follows: (1) flush microfluidic channels with cell culture media; (2) load channels with antibody secreting cells (top) and capture beads (bottom); (3) incubate cells with beads to capture secreted antibody; (4) trap cells and beads with sieve valves and flush out unbound antibody by blowing buffer over cell-bead mixture; (5) flow fluorescently-labeled antigen over trapped cells and beads; and (6) flush out unbound antigen by blowing buffer over trapped cells and beads and image fluorescent beads.

Data Analysis.

Fluorescent images were analyzed using MaximDL 4 imaging software. Fluorescent intensities were measured by selecting line profiles through the beads and recording the maximum intensity at the bead surface. During protein binding experiments, line profiles were constructed through the same beads at each measurement time point in order to avoid any systemic variations caused by differences in bead-to-bead binding capacity, variation in position in the flow channel and non-uniform illumination over the field of view. The measured fluorescence bead intensities were assumed to be proportional to the concentration of antibody-antigen complex ([AbAg]) and were fit to the following first-order, mass action and Langmuir isotherm equations using nonlinear least squares minimization:

$$F(t) = (F_{max} - F_0)\frac{[Ag]_o}{[Ag]_o + K_d}\left(1 - e^{-(k_{on}[Ag]_0 + k_{off})t}\right) + F_0 \quad \text{(equation 1)}$$

$$F(t) = (F_{max} - F_0)\frac{[Ag]_o}{[Ag]_o + K_d}e^{-k_{off}t} + F_0 \quad \text{(equation 2)}$$

$$F(t) = (F_{max} - F_0)\frac{[Ag]_o}{[Ag]_o + K_d} + F_0 \quad \text{(equation 3)}$$

where F(t) represents the measured bead fluorescence at time t, F_0 and F_{max} represent the background and maximum bead fluorescence, respectively, $[Ag]_0$ represents the solution concentration of antigen (in M), and, k_f and k_r represent the intrinsic association and dissociation rate constants, in units of $M^{-1}s^{-1}$ and s^{-1}, respectively.

EXAMPLES

The following examples describe embodiments of the invention detailed herein.

Example 1. Measurement of Antibody-Antigen Binding Kinetics on Beads

The binding kinetics of the D1.3 mouse monoclonal antibody (mAb) to fluorescently-labeled hen egg lysozyme (HEL) was measured using the methodologies and techniques described herein. See: FIG. **3**A and Table 1 herein.

TABLE 1

Antibody-antigen binding kinetics measured using the microfluidic fluorescence bead assay.

Antibody/Antigen interaction	k_{on} ($M^{-1}s^{-1}$)	k_{off} (s^{-1})	K_d
D1.3 mAb/HEL-Dylight488	$1.87 \pm 0.48 \times 10^6$	$2.10 \pm 0.25 \times 10^{-3}$	1.20 ± 0.42 nM
D1.3 mAb/HEL-Dylight633	$1.27 \pm 0.22 \times 10^6$	$2.15 \pm 0.23 \times 10^{-3}$	1.75 ± 0.46 nM
HyHEL-5 mAb/HEL-Dylight633	$5.75 \pm 0.71 \times 10^6$	$1.69 \pm 0.30 \times 10^{-4}$	30.0 ± 7.4 pM
LGB-1 mAb/EGFP	$5.00 \pm 0.72 \times 10^4$	$5.15 \pm 0.89 \times 10^{-3}$	106 ± 28 nM

The measured association and dissociation rate constants for the D1.3/HEL interaction were $1.87\pm0.48\times10^6$ $M^{-1}s^{-1}$ and $2.10\pm0.25\times10^{-3}$ s^{-1}, respectively, and were consistent with values of $1.0\text{-}2.0\times10^6$ $M^{-1}s^{-1}$ and $1.15\text{-}3.04\times10^{-3}$ s^{-1} previously measured using surface plasmon resonance (SPR) spectroscopy, stopped-flow fluorescence quenching, and competitive ELISA. See, for e.g., Batista, F. D. and Neuberger, M. S. (1998), *Immunity* 8: 751-759 and Ito, W. et al. (1995), *Journal of Molecular Biology* 248: 729-732. A ten-fold smaller association rate constant previously reported for the D1.3/HEL interaction (1.67×10^5 $M^{-1}s^{-1}$) can likely be attributed to differences between the full D1.3 mAb used in our microfluidic bead-based measurements and the recombinant single-chain antibody fragment used by Bedouelle and coworkers (England et al. (1999) *J. Immunol.* 162: 2129-2136).

Additionally, indirect, label-free measurements of the D1.3 mAb/HEL dissociation rate constant using a variation of our microfluidic bead assay were performed using the methodologies and techniques described herein. See: FIGS. **1**D and **3**D herein. In this assay, D1.3 mAbs immobilized on beads were first saturated with unlabeled HEL and subsequently washed with fluorescently-labeled HEL. Measurements of the accumulated bead fluorescence faithfully reflected the D1.3/HEL dissociation kinetics provided the labeled HEL was at a sufficiently high concentration to ensure that dissociation was rate-limiting (i.e. $k_{on}[Ag]>k_{off}$, or, equivalently, $[Ag]>K_d$). Using this method, the dissociation rate constant of D1.3 and unlabeled HEL was measured to be $1.45\pm0.30\times10^{-3}$ s^{-1}, in close agreement with direct dissociation measurements between D1.3 and fluorescently-labeled HEL. See Table 1 herein.

The microfluidic bead assay was used to measure the binding kinetics of HEL and HyHEL-5, a distinct mouse mAb with significantly stronger binding affinity to HEL than D1.3. In comparison to the D1.3 mAb, HyHEL-5 bound HEL with a nearly four-fold larger association rate constant ($5.75\pm0.71\times10^6$ $M^{-1}s^{-1}$) and ten-fold smaller dissociation rate constant ($1.69\pm0.30\times10^{-4}$ s^{-1}). See: FIG. **3**B herein. Thus, HyHEL-5 bound HEL with a ~40-fold smaller equilibrium dissociation constant than D1.3 (30 pM vs. 1.2 nM). See: Table 1 herein. Compared with the microfluidic bead assay, previous measurements of the HyHEL-5/HEL inter-

action using solution-phase fluorescence anisotropy resulted in a similar dissociation rate constant (2.2×10^{-4} s^{-1}), but a three- to five-fold larger association rate constant ($1.5\text{-}3.3\times10^{7}$ $M^{-1}s^{-1}$). See, for e.g., Xavier, K. A. and Willson, R. C. (1998) *Biophys. J.* 74: 2036-2045. Since HyHEL-5 mAb binds HEL with near diffusion-limited association kinetics, immobilization of the mAb in the microfluidic bead assay could potentially result in slower association kinetics when compared with solution-phase fluorescence anisotropy measurements. However, since the diffusion constant of HEL is approximately three times larger than that of the mAb, immobilization of the HyHEL-5 mAb would reduce the effective diffusion coefficient ($D\cong D_{mAb}+D_{HEL}$) and, hence, the apparent association rate constant by at most 25%. See, for e.g., Tyn, M. T. and Gusek, T. W. (1990), *Biotechnology and Bioengineering* 35: 327-338 and He, L. and Niemeyer, B. (2003), *Biotechnol. Prog.* 2003, 19: 544-548. Therefore, the difference in measured and reported association rate constants is likely a result of different buffer solutions, as the HyHEL-5 and HEL binding interaction is known to be very sensitive to solution pH and buffer salt concentration. See, for e.g., Xavier, K. A. and Willson, R. C. (1998) *Biophys. J.* 74: 2036-2045 and Dlugosz et al. (2009), *The Journal of Physical Chemistry* 113: 15662-15669.

The binding kinetics of a commercially available mouse monoclonal antibody (LGB-1, Abcam) to enhanced green fluorescent protein (eGFP) were also measured using the methodologies and techniques described herein. See: FIG. **3** herein. This binding interaction was chosen to demonstrate that the bead-based assay can be used to measure binding kinetics of a previously uncharacterized antibody without optimizing the bead immobilization chemistry. In this instance, native eGFP fluorescence was measured without an exogenous fluorescent label. The measured association and dissociation rate constants for the LGB-1/eGFP interaction were $5.00\pm0.72\times10^{4}$ $M^{-1}s^{-1}$ and $5.15\pm0.89\times10^{-3}$ s^{-1}, respectively. See: Table 1 herein.

Collectively, the measured binding kinetics of the anti-lysozyme and anti-eGFP mAbs span nearly four orders of magnitude in equilibrium dissociation constants (30 pM-100 nM), with association rate constants varying from 5×10^{4}-10^{6} $M^{-1}s^{-1}$ and dissociation rate constants ranging from 10^{-3}-10^{-4} s^{-1}. See: Table 1 herein. In principle, the microfluidic bead-based assay can be used to characterize stronger antibody-antigen interactions than the HyHEL-5/HEL interaction; however, binding interactions with dissociation rate constants lower than $10^{-4}s^{-1}$ require measurements to be taken over several days or weeks. On the other hand, the bead-based assay can be readily used to measure binding interactions weaker than the LGB-1/eGFP interaction. Using this assay, the practical upper limit in measurable dissociation rate constants is approximately $10^{-1}s^{-1}$, as a result of the time required to exchange solutions in the microfluidic device. Thus, the microfluidic bead-based assay should enable characterization of antibody-antigen interactions that span greater than six orders of magnitude in equilibrium binding affinity.

Example 2. Simultaneous Measurement of Multiple Antibody-Antigen Binding Kinetics Using Optical and Spatial Multiplexing

The binding kinetics of multiple antibody-antigen interactions were measured simultaneously using both optical and spatial multiplexing of the bead-based assay using the methodologies and techniques described herein. Each antibody was immobilized on a distinct population of beads and, subsequently, beads from each population were sequentially trapped using sieve valves on the microfluidic device. Since beads trapped by the sieve valves remain immobilized throughout the duration of each experiment, the spatial address of beads was tracked in order to identify each antibody. Subsequently, the trapped beads were washed with a mixture of antigens, each labeled with a spectrally distinct fluorophore. The beads were then imaged with different fluorescence filter sets designed to coincide with each fluorescent antigen. In this manner, the binding kinetics of 3 different monoclonal antibodies (D1.3, HyHEL-5 and LGB-1) to two different fluorescent antigens (HEL-Dylight488 and eGFP) were simultaneously measured. See: FIG. **4** herein. By employing this strategy, it was possible to spectrally distinguish which beads were coated with anti-lysozyme mAbs or anti-eGFP mAbs, whereas the two anti-lysozyme mAbs (D1.3 and HyHEL-5) were discriminated based on their unique binding kinetics for HEL. In addition, the fluorescence intensities of HyHEL-5 coated beads were significantly higher than the D1.3 coated beads, consistent with the fact that HyHEL-5 binds HEL with a significantly lower equilibrium dissociation constant than D1.3. See: FIG. **4** herein. This technique can be extended to measure any combination of m×n antibody-antigen interactions in which m antibodies are immobilized on different beads and exposed to a solution of n antigens, each with a spectrally-resolvable fluorescent label. In practice, several hundred antibody-antigen interactions could be measured simultaneously by imaging up to 100 beads in a single field of view with five to six spectrally distinct fluorophores. Multiplexed bead measurements could be used for simultaneously analyzing the binding kinetics and binding specificities of a panel of mAbs to multiple different antigens in serum and other complex mixtures.

Example 3. Microfluidic Bead-Based Fluorescence Measurements Reflect Intrinsic Antibody-Antigen Binding Kinetics

A series of experiments were performed using the methodologies and techniques described herein to verify that bead-based fluorescence measurements reflected intrinsic antibody-antigen binding kinetics, and were unaffected by artifacts arising from fluorescent labeling of the antigen, antibody immobilization, diffusion limitation or mass transport effects. Fluorescent labeling of HEL did not alter the intrinsic D1.3/HEL binding kinetics, as indicated by the agreement between microfluidic bead-based measurements using fluorescently labeled HEL and previously reported measurements using SPR spectroscopy with unlabeled HEL. See, for e.g., Batista, F. D. and Neuberger, M. S. (1998), *Immunity* 8: 751-759 and Ito, W. et al. (1995), *Journal of Molecular Biology* 248: 729-732. Moreover, no differences were observed in bead-based kinetic measurements of the D1.3 mAb binding to HEL labeled with two different fluorophores, Dylight488 and Dylight633 (Pierce). See: Table 1 herein. It was ensured that photobleaching of fluorophores did not affect the measured binding kinetics by measuring the photobleaching rates of the of the fluorescent dyes used in this study (Dylight488, Dylight633, and eGFP) and selecting fluorescence exposure times of less than 100 ms, such that each measurement resulted in less than 5% reduction in bead fluorescence. See: FIG. **7**A herein. Indeed, measured binding kinetics were consistent over a large range of fluorescence exposure times (ms), whereas exposure times of greater than 1 s resulted in substantial photobleach-

ing and an artificial increase in measured association and dissociation binding kinetics when compared to intrinsic kinetics. See FIG. **7**B herein.

To examine the effect of different antibody bead immobilization chemistries, we verified that measured association and dissociation rate constants for the D1.3/HEL interaction were the same when captured on silica or polystyrene beads coated with either rabbit or goat anti-mouse polyclonal antibody. See: FIG. **8** herein. It was further verified that multivalent binding between the rabbit anti-mouse pAbs and fluorescently-labeled D1.3 mAb resulted in no detectable dissociation over the course of 3 days, which would otherwise artificially accelerate the measured antibody-antigen binding kinetics. See: FIG. **9** herein. The nearly irreversible bond between rabbit pAb and the mouse mAbs was critical to successful antibody-antigen binding kinetic measurements as attempts to measure D1.3/HEL binding kinetics using Protein A beads without Rabbit anti-mouse pAbs were unsuccessful due to rapid dissociation (and low affinity) of protein A/mouse mAb complexes.

Several experiments were also conducted to verify that diffusion limitation and mass transport did not affect bead-based measurements of antibody-antigen binding kinetics. In the diffusion-limited regime, antibodies adjacent on the bead surface would compete for fluorescent antigen, thus reducing the apparent association rate constant. Similarly, the apparent rate of antibody-antigen dissociation would be reduced due to antigen rebinding to adjacent antibodies. See, for e.g., Berg, H. C. and Purcell, E. M. (1977), *Biophys. J.* 20: 193-219 and Lauffenburger, D. A. and Linderman, J. (1965) Receptors: Models for Binding, Trafficking, and Signaling; Oxford University Press. Nearly identical association and dissociation kinetics for the D1.3-HEL interaction was measured by varying the amount of bead-immobilized D1.3 mAb over two orders of magnitude. See FIG. **10**B herein. Dissociation kinetics of the D1.3 antibody and fluorescently labeled HEL were also similar both in the presence and absence of a high concentration (~2 mg/mL) of competitive unlabeled HEL antigen. See: FIG. **10** herein. Thus, there was no observable competition between antibodies adjacent to one another on the beads and, hence, no diffusion limitation. It was also confirmed that the association and dissociation rate constants of the D1.3-HEL interaction remained constant over a range of flow rates from 3-15 μL/hr, suggesting no effect of mass transport on the measured kinetics. See: FIG. **11** herein.

Example 4. Bead-Based Kinetic Measurements Exhibit Low Detection Limits and Minimal Sample Consumption

To quantify the detection limit and minimal sample consumption required for microfluidic bead-based measurements of antibody-antigen binding kinetics, antibody-antigen binding kinetics were measured using varying amounts of bead-immobilized mAb along with the methodologies and techniques described herein. The association rate constant of fluorescently-labeled D1.3 mAb binding to Rabbit anti-mouse pAb coated Protein A beads was measured. See: FIG. **5**A herein. Using the measured kinetic on-rate constant for this interaction (k_{on}=1.10±0.11×10^6 M^{-1}s^{-1}) and modulating the loading time of D1.3 mAb, the amount of bead-immobilized D1.3 mAb was varied over two orders of magnitude. Then, the antibody-antigen binding kinetics with as little as 1% of the bead surface covered with D1.3 mAb was successfully measured. See: FIG. **5**B herein. Using the manufacturer's specifications as well as steric considerations, a single 5.5 micron bead can bind 4×10^6 antibody molecules (~6.6 amol); therefore, it was estimated that the detection limit of our microfluidic fluorescence bead assay is to be ~4×10^4 antibodies or ~66 zeptomoles. See: FIG. **5**C herein. In contrast, SPR spectroscopy requires at least 200 pg (~10^9 molecules) of immobilized antibody in order to generate a detectable refractive index change. See, for e.g., Biacore Life Sciences—Biacore 3000 System Information. Website: http://www.biacore.com/lifesciences/products/systems_overview/3000/system_information/index.html. Additionally, D1.3/HEL binding kinetics were successfully measured by loading less than 2 million D1.3 mAb molecules (~3 attomoles) into the microfluidic device. In theory, the minimum sample consumption of the microfluidic bead assay could be reduced even further by reducing losses associated with channel dead volumes and optimizing the capture efficiency of antibodies on beads, as well as using microfluidic pumps to achieve flow rates less than 1 μL/hr. Thus, when compared with alternative techniques and SPR spectroscopy, our microfluidic bead-based assay can measure antigen-antibody binding kinetics with a reduction in both detection limit and sample consumption by four orders of magnitude.

Example 5. Measurement of Binding Kinetics of Antigen and Antibody Secreted from Single Cells

Based on the low detection limit of the bead-based assay and in an effort to measure the antigen binding kinetics of antibodies secreted from single antibody secreting cells, single D1.3 hybridoma cells were loaded adjacent to Rabbit anti-Mouse pAb coated Protein A beads captured in the microfluidic device, and then co-incubated the cells and beads for 1 hour at room temperature. See: FIG. **6** herein. Subsequently, antibody-antigen binding kinetics were measured by recording the fluorescence of a single bead washed with buffer and successively higher concentrations of fluorescent antigen, in a manner analogous to the single-cycle kinetics technique used with SPR spectroscopy. See, for e.g., Biacore Life Sciences—Single-Cycle Kinetics. Website: http://www.biacore.com/lifesciences/technology/introduction/data_interaction/SCK/index.html and Abdiche et al. (2008) *Analytical Biochemistry* 377: 209-217. Using the methodologies and experimental techniques described herein, the association and dissociation rate constants for the D1.3/HEL interaction were successfully measured using antibodies secreted by a single D1.3 hybridoma cell, which were consistent with measurements on purified antibodies. See: FIG. **6** and Table 1 herein.

Antibody-secreting cells are known to secrete thousands of antibodies per second at 37° C., and would, therefore, secrete enough antibodies in approximately one hour to saturate the surface of a single 5.5 μm bead with maximum binding capacity of ~4×10^6 antibody molecules. See, for e.g., Niels Jerne (1984) The Generative Grammar of the Immune System and McKinney et al. (1995) *Journal of Biotechnology* 40: 31-48. While it is reasonable to suspect that the hybridoma cells secrete antibodies at a reduced rate when incubated at room temperature; nonetheless, single D1.3 hybridoma cells secreted sufficient antibody within 1 hour at room temperature for complete kinetic characterization. However, based on the incubation time and detection limit of the assay (~4×10^4 antibodies), it can be inferred that single hybridoma cells secreted greater than 10 antibodies/second when incubated at room temperature in the microfluidic device.

Examples 1-5 show that the methods described herein are suitable for measuring antibody-antigen kinetics in a microfluidic environment from a single cell.

Example 6. Dual Function Beads

An overview of a scheme for preparing dual-capture (i.e., dual function) beads using carbodiimide chemistry is shown in FIG. **14**. A representative experiment utilizing dual function beads is shown in FIG. **15**. Briefly, polystyrene COOH beads (Bangs Labs) were conjugated with Rabbit anti-mouse pAb (Jackson ImmunoResearch) and amine-functionalized oligo(dT)$_{25}$ (Genelink) using carbodiimide chemistry. In FIG. **14**(A), a brightfield image of dual-function beads trapped using a microfluidic sieve valve is shown. In FIG. **14**(B), a fluorescence image of synthetic single-stranded DNA molecules captured on dual-function beads is shown. Synthetic DNA molecules are labeled with Cy5 fluorophore for visualization and also contain a poly(A) tail that binds to the oligo(dT) on the bead surface. In FIG. **14**(C), a fluorescence image of mouse D1.3 monoclonal antibody (mAb) captured on dual-function beads. D1.3 mAbs are labeled with Dylight488 fluorophore for visualization and bind to the Rabbit anti-Mouse pAb on the bead surface.

It will be understood that while carboxylic acid (COOH) beads are disclosed herein, other beads, which make use of alternate chemical interactions, could also be used, See: for e.g., G. T. Hermanson (2008), *Bioconjugate Techniques,* 2nd Edition, Published by Academic Press, Inc. For example, an alternate scheme for preparing thee beads would be to use streptavidin coated beads and to mix these beads with biotinylized rabbit anti-mouse pAbs and biotinylated oligo (dT).

Example 7. Multiplex RT-PCR of the Antibody Heavy and Light Chain Genes

Results from a multiplex RT-PCR of the antibody heavy and light chain genes indicated that a gene product coinciding with the proper molecular size was obtained. Briefly, D1.3 hybridoma cells were lysed using a nonionic detergent (1% NP-40 in 1×PBS) and the lysate was then mixed with rabbit anti-mouse pAb, oligo(dT)-conjugated dual-capture beads for mRNA capture. Generally, a gentle lysis buffer is preferred for cell lysis and can include, in addition to the foregoing: 0.5% NP-40 in 1×PBS or DI water or 0.5% Tween-20 in 1×PBS or DI water. Generally, it is preferable and within the knowledge of those persons skilled in the art to use lysis buffers that can sufficiently lyse the outer membrane of the cell in question, while keeping the nucleus intact. RT-PCR was performed using degenerate primers for both heavy and light chain genes and resulted in bands of the expected size for antibody heaby and light chains (date not shown). The results suggest that dual purpose RNA and antibody beads are capable of capturing RNA suitable for amplification. For comparison, RT-PCR of antibody genes was performed using commercially available oligo(dT) beads and dual-capture beads. The methodology utilized herein is generally as follows:

1) Capture oligo(dT) beads in microfluidic chambers using sieve valves.
2) Load cells in microfluidic chambers.
3) Load antibody-capture beads in chambers.
4) Incubate cells and beads.
5) Measure antibody-antigen binding kinetics.
6) Lyse cells using either a) 1% NP-40 in 1×PBS, or b) alkaline lysis solution (100 mM Tris-HCl, pH 7.5, 500 mM LiCl, 10 mM EDTA, pH 8.0 1% LiDS, 5 mM dithiothreitol (DTT)). During lysis, the cell lysate is flushed over the stack of trapped oligo(dT) beads. The oligo(dT) beads and alkaline lysis solution are from the Dynabead mRNA direct kit developed by Invitrogen, but alternatives to these reagents exist.
7) Wash beads with 1×PBS to remove lysis solution.
8) Open sieve valves.
9) Open microfluidic chamber valves and send beads to an output port (one chamber at a time).
10) Recover beads from output port using a pipette.
11) Pipette beads into 50 microL of one-step RT-PCR mix.
    i) dNTPs;
    ii) mixture of RT and DNA polymerase enzymes;
    iii) degenerate primers for both heavy and light chain genes (PCR reagents from a One-Step RT-PCR kit developed by Qiagen, but could also be prepared ourselves);
12) Perform RT and Touchdown PCR using the following protocol:
    i) RT at 50° C. for 30 min;
    ii) 95° C. for 15 min to inactivate RT enzyme and activate DNA polymerase
    iii) First ten cycles of Touchdown PCR:
    a) 94° C. for 30s;
    b) 55° C. for 1 min (decrease by 1 C each cycle, until 45 C);
    c) 72° C. for 1 min.
    iv) 30 cycles of PCR
    a) 94° C. for 30s;
    b) 45° C. for 1 min;
    c) 72° C. for 1 min.
13) Visualize RT-PCR amplicons on 0.5% DNA agarose gel using SYBRsafe fluorescent dye.
14) Extract amplicons from gel and purify using standard gel extraction kit (Qiagen).
15) Sequence samples.

Example 8. Microfluidic Antibody-Antigen Binding Kinetics Measured Using Dual Function Beads and Antibodies Secreted by Single Hybridoma Cells

Microscope image of D1.3 hybridoma cell adjacent to Rabbit anti-Mouse pAb, oligo(dT)-conjugated polystyrene beads trapped by a microfluidic sieve valve. After a 2 hour incubation the beads with the D1.3 cell, antibody-antigen binding kinetics were measured using fluorescently labeled HEL-Dylight488 conjugate. These results are highlighted in FIG. **16** and show that dual purpose beads are suitable for testing antibody-antigen binding kinetics.

Example 9. Mouse Experiment: Antibody Binding Kinetics and Whole-Cell Heavy Chain RT-PCR with Beads

These experiments were designed to detect antibodies from primary splenocytes harvested from BALB/c immunized mice. The cells were eluted and whole-cell single-plex RT-PCR was performed of heavy and light chain antibody genes. Thereafter, binding kinetics of the antibodies were measured.

Chip.

Bead v6.6 chip with ~3 micron high sieve channels, 2 micron gratings (fabricated: May 29, 2011 with RTV615).

Reagents.

The following reagents were used herein: 1×PBS for reagent flush; FACS-sorted CD138+ primary splenocytes in

RPMI-10-2-ME media; 4.9 micron Rabbit anti-Mouse Protein A beads; 5 microL of stock bead solution resuspended in 100 μL of RPMI-10-2-ME media; and 214 ng/mL HEL488 in 1×PBS.

Experimental Protocol.

The following experimental protocol was followed: washed chip with 1×PBS; closed sieve valves; spun down primary cells and decanted ~400 of 500 pt of media; and re-suspended cells in remaining media.

Thereafter, the cells were loaded in all chambers sequentially with deliberate negative controls included (e.g., R1C14 and R0C02); load 4.9 micron Rabbit anti-Mouse Protein A beads in all chambers sequentially; incubate cells and beads for 1 h 20 min; and wash all chambers with 214 ng/mL HEL488 for 5 min. Thereafter, chamber intensities were analyzed using Image Analysis. Positive chambers were determined as follows: R0004, R0008, R2C02, R2C04, R2C07, R2C12, R2C13, R3C06, R4C01, R4C03, R4C05, R5C08, R5C09, R5C12, R5C14, R6C01, R6C02, R6C09, R6C10, R6C11, and R7C05.

RT-PCR mix without primers was prepared from a One-Step RT-PCR kit (Qiagen). The mix comprised: 10 μL 5×RT-PCR buffer×16=160 μL; 21 μL RNase-free water×16=336 μL; 2 μL dNTPs×16=32 μL; 2 μL Enzyme mix×16=32 μL. The RT-PCR mix without primers was aliquoted into 8 tubes of 70 μL each (2 reaction volumes, not including primer volume).

Prepared primer solutions to be mixed with RT-PCR after cell elution were as follows: Heavy chain—7.5 μL 8 μM 3' IgH first primer×8=60 μL; and 7.5 μL 8 μM 5' IgH first primer×8=60 μL. Kappa chain—7.5 μL 8 μM 3' IgK first primer×8=60 μL; and 7.5 μL 8 μM 5' IgK first primer×8=60 μL. 15 μL of primer mixes were aliquoted into each of 8 tubes. The primers used herein were selected based on what is taught in Table II of Tiller et al. (2009) *J. Immunol. Methods* 350: 183-193, which is incorporated herein by reference. Those persons skilled in the art that variants to the primers defined in Table II could be used under certain circumstances including, for example, the primers in Table III in Tiller et al. (2009).

Eight (8) of the brightest chambers [R0004, R2C04, R2C07, R3C06, R5C12, R5C14, R6C01, R6C10] were eluted. The eluted cell samples were pipetted directly into 70 μL RT-PCR mix without primers. The RT-PCR/cell mix was split into two (2) equal parts of 35 μL and mixed with kappa and heavy chain primers, respectively. RT-PCR was performed using a thermal cycler. Briefly, the "NEST1ST5" protocol was used for the kappa chain reactions, comprising: RT step: 50° C. for 30 min; Hotstart/RT inactivation: 95° C. for 15 min; and 50 Cycles (denaturation: 94° C. for 30s; anneal: 50° C. for 30s; and extension: 72° C. for 55s). Then, there was a final extension: 72° C. for 10 min. Heavy chain reactions performed using the "NEST1H" protocol, comprising: RT step: 50° C. for 30 min; Hotstart/RT inactivation: 95° C. for 15 min; and 50 Cycles (denaturation: 94° C. for 30s; anneal: 56° C. for 30s; extension: 72° C. for 55s). Then, there was a final extension: 72° C. for 10 min.

Thereafter, kinetics were measured on each of the eluted chambers. A summary of the kinetics data is shown in FIG. **17**. Representative kinetics sample data is shown in each of FIGS. **18**A-E herein. Dissociation kinetics were measured and then association kinetics were measured using freshly loaded HEL488. Thereafter, a second round of single-plex RT-PCR was performed using nested second round primers. The heavy chain mix comprised of: 10 μL 5×RT-PCR buffer×8=80 μL; 21 μL RNase-free water×8=168 μL; 2 μL dNTPs×8=16 μL; 2 μL Enzyme mix×8=16 μL; 7.5 μL 8 μM 3' IgH second primer×8=45 μL; and 7.5 μL 8 μM 5' IgH second primer×8=45 μL. The kappa chain mix comprised of: 10 μL 5×RT-PCR buffer×8=80 μL; 21 μL RNase-free water×8=168 μL; 2 μL dNTPs×8=16 μL; 2 μL Enzyme mix×8=16 μL; 7.5 μL 8 μM 3' IgK second primer×8=45 μL; and 7.5 μL 8 μM 5' IgK second primer×8=45 μL. Thereafter, 3.5 μL of template from each of the first round reactions was added and RT-PCR was performed on a thermal cycler. Kappa chain reactions were performed using the "NEST2K" protocol. Briefly, there was no RT step; hotstart/RT inactivation was at 95° C. for 15 min followed by 50 cycles (denaturation: 94° C. for 30s; anneal: 45° C. for 30s; and extension: 72° C. for 55s). Then, there was a final extension: 72° C. for 10 min.

Heavy chain reactions performed using the "NEST2H" protocol. Briefly, there was no RT step; hotstart/RT inactivation: 95° C. for 15 min, followed by 50 cycles (denaturation: 94° C. for 30s; anneal: 60° C. for 30s; and extension: 72° C. for 55s). Then, there was a final extension: 72° C. for 10 min. The RT-PCR products for both first and second round reactions were run on a gel. Kappa chain results from the first round are shown in FIG. **19**A. Kappa chain results from the second round are shown in FIG. **19**B. Heavy chain results from the first round are shown in FIG. **19**C. Heavy chain results from the second round are shown in FIG. **19**D. The gel products were sequenced by standard procedures known to those skilled in the art. Based on the sequence data generated, variants in antibody sequences were detectable. As a representative example, mutations in the R00C04 sample are shown in Table 2 herein.

TABLE 2

R00C04 (9 non-synonymous mutations)

Position (from IMGT)	Situation (from IMGT)	Germline Ab residue	R00C04 Ab residue
L-36	CDR1-L	S	N
L-92	FR3-L	S	T
H-17	FR1-H	A	D
H-36	CDR1-H	S	R
H-40	FR2-H	H	L
H-64	CDR2-H	N	K
H-65	CDR2-H	T	S
H-83	FR3-H	S	I
H-94	FR3-H	P	L

Example 10. Microfluidic Device

A microfluidic device has been developed for assaying a binding interaction between a protein produced by a cell and a biomolecule. The device has a chamber having an aperture and a channel for receiving a flowed fluid volume through the chamber via said aperture. The channel provides for size selection for a particle within the fluid volume. Alternately, another embodiment of the microfluidic device has a chamber having an aperture and a reversible trap. The reversible trap has spaced apart structural members extending across the chamber. The structural members are operable to allow a fluid volume to flow through the chamber while providing size selection for a particle within the fluid volume. See, for example: FIG. **20** herein.

Although various embodiments of the invention are disclosed herein, many adaptations and modifications may be made within the scope of the invention in accordance with the common general knowledge of those skilled in this art. Such modifications include the substitution of known

equivalents for any aspect of the invention in order to achieve the same result in substantially the same way. Numeric ranges are inclusive of the numbers defining the range. The word "comprising" is used herein as an open-ended term, substantially equivalent to the phrase "including, but not limited to", and the word "comprises" has a corresponding meaning. As used herein, the singular forms "a", "an" and "the" include plural referents unless the context clearly dictates otherwise. Thus, for example, reference to "a thing" includes more than one such thing. Citation of references herein is not an admission that such references are prior art to the present invention. The invention includes all embodiments and variations substantially as hereinbefore described and with reference to the examples and drawings. Further, citation of references herein is not an admission that such references are prior art to the present invention nor does it constitute any admission as to the contents or date of these documents.

What is claimed is:

1. A method of assaying a secreted monoclonal antibody produced by a single antibody producing cell (APC) and an antigen, the method comprising:

retaining the single APC within a chamber having a volume of from 100 pL to 100 nL, a solid wall, and an aperture that defines an opening of the chamber;

incubating the single APC within the chamber to produce a secreted monoclonal antibody;

exposing the secreted monoclonal antibody to a first removeable capture substrate, wherein first the removeable capture substrate is in fluid communication with the secreted monoclonal antibody and wherein the first removeable capture substrate is capable of binding the secreted monoclonal antibody;

incubating the secreted monoclonal antibody with the first removeable capture substrate to produce a bound antibody;

exposing a first fluid volume comprising the antigen in fluid communication with the bound antibody;

determining whether the bound antibody binds the antigen; and

lysing the single APC and capturing the nucleic acids of the single APC on a second removeable capture substrate.

2. The method of claim **1**, wherein the single APC is a primary B cell or a memory B cell.

3. The method of claim **1**, wherein the single APC is a primary plasma cell.

4. The method of claim **1**, wherein the single APC is from a human, a rabbit, a rat, a mouse, a sheep, an ape, a monkey, a goat, a dog, a cat, a camel, or a pig.

5. The method of claim **1**, wherein the first removeable capture substrate comprises an anti-Ig bead.

6. The method of claim **1**, wherein the second removeable capture substrate comprises an oligo(dT) mRNA capture bead capable of binding mRNA from the single APC.

7. The method of claim **5**, wherein the second removeable capture substrate comprises an oligo(dT) mRNA capture bead capable of binding mRNA from the single APC.

8. The method of claim **1**, wherein the second removeable capture substrate is capable of binding nucleic acids encoding the variable regions of the secreted monoclonal antibody and capturing the nucleic acids comprises capturing nucleic acids encoding the variable regions of the secreted monoclonal antibody.

9. The method of claim **5**, wherein the second removeable capture substrate is capable of binding nucleic acids encoding the variable regions of the secreted monoclonal antibody and capturing the nucleic acids comprises capturing nucleic acids encoding the variable regions of the secreted monoclonal antibody.

10. The method of claim **1**, further comprising washing the second removeable capture substrate after lysing.

11. The method of claim **5**, further comprising washing the second removeable capture substrate after lysing.

12. The method of claim **6**, further comprising washing the second removeable capture substrate after lysing.

13. The method of claim **7**, further comprising washing the second removeable capture substrate after lysing.

14. The method of claim **8**, further comprising washing the second removeable capture substrate after lysing.

15. The method of claim **1**, further comprising recovering the second removeable capture substrate.

16. The method of claim **1**, further comprising recovering the first removeable capture substrate and the second removeable capture substrate.

17. The method of claim **5**, further comprising recovering the second removeable capture substrate.

18. The method of claim **6**, further comprising recovering the second removeable capture substrate.

19. The method of claim **8**, further comprising recovering the second removable capture substrate.

20. The method of claim **1**, wherein the antigen is fluorescently labeled.

21. The method of claim **1**, wherein determining whether the bound antibody binds the antigen comprises measuring an antigen-antibody binding kinetic property between the antigen and the bound antibody.

22. The method of claim **21**, wherein the antigen-antibody binding kinetic property is a K_{on} rate; a K_{off} rate, a dissociation constant, or a combination thereof.

23. The method of claim **1**, wherein determining whether the bound antibody binds the antigen comprises measuring the affinity of the bound antibody and the antigen.

24. The method of claim **1**, wherein determining whether the bound antibody binds the antigen comprises measuring the avidity of the bound antibody and the antigen.

25. The method of claim **1**, wherein the antigen is a cell fragment, a bacterium, a virus, a viral fragment, or a protein.

26. The method of claim **1**, wherein the aperture serves as the inlet and the outlet of the chamber.

27. The method of claim **1**, wherein determining whether the bound antibody binds the antigen comprises fluorescence imaging of the chamber.

28. The method of claim **1**, wherein determining whether the bound antibody binds the antigen comprises a surface plasmon resonance (SPR) spectroscopy, fluorescence anisotropy, interferometry or fluorescence resonance energy transfer (FRET) measurement.

29. The method of claim **1**, further comprising performing a reverse transcription polymerase chain reaction (RT-PCR) on the nucleic acids of the single APC to amplify the heavy and light chain genes of the secreted monoclonal antibody.

30. The method of claim **5**, further comprising performing a reverse transcription polymerase chain reaction (RT-PCR) on the nucleic acids of the APC to amplify the heavy and light chain genes of the secreted monoclonal antibody.

* * * * *

Exhibit 4

OUR MISSION

We find the best cells.

Discovery of cellular therapies, biopharmaceuticals, and other cell-based products depends on precise, time-consuming, cell-by-cell manipulations. But biologists need to move faster and more efficiently to meet today's scientific demands. Our mission is to accelerate the use of cell-based products by providing researchers access to the Berkeley Lights Platform to find the best cells in a fraction of the time and at a fraction of the cost of traditional methods.

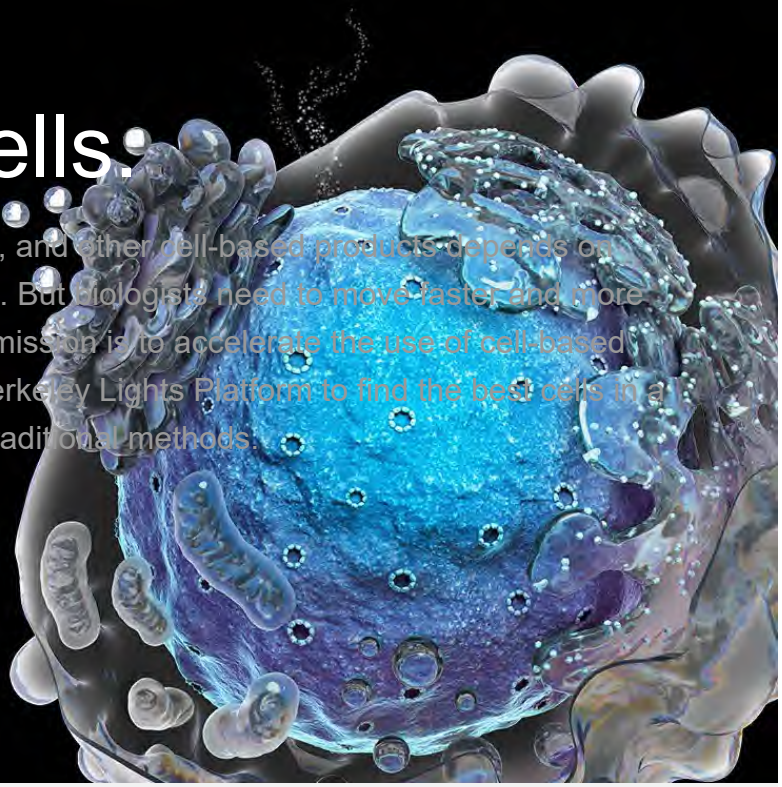

Browse Our Products

OUR PRODUCTS

Our workflows are our products.

Sift through thousands of cells at once and get deep profiling with more relevant phenotypic, genotypic and imaging information for each single cell, across a number of dimensions.

Browse Our Workflows

Link Function to Genotype

Cell Therapy Development

Breakthrough Discoveries

Synthetic Biology

OUR STORY

Understand how we not only find but deliver the best cells.

Our products enable biologists to functionally screen and recover individual living cells. We deliver more information about cell function than any other technology currently available and can link that function to the underlying genomics at a single cell level.

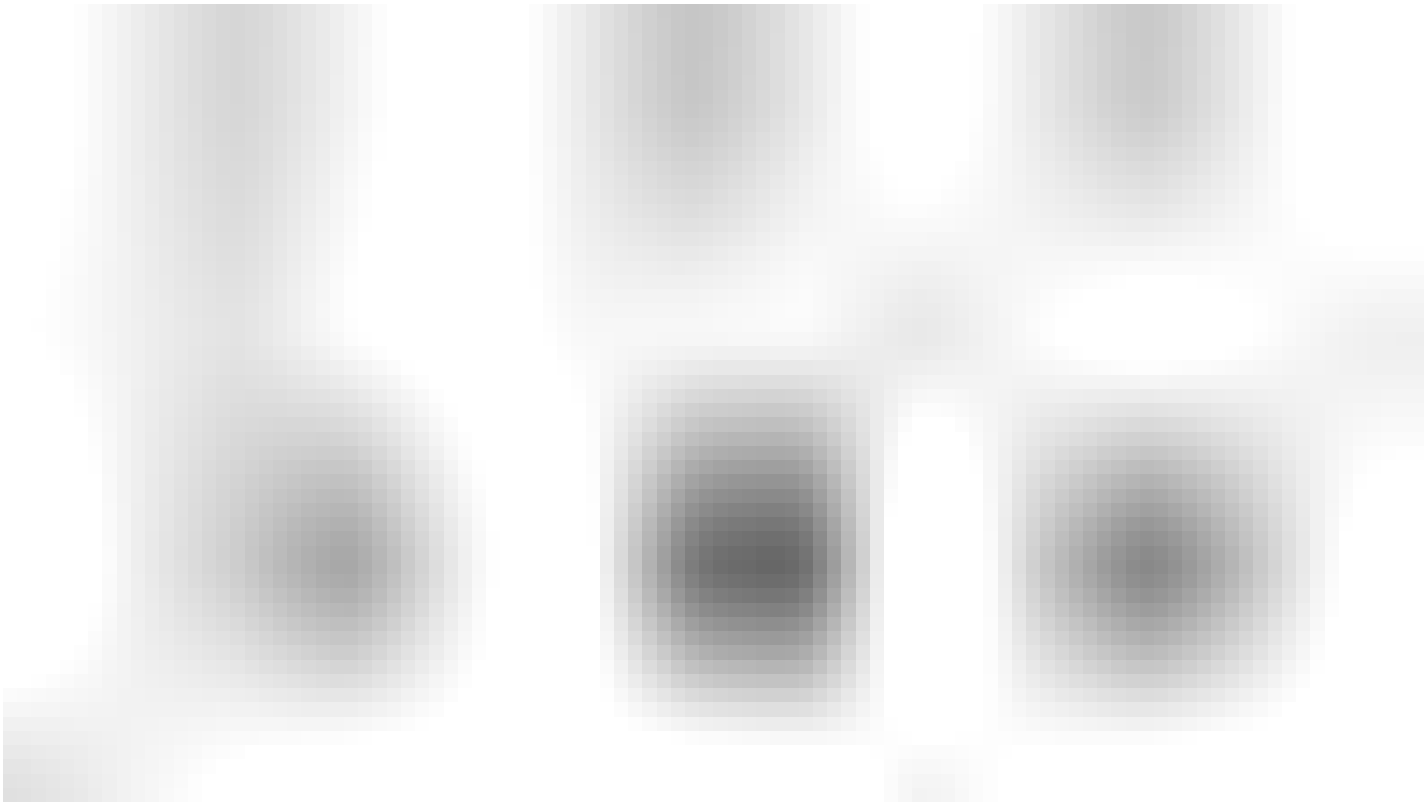

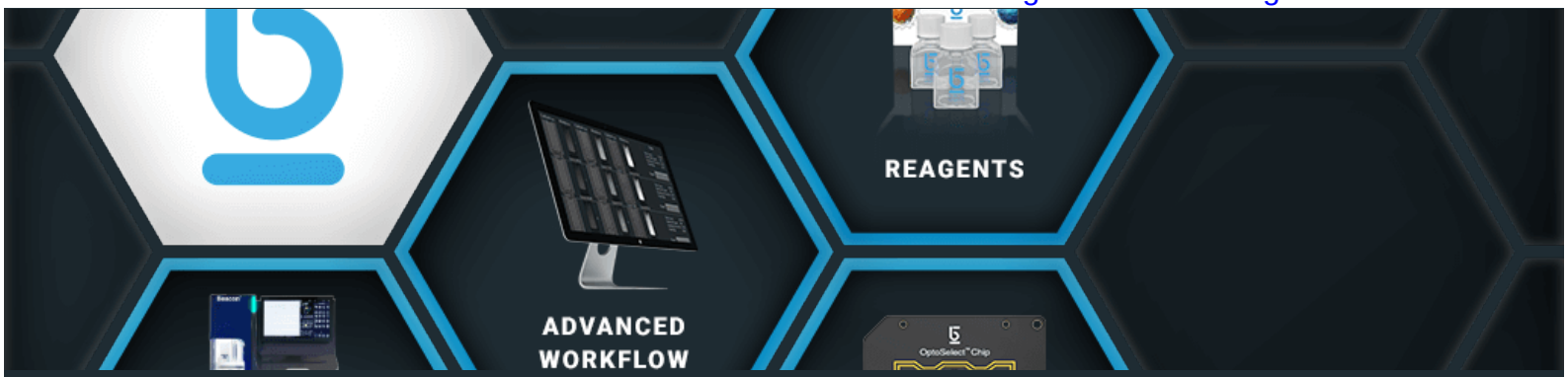

PLATFORM OVERVIEW

The Berkeley Lights Platform can move you toward cell-based breakthroughs faster than you can imagine.

Our platform is a fully integrated, end-to-end solution, comprised of proprietary consumables, including our OptoSelect chips and reagent kits, advanced automation systems, and application software.

View Platform

Most Recent

General Inquiries

info@berkeleylights.com
+1 (510) 858-2855

Tech Support

techsupport@berkeleylights.com
+1 (888) 254-5595 / Ext. 4

Exhibit 5

TECHNOLOGY

Optofluidic Technology is the Key to Faster Workflows and Deeper Data.

See how opto-electropositioning (OEP™) technology moves Cell Biology to light speed.

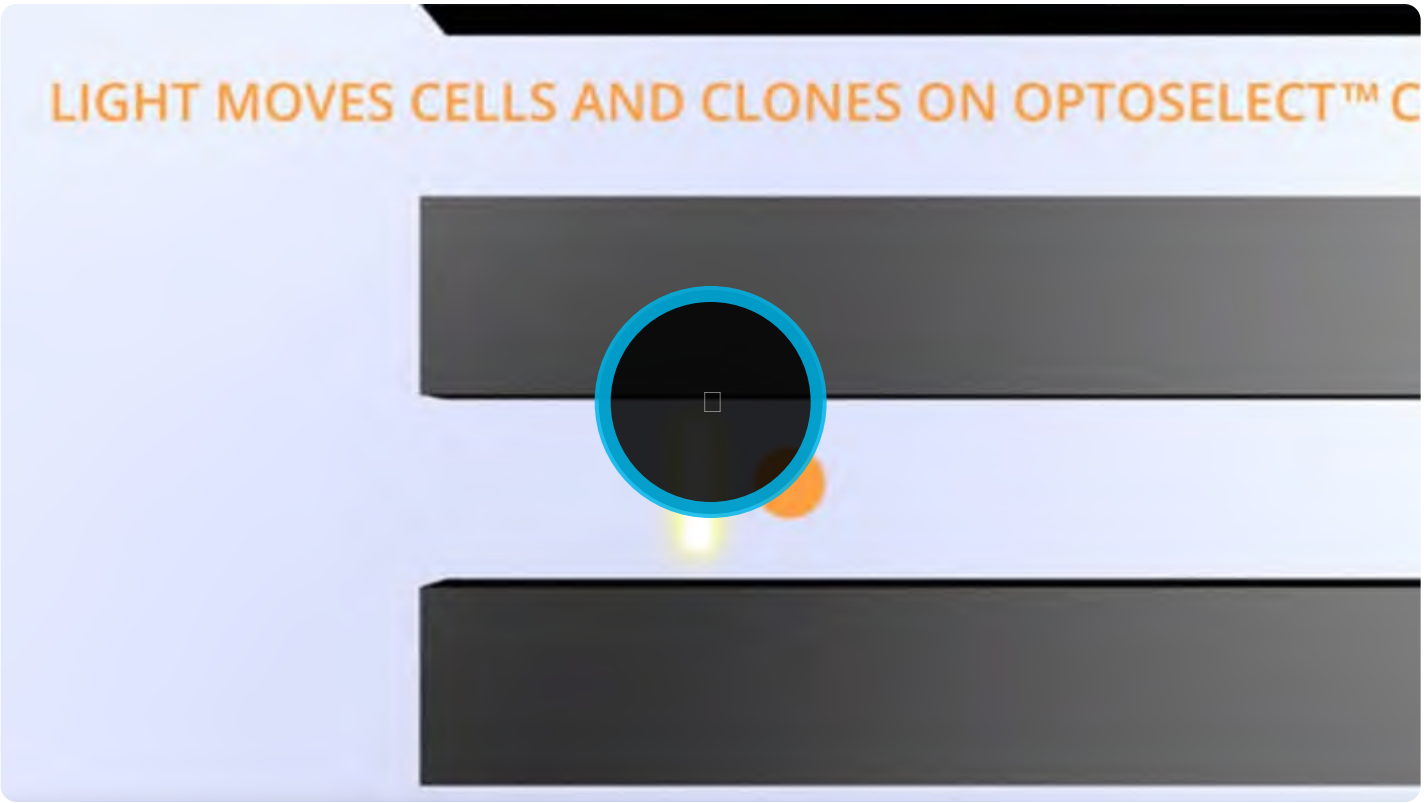

LIGHT MOVES CELLS

Our technology combines precise cell processing, time-saving workflow automation, and rich, deep profiling.

Watch this video animation, to see how Berkeley Lights advanced technology works. Welcome to the future.

The Workflow Modules

Simple, yet powerful onboard modules.

OEP fluidics uses light and millions of light-actuated pixels to move individual cells so they can be isolated, cultured, assayed and exported. Each cell or clone is imaged and monitored in real-time in a NanoPen™ chamber on our OptoSelect™ chips to provide rich visual data early and often. Our full platform and software suite deliver cell processing and deep profiling with more information about cell function than any other technology.

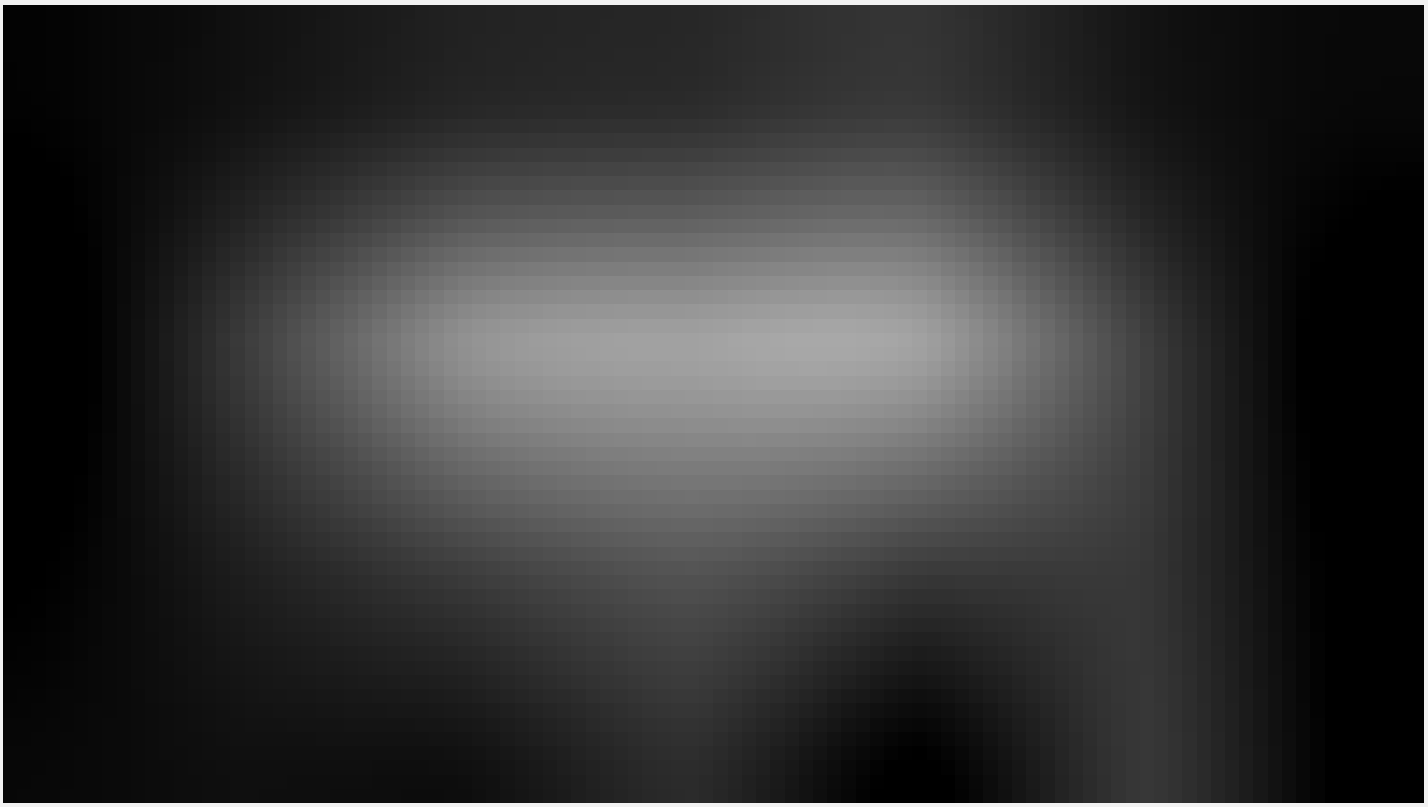

1. Import

Our software automatically identifies single cells and directs them into NanoPen chambers all at once. Chips are loaded with cells in less than 30 minutes.

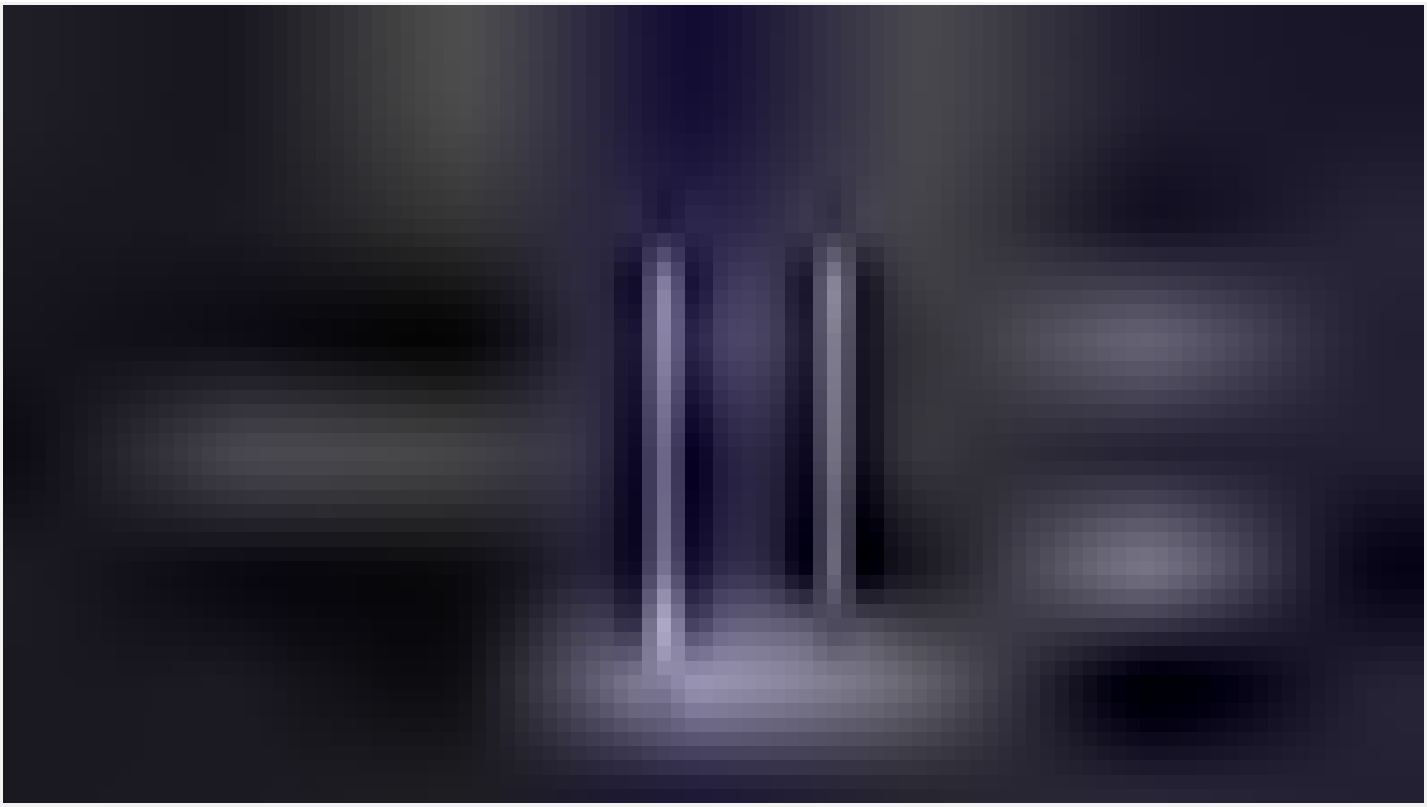

2. Culture

As cells proliferate, nutrients diffuse in, waste diffuses out, and software images the chip continuously to count cells and calculate growth rate.

3. Assay

Test individual cells immediately and repeatedly in our NanoPen chambers, instead of culturing for weeks to reach a minimum number of cells for assay.

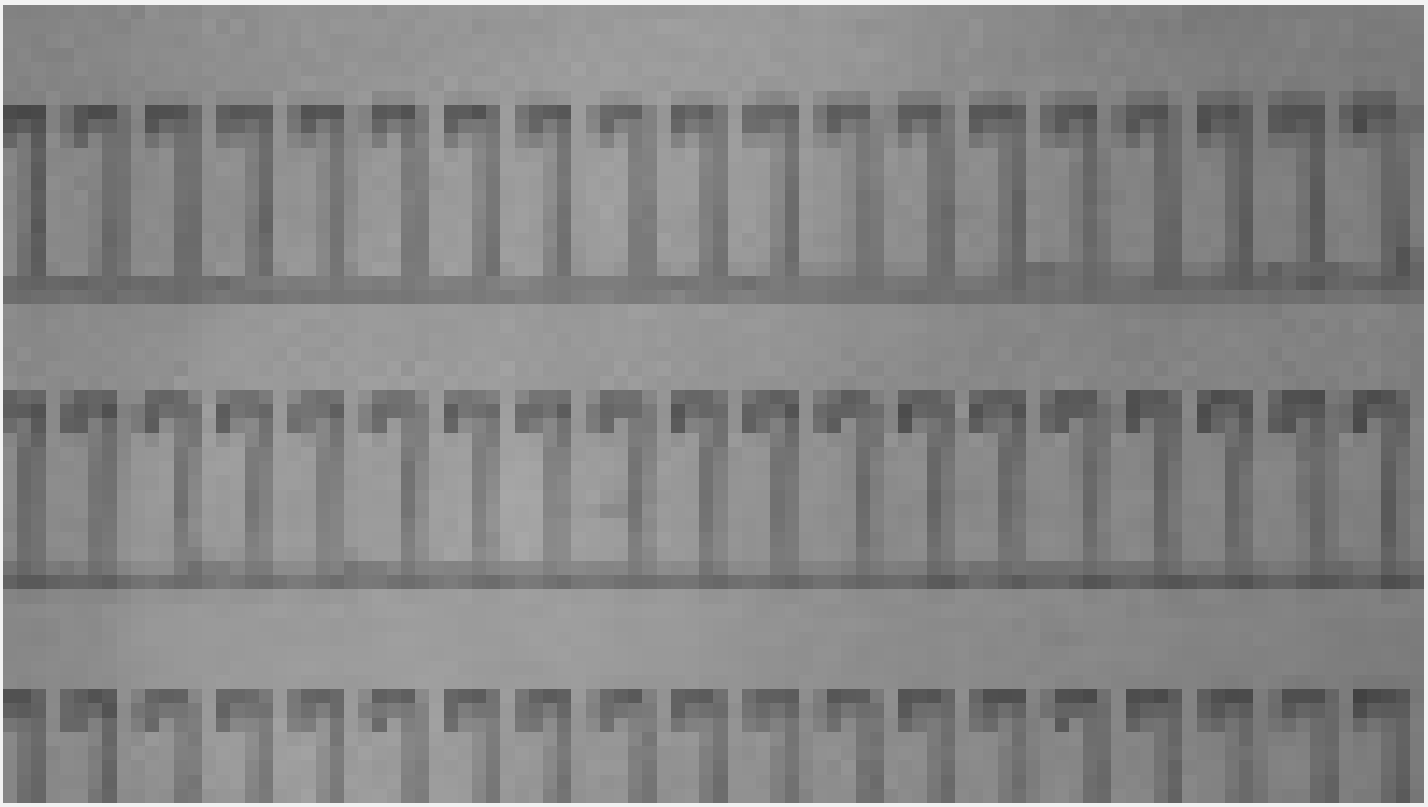

4. Export

Choose your cells of interest. Light patterns move them into position for export to a well plate.

Assays

Assays can be performed quickly with as little as a single cell.

NanoPen chambers are 100,000 times smaller in volume than a microwell. Isolate and assay a single cell within minutes. You won't need to wait weeks for a larger quantity of cells. You have complete flexibility to run fully-automated assays, sequentially or simultaneously, as frequently as you choose.

Supported Cellular Assay Types:

- Real-time lgG Secretion
- Multiplex Assays
- Multiple Antigen Screening
- Multiple Species Binding
- Growth Rate
- Surface Markers
- Viral Neutralization Assays
- Reporter Cell Assays
- Ligand Blocking Assay
- Cell/Cell Interaction
- Cytokine Assays
- Apoptosis Assays
- Tumor Killing Assays
- Other Functional Assays

TYPICAL NANOPEN ASSAYS

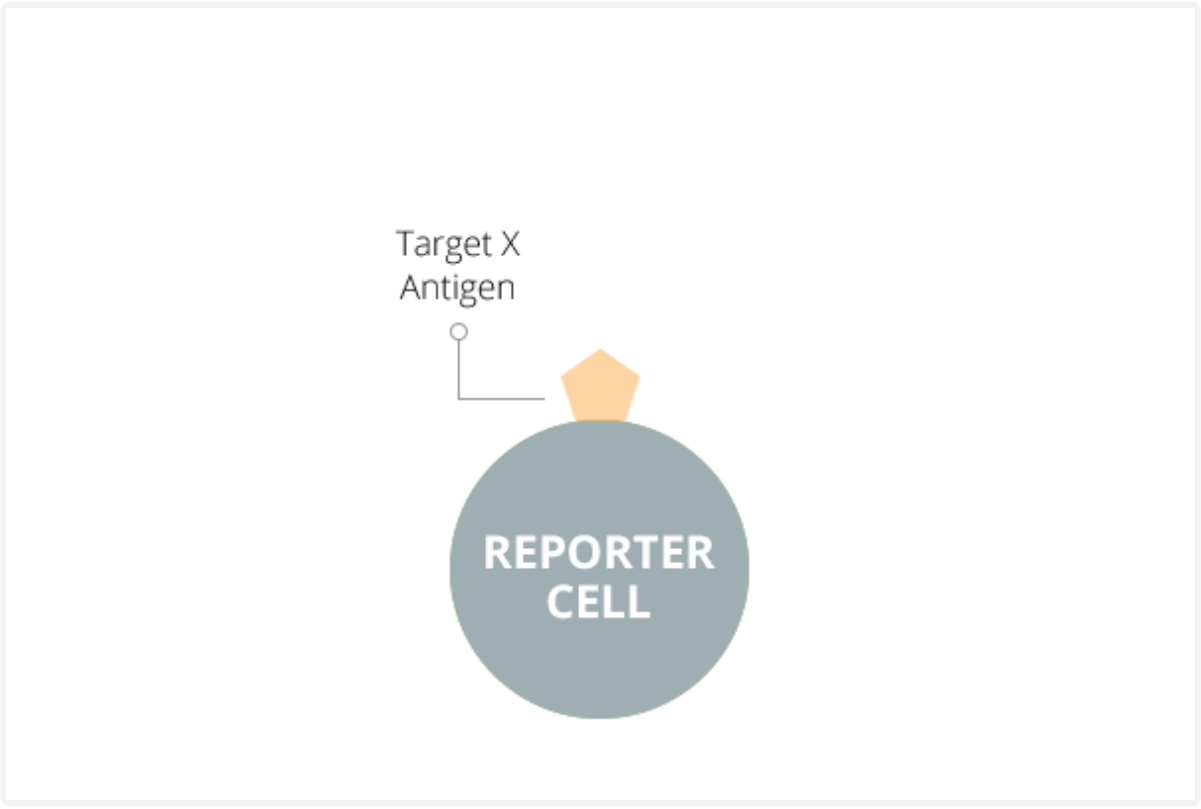

Functional Assay

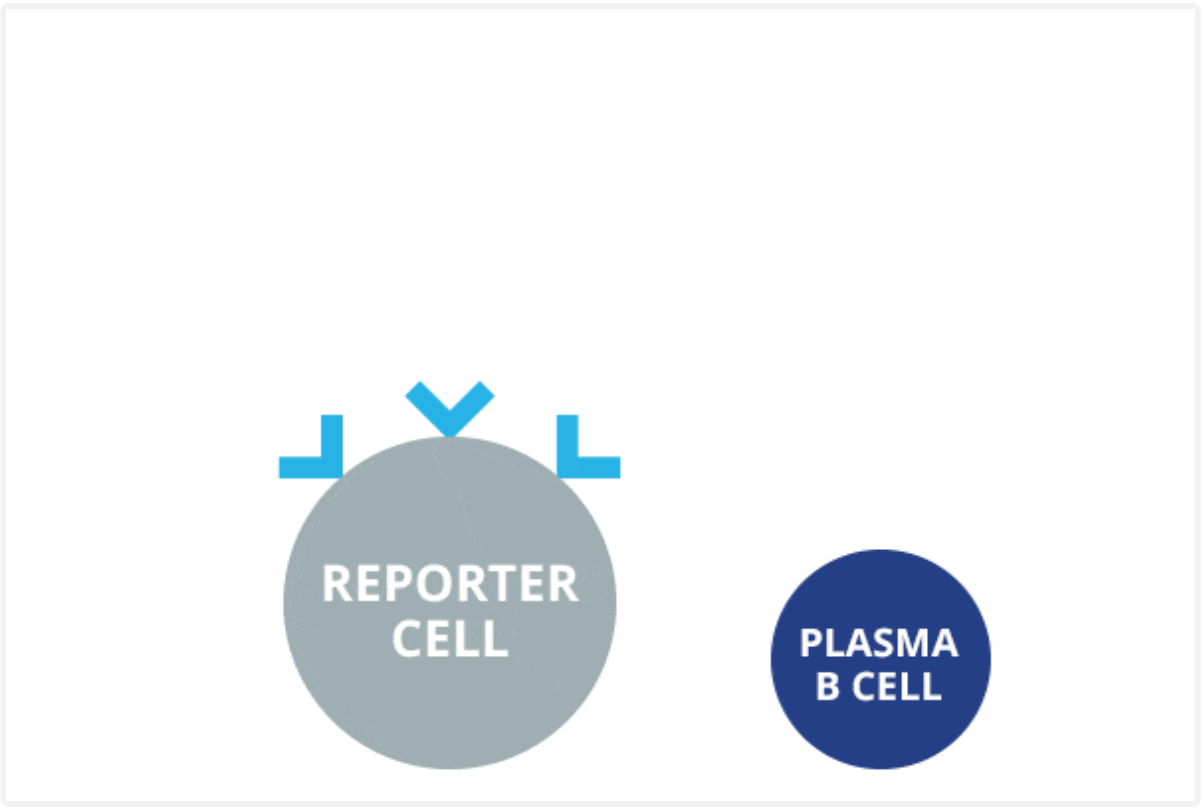

Ligand Blocking Assay

Cross-Species Assay

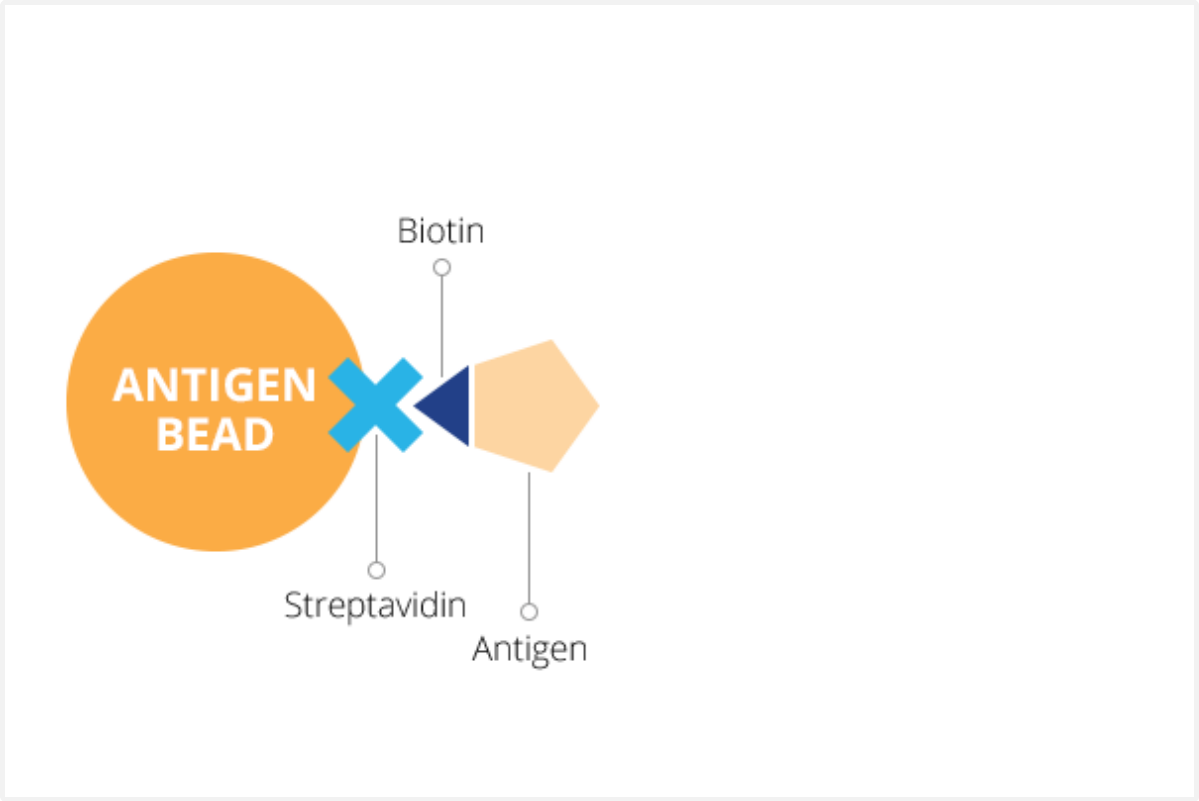

Antigen Specific Bead Assay

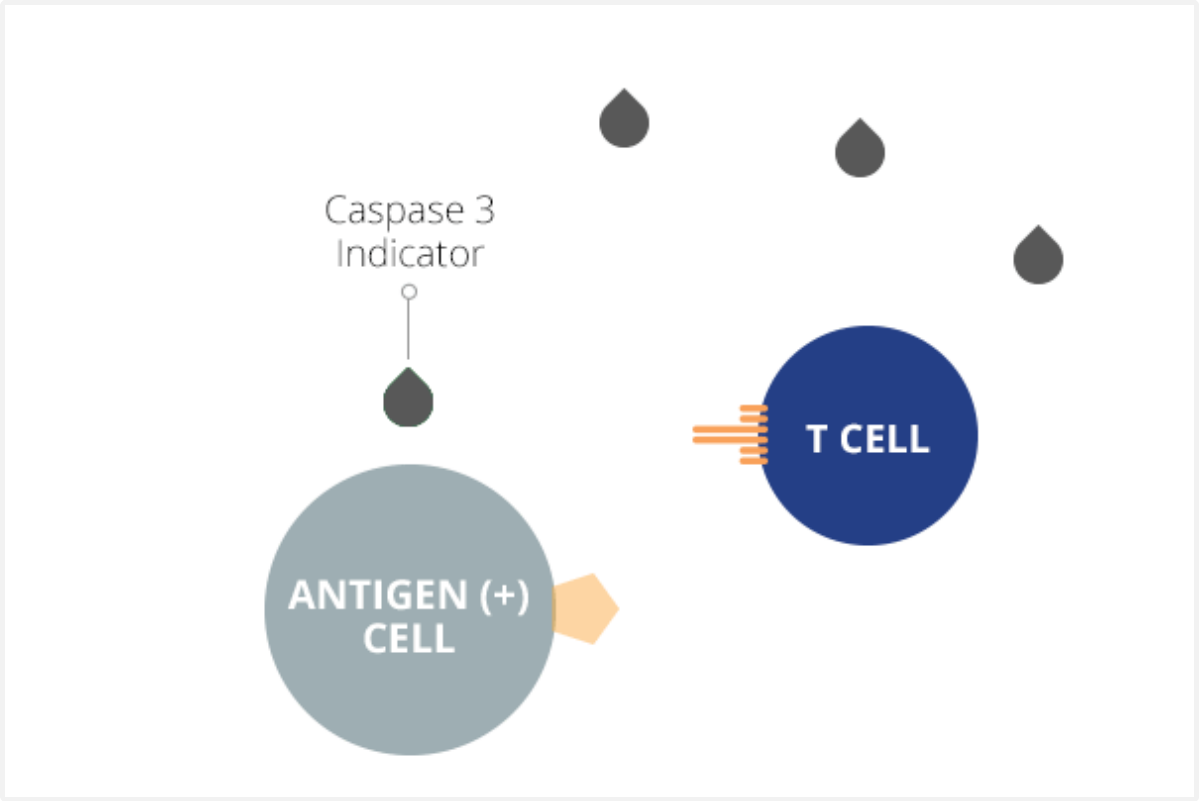

Tumor Cell Killing Assay

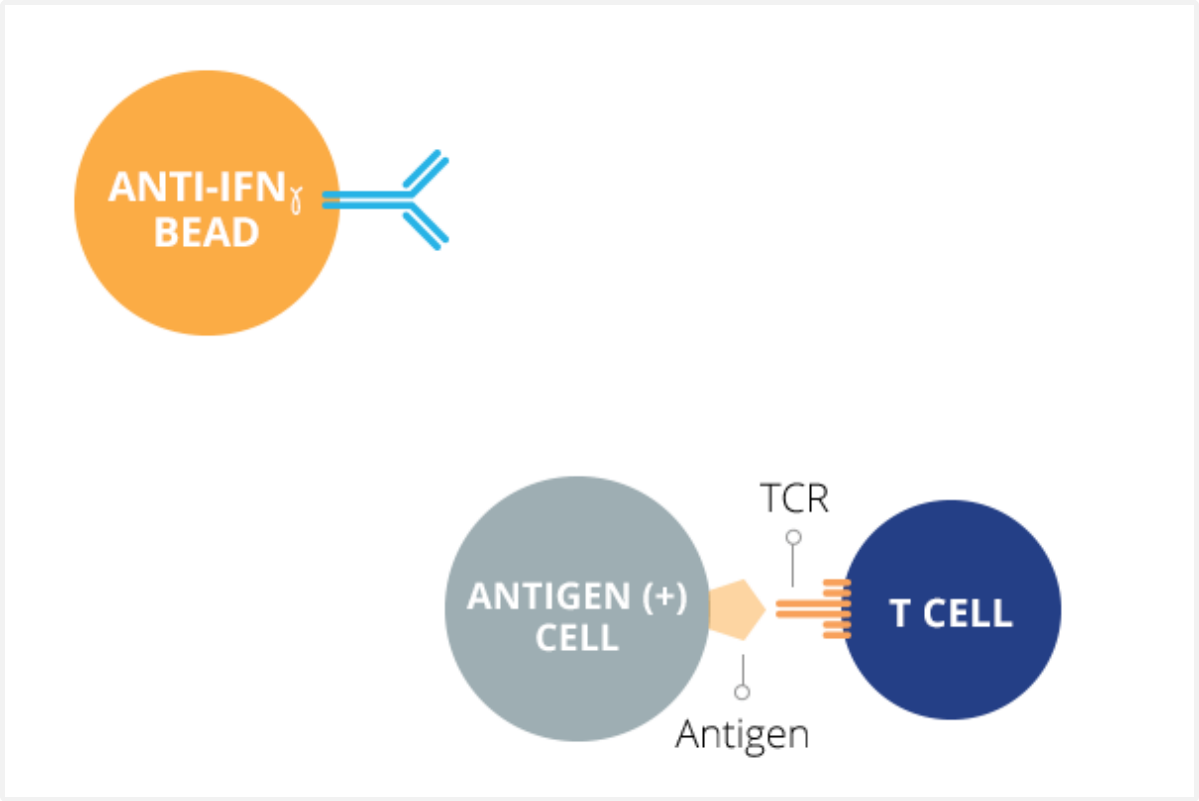

Cytokine Assay

DEEP PROFILING

For every single cell or clone couple phenotypic data, genome, and transcriptome in a scalable way.

Measure individual cells over time and over many assays, stack their performance against each other and only export the cells of interest. The OptoSeq™ Single Cell 3′ mRNA Library kit integrates single cell sequencing library preparation into cell profiling workflows on the Beacon® and Lightning™ optofluidic systems. Live cell phenotypic data can now be directly linked to genomic data using a single, innovative and scalable instrument.

Berkeley Lights Workflows

Our technology wouldn't matter if it didn't have applications that will change the way you can use and deploy cell-based products.

Below are some examples of proven workflows where we can and have made a difference. We drastically reduce time to results for each of these application workflows while providing detailed measurements on each cell, enabling a whole new perspective with deep understanding of each cell's behavior. Pick your workflow and see the difference.

Access Greater Diversity

Antibody Discovery

Best Production Cell Lines

Cell Line Development

Link Function to Genotype

Cell Therapy Development

Breakthrough Discoveries

Synthetic Biology

Get in Touch with Berkeley Lights

Let us know what you are looking for and one of our experts will contact you promptly to follow up on your request.

Learn More

General Inquiries

info@berkeleylights.com
+1 (510) 858-2855

Tech Support

techsupport@berkeleylights.com
+1 (888) 254-5595 / Ext. 4

Exhibit 6

SYSTEM

The Beacon® Optofluidic System

1000s of cells. 100x the insights. 10x faster. The Beacon system is a better, more advanced way to process and analyze cells.

With the Beacon system's light-speed workflows, you'll gain insights, iterate and innovate as fast as your inspiration.

- Replace a roomful of equipment with the Beacon system
- Work with individual cells radically faster than using other technologies
- Perform assays at any time, as often as you need
- Track phenotype and genotype of single cells or clones
- Automate and scale workflows far beyond manual, time-intensive analysis
- Generate greater insights through deep profiling of each cell or clone

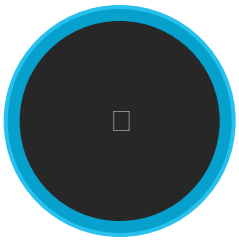

OVERVIEW

In the race to find important cells, the Beacon system saves time, money and effort.

Imagine how much further you can take your product development with a single cell-based workflow that shortens the selection process to just days. Bring the right biologic therapies into clinical testing faster. Identify the cells that matter much sooner. Move any field light-years ahead.

"The Beacon system paired with ingenious protein chemistry, will facilitate a high-throughput approach to identifying highly potent and rare 'needle-in-a-haystack'- antibodies that would be ideal biotherapy candidates that have been difficult or impossible to find with previously available technology."

Stephen Wilson, Ph.D., Executive Vice President and Chief Operating Officer at La Jolla Institute

The Beacon System Workflows

Beacon system enables game changing process improvements and is most popular for the following workflows. Pick your workflow and see the difference:

Access Greater Diversity

Antibody Discovery

Best Production Cell Lines

Cell Line Development

Breakthrough Discoveries

Synthetic Biology

Link Function to Genotype

Cell Therapy Development

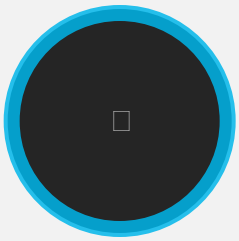

MORE INSIGHTS

The Beacon system's deep profiling reveals 100x the insights of legacy technologies.

The Beacon system can capture bright field and fluorescence images of each NanoPen™ in an OptoSelect™ chip at any time. Track and assay the same individual cell across multiple time points to reveal **deep profiling—richly detailed "fingerprints" of cells and clones** you can't get any

other way.

BEACON TECHNOLOGY

At the core of the Beacon system is a combination of optics and nanofluidics called optofluidics.

The OptoSelect chips replace typical well plates. Each OptoSelect chip contains thousands of NanoPen chambers, which are like wells on a microplate. This is where cells are deposited, where they grow and where they are characterized using a myriad of proprietary Berkeley Lights assay.

Beacon Workflow Modules

Screening 1000s of cells is an automated and process process on the Beacon system with our four workflow modules: Import, Culture, Assay and Export. These modules can be adapted, interchanged and deployed with a variety of single-cell assays to address specific applications and a variety of cell types.

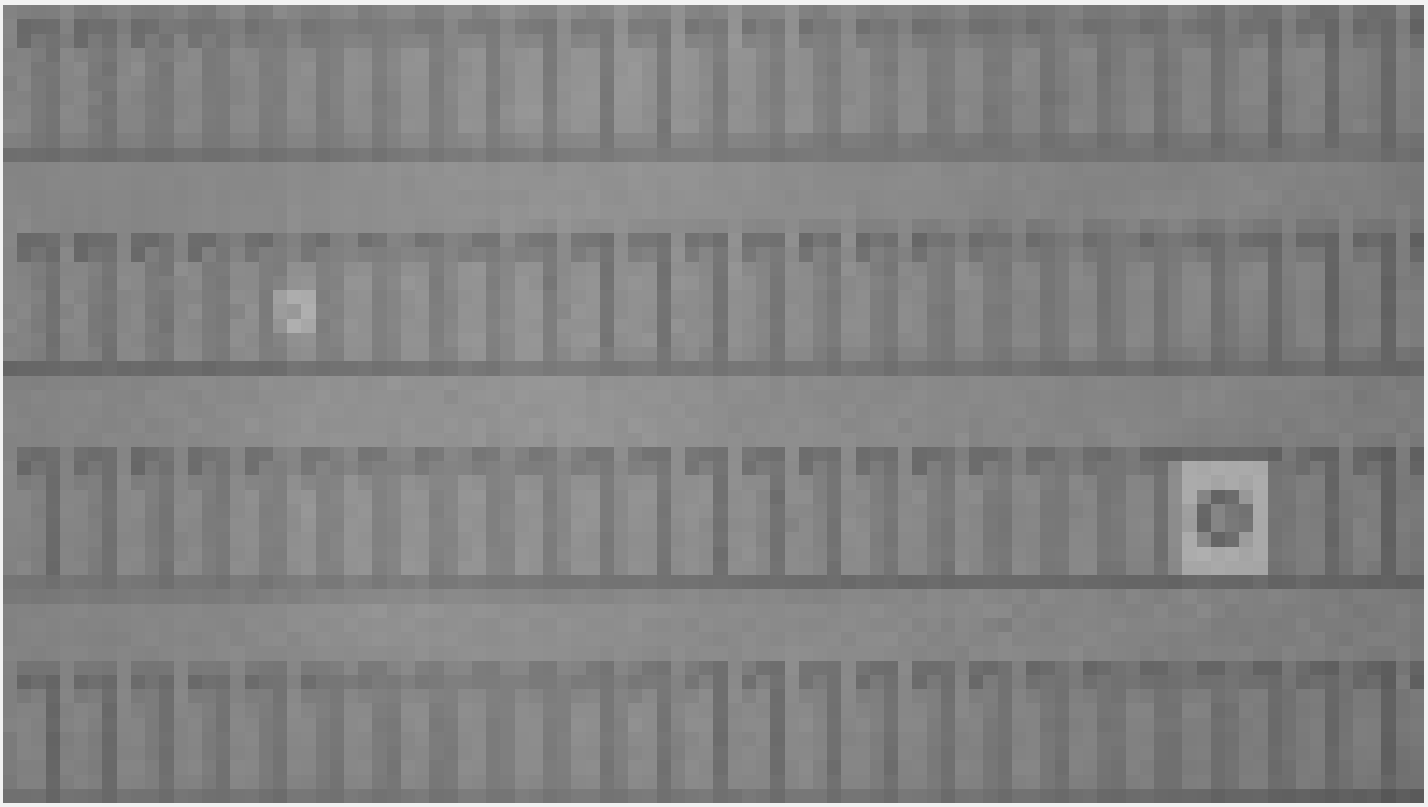

Import

Our software automatically identifies single cells and directs them into NanoPen chambers all at once. Chips are loaded with cells in less than 30 minutes.

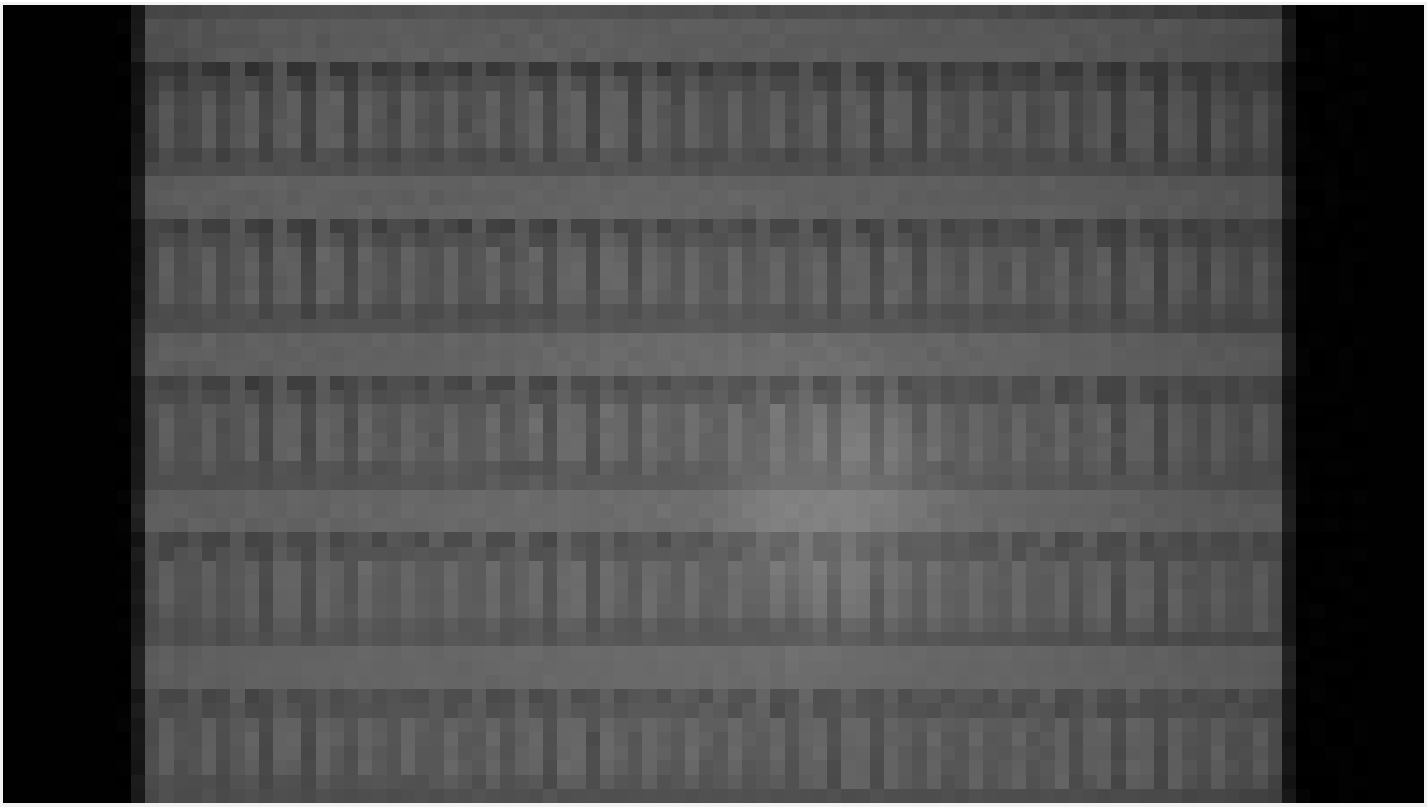

Culture

As cells proliferate, nutrients diffuse in, waste diffuses out, and software images the chip continuously to count cells and calculate growth rate.

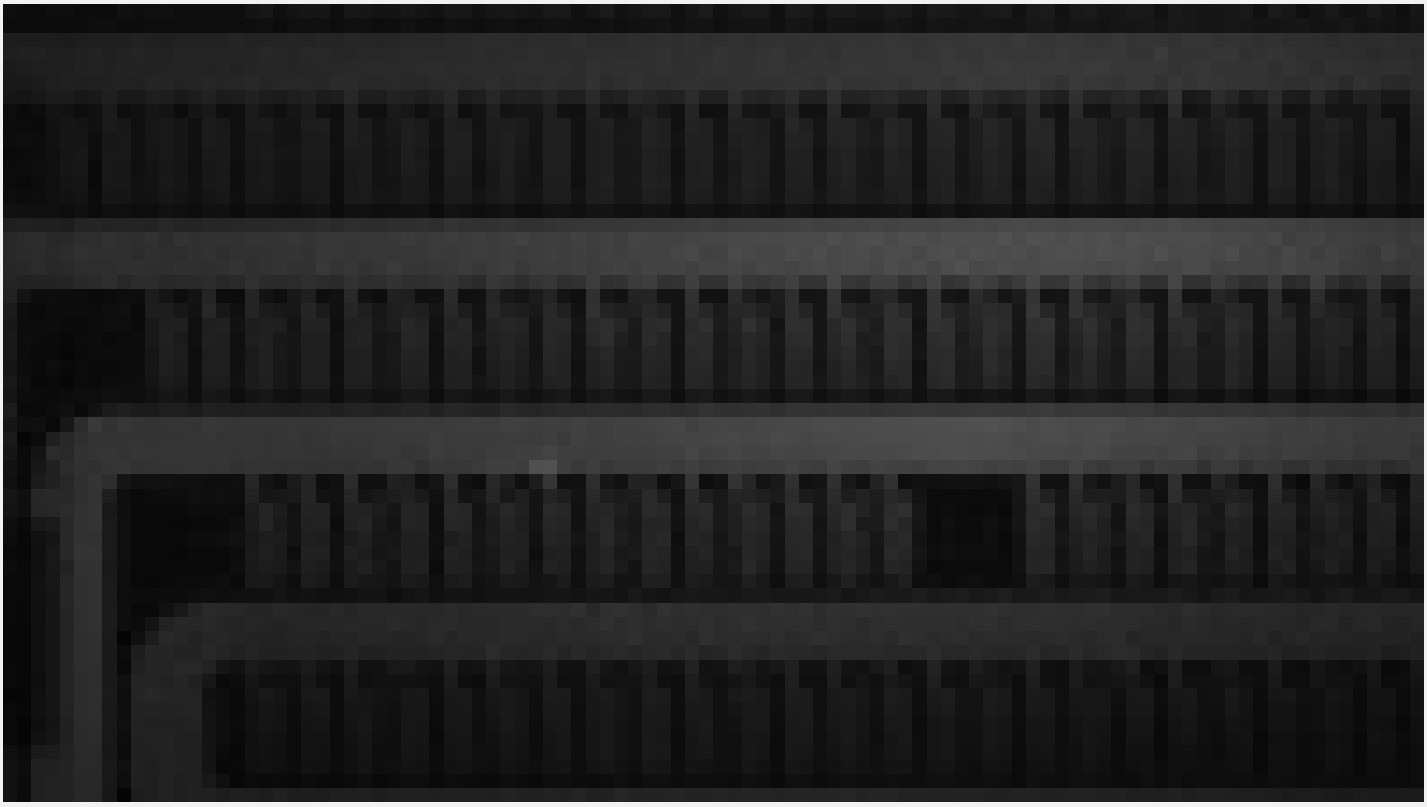

Assay

Test individual cells immediately and repeatedly in our NanoPen chambers, instead of culturing for weeks to reach a minimum number of cells for assay.

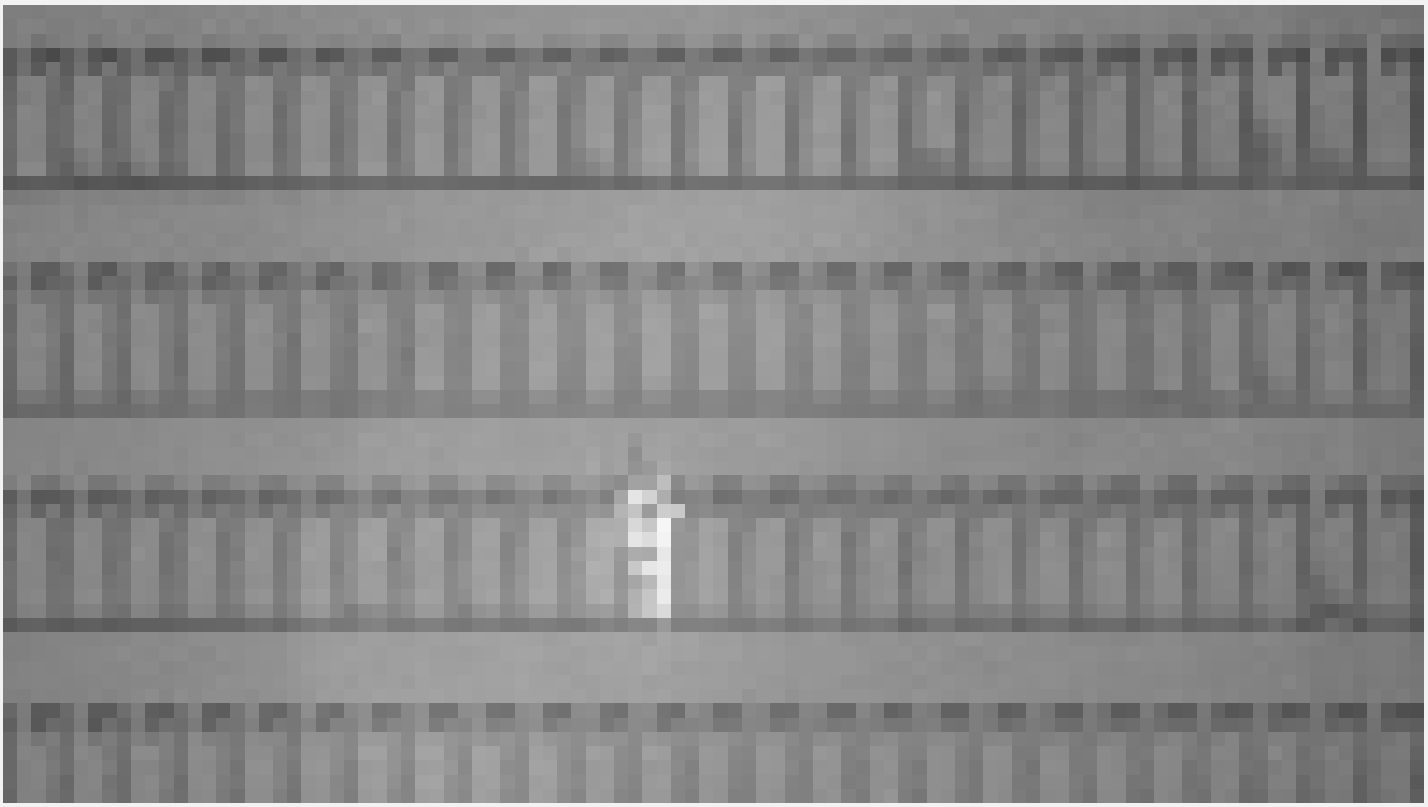

Export

Choose your cells of interest. Light patterns move them into position for export to a well plate.

SAMPLE BEACON ASSAYS

NanoPen chambers are 100,000 times smaller in volume than a microwell.

That means a single cell can be isolated and assayed in its own discrete chamber. There's no need to wait weeks for a large quantity of cells to assay. Perform secretion assays with both soluble or membrane bound targets within hours of cloning. You have complete flexibility to run fully-automated assays, sequentially or simultaneously, as frequently as you choose.

Antigen-Specific Bead Assay

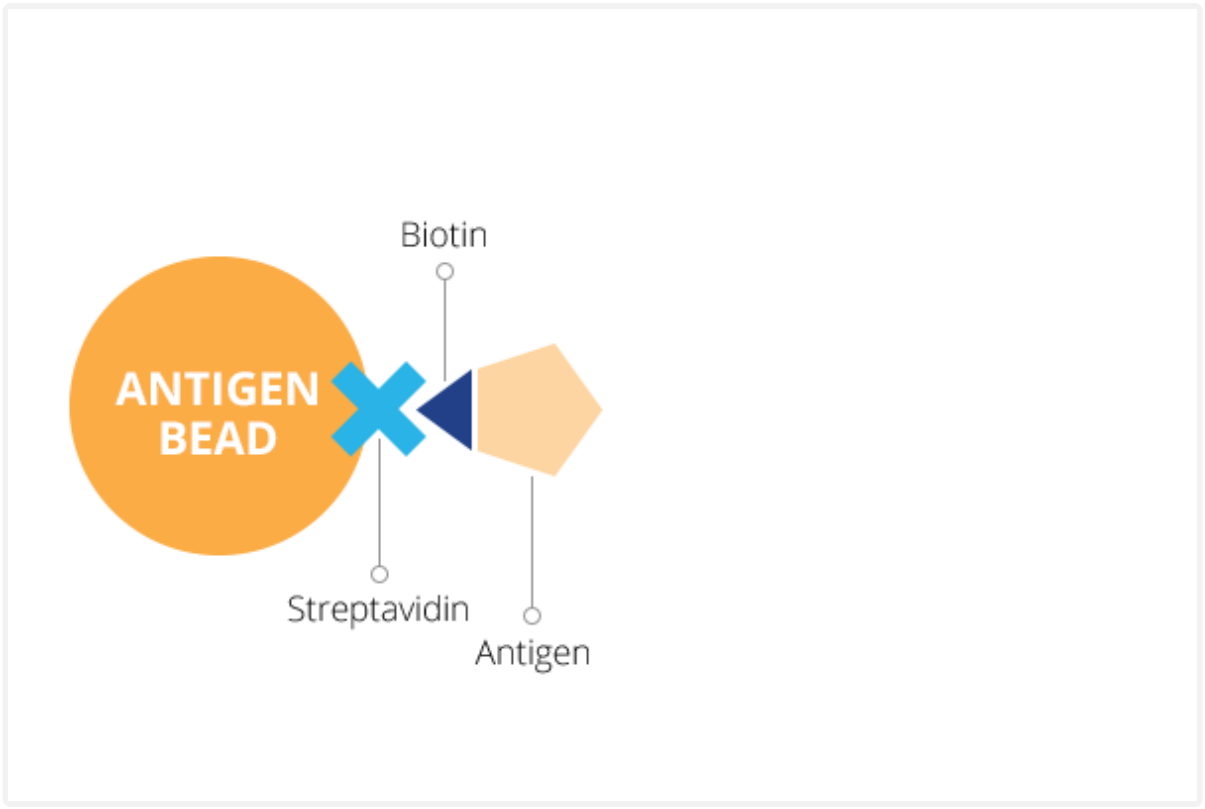

Mutliplex IgG Capture Assay

High Throughput Chips

Depending on your assay and throughput needs, different chips with different throughput and NanoPen chamber shapes are available for the Beacon system. You can run up to 4 chips at the same time and the Culture Station instrument can be used for culturing cells on chips offline.

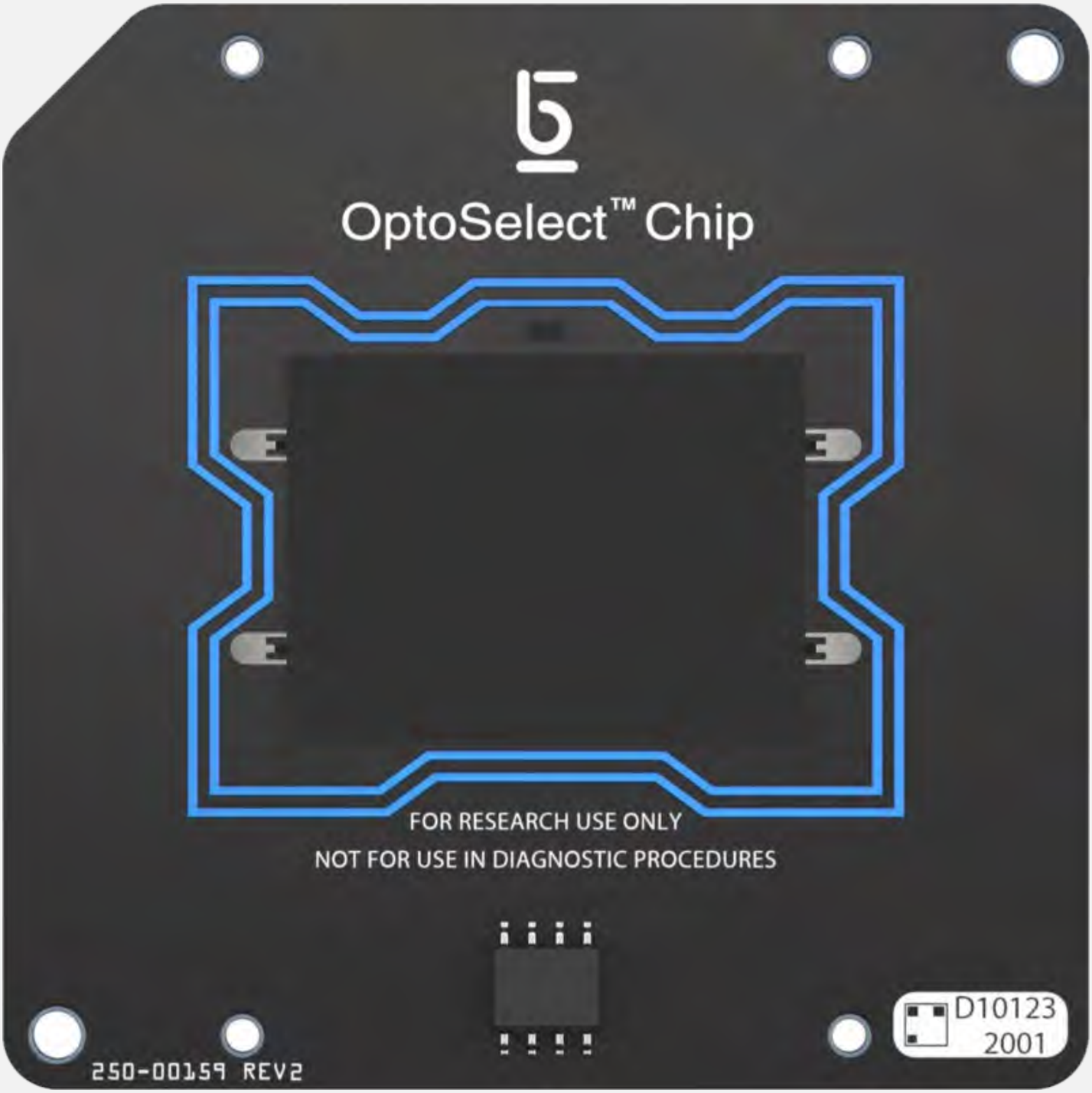

OptoSelect 1750 Chip

1.7 nL NanoPen chambers are ideal for longer term culture experiments including cell line

development and adherent cell cloning.

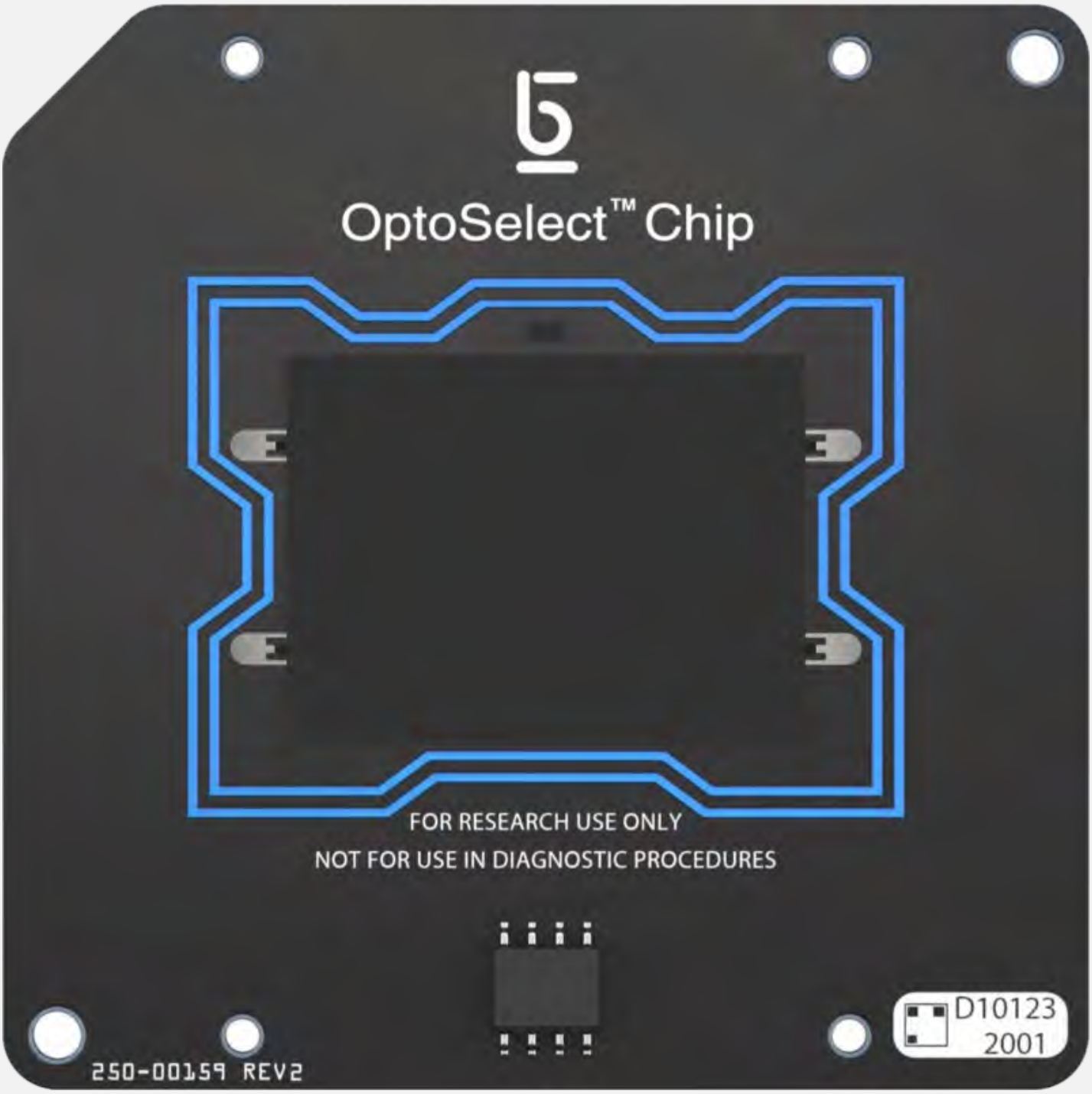

OptoSelect 3500 Chip

0.75 nL NanoPen chambers enable some cell division and higher clone throughput.

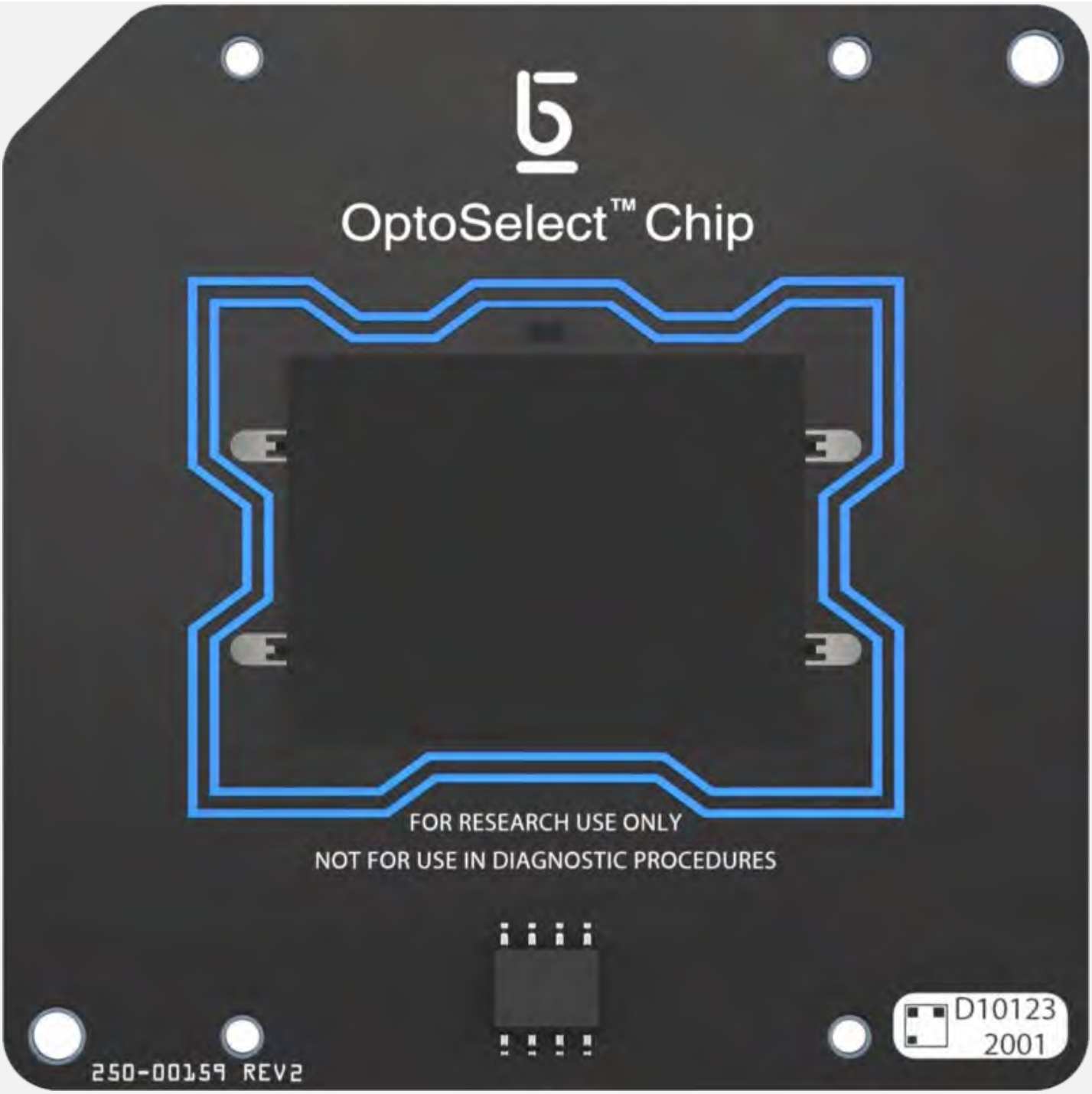

OptoSelect 11K Chip

0.32 nL NanoPens are designed for the highest throughput of single cell screening.

Related Resources

View All Beacon System Resources

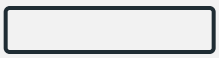

Get in Touch with Berkeley Lights

Let us know what you are looking for and one of our experts will contact you promptly to follow up on your request.

Learn More

General Inquiries

info@berkeleylights.com
+1 (510) 858-2855

Tech Support

Support

techsupport@berkeleylights.com

+1 (888) 254-5595 / Ext. 4

Get In Touch

Exhibit 7

WORKFLOW

Antibody Discovery

More diversity, functional leads–in just 24 hours.

B-Cell Antibody Discovery Workflow

Access broad B cell diversity to select better antibody lead candidates in just days.

"In less than 24 hours, using the Beacon single-cell system, GenScript ProBio completed immunized mice processing, immune cell isolation and enrichment, single cell sorting, on-

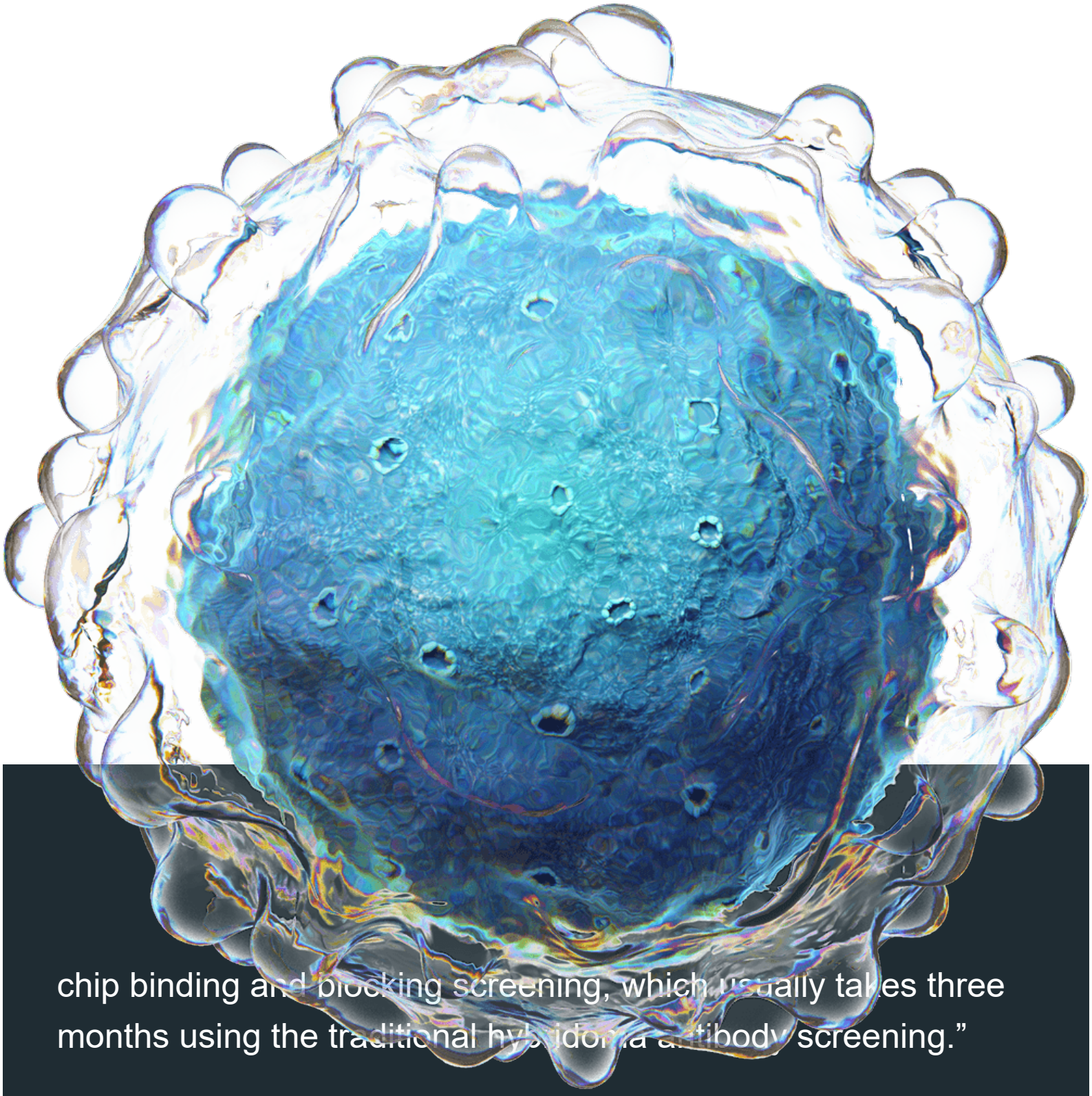

chip binding and blocking screening, which usually takes three months using the traditional hybridoma antibody screening."

Dr. Brian Min, CEO of GeneScript ProBio

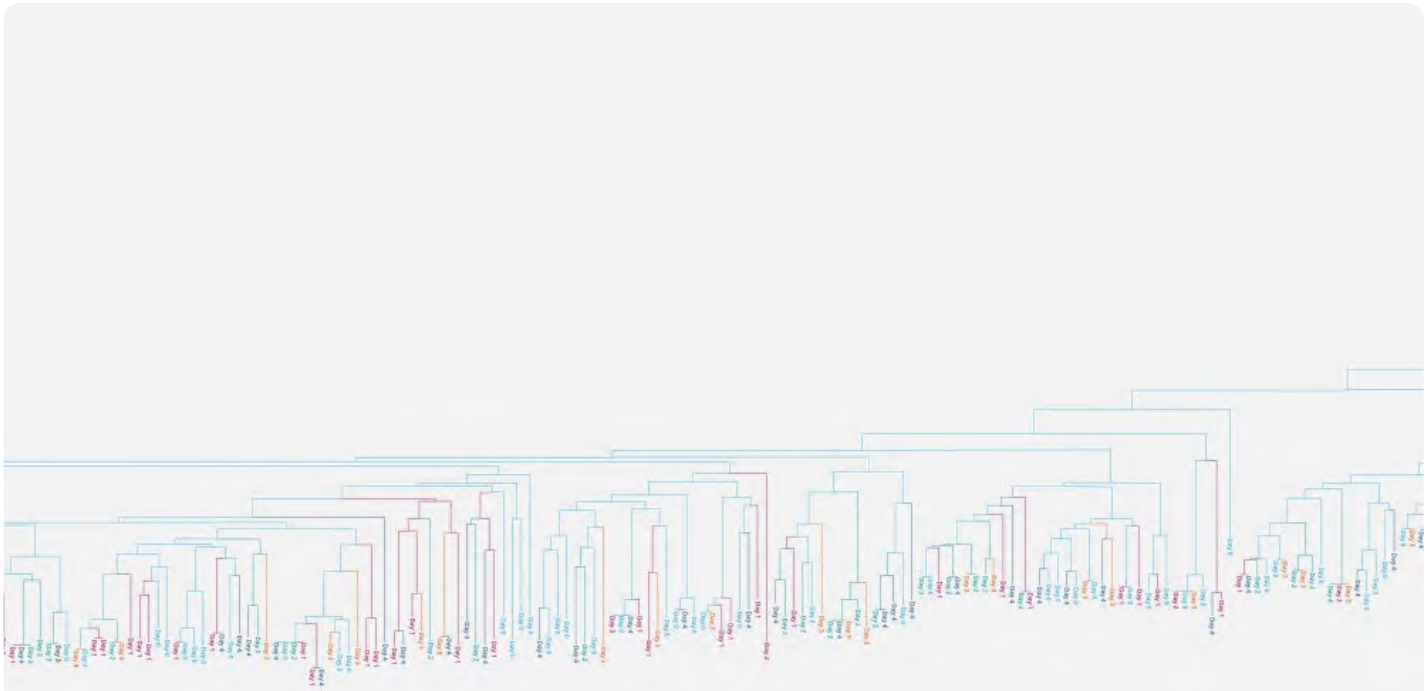

Hover to Zoom In

GREATER B CELL DIVERSITY

With the Opto™ Plasma B Discovery Workflow, everything you need to connect antibody function to gene sequence at the single-cell level is available.

Increase your chances of finding rare functional antibody therapeutic candidates by screening the plasma B cell repertoire using the Berkeley Lights Platform.

Rapid Screening of the B Cell Repertoire

Plasma B discovery using the Beacon® optofluidic system bypasses time-consuming and inefficient

hybridoma fusion.

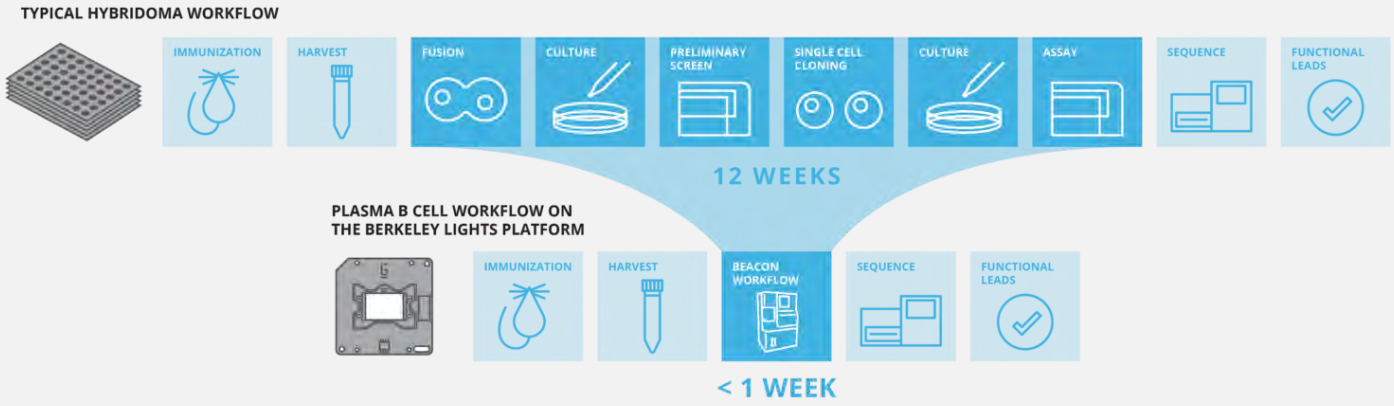

Plasma B cells are screened using binding and functional assays to select only the most qualified antibody lead candidates. OptoSeq™BCR enables automated recovery of broad antibody sequence diversity in under a week.

Down-select Lead Candidates Earlier.

The Opto Plasma B Discovery Workflow enables down-selection of lead candidates through multiple assays for antigen specificity and function.

With a NanoPen™chamber volume of only 250 pico liters, reactions are fast and precise. Complete assays in less than 1 hour, then reset your chips to enable the next assay to begin. Better characterization upfront reduces the expense of having to sequence or clone irrelevant non-functional hits.

ASSAYS THAT RUN IN OUR NANOPEN CHAMBERS

Functional Assay

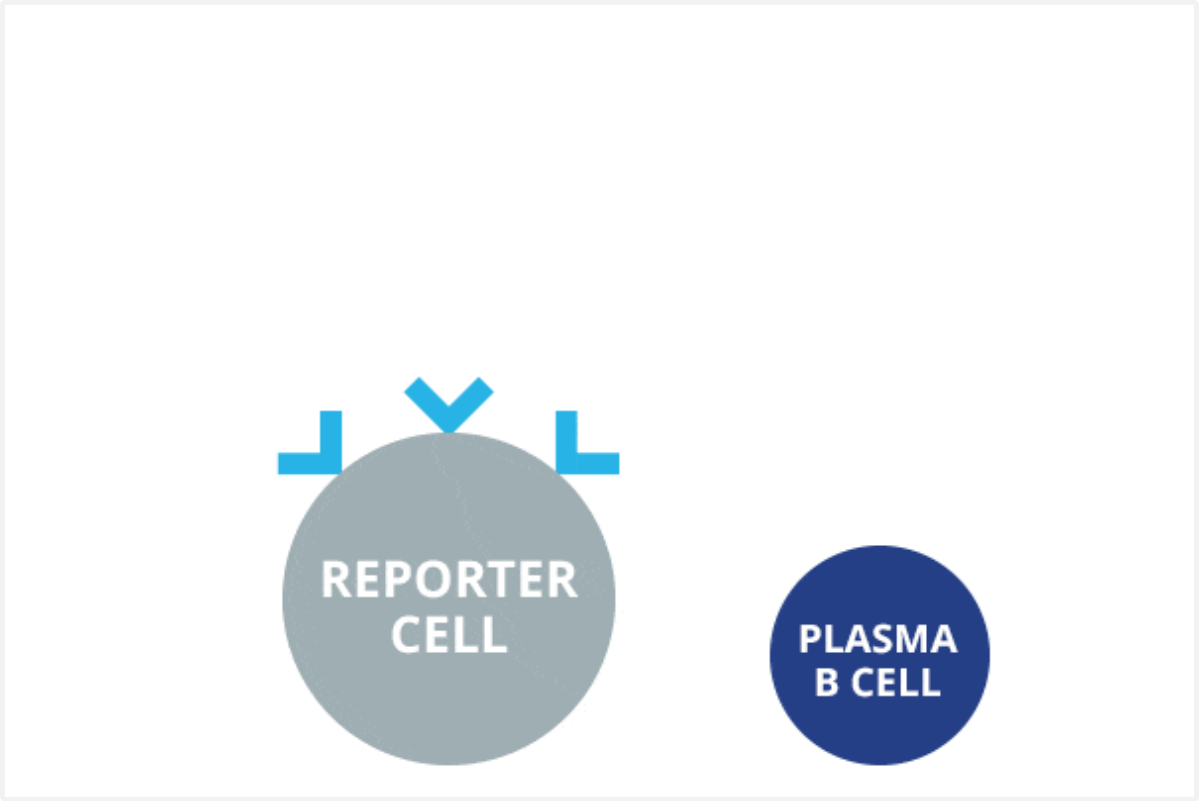

Ligand Blocking Assay

Cross-Species Assay

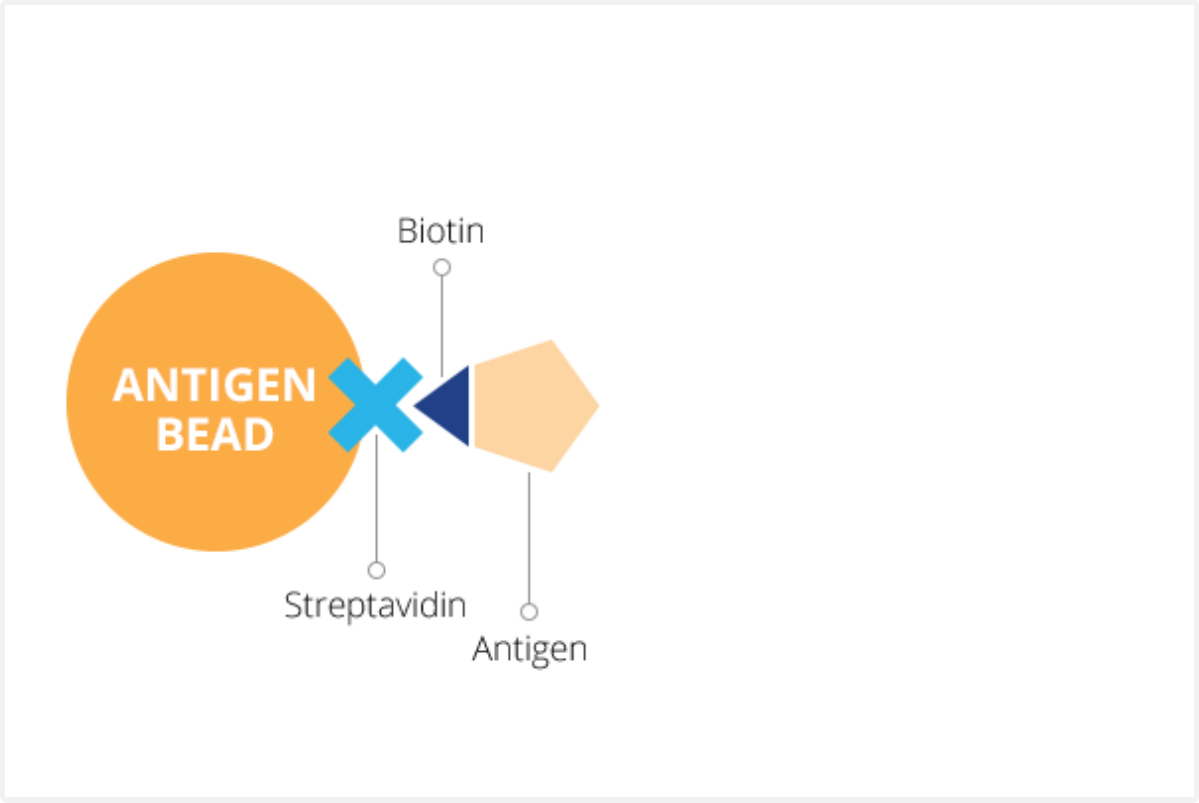

Antigen Specific Bead Assay

Link Sequence With Function in Just Two Days

Every antibody sequence can be mapped directly to a known antibody function. Sequence relationships identify individual mutations that confer antigen specificity, cross-reactivity, and function.

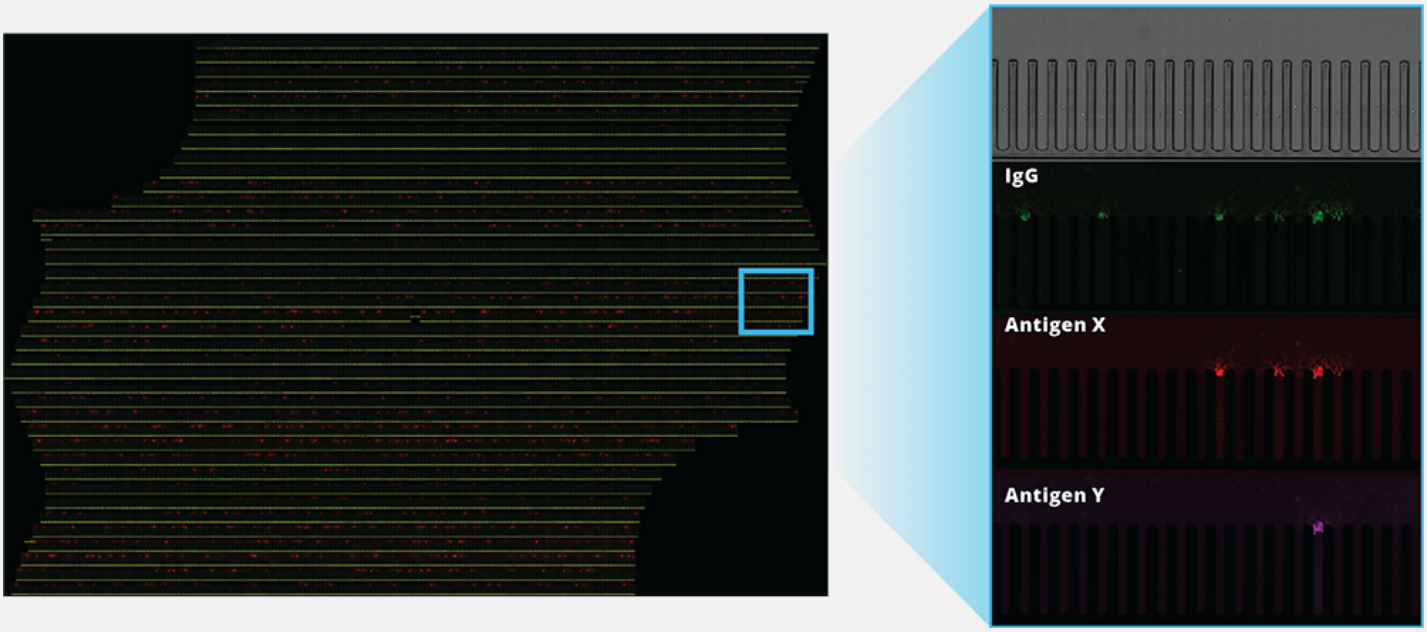

Discover Thousands of Hits in Days, Not Months.

BEACON SYSTEM'S OPTOSELECT™ CHIP

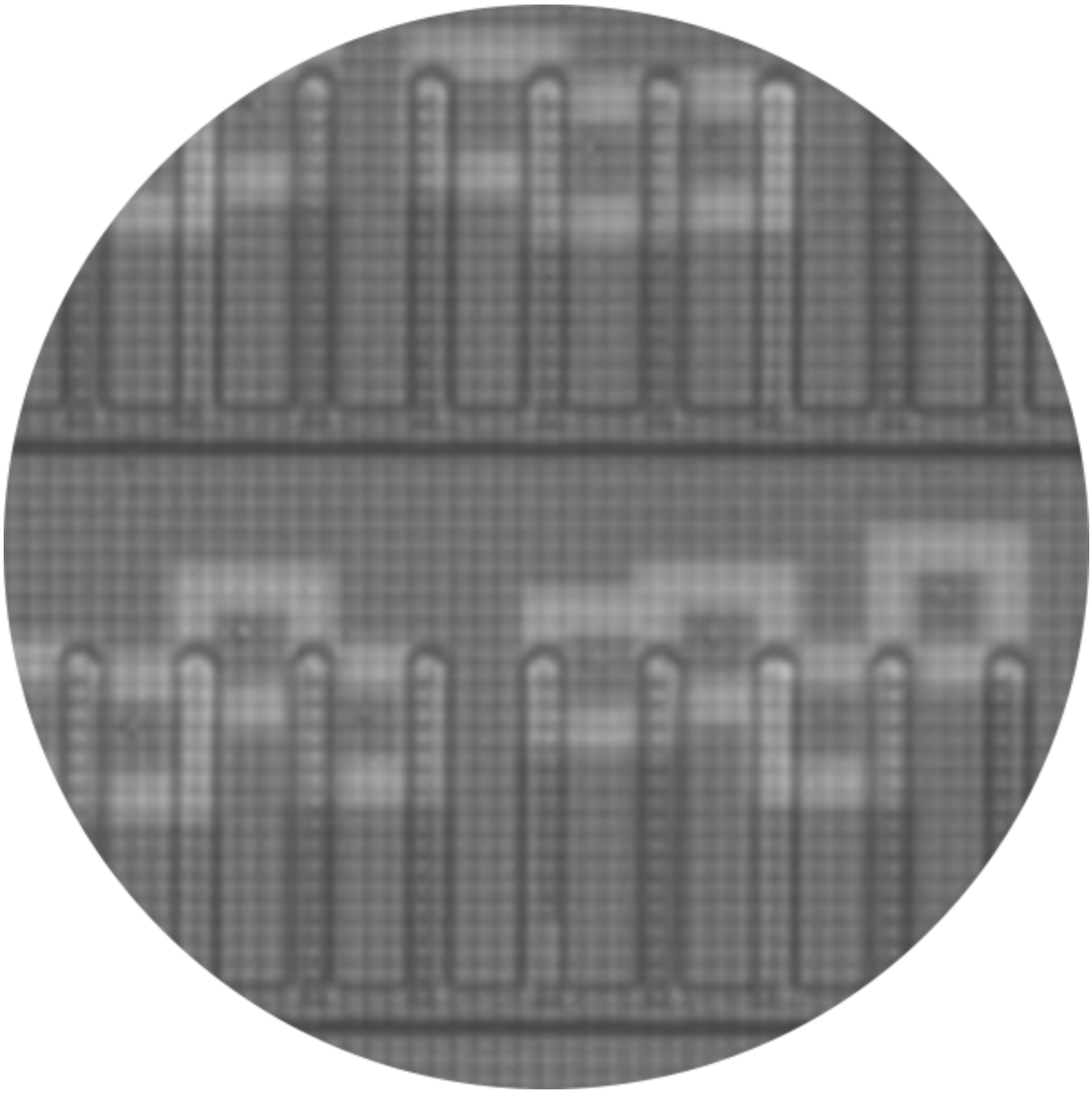

STEP 1: CLONING

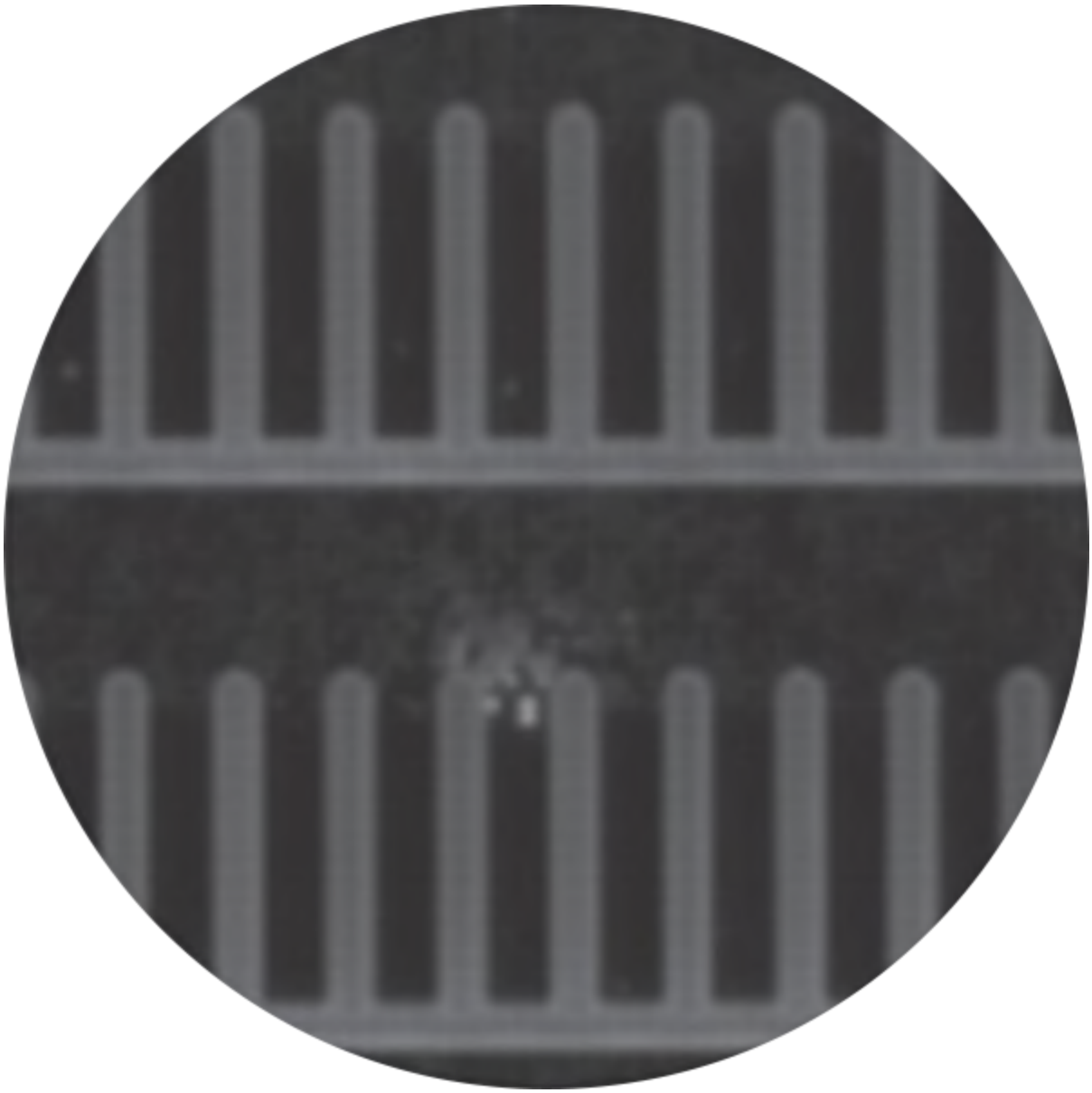

STEP 2: ASSAY

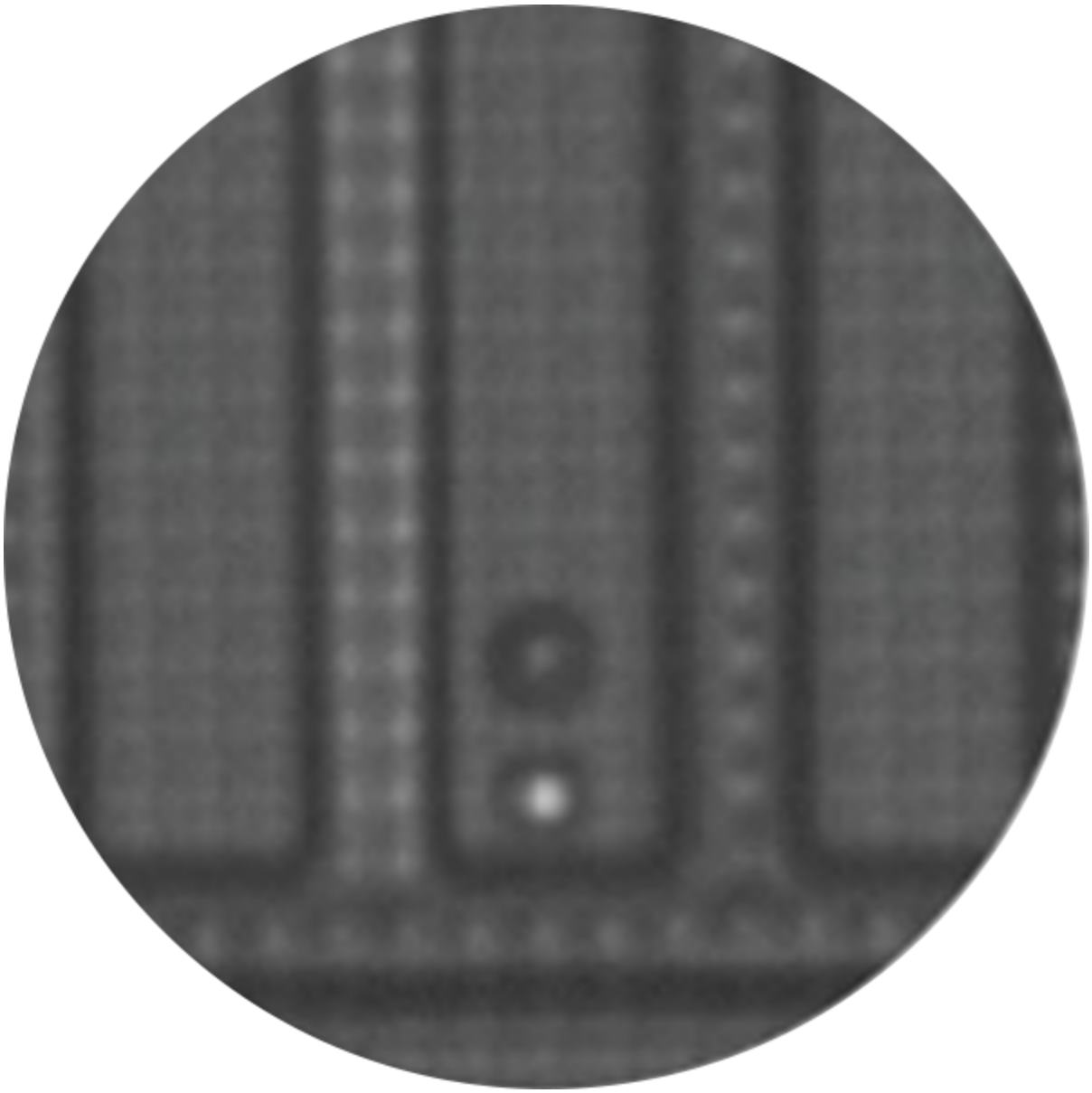

STEP 3: CDNA SYNTHESIS

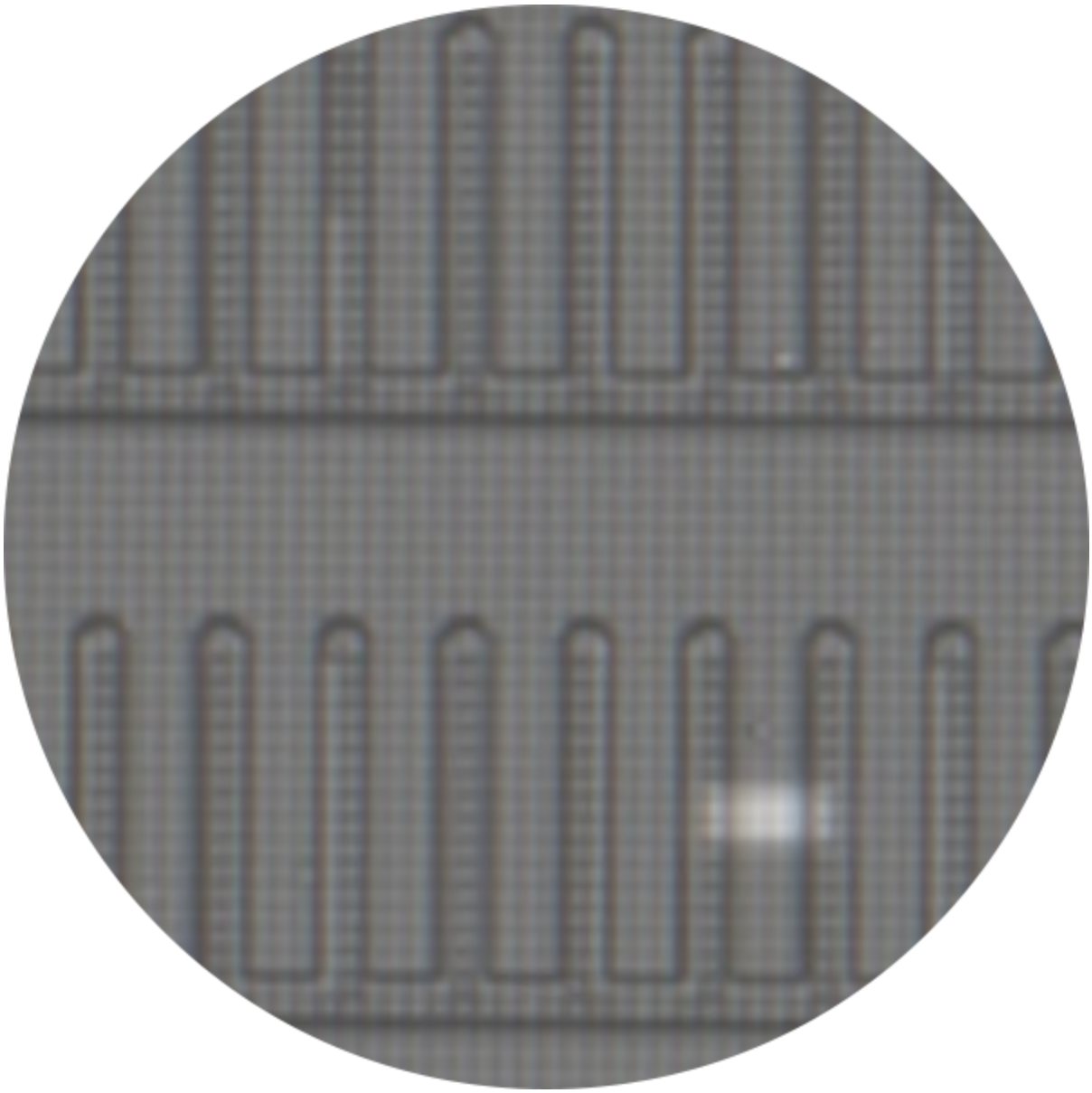

STEP 4: SEQUENCE RECOVERY

Plasma B discovery on the Beacon system enables automated, direct screening of B cells immediately after organ harvest and cell purification.

B cells can be screened from multiple organs (spleen, bone marrow, lymph nodes) and cultured for multiple days in specialized media to enable multiple screens from a single cell sample.

Related Resources

View All Antibody Discovery Resources

Get in Touch with Berkeley Lights

Let us know what you are looking for and one of our experts will contact you promptly to follow up on your request.

Learn More

General Inquiries

info@berkeleylights.com

+1 (510) 858-2855

Resources

Support

Get In Touch

Tech Support

techsupport@berkeleylights.com

+1 (888) 254-5595 / Ext. 4

Privacy Policy • Terms of Use • Patents

Exhibit 8

BIOTECH METHOD

Biotechnology Journal

www.biotechnology-journal.com

Assuring Clonality on the Beacon Digital Cell Line Development Platform

*Kim Le, Christopher Tan, Huong Le, Jasmine Tat, Ewelina Zasadzinska, Jonathan Diep, Ryan Zastrow, Chun Chen, and Jennitte Stevens**

During biomanufacturing cell lines development, the generation and screening for single-cell derived subclones using methods that enable assurance of clonal derivation can be resource- and time-intensive. High-throughput miniaturization, automation, and analytic strategies are often employed to reduce such bottlenecks. The Beacon platform from Berkeley Lights offers a strategy to eliminate these limitations through culturing, manipulating, and characterizing cells on custom nanofluidic chips via software-controlled operations. However, explicit demonstration of this technology to provide high assurance of a single cell progenitor has not been reported. Here, a methodology that utilizes the Beacon instrument to ensure high levels of clonality is described. It is demonstrated that the Beacon platform can efficiently generate production cell lines with a superior clonality data package, detailed tracking, and minimal resources. A stringent in-process quality control strategy is established to enable rapid verification of clonal origin, and the workflow is validated using representative Chinese hamster ovary-derived cell lines stably expressing either green or red fluorescence protein. Under these conditions, a >99% assurance of clonal origin is achieved, which is comparable to existing imaging-coupled fluorescence-activated cell sorting seeding methods.

1. Introduction

The development of biotherapeutics relies on manipulating mammalian cells to secrete desired proteins. To ensure maximal productivity and as part of the overall control strategy, regulatory agencies require that all biomanufacturing cell lines be "cloned from a single cell progenitor" to ensure safety and consistent product quality.[1–3] Additionally, guidelines from the FDA released over the past few years also established an expectation for industrial sponsors to provide high assurance of clonality.[4–6] Historically, subcloning was performed through limiting dilution plating, and clonality assurance was assessed based on statistical arguments.[7,8] To improve assurance, multiple rounds of limiting dilution were often performed to obtain a desired probability of clonal derivation.[9,10] Modern cloning approaches instead employ specialized instruments to ensure that a single cell is seeded into microtiter plates through interrogation of cells at the point of deposit. These include fluorescence-activated cell sorting (FACS), Cytena single-cell printer (SCP),[11] and Solentim verified in-situ plate seeding (VIPS).[12–16] In the above examples, cell deposition is usually coupled with the use of microscopic imaging of well plates before deposition, after deposition (within 24 h), and during subsequent colony expansion. Additionally, a manual verification step of these images by one or more trained scientists is performed to confirm single cell origin and select candidate clones for subsequent colony picking.

The emerging, fully integrated Berkeley Lights Beacon nanofluidic technology holds the potential to transform traditional manual cell culture to digital analysis and manipulation. The Beacon platform is equipped with opto-electropositioning (OEP), microfluidics, and microscopy to enable cells to be manipulated, cultured, and assayed on nanofluidic chips.[17–20] We have previously demonstrated that the Beacon instrument can be employed to generate high quality cell lines with reduced resource requirements compared to traditional FACS-based methods. However, no reported clonality assessment has been published for the Berkeley Lights Beacon platform.[21]

Each nanofluidic chip contains 1758 NanoPen chambers arrayed along four continuous channels. The NanoPens have a narrow opening to the channel for nutrients and cellular waste diffusion and are not completely separated by physical barriers, leading to the possibility that on-chip mixing of cells from one NanoPen to another can occur. The Beacon platform prevents on-chip mixing of cells from one NanoPen to another in two ways. First, the nanofluidic chips are tilted at a small angle from horizontal so that cells settle to the bottom of NanoPens and

K. Le, C. Tan, H. Le, J. Tat, E. Zasadzinska, J. Diep, R. Zastrow, C. Chen, J. Stevens
Drug Substance Technologies
Process Development
Amgen, Inc.
One Amgen Center Drive, Thousand Oaks, CA 91320, USA
E-mail: jennitte@amgen.com

The ORCID identification number(s) for the author(s) of this article can be found under https://doi.org/10.1002/biot.201900247

DOI: 10.1002/biot.201900247

away from the narrow opening to the channel. Second, the chips are engineered so that there is no net flow into or out of the NanoPens. The fluidic regime, whether laminar or turbulent, can be assessed by the non-dimensional Reynolds number which is a ratio of inertial forces to viscous forces. For a typical Beacon flow rate of 1 μL s^{-1} through the chip's channels, the Reynolds number is ≈1.2, whereas the accepted transition to turbulent flow begins to occur at a Reynolds number of 2300. Thus, we can assume that all flows in these channels are laminar and that cells can only be moved into and out of the NanoPens using light-based manipulation. However, whether these methods are sufficient to prevent on-chip mixing and to ensure clonality when culturing and exporting highly optimized production cell lines has not been previously published. In this manuscript, we describe how the Beacon's integrated imaging capability, in combination with in-process controls, is employed to generate a reliable clonality data package. Using a representative Chinese hamster ovary (CHO) model system that constitutively expresses either green fluorescent protein (GFP) or red fluorescence protein (RFP), we have validated this workflow and present unrivaled clonality assurance compared to FACS and limiting dilution-based procedures.

2. Experimental Section

2.1. Cells and Cell Culture

Model cell lines were generated by transfecting a clonal CHO host with plasmid DNA encoding either a GFP or an RFP and a selection marker. Following transfection, stably expressing pool populations were generated through repeated passaging under selection pressure until the cells reached above 90% viability. Selection pressure was then removed, and the cells were monitored for stable expression of GFP or RFP through fluorescence microscopy. Pools were then re-transfected with plasmid DNA encoding heavy and light chains from a human monoclonal antibody with a metabolic selection marker through a process typical of a standard cell line development campaign. Antibody secreting pools were selected through passaging in a selective seed-train growth medium until the cells reached above 90% viability and maintained consistent doubling times. Subclones were isolated from pools through three rounds of sequential limiting dilution, fluorescence-activated cell sorting (FACS), and Berkeley Lights Instrument (BLI) subcloning methods. Isolated clones were expanded and screened for stable fluorescent protein expression. Throughout the process, the cells were cultured in either 96-well, 24-well, or 24-deepwell microtiter plates (Corning, Corning, NY), 125 mL shake flasks (Corning, Corning, NY), T-175 flasks (Corning, Corning, NY), or 50 mL spin tubes (TPP, Trasadingen, Switzerland) in growth media at 36°C, 5% CO_2 and 85% humidity. Cells were maintained by passaging multiple times a week at a target seed density.

2.2. Single Cell Cloning by Limiting Dilution

Limiting dilution cloning was performed through measurement of viable cell density of a stable culture using a trypan blue dye exclusion cell analyzer (Vi-Cell XR, Beckman Coulter, Brea, CA), dilution in custom cloning media at a target density of approximately 0.7 cells per 180 μL per well and transferring into a sterile 96-well microtiter plate (Corning, Corning NY).

2.3. Single Cell Cloning by Flow Cytometry

The FACS AriaIIu (Becton Dickinson, Franklin Lakes, NJ) cell sorter was used to isolate and deposit single cells from stable transfected pools directly into 96-well microtiter plates (Corning, Corning, NY) prefilled with a custom cloning medium. Sorting parameters were set for three doublet discrimination gates, the highest stringency conflict resolution setting, and flow rates that conferred optimal purity. Manual verification of single cells sorted on a glass slide by microscopy was performed to increase sorting stringency (if doublets or aggregates were detected) until zero doublets were observed. Following optimized instrument set-up, single cell sorting into the wells of a 96-well microtiter plate commenced. Internal plate control wells include wells bulk sorted with single color cells.

2.4. Imaging and Image Verification after FACS or Limiting Dilution Seeding

After depositing, plates were centrifuged and immediately imaged on a high-throughput microscopic imager (Cell Metric, Solentim, Dorset, UK or CloneSelect Imager, Molecular Devices, San Jose, CA). Imaging was performed periodically post seeding to track the formation of a single colony. Clonally derived cell lines were confirmed using several criteria: 1) clear proof of a single cell on day 0; 2) absence of significant artifacts in the well; 3) formation of single round colony; and 4) independent verification by two different scientists.

2.5. Single Cell Cloning by Berkeley Lights Beacon Instrument

Stable pools were single cell loaded on OptoSelect chips (Design 1750, Berkeley Lights, Emeryville, CA) using the Beacon instrument (Berkeley Lights, Emeryville, CA). OEP settings and scripts for loading and exporting cells were provided by BLI. Cells were cultured on the chips for 4 days using seed train growth medium containing additional growth supplements and manufacturer-recommended settings. Repeated imaging and cell counting were performed using the integrated 4× microscope and camera on the Beacon instrument. Cell counting algorithms were provided by BLI. Evidence of clonal derivation was achieved by an image of a single cell in a NanoPen. Selected pens were exported using OEP to guide between 2–20 cells out of NanoPens into the main channel, followed by flushing off the chip into a 96-well microtiter plate prefilled with a custom cloning medium. Blank exports were performed before and after each export where an equal volume line sample is deposited into even-column wells. Exports and blank samples are incubated for at least 14 days to monitor growth and contamination events in the system lines. Fluorescence in plates was monitored using the Cell Metric FL imaging system (Solentim, Dorset, UK) using the manufacturer supplied "monitor clonality scripts." Detection of RFP and GFP expressing were optimized through single color controls and validation using the EVOS FL Cell Imaging Microscope (Thermo Fisher, Waltham, MA)

Table 1. Validation of the Beacon cloning process steps and the overall clonality assurance rates.

Process step	True positive	False positive	Negative	Assurance rate
Beacon loading	1205	3	550	99.7%
Beacon NanoPen Isolation	1758	0	n.a.	100%
Beacon export purity	112	0	n.a.	100%

Scores of true positive, false positive, and negative events for individual workflow steps described in Figure 2. For Beacon Loading, true positive event is defined as single cell of known phenotype, false positive is defined as single cell of unknown phenotypic identity, negatives defined as blank pen (280), pen loaded with multiple cells (182), or incorrectly categorized by BLI algorithm as blank (88). For Beacon NanoPen Isolation, true positive defines pens that maintained homogenous phenotypic identity on day 4 when compared to day 0. For Beacon Export Purity, true positive is defined as clone of homogenous phenotypic identity that is consistent with phenotypic identity of clone selected for export.

2.6. Calculation of Clonality Probability

To evaluate clonality assurance, the probability of clonality (PoC) was calculated by estimating the percentage of true positives among all clone candidates.[22] Among clone candidates that have passed all bright field imaging and verification criteria, true positive and false positive are determined by using independent fluorescent imaging at least 14 days of outgrowth to check whether the culture has a single-color phenotype. Clones that have passed verification criteria and later determined to have a dual-color phenotype are false positives. To compensate for the inability to see wells that contain cells of the same color, the number of false positive wells were doubled (2×). To account for the effect of sample size, the Wilson method was used as previously described.[23] Briefly, a one-sided upper 95% confidence interval for the probability was calculated as a conservative estimate. The data in **Table 1** was used to calculate the confidence interval using the Wilson method:

95% upper confidence limit probability

$$= \frac{\hat{p} + \frac{z_{1-\alpha}^2}{2n} + z_{1-\alpha}\sqrt{\frac{\hat{p}(1-\hat{p})}{n} + \frac{z_{1-\alpha}^2}{4n^2}}}{1 + \frac{z_{1-\alpha}^2}{n}},$$

where n is the total number of observed wells, $z_{1-\alpha}$ is the $(1-\alpha)$th percentile of the standard normal distribution; $1-\alpha$ is the target confidence level, and $\hat{p}$ is the observed proportion of false positives among all wells.

3. Results and Discussion

3.1. The Beacon Platform Provides a Complete Image Data Package for Clonal Assurance

A common paradigm used to assure a single cell progenitor is to establish assurance of single cell deposition into a culture vessel, assurance of culture isolation through the duration of the culture, and assurance of purity when transferred out (**Figure 1**A). Typically, cloning processes occur in a single well of a microtiter plate. Assurance of single cell deposition (Figure 1A, blue box, i) is determined through a statistical distribution assumption for limiting dilution, imaging during deposition (SCP), or experimentally measured and calculated (FACS).[23] To improve assurance, microscopic imaging at the bottom of the well (Figure 1A, green boxes) within 24 h of plating provides evidence of single cell isolation and deposition. Images are often taken before (iii) and after cell seeding (iv), followed by repeated imaging to monitor growth of a localized colony (v). The probability of cells that may reside outside of the image area (Figure 1A, red box, ii) is experimentally determined and calculated as "ghost" wells.[24] Together, the plurality of data is manually verified and accepted as clonally derived.

The Berkeley Lights Beacon platform follows a similar clonality assurance paradigm through microscopic imaging and manual verification (Figure 1A, Bottom). The platform provides improved integrated imaging capability in combination with in-process quality controls compared to microtiter plate based cloning approaches. An OptoSelect NanoPen is over 100 000× smaller in volume (≈1.7 nL) than a well in a 96-well microtiter plate (≈200 µL). This size reduction results in improved image quality due to minimal z-depth (≈40 µm), clear edges, and reduced debris and artifacts. Automated focus and calibration capability combined with artificial intelligence (AI) cell identification simplifies the imaging workflow, enabling near real-time image analysis.

The initial cell deposition step utilizes an AI algorithm for cell detection followed by OEP to guide single cells into NanoPens (vii). The entire chip imaged before (viii) and immediately after cell loading is completed to provide pictorial proof of a single cell progenitor (ix). In the second stage of on-chip cell culturing and characterization, the fluidic flow in channels outside NanoPens is optimized to maintain completely in laminar regime with no occurrence of turbulence within the NanoPens where the cells are growing or in the chip channels. Time-course imaging and an AI cell count algorithm are used as in-process monitoring tools to ensure the empty NanoPens remain empty (xi) and cells do not expand beyond the maximum recommended height inside the NanoPen (x). In case when overgrowth occurs, there is a risk that the growing clones will expand into the channels and contaminate the export flow path. This risk is mitigated through strict monitoring of growth and ensuring that exports are performed before the cells expand beyond the recommended height (roughly ¾ of pen height filled). In the last stage of export for each clone, the complete export flow path is thoroughly flushed. Pen images are taken before (xii), during (xiii), and immediately after (xiv) export, as well as the export well plate (xv) to account for all cells on the chip. Throughout the export procedure, in-process fluidic samples are taken before and after each export. These in-process samples are deposited into a medium containing well on the same well plate to assess for clonal contamination or cross contamination in system lines. The well plate is further incubated for 2 weeks and re-imaged to ensure growth only in the intended wells and not in the in-process fluid control samples (xvi-red boxes). Manual verification of images is performed as a last step for data verification together with a complete image data set tracking cells

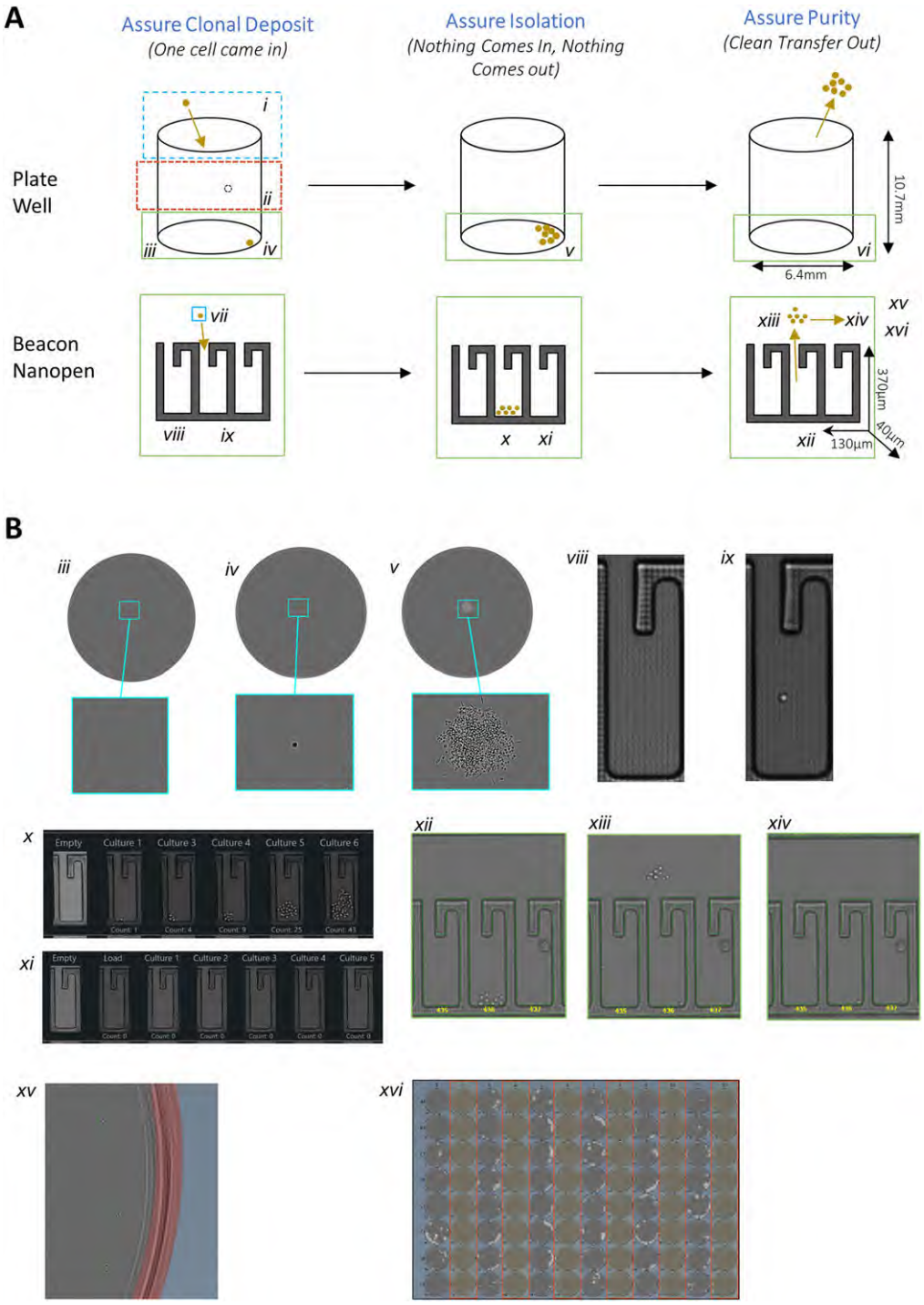

Figure 1. Subcloning workflow and single cell progenitor controls. A) Schematic of comparing single cell cloning workflows associated with microtiter plate-based cloning (top) and Beacon platform (bottom). Blue squares designate primary cell isolation and deposition methods steps. Green squares designate microscopic imaging image evidence and respective imaging areas captured. Red dotted square represent areas unable to capture using imaging and assurance is provided through measurement of "ghost-well" rates. Roman numerals indicate specific image data points or statistical measurements. B) Examples of image evidence used to support single cell progenitor assurance. Evidence from plate sorting methods include image prior to seeding (iii), image directly after seeding (iv), and image of a single localized colony (v). Evidence from Beacon cloning involve image of empty NanoPen prior to seeding (viii), image of single cell after OEP seeding (ix), time series of NanoPen growth (x), evidence of zero cross-contamination on chip through time series of adjacent empty NanoPens (xi), image record of OEP export including before (xii), after unpenning (xiii) and after flushing into well plates (xiv), image evidence of cells deposited into well plates (xv), evidence of growing culture after incubation (xvi), evidence of lack of contamination from cultured in process fluidic samples (xvi wells in red boxes)

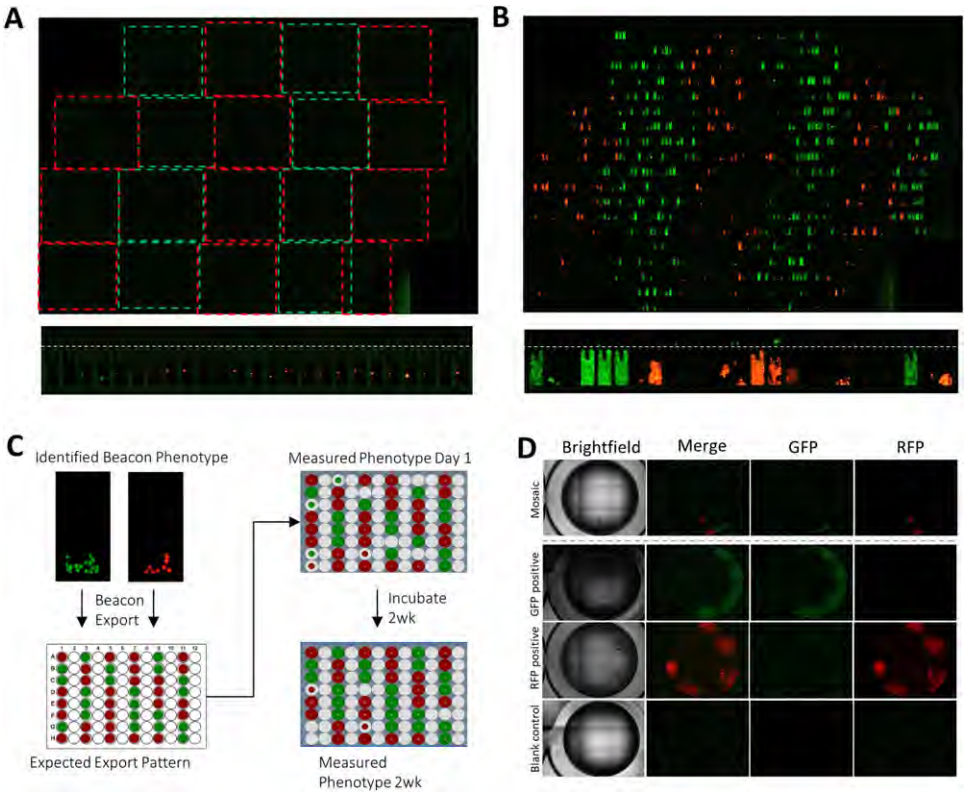

Figure 2. Validation of workflow steps using representative model CHO system. A) Single cells expressing expected fluorescent protein (GFP or RFP) were loaded onto the desired zones (dotted boxes) on the chip. Red and green fluorescence are measured and merged in example image of entire chip (top) and zoomed section (bottom). B) Cells are cultured over extended time to monitor and confirm that there is no mixing between pens during laminar flow of culture media. White dotted line depicts the border between flowing channel (above line) and inside NanoPens (below line). C) Cells with the expected phenotype were exported as shown by imaging of well plates post export using a fluorescence enable plate imager. D) Example images of clones expressing fluorescent proteins acquired after export into well plates. Images corresponding to mixed colony were acquired and scaled independently.

on and off the Beacon that enables rapid data verification and documentation.

4. Validation of Beacon Cloning Process Using Representative Model CHO System

To validate that the process described earlier does assure for clonal derivation, we used two representative CHO model cell lines that constitutively express either GFP or RFP. They were developed following a standard cell line development workflow, subcloned multiple times with multiple techniques, and the final clones were selected to have similar growth phenotypes and a stable fluorescent phenotype. In **Figure 2**A, the Beacon instrument's ability to correctly deposit single cells of known fluorescent phenotypes into desired pen locations was assessed. As shown in Table 1, single red and single green cells were placed into the desired zones on the chip. Immediately after load, pens were interrogated with the integrated fluorescent imaging capabilities to verify correct loading and tracking of cell origins. The Beacon correctly loaded, identified and documented a single clone with a single color 99.7% of the time.

Figure 2B illustrates the monitoring of cross-contamination events during cell culturing. Here the chip was cultured for an extended duration (10 days), which is two times longer than typical process (5 days) and imaged daily. Zero instances of multi-fluorescence pens or altered fluorescence pens were observed. Finally, the export purity rate off the instrument was determined (Figure 2C). Fluorescence identity of pens was determined and selected for export at days 4–6. Fluorescence imaging was performed on the exported well plates after export was complete and 2 weeks after (Figure 2D). All export colors and expected blank wells out of 112 attempts were as expected. Results are summarized in Table 1.

To measure the overall clonality assurance on the Beacon platform and compare to industry standard microtiter plate-based cloning approaches (limiting dilution and FACS), an equal volume mixture of the GFP- and RFP-expressing cells was subcloned using one of the three methods: limiting dilution seeding combined with plate image verification, FACS assisted cell deposition combined with plate image verification, and Beacon with integrated imaging and process controls (**Table 2**). After each process output, clones were manually assessed for positive evidence of clonality using the described process in Figure 1. Verified clones were then reassessed using a second independent instrument (Solentim CellMetric FL) to determine the number of single-color output cultures and multi-color output cultures. The number of multi-color output cultures provides a surrogate

Table 2. Overall clonality assurance rates.

Cloning process	True positive	False positive	Negative	No cell	Attempts	Assurance rate	Wilson assurance
Beacon cloning process	419	0	26	349	794	100%	99.36%
FACS cloning process	179	0	219	1226	1624	100%	98.52%
Limiting dilution cloning process	66	0	311	775	1152	100%	96.08%

An equal ratio of cells stably expressing either GFP or RFP proteins were cloned using one of three approaches: limiting dilution, FACS, and Beacon. True positives are defined as clones that have passed clonal verification acceptance criteria and then measured to have a single color phenotype. False positives have passed clonal verification acceptance criteria and measured to have a multi-color phenotype. Negatives are clones that have failed acceptance criteria defined by each method. "No cell" refers to the number of wells that show no growth after seeding or exporting.

to estimate the false positives, which is needed to calculate the probability of clonality (PoC).[22,24] To calculate the probability that the process ensures a single cell origin, we calculate the measured probability of clonality (number of true positives/(number of true positives + false positives)).[22] The probability is also calculated using one-sided upper 95% confidence interval by Wilson method to take in account for sample size.[7,23] The Beacon platform was shown to provide equivalent clonality assurance to reported methods (100% and 99.33%, respectively). This coincides with a similar monoclonal probability assessment performed by the instrument manufacturer. When comparing between growing colonies, the Beacon cloning and confirmation process calls 94% of exported cultures as positive that they were clonally derived. This is compared to 45% for a FACS and 17% for a limiting dilution process. These lower rates are due to a number of reasons including multiple cells seeded in a single well, strict imaging acceptance criteria (e.g., away from well edge, focus, high contrast, round cell shape), difficulty ensuring a high-quality day zero image, and maintaining a single localized colony over the imaging time frame. Additionally, Beacon clones that have been selected for export into 96-well microtiter plates have a higher recovery rate (56%) (positive + negative / attempts) compared to FACS (24%) and limiting dilution (33%) in the same plate format. The improved recovery can be attributed to preselection of healthy, growing clones on the chip, and the fact that multiple cells are seeded into plates from the Beacon process. In comparison, the direct well plate seeding methods require a single cell clonality image inside a well, and therefore must recover from a lower effective density, that is, a single cell. Together, the overall cloning efficiency (true positive, clonal verified, growing colonies/attempted seeded wells) is 52% for Beacon, 11% for FACS, and 5.7% for limiting dilution.

5. Conclusions

It is well established that manufacturing cell line clonality derivation can be assured using microscopic imaging and verification. Clonality assurance on the Berkeley Lights Beacon platform follows the same imaging and validation paradigm. However, through improved integrated imaging capability, cell detection algorithms, and in-process quality controls, the Beacon provides an overall stronger data package for single cell progenitor assurance. Using a representative CHO model system, we have demonstrated the Beacon platform provides improved efficiency over FACS and limiting dilution approaches, while offering comparable assurances of single cell derivation.

Acknowledgements

The authors would like to thank Tanner Neville, Keith Breinlinger, and contributors from Berkeley Lights, Inc. for insights, technical support, and thoughtful discussion. The authors also thank their colleagues in Amgen Drug Substance Technologies and Attribute Sciences for project support.

Conflict of Interest

The authors declare no conflict of interest.

Keywords

Berkeley Lights, cell line development, Chinese hamster ovary cells, clonality assurance, digital cell culture

Received: June 1, 2019
Revised: September 27, 2019
Published online: November 27, 2019

[1] M. Plavsic, *ICH Q5D Derivation and Characterization of Cell Substrates Used for Production of Biotechnological/Biological Products*, European Medicines Agency, Amsterdam **2017**.
[2] *Quality, Non-Clinical and Clinical Aspects of Medicinal Products Containing Genetically Modified Cells*, European Medicines Agency, Amsterdam **2012**.
[3] J. Y. Baik, K. H. Lee, *Biotechnol. J.* **2018**, *13*, 1700230.
[4] S. Kennett, presented at WCBP 2014, Washington, DC, January **2014**.
[5] R. Novak, *CDER/OPQ/OBP/DBRRI*, **2017**. https://cdn.ymaws.com/www.casss.org/resource/resmgr/cmc_no_am_jan_spkr_slds/2017_CMCJ_Novak_Rachel.pdf (accessed: May 2019).
[6] J. Welch, *CDER/OPQ/OBP/DBRRIV*, **2017**. https://cdn.ymaws.com/www.casss.org/resource/resmgr/ce_pharm_speaker_slides/2017_CE_Pharm_-_Welch_Slides.pdf (accessed: May 2019).
[7] H. A. Coller, B. S. Coller, *Hybridoma* **1983**, *2*, 91.
[8] J. Quiroz, Y.-S. Tsao, *Biotechnol. Prog.* **2016**, *32*, 1061.
[9] Y. Zhou, D. Shaw, C. Lam, J. Tsukuda, M. Yim, D. Tang, S. Louie, M. W. Laird, B. Snedecor, S. Misaghi, *Biotechnol. Prog.* **2018**, *34*, 559.
[10] T. Lai, Y. Yang, S. K. Ng, *Pharmaceuticals* **2013**, *6*, 579.
[11] M. Yim, D. Shaw, *Biotechnol. Prog.* **2018**, *34*, 1454.
[12] T. Kelly, A. M. Tuckowski, K. D. Smith, presented at the 26th ESACT Meeting, Copenhagen, Denmark, May **2019**, P-154.
[13] F. Boldog, S. Rajendran, S. Balasubramanian, L. Webster, M. Lee, A. Gough, C. Richards, T. Purcell, E. Hart, M. Fox, D. Vavilala, N. Kulikov, J. Minshull, O. Beske, presented at the 26th ESACT Meeting, Copenhagen, Denmark, May **2019**, P-173.

[14] A. Gough, C. Richards, I. Taylor, presented at the 26th ESACT Meeting, Copenhagen, Denmark, May **2019**, P-595.
[15] A. Gough, C. Richards, I. Taylor, presented at the 26th ESACT Meeting, Copenhagen, Denmark, May **2019**, P-449.
[16] J. Fieder, P. Schulz, I. Gorr, H. Bradl, T. Wenger, *Biotechnol. J.* **2017**, *12*, 1700002.
[17] H. Y. Hsu, A. T. Ohta, P. Y. Chiou, A. Jamshidi, S. L. Neale, M. C. Wu, *Lab Chip* **2010**, *10*, 165.
[18] A. Mocciaro, T. L. Roth, H. M. Bennett, M. Soumillon, A. Shah, J. Hiatt, K. Chapman, A. Marson, G. Lavieu, *Commun. Biol.* **2018**, *1*, 41.
[19] M. Jorgolli, T. Nevill, A. Winters, I. Chen, S. Chong, F. F. Lin, M. Mock, C. Chen, K. Le, C. Tan, P. Jess, H. Xu, A. Hamburger, J. Stevens, T. Munro, M. Wu, P. Tagari, L. P. Miranda, *Biotechnol. Bioeng.* **2019**, *116*, 2393.
[20] A. Winters, K. McFadden, J. Bergen, J. Landas, K. A. Berry, A. Gonzalez, H. Salimi-Moosavi, C. M. Murawsky, P. Tagari, C. T. King, *mAbs* **2019**, *11*, 1025.
[21] K. Le, C. Tan, S. Gupta, T. Guhan, H. Barkhordarian, J. Lull, J. Stevens, T. Munro, *Biotechnol. Prog.* **2018**, *34*, 1438.
[22] C. Chen, K. Le, H. Le, K. Daris, N. Soice, J. Stevens, C. T. Goudar, *Biotechnol. J.* **2019**, 1900289.
[23] K. Evans, T. Albanetti, R. Venkat, R. Schoner, J. Savery, G. Miro-Quesada, B. Rajan, C. Groves, *Biotechnol. Prog.* **2015**, *31*, 1172.
[24] D. Shaw, M. Yim, J. Tsukuda, J. C. Joly, A. Lin, B. Snedecor, M. W. Laird, S. E. Lang, *Biotechnol. Prog.* **2018**, *34*, 584.

Exhibit 9

AIChE

A Novel Mammalian Cell Line Development Platform Utilizing Nanofluidics and OptoElectro Positioning Technology

Kim Le
Drug Substance Technologies, Process Development, Amgen Inc., Thousand Oaks, CA, 91320

Christopher Tan
Drug Substance Technologies, Process Development, Amgen Inc., Thousand Oaks, CA, 91320

Shivani Gupta
Drug Substance Technologies, Process Development, Amgen Inc., Thousand Oaks, CA, 91320

Trupti Guhan
Drug Substance Technologies, Process Development, Amgen Inc., Thousand Oaks, CA, 91320

Hedieh Barkhordarian
Drug Substance Technologies, Process Development, Amgen Inc., Thousand Oaks, CA, 91320

Jonathan Lull
Drug Substance Technologies, Process Development, Amgen Inc., Thousand Oaks, CA, 91320

Jennitte Stevens
Drug Substance Technologies, Process Development, Amgen Inc., Thousand Oaks, CA, 91320

Trent Munro
Attribute Sciences, Process Development, Amgen Inc.Thousand Oaks, CA, 91320

DOI 10.1002/btpr.2690
Published online September 19, 2018 in Wiley Online Library (wileyonlinelibrary.com)

Generating a highly productive cell line is resource intensive and typically involves long timelines because of the need to screen large numbers of candidates in protein production studies. This has led to miniaturization and automation strategies to allow for reductions in resources and higher throughput. Current approaches rely on the use of standard cell culture vessels and bulky liquid handling equipment. New nanofludic technologies offer novel solutions to surpass these limits, further miniaturizing cell culture volumes (10^5 times smaller) by growing cells on custom nanofluidic chips. Berkeley Lights' OptoElectro Positioning technology projects light patterns to activate photoconductors that gently repel cells to manipulate single cells on nanofluidic culturing chips. Using a fully integrated technology platform (Beacon), common cell culture tasks can be programmed through software, allowing maintenance and analysis of thousands of cell lines in parallel on a single chip. Here, we describe the ability to perform key cell line development work on the Beacon platform. We demonstrate that commercial production Chinese hamster ovary cell lines can be isolated, cultured, screened, and exported at high efficiency. We compare this process head to head with a FACS-enabled microtiter plate-based workflow and demonstrate generation of comparable clonal cell lines with reduced resources. © 2018 American Institute of Chemical Engineers *Biotechnol. Prog.*, 34:1438–1446, 2018
Keywords: Cell line development, automation, nanofluidics

Introduction

The development of a successful therapeutic biologic is a lengthy, multiple step process which begins with isolation of a highly productive mammalian cell line to generate a cell line bank for future clinical and commercial production. Typical mammalian cell line development processes are resource intensive and require lengthy timelines because of the slow recovery of cells during selection, single cell subcloning, and the need to perform multiple screening assays to identify suitable production hosts.[1] Additionally, regulatory agencies require that clinical trials be initiated with material from clonally derived cell lines and banks.[2]

A typical cloning and clone selection process is among the most labor-intensive steps during cell line development as a result of the several technical challenges. First, single-cell isolation is inefficient. Single cells are deposited in individual wells of a cell culture plate by limiting dilution,[3] single cell printing,[4] or

Kim Le and Christopher Tan contributed equally to this work.

Correspondence concerning this article should be addressed to Kim Le at khle@amgen.com

fluorescence-activated cell sorting (FACS).[5,6] Each of these methods have degrees of error in isolating individual cells and clonality must be verified by manual imaging of each individual well, followed by visual confirmation of the presence of a single cell in the well.[7] Second, individual cells grow poorly in microtiter plates likely as a result of the loss of cell-to-cell signaling, or the dilution of autocrine and paracrine factors secreted into the media and require time to recapitulate a healthy culture.[8] Finally, the lack of good high-throughput methods for analyzing protein secretion at the single-cell level that can predict large-scale production titers requires scaling of clones to large scale to allow for protein analytics and screening of product titer and quality.[9] As increasing the number of clones analyzed increases the likelihood of identifying rare clones with high titer and product quality attributes, hundreds if not thousands of clones must be carried from single cell to large scale cell cultures.

To address these challenges, significant efforts have been employed integrating miniaturized cell culture systems with high-throughput liquid handling automation.[10] These systems are usually coupled with microliter scale high throughput analytics to quickly identify potential candidate cell lines for manufacturing.[11] For example, a common miniaturization platform is to use shaken microtiter plates coupled with automated liquid handling.[12,13] However, when increasing throughput (number of wells per plate), technical limitations such as evaporative loss, increased aeration and agitation requirements, low density recovery efficiency, pipetting accuracy at submicroliter volumes, parallel processing liquid handling, and low limits of protein detection (ng) required limit the improvement of these approaches.[14]

Nanofluidic technologies offer a promising solution to further miniaturize cell culture processes.[15] One such technology platform has been developed by Berkeley Lights.[16] Their Beacon platform combines the use of nanofluidics on a temperature-controlled chip arrayed with 1758 pens (OptoSelect™ Chips), single cell manipulation though OptoElectro Positioning™ (OEP),[17–19] and high-resolution fluorescence imaging for downstream analytics. OEP can manipulate hundreds of cells in parallel on OptoSelect™ Chips, allowing multiplexed depositing of single cells into an array of individual pens with nanoliter volumes (nanopen). The entire chip can be imaged in 8 min, and coupled with artificial intelligence-based cell counting, allows for efficient monitoring of clonality and growth of all clones on the chip.[3] Additionally, bead and diffusion-based fluorescent assays can be adapted for scoring secreted antibody on chip. Thus, relative protein productivity can be established on the instrument and only clones with acceptable productivity can be selected for export to microtiter plates and scaled-up for further studies. Captured data can then combined to document cell growth measurements, proof of clonal origin, single-cell secretion, and overall population compositions.

To assess the potential of the Beacon platform in production cell line development, we compared a Beacon-based subcloning workflow with a traditional FACS-based process. We aimed to compare the throughput, timelines, resource requirement, data quality, and overall performance of cell lines generated.

Materials and Methods

Cell lines

Cell lines were generated by transfection of an Amgen proprietary clonal CHO host cell lines with plasmid DNA encoding for a heavy chain and light chain from a human monoclonal antibody. Following transfection, stably expressing pool populations were created through the repeated passaging in selective growth media until cells reach percent viabilities greater 90% and maintain consistent doubling times. Further selection using increasing levels methotrexate is also applied to improve productivity. Cells were cultured in either 96-well, 24-well, or 24-deepwell microtiter plates (Corning, Corning, NY), 125 mL shake flasks (Corning, Corning, NY), T-175 flasks (Corning, Corning, NY), or 50 mL TubeSpin (TPP, Trasadingen, Switzerland) in Amgen proprietary media at 37°C, 5% CO_2, and 85% humidity. Cells were maintained by passaging multiple times a week at a targeted seed density.

Single cell cloning by flow cytometry and imaging

A FACSAriaIIu (Becton Dickinson, Franklin Lakes, NJ) cell sorter was used to isolate and deposit single cells from a stable transfected cell line directly into 96-well microtiter plates prefilled with proprietary cloning medium. Sorting conditions were set to internally determined parameters that encourage high assurance of single cell isolation. After depositing, plates were centrifuged and immediately imaged on a high-throughput microscopic imager (Cell Metric, Solentim, Dorset, UK). Imaging was performed periodically to track the formation of a single colony. Clonally derived cell lines are confirmed using a criterion of (1) clear proof of a single cell, (2) absence of other significant artifacts in the well, (3) formation of single round colony, and (4) verification by two scientists.

Berkeley lights beacon instrument

Cell lines were single cell loaded on OptoSelect™ Chips (Design 1750, Berkeley Lights, Emeryville, CA) using the Beacon Instrument (Berkeley Lights, Emeryville, CA). OptoElectro positioning settings and scripts for loading and exporting cells were provided by Berkeley Lights Inc. Cells were cultured on the OptoSelect™ chips for up to 4 days using proprietary growth media and manufacturer recommended settings. Repeated imaging and cell counting were performed using the integrated 4X microscope and camera on the Beacon instrument. Evidence of clonal derivation is achieved by image of a single cell in a nanopen (0.05 mm^2 area, and 0.002 mm^3). Secretion assays were performed using the Spotlight HuIg2 Assay (Berkeley Lights, Emeryville, CA) with supplied method scripts and assay analyzer software (Cell Analysis Suite, Build 30552). Selected pens were exported using OEP to move cells out of pens followed by flushing off the chip into a 96-well microtiter plate prefilled with proprietary cloning media.

Scale up of exported subclones

Exported cells were scaled up through dilution into proprietary passaging medium into increasing sized microtiter plates and cultured in static incubators at 37°C, 5% CO_2**.** Transfer steps were assisted using a Biomek Fx^P liquid handling robot (Beckman Coulter, Brea, CA). Cells were transitioned to suspension culturing using shaken 24-deepwell plates (Corning, Corning, NY) and 50 mL TubeSpin bioreactors (TPP, Trasadingen, Switzerland). Growth in microtiter plates was monitored using the Cell Metric imaging system (Solentim, Dorset, UK).

Small-scale production cultivation

Fed-batch evaluations were performed in TubeSpin bioreactors (TPP, Trasadingen, Switzerland). Individual tubes were set up with a working volume of 30 mL of production media, incubated at 36°C, 5% CO_2, 85% relative humidity, and shaken at 225 rpm with at 50 mm orbital diameter in a large-capacity ISF4-X incubator (Kuhner AG, Basel, Switzerland). Cultures were inoculated at a target cell density ranging from 8×10^5 to 1×10^6 cells/mL and were fed a single bolus feed at Days 3, 6, and 8. In-process samples were taken from cultures on Days 0, 3, and 6–10 for analysis. Cell concentrations and viability of cultures were determined using a Vi-Cell XR cell counter (Beckman Coulter, Brea, CA). Antibody titers were measured by affinity Protein A high-performance liquid chromatography.

Bioreactor production

Seven-liter Bioreactors (Applikon, Foster City, CA) were used for a standard production culture with a 4.4 L working volume. Temperature set-point and agitation were controlled by digital control units. pH set-point was controlled automatically by CO_2 or 1 M Na_2CO_3 addition. Dissolved oxygen set-point was controlled by sparging oxygen through a drilled-tube and a sintered-steel spargers. Proprietary production medium were used. Daily samples were analyzed for viable cell density (VCD) and viability (%) using a Bioprofile CDV (Nova Biomedical, Waltham, MA), glucose, lactate, NH4+ and osmolality using BioProfile Flex Analyzer (Nova Biomedical, Waltham, MA), and pH, pCO_2, and pO_2 using Corning 248 blood gas analyzer (Medfield, MA). Supernatant samples were also analyzed for titer.

Results

The Beacon can efficiently clone and recover production CHO cell lines

To determine how the nanofluidic platform would best fit into an industrial cell line development platform, we closely examined each cell line development step. We identified subcloning operations as the most impactful application of the technology because of the (1) high-throughput cell culture needs, (2) requirement to proving clonal derivation and tracking, and (3) the greatest potential for resource and timeline savings through the early decision of a final clone.

To explore the efficiency of performing the cloning workflow on the Beacon instrument, we evaluated the ability to efficiently isolate single cells and document clonality, growth of the cells on the chip under perfusion culture, export of the cells into microtiter plates, and outgrowth and performance of the resulting cell lines. To ensure that there were no product or cell line specific influences on growth and export, 17 unique CHO cell lines were tested from host different lineages, selective pressures, expressing three modalities (monoclonal antibody, a-glycosylated antibody, and bispecific antibody), with a range of titers. We examined efficiency for the four major steps of the workflow (Figure 1A), such as isolation of single cells (Figure 1B), growing clonally derived cells in nanopens (Figure 1C), exporting grown populations out of nanopens into microtiter plates (Figure 1D), and expanding cultures in microtiter plates (Figure 1E). A total of 10 chips with 1,758 pens each were OEP-loaded with the described cell lines to achieve an average of 1,038 single cells per chip (59%), with a range 820–1,258 clones (46%–71%) (Figure 1B). Out of 9,365 single clones, 65% show at least one doubling after 3 days (Figure 1C). Figure 1D describes the range of cell numbers that can moved out of the pen using OEP. Out of 221 unpen attempts (move cultures outside of pen), OEP was able to remove 209 of pens (94%) with at least 3 cells. Following unpenning, cell populations were deposited into 96-well microtiter plates. Of the attempted depositions, 81% form viable colonies in plates (Figure 1E). In total, a single chip can generate from 406–623 viable clones from a single load (or 23%–35% to available pens).

The Beacon workflow can isolate and screen clones for productivity

We next compared subcloning procedures on a cell line expressing a secreted biologic with traditional microtiter plate-based methods vs. a nanofluidic workflow on the Beacon Instrument. Figure 2 describes a standard subcloning operation where a starting heterogenous population is isolated and deposited into microtiter plates using FACS-based cell sorting. Immediately after deposition, high-quality, high-throughput whole well imaging is used to verify a single cell in a well as described above. After growth and repeated imaging, colonies are picked and consolidated using automation liquid handlers. As secretion and growth rates are difficult to measure early on, dozens of clones are scaled up to perform a high-throughput small scale production assay. In contrast, single cell isolation, growth assessment, and high-throughput screen are performed while on the chip (dotted box) in the nanofluidic workflow, and only those clones that meet the desired criteria are exported and expanded for further evaluation.

High expressing CHO stable pools secreting an antibody fusion modality were subcloned using a FACS-based cloning method, and the same pools were cloned and analyzed on the Beacon platform. A total of 1,920 wells (20 plates) were seeded using the standard process as compared to 3,518 pens (2 Chips) on the Beacon process. The FACS process resulted in 360 wells with single cell-derived colonies that passed a stringent image analysis screening that consists of repeated image tracking of colony outgrowth originating from a verified single cell. Alternatively, for the Beacon process, 1,603 clones were derived from single cells as determined by high quality imaging of each pen after loading on the OptoSelect™ chips. Cells were then assessed for growth for up to 4 days though repeated bright-field imaging of pens and the use of a cell counting algorithm. (Figure 3A). To measure secreted antibody, a diffusion-based assay was employed (Spotlight Assay). In this assay, nanopens are first saturated with a fluorophore-tagged small molecule targeting human IgG Fc. Following equilibration of fluorescent signal between the pen and the channel, the chip is flushed to clear signal from the channel and diffusion of the fluorescent molecule out of the pens is observed. Pens containing secreted antibody have the fluorescent small molecule bound to the antibody forming a complex that diffuses slower as a result of its high molecular weight as compared with pens with little or no antibody where most of the fluorescent signal diffuses quickly. This difference in diffusion rates is measured and quantified on the Beacon platform (Figure 2). A total of 51 clones were exported for scale up (highlighted) which exhibited a wide range of growth (Figure 3B) and productivity characteristics (Figure 3A). Following export, populations were scaled to suspension culture for small-scale fed-batch screening.

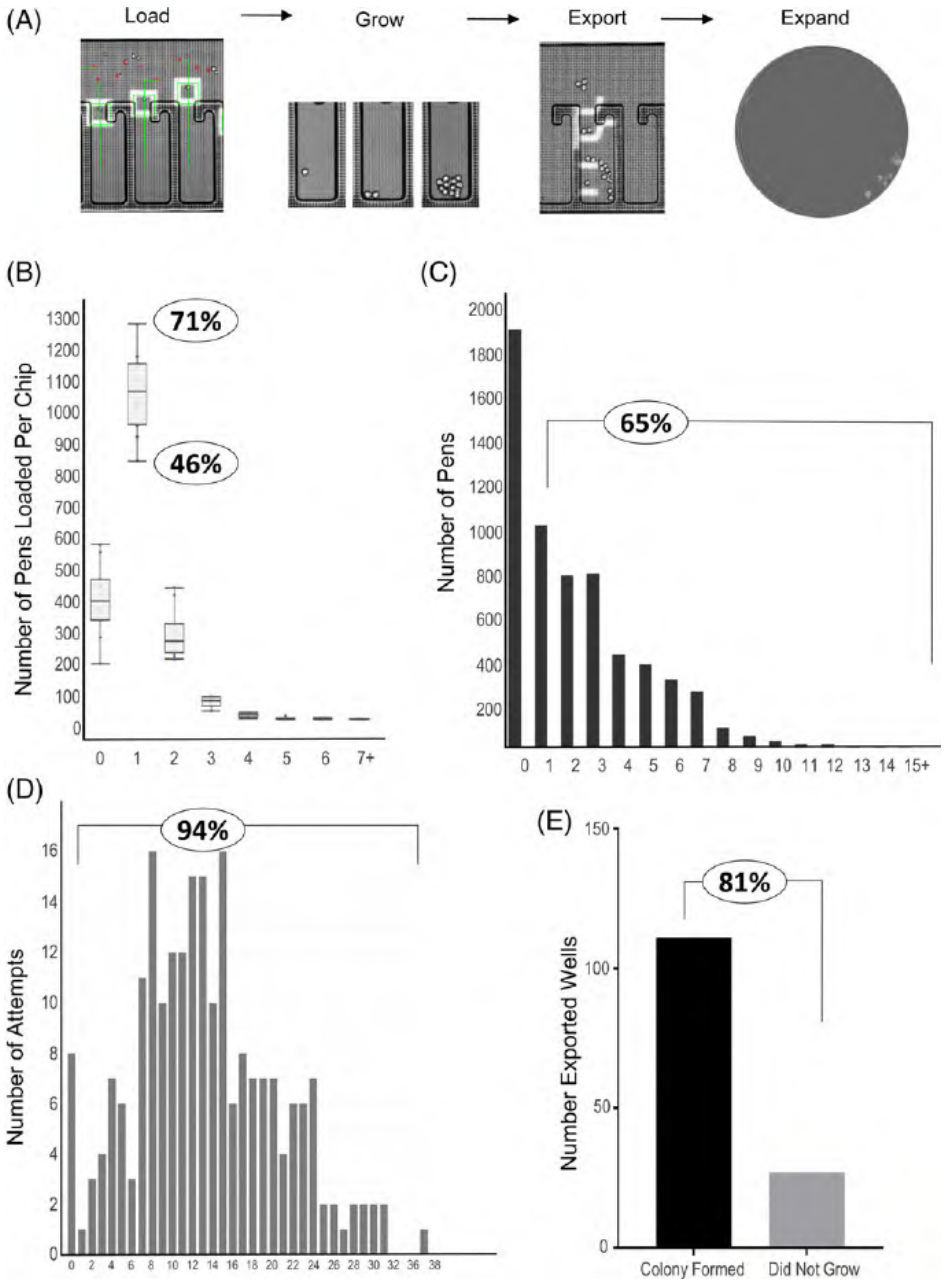

Figure 1. Assessment of workflow efficiency of the Beacon platform. (A) Representation of workflow with images of cells and colonies. (B) Number of pens that contain empty, single, or multiple cells per chip after loading operation. Percentage denotes highest and lowest percent singles loaded. (C) Cell count of pens after 3 days from single cell loads. Percentage denotes number of single clones with positive cell growth. (D) Counts of unpenned cells after export workflow. Percentage denotes numbers of pens with exports greater than three cells. (E) Count of wells with growth after export.

To determine whether the Spotlight assay is predictive of larger scale fed-batch productivity, the Spotlight titer measurements for each clone were compared to resulting 10-day fed-batch specific productivity following approximately 50 days of scaleup. Plotted in Figure 3C is the comparison of early Spotlight assay score (*x*-axis) vs. the specific productivity of each clone during fed-batch (*y*-axis). Overall, we see decent correlation of titer scores with the final productivity of cells (Pearson product correlation coefficient = 0.7395).

The Beacon cell line development workflow generates comparable cell lines as traditional methods

Beacon generated cell lines were compared with equal numbers of clones expanded from FACS-based workflow. The overall total time from seeding to suspension screening start was comparable between processes. Clones from both processes were run side by side in a small-scale fed-batch screening experiment. On average, the plate-based process yielded clones with an average normalized titer of 1.0 and range from 0.1 to 2.2. The Beacon clones on average had a normalized titer of 1.25 with a range of 0.3 to 2.9 (Figure 4A). Following small scale fed-batch screening, the top three clones from each process were run on bench scale bioreactors. VCD, viability, cumulative titer, and specific productivity vs. process duration (respectively clockwise, left to right) are plotted in Figure 3C. The top Beacon clones (black) perform similarly to top standard clones (white) in terms of titer and viability. Two Beacon isolated clones show higher specific productivity by achieving comparable titer with lower total cell mass. Overall, the top beacon clone

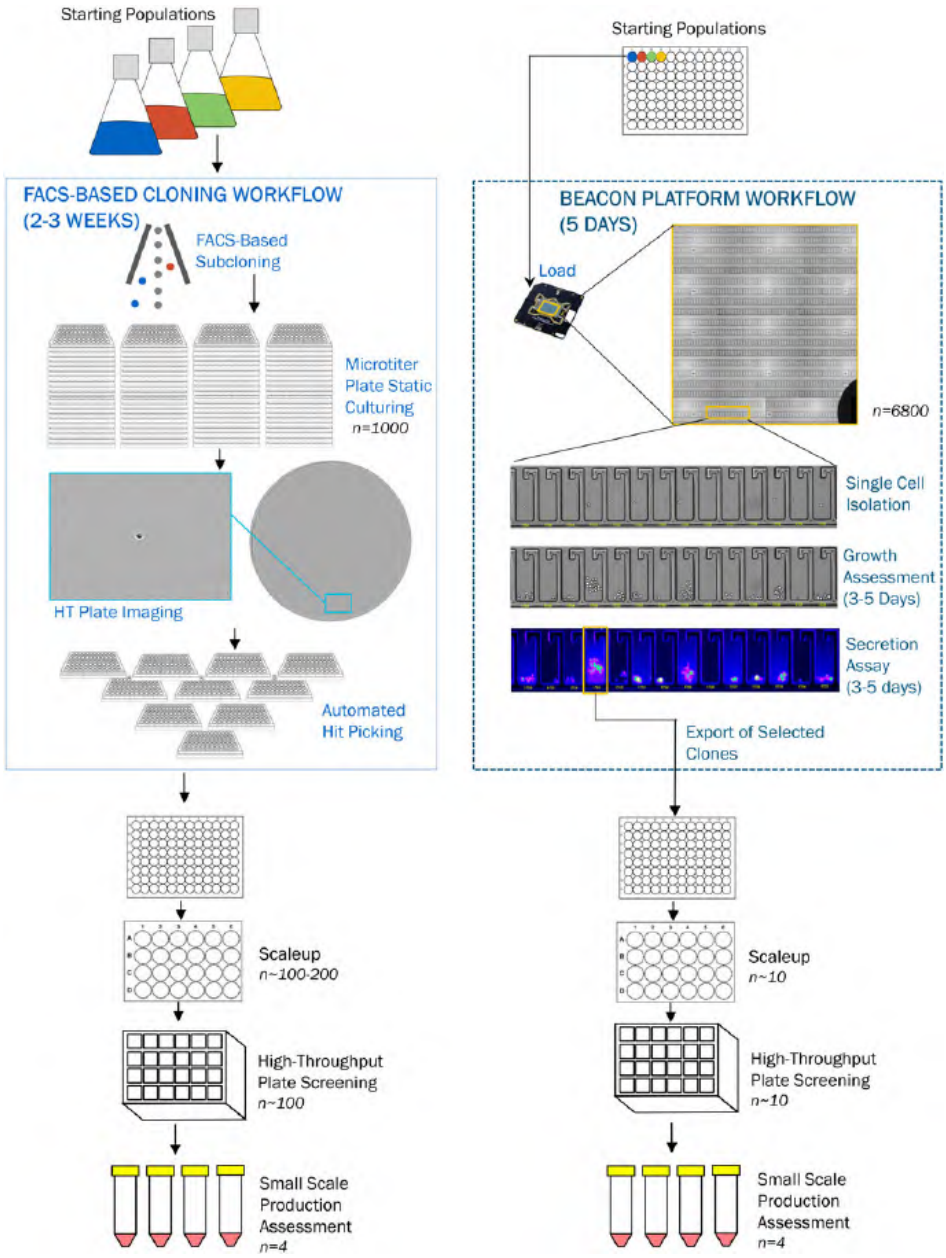

Figure 2. Comparison of a microtiter plate-based cloning workflow vs. a nanofluidic chip subcloning workflow. A depiction of the steps involved in performing a clonal isolation and expansion workflow using two approaches. Differences are highlighted in boxes for FACS-based workflow(solid) and Beacon workflow (dotted).

(Beacon-A) performed comparable to the top plate-derived clone (FACS-B).

The Beacon platform can generate high expressing production cell lines with reduced resources

As the Spotlight secretion measurements have been shown to correlate with later clone productivity, it can be employed to preselect top clones and therefore reduce the numbers of clones needed to scale up and analyze. To demonstrate this, the Beacon was again compared side by side to a standard FACS process for a new model monoclonal antibody. In this case, a standard FACS-based process yielded a total of 157 mature clonally-derived candidate cell lines. For the Beacon process, only 10 clones were scaled and evaluated. These 10 clones were preselected by the Spotlight assay and growth on the chip and represented the top 25% of secretors and top 50% of doubling times. The fed-batch screening was performed resulting in the FACS-based process analyzed 92 clones with an average normalized titer of 1.0 and range from 0.01 to 2.0. The 10 Beacon clones had an average normalized titer of 1.19 with a range of 0.5–1.6. The top 4 clones of each process were then run in an alternative intensified process that favors higher cell mass accumulation and higher viability. Top Beacon clones performed similarly to top standard clones in terms of titer and viability. Similar to the previous study, the two Beacon clones were identified having higher specific productivity. Overall, the Beacon process was able to achieve comparable clones as the FACS-based process despite scaling up a fraction of the number of clones.

The Beacon platform allows for rich analysis of data

In addition to execution of existing cell line workflows at higher efficiency, the Beacon platform generates a richer data

Biotechnol. Prog., 2018, Vol. 34, No. 6

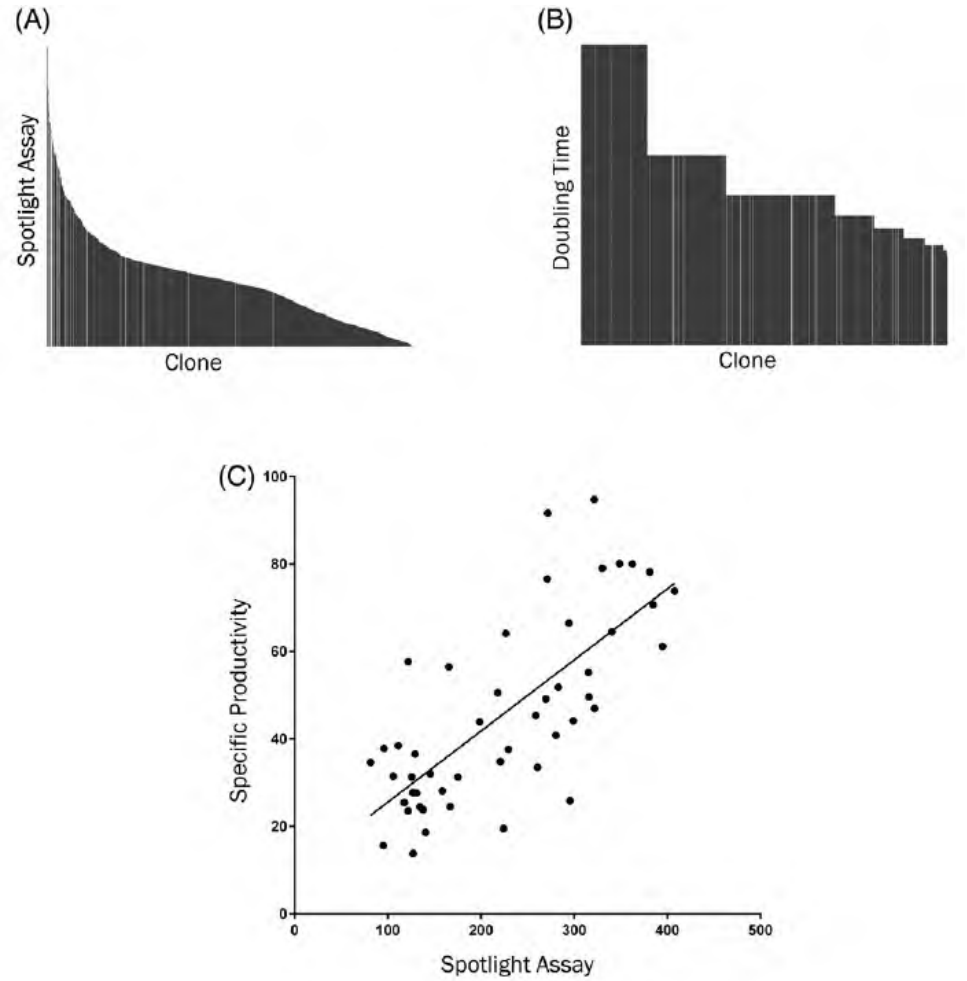

Figure 3. Correlation of Spotlight Titer analysis of early clones with fed-batch specific productivity of mature clones. (A) Secretion and growth measurements measured on OptoSelect™ chips. The Spotlight secretion assay generates a ranked assay score. (B) Growth assessment on chip is performed through performing cell counts and calculation of doubling time. Selected clones with a wide range of growth and secretion highlighted in white. (C) Scatter plot of individual clones analyzed early on the Beacon using Spotlight Assay (X-axis-Titer score) and analyzed 50 days later in a suspension fed-batch production experiment (Y-axis-Relative specific productivity).

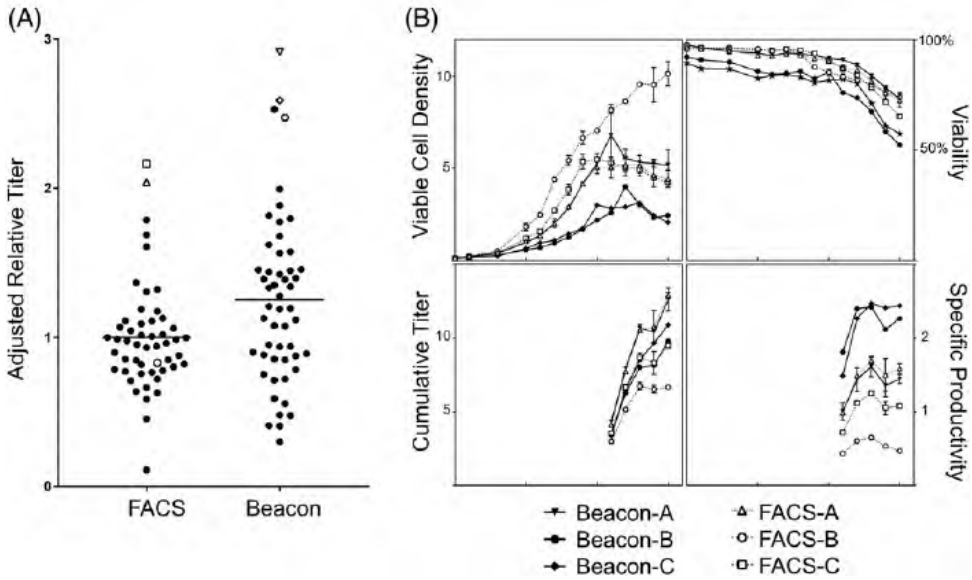

Figure 4. Comparison of clonally derived cell lines from FACS-based and Beacon Workflows. (A) Fed-batch screening of mature clones. Clones from both methods screened using a fed-batch production screen and accumulated titer measured (Normalized grams/liter). Top clones from each method highlighted with open circles. (B) Bioreactor screening of top clones. Top 3 Beacon clones (Black) screened with top 3 FACS-based clones (white). Plot of VCD (Top Left), viability (Top Right), accumulated titer (Bottom Left), and specific productivity (Bottom Right) over process duration.

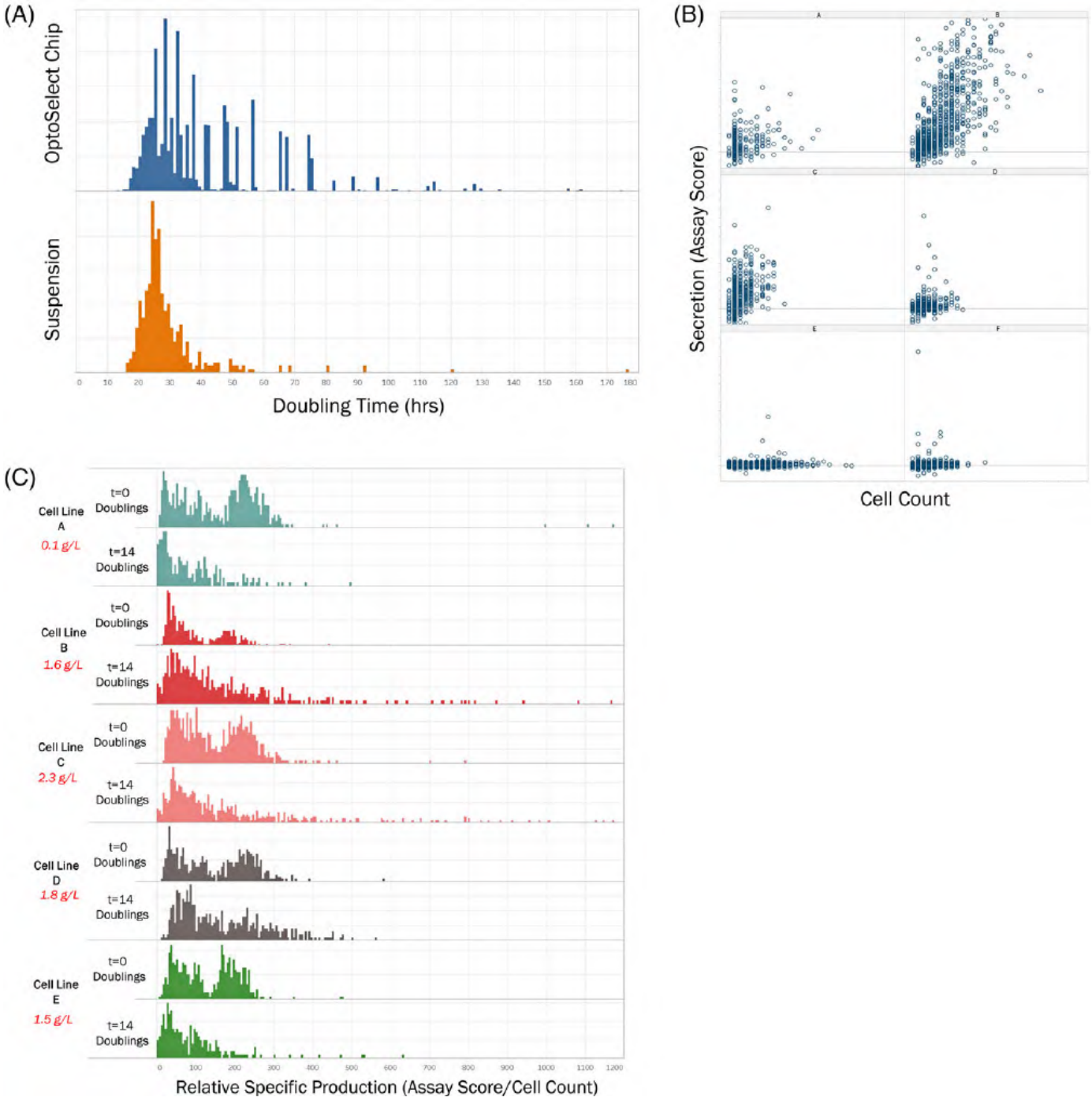

Figure 5. Assessment of stable cell lines on the Beacon platform. (A) Interrogating cell growth from single cells (blue) vs. shaken suspension pools (orange). (B) Single clone analysis of stable populations for growth and secretion. Plot of cell numbers after 3-day growth vs. spotlight secretion assay score. (C) Specific productivity profiles of five stable pools after culturing.

package as compared to FACS or batch screening data. Unlike typical FACS analysis, the Beacon platform allows for the assessment of secretion and growth at a single cell level. As a result, a better understanding of the dynamics of the overall populations and subpopulations is visualized. Figure 5A compares the doubling time of a selected antibody-expressing pool population. The cell line was either passaged in shaken suspension (shake flasks) vs. clonally isolated and grown in individual nanopens. While the median doubling time on the Berkeley Lights instrument was marginally higher (28 vs. 26 h) than shake flask doubling time, the overall distributions were similar, indicating that production CHO lines are capable of comparable growth on the instrument. The lower mean growth rate on the instrument is not surprising as shake flasks represent a large population of cells where faster growing cells will outgrow slower growing cells and be over-represented in the culture. Indeed, rare clones with doubling times of >100 hours can be seen on the instrument and represent an interesting population of cells we have not previously been able to isolate because of the masking by the faster growing cells in microtiter plates.

The Beacon data set also allows single cell population comparisons across multiple pools. Figure 5B plots secretion vs. 3-day growth of individual pens for an unamplified vs. methotrexate (MTX) amplified pool expressing a monoclonal antibody. This analysis provides a full view of a population

heterogeneity of not only relative expression but also doubling times. For example, the unamplified pool A is primarily constituted by a fast-growing population with relatively low expression and a few rare slower growing outliers, while some have high productivity. Upon amplification to 150 nM MTX, population B profile changes dramatically, with a shift to a higher producing, faster growing population. Importantly one can then potentially isolate cells with a unique growth and productivity profile. Interestingly, a 300 nM MTX amplified pool (C) shows a population centered around lower growth population relative to the 150 nM pool, suggesting increasing levels of MTX lead to diminishing productivity returns. In panels D–F, a separate cell line profile shows that one of the populations has a low productivity and rapidly dividing subpopulation (E), population (F) exhibits a slow-growing high-productive phenotype, and population (D) has a combination of growth and secretion.

Figure 5C further visualizes the distribution of specific productivity in a pooled population. Here, four stable pool cell populations are secreting the same protein and only differ by transfection event. The productivity profiles generated on the Beacon correlate well with the measured batch titers at the later time point. Interestingly one can observe how these pools change over time in culture as pool B and C appears to have higher production populations that are emerging during the culture period. These figures exemplify how richer data obtained from the Beacon gives insight into the interrogated population, allowing for stronger assessments and decision making.

Discussion

We have demonstrated the feasibility of performing a cell line development workflow on a novel nanofluidic platform utilizing software driven OEP and fluorescent detection. As a result, a simplified workflow to maintain and screen over 3,000 subclones simultaneously, document clonality, and efficiently select highly productive clones and export clonal cell lines is achievable.

The case study described demonstrates the ability to reduce overall resources by dramatically decreasing the total number of subclones that need to be individual maintained, scaled, and analyzed. Through screening early on chip, we show that it is only necessary to isolate a fraction of Beacon-selected clones as compared to FACS based methods to achieve higher average fed-batch titers though the elimination of poor producing clones (less than 0.5 relative titer). Screening significantly fewer clones in plate-based formats results in a corresponding decrease in cell culture load that translates to reduced labor, required incubator space, and laboratory footprint.

Another critical resource advantage of utilizing an integrated nanofluidic device for commercial cell line development is the ability to generate high quality images throughout the entire subcloning process for generating complete proof of clonality reports. Time lapse imaging of growth from the single cell stage to export provides confidence of clonal origin, a complete record of cell growth, and secretion phenotypes. Simultaneous imaging of empty pens allows for the in process monitoring of cross-contamination throughout the duration of the experiment. Exports are tracked by on-instrument imaging at each step of the OEP export process and complemented by subsequent off-instrument imaging of export plates. Together, a complete image documentation package can be created to provide to regulatory agencies to assure clonal derivation.

In addition to streamlining the cloning process and reducing resources, this study also potentially highlights the power of the Beacon to select cells with rare phenotypes or desirable traits. For example, in both case studies, the Beacon workflow derived clones had the highest specific productivity. While plate subcloning and production screening selection can be biased towards faster growing clones, slower growing clones with higher specific productivity can be interrogated in the nanofluidic environment for use in long-term perfusion-based manufacturing platforms where steady growth is optimal for example. Further, the single cell data obtained from cell lines provides insights into defining population characteristics of the production cell lines that are not currently possible with the traditional FACS-based methods. Data generated in this study provide additional understanding of rapidly shifting populations dynamics that occur during prolonged culturing of cells in vitro (Figure 5). Ultimately, this data can be combined holistically with manufacturing data to develop predictive models for cell line selection.

Top clone selection is arguably one of the most important decisions made over the lifecycle of bringing a novel biotherapeutic to patients. The resulting master and working cell banks are used over the entire life-cycle of the marketed product that can last multiple decades. Currently, a great deal of effort and scrutiny is involved in the selection of the top clone through assessment of performance and product quality in small scale production runs followed by protein analytics. The Beacon platform offers an opportunity to obtain large amounts of similar information from thousands of clones at the point of cloning. As described in the Figure 1, we can obtain detailed growth information, secreted antibody titers, and specific productivity. Additional information can be obtained through modulating the culturing conditions on chip such as media, temperature, gasses, and treatments. Bead-based capture and diffusion assays can also be developed to interrogate product quality immediately after secretion. Together, this package may potentially be used as surrogate data for the selection of the final master cell bank and therefore significantly reduce resources.

Conclusions

Developing a commercial production cell line usually involves three general activities, the culturing of CHO cells, the sterile manipulation of cell culture, and the cellular analytics. The nanofluidic platform offered by Berkeley Lights provides the ability to do all three activities efficiently within an integrated workflow. For the first time, we have shown this type of technology can be directly applied to generate clonal CHO cells suitable for commercial development. We show this is particularly effective when applied to the subcloning workflow. When compared to a traditional plate-based workflow, the Beacon platform is capable of efficiently producing comparable manufacturing cell lines. Additionally, a rich data set is generated to support clonality, tracking, and population understandings and enable early decisions and identify high performing cell lines.

Acknowledgments

The authors thank Tanner Neville, Troy Lionberger, Gang Wang, and contributors from Berkeley Lights Inc. for insights and technical support. The authors also thank their colleagues

in Amgen Drug Substance Technologies and Attribute Sciences for project support.

Literature Cited

1. Wurm FM. Production of recombinant protein therapeutics in cultivated mammalian cells. *Nat Biotechnol.* 2004;22(11):1393–1398.
2. Frye C, Deshpande R, Estes S, Francissen K, Joly J, Lubiniecki A, Munro T, Russell R, Wang T, Anderson K. Industry view on the relative importance of "clonality" of biopharmaceutical-producing cell lines. *Biologicals*. 2016;44(2):117–122.
3. Zhou Y, Shaw D, Lam C, Tsukuda J, Yim M, Tang D, Louie S, Laird MW, Snedecor B, Misaghi S. Beating the odds: the poisson distribution of all input cells during limiting dilution grossly underestimates whether a cell line is clonally-derived or not. *Biotechnol Progress*. 2017.
4. Gross A, Schoendube J, Zimmermann S, Steeb M, Zengerle R, Koltay P. Technologies for single-cell isolation. *Int J Mol Sci.* 2015;16(8):16897–16919.
5. DeMaria CT, Cairns V, Schwarz C, Zhang J, Guerin M, Zuena E, Estes S, Karey KP. Accelerated clone selection for recombinant CHO CELLS using a FACS-based high-throughput screen. *Biotechnol Progress*. 2007;23(2):465–472.
6. Misaghi S, Shaw D, Louie S, Nava A, Simmons L, Snedecor B, Poon C, Paw JS, Gilmour-Appling L, Cupp JE. Slashing the timelines: opting to generate high-titer clonal lines faster via viability-based single cell sorting. *Biotechnol Progress*. 2016;32(1):198–207.
7. Evans K, Albanetti T, Venkat R, Schoner R, Savery J, Miro-Quesada G, Rajan B, Groves C. Assurance of monoclonality in one round of cloning through cell sorting for single cell deposition coupled with high resolution cell imaging. *Biotechnol Progress*. 2015;31(5):1172–1178.
8. Lim UM, Yap MG, Lim YP, Goh LT, Ng SK. Identification of autocrine growth factors secreted by CHO cells for applications in single-cell cloning media. *J Proteome Res.* 2013;12(7):3496–3510.
9. Arkin MR, Glicksman MA, Fu H, Havel JJ, Du Y. Inhibition of protein-protein interactions: non-cellular assay formats. In: Sittampalam GS, Coussens NP, Brimacombe K, Grossman A, Arkin M, Auld D, Austin C, Baell J, Bejcek B, TDY C, Dahlin JL, Devanaryan V, Foley TL, Glicksman M, Hall MD, Hass JV, Inglese J, Iversen PW, Kahl SD, Kales SC, Lal-Nag M, Li Z, McGee J, McManus O, Riss T, Trask OJ Jr, Weidner JR, Xia M, Xu X, editors. *Assay Guidance Manual*. Rockville, MD: Bethesda; 2004.
10. Woodruff K, Maerkl SJ. A high-throughput microfluidic platform for mammalian cell transfection and culturing. *Sci Rep.* 2016;6:23937.
11. Priola JJ, Calzadilla N, Baumann M, Borth N, Tate CG, Betenbaugh MJ. High-throughput screening and selection of mammalian cells for enhanced protein production. *Biotechnol J.* 2016;11(7):853–865.
12. Chaturvedi K, Sun SY, O'Brien T, Liu YJ, Brooks JW. Comparison of the behavior of CHO cells during cultivation in 24-square deep well microplates and conventional shake flask systems. *Biotechnol Rep.* 2014;1-2:22–26.
13. Markert S, Joeris K. Establishment of a fully automated microtiter plate-based system for suspension cell culture and its application for enhanced process optimization. *Biotechnol Bioeng.* 2017;114(1):113–121.
14. Halldorsson S, Lucumi E, Gomez-Sjoberg R, Fleming RM. Advantages and challenges of microfluidic cell culture in polydimethylsiloxane devices. *Biosens Bioelectron.* 2015;63:218–231.
15. Sackmann EK, Fulton AL, Beebe DJ. The present and future role of microfluidics in biomedical research. *Nature*. 2014;507(7491):181–189.
16. Chiou PY, Ohta AT, Wu MC. Massively parallel manipulation of single cells and microparticles using optical images. *Nature*. 2005;436(7049):370–372.
17. Valley JK, Neale S, Hsu HY, Ohta AT, Jamshidi A, Wu MC. Parallel single-cell light-induced electroporation and dielectrophoretic manipulation. *Lab Chip*. 2009;9(12):1714–1720.
18. Hsu HY, Ohta AT, Chiou PY, Jamshidi A, Neale SL, Wu MC. Phototransistor-based optoelectronic tweezers for dynamic cell manipulation in cell culture media. *Lab Chip*. 2010;10(2):165–172.
19. Mocciaro A, Roth TL, Bennett HM, Soumillon M, Shah A, Hiatt J, Chapman K, Marson A, Lavieu G. Light-activated cell identification and sorting (LACIS) for selection of edited clones on a nanofluidic device. *Commun Biol*. 2018;1(1):41.

Manuscript received Jan. 26, 2018, revision received Jun. 26, 2018, accepted Jun. 27, 2018.

Exhibit 10

mAbs

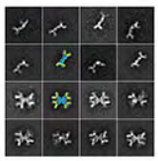

ISSN: 1942-0862 (Print) 1942-0870 (Online) Journal homepage: https://www.tandfonline.com/loi/kmab20

Rapid single B cell antibody discovery using nanopens and structured light

Aaron Winters, Karyn McFadden, John Bergen, Julius Landas, Kelly A. Berry, Anthony Gonzalez, Hossein Salimi-Moosavi, Christopher M. Murawsky, Philip Tagari & Chadwick T. King

To cite this article: Aaron Winters, Karyn McFadden, John Bergen, Julius Landas, Kelly A. Berry, Anthony Gonzalez, Hossein Salimi-Moosavi, Christopher M. Murawsky, Philip Tagari & Chadwick T. King (2019) Rapid single B cell antibody discovery using nanopens and structured light, mAbs, 11:6, 1025-1035, DOI: 10.1080/19420862.2019.1624126

To link to this article: https://doi.org/10.1080/19420862.2019.1624126

Published online: 11 Jun 2019.

MABS
2019, VOL. 11, NO. 6, 1025–1035
https://doi.org/10.1080/19420862.2019.1624126

Taylor & Francis
Taylor & Francis Group

REPORTS

OPEN ACCESS Check for updates

Rapid single B cell antibody discovery using nanopens and structured light

Aaron Winters[a], Karyn McFadden[a], John Bergen[b], Julius Landas[b,c], Kelly A. Berry[b], Anthony Gonzalez[a], Hossein Salimi-Moosavi[a,c], Christopher M. Murawsky[b], Philip Tagari[a], and Chadwick T. King[b]

[a]Department of Therapeutic Discovery, Amgen Research, Thousand Oaks, CA, USA; [b]Department of Therapeutic Discovery, Amgen Research, Burnaby, Canada; [c]Department of Pharmacokinetics & Drug Metabolism, University of British Columbia, Vancouver, Canada

ABSTRACT

Accelerated development of monoclonal antibody (mAb) tool reagents is an essential requirement for the successful advancement of therapeutic antibodies in today's fast-paced and competitive drug development marketplace. Here, we describe a direct, flexible, and rapid nanofluidic optoelectronic single B lymphocyte antibody screening technique (NanOBlast) applied to the generation of anti-idiotypic reagent antibodies. Selectively enriched, antigen-experienced murine antibody secreting cells (ASCs) were harvested from spleen and lymph nodes. Subsequently, secreted mAbs from individually isolated, single ASCs were screened directly using a novel, integrated, high-content culture, and assay platform capable of manipulating living cells within microfluidic chip nanopens using structured light. Single-cell polymerase chain reaction–based molecular recovery on select anti-idiotypic ASCs followed by recombinant IgG expression and enzyme-linked immunosorbent assay (ELISA) characterization resulted in the recovery and identification of a diverse and high-affinity panel of anti-idiotypic reagent mAbs. Combinatorial ELISA screening identified both capture and detection mAbs, and enabled the development of a sensitive and highly specific ligand binding assay capable of quantifying free therapeutic IgG molecules directly from human patient serum, thereby facilitating important drug development decision-making. The ASC import, screening, and export discovery workflow on the chip was completed within 5 h, while the overall discovery workflow from immunization to recombinantly expressed IgG was completed in under 60 days.

ARTICLE HISTORY
Received 8 February 2019
Revised 2 May 2019
Accepted 22 May 2019

KEYWORDS
Monoclonal antibody; antibody generation; structured light; antibody discovery; NanOBlast; nanofluidics; ASC; ELISA; OptoElectro Positioning; OEP

Introduction

The annual number of antibody-based therapeutics to receive approval in either the European Union or the United States reached double digits for the first time in 2017.[1] Moving such therapeutics from early discovery through clinical trials and eventually into the marketplace requires the development and validation of numerous analytical methodologies.[2,3] Ligand binding assays (LBAs) are analytical tools frequently used for pharmacokinetics (PK), pharmacodynamics (PD), and toxicokinetics studies due to their sensitivity, specificity, reproducibility, and relatively simple execution.[4–6] LBAs constructed with high-affinity, neutralizing, and paired capture/detection monoclonal antibody (mAb) reagents are particularly useful for correlating the levels of free-drug with efficacy of the therapeutic candidate.[3,6–8] Anti-idiotype LBAs offer significant advantages over generic anti-Fc or anti–light chain, polyclonal antibody–based assays owing to comparatively less nonrelevant human IgG constant region binding when directly testing human serum samples containing endogenous serum IgG.[8]

Tool antibodies for use in LBAs are most frequently derived from in vivo immunization followed by either immortalization as hybridomas[9,10] or as immune cell libraries for display technologies such as phage or yeast.[11] Despite these methodologies being important and reliable discovery engines, they have notable process limitations. Hybridomas require immortalization of antibody-secreting cells (ASCs) via somatic fusion to a myeloma cell line. Even with optimized electrofusion protocols, only 1 of 5000 input B cells survives fusion, becomes immortalized, and secretes antibody.[12] Additionally, hybridoma methods generally require extensive cell culture, which is labor intensive and dependent on mitosis, further slowing development timelines. Display technologies, which start from antigen-experienced IgG messenger RNA (mRNA) pools, suffer primarily from the loss of the cognate VH and VL pairing of the input repertoire.[11,13,14] This can result in the identification of low-affinity antibodies, and usually necessitates multiple rounds of time-consuming affinity maturation to generate potent molecules.[15] Finally, hybridoma and display technologies both require substantial laboratory space, aseptic and benchtop liquid handling automation, and multiple trained operators to perform antibody discovery campaigns at commercial scales.

Recently, several approaches that effectively used "micro tools" for direct B cell antibody discovery have been described.[16–18] Custom microfluidic chambers,[19] microencapsulation,[20,21] custom microwell devices,[22–24] and microcapillary tubes[25] have all been used to discover mAbs, although with variable success. These methods all allow the direct isolation and screening of ASCs as single cells, thereby

CONTACT Aaron Winters awinters@amgen.com Amgen Research, One Amgen Center Drive, Thousand Oaks, CA 91320, USA

This article has been republished with minor changes. These changes do not impact the academic content of the article.

allowing some phenotypic characterization of the encoded antibody without B cell immortalization or library generation. Recovery of the desired sequences is generally accomplished using single cell polymerase chain reaction (PCR)[26] or, in some cases, barcode-based next-generation sequencing followed by recombinant cloning and expression en masse.[27] These micro tools eliminate the need for immortalization, are species-agnostic, allow high throughput sampling as well as multiparameter phenotyping of the input cells, have reduced reagent consumption compared to hybridoma and display technologies, and maintain the ability to retain the native VH and VL pairings of the original antibody. Despite their many advantages, the aforementioned micro-tool techniques are not widely commercially available; lack the ability to execute back-to-back iterative screens; cannot keep the cells, and therefore the antibody mRNA, viable for extended periods of time; and require an operator to physically pick the individual B cells of interest in subsequent molecular recovery.

Here, we present a nanofluidic optoelectronic B lymphocyte antibody screening technique (NanOBlast) built around Beacon™, a commercially available (Berkeley Lights), integrated culture and imaging platform. Beacon™ leverages a novel, disposable, microfluidic culturing chip (OptoSelect™ OS3500) containing 3513 one nanoliter pens (hereinafter, nanopens) fabricated out of polydimethylsiloxane. The platform allows two-dimentional manipulation of living cells based on the principle of light-induced dieletrophoresis, a process known as OptoElectro Positioning (OEP).[28–30] OEP enables nondestructive maneuvering of individual ASCs into and out of the individual nanopens. Precision microfluidics enables ASC import to and export from the chip; five-color, single-pass fluorescent filter cubes allow multiplexed screening. Beacon has been successfully used for single-cell phenotype and genotype characterization of ovarian cancer patient-derived tumor cells,[31] identification of CRISPR-Cas9–edited primary T cells[32] and for clonal selection of highly productive Chinese hamster ovary (CHO) cell lines.[33] However, to our knowledge, there are no reports of applying the Beacon platform directly for antibody discovery from primary murine ASCs. Therefore, we report here a proof-of-concept experiment of the NanOBlast technique.

Results

Overview of the NanoBlast workflow on Beacon

The fundamental design and features of the Beacon platform, its culturing chip, and OEP technology have been previously described.[32,33] We describe the NanOBlast technique briefly here.

The NanOBlast workflow begins with generating antigen-specific ASCs via in vivo immunization (Figure 1a). ASCs are microfluidically imported into the chip and sequestered into individual nanopens for screening via gravity or OEP. ASCs that secrete antigen-specific IgG are detected using a bead-

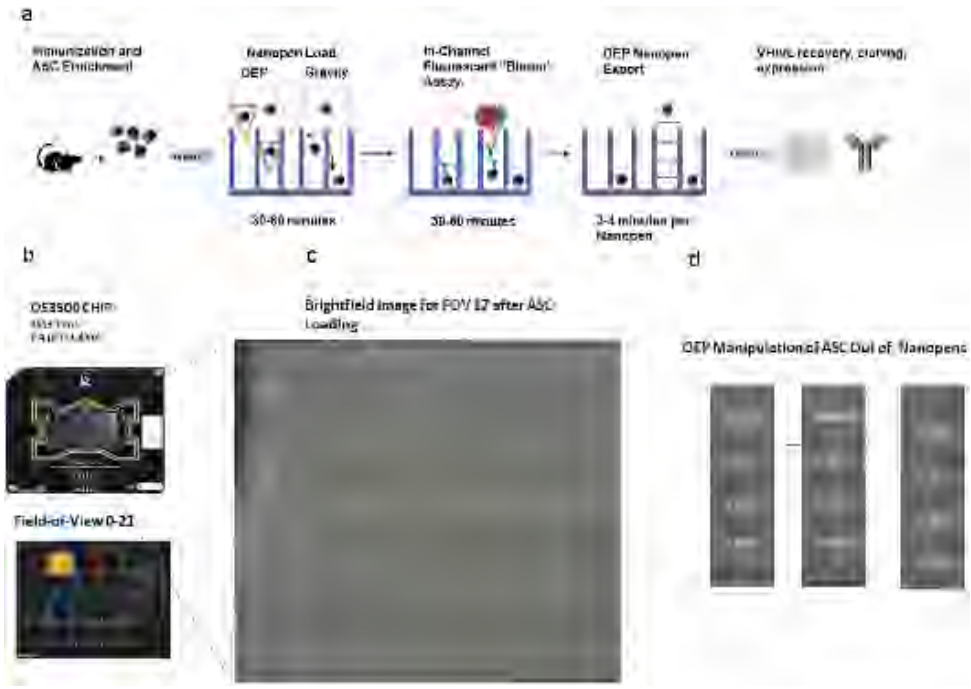

Figure 1. NanOBlast workflow overview. (a). Antigen-experienced immune cells were harvested from wild type mice and enriched using a combination of magnetic negative selection and/or multiparameter FACS sorting. ASCs are loaded into the nanopens of an OptoSelect OS3500 culturing chip via OEP or by inverting the chip and allowing gravity to pull the ASCs downward from the channel into the nanopen. Nanopens are screened for both IgG secretion and antigen specificity using an in-channel multiplex bead-based assay. Immediately after screening, the beads are flushed to waste and the ASC in the selected nanopens is manipulated out of the nanopen using OEP and exported directly into 96-well plates containing lysis buffer using the onboard fluidic system. Single-cell reverse transcriptase (RT) PCR, a modified 5′ RACE amplicon generation step for VH and VL sequence recovery, Golden Gate cloning and recombinant expression using human embryonic kidney 293T cells generate material for binding characterization studies. (b). OS3500 chip from Berkeley Lights containing 3513 polydimethylsiloxane nanopens. The optical train on the Beacon platform subdivides the imaging of the chip into 21 specific FOV. (c). FOV 17 brightfield image showing ASCs sequestered in nanopens after loading overlaid with results of the on-board cell counting algorithm. (d). OEP manipulation of a single ASC out of a nanopen into the channel space of the chip in preparation for export.

based, two-color fluorescent binding assay that produces a characteristic fluorescent bloom. Individual cells of interest are then un-penned using OEP and exported from the chip directly into 96-well plates containing cell lysis buffer. Antibody VH and VL sequences are recovered using single-cell rapid amplification of cDNA ends (RACE), cloned and recombinantly expressed as canonical antibodies using standard methods. The recombinant antibodies are used for binding confirmation and eventual validation in relevant downstream assays. Figure 1b displays the chip and corresponding field of view (FOV) map, Figure 1c is a brightfield image of FOV 17 after loading with ASCs, and Figure 1d demonstrates three sequential images of a single well undergoing OEP export of an individual ASC.

To demonstrate the utility of our NanOBlast antibody discovery workflow, we sought to discover reagent antibodies suitable for bioanalytical assay development in support of therapeutic IgG clinical candidates.

NanoBlast technique proof-of-concept study

Anti-therapeutic IgG ASC enrichment and OptoSelect chip loading

We generated immune animals by challenging CD-1® mice with antigen (i.e., the therapeutic IgG clinical candidate) twice per week over the course of 31 days. We identified animals displaying suitable antigen-specific serum titers using enzyme-linked immunosorbent assay (ELISA). Spleens and lymph nodes (popliteal, inguinal, mesenteric, and brachial) were harvested from the two mice with the highest antigen titer level and processed into single-cell suspensions. ASCs were enriched by a combination of magnetic depletion to remove non-B and surface IgM-expressing B cells and fluorescence-activated cell sorting (FACS) specifically on a B220lo, CD138hi gated population (data not shown). The loss of the B cell marker B220 (also known as CD45R) combined with the high expression of CD138 (Syndecan-1) has traditionally been used to broadly define the antibody-secreting cell population.[34] Enriched ASCs were cultured overnight and imported into an OptoSelect microfluidic chip at a density of 500 cells per microliter. To facilitate expedited screening and minimize the duration cells remained on-chip, the ASCs were penned into individual nanopens using gravity deposition. The chip was then reloaded onto the Beacon platform and imaged to enumerate the overall penning efficiency and the number of cells isolated in each nanopen. In this experiment, 952 cells were isolated into 750 of the available 3513 nanopens (21.3%). Of the 750 loaded nanopens, 615 contained single cells (82%) and 135 contained two or more cells (18%). The penned ASCs were cultured for an additional 75 min by perfusing media through the microfluidic channels before running subsequent anti-idiotypic selective screening assays.

On-chip anti-idiotypic ASC screening

A multiplex, indirect, bead-based competition screening strategy was developed to allow detection of both murine IgG secretion and specific binding reactivity against only the complementarity-determining regions of the human IgG antigen (Figure 2a). A mixture of anti-murine IgG Fc-specific capture beads, an Alexa Fluor 568–conjugated secondary antibody to the murine IgG H + L, and the target antigen linked to Alexa Fluor (AF) 647–conjugated streptavidin was loaded onto the chip in the presence of 10% human serum. Human serum was included to simulate the

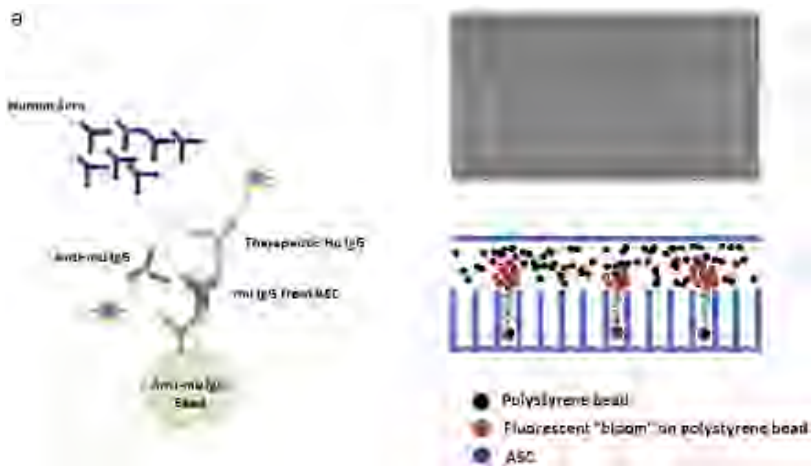

Figure 2. NanOBlast on-chip screening. (a). Cartoon schematic and representative brightfield image of the channel and nanopen space depicting the homogenous bead-based assay design for detection of IgG secretion and antigen specificity in the channel of the OS3500 chip. 3.2-micron polystyrene beads precoated with goat anti-murine IgG, Fc-specific polyclonal antibodies were mixed with AF 568–labelled, goat, anti-murine IgG H+L–specific, polyclonal antibodies; biotin-labelled therapeutic human IgG; streptavidin AF 647; and 10% human serum were imported into the channel space of the chip via onboard fluidics. (b). 45-min (final in the assay series) images of all 21 FOV stitched together depicting the blooms generated for the IgG secretion AF 568 signal as captured in the TRED filter cube of the Beacon. Magnification view of 60 individual nanopens on the chip demonstrating fluorescent bloom formation at the mouth of the nanopen. Time course of bloom formation for nanopen 928 (clone 1A3) demonstrating the change in intensity and size over the duration of the screen. (c). 45-min (final in the assay series) images of all 21 FOV stitched together depicting the blooms generated for the antigen-specific secretion AF 647 signal as captured in the Cy5 filter cube of the Beacon. Magnification view of 60 individual nanopens on the chip demonstrating fluorescent "bloom" formation at the mouth of the nanopen. Time course of bloom formation for nanopen 928 (clone 1A3) demonstrating the change in intensity and size over the duration of the screen. (d). 45-min timepoint images for antigen specificity and IgG secretion of the 13 nanopens from recovered mouse IgGs after constraining the panel to only single exported ASCs.

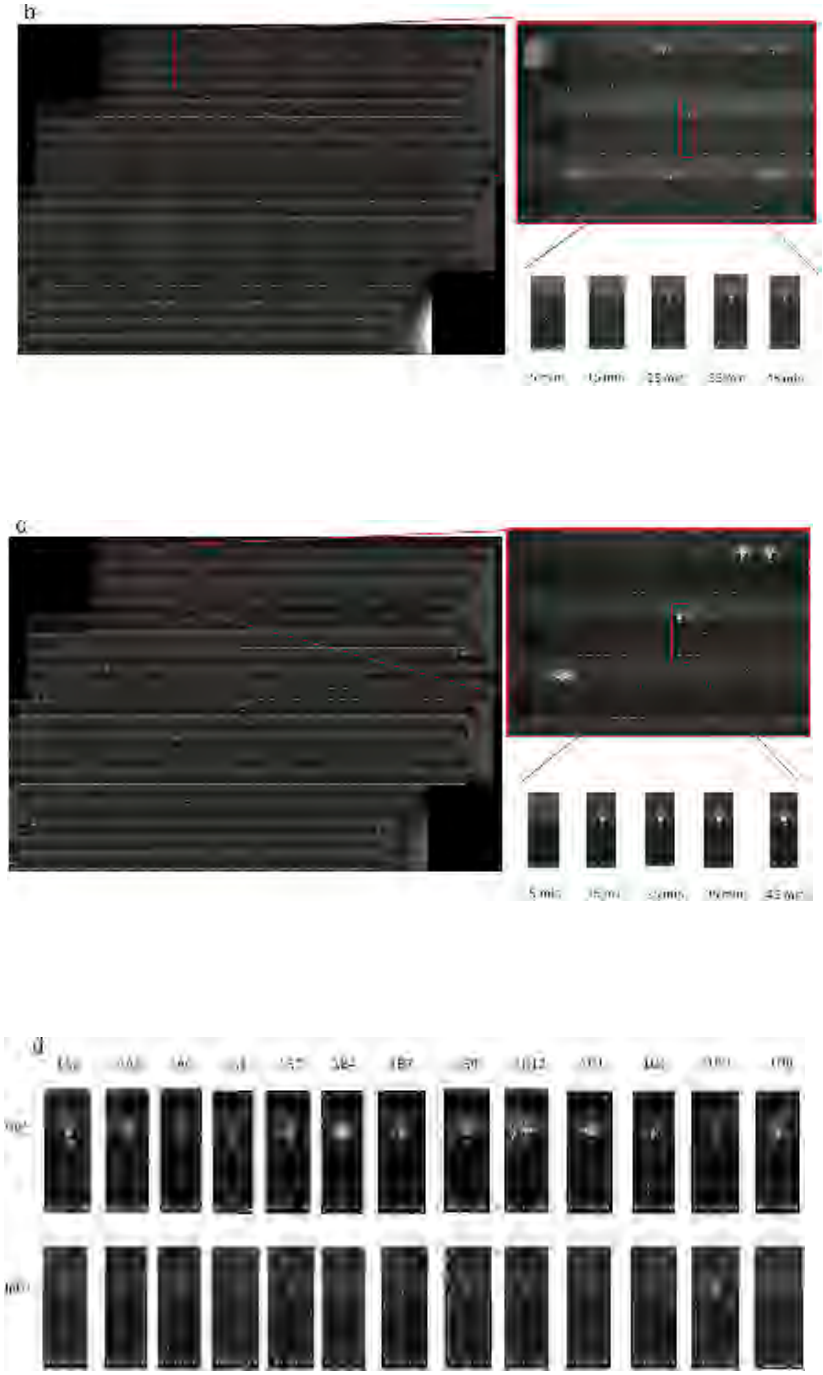

Figure 2. Continued.

complex matrix that will be present in the final LBA, and to ensure that the binding of any mouse antibodies reactive against the constant regions of the therapeutic human IgG would not interfere with the detection of true anti-idiotype antibodies. To identify ASCs producing anti-idiotype antibodies, we imaged each of the 22 FOVs of the chip in both the Cy5 (AF 647) and the TRED (AF 568) fluorophore channels every 5 min over a total duration of 45 min. There were 396 individual images 198 per fluorophore channel) collected over the course of the 45-min assay. Both the TRED and the Cy5 channel images were analyzed using onboard image detection software algorithms and manually verified for the presence of a characteristic fluorescent "bloom" that forms at the mouth of the nanopen (TRED Figure 2b, Cy5 Figure 2c). The presence of anti-idiotypic murine IgG was detected in some nanopens at 5 min, the earliest time point measured (Figure 2c). When the complete chip was analyzed, 201 individual murine IgG-secreting blooms were identified (21% of the total cells penned, Table 1). Importantly, 51 of the IgG-secreting nanopens also displayed reactivity to the therapeutic human antibody (Table 1). Thus, 25% of total IgG-secreting nanopens harbored antibodies that were specific for the antigen and were likely to be therapeutic antibody idiotype–reactive.

Table 1. IgG vs Antigen-specific ASC results per OS3500 Field of View.

Field of View (FOV)	Number of Pens	IgG secreting (AF 568 bloom)	Antigen binding (AF 647 bloom)
0	172	17	5
1	200	9	2
2	200	2	1
3	180	4	2
4	90	8	3
5	192	11	2
6	200	10	3
7	196	13	2
8	200	8	1
9	155	5	1
10	83	2	0
11	160	12	5
12	200	14	2
13	200	11	3
14	200	13	4
15	145	2	2
16	73	12	1
17	151	19	7
18	160	9	1
19	160	6	2
20	132	10	1
21	64	4	1
All	3513	201	51

VH and VL recovery, cloning, and recombinantexpression

To recover the potential anti-idiotype antibodies identified using NanOBlast, the individual cells located within 44 of the 51 antigen-specific nanopens were unpenned using OEP and exported directly into a 96-well plate containing cell lysis buffer. The antigen-specific ASCs in the remaining seven nanopens were not exported because the bloom intensity of the antigen-specific signal, although detectable, was relatively weak compared to other nanopens (data not shown). To confirm successful export, brightfield image analysis of the channel space immediately after unpenning, but directly before export, was performed (data not shown). Figure 2d displays IgG secretion and antigen-specific bloom images for 13 representative nanopens visually confirmed to contain single ASCs.

A total of 30 paired VH and VL sequences from the 44 exported ASCs were successfully recovered. We constrained our analysis, and subsequent efforts, to focus only on nanopens containing single cells to eliminate the recovery of noncognate VH and VL pairs caused by multiple ASCs within a single nanopen. Comparison of the recovered sequences indicated 13 unique antibody sequences that arose from at least 10 different V-(D)-J recombination events (Figure 3a; Table 2).

Characterization of rescued antibodies and selection of tool reagents for the therapeutic bioanalytical method

The 13 recovered sequences were cloned into an expression vector using a murine IgG2a isotype, transiently transfected into human embryonic kidney 293T cells and the antibody-containing, conditioned media was harvested 5 days later. The supernatants were quantified and displayed a range of concentrations (2.3–117 µg/ml (Table 1)), typical of murine IgGs.[26]

Normalized antibody samples were assayed for antigen-specific binding using an IgG-capture ELISA, like that used in the on-chip, bead-based NanOBlast strategy (Figure 3b). To differentiate the antibodies based on their relative binding strength and to ensure the relative binding affinity was strong enough for downstream LBA development, the antigen concentration was titrated from 6.6 nM to 66 pM. Under these limited antigen conditions, all 13 recombinant IgGs bound antigen in a dose-responsive manner (Figure 3c).

To select antibodies appropriate for bioanalytical method development, the recombinant murine antibodies were purified and biotinylated. For this bioanalytical assay, a pair of unique and complementary anti-idiotype antibodies are required to enable simultaneous capture and detection of the fully human therapeutic in the presence of human IgG-containing serum. Iterative combinations of each of the NanOBlast-derived antibodies, as either capture or biotin-detection reagents, were assayed via sandwich ELISA (Figure 3d). Under these conditions, antibody 1A3 was observed to be the most appropriate capture reagent as it showed no serum matrix effects and permitted a highly sensitive LBA construction with the flexibility of using multiple detection antibodies. When paired with antibodies 1B4, 1B9, or 1C1, antigen capture via 1A3 enabled the construction of a specific LBA with a lower limit of quantitation below 1 ng/ml (Figure 3e), thereby establishing a robust LBA easily capable of quantifying the free therapeutic IgG levels expected in first-in-human clinical studies.

Discussion

Although the NanOBlast workflow described here shares some similarities with previously described single-cell ASC discovery methods,[13–22] it introduces an entirely novel nanofluidic culture and screening paradigm using the Beacon platform. To our knowledge, Beacon is the only tool that enables massively parallel, precise, digitally driven control over the import, culture, screening, analysis, and export of non-immortalized primary antigen-specific ASCs. The ability to rapidly sequester and culture single, primary ASCs in individual, software-tracked nanopens; screen the secreted antibodies for desired phenotypes; and digitally document the entire workflow enables unprecedented speed and utility for commercial antibody discovery.

While dependent on the immunogenicity of the antigen and the exact conditions of the immunization campaign, antigen-specific ASCs in wild-type hyperimmunized mice are typically present at frequencies <0.1% (Ref. 29, Amgen unpublished data). As such, enrichment of immune cells for relevant ASCs is necessary prior to initiate NanOBlast to efficiently use the 3513 nanopens of an OS3500 chip. Applying both magnetic negative selection and a multiparameter FACS sort to primary mouse lymphocytes enabled us to reduce the initial ~10^8 mixed population of cells to ~10^4 ASCs with the desired characteristics. The current NanOBlast workflow would not be possible using an unenriched population of lymphocytes due to the low frequency of ASCs amongst primary lymphocytes and the fixed number of nanopens on a chip (3513). Increasing the antigen-specific ASC enrichment effectiveness before chip loading is of obvious value in terms of efficiency and recoverable antibody panel size. Specific immunization and enrichment strategies will need to be developed for the particular in vivo model or antibody generation platform, as well as for the specific B cell compartment targeted. A successful strategy must balance ASC generation, enrichment (e.g., purity, yield) and cellular viability such that they can be manipulated and screened on Beacon.

Loading single cells into individual nanopens is a critical requirement of our NanOBlast workflow. A nanopen containing more than 1 ASC potentially complicates the interpretation

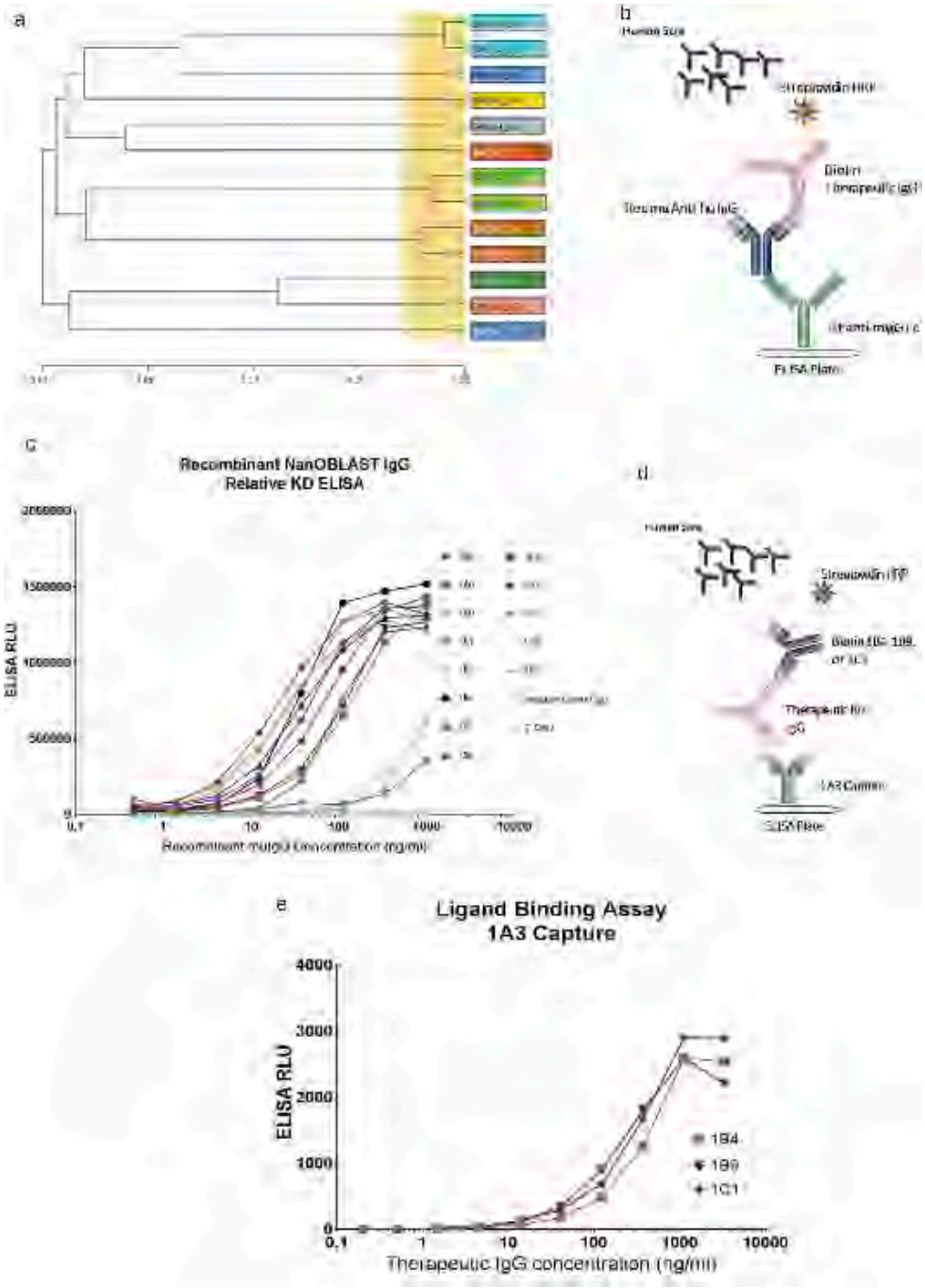

Figure 3. Recombinant Mouse IgG Characterization. (a). VH and VL V(D)J dendrogram illustrating the sequence diversity of the single-cell, recovered, antigen-specific clones. The yellow box indicates a chosen maximum distance between two antibodies to allow grouping and is based on a calculation of similarity equal to the number of mismatches divided by the sequence length. The tree length is on the x-axis and antibodies with a distance less than 0.1 from each other were grouped together resulting in 10 separate antibody clades. (b). Plate-based immunoassay design for verification of antigen specificity and relative affinity of the recombinantly expressed antitherapeutic murine IgGs. (c). Dose response, antigen-specific immunoassay binding curves using a limiting concentration of 66 pM of the therapeutic IgG. (d). Design of the completed LBA for evaluation of free therapeutic IgG in human serum. E. LBA with lower limit of quantification < 1ng/ml using 1A3 as the capture antibody on the plate and either 1B4, 1B9, or 1C1 as the detection antibody in a matrix of human serum.

of fluorescent blooms because the signal may be generated by more than one specific antibody. It can also confound the downstream analysis if noncognate pairs of VH and VL are combined for recombinant expression. The efficiency of loading single cells in the nanopens is directly related to the density of the ASCs imported into the channel of the chip and the percentage of clumped cells in the preparation. Software-driven OEP nanopen loading offers enhanced precision compared to gravity loading due to the image detection and targeting control that the Berkeley Lights Cell Analysis Suite (CAS) version 1.3 software provides. We have successfully performed this semi-automated loading strategy on ASCs harvested from wild-type mice, transgenic mice (e.g., XenoMouse®), and hybridomas (unpublished data). However, optimization of the exact voltage and frequency of the current applied to the chip, duration of application, and temperature of the chip are necessary to

Table 2. Anti-Idiotypic IgG Recovery and Expression.

Molecular Recovery of Antibody[a]						
Pen ID	Export plate well	VH germline	% Identify	VL germline	% Identify	Recombinant IgG μg/mL[b]
928	1A3	VK1|1–110*01/JK4|4*01	98.8	VH1|1–82*01/D2|2–11*01|RF1/JH3|3*01	94.3	16.6
2770	1A6	VK6|6–13*01/JK2|2*01	92.6	VH1|1–14*01/D4|4–1*02|RF3/JH4|4*01	98.9	4.7
1204	1A9	VK8|8–21*01/JK5|5*01	97.5	VH5|5–6*01/D4|4–1*02|RF3/JH2|2*01	95.4	2.3
3445	1B1	VK6|6–23*01/JK4|4*01	97.5	VH2|2–6-1*01/D4|4–1*02|RF1/JH4|4*01	95.4	117.1
1593	1B2	VK6|6–17*01/JK1|1*01	97.5	VH4|4–1*01/D4|4–1*01|RF3/JH2|2*01	96.6	37.4
60	1B4	VK5|5–43*01/JK4|4*01	96.3	VH9|9–3*01/D4|4–1*01|RF1/JH2|2*01	98.9	14.1
3011	1B7	VK4|4–68*01/JK5|5*01	98.8	VH1|1–14*01/D2|2–2*01|RF2/JH2|2*01	95.4	2.4
221	1B9	VK4|4–74*01/JK2|2*01	100.0	VH1|1–34*02/D4|4–1*02|RF3/JH4|4*01	95.4	5.1
517	1B12	VK4|4–91*01/JK2|2*01	97.5	VH2|2–9-1*01/D4|4–1*01|RF1/JH4|4*01	96.6	40.5
523	1C1	VK6|6–13*01/JK2|2*01	93.8	VH1|1–14*01/D4|4–1*02|RF3/JH4|4*01	98.9	43.9
3230	1C4	VK5|5–43*01/JK4|4*01	96.3	VH9|9–3*01/D4|4–1*01|RF1/JH2|2*01	93.1	12.5
2738	1C9	VK1|1–110*01/JK2|2*01	100.0	VH1|1–61*01/D4|4–1*01|RF3/JH3|3*01	93.1	4.6
1682	1D8	VK6|6–17*01/JK1|1*01	98.8	VH4|4–1*01/D4|4–1*01|RF3/JH2|2*01	96.6	40.4

[a]Germline analysis based on IMGT database. [b]Quantification of IgG in HEK293T supernatants determined by Forte Bio.

effectively use OEP manipulation without damaging fragile ASCs. The precise combination of optimal conditions will likely depend on the harvested B cell compartment, enrichment processing, and culture media formulations. Optimizing semi-automated OEP is the subject of continued experimentation in our lab. Moreover, primary murine ASCs frequently aggregate in ex vivo culture (data not shown), and we speculate that the use of deoxyribonuclease or other de-clumping reagents may encourage ASCs to remain as singlets during pre-chip processing. More homogenous single-cell suspensions will undoubtedly enable more efficient single-cell nanopen loading for both OEP and gravity methodologies.

The strategies underpinning our NanOBlast on-chip screening assays were threefold: 1) identify nanopens containing ASCs secreting antibodies of the IgG isotype, 2) multiplex the assays to reduce overall on-chip processing time, and 3) identify ASCs secreting anti-idiotypic (not framework-specific) antibodies by executing the bead-based assay in the presence of 10% human sera. By performing the assay in an excess of unlabeled human IgG along with the labeled target antigen, a competitive binding environment was established. Nanopens containing ASCs producing antibodies specific for common epitopes present on human antibodies (e.g., constant domains) were unable to bind to the target antigen and therefore could not form fluorescent immune complexes (i.e., blooms). This assay format allowed us to identify ASCs secreting antibodies that were likely to be anti-idiotypic toward our therapeutic IgG antigen.

Quantitative ranking of the binding of antibodies is frequently used to characterize candidate molecules and can be accomplished using ELISA, FACS, surface plasmon resonance systems (e.g., Biacore), and other methodologies.[7,8,11,15,26,35–40] As of early 2019, the Beacon software was unable to generate quantitative values for fluorescent blooms. Despite the high-content imaging capabilities, this limited the built-in analysis to a binary (yes/no) result. The bloom size, intensity and rate of change resulting from the accumulation of antibody/antigen complexes are likely governed by multiple factors, including assay design, IgG secretion rate, actual location of the ASC within the pen, and the binding kinetics (i.e., determination of association [k_{on}] and dissociation [k_{off}]) of the IgG molecule to its cognate antigen. This blend of variables (known and unknown), makes it challenging to determine the role that affinity of the ASC-derived IgG plays in bloom formation. While it is tempting to analyze the bloom images and extrapolate relative rankings of nanopens based on factors such as bloom intensity and size, we do not yet have data that validates this approach. The application of advanced machine learning algorithms, combined with training data sets of verified recombinant NanOBlast IgGs, may be necessary to confidently enable automated ranking on the Beacon™ platform.

Although the goal of this study was not to make direct quantitative comparisons to other antibody discovery methods, we can speculate how NanOBlast might compare to traditional hybridoma generation workflows, specifically in terms of total quantity and diversity of recovered antibody sequences. In 1989, Schmitt et. al described an optimized hybridoma electrofusion protocol capable of generating one hybridoma from 5000 input splenic lymphocytes.[12] Even if we assume that hybridoma process optimization over the last 30 years resulted in protocols with 50X greater hybridoma generation efficiency (e.g., one hybridoma for every 100 input ASCs), the 615 single ASCs identified here would have translated to only six IgG secreting hybridomas. Using data generated in this study (Table 1) as a guide, 25% of these recovered hybridomas would secrete antigen-specific antibodies, resulting in a total of 1–2 hybridomas available for further analysis. The 615 single-penned ASCs analyzed in our NanOBLast workflow represented less than 10% of the total ASCs recovered from our FACS-based enrichment process, yet we still recovered 13 unique antibody sequences representing 10 distinct clades. We feel confident that as we advance the NanOBLast workflow in terms of enrichment efficiency and screening scale, we will be able to sample increasingly larger portions of the immune repertoire of hyperimmunized animal models with an efficiency that is simply not possible with even the most highly optimized hybridoma generation methods.

Taken together, our data indicate that NanOBlast is a rapid and effective method for isolating, characterizing, and recombinantly producing antibodies in less than 60 days directly from antigen-experienced murine ASCs. Although indispensable for the successful development of protein therapeutics, our focus on identification of tool reagents from wild-type mice represents a jumping-off point for antibody discovery from in vivo-derived ASCs using this technique. Therapeutic antibody discovery leveraging transgenic mouse platforms, such as XenoMouse®,[41] would be of great value, as would

the direct characterization and recovery of human ASCs harvested from the peripheral blood of patients undergoing active disease. Indeed, the species-agnostic nature of NanOBlast opens the door to de novo antibody discovery from any species where antigen-experienced ASCs can be identified and enriched. Expanding the library of reliable, effective and high-content on-chip assays (e.g., receptor-ligand blocking, antibody competition, epitope binning, affinity assays) using the nanopen architecture and the five-color imaging capability of the Beacon platform will be a necessary next step to realizing the full potential of NanOBlast. In this regard, we have already made significant progress using antigen-expressing cells in place of the soluble antigen-bead system described here. This raises the possibility of more physiologically relevant screening scenarios for therapeutically interesting complex membrane targets, as well as functional, reporter-style, cell-dependent assays. Concurrent with expansion of the operational assay catalogue, ongoing platform and software improvements for the Beacon platform achieved by Berkeley Lights continue to increase tool functionality and quantitative ranking of nanopen assays. Moreover, we feel the overall workflow timeline can be executed even more rapidly. Successful VH and VL recovery and recombinant expression in 5–7 days have been demonstrated,[35,37,38] as have rapid immunization strategies.[42,43] Combining approaches such as these with the 1-day screening process of the NanOBlast method described here, complete antibody discovery workflows using antigen-experienced, affinity-matured ASCs could be executed in as little as 3–4 weeks. We anticipate that this novel methodology will ultimately advance the discovery of critically important tool and therapeutic antibodies, better enabling the treatment of human diseases.

Materials and methods

Antigen supply and immunization

A human IgG1 mAb clinical candidate that targets a cell membrane antigen was used as the antigen in this study. This mAb was generated by gene synthesis and recombinant expression in CHO host cells. It was recovered from the clarified CHO cell condition media using a three-step process including 1) affinity capture using MabSelect SuRe (GE Healthcare Life Sciences), 2) purification on an SP HP column (GE Healthcare Life Sciences), and 3) dialysis into sodium acetate buffer (A52Su: 10 mM acetic acid, 9% sucrose, pH 5.2) for long-term stability.

Mice were housed in groups at an Association for Assessment and Accreditation of Laboratory Animal Care International–accredited facility. Animals were cared for in accordance with the *Guide for the Care and Use of Laboratory Animals*, 8th Edition. All research protocols were reviewed and approved by the Amgen Institutional Animal Care and Use Committee. Ten CD-1 mice (Charles River Laboratories) were immunized with antigen a total of 10 times over 31 days. Boost 1 consisted of 5 µg of antigen emulsified in 100 µL Complete Freund's Adjuvant (Sigma Aldrich) delivered to four spots subcutaneously. Boosts 2–10 were delivered every 3 to 4 days and consisted of 5 µg antigen emulsified into 300 µL Sigma Adjuvant System (Sigma Aldrich) delivered subcutaneously to six spots alternately each time between dorsal and ventral sides of the mouse. Submandibular check bleeds of 150 µL were taken on day 25 for serum titer analysis. Mice 8, 9, and 10 were boosted intraperitoneally on day 27 with 50 µg of the human IgG antigen resuspended in Dulbecco's phosphate-buffered saline (PBS) (Gibco Life Sciences). On day 31, mice 8 and 9 were euthanized, and spleens and LNs harvested for B cell processing. The remaining eight mice not harvested were euthanized immediately after the development of the LBA was validated.

Immunogen biochemical conjugation

Biotinylated forms of the therapeutic IgG were generated by buffer-exchanging the human IgG into PBS using Zeba columns (Thermo Fisher Scientific), and then adding a 10-fold molar excess of NHS-PEG-Biotin (Thermo Fisher Scientific) to the antigen. After 60 min incubation at RT, excess biotin was removed again using a Zeba column and the concentration confirmed via A280. The horseradish peroxidase (HRP) form of the antigen was generated by adding a 10-fold molar excess of SAT-PEO4 (Thermo Fisher Scientific) to the antigen in Dulbecco's PBS and incubating for 60 min at room temperature. 50 mM hydroxylamine-HCl was added to the preparation and incubated for 90 min again at room temperature. Excess hydroxylamine-HCL and SAT-POE4 were removed using Zeba column. A 4-fold molar excess of maleimide-activated HRP (Thermo Fisher Scientific) was added to the preperation and incubated for 60min at RT. The excess unreacted malemide HRP was not removed and the final concentration of the conjugate was estimated assuming 90% recovery of the starting concentration of human IgG.

ELISA serum characterization

384-well plates were coated with 2 µg/mL of a fibrinogen-streptavidin dextran conjugate in PBS overnight at 4°C. Plates were washed with PBS plus 0.05% Tween20 (Sigma) and blocked with 50 µL per well of Superblock (Thermo Fisher Scientific). 20µL per well of a mixture of 250 ng/mL each of biotin- and HRP-conjugated therapeutic antibody diluted in Superblock buffer containing 20% human serum (Calbiochem) was added to each well. 20 µL per well of serially diluted murine antiserum was then added to the plate and incubated overnight. The following morning, plates were washed 4 times and 25 µL per well of Femto substrate (Thermo Fisher Scientific) was added to each well. The plate was read on a Spectramax M5 (Molecular Devices) reader using 25 ms integration time.

ASC harvest and enrichment

Selected mice were boosted by injecting 150 µL PBS (Gibco) containing 50 µg of therapeutic IgG antigen intraperitoneally. Four days after boost, spleen and mesenteric, popliteal, inguinal, and brachial lymph nodes were harvested from each animal. The spleen and lymph nodes were then processed into a single cell suspension using a GentleMACS cell dissociator (Miltenyi Biotech). The cell suspension was washed twice in PBS plus 2% fetal bovine serum (FBS) before red blood cell lysis with 8.3 g/L ammonium chloride in 10 mM

trisaminomethane-HCL, pH 7.2 for 5 min at room temperature. Non-B cells and IgM-expressing B cells were removed using an EasySep Mouse Pan B Isolation kit (StemCell) following the manufacturer's protocol with a slight modification. Briefly, a biotinylated rat anti-IgM mAb (Amgen) was added to the Pan B isolation antibody cocktail mixture step at a final concentration of 5 μg/mL. The isolated B cells were then counted and stained for sorting. The B cells were blocked with Mouse BD Fc Block™ purified anti-mouse CD16/CD32 mAb 2.4G2 (BD Bioscience) for 5 min at 4°C. The cells were incubated with APC-H7 Rat Anti-Mouse B220 (clone RA3-6B2, BD Bioscience) and PE Rat Anti-Mouse CD138 (clone 281–2, BD Bioscience) for 30 min at 4°C. The samples were washed with PBS plus 2% FBS twice and incubated with 7AAD (BD Bioscience) for 10 min on ice. All antibodies were used at a final concentration of 1 μg of antibody per 1 million cells. The B220low, CD138Hi population was sorted on a BD FACS Melody (BD Bioscience) using the manufacturer's recommended settings. The sorted cells were incubated in a 37°C incubator with 5% CO_2 until needed.

Beacon ASC import, assay, and export

OptoSelect 3500 chip was loaded onto Beacon, and the wet chip Python script was executed using the one-step priming reagent (Berkeley Lights Inc.) and 0.1% Pluronic F127 rinse (Invitrogen). The fluidics were primed with cell culture media consisting of Iscove's Modified Dulbecco's Media basal media (Gibco Life Technologies), 15% low IgG FBS (Gibco), 10mM HEPES (Gibco), one part NEAA (Gibco), 55uM 2-mercaptoethanol (Gibco), one part Penicillin-Streptomycin-Glutamine (Thermo Fisher Scientific), and a proprietary blend of additional supplements designed to enhance ex-vivo ASC survival.

Enriched ASCs were imported using the small volume import script with 0μL leading volume, 6 μL package volume, and 10μL lagging volume. Cells were cultured at 36°C during the duration on the chip. The antigen-screening mixture consisted of 900 μL of growth media, 100μL of human serum, 1 μL of goat anti-mouse IgG H + L AF 568 (Invitrogen), 1μg/mL of biotinylated therapeutic IgG, and 500 ng/mL of Streptavidin AF 647 (Invitrogen). 300μL of 3.2 μM polystyrene beads coated with a goat polyclonal antibody specific to the Fc regions of mouse IgG (Spherotech #MPFc-30–5) were rinsed 1 time in PBS and resuspended in 30μL of the antigen screening mixture. The beads were resuspended and 20 μL of the mixture was imported directly into the chip at 1 μL/sec using the manual Nest pump functions of CAS.

The screening assay was initiated using the multiplex assay script on the CAS using channel priority with image capture iterations every 5 min for a total of 10 iterations. The Texas Red channel for the AF 568 fluorophore was set to 1500 ms exposure time, and the CY5 channel for the AF 647 fluorophore was set to 2000 ms. The freeze valve was turned on during the entire length of the assay. Immediately following assay completion, the chip was flushed 3 times with culture media to remove beads from the fluid path. Fluidic lines were flushed further by removing the OS3500 chip from the nest, pumping 10 cycles of deionized water through the lines of Beacon, reloading a flush chip and priming the lines once again with culture media 4 times. The OS3500 chip containing the ASCs was reloaded on the nest, recalibrated in the CAS and flushed another 3 times with culture media in preparation for export. A 96-well forensic grade PCR plate (Eppendorf) was prepared to receive nanopen exports by adding 5 μL of TCL buffer (Qiagen) supplemented with 5 mM dithiothreitol (Thermo Fisher Scientific) to each well. 15 μL of mineral oil (Sigma) was finally added to the top of each well, and the entire plate was centrifuged for 1 min at 600 g. The plate was loaded in the incubator WP1 of Beacon, and the small volume PCR export script was executed using manually imported nanopen IDs. OEP was set to 4.2v and 1200kHz, the temperature of the chip was reduced to 18°C and 5 μL of total volume containing the nanopen contents was exported using the automated script. The plate was immediately frozen at −80c after all exports were completed.

Molecular recovery

RNA purification and reverse transcriptase (RT) PCR were performed using a modified protocol provided by Berkeley Lights Inc. RNA was purified using AMPure RNA Clean XP kit and eluted directly into a 9 μL RT reaction with Maxima RNaseH minus RT. A dT primer with adaptor (P1) and a 5′ template switching primer (P2) was used in the RT reaction. The RT reaction was incubated at 42°C for 90 min, followed by 10 cycles of 50°C for 2 min followed by 42°C for 2 min, then heat-inactivated at 75°C for 15 min and left at 4°C until the next step. The 9 μL RT reaction product was added to a PCR mix using KAPA HiFi HotStart Readymix with primer P3 in a reaction, amplifying the complementary DNA (cDNA) in 30 μL total. The cDNA amplification was performed at 98°C for 3 min, followed by 20 cycles of 98°C for 15 s, 65°C for 30 s, 72°C for 6 min, with a final incubation at 72°C for 10 min, and left at 4°C until the next step. A 1 μL portion of the cDNA amplification product was used to amplify the gamma and kappa chains in separate 15 μL reactions with primers in the antibody constant regions (MoG_AS and MoK_AS) and P4 to obtain the specific product for sequencing. PCR conditions were 98°C for 3 min, followed by five cycles of 98°C for 20 s – 65°C for 45 s – 72°C for 45 s, 10 cycles of 98°C for 20 s – 60°C for 45 s – 72°C for 45 s, 10 cycles of 98°C for 20 s – 58°C for 45 s – 72°C for 45 s and final extension of 5 min at 72°C. The specific PCR products were sequenced at Genewiz with the corresponding antibody constant region primers (MoG or MoK). Sequence analysis was performed using in-house software and aligned to the international ImMunoGeneTics information system® (http://www.imgt.org) database for germline determination.

Cloning and recombinant antibody expression

Sequences from the unique variable regions were synthesized with adaptors for cloning at Integrated DNA. Cloning was performed using BsmBI restriction sites into in-house vectors for expression. Transfection into human embryonic kidney 293T cells (CRL-3216,™ ATCC) was performed using 293Fectin according to manufacturer's protocols, modified to include 1 μL of 293Fectin per 1 μg of DNA in total precomplex volume of 100 μL. Supernatants were harvested

5 days after transfection and quantified via Forte Bio Octet (Molecular Devices) using anti-moFv AMQ sensors and a murine IgG2a isotype standard curve.

Relative affinity ELISA of recombinant anti-idiotypic IgGs

384-well plates were coated with 2 µg/mL of goat anti-murine IgG,-Fc specific polyclonal antibody (Thermo Fisher Scientific Cat # 31170) in PBS overnight at 4°C. Plates were washed with PBS plus 0.05% Tween20 (Sigma) and blocked with 50 µL per well of Superblock (Thermo Fisher Scientific). 20 µL per well of serially diluted recombinant antitherapeutic IgGs were added to the plates and incubated for 60 min at room temperature. Plates were washed 2 times and 20 µL per well of a 10 ng/mL solution of HRP labelled therapeutic IgG suspended in 20% human serum (Calbiochem) and Superblock (Thermo Fisher Scientific) was added to the plate. After a 60-min incubation, plates were washed 4X and 25 µL/well of Femto substrate (Thermo Fisher Scientific) was added to each well. The plate was read on a Spectramax M5 (Molecular Devices) reader using 25 ms integration time.

Bioanalytical LBA screening

The anti-IgG therapeutic antibodies were purified by protein G affinity purification (GE Healthcare) from 50 mL conditioned media and eluted by 0.5 M acetic acid, and then neutralized immediately with 2 M phosphate buffer with pH of 8.2. The concentration of the antibodies was measured by spectrophotometer at 280 nm.

The purified antibodies were screened in combinatorial approach as previously described.[8] Briefly, an ELISA plate (Corning 3690) was coated with antitherapeutic antibodies at 1 µg/mL in one part PBS and incubated overnight at 4°C. The ELISA plates were washed and blocked with I-Block™ (Applied Biosystems) buffer (one part PBS plus 0.2% I-Block and 0.05% Tween20) for 1 h at room temperature before use. Standards were prepared by spiking the therapeutic antibody into 100% serum from different species (mouse, rat, cynomolgus monkey, and human). The prepared standards samples were then diluted 1:10 (or 1:4 for high sensitivity assay) in the assay buffer (I-Block with 5% BSA). Then, 50 µL of diluted standards samples were loaded into each well of the ELISA plate coated with antitherapeutic antibodies and allowed to incubate for 1.5 h at room temperature. After a wash step, 50 µl of biotin conjugated of antitherapeutic antibodies at a concentration of 100 ng/mL in the assay buffer was added to each well of the plate and incubated for 1.5 hr. After a wash step, 50 µl of streptavidin conjugated to horseradish peroxidase at 200 ng/mL in the assay buffer was added to each well of the plate and incubated for 15 min. After a final wash step, a tetramethylbenzidine peroxidase substrate solution (KPL Inc) was added to each well and absorbance of the developed color was measured by kinetic read at 650 nm by a colorimetric plate reader SpectraMax (Molecular Devices).

Acknowledgments

The authors wish to thank Keith Breinlinger, Tanner Neville, Dina Sirypangno, Phillip Jess, Hariharasudhan Chirra Dinakar, Daniel Yang, Goeffrey Hess, Adriene Higa, Ravi Ramenani, Hayley Bennett, Minha Park, John Tenney and the rest of the Berkeley Lights Inc team for their consistent collaborative support with the Beacon system operation and development. We would like to thank the Amgen SPARC organization for their execution of the in-vivo protocols as well as the Pre-Pivotal DS, Hybrid Modalities and Biologics Optimizations organizations for their collaborative discussions on commercial implementation of the Beacon technology. Tim Peoples of Amgen provided editorial assistance.

Disclosures

A.W., K.M., J.B., K.A.B, A.G., H.S.-M., C.M.M., P.T., and C.T.G. are employees and stockholders of Amgen Inc. J.L. is a former employee of Amgen Inc.

Funding

This work was supported by Amgen Inc. [NA].

ORCID

Karyn McFadden http://orcid.org/0000-0002-7972-9122
Julius Landas http://orcid.org/0000-0001-9381-5951
Anthony Gonzalez http://orcid.org/0000-0003-2452-539X
Christopher M. Murawsky http://orcid.org/0000-0002-9698-052X

References

1. Kaplon H, Reichert JM. Antibodies to watch in 2018. MAbs. 2018;10:183–203.
2. Lagasse HA, Alexaki A, Simhadri VL, Katagiri NH, Jankowski W, Sauna ZE, Kimchi-Sarfaty C. Recent advances in (therapeutic protein) drug development. F1000Res. 2017;6:113.
3. Lee JW, Salimi-Moosavi H. Bioanalysis of target biomarker and pk/pd relevancy during the development of biotherapeutics. Bioanalysis. 2012;4:2513–23.
4. DeSilva B, Smith W, Weiner R, Kelley M, Smolec J, Lee B, Khan M, Tacey R, Hill H, Celniker A. Recommendations for the bioanalytical method validation of ligand-binding assays to support pharmacokinetic assessments of macromolecules. Pharm Res. 2003;20:1885–900.
5. Kuang B, King L, Wang HF. Therapeutic monoclonal antibody concentration monitoring: free or total? Bioanalysis. 2010;2:1125–40.
6. Talbot JJ, Calamba D, Pai M, Ma M, Thway TM. Measurement of free versus total therapeutic monoclonal antibody in pharmacokinetic assessment is modulated by affinity, incubation time, and bioanalytical platform. Aaps J. 2015;17:1446–54.
7. Li H, Ortiz R, Tran L, Hall M, Spahr C, Walker K, Laudemann J, Miller S, Salimi-Moosavi H, Lee JW. General lc-ms/ms method approach to quantify therapeutic monoclonal antibodies using a common whole antibody internal standard with application to preclinical studies. Anal Chem. 2012;84:1267–73.
8. Salimi-Moosavi H, Winters A, Abbott C, Patel J, Hager T, Patel V, Shih J, Zhuang Y, Ma M. A multifactorial screening strategy to identify anti-idiotypic reagents for bioanalytical support of antibody therapeutics. Anal Biochem. 2015;470:52–60.
9. Basalp A, Yucel F. Development of mouse hybridomas by fusion of myeloma cells with lymphocytes derived from spleen, lymph node, and bone marrow. Hybrid Hybridomics. 2003;22:329–31.
10. Kohler G, Milstein C. Continuous cultures of fused cells secreting antibody of predefined specificity. Nature. 1975;256:495–97.
11. Bradbury AR, Sidhu S, Dubel S, McCafferty J. Beyond natural antibodies: the power of in vitro display technologies. Nat Biotechnol. 2011;29:245–54.
12. Schmitt JJ, Zimmermann U, Neil GA. Efficient generation of stable antibody forming hybridoma cells by electrofusion. Hybridoma. 1989;8:107–15.
13. Clackson T, Hoogenboom HR, Griffiths AD, Winter G. Making antibody fragments using phage display libraries. Nature. 1991;352:624.

14. Meijer PJ, Andersen PS, Haahr Hansen M, Steinaa L, Jensen A, Lantto J, Oleksiewicz MB, Tengbjerg K, Poulsen TR, Coljee VW, et al. Isolation of human antibody repertoires with preservation of the natural heavy and light chain pairing. J Mol Biol. 2006;358 (3):764–72.
15. Hu D, Hu S, Wan W, Xu M, Du R, Zhao W, Gao X, Liu J, Liu H, Hong J. Effective optimization of antibody affinity by phage display integrated with high-throughput DNA synthesis and sequencing technologies. PLoS One. 2015;10:e0129125.
16. Fitzgerald V, Leonard P. Single cell screening approaches for antibody discovery. Methods. 2017;116:34–42.
17. Seah YFS, Hu H, Merten CA. Microfluidic single-cell technology in immunology and antibody screening. Mol Aspects Med. 2018;59:47–61.
18. Voigt A, Semenova T, Yamamoto J, Etienne V, Nguyen CQ. Therapeutic antibody discovery in infectious diseases using single-cell analysis. Adv Exp Med Biol. 2018;1068:89–102.
19. Lecault V, Vaninsberghe M, Sekulovic S, Knapp DJ, Wohrer S, Bowden W, Viel F, McLaughlin T, Jarandehei A, Miller M, et al. High-throughput analysis of single hematopoietic stem cell proliferation in microfluidic cell culture arrays. Nat Methods. 2011;8 (7):581–86.
20. Mazutis L, Gilbert J, Ung WL, Weitz DA, Griffiths AD, Heyman JA. Single-cell analysis and sorting using droplet-based microfluidics. Nat Protoc. 2013;8:870–91.
21. Liu X, Painter RE, Enesa K, Holmes D, Whyte G, Garlisi CG, Monsma FJ, Rehak M, Craig FF, Smith CA. High-throughput screening of antibiotic-resistant bacteria in picodroplets. Lab Chip. 2016;16:1636–43.
22. Story CM, Papa E, Hu CC, Ronan JL, Herlihy K, Ploegh HL, Love JC. Profiling antibody responses by multiparametric analysis of primary b cells. Proc Natl Acad Sci U S A. 2008;105:17902–07.
23. Jin A, Ozawa T, Tajiri K, Obata T, Kondo S, Kinoshita K, Kadowaki S, Takahashi K, Sugiyama T, Kishi H, et al. A rapid and efficient single-cell manipulation method for screening antigen-specific antibody-secreting cells from human peripheral blood. Nat Med. 2009;15(9):1088–92.
24. Ronan JL, Story CM, Papa E, Love JC. Optimization of the surfaces used to capture antibodies from single hybridomas reduces the time required for microengraving. J Immunol Methods. 2009;340:164–69.
25. Fitzgerald V, Manning B, O'Donnell B, O'Reilly B, O'Sullivan D, O'Kennedy R, Leonard P. Exploiting highly ordered subnanoliter volume microcapillaries as microtools for the analysis of antibody producing cells. Anal Chem. 2015;87:997–1003.
26. Tiller T, Busse CE, Wardemann H. Cloning and expression of murine ig genes from single b cells. J Immunol Methods. 2009;350:183–93.
27. Haessler U, Reddy ST. Using next-generation sequencing for discovery of high-frequency monoclonal antibodies in the variable gene repertoires from immunized mice. Methods Mol Biol. 2014;1131:191–203.
28. Valley JK, Neale S, Hsu HY, Ohta AT, Jamshidi A, Wu MC. Parallel single-cell light-induced electroporation and dielectrophoretic manipulation. Lab Chip. 2009;9:1714–20.
29. Chiou PY, Ohta AT, Wu MC. Massively parallel manipulation of single cells and microparticles using optical images. Nature. 2005;436:370–72.
30. Hsu HY, Ohta AT, Chiou PY, Jamshidi A, Neale SL, Wu MC. Phototransistor-based optoelectronic tweezers for dynamic cell manipulation in cell culture media. Lab Chip. 2010;10:165–72.
31. Beaumont KG, Hamou W, Bozinovic N, Silvers TR, Shah H, Dave A, Allette K, Strahl M, Wang Y-C, Arib H, et al. Multiparameter cell characterization using nanofluidic technology facilitates real-time phenotypic and genotypic elucidation of intratumor heterogeneity. bioRxiv. 2018;457010.
32. Mocciaro A, Roth TL, Bennett HM, Soumillon M, Shah A, Hiatt J, Chapman K, Marson A, Lavieu G. Light-activated cell identification and sorting (lacis) for selection of edited clones on a nanofluidic device. Commun Biol. 2018;1:41.
33. Le K, Tan C, Gupta S, Guhan T, Barkhordarian H, Lull J, Stevens J, Munro T. A novel mammalian cell line development platform utilizing nanofluidics and optoelectro positioning technology. Biotechnol Prog. 2018;34:1438–46.
34. Smith KG, Hewitson TD, Nossal GJ, Tarlinton DM. The phenotype and fate of the antibody-forming cells of the splenic foci. Eur J Immunol. 1996;26:444–48.
35. Kurosawa N, Yoshioka M, Isobe M. Target-selective homologous recombination cloning for high-throughput generation of monoclonal antibodies from single plasma cells. BMC Biotechnol. 2011;11:39.
36. Tiller T. Single b cell antibody technologies. N Biotechnol. 2011;28:453–57.
37. Clargo AM, Hudson AR, Ndlovu W, Wootton RJ, Cremin LA, O'Dowd VL, Nowosad CR, Starkie DO, Shaw SP, Compson JE, et al. The rapid generation of recombinant functional monoclonal antibodies from individual, antigen-specific bone marrow-derived plasma cells isolated using a novel fluorescence-based method. MAbs. 2014;6(1):143–59.
38. Starkie DO, Compson JE, Rapecki S, Lightwood DJ. Generation of recombinant monoclonal antibodies from immunised mice and rabbits via flow cytometry and sorting of antigen-specific igg+ memory b cells. PLoS One. 2016;11:e0152282.
39. Ouisse LH, Gautreau-Rolland L, Devilder MC, Osborn M, Moyon M, Visentin J, Halary F, Bruggemann M, Buelow R, Anegon I, et al. Antigen-specific single b cell sorting and expression-cloning from immunoglobulin humanized rats: A rapid and versatile method for the generation of high affinity and discriminative human monoclonal antibodies. BMC Biotechnol. 2017;17(1):3.
40. Pracht K, Meinzinger J, Daum P, Schulz SR, Reimer D, Hauke M, Roth E, Mielenz D, Berek C, Corte-Real J, et al. A new staining protocol for detection of murine antibody-secreting plasma cell subsets by flow cytometry. Eur J Immunol. 2017;47(8):1389–92.
41. Green LL. Antibody engineering via genetic engineering of the mouse: xenomouse strains are a vehicle for the facile generation of therapeutic human monoclonal antibodies. J Immunol Methods. 1999;231:11–23.
42. Kilpatrick KE, Wring SA, Walker DH, Macklin MD, Payne JA, Su JL, Champion BR, Caterson B, McIntyre GD. Rapid development of affinity matured monoclonal antibodies using rimms. Hybridoma. 1997;16:381–89.
43. Wring SA, Kilpatrick KE, Hutchins JT, Witherspoon SM, Ellis B, Jenner WN, Serabjit-Singh C. Shorter development of immunoassay for drugs: application of the novel rimms technique enables rapid production of monoclonal antibodies to ranitidine. J Pharm Biomed Anal. 1999;19:695–707.

Exhibit 11

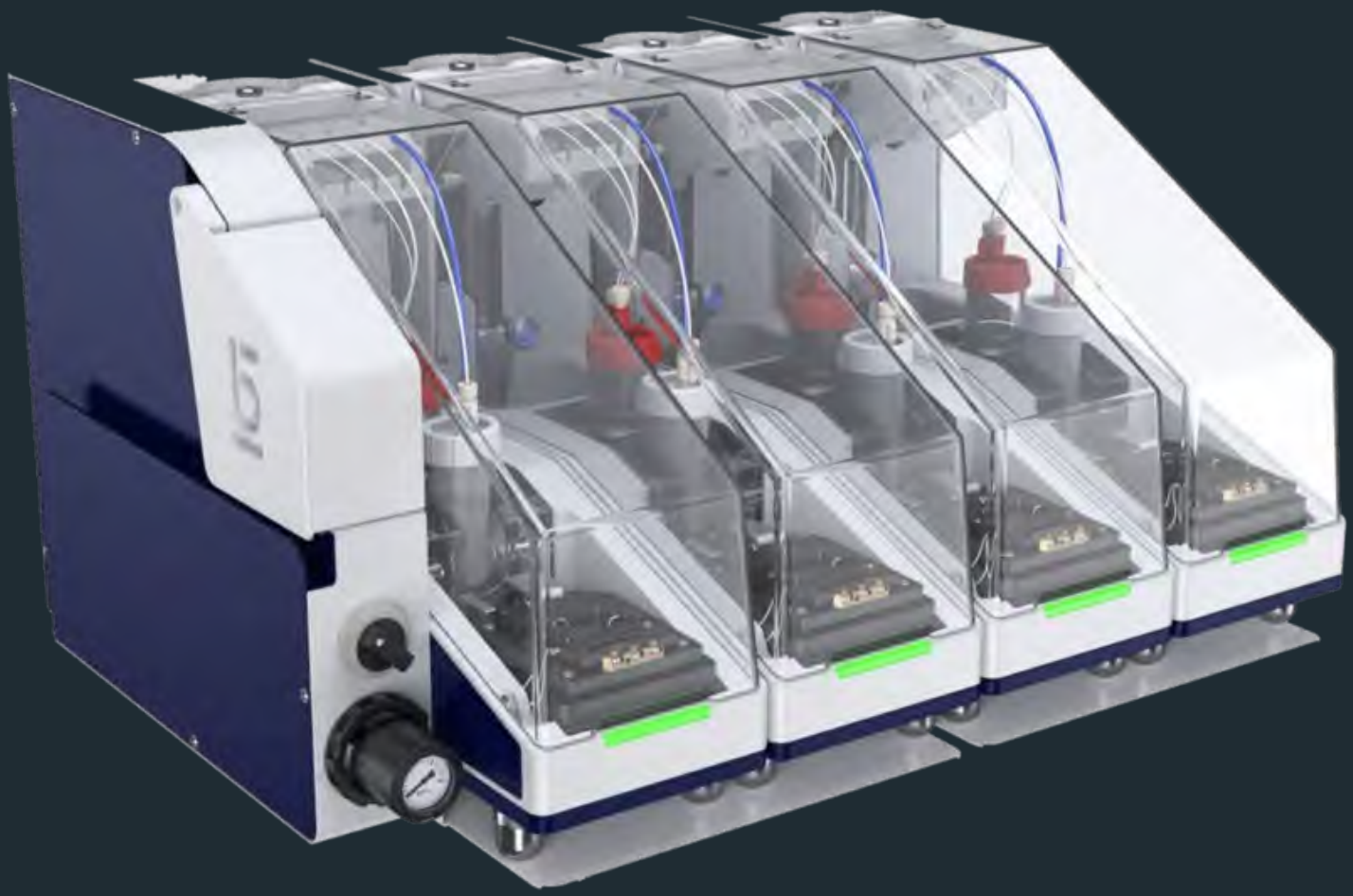

SYSTEM

The Culture Station™ System

Expand Scope, Scale, and Throughput of your Beacon® or

Lightning™ optofluidic system.

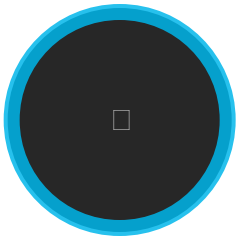

OVERVIEW

Find the cells you are looking for even faster.

The Culture Station lets you free up your Beacon or Lightning system during cell culture and get results faster by running multiple chips in parallel. Save time by running larger experiments with more cells. Optimize experimental conditions more quickly by running 4 chips with independent media types and get your results faster.

DESIGN THE PROCESS

Expand the scope and throughput of your single-cell analysis.

The Culture Station lets you transfer up to 4 OptoSelect™ chips to a culture module with independent media, fluidics and software, and can be seamlessly integrated into Beacon and Lightning workflows. Run media optimization or free up your Beacon or Lightning system to run other experiments during culture stages of an experiment. Once culture has completed, the OptoSelect chips can be moved back to the Beacon or Lightning instruments for further analysis.

This creates a seamless interface between systems and increases throughput when cell culture becomes a constraint. Parallel processing of culture while simultaneously running assays on Beacon or Lightning reduces the product development cycle time and lowers cost, maximizing benefits to the system user. Expand your Culture Station to include capacity for up to 8 chips by linking 2 instruments together on the same computer.

Related Resources

View All Beacon System Resources

Explore Our Technology

Our technology combines precise cell processing, time-saving workflow automation, and rich, deep profiling.

Learn More

General Inquiries
info@berkeleylights.com
+1 (510) 858-2855

Tech Support
techsupport@berkeleylights.com
+1 (888) 254-5595 / Ext. 4

Exhibit 12

Phone: 1 (888) 254-5595 ext. 4 | Email: techsupport@berkeleylights.com

BERKELEY LIGHTS

MENU +

BERKELEY LIGHTS SUPPORT PORTAL.

Digital Cell Biology at Light Speed

LEARN MORE

Search

WELCOME TO THE SERVICE PORTAL.
POWERFUL SUPPORT FROM THE BERKELEY LIGHTS TEAM.

File Case

Submit a request for instrument or workflow help

Knowledge Base

Browse manuals, protocols, user guides and FAQs

Videos

Watch BLI instructional videos

Forum

Submit questions and answers to other users

Troubleshooting

Find the answer to your workflow question